Design, Synthesis and Pharmacological Evaluation of Novel Phosphodiesterase-4 Inhibitors for their Anti-Depressant and Anxiolytic Potential

THESIS

Submitted in partial fulfilment
of the requirements for the degree of
DOCTOR OF PHILOSOPHY

by

MUTHU VENKATESH SUDALI

Under the Supervision of
Prof. R. MAHESH

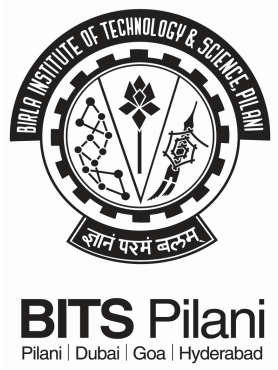

BIRLA INSTITUTE OF TECHNOLOGY & SCIENCE, PILANI
2015

DEDICATED TO MY BELOVED PARENTS & FAMILY

Table of Contents

Contents		***Page No.***
Certificate		*i*
Acknowledgments		*ii*
List of Abbreviations and Symbols		*iv*
List of Figures		*xi*
List of Tables		*xvi*
Abstract		*xviii*
Chapter 1	Introduction	1
Chapter 2	Literature review	30
Chapter 3	Objectives and Plan of Work	57
Chapter 4	Experimental methods	62
Chapter 5	Results and Discussions	134
Chapter 6	Summary and Conclusions	235
Chapter 7	Bibliography	242
Appendix I	*List of Publications and Presentations*	*A-1*
Appendix II	*Biographies*	*A-2*

BIRLA INSTITUTE OF TECHNOLOGY & SCIENCE, PILANI

CERTIFICATE

This is to certify that the thesis entitled **"Design, Synthesis and Pharmacological Evaluation of Novel Phosphodiesterase-4 Inhibitors for their Anti-Depressant and Anxiolytic Potential"** and submitted by **Muthu Venkatesh Sudali** ID No. **2010PHXF010P** for award of Ph.D. Degree of the Institute embodies original work done by him under my supervision.

Signature of the Supervisor:

Name in capital letters: **Prof. R. MAHESH**

Designation: **Professor, Department of Pharmacy &**

Dean, Faculty Affairs,

Birla Institute of Technology & Science, Pilani

Pilani Campus

Date:

Acknowledgments

I am grateful to my research advisor **Prof R. Mahesh**, Dean, Faculty Affairs, BITS Pilani, Pilani Campus for providing valuable wealth of information due to his versatile expertise which immensely contributed to improve my research and prepare me for future challenges. I owe him huge debt of gratiude for providing constant support and freedom to express my capability in research. I could not have it without him. Thanks **Prof R. Mahesh**.

I am grateful to **Prof. B.N. Jain**, Vice-Chancellor, BITS Pilani and **Prof. G. Raghurama**, Director, BITS Pilani, Pilani Campus for permitting me to pursue my research work in the Institute.

I express my earnest thanks to **Prof. R. N. Saha**, Director, BITS Pilani, Dubai Campus for his valuable suggestions and impetus during my research work. I am grateful to **Prof. S. K. Varma**, Dean (RCD) for his motivation, constant support and encouragement.

I would like to thank my doctoral approval committee (DAC) members **Dr. S. Murugesan**, Head, Department of Pharmacy, Pilani Campus and **Dr. Hemant R. Jadhav**, Associate Dean, Academic Research Division for helpful discussions and suggestions during the dissertation. I am highly indebted to **Prof. Vijay K. Chaudhary**, Department of Biochemistry, University of Delhi South Campus, New Delhi for permitting me to use their instrumentation facility (Elisa Reader) and **Mr. Kapil Mathur** Research Scholar in department of Biochemistry for assistance provided in handling the instrument. I would also like to heartily thank **Dr. Jyoti**, **Mr. Samir Singh** and **Ms. Pooja Shah** for their untiring support during the patent process of my research work.

I would like to specially thank **Dr. T. Devadoss**, **Dr. Senthil Kumar** and **Mr. Sampath** for the enormous assistance provided throughout my research work.

I would also like to acknowledge **Dr. Srikant Charde**, Head, Department of Pharmacy, Hyderabad Campus, **Dr. Atish Paul**, Convener, Departmental Research Committee, **Dr. Anil Gaikwad**, and **Dr. Rajeev Taliyan** for their assistance during the dissertation. I am highly indebted to **Mr. Ashok P** and **Mr. Arghya** for the enthusiasm, support and timely guidance given by them during all the stages of my work. I would like to thank **Mr. Ankur** for his assistance during my animal studies.

My special thanks to **Dr. R. P. Pareek**, **Dr. Sushil Yadav**, **Dr. Sunil Dubey**, **Dr. Anil Jindal**, **Dr. Anupama Mittal**, **Dr. Deepak Chitkara**, **Mr. Mahaveer Singh**, **Mr. Shvetank Bhatt**, **Mr. Murli M. Pandey**, **Mr. Gautam Singhvi**, **Ms. Priti Jain**, **Ms. Archana Kakkar** and **Mr. Baldev Gautam** for their helpful advices.

I always had a hearty inspiration from **Mr. Jaipal A**, **Mr. Emil**, **Mr. Prashant**, **Mr. Satish**, **Mr. Yeshwant**, **Mr. Ashok Sharma** for the wonderful moments we have shared and making my stay in Pilani, a pleasant and memorable one.

I express heartiest gratitude to all my dear friends and colleague research scholars of Department of Pharmacy **Mr. Vadiraj**, **Mr. Santosh**, **Ms. Garima**, **Ms. Vibhu**, **Ms. Deepali**, **Mr. Pankaj**, **Mr. Subhash**, **Mr. Sridhar**, **Mr. Almesh**, **Mr. Saurabh**, **Mr. Sorabh**, **Ms. Anuradha**, **Ms. Sruthi** and **Dr. Pallavi** for timely help and their friendship shall always be remembered.

I thank the non-teaching staff **Mr. Hari**, **Mr. Pradeep**, **Mr. Ram Suthar**, **Mr. Puran**, **Mr. Sajjan**, **Mr. Mahender**, **Mr. Naveen**, **Mr Tarachand**, **Mr. Laxman**, **Mr. Sitaram**, **Mr. Vishal**, **Mr. Shyam**, **Mr. Mukesh** and **Mr. Shiv** and all the students of Pharmacy departmentfor their valuable help at each stage of the research work.

My special thank to **Mr. Avthar Singh** and **SAIF**, **Panjab University**, Chandigarh for providing analytical facilities related to my research work.

I would like to thank **Department of Biotechnology**, New Delhi for funding the research work and providing the fellowship and later from **University Grants Commission** for Basic Science Research.

Last but not least, I would also like to thank **Department of Pharmacy** and **BITS Pilani University** for giving me an opportunity to carry out my research successfully.

I would be failing in my duties if I forget those pretty **animals** which were part of my research work.

My sincere thanks and regrets to all friends and people I missed to acknowledge who had directly or indirectly helped me to accomplish this task.

Finally, I would like to express my heartfelt thanks to my parents **S. Sudalai** and **S. Esakiammal**, sister **S. Nambi Nachiyar** wife **A. Priya** and my beloved son **M. V. Pranesh**

Last but not the least; it is GOD, the 'Almighty' who graced me in finishing this task.

Muthu Venkatesh Sudali

List of Abbreviations and Symbols

AA	Amino acid
Ach	Acetylcholine
AC	Adenylyl cyclases
ADMET	Absorption, distribution, metabolism, excretion, toxicity
AKAP	A-kinase anchor proteins
AMP	Adenosine monophosphate
AM1	Austin model 1
ANOVA	Analysis of variance
APA	American psychiatric association
ATP	Adenosine triphosphate
BBB	Blood brain barrier
BDNF	Brain-derived neurotrophic factor
BFGS	Broyden-Flecher Gold Farbshanno
BnBr	Benzyl bromide
BZD	Benzodiazepine(s)
CAM	Complementary and alternative medicine(s)
Ca^{2+}	Calcium ions
cAMP	cyclic Adenosine monophosphate
CBT	Cognitive behavior psychotherapy
cGMP	cyclic Guanosine monophosphate
$CDCl_3$	Deuterated chloroform
CN	Cyclic nucleotide(s)
CNS	Central nervous system
COPD	Chronic obstructive pulmonary disease
CREB	cAMP response-element binding protein

CYP	Cytochrome
DA	Dopamine
DAG	Diacylglycerol
DCM	Dichloromethane
DMSO	Dimethyl sulfoxide
DS	Discovery studio
DSM	Diagnostic and statistical manual of mental disorders
EC	Enzyme commission
ECT	Electro-convulsive shock therapy
ELISA	Enzyme-linked immunosorbent assay
EPAC	Exchange proteins activated by cAMP
EPM	Elevated plus-maze
ERK	Extracellular signal-regulated kinases
ESI	Electron spray ionization
EtOAc	Ethyl acetate
EtOH	Ethanol
FAM	Carboxyfluorescein
FDA	Food and drug administration
FP	Fluorescence polarization
FST	Force swim test
FTIR	Fourier transform infrared
GABA	Gamma amino butyric acid
GAD	Generalized anxiety disorder
GDP	Guanosine diphosphate
GMP	Guanosine monophosphate
GPCR	G-protein-coupled receptors

G_i	G-protein inhibitory
G_s	G-protein stimulatory
GSK	Glaxo Smithkline Beehcam
GTP	Guanosine triphosphate
HARBS	High affinity rolipram binding site
HBA	Hydrogen bond acceptor
HBD	Hydrogen bond donor
HIA	Human intestinal absorption
HOBt	1-hydroxybenzotriazole
HPA	Hypothalamic-pituitary-adrenal
^{1}H NMR	Proton nuclear magnetic resonance
5-HT	Serotonin/5-hydroxytrytophan
IAEC	Institutional Animal Ethics Committee
IP_3	Ionositol triphosphate
IR	Infrared
I.V	Intravenous
K_m	Michaelis constant
LARBS	Low affinity rolipram binding site
Log P	Log of oil/water partition coefficient
LR	Linker region
M	Molar
MAOI	Monoamine oxidase inhibitor(s)
MDD	Major Depression disorder
MeOH	Methanol
Me^{2+}	Metal ions
Mg^{2+}	Magnesium ions

MS	Mass spectrometer
MW	Molecular weight
NCE	New chemical entity
NDRI	Nor-adrenaline and dopamine re-uptake inhibitor
NE	Norepinephrine/Noradrenaline
NMP	Nucleotide monophosphate
NO	Nitric oxide
OCD	Obsessive compulsive disorder
OFT	Open field test
PD	Panic disorder
PDB	Protein Data Bank
PDE	Phosphodiesterase
PFC	Prefrontal cortex
pH	Negative log to the base 10 of hydrogen ion concentration
PK	Pharmacokinetic(s)
PKA	Protein kinase-A
PKG	Protein Kinase-G
PLP	Piecewise Linear Potential
PPB	Plasma protein binding
PTSD	Post traumatic stress disorder
QOL	Quality of life
R_f	Retention factor
RA	Rheumatoid arthritis
RBF	Round bottom flask
RCSB	Research collaboratory for structural bioinformatics
RMSD	Root mean square deviation

Rt	Room temperature
SAD	Separation anxiety disorder
SAR	Structure activity relationship
SD	Standard deviation
Sec/s	Seconds
SEM	Standard error of mean
SLA	Spontaneous locomotor activity
SNRI	Selective nor-epinephrine re-uptake inhibitor
SP	Specific phobia
SSRI	Selective serotonin re-uptake inhibitor
TCA	Tricyclic anti-depressants
TeCA	Tetracyclic anti-depressant
TEA	Triethyl amine
THF	Tetrahydrofuran
TMS	Tetramethylsilane
TST	Tail suspension test
UCR	Upstream conserved regions
TLC	Thin layer chromatography
UCR	Upstream conserved region
UV	Ultraviolet
Zn^{2+}	Zinc ions
Á	Angstrom (10^{-10} meter)
°C	Degree centigrade
λ_{max}	Wavelength of maximum absorbance
%	Percentage
=	Equal to

<	Less than
>	More than
s	Singlet
d	Doublet
t	Triplet
q	Quartet
m	Multiplet
J	Coupling constant
σ	Sigma
π	Pi
α	Alpha
β	Beta
γ	Gamma
δ	Delta
µM	Micro molar
µl	Micro liter
µg/l	Microgram per liter
µg/ml	Microgram per milliliter
bend	Bending
conc.	Concentration
calcd.	Calculated
cm	Centimeter
cm^{-1}	Centimeter inverse
g	Gram
H	Hydrogen
hr	Hour

i.p.	Intraperitoneal
L	Liter
Mg	Milligram
mg/Kg	Milligram per kilogram
MHz	Mega Hertz
Min	Minutes
Ml	Milli liter
mM	Millimolar
m/z	Mass per charge ratio
nM	Nanomolar
p.o.	Per-oral
str	Stretching
v/v	Volume by volume
w/v	Weight by volume
3D	Three dimension

List of Figures

Fig. No.	*Caption*	*Page No.*
1a	Cell signaling pathway	2
1b	Signal pathway of cAMP and cGMP and its role in physiological process	2
2	PDE-catalyzed hydrolysis of cAMP and cGMP	3
3	Schematic representation of mechanism of cellular signaling by cAMP	5
4	Domain structures of PDE 1-11	6
5	PDE families based on their substrate specificity	6
6	Diagrammatic representations of architecture of PDE enzyme	8
7	The glutamine switch mechanism	9
8	Important residues involved in hydrolysis of cAMP catalyzed by PDE4B	10
9	A putative mechanism for the phosphodiester bond hydrolysis by PDEs	11
10	Molecular characteristics of catalytic regions in PDE4 enzyme	13
11	Structures of some MAOIs	23
12	Structures of some TCAs	24
13	Structures of some SSRIs	25
14	Structures of some atypical and second-generation anti-depressant	26
15	Structures of some benzodiazepines	27
16	Structures of some azaspirones	28
17	Structures of miscellaneous compounds	28
18	Structural classification of PDE4 inhibitors	30
19	Plausible interaction of rolipram in PDE4 active site	32
20	Plausible modifications on rolipram to design better PDE4 inhibitors	33
21	Plausible interaction of nitraquazone in PDE4 active site	43

Fig. No.	*Caption*	*Page No.*
22	Plausible interaction of theophylline in PDE4 active site	52
23	Assay by fluorescent polarization principle	124
24	Difference between 'potency' (affinity) and 'efficacy' (activity)	125
25	Validation of docking methodology	128
26	Nitraquazone derivatives selected for building pharmacophore model	134
27	Novel pharmacophoric model for designing novel PDE4 inhibitors	136
28	Pharmacophoric comparison of Nitraquazone derivatives and QC (A – F) series and QZ (A – B) series	138
29	Mechanism of ethyl 3-oxo-3,4-dihydroquinoxaline-2-carboxylate formation	139
30	Mechanism of ethyl 4-benzyl/substituted benzyl 3-oxo-3,4-dihydroquinoxaline-2-carboxylate formation	140
31	Mechanism of 2-amino-*N*-benzyl/substituted benzylbenzamide formation	140
32	Mechanism of ethyl 3-benzyl/substituted benzyl-4-oxo-3,4-dihydroquinazoline-2-carboxylate formation	141
33	2D interaction of QCA-1 at the active site of PDE4D	147
34	2D interaction of QCA-1 at the active site of PDE4B	147
35	2D interaction of QCA-8 at the active site of PDE4D	148
36	2D interaction of QCA-14 at the active site of PDE4D	148
37	2D interaction of QCA-4 at the active site of PDE4D	149
38	2D interaction of QCA-10 at the active site of PDE4D	149
39	2D interaction of QCA-11 at the active site of PDE4D	150
40	2D interaction of QCA-13 at the active site of PDE4D	150
41	2D interaction of QCA-15 at the active site of PDE4B	150
42	ADMET Plot for QCA Series	153

Fig. No.	*Caption*	*Page No.*
43	2D interaction of QCB-11 at the active site of PDE4D	166
44	2D interaction of QCB-7 at the active site of PDE4D	166
45	2D interaction of QCB-6 at the active site of PDE4D	167
46	2D interaction of QCB-6 at the active site of PDE4B	167
47	2D interaction of QCB-16 at the active site of PDE4D	168
48	2D interaction of QCB-13 at the active site of PDE4D	168
49	2D interaction of QCB-12 at the active site of PDE4D	169
50	2D interaction of QCB-18 at the active site of PDE4D	169
51	2D interaction of QCB-14 at the active site of PDE4B	169
52	ADMET Plot for QCB Series	174
53	2D interaction of QCC-12 at the active site of PDE4D	183
54	2D interaction of QCC-10 at the active site of PDE4D	183
55	2D interaction of QCC-2 at the active site of PDE4D	184
56	2D interaction of QCC-11 at the active site of PDE4D	184
57	2D interaction of QCC-5 at the active site of PDE4D	185
58	2D interaction of QCC-3 at the active site of PDE4D	185
59	2D interaction of QCC-1 at the active site of PDE4D	185
60	2D interaction of QCC-1 at the active site of PDE4B	185
61	2D interaction of QCC-16 at the active site of PDE4D	186
62	2D interaction of QCC-8 at the active site of PDE4B	186
63	ADMET Plot for QCC Series	188
64	2D interaction of QCD-16 at the active site of PDE4D	193
65	2D interaction of QCD-16 at the active site of PDE4B	193
66	2D interaction of QCD-4 at the active site of PDE4D	193
67	2D interaction of QCD-3 at the active site of PDE4D	193

Fig. No.	*Caption*	*Page No.*
68	2D interaction of QCD-8 at the active site of PDE4D	194
69	2D interaction of QCD-15 at the active site of PDE4D	194
70	2D interaction of QCD-5 at the active site of PDE4D	194
71	ADMET Plot for QCD Series	197
72	2D interaction of QCE-5 at the active site of PDE4D	202
73	2D interaction of QCE-5 at the active site of PDE4B	202
74	2D interaction of QCE-7 at the active site of PDE4D	202
75	2D interaction of QCE-7 at the active site of PDE4B	203
76	2D interaction of QCE-6 at the active site of PDE4D	203
77	2D interaction of QCE-6 at the active site of PDE4B	203
78	2D interaction of QCE-13 at the active site of PDE4D	204
79	2D interaction of QCE-8 at the active site of PDE4D	204
80	2D interaction of QCE-18 at the active site of PDE4D	204
81	2D interaction of QCE-10 at the active site of PDE4D	204
82	2D interaction of QCE-12 at the active site of PDE4D	205
83	2D interaction of QCE-11 at the active site of PDE4D	205
84	ADMET Plot for QCE Series	207
85	2D interaction of QCF-10 at the active site of PDE4D	212
86	2D interaction of QCF-10 at the active site of PDE4B	212
87	2D interaction of QCF-18 at the active site of PDE4D	212
88	2D interaction of QCF-2 at the active site of PDE4D	213
89	2D interaction of QCF-17 at the active site of PDE4D	213
90	2D interaction of QCF-16 at the active site of PDE4D	213
91	2D interaction of QCF-5 at the active site of PDE4D	214
92	2D interaction of QCF-5 at the active site of PDE4B	214

Fig. No.	*Caption*	*Page No.*
93	2D interaction of QCF-4 at the active site of PDE4D	214
94	2D interaction of QCF-8 at the active site of PDE4D	214
95	ADMET Plot for QCF Series	217
96	2D interaction of QZA-10 at the active site of PDE4D	222
97	2D interaction of QZA-15 at the active site of PDE4D	222
98	2D interaction of QZA-3 at the active site of PDE4D	223
99	2D interaction of QZA-12 at the active site of PDE4D	223
100	2D interaction of QZA-14 at the active site of PDE4D	223
101	2D interaction of QZA-4 at the active site of PDE4D	224
102	ADMET Plot for QZA Series	226
103	2D interaction of QZB-5 at the active site of PDE4D	231
104	2D interaction of QZB-11 at the active site of PDE4D	231
105	2D interaction of QZB-2 at the active site of PDE4D	231
106	2D interaction of QZB-3 at the active site of PDE4D	231
107	2D interaction of QZB-4 at the active site of PDE4B	232
108	2D interaction of QZB-6 at the active site of PDE4B	232
109	ADMET Plot for QZB Series	234

List of Tables

Table No.	*Caption*	*Page No.*
1	The phosphodiesterase superfamily	7
2	PDEs and their conserved glutamine residues	10
3	Conserved hydrophobic clamp residues in PDE family	11
4	Distances between the pharmacophoric elements of selected nitraquazone derivatives and standard PDE4 inhibitors	135
5	Distances between the pharmacophoric elements of the designed series	137
6	In-vitro data of QCA series	143
7	Docking results of QCA series for PDE4D	145
8	Docking results of QCA series for PDE4B	146
9	ADME properties of QCA Series	152
10	Pharmacological data of QCA series analogues for SLA and its anti-depressant activity in FST mice model	155
11	Anti-depressant activity of QCA series analogues in TST mice model	157
12	Effect of QCA series analogues and diazepam on the behavior of mice in EPM test	159
13	Effect of QCA series analogues and diazepam in dark-light mice model	161
14	Effect QCA series analogues and diazepam on the behavior of mice in OFT	163
15	In-vitro data of QCB series	165
16	Docking results of QCB series for PDE4D	170
17	Docking results of QCB series for PDE4B	171
18	ADME properties of QCB Series	173
19	Pharmacological data of QCB series analogues for SLA and its anti-depressant activity in FST and TST mice model	177
20	In-vitro data of QCC series	179

Table No.	*Caption*	*Page No.*
21	Docking results of QCC series for PDE4D	181
22	Docking results of QCC series for PDE4B	182
23	ADME properties of QCC Series	187
24	In-vitro data of QCD series	190
25	Docking results of QCD series for PDE4D	191
26	Docking results of QCD series for PDE4B	192
27	ADME properties of QCD Series	196
28	In-vitro data of QCE series	199
29	Docking results of QCE series for PDE4D	200
30	Docking results of QCE series for PDE4B	201
31	ADME properties of QCE Series	206
32	In-vitro data of QCF series	209
33	Docking results of QCF series for PDE4D	210
34	Docking results of QCF series for PDE4B	211
35	ADME properties of QCF Series	216
36	In-vitro data of QZA series	219
37	Docking results of QZA series for PDE4D	220
38	Docking results of QZA series for PDE4B	221
39	ADME properties of QZA Series	225
40	In-vitro data of QZB series	228
41	Docking results of QZB series for PDE4D	229
42	Docking results of QZB series for PDE4B	230
43	ADME properties of QZB Series	233

Abstract

Phosphodiesterase-4(PDE4), an important component of the cyclic adenosine monophosphate (cAMP) cascade, selectively metabolizes cAMP in the brain to the inactive monophosphate. Their inhibitors may offer novel strategies in the treatment of depression. However, its development as antidepressant drugs has been encumbered by their side effects profile of non-selective PDE inhibitors like nausea, emesis, gastrointestinal side-effects, and vascular toxicity. These side-effects can be minimized by specifically targeting isozymes in the particular tissue or the cell of interest. So, we were interested in developing novel, PDE4 inhibitors with better isozyme selectivity and further explore their potential as anti-depressant and anxiolytics.

The novel pharmacophoric requirements derived from nitraquazone and its related compounds as potential PDE4 inhibitors that include key elements: a) a planar scaffold providing a HBA and b) two hydrophobic substituent's with their corresponding linker (1 and 2). On the basis of the proposed pharmacophore, six different series of N4 substituted quinoxaline based carboxamides with variations on linker-1 and/or unsubstituted/substituted hydrophobe, and while two series of N3 substituted quinazoline based carboxamides which are positional isomer of quinoxaline-carboxamides were designed as per the pharmacophoric requirements as novel PDE4 inhibitors.

The first series comprises of linker-1 having alkyl group and unsubstituted hydrophobe i.e., benzyl (QCA), while in second series substituted hydrophobe having strong activating group (OCH_3) at para-position i.e., 4-methoxybenzyl (QCB), and in third series substituted hydrophobe having strong deactivating group (CN) at para-position i.e., 4-cyanobenzyl (QCC) were designed and synthesized. Similarly unsubstituted hydrophobe with linker-1 having carbonyl group viz., benzoyl (QCD), or having both alkyl and carbonyl group i.e., 2-phenylacetyl (QCE), or (*n = 2*) increased alkyl chain length i.e., phenethyl (QCF), while two series of N3 substituted quinazoline based carboxamides which are positional isomer of QCA and QCB series viz. benzyl (QZA), 4-methoxybenzyl (QZB) were also designed and synthesized.

The novel designed NCE's adhered to the pharmacophoric features and distances in accordance with the designed pharmacophoric model. "Lipinski's rule of five" was considered to attain better pharmacokinetic profile. The proposed compounds were mapped, In order to find the best fit among compounds that are capable of binding to PDE4 with a similar or better set of interactions. On comparison between pharmacophoric model and the designed series, the RMSD values indicate that all the

proposed compounds had high fit value. The designed NCE's were then synthesized and evaluated for their PDE4 inhibitory activity. The quinoxaline-carboxamides were synthesized from the starting material, *o*-phenylenediamine in a sequence of reactions; while the quinazoline-carboxamides were synthesized from the starting material, isatoic anhydride in a sequence of reactions; the structures of these synthesized molecules were confirmed by spectral data and the purity was assessed by thin layer chromatography. The synthesized compounds were further subjected to *in-vitro* assay by PDE4D and PDE4B isoform elisa-kit using fluorescence polarization (FP) principle.

Most of the synthesized compounds exhibited varied PDE4 inhibitory activity and comparably better actives for PDE4D than PDE4B but had showed equal affinity for both the isoforms. Among the N4 substituted quinoxaline-2-carboxamides, 4-cyano derivatives QCC-5, QCC-2 and QCC-17 containing strong deactivating group exhibited prominent inhibition and better affinity for PDE4D than PDE4B isoform. Considering this compound as lead further appropriate modifications could possibly enhance selective inhibition of its isoform. While, among the quinazoline-2-carboxamides, compounds of QZA and QZB displayed notable affinity for PDE4D but were moderate to weak PDE4 inhibitors. On comparing the positional isomeric series, (QCA and QZA) and (QCB and QZB) the quinazoline planar scaffold with HBA is preferred over the quinoxaline scaffold with HBA for selective PDE4D isoform inhibition.

The results indicate that the position of nitrogen and keto group in the planar scaffold including the benzyl group plays a major role in defining the potency and affinity among the isoform. Among the quinoxaline-2-carboxamide series, modification on the linker-1 with alkyl or carbonyl group does not play any crucial role in the activity or affinity. The SAR studies of these analogues synthesized indicate that the substitution at *ortho*-position on the phenyl ring is better tolerated for PDE4D inhibitory activity. These moieties have markedly lower affinity and inhibitory activity for PDE4B isoform. The molecular docking studies were performed using LigandFit and the ADMET properties were computed using the ADME descriptors module in Accelrys (D.S 3.5) software. The interactions of these ligands were analyzed inside the binding site and its drug-like properties have been predicted and reported.

After evaluating their antagonistic potentials, all the synthesized molecules were subjected for their anti-depressant potentials by using various rodents' test battery like forced swim test in mice model, tail suspension test, etc. The compounds with better PDE4 inhibition and significant anti-depressant effects were selected for their anxiolytic study using elevated plus-maze test, L/D model and open field test. Among the tested

moieties in both FST and TST, few compounds (QCA-1, QCA-8, QCA-14, QCA-15, QCB-3, QCB-5, QCB-12 and QCB-15) showed better anti-depressant activity as compared to vehicle treated group. Compounds QCA-1, QCA-8, QCA-11 and QCA-14 exhibited pronounced potential for their anxiolytic like activity as compared to vehicle treated group in EPM. Further, when subjected to open field test (OFT), compounds QCA-1, QCA-8 and QCA-14 exhibited pronounced effect compared to control.

1. Introduction

1.1. Cellular signaling and phosphodiesterases

1.1.1. *Overview of cell signaling Process*

Cell signaling is a vital process essential to control the biography of cells from their birth, during the process of cell proliferation, their differentiation into definite cell types to perform diverse cell functions, and finally their death through processes such as apoptosis. Cell signaling orchestrates all these cellular activity. Many of these signaling systems regulate development, tissue repair, immunity and normal tissue homeostasis; also control broad range of specific processes in adult cells, such as proliferation, contraction, secretion, metabolism, information processing in neurons and sensory perception. Disruption in these signaling pathways leads to disease. However, understanding these signaling pathways, controlling and/or manipulating it at different rate–limiting may lead to the improvement of newer therapeutic agents.

There are a multitude of intracellular signaling pathways responsible for transmitting information within the cell. Among the intracellular messaging systems, primary and secondary messengers are critical components of the signaling network and essential regulators in central nervous system (CNS) functions. Primary messengers are chemical stimulus which exerts their effects locally, or at a distance sites e.g., neurotransmitters, hormones, growth factors, and extracellular matrix components. Once the signal is received by receptor protein, it undergoes a conformational variation thereby launching a sequence of biochemical responses inside the cell. These intracellular signaling pathways, also called signal transduction cascades are critically essential in controlling the amplitude and duration of the intracellular signals to the receptor it is bound. Activation of receptors leads to the synthesis of second messengers that triggers and harmonizes intracellular signaling pathways. **(Fig. 1a)** Major classes of secondary messengers include cyclic nucleotide (CN) e.g., cAMP and cGMP, ionositol triphosphate (IP_3) and diacylglycerol (DAG), calcium ions (Ca^{2+}) and small molecules such as nitric oxide (NO). Among secondary messengers, CNs are in limelight since their discovery in 1957 by Robison, Butcher and Sutherland.[1] In particular, cAMP signaling is thought to play a major role in depression.[2]

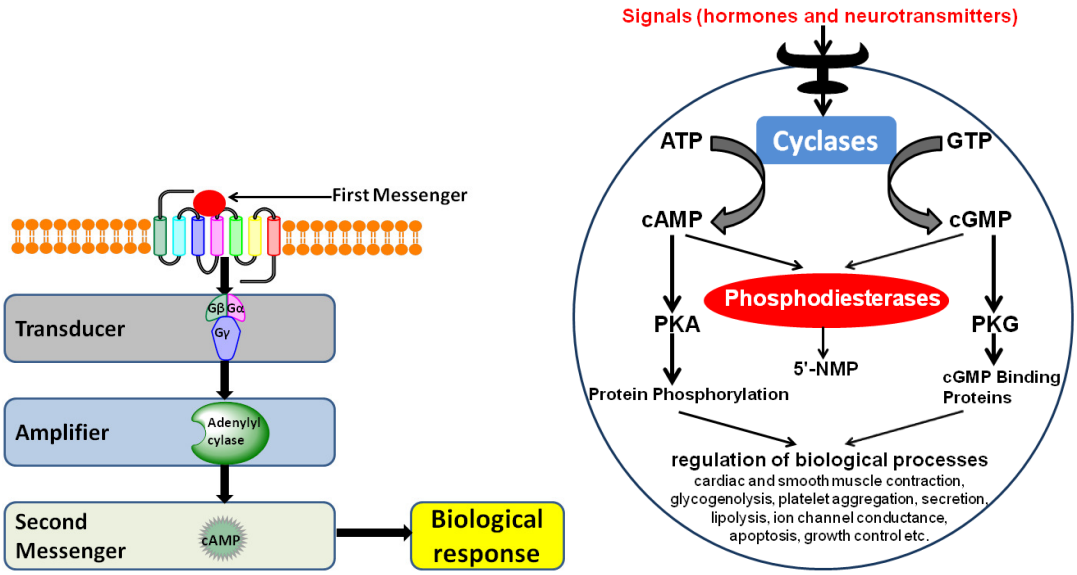

Fig. 1: (a) Cell signaling pathway **(b)** Signal pathway of cAMP and cGMP and its role in physiological process

1.1.2. *Role of cyclic mononucleotides*

Cyclic adenosine monophosphate (cAMP) is a ubiquitous second messenger that regulates a multitude of cellular responses. It mediates the response of cells to a broad array of hormones and neurotransmitters, thereby modulating numerous physiological processes, such as cell growth, differentiation, survival, inflammation, ion channel function, cardiac and smooth muscle contraction, platelet aggregation, secretion, apoptosis, lipogenesis, lipolysis, gluconeogensis and glycogenolysis, etc.[3] **(Fig.1b)**

1.1.3. *Overview of phosphodiesterases*

cAMP, being a conventional second messenger was first discovered by Earl W Sutherland Jr. and Theodore W Rall in 1957, and reported their hydrolytic activities by cyclic nucleotide phosphodiesterases (CN PDEs).[4] Five Nobel award and more than 100,000 publications have been reported on PubMed from the research on cAMP, till date. Application of advanced techniques like fluorescent probes allowed to analyze/visualize and also estimate cAMP signaling at different levels which contributed appreciably in the understanding of this pathway.[5]

CN PDEs is a large multigene family of related metallophosphohydrolases (PDE; EC 3.1.4.17) that selectively catalyzes and hydrolyzes the 3'-cyclic phosphate bonds of adenosine and/or guanosine 3',5'-cyclic monophosphate (cAMP, **1** and cGMP, **3**) to produce the corresponding 5'-monophosphate nucleotide (5'-AMP, **2** and 5'-GMP, **4**) in a variety of tissues.[6] **(Fig.2)** These enzymes display cell type-specific expression patterns and vary distinctly in their forms of regulation, intracellular distribution, relative activities,

and K_m values.[7] Intracellular levels of cAMP in neurons are tightly controlled processes by adenylyl cyclases (ACs) enzymes that regulate its synthesis and degradation by phosphodiesterases (PDEs) which engage machinerys at the receptor and postreceptor levels. Activity of enzymes, such as protein kinases (PK) which transmits signals received at the membrane to the nucleus to switch on and off exact genes and are regulated by cAMP. Transient fluctuations of intracellular cAMP concentrations within a narrow range alter intracellular signaling and maximize biological result.[8]

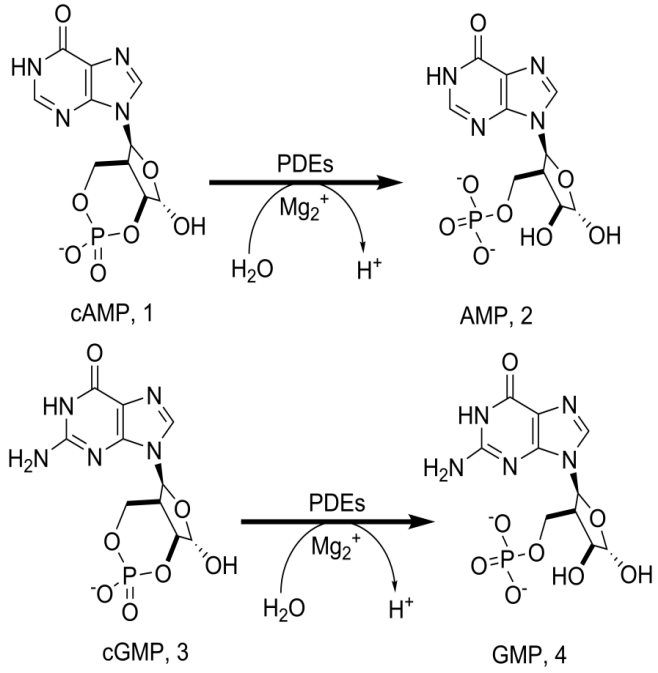

Fig. 2: PDE-catalyzed hydrolysis of cAMP and cGMP

1.1.3.1. *Formation and degradation of cyclic mononucleotides*

cAMP is generated from adenosine triphosphate (ATP) in response to a number of extracellular signals by adenylyl cyclases (ACs), and most of these binds to G_s-protein-coupled receptors (GPCR).[9] The guanine nucleotide-binding regulatory proteins (G-proteins) are a hetero-trimeric complex of G_α, G_β and G_γ subunits, G_α subunits possess GTPase activity. When active, the G_α and $G_{\beta\gamma}$ proteins dissociate from each other and also from the membrane-bound GPCR by exchange of bounded GDP (Guanosine diphosphate) with GTP (Guanosine triphosphate), and activate downstream intracellular signaling cascades. In the case of $G_{\alpha s}$, it signals to a family of proteins called AC, which in turn interacts with a large group of seven-transmembrane-domain receptors.[10] **(Fig.3)** There are in fact 10 members of the AC family including 9 membrane-spanning ACs (AC1-9), and one soluble isoform. Various AC isoenzymes have different regulatory properties, expression patterns, and localization within different domains of the plasma

membrane.[11] Once cAMP is produced by ACs it can affect cellular function by acting through one of three effector systems; cAMP-dependent protein kinase A (PKA), exchange proteins activated by cAMP (EPAC-1 or 2) that activate the small GTP-binding protein Rap1, or cyclic nucleotide gated ion-channels (CN channels).[12] These traids of effectors of cAMP mediate a multitude of cAMP signaling pathways in numerous cells and tissues. **(Fig. 3)** Among the vital substrates for kinase, A-kinase anchor proteins (AKAPs) and PDEs highlight the level of feedback assimilation in these systems. Moreover, a number of receptors inhibit AC by interacting with the inhibitory guanine nucleotide-binding regulatory protein G_i.[12d, 13] Consequences of receptor separation from G-proteins and action of synthetic enzyme cyclases results in accumulation of cyclic mononucleotides with swift modulation of PDEs lead to cAMP degradation.

It is crucial to have mechanism for degradation of these generated intracellular second messengers. In the case of cAMP, this is done uniquely through the action of CN PDEs, which converts cAMP to 5'-AMP. Although several plasma membrane pumps can extrude cAMP from cells, intracellular hydrolysis of cAMP by CN PDEs represents the most prominent mechanism through which this CN is inactivated.[14] **(Fig.3)** It is expected that in influencing local concentrations and compartmentalization, degradation plays a major role than synthesis which further permits PDEs to modify cyclic mononucleotide levels particularly, making them striking drug targets.

In Central nervous system (CNS), cyclic mononucleotide regulates a host of cellular functions involved in signal transduction pathway through PKA, and in synaptic transmission of dopamine/DA, nor-epinephrine/NE, serotonin/5-HT and glutamate neurons. It influences many other functions, such as learning, mood, and nerve growth regeneration.[15] Alterations in availability of CN can contribute to changes in neuronal cell function, thus precipitating, maintaining or exacerbating motor, cognitive or psychiatric disturbances.[16] In the nucleus, cAMP binds to a response-element binding protein (CREB) and affects transcription of many genes including brain-derived neurotrophicfactor (BDNF), thought to be implicated in long-term enhancement of depression and depression-allied brain changes.[15b, 16b, 17]

Thus, PDEs represents an important group of enzymes in this multifaceted dogmatic scheme, and have developed into vital target of greater significance in psychiatric disorders and especially, in depression. Extensive expression of PDEs throughout the brain makes it prospective targets for drug development.[15b, 18]

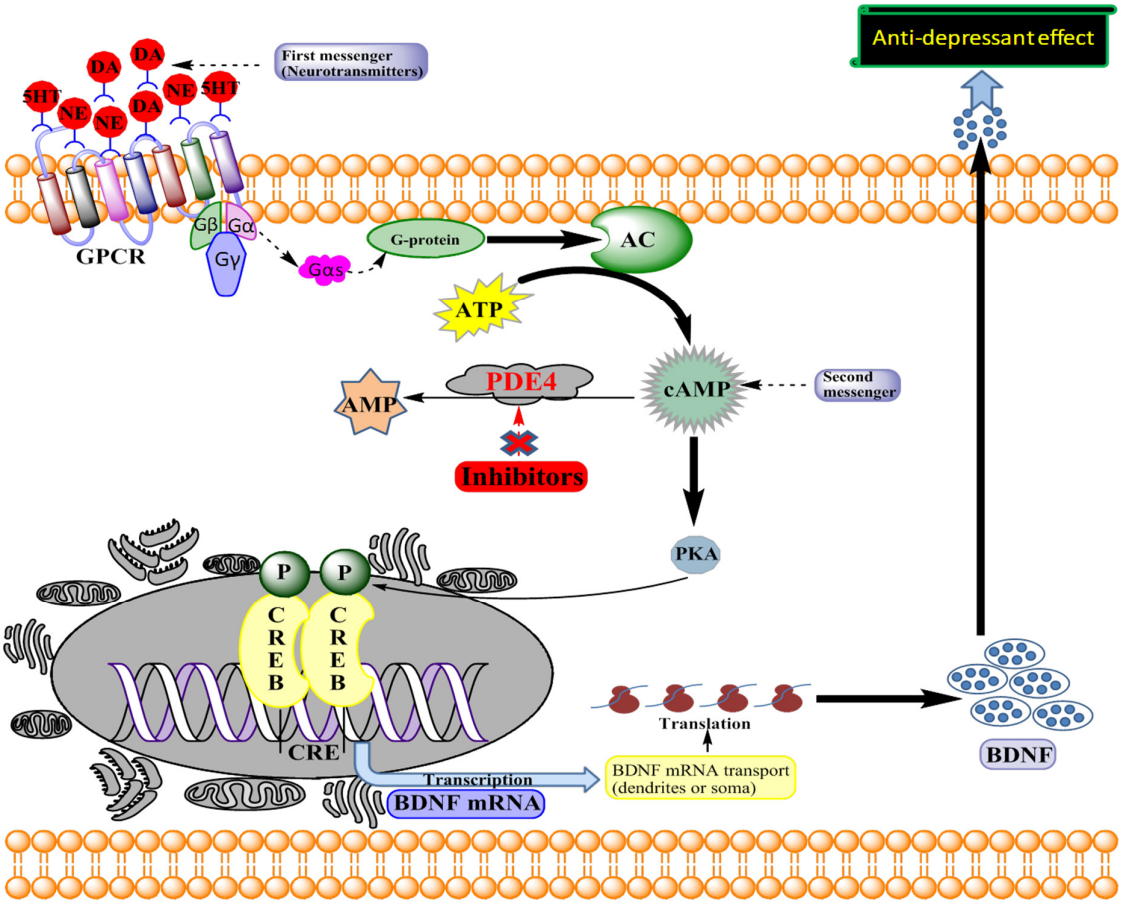

Fig. 3: Schematic representation of mechanism of cellular signaling by cAMP

1.1.4. *Classification of Phosphodiesterases enzyme*

Ever since the initial refinement of venom phosphodiesterase, for nearly six decades PDEs has been widely studied.[19] Beginning with the work of Thompson and Appleman, isolation and characterization of PDEs from diverse tissue and cell types from numerous species have revealed that there are multiple families of PDE isoenzymes.[20] A variety of biochemical studies have revealed the existence of at least eleven diverse mammalian PDE gene families (PDE1–11), including 20 genes and about 50 isoform with 20-25% sequence homology identified on the basis of amino acid (AA) sequence, domain structure, catalytic and regulatory differences.[21] **(Fig. 4)** These families are distinguished according to their substrate specificity (cAMP, cGMP or both nucleotides), modes of regulation, tissue distribution, kinetic properties, allosteric regulators, protein sequence and sensitivity to specific inhibitors.[6a, 18c,22] These multitude PDEs controls the cellular concentrations of cyclic nucleotides in a family-dependent way, mediating array of genetic responses.

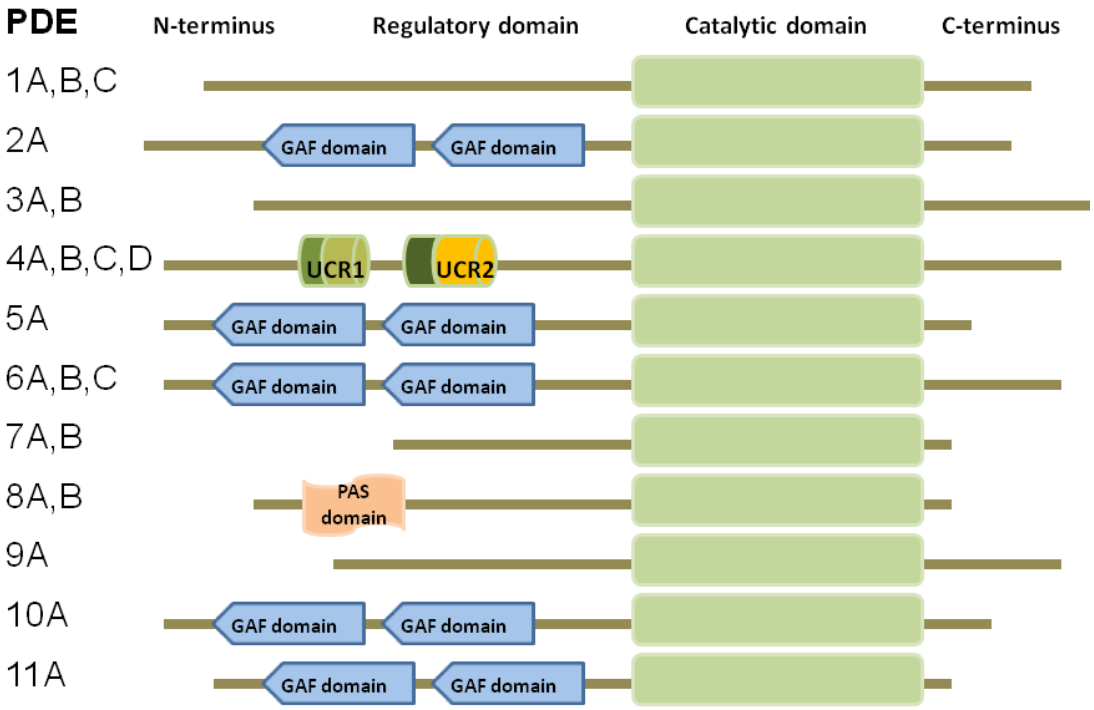

Fig. 4: Domain structures of PDE 1-11

The PDE families are classified based on their substrate specificity: cAMP–specific PDEs, including PDE (4, 7 and 8); cGMP–specific PDEs, including PDE (5, 6 and 9) and dual substrate PDEs, which hydrolyze both cAMP and cGMP, including PDE (1, 2, 3, 10 and 11).[23] **(Fig. 5)** Among every PDE family, 1-4 discrete genes have been recognized, comprising 21 subfamilies or subtypes in mammals. Within the 11 PDE families, PDE4 is the most vital enzyme which controls the concentration of intracellular cAMP with very high affinity, as designated by its low K_m value (1-3 µM), and is extremely precise for cAMP as a substrate, but insensitive to cGMP or Ca^{2+}/calmodulin.[15b] The main characteristics of the PDE families are listed in **Table 1**.

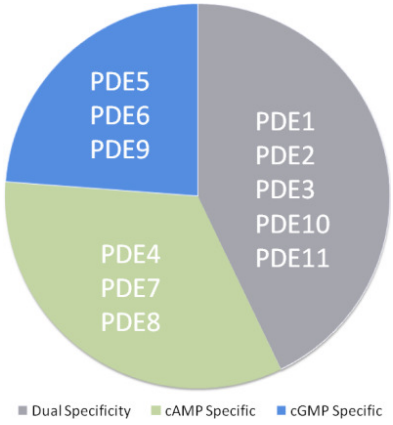

Fig. 5: PDE families based on their substrate specificity

Table 1: The phosphodiesterase superfamily*

Nomenclature	Gene family (preferred substrates)	No. of Gene Products (Splice variants)	Distribution	Selective Inhibitors
PDE1	Ca^{2+}/calmodulin stimulated (cGMP>cAMP)	3 (9)	Brain, heart, kidney	Vinpocetine SCH51866
PDE2	cGMP-stimulated (cGMP≈cAMP)	1 (3)	Brain, adrenals	MEP-1, EHNA
PDE3	cGMP-inhibited (cGMP≈cAMP)	2 (3)	Heart, liver, smooth muscle, adipose tissue	Milrinone, Siguazodan (SKF 94120)
PDE4	cAMP-specific (cAMP>>>cGMP)	4 (16)	Brain, immune system, lung, heart, testis	Rolipram, denbufylline, Ro 20-1724
PDE5	cGMP-specific	1 (3)	Smooth muscle, lung, platelets, spleen	Zaprinast KF31327 Sildernafil
PDE6	Photoreceptor	3 (3)	Retina	Zaprinast
PDE7	cAMP-specific, rolipram-insensitive	2 (3)	Skeletal muscle, brain, heart, liver, lymphocytes	Dipyridamole
PDE8	cAMP-specific, IBMX-insensitive	2 (2)	Gonads, intestines, thyroid	Dipyridamole
PDE9	cGMP-specific	1 (4)	Spleen, small intestine, brain, heart, kidney	SCH 51866
PDE10	Dual substrate (cAMP≈cGMP)	1 (1)	Brain, testis	SCH 51866, dipyridamole

*Data obtained from Conti, 1995; Spina et al., 1998; Soderling et al., 1999; Fischer et al., 1998; Fischer et al., 1998a; Fawcett et al., 2000; Gardner et al., 2000; Hayashi et al., 1998 and Guipponi et al., 1998.[9b, 16b, 18b, 22a, 24]

1.2. Architecture of PDE enzyme

Analysis of the amino acid sequences of the various PDE4 isoform have demonstrated that they have a common overall structure including regions unique to this enzyme family.[25] In fact, through the use of alternate promoter initiation sites and alternate splicing of mRNA, there are more than 50 distinct isoform variants of PDEs.[26] Genetic analyses have shown that the sequence identity within the catalytic domain is high between families of PDEs. It generally lies within the central to C-terminal region of these enzymes. However, the N- and C-terminal sequences are very different, suggesting that these sequences motifs involved in the regulation of PDE catalytic activity and control the localization of PDEs to subcellular locations for intracellular targeting.[7b, 27] **(Fig. 6)** PDE families and their isoform are differentially expressed, and this expression depends on the tissue type and the pathological or physiological condition of the tissue.[23a, 26a] Furthermore, each family, and even the members of the sub-family, reveal distinct tissue, cell, and subcellular expression patterns, hence is likely to contribute in distinct signal transduction mechanisms, involved both in physiological and pathophysiological

processes.[7b, 28] Further insight into the molecular and cellular mechanisms that account for high level of complexity of PDE4 activity, might offer additional opportunities for therapeutic intervention, directed at particular PDE4 isoform with specific localization and function.[10d, 29]

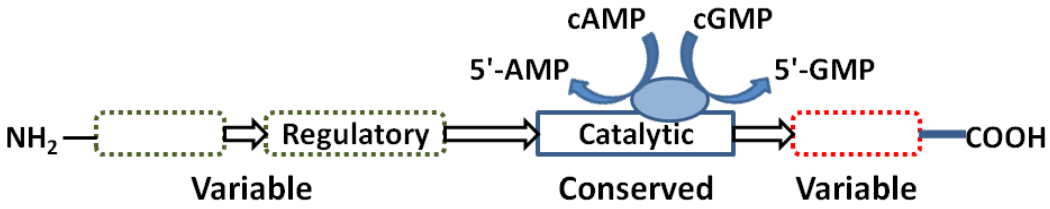

Fig. 6: Diagrammatic representations of architecture of PDE enzyme

1.2.1. *Catalytic Domain in PDEs*

The functional structure of the catalytic domain, which constitutes the core of the PDE, shows clear homology among various PDE4 subfamilies, where the sequence of any catalytic domain family express between 25 to 51% amino acid sequence identity with any other.[8c, 26b, 30] It contains about 250 amino acids that interact with the physiological substrate, cAMP. Inhibitors which share structural similarity with cAMP also bind there. The boundary of the catalytic unit is inferred initially by sequence homology studies and is further supported by single point mutations and truncation analyses.[7b, 31] The understanding of the structure of PDE catalytic units has been dramatically changed with the definition of the three-dimensional structure of the catalytic core of PDE4B.[29b, 32]

The X-ray crystallographic structure of the catalytic domain of nine families of PDEs has been resolved. The catalytic domains assume a compact α-helical structure, comprising 15-17 α-helices, which is divided into three distinct sub-domains. These domains define a deep hydrophobic binding-pocket formed at the border of the three domains where the substrates (cAMP or cGMP) or inhibitors attach.[26b, 31a] cAMP binds within a 440-Å pocket that is lined with both hydrophobic and negatively charged groups that are conserved among the various PDE families. At the base of this binding-pocket are two divalent metal binding sites (Zn^{2+} and Mg^{2+}) which act as an anchor for the three domains to hold them together. The first metal ion is a tightly bound Zn^{2+} ion, thought to be crucial for the catalytic activity of PDE enzymes and the regulation of their function.[26b, 33] The second metal ion, which is readily exchangeable, is probably Mg^{2+} in vivo.[29b, 33] The metal binding site that binds zinc has two histidine and two aspartic acid residues that are extremely preserved amid all PDEs and are liable for interaction with the CN purine. Structural studies have revealed that the CN specificity of the catalytic site depends mainly on single specific invariant glutamine. This glutamine serves as the main specificity determinant by a “glutamine switch” mechanism, which stabilizes the binding

of the purine ring in the binding pocket through hydrogen bonds with either cAMP or cGMP or both, depending on the orientation of the glutamine.[34] Among the two orientations, in one the hydrogen bond (H-bond) complex supports guanine binding leading to cGMP selectivity and in the other supports adenine binding resulting in cAMP selectivity. In twin-definite PDEs, a key histidine residue may aid the invariant glutamine to snap between cAMP and cGMP.[26b, 33-34] **(Fig. 7)**

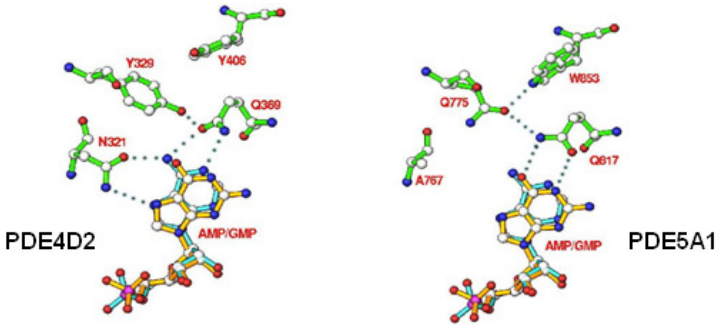

Fig. 7: The glutamine switch mechanism

The catalytic active site of PDEs contains 17 amino acids residue out of which 12 are highly conserved throughout PDE super family. Catalytic site can be further divided in three clusters of amino acids based on three distinct roles: (i) nucleotide reorganization (ii) hydrophobic clamp and (iii) hydrolysis.

The discovery that the catalytic unit of PDE4 isoform is formed from three subdomains pivoted around two Metal ion binding sites provides a basis for the proposals made in various laboratories that PDE4 enzymes can adopt distinct conformational states.[32-33, 35] This is based on the observations that particular PDE4 isoform exhibit very different susceptibilities to inhibition by the PDE4-selective inhibitor rolipram. This has been shown to occur as a consequence of interaction with other proteins,[35-36] phosphorylation,[23b, 37] altered thiol group oxidation state,[38] and association with membranes.[38-39] As the catalytic domain consists of three sub-domains, it is possible that one or more of these is modified in a way that changes the conformation of the inhibitor-binding site such as high affinity rolipram binding site (HARBS) and low affinity rolipram binding site (LARBS), which forms the catalytic core of the enzyme.[31a, 32, 34c]

1.2.1.1. *Nucleotide Reorganization Unit*

Group of residues that decides specificity of PDEs towards cAMP, cGMP or both CNs are part of nucleotide reorganization unit. Glutamine is highly conserved in catalytic site of all PDEs as summarized in **Table 2**. The fate of orientation of the amide group of an invariant glutamine depends on the adjacent environment is provided by this group of amino acids.

Table 2: PDEs and their conserved glutamine residues

PDE	Gln	PDE	Gln	PDE	Gln	PDE	Gln
PDE1A	Q417	PDE4B	Q443	PDE6B	Q771	PDE8B	Q298
PDE1B	Q421	PDE4C	Q597	PDE6C	Q775	PDE9A	Q453
PDE1C	Q427	PDE4D	Q369	PDE7A	Q413	PDE10A	Q716
PDE3B	Q988	PDE5A	Q817	PDE7B	Q374	PDE11A	Q425
PDE4A	Q403	PDE6A	Q773	PDE8A	Q706		

Glutamine amide adopts different orientation by flipping 180°, one to network with cAMP and toggles toward another to network with cGMP. This glutamine switch is restricted by complex of hydrogen bonds near this extremely conserved glutamine.[34a] **(Fig. 8)**

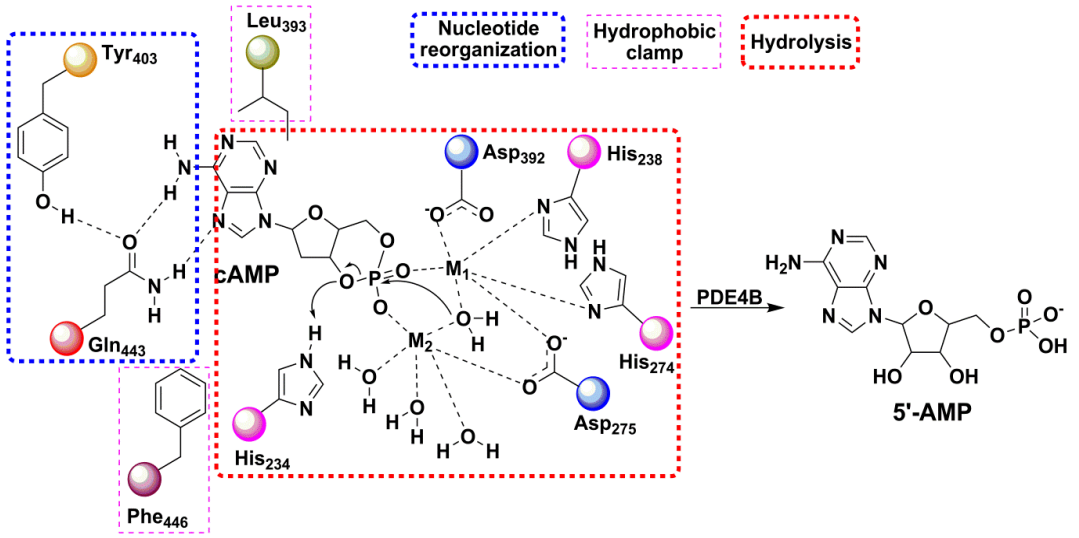

Fig. 8: Important residues involved in hydrolysis of cAMP catalyzed by PDE4B

1.2.1.2. *Hydrophobic Clamp*

Resolved crystal structure of all PDEs reveals the fact that a set of conserved amino acid residues act as hydrophobic clamp to anchor planar aromatic ring adenine or guanine bases of respective cAMP, cGMP or aromatic ring of co-crystallized inhibitor in crystal structure. This clamp comprises of a couple of vastly preserved hydrophobic amino acid residues, where one jaw of the clamp is phenylalanine in all PDE family members. In Contrast, the opposite jaw of the clamp is not highly conserved but by nature is also hydrophobic like valine, phenylalanine, leucine or isoleucine in all PDEs.[30] Residues acting as hydrophobic clamp in PDE family are summarized in **Table 3**.

Table 3: Conserved hydrophobic clamp residues in PDE family

PDE	Clamp-1 (Varies among Val, Leu, Ile)	Clamp-2 (conserved Phe)	PDE	Clamp-1 (Varies among Val, Leu, Ile)	Clamp-2 (conserved Phe)
PDE1A	L384	F420	PDE6A	V734	F776
PDE1B	L388	F424	PDE6B	V732	F774
PDE1C	L394	F430	PDE6C	V737	F779
PDE2A	I826	F862	PDE7A	V380	F416
PDE3A	I968	F1004	PDE7B	V341	F377
PDE3B	I955	F991	PDE8A	I672	F709
PDE4A	I370	F406	PDE8B	I264	F301
PDE4B	I410	F446	PDE9A	L420	F456
PDE4C	I564	F600	PDE10A	I682	F719
PDE4D	I336	F372	PDE11A	V390	W428
PDE5A	V782	F820			

1.2.1.3. *Hydrolysis Unit*

Among the two divalent metal ions, the first one is Zn^{2+}, which is coordinated by highly conserved two histidine and two aspartate residues throughout PDE family and two water molecules. The second one is possibly an Mg^{2+}, which acquires nearly octahedral geometry and is coordinated by the same aspartate that also coordinates with Zn^{2+} and five water molecules, among which one water molecule bridges with Mg^{2+} and Zn^{2+}. **(Fig. 9)**

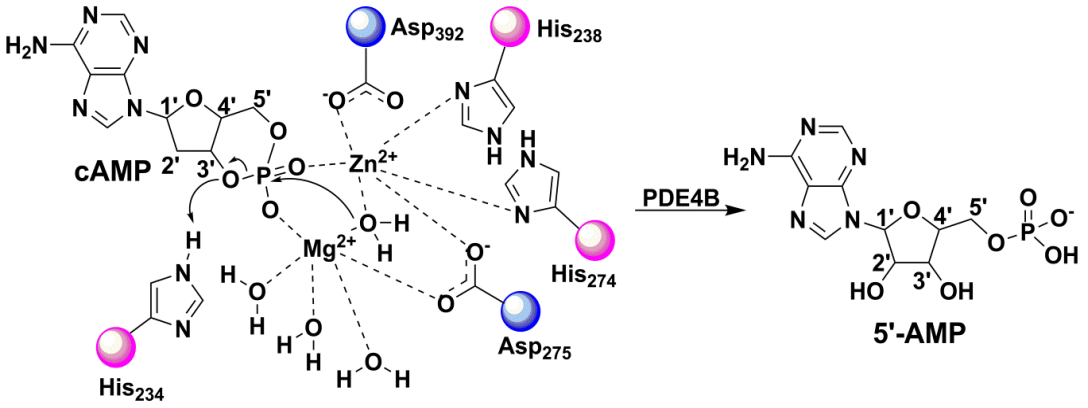

Fig. 9: A putative mechanism for the phosphodiester bond hydrolysis by PDEs

In the proposed hydrolysis model for PDE4B, both metal ions harmonize with the exocyclic phosphoryl oxygen atoms to obtain a better affinity cAMP binding and thus polarize with the phosphodiester bond in turn to increase the electrophilicity of phosphorous atom of phosphate group. Moreover the bridging hydroxide or Mg-synchronized water, acts as the nucleophile and catalysis is more aided by a hydrogen bonding interaction involving the conserved His234 and the O_3' leaving group resulting in the hydrolysis of phosphate diester.[32, 34c, 40]

1.2.2. *The Regulatory domain*

Unlike the catalytic domain, the N-terminus regulatory domain is highly variable between PDEs, resulting in the unique characteristics of each PDE family. Among the numerous domains charted to the N-terminus, three forms are present in several PDE families. These comprise domains for ligand binding, oligomerisation, kinase recognition/ phosphorylation, and regions that auto-inhibit the catalytic domain. Docking domains are also there at the N-terminus.[7b, 27, 41] Various types of protein domains offer regulatory control over the catalytic domains. PDE4 has upstream conserved regions (UCRs), 1 and 2. In the UCR1 region, phosphorylation sites have been identified, while UCR2 corresponds to an auto-inhibitory domain that negatively controls PDE catalytic activity.[23b, 42] **(Fig. 4)** At the N-terminus of UCR1 of all long forms of PDE4, there is a highly conserved motif (RRESF), that can be phosphorylated by PKA, hence leading to better catalytic activity of the enzyme.[7b, 42a, 43]

1.3. Molecular Characteristics of PDE4

Molecular cloning studies revealed that mammalian PDE4 enzyme families are encoded by four genes, which are distributed on three different chromosomes in humans.[37b, 44] The products expressed are termed as PDE4A, PDE4B, PDE4C, and PDE4D.[6b, 25a, 45] The initial naming of the type 4 PDE enzyme family is based on studies done by Reeves et al.[46] In the study, using the ion-exchange chromatography to separate PDE activities from heart, a fourth peak of PDE activity was eluted after the cGMP-inhibited PDE3 activity. This activity is specific for cAMP and sensitive to inhibition by rolipram. Later, Bolger and co-workers showed the presence of four distinct subfamilies of human PDE4 and their rodent equivalents.[25a] Till date, sixteen different isoform, encoded by four genes (4A, 4B, 4C, 4D) have been identified; multiple forms result from each gene due to alternative mRNA splicing.[47] Nomenclature of PDEs includes gene family designation (PDE isozyme 4) followed by the gene product (PDE4D) and lastly the splice variant (PDE4D2).

Unique to the PDE4 enzyme family are two highly conserved regions found in upstream of the catalytic region towards the N-terminals of these enzymes. These have been designated as the Upstream Conserved Regions 1 and 2 (UCR1 and UCR2).[25a, 45a, 48] The UCR1 is separated from the UCR2 by the Linker Region 1 (LR1) and the UCR2 region is separated from the catalytic region by the Linker Region 2 (LR2). PDE4 isoenzymes that contain both the UCR1 and the UCR2 are referred to as “long” forms, whereas variants that lack the UCR1 are referred to as the “short” forms. **(Fig. 10)** Using two-hybrid analysis and biochemical pulldown assays, it has been shown that the UCR1

is able to bind to the UCR2; these may form a regulatory module that influences the structure and function of the catalytic unit. Ser-54 within the UCR1 region can be phosphorylated by protein kinase A (PKA), which increases in catalytic activity of PDE4D3 and changes its sensitivity to rolipram inhibition.[10d, 42a, 47b] It has been suggested that the phosphorylation of Ser-54 places a negatively charged phosphate and triggers a conformational change in UCR1 that leads to the alteration of the conformation of the catalytic unit and hence its activation. This PKA phosphorylation site is conserved among long-form PDE4 variants, and hence likely to regulate their activity.[42a, 48] In addition to these conserved regions, various isoform have specific N-terminal regions. Evidence suggests that the role of N-terminal region is both to achieve intracellular targeting and to exert a regulatory effect.[28, 49]

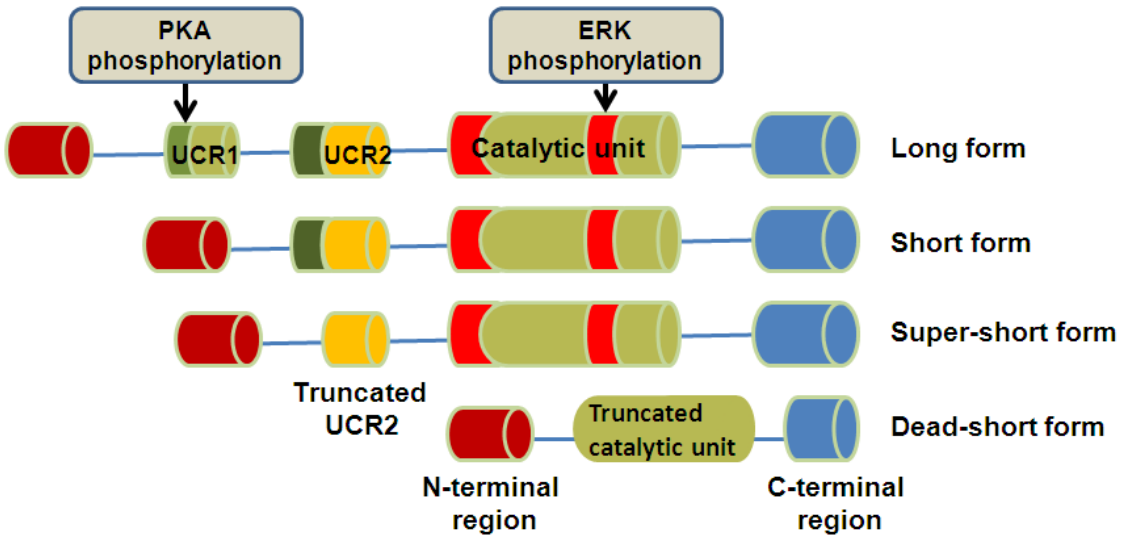

Fig. 10: Molecular characteristics of catalytic regions in PDE4 enzyme[15b]

1.4. Therapeutic implications of cAMP-Specific type 4 PDEs

The cAMP-specific PDE4 enzymes present a particular interest due to their errand in the regulation of several fundamental processes including learning and memory,[18b, 25a, 45] cellular survival[3a, b, 50] and inflammation.[9b, 22a, 51]

In the brain, cAMP has been implicated in various functions ranging from the sensory transduction to synaptic plasticity, activating a considerably complex machinery of intracellular regulation. It has been demonstrated that endogenous cAMP levels, control PDE4 by regulatory processes involving phosphorylation (short-term) and gene expression (long term). An enhanced PDE4 activity, via protein kinase-A (PKA)

mechanism, has been observed within 10-15 min of cAMP cascade activation,[42a, 52] whereas increased PDE4 density, via an increase in gene transcription, results in increase in cAMP after prolonged duration (hours to days).[29a] Such changes in the cAMP pathway, leading to augmentation in the cAMP concentration and subsequent regulation of PDE4, can be achieved by chronic administration of anti-depressants supporting the essential role of PDE4 in the mechanism of action of these agents.[3d, 53] PDE4 selective inhibitors have been proven to display anti-depressant characteristics of their own,[15b, 48, 53a, 54] as well as functions in learning and memory, Parkinson's and multiple sclerosis disease.[6c, 55]

Interest, first focused on these enzymes with the discovery that they can be potently and selectively inhibited by rolipram, a compound that shows anti-depressant activity in humans and in several pre-clinical models.[15b, 56] Specifically, they have been shown to: reduce the duration of immobility in the forced-swim test; diminish rate of response and amplify reinforcement rate below a differential-reinforcement-of-low-rate schedule; reverse the causes of chronic, mild stress; stabilize the behavioral shortages examined in flinders susceptible-line and olfactory-bulbectomized rats; antagonize the causes of reserpine and enhance yohimbine-induced toxicity. Utilizing PDE4 subtype deficient mice, it appears that PDE4D is an essential mediator of the anti-depressant effects of PDE4 inhibitors.[6c]

Further, recent studies have been extended to explore therapeutic potentials of PDE4 inhibitors for other diverse CNS diseases, such as Alzheimer's disease,[57] Parkinson's disease,[58] schizophrenia, stroke, Huntington's disease, autism and tardive dyskinesia.[15b, 18a, 27, 48] With the generation of a host of other PDE4 inhibitors, it was observed that PDE4 inhibitors can also serve as potent anti-inflammatory agents that are of potential therapeutic benefit for a wide range of disorders, including asthma,[59] chronic obstructive pulmonary disease (COPD),[59a, 60] rheumatoid arthritis (RA),[61] and Crohn's disease.[62] On the same note, alterations in PDE4 activity have been attributed to disorders such as diabetes insipidus,[63] diabetes mellitus,[57a, b, 64] atopic dermatitisand psoriasis.[59b] However, side-effects, particularly emesis, have hindered rolipram and other PDE4 inhibitors from further clinical utility.[6c, 15b] Theophylline, a non selective PDE inhibitor, has been used for the treatment of asthma and other pulmonary diseases. The non-selective nature of theophylline not only produces side-effects but also limits its use in selectively inhibiting particular PDE in target tissues[6c].

Such discoveries lead to the proposal of developing new selective inhibitors that could target specific diseases. With the discovery of PDE families and some twenty crystal structures of PDEs available, selective inhibitors of PDEs have been synthesized and

assessed for thier therapeutics potential to treat various human diseases.[48] Successful examples include PDE5 inhibitors sildenafil (Viagra®), vardenafil (Levitra®), and tadalafil (Cialis®) for the treatment of erectile dysfunction.[16b] PDE4 inhibitors have shown great potential for treatment of asthma and COPD, but side-effects such as emesis prevent their practical applications. It is generally believed and hypothesized that side-effects of PDE4 inhibitors arise from inhibition of non-targeted PDE families or lack of selectivity against subfamilies PDE4A, B, C, and D. However, the molecular basis for family and subfamily selectivity of PDE4 inhibitors is poorly understood.[6c]

Cumulative report suggests that cAMP-mediated signaling system is disrupted in several neuropsychiatric disorders[65] and PDE4 enzyme is a rate limiting step in this pathway which can be explored as a better target. This provoked an interest to design and develop novel ligands as better PDE4 inhibitor with subfamily selectivity and devoid or with minimum side-effects. This work will inspire further exploration, translating the role of novel designed and synthesized nitraquazone (quinazoline-2,4-dione) derivatives as better PDE4 inhibitors into novel therapeutic strategies for their neuropsychiatric disorders like depression and anxiety.

1.5. Depression

1.5.1. *Overview of depression*

Described by Hippocrates more than 2400 years ago, 'melancholia,' is derived from the ancient Greek **μελαγχολία** (*melan-chole*) and is defined as "sadness or depression of the spirits; gloom" and now depression. It is a mood disorder and one of the prime causes for illness-related disability worldwide which carries significant social suffering and economic burden in India and worldwide.[66] Report from epidemiological studies suggests that frequency for psychiatric disorders vary from 9.5 to 370/1000 population with prevalence highest among marginalized population. Moreover, the loss of human life remains a solemn reality as suicide rates in depressed patients are anticipated as high as 15%.[66d, 67] Common mental disorders such as depression and anxiety are often co-morbid with other health and psychosocial crisis and are among the most vital causes of morbidity.[68] Therefore it is vital to understand the causes of depression in particular, which is a common and debilitating disorder in an effort to develop treatments to alleviate the symptoms of those sufferings.

Historically feelings of sadness, worthlessness, and despair have been referred to as melancholia. The clinical symptoms of depression had been combined under the umbrella term, "major depressive disorder" (MDD). The nosology of depressive disorder has increased in complexity over time. Indeed, the ever-changing nature of the systematic classification of depression is evident in the five different versions of the Diagnostic and Statistical Manual of Mental Disorders (DSM) published by American Psychiatric Association's (APA). Melancholia appears in the DSM-IV and DSM-V [current version-2013],[69] as one of the four subtypes of MDD: melancholic, atypical, catatonic, and postpartum onset depression. Anhedonia, or the loss of pleasure, is the characteristic defining feature of melancholic depression. However, in another classification system, more focus is placed on melancholia and non-melancholic (atypical, catatonic, and postpartum onset) depression.[69c]

1.5.2. *Aetiology of Depression*

Major depression disorder (MDD) is a recurrent and disabling neuropsychiatric disorder affecting 7% of the population worldwide. Although recognized by mankind hundreds of years ago, the aetiology of MDD is still a mystery. Depression is likely a multifactorial disorder that arises from complex gene-environment interactions. The onset of a depressive episode is hypothesized to occur on a genetic background of increased susceptibility to develop MDD combined with the presence of stressful, adverse life experiences.

Environmental factors, particularly emotional stress, are strongly associated and can precipitate depressive episodes. Postmortem brain studies of depressed individuals revealed dramatic physiological differences from non-depressed control brains including neuronal atrophy and cell loss in limbic brain structures.[67a, 70] Importantly, exposure of animals to environmental stress is sufficient to induce depressive-like behavioral changes in addition to cellular deficits mirroring those seen in postmortem brain.[71] Nonetheless, both genetic and environmental factors are likely to involve common brain regions and molecular pathways. Many researchers have therefore tried to understand the genetics of MDD in an effort to determine which genes underlie susceptibility to MDD and which genes are related to anti-depressant treatment response.[72] Unfortunately, the search for a single gene that causes depression has been thus far inconclusive, and the consensus is that multiple genes are likely involved in the pathophysiology of depression.[73] Delineation of these individual regions and pathways will help to refine our current understanding of underlying causal mechanisms, and will thus aid in the development of novel, targeted treatments for mood disorders.

1.5.3. *Brain regions affected in depression*

Given the complex nature of depression, it is not surprising that current information regarding the specific brain regions underlying the disease is limited. While pathological changes have been observed in the brains of depressed patients, these findings are not categorical, and as such do not represent *bonafide* biomarkers for the disease. Postmortem and structural imaging comparisons have revealed decreased graymatter volumes in subregions of cortex [including prefrontal cortex (PFC)], amygdala, hypothalamus and hippocampus.[74] Frontal cortex and hippocampus controls the cognitive and emotional behavioral aspects, including memory impairments and feelings of worthlessness, hopelessness, guilt, doom and suicide. These results are supported by neuroimaging studies showing alterations in cerebral blood flow and glucose metabolism in areas of the PFC, hippocampus, striatum, amygdala and thalamus.[67a, 75] Reward pathways involving the striatum and amygdala are likely core in mediating depression-associated anhedonia, anxiety and reduced motivation. Hyperactivity of the hypothalamic-pituitary-adrenal axis (HPA axis) may play a role, as imbalances in sleep, appetite and energy in addition to loss of interest in pleasurable activities are prevalent in affected individuals, but the mechanisms underlying this abnormality is uncertain.[66b, 76]

Moreover, connections between these regions via major neurotransmitter pathways highlight putative brain circuitry involved in the pathogenesis and treatment of mood disorders.[66b, 75d] Furthermore, while knowledge of the neuropathology of the depressed

brain has come from postmortem examination, much has been determined by comparing the molecular changes evident following effective anti-depressant treatment.

1.5.4. *Clinical symptoms of depression*

MDD is currently characterized by a triad of clinical symptoms: low or depressed mood, anhedonia, and low energy or fatigue. Other symptoms of depressive illness include sleep and psychomotor disturbance, feelings of guilt, low self-esteem, thoughts of suicide, and dysregulation of food intake and body weight.[66e, 77] Due to its unrelenting nature, depression is an extremely disabling disorder, and is a major cause of morbidity and mortality due to suicide. Many of the symptoms of depression are non-specific and difficult to distinguish from everyday sadness; therefore, MDD is often misdiagnosed or under diagnosed.

1.6. Anxiety

1.6.1. *Overview of anxiety*

Anxiety is also a common neuropsychiatric disorder which is co-morbid with other health and psychosocial problems. It has a premature inception, impose a chronic or relapsing course, cause ample personal agony, diminish quality of life (QOL), harm community and professional purpose and impose a significant monetary load. Anxiety is frequently co-morbid with major depression, bipolar disorder, schizophrenia, substance misuse and physical illness, and is associated with increased risks of suicidal behavior. However, the sources of anxiety disorders continue to be a mystery, which hampers exact diagnosis, the prophecy of prognosis, and the growth of refined treatment approaches.[78]

Diagnosis and classification of anxiety disorders are based on DSM-IV (1994) criteria. Based on the symptoms, anxiety are classified into Generalized anxiety disorder (GAD), Social phobia (social anxiety disorder), Specific phobia (SP), Panic disorder (PD), Obsessive compulsive disorder (OCD), Post traumatic stress disorder (PTSD). It is also suggested that separation anxiety disorder (SAD) may further initiate depressive disorder, agoraphobia, panic disorder, and related anxiety disorder in adulthood.[79]

1.6.2. *Aetiology of anxiety*

It is estimated that about 25% of the population will experience an anxiety disorder at some stage of their life. Women are twice more likely to suffer from an anxiety disorders than men. Unfortunately, only 50% of people receive treatment for their disorders. People with anxiety disorders are also at higher risk of being affected by substance abuse. So symptoms of severe, chronic, debilitating anxiety, need treatment with an anti-anxiety agent. As in depression, the exact pathophysiology of anxiety is uncertain.

Based on animal studies and responses to drug treatment the neurotransmitters like acetylcholine/Ach, serotonin/5HT, nor-epinephrine/NE, and dopamine/DA as well as the intracellular messenger, cAMP have been implicated in the pathogenesis of anxiety disorders. It is proposed that anxiety may be due to imbalance between the activities of the inhibitory, anxiolytic (GABA), and excitatory, anxiogenic (glutamate), systems in mammalian brain.[80]

1.6.3. *Brain regions affected in anxiety*

The brain region affected includes the prefrontal cortex, specifically the orbital and anterior cingulate cortices, the ventral striatum, amygdala, and the brainstem catacholaminergic systems, particularly DA and 5-HT.[78b] It is suggested that the septohippocampal pathway also play a dominant role in physiological function during anxiety.[80]

1.6.4. *Clinical symptoms of anxiety*

Anxiety is usually linked with former 'psychoneurotic' disorders and is unsolved puzzle in biological or psychosomatic terms; existing hypothesis involves hyperactivity of adrenergic system or dysfunction of serotonergic systems in the CNS. Further, symptoms of anxiety are usually related with depression and mainly with dysthymic disorder (chronic depression of moderate severity), PD, agoraphobic and other SP, OCDs, eating disorders and many personality disorders. Twin and family studies imply mutual genetic vulnerability to depression and anxiety.[81]

In clinical practice, numerous patients suffering from anxiety disorders are not recognized or do not present; they receive sub-optimal standard of care; the efficacy of pharmacological and psychological healing manipulations in existing clinical practice can be unsatisfactory. These signify imperative clinical challenges, and hence there is substantial scope for progress in the identification, care and management of patients with anxiety disorders.[78a]

Effectual healings for depression and anxiety also remarkably overlie: therapeutics acting on monoaminergic systems, and psychotherapies based on panic loss and further techniques geared toward decreasing evasion and escalating objective-directed, rewarding behavior. Notably, there is also a familiar neural complex related with these ailments. This complex is essential to the pharmacological and psychological strategies for management and the theory that drive this research of the underlying pathophysiology.[78b] A report on meprobamate by Berger (1954) marked the beginning of investigation of modern sedatives with useful anxiolytic properties. The first anxiolytic agent developed was chlordiazepoxide by Sternbach in 1957.[82]

1.7. Current available treatments (Non-pharmacological and pharmacological therapy) for depression and anxiety

1.7.1. *Non-pharmacological therapy for depression and anxiety*

Diverse therapeutic approaches, both pharmacological and non-pharmacological, have been anticipated for treatment-resistant depression and anxiety.[83] In contrast to the limited understanding of the aetiology and pathophysiology, a variety of psychological interventions for mild depression and anxiety is available which includes psychotherapy, electro-convulsive shock therapy (ECT), pharmacotherapy, complementary and alternative medicine (CAM) therapies,[75d, 75f] while systematic desensitization is effective in greatly reducing or eliminating phobias.[84] Psychotherapeutic interventions are commonly known as talk therapies; cognitive behavior psychotherapy (CBT), interpersonal therapy and psychoanalysis, are examples of different psychotherapies.[85] The aim of CBT is to address the causes of the patient's mood bias toward negative emotions (seen as the primary cognitive dysfunction in MDD) and is extensively thought to be the most effectual psychological strategy for healing anxiety disorders along with pharmacotherapy.[75f, 86] While interpersonal therapy focuses on the relationships of the patient to others, psychoanalysis is based on the theories of Sigmund Freud where the relationship of past experiences to the present are explored.[85c, 87]

Other interventions such as ECT and pharmacotherapy are aimed at fixing biological brain dysfunctions thought to underlie MDD either at the level of neural networks or at the level of neuronal signaling pathways. ECT introduced in 1938, is a procedure in which electric current is passed through electrodes placed on different areas of the patient's head to medically induce seizures in a controlled setting.[88] Although controversial, ECT has been used successfully in severely depressed patients who have demonstrated resistance to other forms of treatment and is thought to work at the level of neural networks.[89] Pharmacotherapy is the first line of treatment with the administration of anti-depressant drugs over a period of months to years. Current anti-depressant drugs are thought to act at the level of neuronal signaling pathways by targeting receptors, enzymes and transporters present at neural synapse.[90] Patients who do not respond to conventional psychotherapy and/or pharmacotherapy might look to CAM therapies which include physical therapies [meditation, exercise, yoga, music therapy (MT), light therapy (LT), sleep deprivation and acupuncture], herbal remedies (St. John's Wort, gingko, free and wanderers plus) and Nutraceuticals [i.e. dietary and nutritional supplements such as vitamins and minerals, omega-3 fatty acids, S-adenosylmethionine (SAM-e), Dehydroepiandrosterone (DHEA) and 5-hydroxytryptophan (5-HT)].[91] Physical therapies are considered to be harmless and are encouraged.[92] The use of herbal teas and

medicines is often discouraged, as drug interactions can occur. Whether alternative forms of therapy are of benefit to patients by impacting depressive symptoms is unclear.[93]

Nonetheless, the disadvantages with these approaches is there late onset of action, response rates varies to great extent among anxiety disorders, non-response to treatment varies between 25-35%. Thus, ideal approaches have been made to increase psychological manipulations, by isolating the important component of therapeutics and by scrutinizing neurobiological moderator and mediators of responses, including neurophysiological and genetic factors.[94]

1.7.2. *Pharmacological therapy/anti-depressants and anxiolytics*

Even now, the diagnosis of MDD is still based on symptoms, including the pervasive low mood, low self esteem, feelings of helplessness and guilt, loss of interest of previously enjoyed activities, and changes in appetite and sleep. Despite the relative lack of knowledge of the aetiology of MDD, there are certain effective treatments available, which include anti-depressant medications.[95] Mild and more severe forms of depression respond to a host of anti-depressants, with a combination of medication and psychotherapy providing optimal treatment. Current anti-depressants are from three major classes:

I) *Monoamine oxidase inhibitors (MAOIs)*: Phenelzine, iproniazid, tranylcypromine, Moclobemide
II) *Tricyclic anti-depressants (TCAs)*: Imipramine, clomipramine, amitriptyline; and
III) *Selective serotonin/nor-epinephrine re-uptake inhibitors (SSRIs, SNRIs)*: fluoxetine, fluvoxamine, citalopram, paroxitine, sertraline

Many drugs, not listed in the anti-depressant category like carbamazepine, sodium valporate and gabapentin have been shown to be beneficial in the treatment of not only bipolar depression but also in the treatment of schizophrenia, schizoaffective disorders, impulse control disorders and PTSD.

Anxiolytics are generally known as minor tranquilizers and are used for the management of anxiety and its associated behavioral and physical indications. Therapeutic treatment has been verified effective and is a less laborious, less rigorous than psychosocial remedies. Several anxiety disorders react well to anti-depressants [mainly the SSRIs, venlafaxine, TCAs and MAOIs] and anti-anxiety agents (especially BZDs).[79, 96]

Currently clinically existing anxiolytics other than anti-depressants are:

I) *Benzodiazepines (BZDs)*: Diazepam, alprazolam, oxazepam, clonazepam, chlordiazepoxide
II) *Azaspirones*: Buspirone, gepiron; and
III) *Miscellanous*: β-blockers (Propranolol), Anti-psychotics (Clozapine, resperidone, olanzapine), α_2-agonists (Clonidine, guanfacine) and Anti-histamine (Cyproheptadine)

1.7.3. *Major hypotheses of anti-depressant action — Monoamines/Biogenic amine theory*

The monoamine hypotheses of depression was proposed by Schildkraut, referring basically to catecholamines.[97] The monoamine or biogenic amine theory proposes that there is a chemical imbalance in the depressed brain, specifically a deficit of monoamines (5HT, NE, and/or DA) and that this monoamine theory of depression was developed in hindsight following the discovery of the mechanism of action of efficacious pharmacotherapy.[66e, 98]

These current anti-depressants and anxiolytics share the same basic mechanism of action–manipulation of the levels of monoamines at the synaptic cleft between neurons in the brain.[90a] 5-HT is assumed to control other neurotransmitter systems; decreased 5-HT activity may allow these systems to act in abnormal and erratic ways. Later pharmacokinetic analysis revealed that these drugs increased levels of biogenic amines through the inhibition of either presynaptic monoamine re-uptake transporters or an enzyme that degrades the monoamines, monoamine oxidase. The role of NE in depression is established by the findings that dysregulation of central NE systems is a hallmark of depression[99] and that selective inhibition of NE re-uptake signifys an efficient treatment strategy.

MAOIs acts by increasing the availability of monoamines at the synapse by inhibiting there degradation in the presynatpic neuron;[100] re-uptake inhibitors amplifying synaptic monoamines by indulging with carriers into the presynaptic neurons, with especially drugs mediating 5-HT or NE to some extent. Few novel therapeutics also directly target definite monoaminergic receptors.

1.7.4. *Classes and mechanisms of action on monoamines*

1.7.4.1. *Monoamine oxidase inhibitors (MAOIs)*

MAOIs were among the first clinically used anti-depressant drugs and were serendipitously discovered over 50 years ago.[75d] Investigators performing clinical trials with the tuberculosis drugs isoniazid (Laniazid®) and iproniazid (Parnate®) in the early 1950s noted that these drugs had an unexpected mood elevating effect leading researchers to speculate their potential use in the treatment of MDD. MAOIs are considered first generation anti-depressants and those currently approved for the treatment of MDD, include the hydrazine derivatives phenelzine (Nardil®) and isocarboxazid (Marplan®) as well as the non-hydrazine derivatives tranylcypromine (Parnate®) and selegiline (Emsam®). **(Fig. 11)**

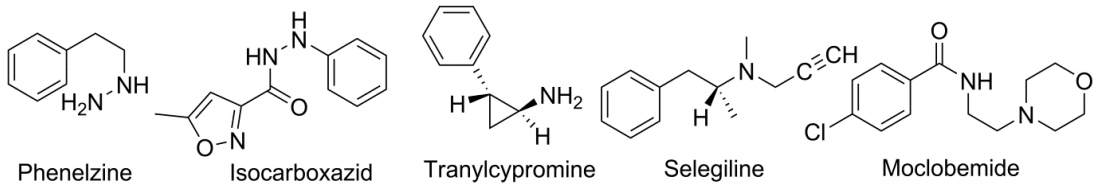

Fig. 11: Structures of some MAOIs

MAOIs have been found to be effective in the treatment of PD with agoraphobia, SP, or mixed anxiety and depression, and PTSD. Phenelzine was found to be a promising anxiolytic used in the treatment of PD, SAD and PTSD.[101] While MAOIs like iproniazid, isocarboxazid, and tranylcypromine can be used in the management of various mood and anxiety disorders. When compared to MAOIs, Moclobemide (Depnil®) is a Reversible Inhibitors of Monoamine Oxidase-A (RIMAs), primarily used to treat GAD, SP and PD possess better side-effect profile and does not require dietary restrictions.[102]

Although these MAOIs exhibit powerful anti-depressant effects, serious adverse effects including food and drug interactions unfortunately limit their use.[103] MAOIs are therefore prescribed to MDD patients who display treatment resistance to first line anti-depressant therapy.[100]

1.7.4.2. *Tricyclics anti-depressants (TCAs)*

TCAs non-specifically block the re-uptake of monoamines by inhibiting the activity of re-uptake transporters present on presynaptic neurons; therefore, these classes of drugs also increase the amount of monoamines available to bind to their respective postsynaptic receptors. The anti-depressant effects of the prototypic TCA, imipramine (Tofranil®), were also discovered by surprise in the late 1950s during trials, to determine whether it could be used as an anti-psychotic agent.[104] These anti-depressants are

referred to as “tricyclic” on the basis of a three-ringed chemical structure. TCAs are also considered first generation anti-depressants but also include some second-generation drugs with those currently approved for the treatment of MDD including amitriptyline (Elavil®), nortriptyline (Pamelor®), amoxapine (Asendin®), doxepin (Sinequan®), desipramine (Norpramin®), protriptyline (Vivactil®), and trimipramine (Surmontil®).[105] **(Fig. 12)**

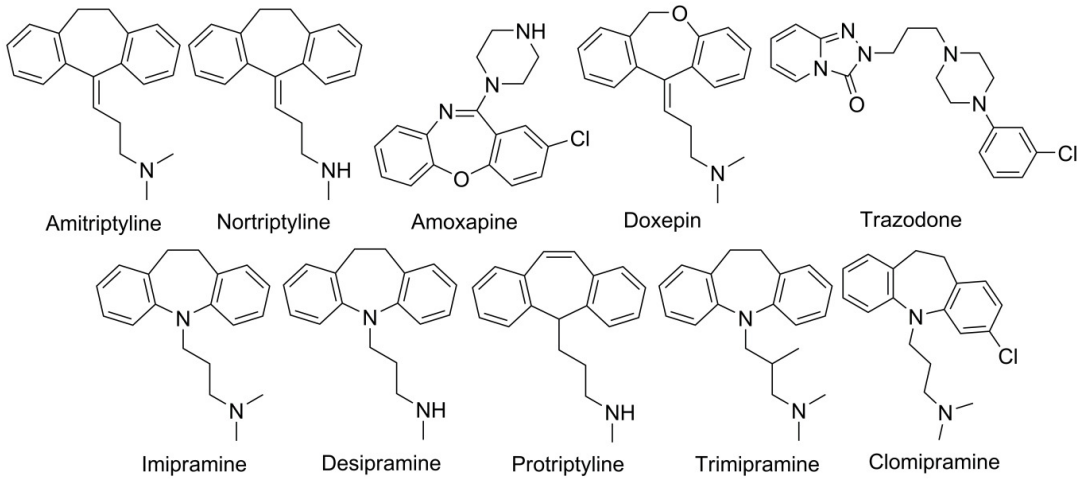

Fig. 12: Structures of some TCAs

By 1970’s and 1980’s it was found that certain TCAs and MAOIs were effective in treating PD. TCAs like clomipramine(Anafranil®) was effective in treating OCD and in the treatment of panic disorder with significant anxiolytic effects.[106] Imipramine was the first tricyclic anti-depressant agent that expressed good anxiolytic activity in panic disorder, effective in treating PTSD and GAD.[107] While other TCAs like doxepin, amitriptyline, and the unrelated trazodone (Desyrel®) are anxiolytics. Generally these agents are preferred when anxiety is co-morbid with depression.[108] **(Fig. 12)**

Like the MAOIs, TCAs are efficacious anti-depressants, but clinical use is limited by their side-effect profile. The anti-cholinergic side-effects of TCAs are related to their blockade of muscarinic acetylcholine receptors and include xerostomia, dry nose, blurry vision, constipation, urinary retention, cognitive, and/or memory impairment, and hyperthermia. Despite their side-effect profile, TCAs display very powerful anti-depressant effects and are therefore prescribed as second-line therapy to patients who have failed to respond to more selective anti-depressant.[104, 109]

1.7.4.3. *Selective serotonin/nor-epinephrine re-uptake inhibitors (SSRIs, SNRIs)*

In the late 1980’s, fluoxetine (Prozac®) was the first SSRI marketed by Eli Lilly and Co., starting the second generation of anti-depressant drug development. This anti-

depressant drug was designed to selectively block the serotonin re-uptake transporter (SERT) to increase the amount of serotonin at the synapse without non-selectively antagonizing other receptors.[110] Based on its comparable efficacy and decreased side-effect profile compared to TCAs, fluoxetine is considered the prototypic SSRI and was the most prescribed anti-depressant for several consecutive years. SSRIs currently approved for the treatment of MDD include citalopram (Celexa®), escitalopram (Lexapro®), paroxetine (Paxil®), and sertraline (Zoloft®). **(Fig. 13)**

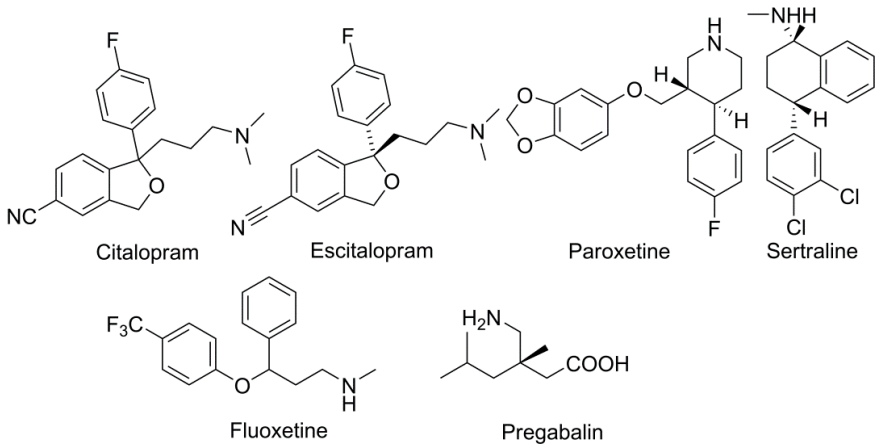

Fig. 13: Structures of some SSRIs

By 1990's and the Current guidelines recommend SSRIs as first line treatment for the pharmacological management of GAD, OCD and PTSD.[111] Both SSRIs and SNRIs, typically used as anti-depressants are currently used as first line drugs for the treatment of anxiety disorders like SAD, OCD and PD, and to a certain extent in GAD and PTSD.[66e, 112] These agents are useful in anxiety co-morbid with depression, which is a major advantage over benzodiazepines and azapirones.[66e, 113] The efficacy of these classes of compounds is well established for the treatment of anxiety disorders. Pregabalin (Lyrica®) may be used as a second line medication in GAD.[114] **(Fig. 13)**

The common side-effects associated with SSRIs are fatigue, nausea, gastro-intestinal upsets and perspiration.[115] SSRIs used in combination with MAOIs, medications used for pain or migraines, or supplements such as St. John's Wort can cause dangerous drug interaction that results in extremely elevated levels of serotonin in the brain and rarely, the potentially deadly "Serotonin Syndrome".[116] The abrupt cessation of SSRIs can result in "Discontinuation Syndrome". To avoid or reduce withdrawal symptoms from the absence of SSRIs, the dose of the drug is gradually tapered off.[117] SSRIs are currently the more widely prescribed anti-depressants because they demonstrate a more favorable side-effect profile and comparable, although not superior, anti-depressant efficacy as compared with MAOIs and TCAs.

1.7.4.4. *Atypical and second-generation anti-depressant*

Following the success of second-generation anti-depressants such as fluoxetine that demonstrated selectivity for the 5-HT transporter, other anti-depressants were developed to selectively inhibit the re-uptake of NE, 5-HT and NE or NE and DA or to block specific 5-HT receptors. The SNRIs currently in testing for the treatment of MDD include reboxetine (Edronax®, Vestra®). Anti-cholinergic symptoms such as xerostomia, perspiration, blurred vision, constipation, and tachycardia are the adverse effects associated with reboxetine.[118] Another atypical anti-depressant that displays strong effects on NE re-uptake is the tetracyclic anti-depressant (TeCAs) maprotiline (Ludiomil®). Maprotiline's anti-histamine action can cause drowsiness and there is increased risk of rashes, seizures, and death from overdose limiting the use of this anti-depressant drug.[118b] Duloxetine (Cymbalta®) and venlafaxine (Effexor®) are selective 5-HT and SNRIs currently approved for the treatment of MDD. Side-effects can include nausea, emesis, dizziness, insomnia, abnormal dreams, constipation, perspiration, xerostomia, yawning, tremor, gas, anxiety, agitation, abnormal vision, sexual dysfunction, and headache.[119] Another atypical anti-depressant, bupropion (Wellbutrin®), is a selective NE and DA re-uptake inhibitor (NDRI) currently approved for the treatment of MDD. Common side-effects of bupropion include agitation, anxiety, insomnia, and weight loss.[119-120] Two structurally similar atypical anti-depressants, trazodone (Desyrel®) and nefazadone (Serzone®) are thought to produce anti-depressant effects via 5-HT modulation, specifically via blockade of type IIA serotonin receptors (5-HT_{2A}R). Nefazodone has now discontinued due to a rare incidence of hepatotoxicity. Side-effects include drowsiness, sedation, induction or exacerbation of arrhythmias, and priapism (painful, prolonged erection).[119] **(Fig. 14)**

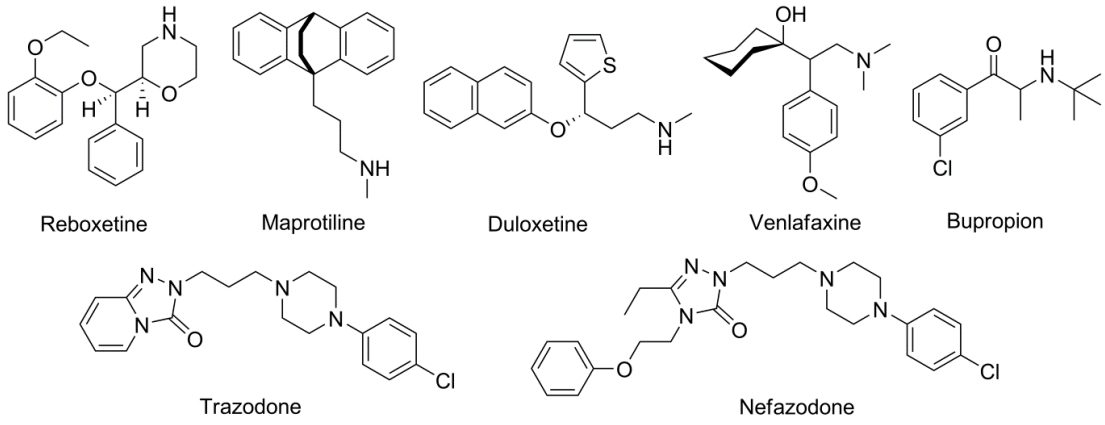

Fig. 14: Structures of some atypical and second-generation anti-depressants

1.7.4.5. *Benzodiazepines (BZs)*

Until 1900's BZDs were the first line of treatment or augmentation for anxiety disorder subtypes. BZDs possess a wide range of therapeutic utility; like anxiolytics, anti-convulsants, sedatives/hypnotics, muscle relaxants and amnestic properties.[121] Electro-physiological and biochemical studies have suggested that BZDs primarily interacts with the key inhibitory neurotransmitters like GABA or glycine which improves the presynaptic inhibitory process in both brain and nervous system; while the radioligand binding indicated their ability to inhibit the binding of [^{3}H]strychnine, a glycine antagonist, to glycine receptors and their clinical efficacy.[80] BZDs like Diazepam (Valium®), chlordiazepoxide (Librium®), and alprazolam (Xanax®) are drugs of choice for the treatment of GAD and SAD. Clonazepam (Linotril® and Clonotril®) is the drug of choice for treatment of SP and PD. **(Fig. 15)**

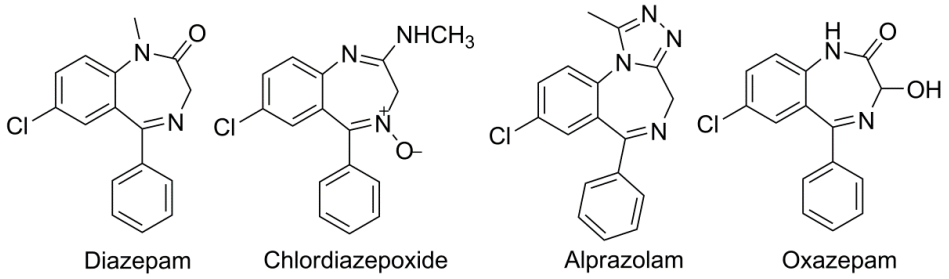

Fig. 15: Structures of some benzodiazepines

Despite their undesirable side-effects such as muscle relaxation, sedation, drowsiness, dizziness, decreased alertness, concentration, and interaction with other drugs,[122] oxazepam (Zaxpam®) is used extensively since the 1960s for the treatment of SP, PTSD, insomnia, premenstrual syndrome and in other conditions.[123] Chronic use of BZDs leads to cognitive impairment, addiction, physical dependency and withdrawal symptoms.[124]

1.7.4.6. *Azaspirones*

Non-benzodiazepine anxiolytics such as buspirone (Buspar®), gepirone (Ariza®) and tandospirone (Sediel®) have efficacy alike benzodiazepines but have less serious adverse effects and hazard of mortality due to overdose.[125] They function as a 5-HT$_{1A}$ receptor partial agonist and are widely used for the treatment of GAD.[126] Their better side-effect profile and no withdrawal effect made them better substitutes to BZDs for the treatment of GAD.[127] Side-effects of azapirones include dizziness, restlessness, headache, nausea and diarrhea. Nevertheless, it takes several weeks to produce their therapeutic effect, which is a major drawback of this class of drugs to treat anxiety.[121, 128] **(Fig. 16)**

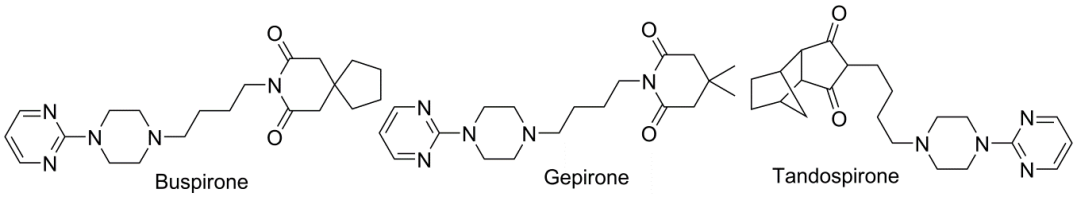

Fig. 16: Structures of some azaspirones

1.7.4.7. *Miscellaneous*

Propranolol (Inderal®), a β-blocker used as anti-hypertensive and anti-anginal has been well known to have anxiolytic properties.[129] They act by inhibiting the autonomic nervous system, thereby relieving the anxiety-induced symptoms, such as palpitation and hand tremor. The side-effects associated with it are asthma, heart failure, peripheral vascular disease and diabetes mellitus.[130] Certain atypical anti-psychotic agents such as clozapine (Clozaril®), olanzapine (Lanzek®) have shown beneficial effects in treating the symptoms of PTSD.[131] α_2-Agonists such as clonidine (Catapres®) and guanfacine (Tenex®) are used to treat anxiety disorder like PTSD and also showed transient anxiolytic effects in PD and GAD.[132] Cyproheptadine (Peritol®), an anti-histamine drug is used to alleviate the nightmares associated with PTSD.[133] **(Fig. 17)**

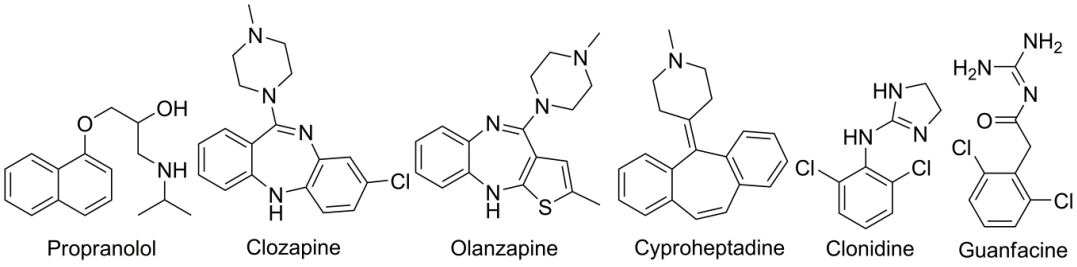

Fig. 17: Structures of miscellaneous compounds

1.7.5. *Detriments in current therapy*

However, several gaps in the monoamine theory of depression began to emerge. Most notably, there is a discrepancy between the acute onset of action on monoamines.[118b] Furthermore, responses to conventional anti-depressants treatment is variable, with 30 to 40% of patients not responding to the treatment,[83, 134] and 60-75% of responders failing to achieve complete remission. Anti-depressants are frequently used notoriously, and with lack of practical data to support their symptoms, off-label to treat other conditions such as anxiety disorders, chronic pain, eating disorders, OCD and some hormone-intervened disorders like dysmenorrhea.[135] Thus, stressing the need to develop better, mechanism-based anti-depressants and anxiolytics in preclinical models and clinical settings for both controlling and maintaining relief from neuropsychotic disorders like depression and anxiety triggered the interest in the current study.[75d, 98, 136]

Till date, the relationships involving alterations in monoamine levels and remedial results of anti-depressant have not been completely revealed. Downstream variations in intracellular messaging systems, transcription, translation and discrepancy in articulation of receptors are most likely moderators of indication development. Currently the specific genes and proteins involved in a wide array of mental processes are being examined including roles for specific neurotransmitters and receptors in psychiatric and neurodegenerative disorders[49, 57c, 137], changes in gene expression that occur with psychiatric disorders and their treatment[138], and molecular changes that accompany learning and memory.[139] One of the molecules suggested; that plays a crucial role in neurotransmission and long-term synaptic change is the second messenger; cyclic adenosine monophosphate (cAMP).[139d, 140] Development of novel anti-depressant therapeutics can be achieved by targeting receptors present postsynaptically and their coupled intracellular messaging systems.[140c, 141]

2. Literature review

From the beginning of 1990s, for several reasons, therapeutic potential utility of isoenzyme selective PDEs inhibitors have been mainly focusing on drugs capable of inhibiting PDE4, a cAMP specific PDE. Among them few important reasons for targeting PDE4 are:

- Tissue distribution of PDE4 strongly implies that pathologies associated to the central nervous and immune systems could be treated through the selective inhibition of PDE4.
- Enhanced intracellular cAMP concentration, the apparent biochemical consequences of PDE4 inhibition, is well characterized in immuno-competent cells, where it acts as a deactivating signal.
- The pathologies related with these biological systems signify some of the more vital therapeutic targets for the next century such as depression, schizophrenia, parkinsonism, asthma, atopy, multiple sclerosis, arthritis, type-II diabetes and AIDS.

With the knowledge that multiple distinct PDE isozymes exist, and they differ in their cellular distribution, leading to the synthesis of a variety of inhibitors that possess marked degree of selectivity among them, thereby raising the possibility, that the unfavorable side-effects profile of non-selective PDE inhibitors like nausea, emesis, gastrointestinal side-effects, and vascular toxicity by specifically targeting these isozymes can be minimized that predominate in the particular tissue or the cell of interest.[142] While a wide diversity of inhibitors has been reported, the success is very minimal till date. On the basis of structural features, selective PDE4 inhibitors are broadly classified into:

1) Catechol ethers: Structural analogues of rolipram **(1)**

2) Heterocyclic and analogues: Structural analogues of nitraquazone **(2)**

3) Xanthine and related compounds: Structural analogues of theophylline **(3)**

4) Miscellaneous selective PDE4 inhibitors: Structurally diverse compounds

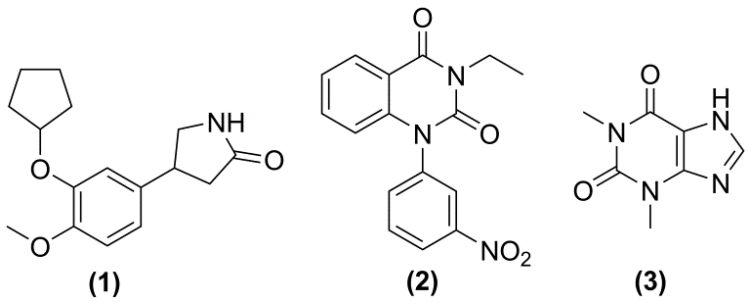

(1) **(2)** **(3)**

Fig. 18: Structural classification of PDE4 inhibitors

2.1. *Rolipram binding site*

Rolipram has been found to bind to a high affinity rolipram binding sites (HARBS) on PDE4, distinct from catalytic site; which is not present in all tissues that contain PDE4 and are co-expressed with human recombinant PDE4 activity. The pharmacological effects of several PDE4 inhibitors correlate better with displacement of rolipram binding than with PDE4 inhibition. Inhibition of PDE4 produces desirable effects on inflammation, anaphylaxis and smooth muscle contraction, while eliciting action on both CNS and GI as side-effects. PDE4 inhibitors also potentially displace [^{3}H] rolipram from a high affinity binding site (HARBS) which is proposed to be an allosteric binding site on PDE4 enzyme. The undesired emetic side-effect of PDE4 inhibitors is hypothesized due to its affinity for rolipram to bind to their allosteric sites comparatively than potency of inhibiting PDE4 enzyme activity. The apparent apprehension regarding the PDE4 inhibitors has emerged from their CNS effect resulting from their anti-depressant activity due to inhibition of PDE4 in brain. Striving efforts have been made to eliminate the emetic effect of PDE4 inhibitors by developing compounds with reducing or abolishing its affinity for HARBS while retaining its PDE4 potency.

Renewed interest to understand the fascinating factor in the mystery of PDE4 activity and its regulation, HARBS in the rat brain were labeled by [^{3}H] rolipram in a stereospecific, stereoselective and saturable manner. It has also been revealed that a monocyte derived recombinant PDE4 has a binding site with an affinity for rolipram approximately 100 times that of catalytic site. Further studies with various PDE4 inhibitors indicate that it binds to catalytic domain which is characteristic of rolipram binding site and possibly may not be an allosteric site but a part of different conformer of PDE4.

2.2. *Catechol-based PDE4 inhibitors or structural analogues to rolipram*

The incidence of the dialkyl catechol motif in PDE4 inhibitors is evident from the earliest illustrated PDE4 inhibitor such as rolipram **(1)** through to clinical candidate apremilast (CC10004) **(4)** and marketed roflumilast (Daliresp®) **(5)**. Molecular modeling and X-ray crystal diffraction studies, suggest the significance of catechol group, since it accepts a double hydrogen bond from the carboxamide of a glutamine residue (the so-called glutamine switch involved in PDE substrate specificity) at the back of the PDE4 catalytic site.[30]

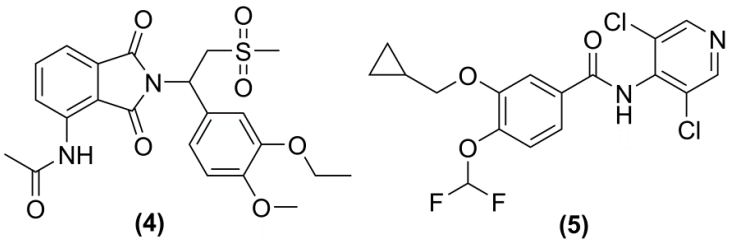

(4) **(5)**

Rolipram (ZK-62711) **(1)** is the prototype of this class and now well exploited of all selective PDE4 inhibitors. It was originally developed as an anti-depressant; potent cAMP-PDE4 inhibitor in brain homogenates.[143] Later, higher selectivity of rolipram and Ro 20-1724 for PDE4 was verified on vascular purified PDE.[144] A thorough SAR study suggested that the catechol-ether of 4-(3,4-dialkoxyphenyl) moiety was important for PDE4 inhibition, as it played a vital function in binding to the enzyme **(Fig. 19)**. The substitutent at the 4-position of the phenyl ring was constrained to small hydrophobic groups, mainly methoxy, indicating that this group might occupy a small hydrophobic compartment. In disparity, various alkoxy substitutents were well tolerated at the 3-position, suggesting that it fills the large hydrophobic cavity of the active site located near the enzyme surface in an optimal manner **(Fig. 19)**. The cyclopentyl group creates the maximal inductive effect for a fairly reasonable bulkiness increasing the inhibitory activity towards PDE4 by ten times, when the *meta*-methoxy group is replaced by a *meta*-cyclopentyl group as in rolipram.[59a] Since the characterization of PDE as a therapeutic target, many pharmaceutical companies started SAR studies to develop a series of rolipram analogues as PDE4 inhibitors and are reported.

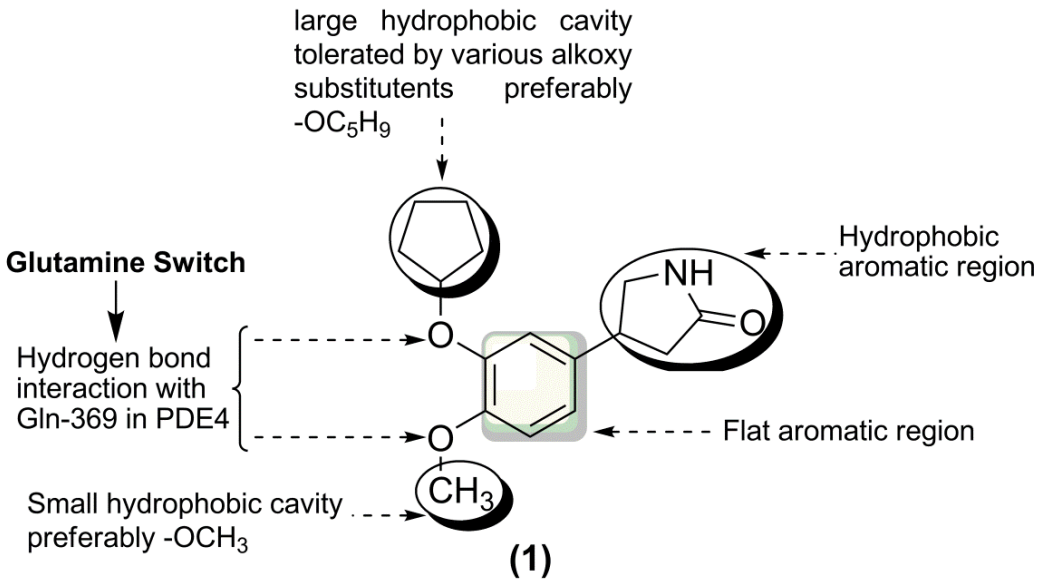

Fig. 19: Plausible interaction of rolipram in PDE4 active site

Rolipram **(1)** has frequently been used as a template for design of new and subtype specific PDE4 inhibitors. Several groups have reported the synthesis of PDE4 inhibitors derived from rolipram, in which the modifications were carried on the pyrrolidinone ring, catechol ring and/or on the linker between them **(Fig. 20)**.

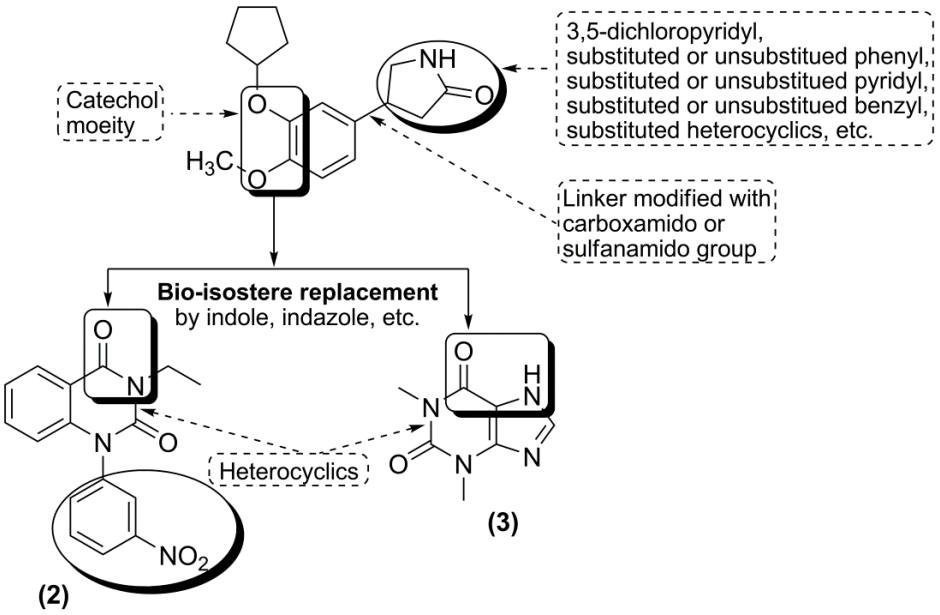

Fig. 20: Plausible modifications on rolipram to design better PDE4 inhibitors

Mesopram (ZK-117137 or SH-636), **(6)** a PDE4 inhibitor topologically similar to rolipram, was developed for the management of relapsing-remitting multiple sclerosis. The immunomodulatory profile of mesopram was reported in pre-clinical rodent models.[145] Ro 20-1724 **(7)** is another potent compound containing the catechol ether moiety, found in rolipram.[146] Studies with rolipram and Ro 20-1724 have exhibited prevalent distribution and principal positional function of PDE4 in control of cAMP levels in human inflammatory cells and in airway smooth muscle[147] inducing their significance in the therapeutic prospective of PDE4 inhibitors as anti-asthmatic agents[148] and thus initiating synthetic interest on the discovery of new PDE4 inhibitors. Notably, similar undesired side-effects profile of rolipram halted the progress of these compounds.

3,5-dichloropyridyl-4-carboxamide was identified as an effective pharmacophore through exhaustive SAR work on the effect of changes to alkoxy groups, amide linkages and *N*-phenyl ring of benzamide moiety on PDE4 inhibition for suitable variations on the pyrrolidinone ring. Several *N*-heterocyclic benzamide derivatives have been demonstrated to show exceptional potency in histamine induced bronchospasm and PDE4 inhibition. Roflumilast **(5)** a benzamide derivative is a potent selective PDE4 inhibitor derived from human neutrophils and similar potent to roflumilast *N*-oxide (major

metabolite formed *in-vivo*) and piclamilast, however more than 100-fold potent than rolipram and cilomilast.[149] It is the first PDE4 inhibitor approved for treatment of COPD.[150]

Piclamilast (RP-73401) **(8)** is a potent benzamide PDE4 inhibitor,[151] that exhibits non-selectivity for inhibiting PDE4 (catalytic site) over the dislodgment of rolipram from its binding site.[152] It acts by down regulating-tumor necrosis factor (TNF) and has shown potent anti-inflammatory activity in *in-vitro* studies using novel human whole blood assay.[150] Pharmacokinetic studies in mice have revealed that this compound undergoes extensive first pass metabolism resulting in less than 5% bioavailability.[153] However, the clinical development of piclamilast has been discontinued.

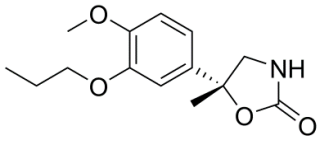

(6)

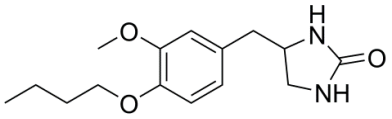

(7)

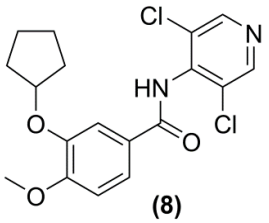

(8)

Since PDE4 needs a divalent metal ion for catalysis and using hydroxamic acid group as a metal chelator, two novel series of rolipram analogues, 3-aryl-2-isoxazoline-5-hydroxamic acids **(9)** and their acyclic counterparts *N*-aroylaminohydroxamic acids, were synthesized and assessed for PDE4 inhibitory activity.[154] Further, a highly potent *N*-phenyl rolipram derivatives **(10)** were synthesized with a hydrophilic substitution in 5-position of inner phenyl ring. These compounds showed potential activity in animal model of airway inflammation and exhibited little selectivity among the isozymes. SAR evaluation had pointed that this site can tolerate diverse substituents lacking deteriorating effects on PDE4 potency.[155]

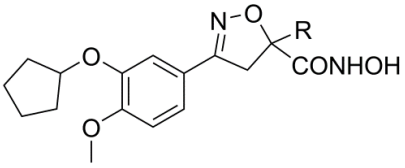

(9)

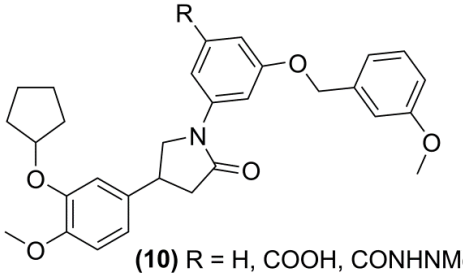

(10) R = H, COOH, $CONHNMe_2$

CDP-840 **(11)** is a potent selective PDE4 inhibitor, derived from rolipram by modifying the pyrrolidinone moiety has revealed effectiveness in phase II allergen test study in asthmatics devoid of adverse effects.[156] It inhibits PDE4 isoenzymes lacking any effect on PDE-1, 2, 3, 5, and 7 while in inhibiting human recombinant isoenzymes like PDE-4A, B, C or D it does not exhibit major selectivity and was equally potent against the isoenzymes lacking UCR1 (PDE-4B2 and PDE-4D2).[157] When compared to rolipram,

CDP-840 operated as a simple competitive inhibitor of all PDE4 isozymes. However, it suffered from extensive metabolism *in-vitro* and thereby a short half-life in vivo.[158] Thus, a very potent and metabolically steady PDE4 inhibitor (L-791,943) **(12)** containing a stable bisdifluoromethoxy catechol and a bistrifluoromethylcarbinol were developed.[159]

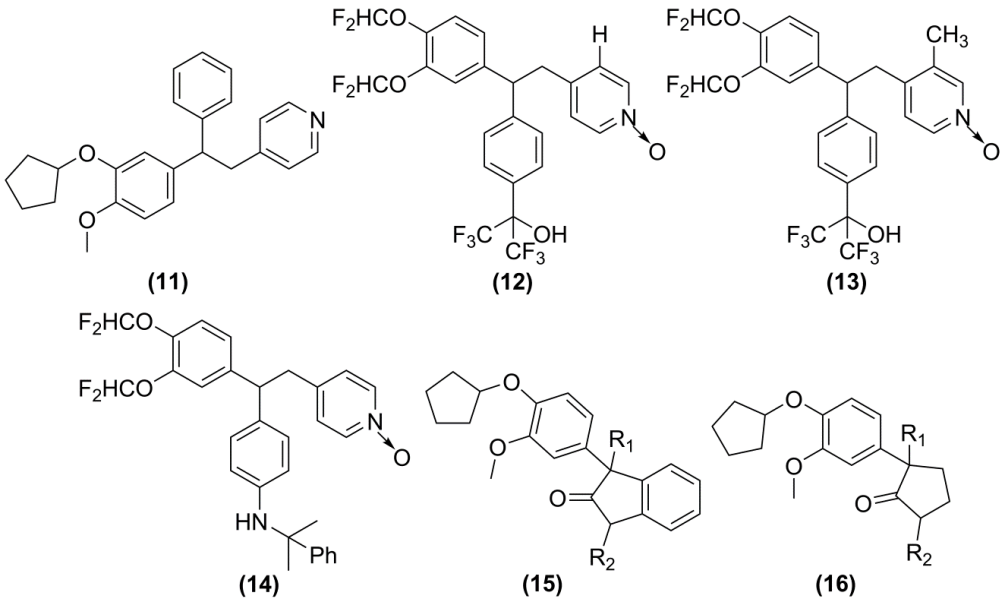

(11) **(12)** **(13)** **(14)** **(15)** **(16)**

The structure **(12)** was further modified to enhance metabolism led to the identification of (L-826,141) **(13)** as a potent PDE4 inhibitor.[160] In order to decrease the half-life further, metabolically resistant phenyl bistrifluoromethylcarbinol of **(12)** was reinstated with substituted aminopyridine residue, and a SAR study lead to the recognition of compound **(14)**. It exhibited a good PDE4 inhibitor activity and an improved pharmacokinetic profile over compound **(12)**.[161] A series of conformationally constrained quaternary substituted oxindole derivatives **(15)** of CDP-840, a potent and selective PDE4 inhibitor were also synthesized and evaluated for their PDE4 inhibitory activities.[162] Owing to their PDE4 activity in submicromolar range and reasonable selectivity for the selectivity catalytic binding site, these compounds had the potential for addressing the emetic side-effects. A series of potent spirocyclic γ-lactum **(16)** was synthesized by the same group and reported that large lipophilic group at R_2 and substitution at R_1 is a definite pre-requisite for better PDE4 inhibitory activity.[163]

The indole[164] or indazole[165] skeleton **(17-19)** was identified as an effective isostere for catechol (3-methoxy-4-cyclopentoxy motif of rolipram). Replacement of catechol like moiety with an indole moiety yields compounds **(17)** that can potently inhibit the activation of inflammatory cells *in-vitro*. It exhibits modest tolerance for steric bulk at R_1 and has a preference for bulky hydrophobic groups at R_2, thereby making the indole skeleton an effectual isostere for the catechol of piclamilast.[164]

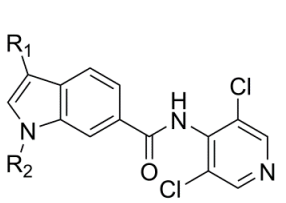

(17)

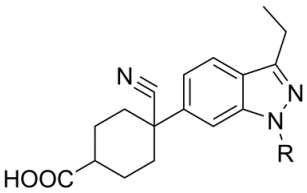

(18a) R =

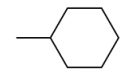

(18b) R =

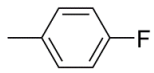

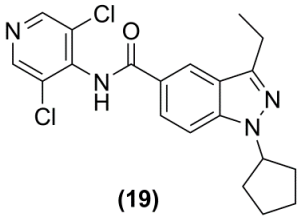

(19)

Modification of the aromatic ring was attempted rather than the pyrrolidinone ring or catechol ring. Both the Methylenedioxy- **(20)** and ethylenedioxyphenyl derivatives **(21)** and also derived cyclohexylidene acetal **(22)** were synthesized and were less or not potent.

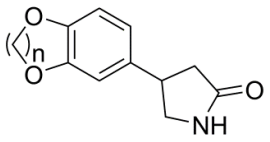

(20) (n=1) **(21)** (n=2)

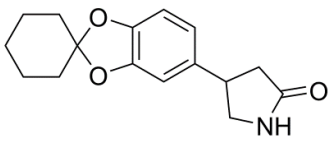

(22)

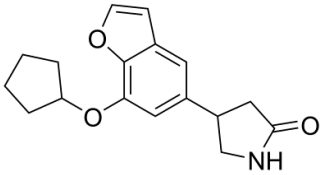

(23)

More radical alteration of the 4-methoxy-phenyl subunit of rolipram were benzofuran **(23)**, dihydrobenzofuran **(24)**, and dihydrobenzopyran **(25-26)** nucleus, isoster for catechol, which were designed and synthesized by simply anchoring the methoxygroup at the 4-position to the ring. These compounds were equipotent to rolipram.[166] On further investigation, 2-alkyl-7-methoxybenzofuran derivatives **(27)**, as potent inhibitors of PDE4, were reported.[167] Later, replacement of 7-methoxybenzofuran moiety of **(27)** by 7-methoxyfuro[2,3-*c*]pyridine **(28)** was reported[168] where the introduction of the nitrogen atom was proposed to enhance the pharmacokinetic properties of this series over the benzofurans. 7-Methoxy substitutent of **(28)**, as indicated by SAR study, was decisive for PDE4 inhibition, and substituting it with a difluoromethoxy group improved the potency.

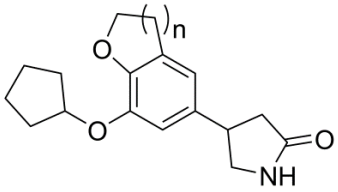

(24) (n = 1) **(25)** (n = 2)

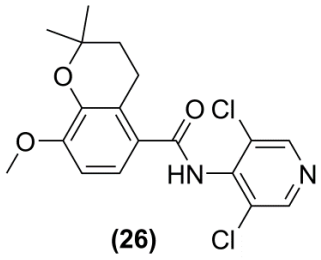

(26)

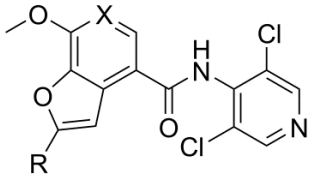

(27) X = CH **(28)** X = N

Interestingly, a novel sulfonamide series **(29)** was identified and designed as an orally active PDE4 inhibitor devoid of nausea/emesis, in man but maintaining the full spectrum of favorable biological actions.[169] These compounds exhibited better selectivity for the PDE4 catalytic site over the HARBS and no emetic side-effect up to the highest dose

tested in ferrets.Investigation of trialkoxybenzenes **(30)** resulted in a highly potent compound **(31)** that contained 3,5-dichloropyridine as metal-binding group. This most active compound on oral dosing in rats was converted into *N*-oxide, an active and equipotent metabolite.[170]

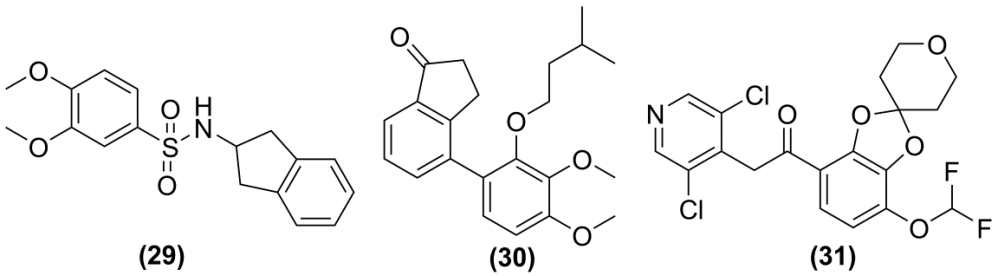

(29) **(30)** **(31)**

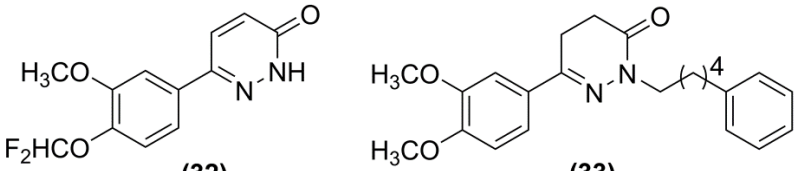

(32) **(33)**

However, the PDE4 activity to rolipram binding ratio of benzimidazole was not acceptable. The pyridazinone derivative, zardaverine **(32)** was reported for their PDE activity, which selectively inhibited PDE3 and PDE4 isozyme. It was introduced as a potent bronchodilator *in-vivo* and *in-vitro*.[171] A conceptually different approach to discover novel PDE4 inhibitors was initiated from zardaverine **(32)**, the core pyridazinone template which was optimized via parallel synthesis and virtual libraries were created after docking and scoring the candidates into the active site of human PDE4D. These virtual libraries covered three variable points of connection of the linker to zardaverine, five simple alkyl linkers and 15 different functional groups. Top scoring compounds were synthesized and evaluated, leading to the identification of better potent compound **(33)**.[172]

Following a similar strategy, a series of catechol benzimidazoles **(34)** were developed from rolipram and analyzed. 2-indanyl analogue was found to be a potent PDE4 inhibitor. SAR studies indicated that manipulation at 3-alkoxy position resulted in alteration of affinity with enhanced PDE4 inhibitory activity while reducing the [^{3}H] rolipram binding site affinity.[173] Bioavailable and efficacious 2-substituted-4-methoxybenzimidazoles **(35)** were designed by replacing 3,4-dialkoxyphenyl group of piclamilast **(8)** and evaluated for their PDE4 inhibitory activity in *in-vivo* models of inflammation.[153] These compounds including their *N*-oxides derivative retained the required inhibitory activity against PDE4 and also expressed good oral bioavailability in mouse.

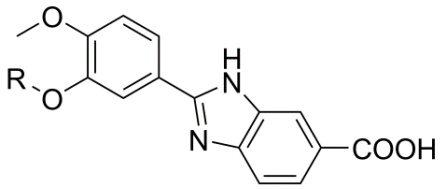

(34)

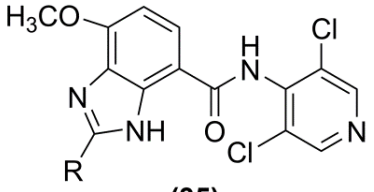

(35)

In a series of 5-(catechol ethers)-2-imidazolidinones, comprising structural features of both rolipram (**1**) and RO 20-1724 (**7**), the substitutents on catechol-3-oxygen were primarily modified to get compound **(36)** and **(37)**. Another series containing bi, tri and tetracyclic hydrocarbons at 3-alkoxy positions of the same parent structure have also been studied; Compound **(38)** and **(39)** were the most potent inhibitors in this series.[148]

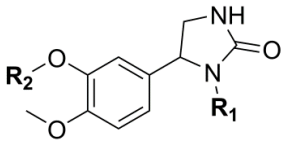

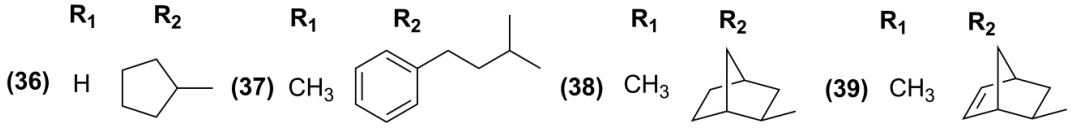

(36) **(37)** **(38)** **(39)**

Tetrahydro-pyrimidinone (Atizoram, CP-80,633) **(40)** was originally developed for oral treatment of asthma and was observed that both the enantiomers were equipotent, but discontinued due to emesis in humans.[174] In phase II clinical trials it showed efficacy for atopic dermatitis. Further studies lead to the synthesis and evaluation of a series of oxime carbonates and carbamates. Of these two compounds, PDA-641 **(41)**[175] and tibenelast (LY-186655) **(42)**[176] were identified to be equipotent to rolipram as PDE4 inhibitors.[148]

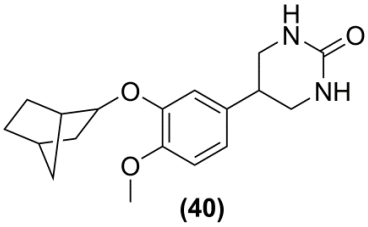

(40)

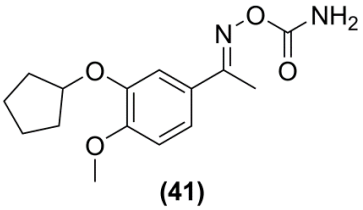

(41)

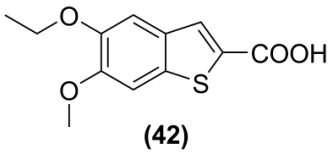

(42)

A novel series of 4-(3-alkoxy-4-methoxy-phenyl)benzoic acids and their corresponding carboxamides have been synthesized and evaluated in an effort to reduce emetic side-effects. Phenylpentoxy derivatives (**43**) was found to exhibit potent PDE4 inhibitory activity and possessed approximately 400 times weaker activity than rolipram for [^{3}H] rolipram binding site and demonstrated a significant reduction in emetic side-effects.[177] Tetomilast (OPC-6535) **(44)**,[178] a pyridyl thiazole derivative that potentially inhibits PDE4

and reported for the treatment of Crohn's disease and ulcerative colitis was associated with adverse effects like headache, nausea and emesis.[179] Similar strategies lead to the development of a potent 'second generation' PDE4 inhibitor with decreased potential for side-effects. Cilomilast (SB-207499; Ariflo®) **(45)** developed by GSK,[180] was approved by FDA in 2003 for both COPD and asthma.[181] It is selective for low-affinity PDE4 over HARBS and reported to be well tolerated; however, the side-effects of nausea and emesis do occur at higher doses.[6c] It is a exclusive compound in clinical phase trials that provided a weak PDE4D selectivity (10 fold as compared to other PDE4 subtypes).[152]

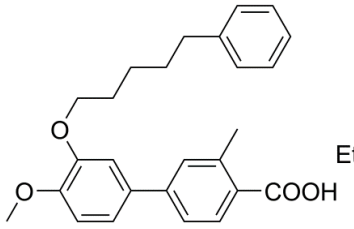

(43)

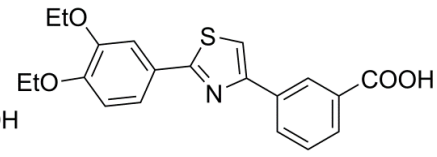

(44)

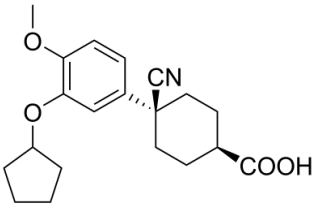

(45)

A series of rolipram derivatives, differently substituted either at the pyrrolidinone ring e.g., *N*-(benzopyranyl)pyrrolidinone **(46)**[182] or at aromatic ring have been synthesized and reported.Among these compounds, rolipram was the most active compound.[183] Oglemilast (GRC-3886) **(47)** and revamilast (GRC-4039) **(48)**, a dibenzofuran derivativewas found to be effective in animal models of rheumatoid arthritis (RA) and for the oral treatment of COPD and asthma.[60, 184] Oglemilast has been discontinued due to discouraging clinical data.

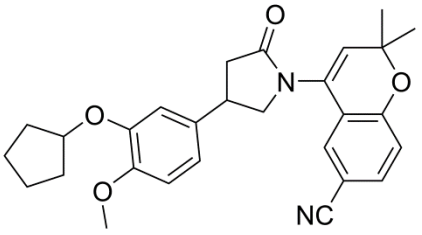

(46)

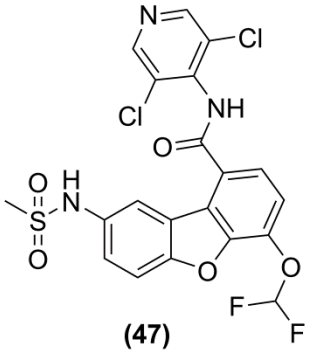

(47)

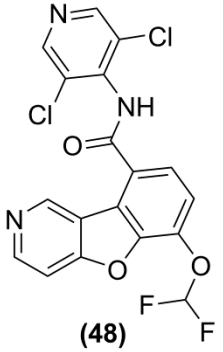

(48)

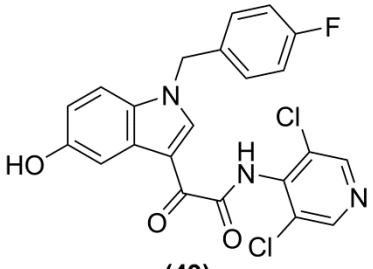

(49)

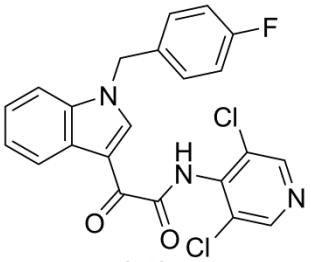

(50)

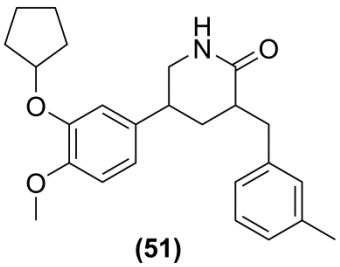

(51)

Potent selective PDE4 inhibitors, ronomilast (ELB-353) **(49)** and AWD-12-281 (Loteprednol) **(50)**, an indole derivatives and its 5-hydroxy analogue having similar topology to oglemilast were indicated for the prevention and treatment of allergic/inflammatory skin diseases. These compounds have the familiar dichloropyridine-amide motif which is also present in roflumilast, and have an acidic moiety on the heterocyclic system. In pre-clinical studies, ronomilast was known as a strong disease modifier for many therapeutic implications like rheumatoid arthritis, COPD, atopic dermatitis, asthma, rhinitis, psoriasis and in cigarette smoke-induced lung inflammation, in mice. Essentially, ronomilast was well tolerated and devoid of side-effects linked with PDE4 inhibitors like CNS and gastrointestinal effects which has been a vital development obstacle till date.[185] Like cilomilast, AWD 12-281 was effective against allergic contact dermatitis in mice and other inflammatory response (Type-1) in mice and guinea pigs indicating its use for atopic dermatitis and psoriasis.[59b, 186] These compounds **(49-50)** exhibited lower emetic potential compared to cilomilast and highest dose was achieved by inhalation route.HT-0712 (IPL-455903) **(51)** was indicated for memory enhancement, by improving cognitive function through cAMP/CREB signaling, restoring the motor skill and cortical function following focal cerebral ischemia. It was efficacious, safe and well tolerated, although preliminary indications like memory and learning failed to show positive statistical effect.[6c]

Structurally diverse class i.e., 2,2-disubstituted indan-1,3-dione **(52)** based cyclic compounds which has conformationally constrained indan ring linker have been reported which lead to the identification of PDE4 inhibitors with nanomolar potency with no emetic and oral activity.[187] Currently, several patents and literatures have appeared specifically claiming deuterated analogues of catechol motifs as PDE4 inhibitors to lower metabolism and increase its plasma levels. Closely related to apremilast, a series of thiophene-containing analogues **(53)** was synthesized which showed potency in submicromolar range for PDE4B and TNFα. PEGylated analogues of apremilast **(54)** were synthesized to modulate the solubility and pharmacokinetic (PK) profile of the molecule by derivatizing the acetamide group resulted in a series of highly potent inhibitors against PDE4B. Substituting the carbamate group for urea was also tolerated although expressed a slight decrease in its activity. However, substitution of the catechol methoxy group with various lengths of PEG chains lead to loss of considerable activity.[54b]

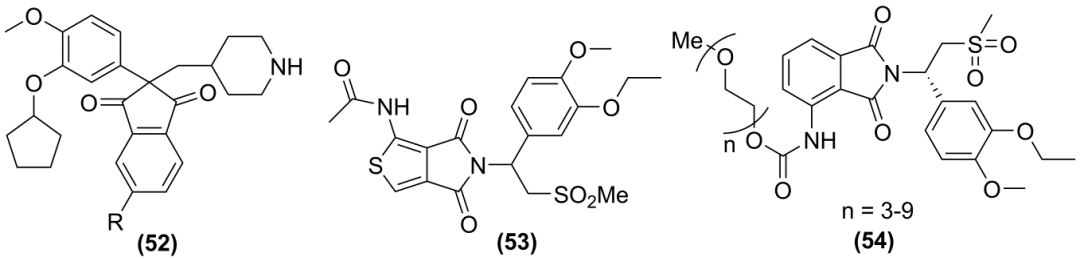

(52) **(53)** **(54)**

Modification in the structure of roflumilast **(5)** withbranching esters in the central linker lead to compounds **(55-57)** as Potent PDE4 inhibitors for inhaled administration, in the treatment of respiratory diseases.[188] The presence of this ester group could potentially help to reduce systemic exposure through hydrolysis, for the compounds desired for topical application.

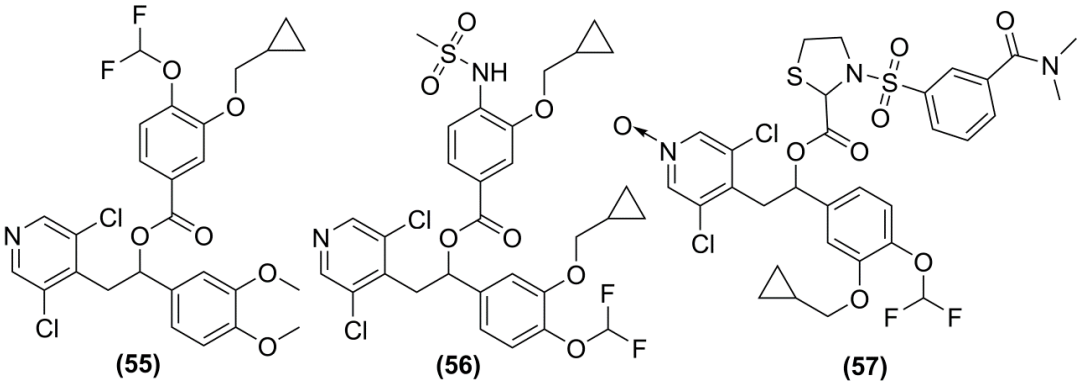

(55) **(56)** **(57)**

The catechol/3,5-dichloropyridine combination was investigated with series of bicyclic compounds in which the linking amide group of roflumilast was substituted with isosteric 4-aminoquinolones **(58)**. Some compounds showed better topical applications as solutions, due to their additional long chain, basic amino groups as exemplified by compound **(59)** and also had better long-term stability.[54b]

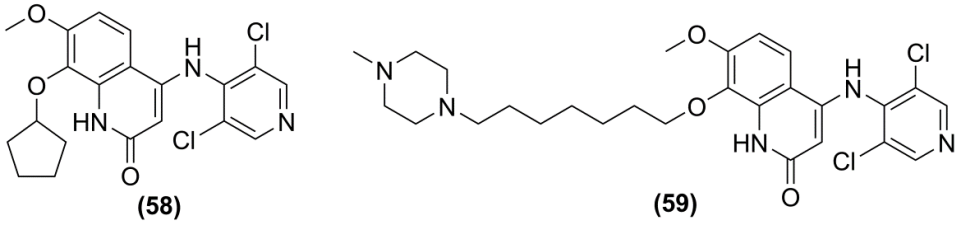

(58) **(59)**

Benzodiazepinone-derived catechols **(60)**, lipophilic amines in which the chain was extended from the *para*-position of a benzodiazepinone-5-phenyl ring, with a spacer of 1-5 carbons were synthesized.[54b] A potent PDE4 inhibitors based upon a benzodiazepine template was successfully identified[189] and SAR of this series indicate that both benzamide **(61)** and heteroarylamide substituents, as in compound CI-1018 **(62)**, representing a novel PDE4 inhibitor with improved activity and selectivity compared to

other PDEs.[190] Analogues of this compound exhibited potent PDE4 inhibitory activity with better selectivity towards PDE4 and lower affinity for HARBS.[191] Optimization provided a back-up compound CI-1044 **(63)** to CI-1018, expressing potent inhibition of PDE4 activity both *in-vitro* and *in-vivo* and maintaining the good safety profile.[192] Pyridylamide compounds were observed to be 3-fold more potent than rolipram.[190]

Despite its teratogenic properties, thalidomide **(64)** has effective immunomodulatory properties. Using PDE4 inactive thalidomide as a lead structure, its homologous, CC-1088 **(65)** and apremilast **(4)** derived from 3-amino-3-arylpropionic acids were synthesized and found to be potent inhibitors of TNF-α and PDE4.[193] In this series, the sulfone moiety was a better isostere for the carboxylic acid moiety, while swapping the phthalimide group at 4-position did not have major impact on PDE4 inhibitory activity in the enzymatic assay. Nonetheless, addition of the *N*-acetylamino group lead to the identification of apremilast **(4)**, which had improved potency in cell based assays.[194] Among these analogues, apremilast is the most advancedoral PDE4 inhibitor for the treatment of psoriasis, psoriatic arthritis and several other autoimmune diseases such as ankylosing spondylitis, Behcet's disease and rheumatoid arthritis (RA).[54b]

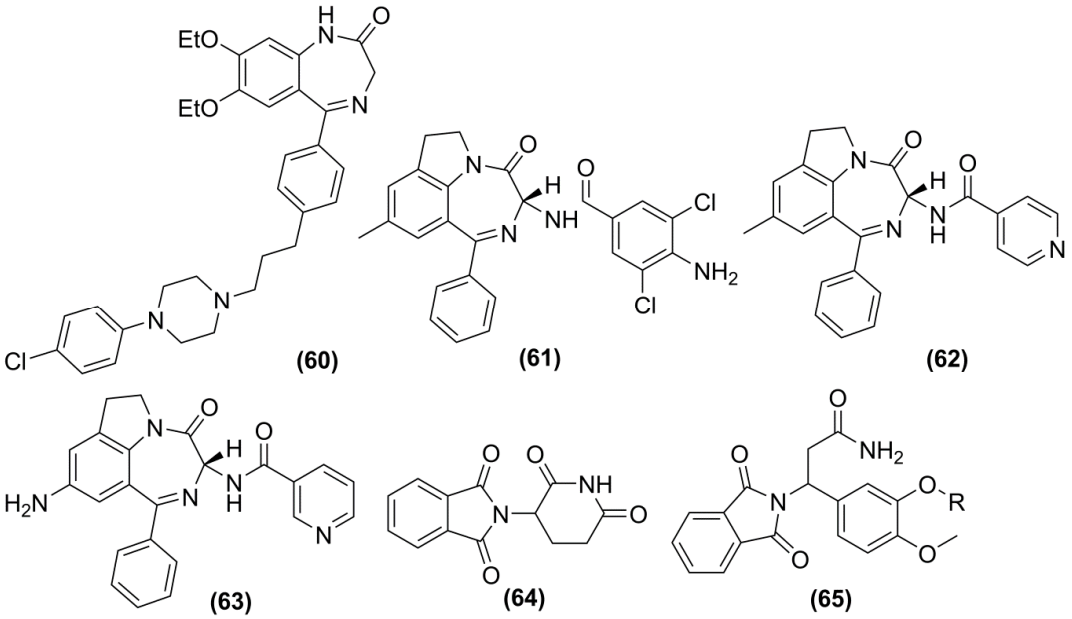

In pre-clinical tests of cognition in several species, MEM 1414 reversed memory deficits and established major and continuous developments in cognitive function over a broad dose range. However, MEM 1414 was linked with typical adverse event profile of PDE4 inhibitors, namely nausea and emesis, though there were mild and self-limiting side-effects. MEM 1917 demonstrated a potential candidate for the treatment of depression. They shared a pathway in memory formation and depression, by inhibiting the action of

PDE4 and increasing levels of cAMP may restore the imbalances in neurotransmitter and the cognitive impairments in depressed patients, although the mechanism was not well understood.[195] Structures of these compounds have not been revealed to date.

2.3. *Heterocyclics and Analogues*

The catechol-binding motif can also be mimicked in a range of heterocycles, whereby one of the catechol alkoxy groups is replaced by a heterocyclic nitrogen atom. This is a bioisosteric replacement and thus can maintain the same Hydrogen bond interaction with 'glutamine switch' of the PDE4 enzyme **(Fig. 20)**.[54b] This class of PDE4 inhibitors is exemplified by nitraquazones (TVX 2706) **(2)**. It was hypothesized that the nitro group of nitroquazone **(2)** could overlay the lactum moiety of rolipram to explain its PDE4 activity. Nitraquazone and congeners exhibited rolipram binding site affinity in nanomolar range (rolipram K_d = 1-2 nM). It is expected that HARBS is responsible for emesis and nausea, so it becomes important to ascertain selectivity for PDE4 inhibitory activity over this binding site. The compound nitraquazone **(2)** is familiar for its prominent anti-inflammatory and analgesic pharmacological profile. Several compounds structurally related to nitraquazone have been synthesized and evaluated as PDE4 inhibitors.

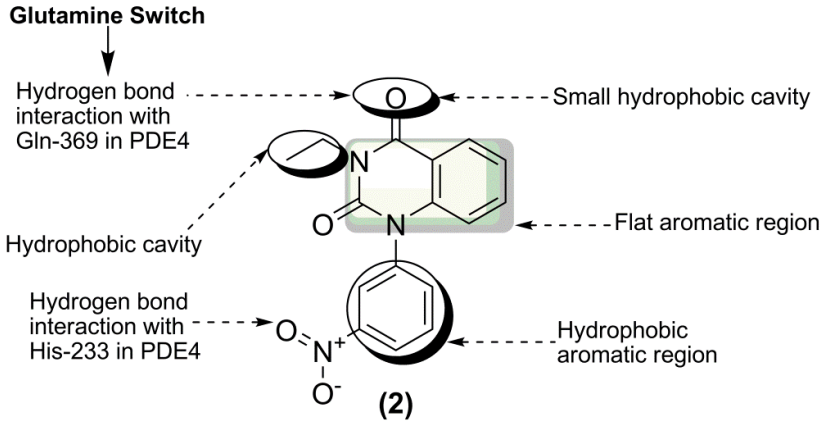

Fig. 20: Plausible interaction of nitraquazone in PDE4 active site

The quinazolinediones are topologically diverse from rolipram but may be categorized along with denbufylline **(133)**, for SAR as "fused ring" compounds. Compounds related to nitraquazone **(2)** have been evaluated and substitutions of the *N*-ethyl group with better lipophilic groups were revealed to augment PDE4 inhibitory potency. Pruning dione in the structure may not essentially affect the inhibitory activity although little activity was preserved even after modification of the fused ring structure.[196]

The archetypical quiazolin-2,4-dione moiety of compound **(2)** has been extensively manipulated to afford a variety of structure derived compounds. 3'-NO_2 group of

compounds **(2)** have been replaced by different nonprotic, electron-withdrawing functionalities like halogens (Cl, Br) , esters, etc., to study its SAR.[197] Corresponding acid and *N*-methyl amide produced a substantial and complete loss in potency, respectively.

Pyridopyrimidinediones analogues have been reported for their PDE4 inhibitory activity. Although benzene-pyridine isosteric replacement lead to decrease in potency in case of compound **(66),** as compared to compound **(67),** but an acid or *N*-methylamide were inactive. However, introduction of bulkier (higher lipophilic) groups at N_3 afforded compound (CP-77059) **(68)**, **(69)** and **(70)** with substantially increased potency.[54a] These compounds showed interesting anti-inflammatory properties in the carrageenan-induced rat paw edema.[198] The corresponding 4-pyridyl derivative (RS-25344) **(71)** proved to be four times potent inhibitor of PDE4 with respect to the prototype **(66)**.[199]

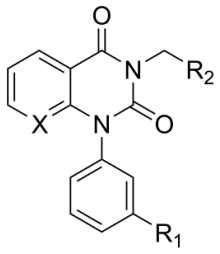

	X	R_1	R_2
(66)	N	$COOCH_3$	CH_3
(67)	CH	$COOCH_3$	CH_3
(68)	N	$COOCH_3$	phenyl
(69)	N	$COOCH_3$	cyclopentyl
(70)	N	$COOCH_3$	norbornyl
(71)	N	NO_2	4-pyridyl

Compounds of the type **(72)** containing pyridopyridazinone nucleus are nanomolar selective inhibitors of PDE4. The associated enhance in side-effects restricted their improvement. Attempts were made to diminish these adverse effects and compounds were synthesized by replacing pyridine with a series of heterocyclic systems like pyrrole, pyrazole, 1,2-dihydropyridine and thiophene.[200] These compounds showed significantly better balance between PDE4 inhibition and emetic side-effects. Slight modification lead to some structurally related compounds, RS-17597 **(73)**,RS-14203 **(74)**, and RS-14491 **(75)**, which inhibited PDE4 activity and improved intracellular cAMP in intact 43D cells in a concentration-dependant manner. The elevated concentration and the lower efficacy in cells indicate reduced capability of these compounds to traverse the plasma membrane and hinder cytosolic PDE4.[201]

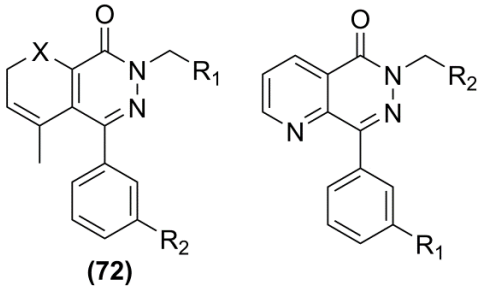

(72)

	R_1	R_2
(73)	NO_2	
(74)	NO_2	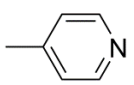
(75)	Cl	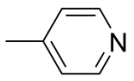

Further simplification of these compounds lead to quinoline derivatives of RS-14203 **(76)** as one of the most potent PDE4 inhibitors.[202] Further, replacement of 3'-nitrophenyl group by benzotriazole resulted in formation of compound **(77)**.[197] GSK-256066 **(78)**, a quinoline derivative was observed to be better PDE4 inhibitor with extremely high affinity and enhanced selectivity with IC_{50} of 3.2 pM for PDE4B over other PDEs. This compound has been evaluated for asthma, COPD and allergic rhinitis. Without disclosing the reason, the progress of this compound was put on hold.[203]

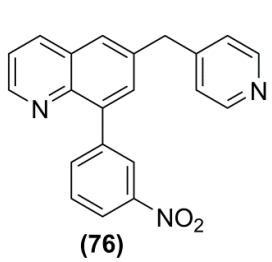

(76)

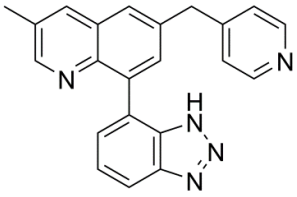

(77)

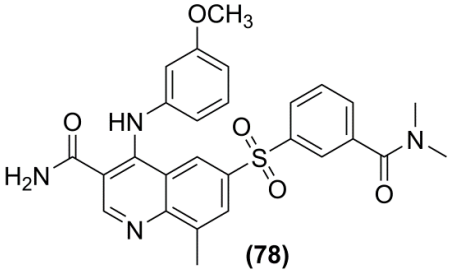

(78)

Quinoline carboxamide **(79)** and sulfonamide **(80)** derivatives and their corresponding *N*-oxides were specifically assessed for their PDE4 and TNF-α inhibitory activity.[204] Biological data were not reported but 8-methoxy-2-trifuoromethylquinoline-5-carboxylic acid derivative was found to be selective PDE4 inhibitor for the treatment of inflammatory disease.[205]

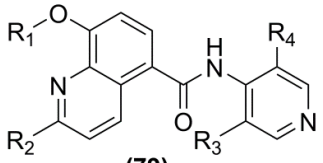

(79)

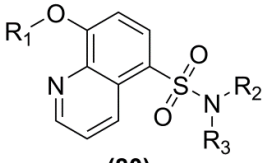

(80)

By amalgamation of the known pharmacophores,8-biarylquinolines[206] specifically, L-454560 that showed low incidence of emesis with high potency, were recognized as a novel class of PDE4 inhibitors and the lead molecule **(81)** was chosen as a development candidate.[207] However, the chance of potential drug-drug interaction and isomerization associated issues prompted a backup attempt. Accordingly, two compounds **(82-83)** were identified that tackled the problems linked with **(81)** and found to be less emetic. The acid **(83)** displayed better efficacy in guinea pig model of bronchoconstriction. Further effort lead to the identification of compound **(84)** as a potent PDE4 inhibitor by substituting the olefin moiety of **(81)** by an appropriate linker, where the group having amide moiety was found to be most potential.[208]

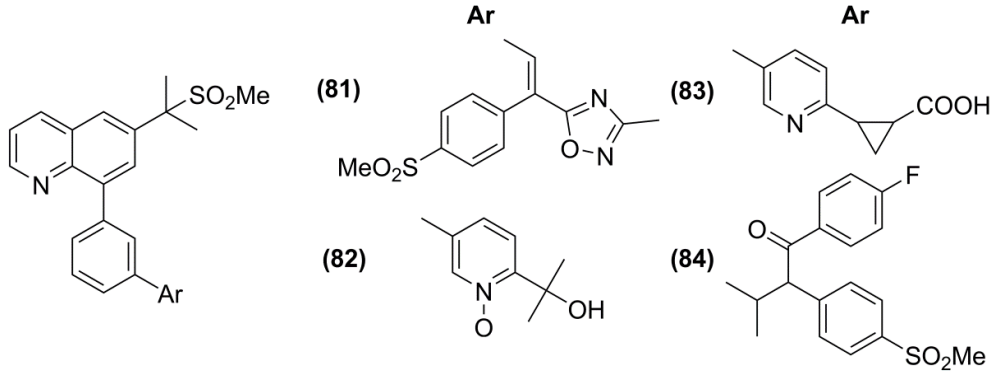

In the course of identifying an emetic probe, it was observed that a large substitutent at the 3'-position of an 8-arylquinoline derivatives lead to compound **(85-86)** with better emetic threshold while retaining the similar potency. Thus, integrating the structural attributes from CDP-840 **(11)**, which were diverse from rolipram, into 3'-position of the 8-arylquinoline afforded better potent PDE4 inhibitors.[209]

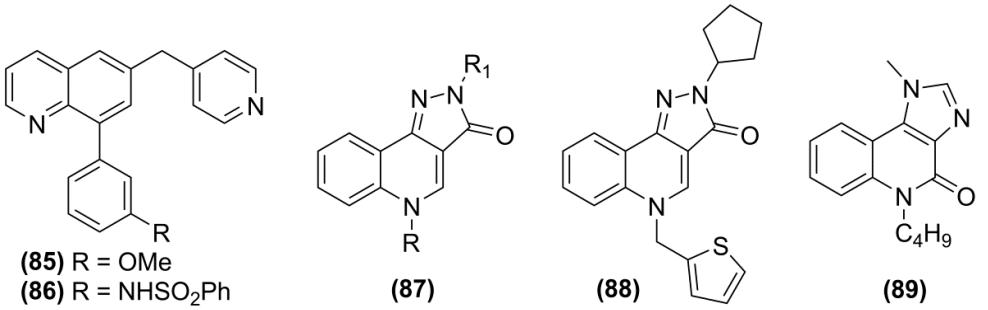

The pharmacophores of nitraquazone **(2)** and arofylline **(134)** were used to design a novel series of 2,5-dihydropyrazolo[4,3-*c*]quinolin-3-one (DHPQ) **(87)** derivatives as PDE4 inhibitors. These compounds exhibited good PDE4 inhibitory activity with weak affinity for rolipram's binding site and good anti-inflammatory profile without emetic side-effects.[210] It was observed that lipophilic group at *N2* position was requisite for PDE4 activity. Compound **(88)**, with 2-thienylmethyl group at *N*5 position and a cyclopentyl group at *N2* position displayed PDE4 activity alike to rolipram and an enhancement of HARBS/PDE4 ratio greater than 100 fold.[21b, 211] Similarly, 7,5-disubstituted 1*H*-imidazo[4,5-*c*]quinolin-4[5*H*]-ones **(89)** were synthesized, the most active compound had *n*-butyl group at 5-postions on the aromatic ring which showed weak adenosine antagonism and PDE inhibition.[212]

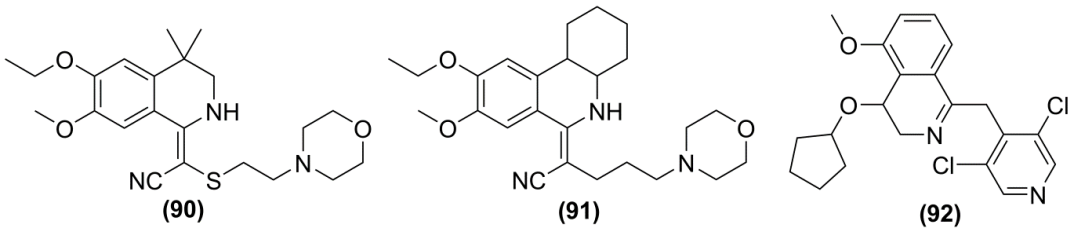

(90) **(91)** **(92)**

A novel tetrahydroisoquinoline **(90-91)** and dihydroisoquinoline **(92)** derivatives as selective PDE4 inhibitors having IC_{50} value in nanomolar range than for PDE2, PDE3 and PDE5 were reported for the treatment of asthma, COPD and rheumatoid arthritis. Further, a series of furoisoquinoline derivatives as PDE4 inhibitors were investigated for treating and preventing diseases caused by inflammation.[211]

Trequinsin-like PDE3/4 inhibitors, RPL554 **(93)** and RPL565 **(94)** were evaluated in array of *in-vitro* and *in-vivo* assays exhibiting a long-acting inhibition for bronchoprotective and anti-inflammatory activities.[213]

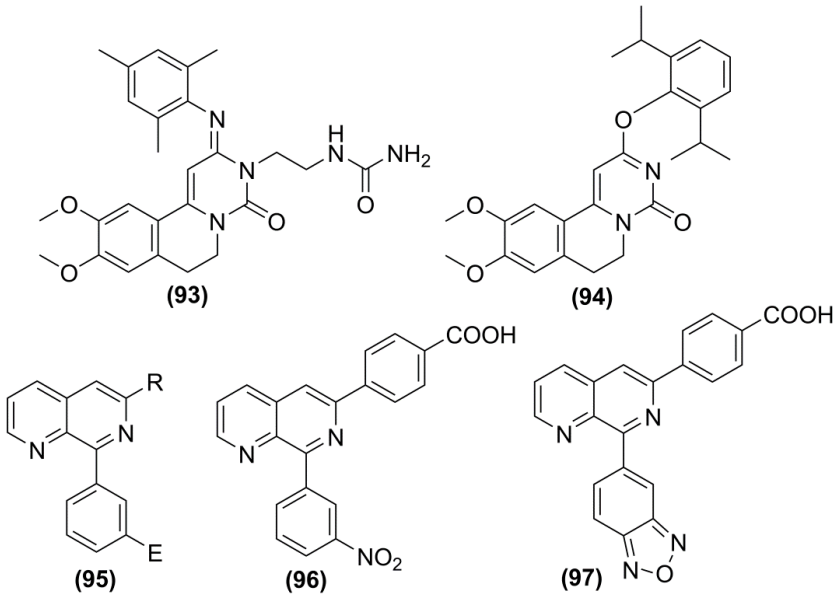

(93) **(94)** **(95)** **(96)** **(97)**

Synthesis and SAR of 6,8-disubstituted-1,7-naphthyridines **(95)** as potent PDE4D subtype-selective inhibitors suggested its potential as an oral therapy for treating asthma. It was reported that a suitable substitution at *C8* with NO_2, Cl and CN groups are vital for better PDE4A-D inhibitory activity, while compounds with a small group, such as H or NH_2 at *C6* resulted in a weak micromolar PDE4A-D activity. Introduction of bulkier group at this site improved the inhibitory potency towards PDE4B and PDE4D. The benzoic acid derivative **(96)** were nonselective and found to be about twice as potent in inhibiting high-affinity [^{3}H]rolipram binding site as compared to inhibiting PDE4D catalytic activity, a profile similar to cilomilast **(45)**.[214] Nevertheless, this compound contained a

sterically non-hindered aromatic nitro functionality known to be responsible for potential mutagenic and carcinogenic properties, and consequently, a suitable substitute of the nitro group was required. Thus, a new series of compounds were evaluated and among them, compound (NVP-ABE 171) **(97)**[215], was found to be more active for PDE4D isoform and 40-times more potent than cilomilast **(45)**.[216]

A novel series of 1,8-naphthyridin-4[1*H*]-ones derivatives were reported to selectively inhibit the PDE4D isozyme.[217] Further modifications lead to a series of 1-biaryl and alkyne-aryl-naphtyridine-4-[1*H*]-one derivatives.[218] 4-hydroxy-2(*1H*)-oxo-1-phenyl-1,8-naphthyridine-3-carboxamides **(98)** were synthesized and reported for their anti-inflammatory activity. It was observed that the nature of substitutents on the amide nitrogen had a distinct effect on anti-inflammatory activity.[219] Considering it as a lead, further modification of the compound lead to 5-phenylimidazo[4,5-*c*][1,8]naphthyridin-4(5H)-one derivatives **(99)**, KF-17625 **(100)** and KF-19514 **(101)**. There anti-inflammatory properties were influenced by the position and nature of substituents on imidazole. Minor modification in the structure of **(101)** lead to compound (KF-18280) **(102)** with decreased toxicity and better anti-inflammatory activity.[220]

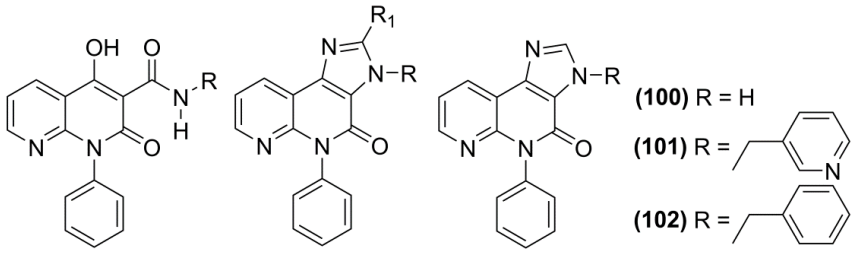

(98) **(99)**

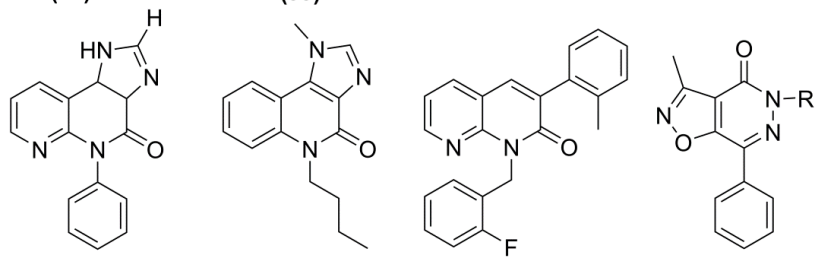

(103) **(104)** **(105)** **(106)**

Novel series of tricyclic heterocyclics imidazo[4,5-*c*][1,8]naphthyridin-4-(*5H*)-ones were designed and synthesized. Compound **(103)** relaxed tracheal preparation spontaneously isolated from guinea pig with 4-16 fold greater potency than aminophylline. It inhibited PDE4 and concanavalin-A-induced histamine release from rat mast cells.[221] Series of 1*H*-imidazo[4,5-*c*]quinolin-4(5*H*)-ones were designed, synthesized and evaluated as PDE4 inhibitors for their bronchodilatory activity. Compound (KF-15570) **(104)** was more effective than aminophylline with fewer side-effects. It exhibited PDE4 inhibition and weak adenosine antagonism.[212] Naftiridinones **(105)** resulted from a lesser structural

simplification of nitraquazone.[197] Heterocyclic fused 3[2H]-4 pyridazinones **(106)** have been synthesized and reported to have potent selective PDE4 inhibitory activity and reduced affinity for rolipram high affinity binding site.[222]

Nicotinamide ethers i.e., a series of 2-aryloxypyridine-3-carboxamides **(107)** and ring opened variants of pyridopyrimidinediones **(68)** have aroused renewed interest in inhibition of PDE4 with reduced emetic side-effects. A variety of substituents X = F, Cl, OCH_3, OC_2H_5, CN and CF_3 were found to be favorable in the *meta*- and *para*- whereas *ortho*-positions on the aromatic ring was not favoured.[223] Recently, PDE4 inhibitors based on pyrido[2,3-*d*]pyrazino **(108)** backbone have been disclosed.

Nitraquazone like inhibitors based on flat heteroaromatic ring system consisting of one (hetero) aromatic or a cycloalkyl systems connected to the flat portion through the methyl spacer with an electron withdrawing substituent represents the best pharmacophore model **(109)**.[197] Challenge in this class of PDE4 inhibitors is to have the selectivity in nanomolar potency with strongly reduced affinity for HARBS to improve the therapeutic index.

A fresh approach to improve therapeutic window of PDE4 inhibitors is intended at identifying the specific targets of emesis and efficacy. An emetic, efficacious and competitive PDE4 inhibitor **(110)** upon photoactivation competent of covalently tagging its biological targets has been synthesized. Efficacious and highly emetic PDE4 photoaffinity probe has been reported which would be highly valuable for recognition of relevant targets through which PDE4 specific inhibitors produce their efficacy and also cause emesis.[224]

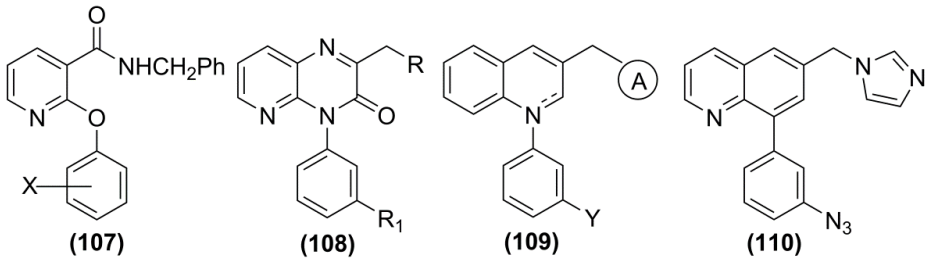

(107) **(108)** **(109)** **(110)**

Among the series, of substituted phthalazin-1-ones **(111)**,[142] 4-aryl-substituted tetra- and hexahydro-2*H*-phthalazin-1-ones**(112)**[225] and pyridazin-3-ones **(113)**[226] with PDE4 inhibitory activity are reported. In both the phthlazinone and pyridazinone series, *N*-substitution is favorable for PDE4 inhibitory activity, while the pyridazinone series is responsible for PDE4 selectivity. A molecular modeling study indicated that the *cis*-fused cyclohexa(e)ne rings occupies a region in space diverse from that occupied by the other fused (un)saturated hydrocarbon rings possibly due to steric interactions of these rings where the binding site plays an vital role in enzyme inhibition.[142, 226] The *cis*-4-aryl

phthalazinone **(114)** was identified as a potent PDE4 inhibitor and exhibited better *in-vivo* anti-inflammatory activites. The *cis*-fused cyclohexane ring played an important role in enzyme inhibition.[225b]

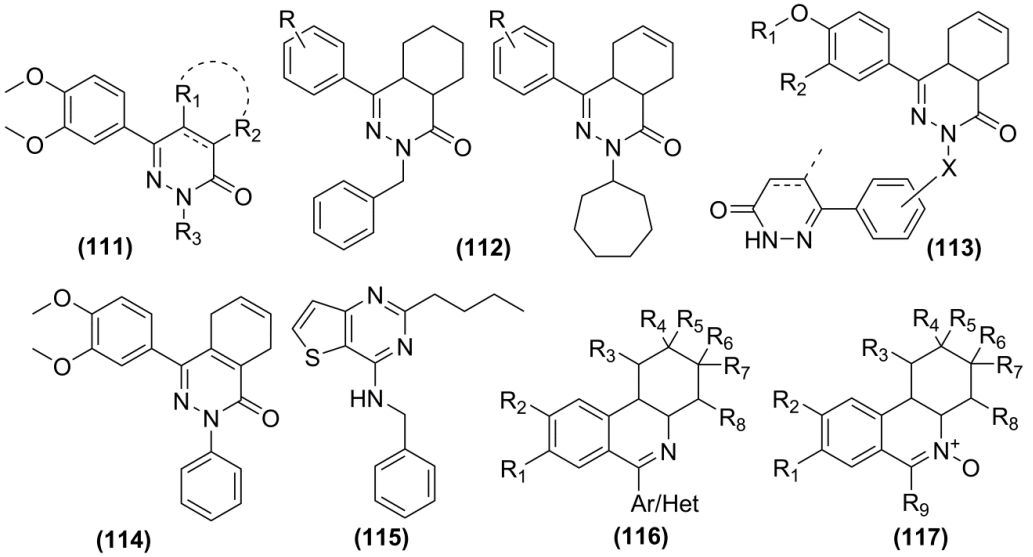

A series of novel heteroaromatic compounds was designed, synthesized and evaluated for their PDE4 inhibitory activities using the common pharmacophore derived from nitraquazone related compounds. Thienopyrimidine **(115)** was selected as a lead compound and a number of compounds with various lipophilic and aromatic groups in both *C2* and *C4* position were synthesized. These compounds displayed good activity for both PDE4 inhibition and cAMP potentiation and also exhibited an improved ratio with respect to the [^{3}H]rolipram specific binding site.[227] Several novel phenanthridine **(116)** and phenanthridine-*N*-oxide derivatives **(117)** were also reported as selective PDE4 inhibitors.[211]

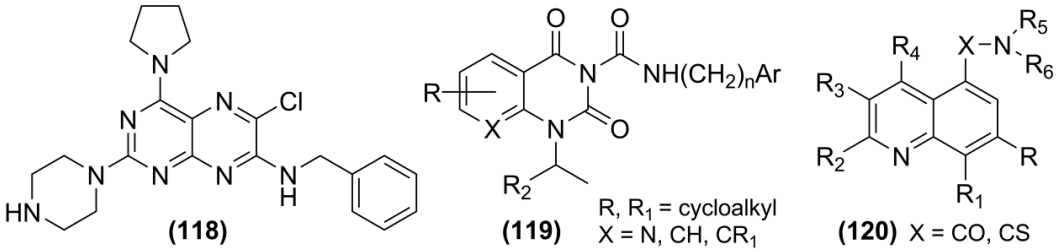

Order of reactivity of pteridine carbon atoms towards secondary amines have been elucidated and alkylamino substituted pteridines **(118)** free of positional isomers, have been proposed.[228] A novel class of inhibitor like compounds **(119)** and **(120)** based on same quinolone and naftiridinone template with the carboxamido or sulfonamido groups have been reported.[229]

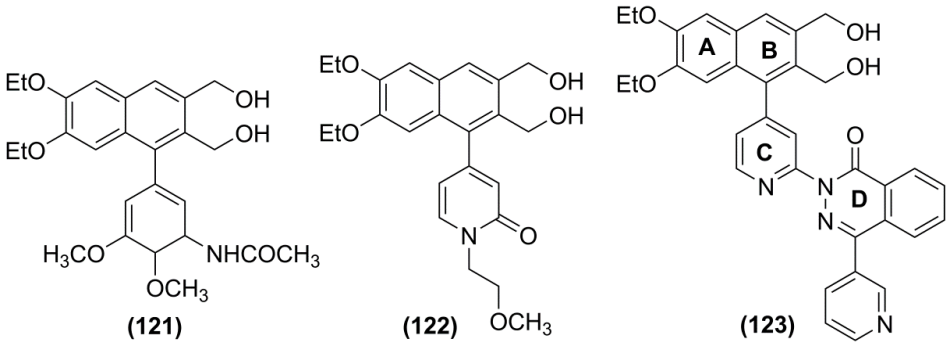

(121) **(122)** **(123)**

A series of 1-aryl-2,3-bi(hydroxymethyl)naphthalene ligand was synthesized and evaluated for their ability to selectively inhibit PDE4. Replacement of 1-phenyl ring as in compound **(121)** by a pyridone ring (T-440) **(122)** lead to marked improvement of their selectivity for PDE4 over PDE3. These compounds were chosen as lead candidates for further pharmacological evaluation.[230]

Amalgamation of compound of **(121)** and compound **(122)** lead to 1-pyridylnaphthalene analogues which were designed to enhance the potency and selectivity for PDE4 inhibition.[231] In this approach, (i) the naphthalene part (A,B-ring) was fixed, (ii) the heterocyclic compound having a carbonyl group (D-ring) was introduced, and (iii) the pyridyl group (C-ring) was preferred on the basis of the possibility of chemical alteration. Accordingly, compound **(123)** exhibited potent anti-spasmogenic activities without significant changes in heart rate and also induced notably weaker emetic effects than piclamilast on both orally and intravenous administration, hence was preferred for further assessment as an anti-asthmatic agent.[232]

2.4. *Xanthine and related compounds*

Alkylated xanthines were the first recognized inhibitors for their CN PDE activity and have been widely used as tools to evaluate the role of CNs in the actions of a large number of agents that increase the rate of synthesis of cAMP or cGMP. Unfortunately, the use of alkylxanthines or probably any other type of PDE inhibitor is complicated by the ability of these agents to inhibit the hydrolysis of both cAMP and cGMP. Additionally, xanthenes have effects on other pathways that are unrelated to, but may be confused with, PDE inhibition.[233] One way to avoid the pitfalls of uninterpretable or misinterpreted results arising from effects of alkylxanthines that are unrelated to inhibition of CN hydrolysis is to use a series of compounds with a wide range of potencies and selectivities as inhibitors of the various forms of PDEs. Then, to the extent that inhibition of a specific PDE isozyme is responsible for a second biological event, the rank orders of potency for inhibition of the specific form of PDE and for producing the second effect should correspond. Such correspondence is very unlikely in the event that the two effects are mechanistically unrelated.[234]

Theophylline **(3)** represents a class of weak non-selective PDE4 inhibitors, used extensively as bronchodilators in the treatment of asthma and anti-inflammatory agents. Therapeutic applications of xanthines are limited to narrow therapeutic index due to variety of physiological effects like gastrointestinal, tachycardia, bronchodilation, CNS stimulation and cardiotonic activity. Inhibition of PDE in heart, brain and lungs may be the mechanism by which xanthines exert their effects.[235] The efficacy of theophylline can be coupled with drugs to improve side-effects profile and therapeutic index could be an important advancement in the treatment of asthma. Attempts are made to improve therapeutic profile by synthesizing new xanthine analogues without specifically focusing on PDE inhibitory activity but so far these efforts have not been successful.[236]

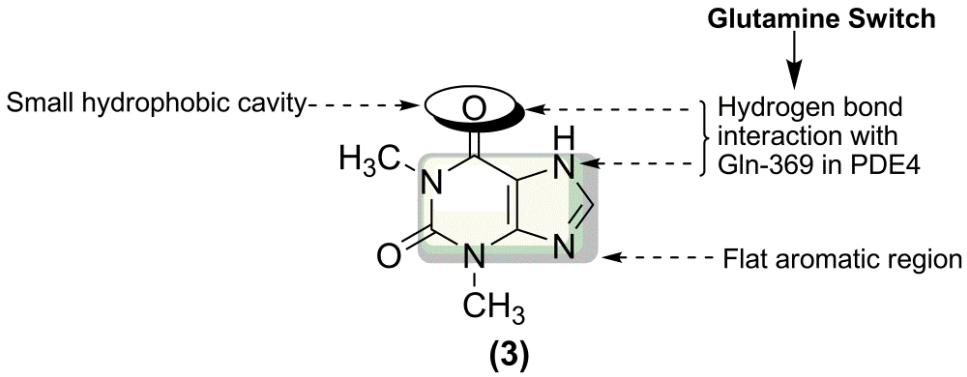

(3)

Fig. 21: Plausible interaction of theophylline in PDE4 active site

An alternative approach towards developing an 'improved theophylline' has emerged recently. Using xanthine skeleton, attempts have been made to design and synthesize novel compounds as selective PDE4 inhibitors which will retain the therapeutic efficacy of theophylline **(Fig. 21)**. It may mimic the PDE substrate to bind and block the highly conserved catalytic site of the enzyme. SAR of this class of compounds were reported and an interesting series of heterocyclic fused xanthines were derived.[237] A series of xanthines with varied substituents at the 1,3 and 8 positions have been prepared in order to understand the SAR for alkyl xanthines as inhibitors of PDE.[238]

Much effort has been made with regard to the modification of the substituents at the *N7* of xanthine. Though this modification has allowed many groups to develop 7-alkylated derivatives of theophylline such as diphylline **(124)**, doxophylline **(125)**; thioanalogues of doxophylline **(126)**, proxyphylline **(127)**, acephylline **(128)**, etophylline **(129)**, tazifylline **(130)**, and bamiphylline **(131)** have been synthesized and studied. These compounds were reported to possess more potent activity and less toxicity.[239] Among the therapeutically useful synthetic xanthine analogues, diphylline, bamiphylline and doxophylline have been approved and marketed as an anti-asthmatic drug.[240] These

derivatives are generally less active and exhibit low or moderate PDE4 inhibitory activity than theophylline but are stable in solution and *in-vivo*. These possess similar side-effects profile as that of theophylline.[241]

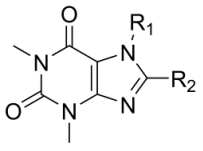

	R_1	R_2
(124)	$CH_2CH(OH)CH_2OH$	H
(125)	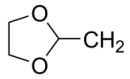	H
(126)	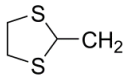	H

	R_1	R_2
(127)	$CH_2CH(OH)CH_3$	H
(128)	CH_2COOH	H
(129)	CH_2CH_2OH	H
(130)	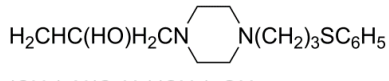	H
(131)	$(CH_2)_2N(C_2H_5)(CH_2)_2OH$	$CH_2C_6H_5$

Previous studies have suggested that introduction of a lipophilic moiety into xanthine skeleton enhances its pharmacological activity to some extent. Enprofylline **(132)**, is a weak adenosine receptor antagonist, exhibits similar pulmonary effect as that of theophylline.[239] Denbufylline (BRL 30892) **(133)**, a selective PDE4 inhibitor shows low adenosine receptor affinity common to many alkyl xanthines. Improvements of these compounds were discontinued due to poor pharmacokinetics.[242] Arofylline (LAS-31025) **(134)** was in clinical trials for oral asthma therapy. It is a weak but selective inhibitor of PDE4 as compared to theophylline. It is 25-30 fold less emetic as compared to rolipram. Arofylline demonstrated significant improvement of pulmonary function, as well as safe profile. Structural analogues of arofylline have been reported by a chiroscience group. The compounds showed improved ratio for PDE4 inhibitory activity versus emetic side-effects.[59b]

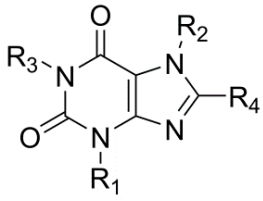

	R_1	R_2	R_3	R_4
(132)	nC_3H_7	H	H	H
(133)	nC_4H_9	CH_2COCH_3	nC_4H_9	H
(134)	$pClC_6H_4$	H	nC_3H_7	H

New heterocyclic compounds 3*H*-imidazo[4,5-*c*]quinolin-4(*5H*)-ones **(135)** have been designed and evaluated for its PDE4 inhibitory activity. This tricyclic heterocyclic can be regarded as a fusion compound of a benzene ring to the bond between 2 and 3 position of 7-substituted xanthine. 5-ethyl-3-methyl derivatives were found to be 5-fold more active than theophylline for their protective effect against antigen induced contraction of trachea in guinea pig.[239] Derivatization at the *N7* or *C8* amino sites of theophylline lead to compound cipamphylline (BRL 61063) **(136)**, the prototype with varying degrees of PDE4, adenosine receptor and high-affinitiy rolipram binding site activity.[243] Sulfonation of cipamphylline at 7- and 8-positions increased potency against PDE5A as compared to PDE4 isozymes.[244] 8-substituted piperazine derivatives have been synthesized and

reported to possess a combination of anti-allergic and anti-histaminic properties.[245] They also displayed potent bronchodilatory activity with enhanced duration of action. Among these, 1-methyl-3-isobutyl-8-(4-benzhydrylpiperazinoethyl) xanthine (S9795) **(137)** exhibited inhibitory action on mast cell degranulation and PDE enzyme.[246]

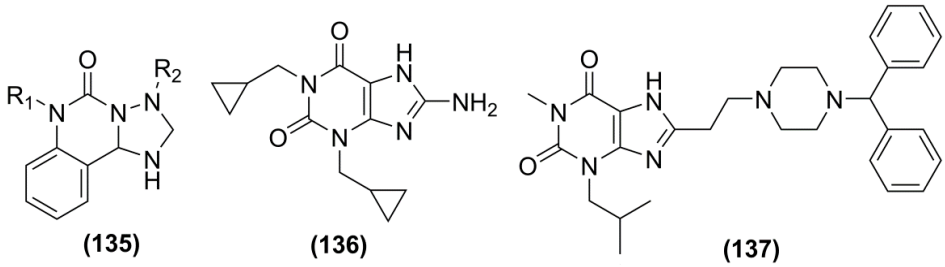

(135) **(136)** **(137)**

Earlier reports suggest that 9-benzyladenine derivative (BWA78U) **(138)** possess anti-convulsant effects in addition to anxiolytic and sedative properties, a series of 9-substituted adenines were synthesized and tested for PDE inhibitory activity.[247] Compound (NCS 613) **(139)** was identified as highly selective inhibitor of PDE4 which binds to catalytic site other than the HARBS, which is allosteric site (partially overlapped with the cAMP binding site) in PDE4 was postulated for this adenine derivative.[248] Extensive SAR studies of the purine ring skeleton mainly at *N3*, *C8*, and the amino group had lead to the identification of lead structure V11294 **(140)** and especially the "rolipram-like" disubstituted catechol moiety at *N3*. During the synthesis of V11689 **(141)** the 8-hydroxy human metabolite of V11294,[249] the 8-benzyloxy analogue **(142)** were also synthesized which was 30 times potent in PDE4B and 4D assays than its parent in the mixed PDE4 assay.[250]

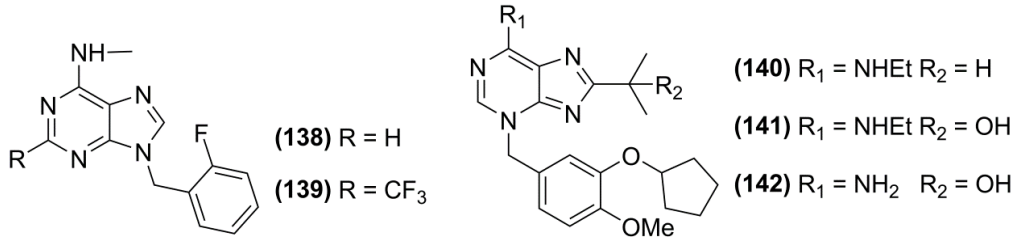

(138) R = H

(139) R = CF_3

(140) R_1 = NHEt R_2 = H

(141) R_1 = NHEt R_2 = OH

(142) R_1 = NH_2 R_2 = OH

A series of benzoseparated purine compounds have been synthesized and reported for their PDE4 inhibitory activity derived from bovine tracheal smooth muscle. Depending upon the substituents at *C7*, *C8* or *C1* positions, these benzoseparated linear derivatives of 3-isobutyl-1-methylxanthine (IBMX) **(143)** expressed PDE inhibitory activity.[251] Xanthine analogues ibudilast **(144)**, a non-selective and moderate inhibitor of CN PDE was implicated for both ischemic stroke and bronchial asthma. It shares several biological actions similar to that of rolipram but still its principal cellular mechanism of action remains, to be defined.[252]

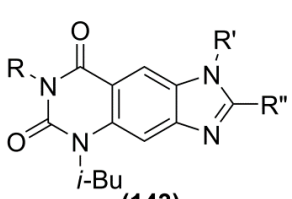

(143)

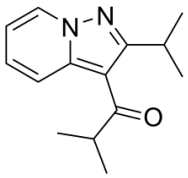

(144)

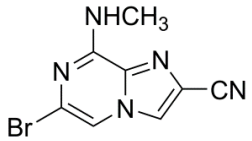

(145)

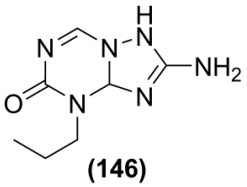

(146)

SCA 40 **(145)** was reported to be a potent smooth muscle relaxant when precontracted by different spasmogens and also as effective anti-bronchospastic than theophylline.[253] The presence of bromine on *C6* and an amino or alkylamino group on *C8* plays a critical role in inhibiting CN PDE 3/4 isozyme. All derivatives of this compound were moderately potent in inhibiting PDE4. Compound with cyano group on *C2* was potent in inhibiting PDE3 isoenzyme.[254] ICI-63197 **(146)** is a weak selective inhibitor of PDE4 which displayed alike potency and efficient in escalating cAMP concentrations in rat cerebral cortex and was at least tenfold more potent than Ro 20-1724 in producing anti-depressant-like effects.[255] It also displays relatively high affinity for the HARBS.[256]

Among the hybrid structures between the xanthine skeleton and rolipram, V11294A **(147)** and RPR 132703 **(148)** are the most interesting examples reported to be selective PDE4 inhibitors. V11294A is well absorbed orally and are non-emetic.[257] Compound RPR 132703 which is structurally similar to rolipram, containing a 1,4-phenolic ether and 3,5-disubstituted pyridine fragment of piclamilast, had been reported as potent orally active inhibitor of LPS-induce TNF-α release in an allergic rat models.[197]

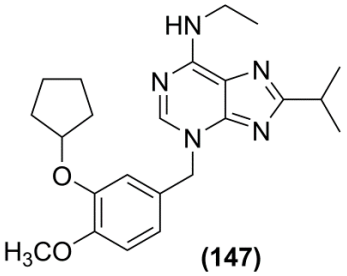

(147)

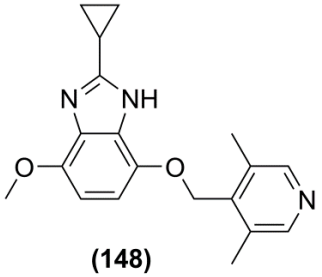

(148)

2.5. *Miscellaneous Selective PDE4 Inhibitor*

Analogues based on pyrazolo[3,4-*c*]pyridine **(149)** nucleus have been reported as PDE4 inhibitors.[258] AN2728 **(150)** and AN-2898 **(151)** are novel oxaborole compounds that decrease TNFα release through inhibition of PDE4. These compounds were effective in both *in-vitro* and *in-vivo* anti-inflammatory studies and were evaluated for atopic dermatitis (AD) and psoriasis.[259] Lirimilast (BAY-19-8004) **(152)**, a benzofuran derivative implicated for the treatment of asthma and has been discontinued, though it did not show emetic responses at doses 30 to 60 fold more than the efficacy dose.[260]

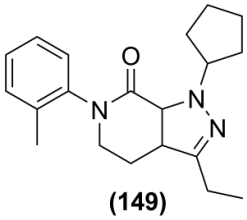

(149)

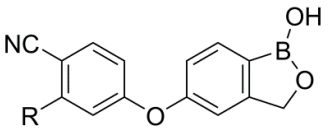

(150) R = H **(151)** R = CN

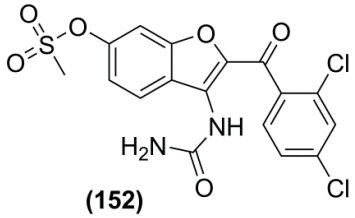

(152)

2.6. *Natural products as PDE4 inhibitors*

The catechol motif is found in some classes of natural products, and also displays PDE4 inhibitory activity. Mesembrine **(153)** and unsaturated analog mesembrenone **(154)** isolated from Kanna (*Sceletium tortuosum*) exhibited PDE4 inhibitory activity. Flavonoid natural products based on a polyphenolic structure containing the catechol motif like hesperetin-7,3'-*O*-dimethylether (HDME) **(155)** have shown to inhibit PDE4. Non-catechol based alkoxy-tricyclics derivatives like 8-methoxycarbazole **(156)** derived from the bark of the curry tree (*murraya koenigii*) showed PDE4 inhibitory activity.[54b]

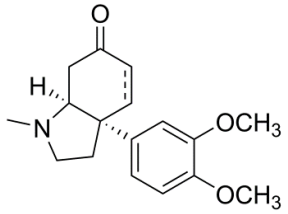

(153) ($-CH_2-CH_2-$) **(154)** (-CH=CH-)

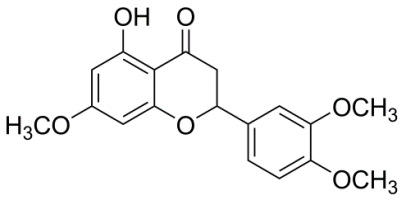

(155)

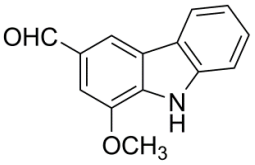

(156)

3. OBJECTIVES AND PLAN OF WORK

Clinically existing anti-depressants and anxiolytics are plagued with one or more drawbacks. As a part of our enduring effort to identify better anti-depressants and anxiolytics with improved therapeutic utility, novel PDE4 inhibitors were designed and evaluated for their therapeutic potential. Clinical studies of existing PDE4 inhibitor like rolipram and second-generation inhibitors like cilomilast and roflumilast were restricted by dose-limiting side effects, namely nausea, vomiting, headache and diarrhea.

No chemotypes differentiate amid the PDE4 subtypes (A, B, C, D), while research from knockout mice along with siRNA targeting and distribution studies, demonstrated that PDE4 subtypes have distinct functional role in therapeutic response. To minimize the side-effects and enhance the therapeutic window of efficacy, it is important to target one of the four subtypes. Among the isoform, PDE4D has been implicated in the mediation of anti-depressant activity and memory, while PDE4B is more likely involved in dopamine-associated and stress-related processes like schizophrenia, anti-psychotic activity and anxiety. It is also observed that the CNS side-effects are associated with PDE4D isoform are still unclear. Its emerging therapeutic potential rekindled our interest to identify better PDE4 inhibitors with subtype selectivity and with minimum or devoid of its side-effects.[15b-261]

Keeping all these aspects in consideration, following prime objectives were set for the present study.

- To design novel PDE4 inhibitors by ligand-based approach based on pharmacophoric templates.
- To synthesize the designed new chemical entities using appropriate organic synthesis approach.
- To evaluate the synthesized new chemical entities (NCE's) for their PDE4 inhibitor potential using *in-vitro* assay techniques.
- Assessment of the synthesized PDE4 inhibitors in various validated animal models of depression and anxiety.

3.1. Plan of work

3.1.1. Design of new chemical entities (NCE's)

In the present work, several compounds related to nitraquazone structure as discussed in the literature review, were initially studied to design the pharmacophore. The pharmacophore was derived using pharmacophore module in Discovery Studio ver 3.5. Identifying the common features of nitraquazone derivative PDE4 inhibitors, the interfeature distances were measured and considered for designing novel modified pharmacophore model. Using this model, novel PDE4 inhibitors were designed which may be potent, better isoform selective and plausibly with minimum side effects.

The pharmacophore model includes the interfeature distances between

a) Planar scaffold providing a hydrogen bond acceptor (HBA) and the hydrophobe connected through linker-1 **(A-B)** (~6.574 Å to ~8.405 Å),
b) Planar scaffold with HBA and hydrophobe connected through linker-2 **(A-C)** (~6.820 to ~7.696 Å) and
c) Between the two hydrophobes **(B-C)** (~8.5 to ~9.136 Å), respectively.

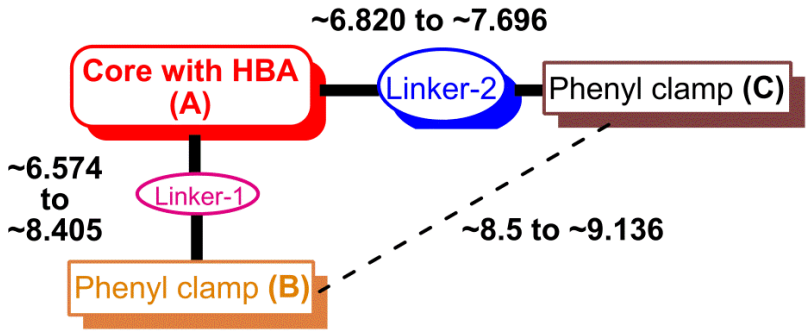

The novel modified pharmacophore consists of key elements: a) a planar scaffold providing a hydrogen bond acceptor (HBA) **(A)** and b) two hydrophobic substituent's **(B and C)** connected with linker-1 and 2, respectively. Based on this pharmacophore model, New Chemical Entities (NCE's) were designed, synthesized and evaluated for their PDE4 inhibitory activity.

3.1.2. Molecular docking and ADMET prediction

Molecular docking studies were performed on the synthesized compounds to sort rationale amid the acquired biological results which will help us to understand the diverse interactions linking the ligands and enzyme active site. The docking method used in this study was LigandFit (Discovery studio 3.5) software.[262] LigandFit was executed for accurate orientation of the ligands into the protein active site. The scored poses were then ranked and analyzed for their interactions inside the binding site. The ADMET

properties of designed molecules were computed using the ADME descriptors module, available in (D.S 3.5) software package from Accelrys[262b] to envisage array of drug-like properties for the compounds. The following classes of properties, were computed, i.e., aqueous solubility, blood-brain barrier penetration (BBB), cytochrome P450 (CYP450) *2D6* inhibition, hepatotoxicity, human intestinal absorption (HIA), and plasma protein binding. Furthermore, key issue was to calculate the BBB and other factors as the drugs should pass through the BBB to react with the receptor protein to treat central nervous system (CNS) disorders. All the designed molecules adhered to "Lipinski's rule of 5".

3.1.3. Synthesis of new chemical entities (NCE's)

Thus, in the present study, different 4-substituted 3-oxo-3,4-dihydroquinoxaline-2-carboxamides and different 3-substituted 4-oxo-3,4-dihydroquinazoline-2-carboxamides as a new series of congener compounds were designed and evaluated for its PDE4 inhibitory activity and isoform selectivity which were further screened for their anti-depressant and anxiolytic potential.

The basic structures of the proposed molecules (series-QCA to QCF) and (series-QZA and QZB) are depicted below. Where, R_1 = H, OCH_3, CH_3, Cl, C_2H_5, $CH_2CH_2CH_3$, $CH(CH_3)_2$, CF_3, etc.

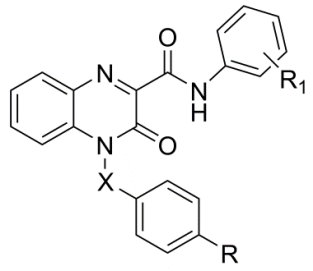

QC (A-F)

Series	X	R	Compounds
QCA	CH_2	H	1-16
QCB	CH_2	4-OCH_3	1-18
QCC	CH_2	4-CN	1-19
QCD	CO	H	1-18
QCE	CO-CH_2	H	1-19
QCF	CH_2-CH_2	H	1-19

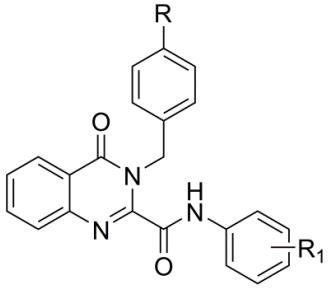

QZ (A-B)

Sr. No.	R	Compounds
QZA	H	1-15
QZB	4-OCH_3	1-18

On the basis of the pharmacophore designed,

- Quinoxaline scaffold with a hydrogen bond acceptor (HBA), benzyl moiety (methylene group as linker-1), and carboxamide as linker-2 along with a substituted hydrophobe distally placed lead to QCA series analogues.

- Further, modification on the benzyl ring by introducing a strong activating [methoxy group (-OCH_3)] or deactivating group [nitrile group (-CN)] at the *para*-position lead to QCB series and QCC series, respectively.
- Additional modification at linker-1 was attempted to understand the significance of the methylene (-CH_2-) group which was suitably replaced with the carbonyl (>C=O) group i.e., benzoyl moiety lead to QCD series.
- Whereas, introduction of both the methylene group and carbonyl group at linker-1, lead to QCE series.
- Increasing the chain length from methylene to ethylene (-C_2H_4-) at linker-1 i.e., phenacyl moiety, lead to QCF series.
- When the quinoxaline scaffold was substituted with positional isomeric quinazoline scaffold, benzyl group (methylene group at linker-1) and carboxamide as linker-2 along with a substituted hydrophobe distally placed lead to QZA series analogues. This series was regiosiomeric to the QCA series.
- Further, modification of the QZA series by introducing a strong activating group [methoxy group (-OCH_3)] at the *para*-position of the benzyl ring lead to QZB series which is positional isomeric to QCB series.

Among the R_1 chosen containing OR (R = alkyl) (linear or branched), at different position (*ortho*, *meta*, *para*); which is a ring activator and electron donating group due to strong resonance effect, while R (R = alkyl) of different chain length, used alone or in combination, at different position which is also a ring activator and electron donating group but has a weak resonance effect. Similarly X (X = halogen preferably chlorine), alone or in combination with R (R = alkyl), at different position, which is a ring deactivator and electron withdrawing group due to its strong inductive effect. These groups were selected in-order to substantially understand the SAR i.e., role of these group pertaining to activity.

3.1.4. Characterization of new chemical entities

The purity of the synthesized molecules were assessed by TLC, in at least two different solvent systems and detected by UV/I_2 chamber using ninhydrin reagent. The structures of the synthesized compounds were confirmed by spectral (IR, NMR and MS) data.

3.1.5. Assay for PDE4 inhibitory activity

All the synthesized compounds were evaluated in *in-vitro* analysis using PDE4B and PDE4D isoform elisa kit using fluorescence polarization. The standard assay protocol provided by the supplier was followed. Fluorescence intensity was measured at an excitation of 485 nm and an emission of 528 nm using a SpectroMax *M5* microplate

reader (Molecular Device, USA). All samples and controls were tested in duplicates and blank values subtracted from all other values. The percent activity in the presence of the compound was calculated according to the following equation

$$Percentage\ Inhibitory\ Activity = \frac{FP - FP_b}{FP_t - FP_b} \times 100$$

Where, *FP* is the fluorescence polarization in the presence of the compound, FP_t is the positive controland FP_b is blank. The percentage of PDE4B and PDE4D inhibitory activity of the synthesized compounds were consequently calculated.

3.1.6. Preliminary pharmacological screening assay

3.1.6.1. Spontaneous locomotor activity (SLA)

SLA test was carried out to determine the actives and eliminate the false positives using actophotometer and digital locomotor scores were recorded for ten minutes. It was also used for the selection of appropriate doses of the test drugs.

3.1.6.2. Preliminary anti-depressant screening

All the synthesized compounds were subjected to screening for their anti-depressant activity in various standardized rodent (mice) models like forced swim test (FST) and tail suspension test (TST) to assess their therapeutic potential. The duration of immobility (i.e., behavioral despair is when the mice give up the hope of 'escaping' a symptom which is clinically identical to depressive disorders) were analyzed.

3.1.6.3 Preliminary anxiolytic screening

In order to determine the anxiolytic potential of the new chemical entities, the molecules were further subjected to various screening in standardized rodent (mice) models like Elevated Plus-Maze test (EPM), Open Field Test (OFT) and Light/Dark (L/D) aversion Test. Increase in the values indicate their anxiolytic potential.

Selected compounds with better PDE4 inhibitory activity and significant anti-depressant values were subjected to elevated plus-maze test in mice. Percentage time spent in open arm was recorded. Compounds with significant anxiolytic effect in elevated plus-maze test were further subjected to Open Field Test (OFT). The number of square crossed and rearing was recorded. Further, compounds were subjected to anxiolytic screening like L/D aversion Test in which time spent in light chamber was recorded. Movement away from the (walls) periphery i.e., towards center was considered as an anxiolytic activity whereas movement along the (walls) periphery was considered as anti-depressant activity.[263]

4. EXPERIMENTAL WORK

4.1. Materials and Methods: Chemistry

All the chemicals and reagents were obtained from Spectrochem Pvt. Ltd. (India), S. D. Fine Chem Limited (India) and Aldrich (USA). Reactions were monitored by TLC, which was performed with 0.2 mm Merck pre-coated silica gel 60 F_{254} aluminum sheets. Compounds were detected by UV, iodine chamber and by dipping the TLC plates in ethanolic solution of ninhydrin and heating. Melting points (uncorrected) were determined on Buchi 530 melting point apparatus. IR spectra (ν_{max} in cm^{-1}) were recorded on Schimadzu IR Prestige-21 FT-IR spectrophotometer, ^1H NMR spectra were recorded at 400 MHz on a Bruker Avance-II, FT-NMR spectrometer using TMS as internal standard (chemical shifts in δ, ppm). Mass spectra were obtained on a Micromass/Waters VG analytical 70–250S instrument using electron spray ionization (ESI) technique (positive and negative mode). Column chromatography was carried out using silica gel 60-120/100-200 mesh as an adsorbent and ethyl acetate/hexane or DCM/MeOH as eluent.

4.2. Synthesis

Series of synthetic schemes were designed, protocols optimized and molecules synthesized, which are briefly discussed here under

Series-1: 4-benzyl-3-oxo-*N*-phenyl-3,4-dihydroquinoxaline-2-carboxamide analogues **(QCA-1 to 16**)

Series-2: 4-(4-methoxybenzyl)-3-oxo-*N*-phenyl-3,4-dihydroquinoxaline-2-carboxamide analogues **(QCB-1 to 18)**

Series-3: 4-(4-cyanobenzyl)-3-oxo-*N*-phenyl-3,4-dihydroquinoxaline-2-carboxamide analogues **(QCC-1 to 19)**

Series-4: 4-benzoyl-3-oxo-*N*-phenyl-3,4-dihydroquinoxaline-2-carboxamide analogues **(QCD-1 to 18)**

Series-5: 3-oxo-*N*-phenyl-4-(2-phenylacetyl)-3,4-dihydroquinoxaline-2-carboxamide analogues **(QCE-1 to 19)**

Series-6: 3-oxo-4-phenethyl-*N*-phenyl-3,4-dihydroquinoxaline-2-carboxamide analogues **(QCF-1 to 19)**

Series-7: 3-benzyl-4-oxo-*N*-phenyl-3,4-dihydroquinazoline-2-carboxamide analogues **(QZA-1 to 15)**

Series-8: 3-(4-methoxybenzyl)-4-oxo-*N*-phenyl-3,4-dihydroquinazoline-2-carboxamide analogues **(QZB-1 to 18)**

4.3. Synthesis of different 4-substituted 3-oxo-3,4-dihydroquinoxaline-2-carboxamides (QCA - QCF series)

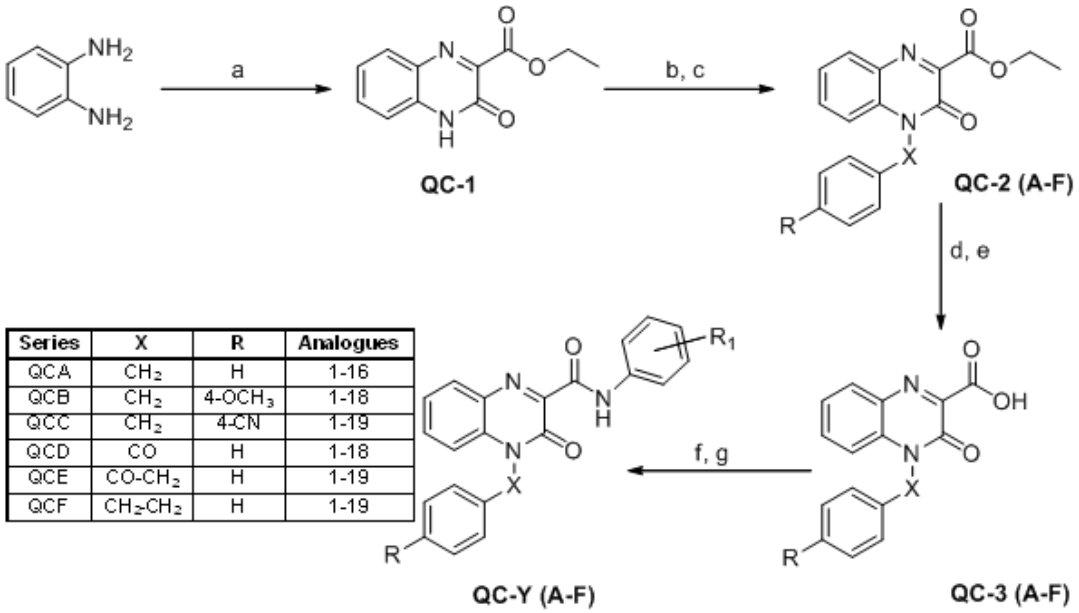

Series	X	R	Analogues
QCA	CH_2	H	1-16
QCB	CH_2	4-OCH_3	1-18
QCC	CH_2	4-CN	1-19
QCD	CO	H	1-18
QCE	CO-CH_2	H	1-19
QCF	CH_2-CH_2	H	1-19

Where, R_1 = H, OCH_3, CH_3, Cl, C_2H_5, $CH_2CH_2CH_3$, $CH(CH_3)_2$, CF_3, etc.

Reagents and conditions: (**a**) Diethyl ketomalonate, EtOH, reflux, 6 hr.; (**b**) K_2CO_3, DMF, rt, 1 hr., then BnBr/4-OMeBnBr/4-CNBnBr/$PhCOCH_2Br$/PhC_2H_5Br, 6hr.; (**c**) only for Benzoyl chloride: TEA, DCM, then C_6H_5COCl, 0 °C–rt, 2hr.; (**d**) 10% aq. NaOH, rt, 2 hr.; or Na_2CO_3, reflux, 6 hr.; (**e**) Conc. HCl, 50%; (**f**) EDC·HCl, HOBt, THF, N_2, 0 °C–rt, 1hr.; (**g**) amines, rt, 6 hr.

4.3.1. Series-1: 4-benzyl-3-oxo-*N*-phenyl-3,4-dihydroquinoxaline-2-carboxamide analogues (QCA-1 to 16)

Ethyl 3-oxo-3,4-dihydroquinoxaline-2-carboxylate (QC-1)

20 g (0.185 mol) of 1,2-phenylenediamine was taken in a 1 L RBF equipped with a mechanical stirrer and a thermocouple. 200 mlof EtOH was added to the reactor and the mixture was stirred for 30 min. To the above reaction mass, 33.90 g (0.195 mol) of diethyl ketomalonate was added in portions over 30 min and the mixture was refluxed for 6 hr. The reaction mixture was cooled and the solvent removed under vacuum; the obtained residue was washed with cold water and recrystallized with EtOH to afford the desired compound.

TLC (EtOAc:Hex 50:50); Yield: 60%; Pale yellow solid; mp: 164-166 °C; IR (KBr, *v* cm^{-1}): 3440 (quinoxaline N-H str.), 3040 (aromatic C-H str.), 1750 (ester C=O str.), 1660 (keto C=O str.), 1570, 1490 (C=C, C=N ring str.), 1465 (CH_2 bend.), 1375 (CH_3 bend.), 1300, 1100 (C=C bend.), 1095, 1044 (ether C-O bend.); ^{1}H NMR (400 MHz, $CDCl_3$) δ 12.95 (s, 1H, NH), 7.93 (m, 1H, quinoxaline), 7.61 (m, 1H, quinoxaline), 7.47 (m, 1H, quinoxaline), 7.39 (m, 1H, quinoxaline), 4.54 (q, 2H, OCH_2CH_3), 1.46 (t, 3H, OCH_2CH_3).

Ethyl 4-benzyl-3-oxo-3,4-dihydroquinoxaline-2-carboxylate (QC-2A)

In a 250 ml RBF, 5 g (0.023 mol) of ethyl 3-oxo-3,4-dihydroquinoxaline-2-carboxylate was dissolved in 75 ml of DMF by stirring at room temperature for 30 min. To the above solution, 9.50 g (0.069 mol) of potassium carbonate was added and the mixture stirred at room temperature for 1hr. 3.92 g (0.023 mol) of benzyl bromide (BnBr) was gradually added in portions and stirring was continued at room temperature overnight. The obtained suspension was poured into 200 ml of cold water and product extracted with ethylacetate (3 × 25 ml). The combined extracts were washed with brine solution and dried over sodium sulfate. Evaporation of solvent gave crude compound and the resultant solid residue was then washed with hexane, filtered, to afford the desired compound. TLC (EtOAc:Hex 25:75); Yield: 65%; Pale yellow solid; mp: 210-212 °C; IR (KBr, *v* cm^{-1}): 3043, 2357, 2339 (aromatic C-H str.), 1732 (ester C=O str.), 1680 (keto C=O str.), 1570, 1490 (C=C, C=N ring str.), 1465 (CH_2 bend.), 1375 (CH_3 bend.), 1300, 1100 (C=C bend.), 1087, 1035 (ether C-O bend.); ^{1}H NMR (400 MHz, $CDCl_3$) δ 7.86 (dd, *J* = 8.0, 1.4 Hz, 1H, quinoxaline), 7.44 (m, *J* = 8.7, 7.3, 1.5 Hz, 1H, quinoxaline), 7.21 (dtd, *J* = 8.6, 7.7, 1.2 Hz, 7H, (2H)-quinoxaline, (5H)-benzyl), 5.42 (s, 2H, benzylic methylene), 4.44 (q, *J* = 7.1 Hz, 2H, OCH_2CH_3), 1.37 (t, *J* = 7.1 Hz, 3H, OCH_2CH_3).

4-benzyl-3-oxo-3,4-dihydroquinoxaline-2-carboxylic acid (QC-3A)

In a 100 ml RBF, 1 g (0.0032 mol) of ethyl 4-benzyl-3-oxo-3,4-dihydroquinoxaline-2-carboxylate was dissolved in 5 ml of dry THF. To the reaction mixture, 50% aqueous sodium hydroxide solution (*pH*>10) was added and stirred at room temperature for 2 hr. The solvent was removed under vacuum; residue washed with ethylacetate and the aqueous portion acidified with dil. HCl (*pH*=5). The obtained solid residue was washed with cold water, filtered and recrystallized with EtOH to afford the desired compound. TLC (EtOAc:Hex 25:75); Yield: 80%; Pale Yellow solid; mp: 223-226°C; IR (KBr, *v*cm^{-1}): 3460 (broad O–H str. COOH), 3043, 2561 (aromatic C-H str.), 1732 (acid C=O str.), 1680 (keto C=O str.), 1537, 1490 (C=C, C=N ring str.), 1273, 1100 (C=C bend.); ^{1}H NMR (400 MHz, $CDCl_3$) δ 14.16 (s, 1H, acid), 8.28 (dd, *J* = 8.1, 1.4 Hz, 1H, quinoxaline), 7.74 (dtd, *J* = 8.6, 7.3, 1.6 Hz, 1H, benzyl), 7.58 – 7.47 (m, 2H, benzyl), 7.39 – 7.32 (m, 3H, (2H)-benzyl, (1H)-quinoxaline), 7.26 (t, *J* = 7.4 Hz, 2H, quinoxaline), 5.64 (s, 2H, benzylic methylene). MS (EI): *m/z* [M^+] for $C_{16}H_{12}N_2O_3$= 281.

General procedure for the synthesis of New Chemical Entity's (NCE's) i.e. quinoxaline-2-carboxamide analogues (QCA-1 to 16)

To 0.5 g (0.0018 mol) of 4-benzyl-3-oxo-3,4-dihydroquinoxaline-2-carboxylic acid taken in a 100 ml RBF, 0.41 g (0.0021 mol) of EDC·HCl was added and stirred with 5 ml of dry THF in an inert atmosphere (nitrogen) at 0 °C for 15 min. To the above reaction mixture, 0.41 g (0.0027 mol) 1-hydroxybenzotriazole (HOBt) was added and stirred for another 45 min. To the above mixture, 1 equivalent of appropriate amines were added and stirred continuously for 6 hr. The reaction mixture was concentrated under reduced pressure; the resultant mass diluted with DCM/ethyl acetate, washed with aqueous sodium bicarbonate (2 × 50 ml), saturated brine solution (2 × 50 ml) and dried over anhydrous sodium sulfate.The solvent was then evaporated under reduced pressure to afford the desired compounds. The obtained compounds were purified by recrystallization with EtOH/MeOH/column chromatography over silica gel.

4-benzyl-3-oxo-*N*-phenyl-3,4-dihydroquinoxaline-2-carboxamide (QCA-1)

TLC (EtOAc:Hexane 30:70); Yield: 74%; White solid; mp: 156-158°C; IR (KBr, *v* cm^{-1}): 3250 (sharp, N–H str.), 3126, 3068 (aromatic C-H str.), 1693 (keto C=O str.), 1680 (amide C=O str.), 1591, 1556 (C=C, C=N ring str.), 1465 (CH_2 bend.), 1325, 1165 (C=C bend.); ^{1}H NMR (400 MHz, $CDCl_3$) δ 11.83 (s, 1H, amide), 8.18 (dd, *J* = 8.1, 1.3 Hz, 1H, quinoxaline), 7.77 (d, *J* = 7.7 Hz, 2H, phenyl), 7.59 – 7.51 (m, 1H, phenyl), 7.43 – 7.36 (m, 1H, phenyl), 7.31 (dd, *J* = 14.2, 5.9 Hz, 5H, benzyl),7.27 – 7.22 (m, 2H, (1H)-quinoxaline, (1H)-phenyl), 7.19 (s, 1H, quinoxaline), 7.09 (t, *J* = 7.4 Hz, 1H, quinoxaline), 5.56 (s, 2H, benzylic methylene). MS (EI): *m/z* [M^+] for $C_{22}H_{17}N_3O_2$= 356.

4-benzyl-*N*-(4-methoxyphenyl)-3-oxo-3,4-dihydroquinoxaline-2-carboxamide (QCA-2)

TLC (EtOAc:Hexane 25:75); Yield: 78%; White solid; mp: 128-130 °C; IR (KBr, *v* cm^{-1}): 3250 (sharp, N–H str.), 3128, 3074 (aromatic C-H str.), 1693 (keto C=O str.), 1680 (amide C=O str.), 1587, 1537 (C=C, C=N ring str.), 1462 (CH_2 bend.), 1323, 1166 (C=C bend.), 1037 (ether C-O bend.); ^{1}H NMR (400 MHz, $CDCl_3$) δ 11.83 (s, 1H, amide), 7.90 (dd, *J* = 8.0, 1.4 Hz, 1H, quinoxaline), 7.51 – 7.45 (m, 6H, (4H)-phenyl, (2H)-benzyl), 7.32 – 7.18 (m, 6H, (3H)-benzyl, (3H)-quinoxaline), 5.45 (s, 2H, benzylic methylene), 3.99 (s, 3H, OCH_3). MS (EI): *m/z* [M^+] for $C_{23}H_{19}N_3O_3$= 386.

4-benzyl-*N*-(2-ethylphenyl)-3-oxo-3,4-dihydroquinoxaline-2-carboxamide (QCA-3)

TLC (EtOAc:Hexane 25:75); Yield: 82%; White solid; mp: 203-206 °C; IR (KBr, *v* cm^{-1}): 3300 (sharp, N–H str.), 3086, 3030 (aromatic C-H str.), 1737 (keto C=O str.), 1651

(amide C=O str.), 1587, 1537 (C=C, C=N ring str.), 1469 (CH_2 bend.), 1346 (CH_3 bend.), 1257, 1095 (C=C bend.); ^{1}H NMR (400 MHz, $CDCl_3$) δ 11.82 (s, 1H, amide), 8.18 (dd, *J* = 8.1, 1.3 Hz, 1H, quinoxaline), 7.56 – 7.49 (m, 1H, phenyl), 7.40 – 7.33 (m, 3H, benzyl), 7.27 (t, *J* = 8.1 Hz, 1H, phenyl), 7.24 – 7.20 (m, 2H, phenyl), 7.17 (d, *J* = 7.6 Hz, 4H, (2H)-benzyl, (2H)-quinoxaline), 7.06 (s, 1H, quinoxaline), 5.57 (s, 2H, benzylic methylene), 2.74 (q, *J* = 7.5 Hz, 2H, CH_2CH_3), 1.24 (t, *J* = 7.5 Hz, 3H, CH_2CH_3). MS (EI): *m/z* [M^+] for $C_{24}H_{21}N_3O_2$= 384.

4-benzyl-*N*-(2-chloro-4-methylphenyl)-3-oxo-3,4-dihydroquinoxaline-2-carboxamide (QCA-4)

TLC (EtOAc:Hexane 25:75); Yield: 84%; White solid; mp: 208-210 °C; IR (KBr, *v* cm^{-1}): 3473 (sharp, N–H str.), 3290, 2956 (aromatic C-H str.), 1745 (keto C=O str.), 1600 (amide C=O str.), 1587, 1504 (C=C, C=N ring str.), 1392 (CH_2 bend.), 1257, 1170 (C=C bend.); ^{1}H NMR (400 MHz, $CDCl_3$) δ 12.14 (s, 1H, amide), 8.53 (d, *J* = 8.4 Hz, 1H, quinoxaline), 8.18 (dd, *J* = 8.1, 1.4 Hz, 1H, phenyl), 7.54 (ddd, *J* = 8.6, 7.3, 1.5 Hz, 1H, phenyl), 7.43 – 7.34 (m, 1H, phenyl), 7.32 – 7.27 (m, 3H, benzyl), 7.23 (d, *J* = 7.1 Hz, 2H, benzyl), 7.19 (d, *J* = 1.6 Hz, 3H, quinoxaline), 5.59 (s, 2H, benzylic methylene), 2.27 (s, 3H, CH_3).

4-benzyl-*N*-(2-chloro-5-methylphenyl)-3-oxo-3,4-dihydroquinoxaline-2-carboxamide (QCA-5)

TLC (EtOAc:Hexane 25:75); Yield: 75%; White solid; mp: 186-188 °C; IR (KBr, *v* cm^{-1}): 3300 (sharp, N–H str.), 3086, 2954, 2511 (aromatic C-H str.), 1741 (keto C=O str.), 1651 (amide C=O str.), 1556, 1537 (C=C, C=N ring str.), 1346 (CH_2 bend.), 1259, 1095 (C=C bend.); ^{1}H NMR (400 MHz, $CDCl_3$) δ 12.10 (s, 1H, amide), 8.50 (s, 1H, quinoxaline), 8.17 (dd, *J* = 8.1, 1.2 Hz, 1H, phenyl), 7.57 – 7.51 (m, 1H, phenyl), 7.38 (t, *J* = 7.3 Hz, 1H, phenyl), 7.31 – 7.16 (m, 7H, (5H)-benzyl, (2H)-quinoxaline), 6.84 (dd, *J* = 8.1, 1.4 Hz, 1H, quinoxaline), 5.59 (s, 2H, benzylic methylene), 2.31 (s, 3H, CH_3).

4-benzyl-*N*-(3-chloro-2-methylphenyl)-3-oxo-3,4-dihydroquinoxaline-2-carboxamide (QCA-6)

TLC (EtOAc:Hexane 25:75); Yield: 77%; White solid; mp: 220-222 °C; IR (KBr, *v* cm^{-1}): 3321 (sharp, N–H str.), 3010, 2308 (aromatic C-H str.), 1685 (keto C=O str.), 1680 (amide C=O str.), 1593, 1515 (C=C, C=N ring str.), 1435 (CH_2 bend.), 1253, 1028 (C=C bend.); ^{1}H NMR (400 MHz, $CDCl_3$) δ 11.87 (s, 1H, amide), 8.19 (dd, *J* = 8.1, 1.2 Hz, 1H, quinoxaline), 7.58 – 7.53 (m, 1H, phenyl), 7.42 – 7.37 (m, 1H, benzyl), 7.28 (dt, *J* = 13.0, 7.7 Hz, 4H, benzyl), 7.20 – 7.12 (m, 5H, (2H)-phenyl, (3H)-quinoxaline), 5.58 (s, 2H, benzylic methylene), 2.44 (s, 3H, CH_3).

4-benzyl-*N*-(4-chloro-2-methylphenyl)-3-oxo-3,4-dihydroquinoxaline-2-carboxamide (QCA-7)

TLC (EtOAc:Hexane 25:75); Yield: 71%; White solid; mp: 212-214 °C; IR (KBr, *v* cm^{-1}): 3344 (sharp, N–H str.), 3062, 2974, 2781 (aromatic C-H str.), 1760 (keto C=O str.), 1703 (amide C=O str.), 1591, 1556 (C=C, C=N ring str.), 1402 (CH_2 bend.), 1290, 1035 (C=C bend.); ^{1}H NMR (400 MHz, $CDCl_3$) δ 11.85 (s, 1H, amide), 8.19 (dd, *J* = 8.1, 1.1 Hz, 1H, quinoxaline), 7.58 – 7.51 (m, 1H, phenyl), 7.39 (t, *J* = 7.3 Hz, 1H, phenyl), 7.32 – 7.24 (m, 4H, benzyl), 7.16 (dd, *J* = 15.1, 7.7 Hz, 5H, (1H)-phenyl, (1H)-benzyl, (3H)-quinoxaline), 5.57 (s, 2H, benzylic methylene), 2.36 (s, 3H, CH_3).

4-benzyl-3-oxo-*N*-(2-propylphenyl)-3,4-dihydroquinoxaline-2-carboxamide (QCA-8)

TLC (EtOAc:Hexane 25:75); Yield: 68%; White solid; mp: 210-212°C; IR (KBr, *v* cm^{-1}): 3203 (sharp, N–H str.), 3032, 2970 (aromatic C-H str.), 1691 (keto C=O str.), 1694 (amide C=O str.), 1587, 1524 (C=C, C=N ring str.), 1371 (CH_3, CH_2 bend.), 1165, 1074 (C=C bend.); ^{1}H NMR (400 MHz, $CDCl_3$) δ 11.86 (s, 1H, amide), 8.19 (dd, *J* = 8.1, 1.4 Hz, 1H, quinoxaline), 7.54 (ddd, *J* = 8.6, 7.3, 1.5 Hz, 1H, phenyl), 7.42 – 7.36 (m, 1H, phenyl), 7.34 – 7.19 (m, 8H, (5H)-benzyl, (2H)-phenyl, (1H)-quinoxaline), 7.15 (dd, *J* = 7.6, 1.4 Hz, 1H, quinoxaline), 7.05 (td, *J* = 7.5, 1.2 Hz, 1H, quinoxaline), 5.57 (s, 2H, benzylic methylene), 2.75 – 2.66 (m, 2H, $CH_2CH_2CH_3$), 1.65 – 1.59 (m, 2H, $CH_2CH_2CH_3$), 0.94 (t, *J* = 7.3 Hz, 3H, $CH_2CH_2CH_3$).

4-benzyl-*N*-(3-chlorophenyl)-3-oxo-3,4-dihydroquinoxaline-2-carboxamide (QCA-9)

TLC (EtOAc:Hexane 25:75); Yield: 73%; White solid; mp: 210-212°C; IR (KBr, *v* cm^{-1}): 3323 (sharp, N–H str.), 3140, 2954 (aromatic C-H str.), 1639 (keto C=O str.), 1585 (amide C=O str.), 1485, 1454 (C=C, C=N ring str.), 1321 (CH_2 bend.), 1166, 1099 (C=C bend.); ^{1}H NMR (400 MHz, $CDCl_3$) δ 12.22 (s, 1H, amide), 8.18 (d, *J* = 7.9 Hz, 1H, quinoxaline), 7.55 (t, *J* = 7.6 Hz, 1H, phenyl), 7.39 (d, *J* = 3.4 Hz, 1H, phenyl), 7.32 – 7.18 (m, 10H, (2H)-phenyl, (5H)-benzyl, (3H)-quinoxaline), 5.60 (s, 2H, benzylic methylene).

4-benzyl-*N*-morpholino-3-oxo-3,4-dihydroquinoxaline-2-carboxamide (QCA-10)

TLC (EtOAc:Hexane 25:75); Yield: 74%; White solid; mp: 165-168 °C; IR (KBr, *v* cm^{-1}): 3361 (sharp, N–H str.), 3026, 2960 (aromatic C-H str.), 1693 (keto C=O str.), 1633 (amide C=O str.), 1591, 1512 (C=C, C=N ring str.), 1417 (CH_2 bend.), 1282, 1166 (C=C bend.); ^{1}H NMR (400 MHz, $CDCl_3$) δ 10.51 (s, 1H, amide), 8.17 (dd, *J* = 8.1, 1.4 Hz, 1H, quinoxaline), 7.40 – 7.35 (m, 1H, benzyl), 7.29 – 7.23 (m, 5H, (4H)-benzyl, (1H)-quinoxaline), 7.14 (d, *J* = 6.8 Hz, 2H, quinoxaline), 5.51 (s, 2H, benzylic methylene), 3.87 – 3.79 (m, 2H, morpholine), 3.03 – 2.98 (m, 2H, morpholine).

4-benzyl-*N*-(2-isopropylphenyl)-3-oxo-3,4-dihydroquinoxaline-2-carboxamide (QCA-11)

TLC (EtOAc:Hexane 25:75); Yield: 77%; White solid; mp: 160-162°C; IR (KBr, *v* cm^{-1}): 3000 (sharp, N–H str.), 2949, 2360, 1975 (aromatic C-H str.), 1745 (keto C=O str.), 1697 (amide C=O str.), 1539, 1455 (C=C, C=N ring str.), 1350 (CH_2 bend.), 1197, 1056 (C=C bend.); ^{1}H NMR (400 MHz, $CDCl_3$) δ 10.71 (s, 1H, amide), 6.47 – 6.43 (m, 1H, quinoxaline), 6.32 – 6.27 (m, 1H, phenyl), 6.22 – 6.17 (m, 4H, benzyl), 6.17 – 6.08 (m, 6H, (1H)-benzyl, (3H)-phenyl, (2H)-quinoxaline), 6.04 (td, *J* = 7.5, 1.3 Hz, 1H, quinoxaline), 4.50 (s, 2H, benzylic methylene), 1.11 (d, *J* = 6.8 Hz, 1H, $CH(CH_3)_2$), 0.17 (d, *J* = 6.8 Hz, 6H, $CH(CH_3)_2$).

4-benzyl-*N*-(4-isopropylphenyl)-3-oxo-3,4-dihydroquinoxaline-2-carboxamide (QCA-12)

TLC (EtOAc:Hexane 25:75); Yield: 85%; White solid; mp: 137-140°C; IR (KBr, *v* cm^{-1}): 3242 (sharp, N–H str.), 2924, 2840 (aromatic C-H str.), 1741 (keto C=O str.), 1651 (amide C=O str.), 1556, 1469 (C=C, C=N ring str.), 1348 (CH_2 bend.), 1259, 1163 (C=C bend.); ^{1}H NMR (400 MHz, $CDCl_3$) δ 11.77 (s, 1H, amide), 8.18 (dd, *J* = 8.1, 1.2 Hz, 1H, quinoxaline), 7.68 (d, *J* = 8.5 Hz, 2H, phenyl), 7.58 – 7.49 (m, 1H, benzyl), 7.38 (t, *J* = 7.7 Hz, 1H, benzyl), 7.29 (dd, *J* = 12.5, 5.7 Hz, 3H, (2H)-benzyl, (1H)-quinoxaline), 7.18 (d, *J* = 8.9 Hz, 5H, (2H)-phenyl, (1H)-benzyl, (2H)-quinoxaline), 5.55 (s, 2H, benzylic methylene), 2.84 (dt, *J* = 13.8, 6.9 Hz, 1H, $CH(CH_3)_2$), 1.19 (d, *J* = 6.9 Hz, 6H, $CH(CH_3)_2$).

4-benzyl-3-oxo-*N*-(2-(trifluoromethyl)phenyl)-3,4-dihydroquinoxaline-2-carboxamide (QCA-13)

TLC (EtOAc:Hexane 25:75); Yield: 65%; White solid; mp: 168-170°C; IR (KBr, *v* cm^{-1}): 3252 (sharp, N–H str.), 3080, 3030 (aromatic C-H str.), 1690 (keto C=O str.), 1633 (amide C=O str.), 1593, 1531 (C=C, C=N ring str.), 1454 (CH_2 bend.), 1338, 1165 (C=C bend.); ^{1}H NMR (400 MHz, $CDCl_3$) δ 12.07 (s, 1H, amide), 8.49 (d, *J* = 8.3 Hz, 1H, quinoxaline), 8.16 (dd, *J* = 8.1, 1.4 Hz, 1H, phenyl), 7.61 (d, *J* = 7.9 Hz, 1H, phenyl), 7.55 (ddd, *J* = 8.7, 7.3, 1.6 Hz, 2H, phenyl), 7.41 – 7.35 (m, 1H, benzyl), 7.32 – 7.25 (m, 4H, benzyl), 7.24 – 7.21 (m, 2H, quinoxaline), 7.19 (d, *J* = 2.9 Hz, 1H, quinoxaline), 5.58 (s, 2H, benzylic methylene).

4-benzyl-*N*-(2-methoxyphenyl)-3-oxo-3,4-dihydroquinoxaline-2-carboxamide (QCA-14)

TLC (EtOAc:Hexane 25:75); Yield: 64%; White solid; mp: 224-226°C; IR (KBr, *v* cm^{-1}): 3182 (sharp, N–H str.), 3059, 2916 (aromatic C-H str.), 1703 (keto C=O str.), 1643 (amide C=O str.), 1573, 1462 (C=C, C=N ring str.), 1415 (CH_2 bend.), 1172, 1149 (C=C bend.), 1028 (ether C-O bend.); ^{1}H NMR (400 MHz, $CDCl_3$) δ 11.93 (s, 1H, amide), 8.53 (d, *J* = 8.0 Hz, 1H, quinoxaline), 8.06 (dd, *J* = 8.3, 1.2 Hz, 1H, phenyl), 7.59 (dd, *J* = 11.5, 4.2 Hz, 1H, benzyl), 7.41 (dd, *J* = 8.0, 5.2 Hz, 2H, benzyl), 7.25 (dd, *J* = 13.7, 7.0 Hz, 5H, (2H)-benzyl, (3H)-phenyl), 7.06 (dd, *J* = 11.7, 4.0 Hz, 1H, quinoxaline), 6.96 – 6.90 (m, 2H, quinoxaline), 5.61 (s, 2H, benzylic methylene), 3.90 (s, 3H, OCH_3).

4-benzyl-*N*-(3-methoxyphenyl)-3-oxo-3,4-dihydroquinoxaline-2-carboxamide (QCA-15)

TLC (EtOAc:Hexane 25:75); Yield: 60%; White solid; mp: 162-164°C; IR (KBr, *v* cm^{-1}): 3190 (sharp, N–H str.), 3039, 2875 (aromatic C-H str.), 1681 (keto C=O str.), 1633 (amide C=O str.), 1598, 1525 (C=C, C=N ring str.), 1421 (CH_2 bend.), 1321, 1170 (C=C bend.), 1035 (ether C-O bend.); ^{1}H NMR (400 MHz, $CDCl_3$) δ 11.82 (s, 1H, amide), 8.17 (d, *J* = 7.8 Hz, 1H, quinoxaline), 7.60 (s, 1H, phenyl), 7.55 (t, *J* = 7.5 Hz, 1H, phenyl), 7.39 (t, *J* = 7.6 Hz, 1H, phenyl), 7.27 (td, *J* = 14.0, 7.6 Hz, 6H, (5H)-benzyl, (1H)-quinoxaline), 7.16 (s, 2H, quinoxaline), 6.65 (dd, *J* = 7.5, 3.9 Hz, 1H, phenyl), 5.55 (s, 2H, benzylic methylene), 3.77 (s, 3H, OCH_3).

4-benzyl-*N*-(2-chloro-6-methylphenyl)-3-oxo-3,4-dihydroquinoxaline-2-carboxamide (QCA-16)

TLC (EtOAc:Hexane 25:75); Yield: 64%; White solid; mp: 190-192°C; IR (KBr, *v* cm^{-1}): 3300 (sharp, N–H str.), 3086, 2954, 2511 (aromatic C-H str.), 1741 (keto C=O str.), 1651 (amide C=O str.), 1556, 1537 (C=C, C=N ring str.), 1346 (CH_2 bend.), 1259, 1095 (C=C bend.); ^{1}H NMR (400 MHz, $CDCl_3$) δ 11.78 (s, 1H, amide), 8.18 (dd, *J* = 8.1, 1.4 Hz, 1H, quinoxaline), 7.65 (d, *J* = 8.0 Hz, 1H, phenyl), 7.60 – 7.51 (m, 2H, benzyl), 7.43 – 7.37 (m, 1H, benzyl), 7.29 (ddd, *J* = 14.9, 9.7, 6.0 Hz, 4H, (2H)-benzyl, (1H)-phenyl, (1H)-quinoxaline), 7.22 – 7.16 (m, 3H, (2H)-quinoxaline, (1H)-phenyl), 5.56 (s, 2H, benzylic methylene), 2.61 (q, *J* = 7.6 Hz, 3H, CH_3).

4.3.2. Series-2: 4-(4-methoxybenzyl)-3-oxo-*N*-phenyl-3,4-dihydroquinoxaline-2-carboxamide analogues (QCB-1 to 18)

Ethyl 4-(4-methoxybenzyl)-3-oxo-3,4-dihydroquinoxaline-2-carboxylate (QC-2B)

5 g (0.023 mol) of ethyl 3-oxo-3,4-dihydroquinoxaline-2-carboxylate was dissolved in 75 ml of DMF in a 250 ml RBF and stirred at room temperature for 30 min. To the above solution, 9.50 g (0.069 mol) of potassium carbonate was added and the mixture stirred at room temperature for 1 hr. 3.59 g (0.023 mol) of 4-methoxybenzyl bromide was gradually added in portions and stirring was continued at room temperature overnight. The obtained suspension was poured into 200 ml of cold water and product extracted with ethylacetate (3 × 25 ml). The combined extracts were washed with brine solution and dried over sodium sulfate. Evaporation of solvent gave crude compound and the resultant solid residue was then washed with hexane, filtered, to afford the desired compound. TLC (EtOAc:Hexane 25:75); Yield: 57%; liquid, hygroscopic; IR (KBr, *v* cm^{-1}): 3020, 2754, 2557, 2364 (aromatic C-H str.), 1720 (ester C=O), 1698 (keto C=O str.), 1560, 1480 (C=C, C=N ring str.), 1565 (CH_2 bend.), 1495, 1384, 1178 (C=C bend.); 1097, 1030 (ether C-O bend.); ^{1}H NMR (400 MHz, $CDCl_3$) δ 8.27 (dd, *J* = 8.5, 1.4 Hz, 1H, quinoxaline), 7.78 – 7.72 (m, 2H, benzyl), 7.52 (dd, *J* = 7.8, 6.6 Hz, 1H, quinoxaline), 7.28 – 7.20 (m, 2H, quinoxaline), 6.92 – 6.84 (m, 2H, benzyl), 5.52 (s, 2H, benzylic methylene), 4.40 (q, *J* = 7.1 Hz, 2H, OCH_2CH_3), 3.78 (s, 3H, OCH_3), 1.35 (t, *J* = 7.1 Hz, 3H, OCH_2CH_3).

4-(4-methoxybenzyl)-3-oxo-3,4-dihydroquinoxaline-2-carboxylic acid (QC-3B)

1 g (0.0030 mol) of ethyl 4-(4-methoxybenzyl)-3-oxo-3,4-dihydroquinoxaline-2-carboxylate was dissolved in 5 ml of dry THF in a 100 ml RBF. To this mixture, 50% aqueous sodium hydroxide solution (*pH*>10) was added and stirred at room temperature for 2 hr. The solvent was removed under vacuum; residue washed with ethylacetate and the aqueous portion acidified with dil. HCl (*pH* = 5). The obtained solid residue was washed with cold water, filtered and recrystallized with ethanol to afford the desired compound. TLC (EtOAc:Hexane 20:80); Yield: 75%; Pale Yellow solid; mp: 204-206 °C; IR (KBr, *v* cm^{-1}): 3390 (broad O–H str. COOH), 3186, 3052, 2974, 2885, 2830, 2620 (aromatic C-H str.), 1766 (acid C=O str.), 1693 (keto C=O str.), 1587, 1537 (C=C, C=N ring str.), 1462 (CH_2 bend.), 1323, 1166 (C=C bend.), 1097, 1035 (ether C-O bend.); ^{1}H NMR (400 MHz, $CDCl_3$) δ 14.24 (s, 1H, acid), 8.27 (dd, *J* = 8.5, 1.4 Hz, 1H, quinoxaline), 7.79 – 7.72 (m, 1H, quinoxaline), 7.55 (dd, *J* = 7.8, 6.6 Hz, 2H, benzyl), 7.28 – 7.20 (m, 2H, quinoxaline), 6.92 – 6.84 (m, 2H, benzyl), 5.58 (s, 2H, benzylic methylene), 3.78 (s, 3H, OCH_3).

General procedure for the synthesis of New Chemical Entity's (NCE's) i.e. quinoxaline-2-carboxamide analogues (QCB-1 to 18)

To 0.5 g (0.0016 mol) of 4-(4-methoxybenzyl)-3-oxo-3,4-dihydroquinoxaline-2-carboxylic acid taken in a 100 ml RBF, 0.37 g (0.0019 mol) of EDC·HCl was added and stirred with 5 ml of dry THF in an inert atmosphere (nitrogen) at 0 °C for 15 min. To the above reaction mixture, 0.37 g (0.0024 mol) HOBt was added and stirred for another 45 min. To the above mixture, 1 equivalent of appropriate amines were added and stirred continuously for 6 hr. The reaction mixture was concentrated under reduced pressure; the resultant mass diluted with DCM/ethyl acetate, washed with aqueous sodium bicarbonate (2 × 50 ml), saturated brine solution (2 × 50 ml) and dried over anhydrous sodium sulfate. The solvent was then evaporated under reduced pressure to afford the desired compounds. The obtained compounds were purified by recrystallization with EtOH/MeOH/column chromatography over silica gel.

4-(4-methoxybenzyl)-3-oxo-*N*-phenyl-3,4-dihydroquinoxaline-2-carboxamide (QCB-1)

TLC (EtOAc:Hexane 30:70); Yield: 64%; White solid; mp: 188-190 °C; IR (KBr, *v* cm^{-1}): 3261 (sharp, N–H str.), 3197, 3136, 3041, 2972, 2839 (aromatic C-H str.), 1689 (keto C=O str.), 1678 (amide C=O str.), 1653, 1591 (C=C, C=N ring str.), 1444 (CH_2 bend.), 1338, 1251, 1178, 1163 (C=C bend.), 1097, 1028 (ether C-O bend.); ^{1}H NMR (400 MHz, $CDCl_3$) δ 11.95 (s, 1H, amide), 8.26 (d, *J* = 7.7 Hz, 1H, quinoxaline), 7.85 (d, *J* = 7.7 Hz, 2H, phenyl), 7.65 (t, *J* = 7.7 Hz, 2H, phenyl), 7.42 (dt, *J* = 15.7, 7.6 Hz, 3H, (2H)-benzyl, (1H)-phenyl), 7.22 (d, *J* = 8.6 Hz, 2H, benzyl), 7.17 (t, *J* = 7.4 Hz, 1H, quinoxaline), 6.88 (d, *J* = 8.7 Hz, 2H, quinoxaline), 5.57 (s, 2H, benzylic methylene), 3.78 (s, 3H, OCH_3).

4-(4-methoxybenzyl)-*N*-(2-methoxyphenyl)-3-oxo-3,4-dihydroquinoxaline-2-carboxamide (QCB-2)

TLC (EtOAc:Hexane 30:70); Yield: 48%; White solid; mp: 152-154°C; IR (KBr, *v* cm^{-1}): 3001 (sharp, N–H str.), 2962, 2885, 2829, 2623, 2557 (aromatic C-H str.), 1746 (keto C=O str.), 1697 (amide C=O str.), 1573, 1514 (C=C, C=N ring str.), 1454 (CH_2 bend.), 1301, 1274, 1180, 1163 (C=C bend.), 1099, 1035 (ether C-O bend.); ^{1}H NMR (400 MHz, $CDCl_3$) δ 11.90 (s, 1H, amide), 8.26 (d, *J* = 7.7 Hz, 1H, quinoxaline), 7.85 (d, *J* = 7.7 Hz, 1H, phenyl), 7.65 (t, *J* = 7.7 Hz, 1H, benzyl), 7.42 (dt, *J* = 15.7, 7.6 Hz, 4H, (1H)-benzyl, (3H)-quinoxaline), 7.22 (d, *J* = 8.6 Hz, 2H, phenyl), 7.17 (t, *J* = 7.4 Hz, 1H, phenyl), 6.88 (d, *J* = 8.7 Hz, 2H, benzyl), 5.57 (s, 2H, benzylic methylene), 3.78 (s, 6H, OCH_3).

4-(4-methoxybenzyl)-*N*-(3-methoxyphenyl)-3-oxo-3,4-dihydroquinoxaline-2-carboxamide (QCB-3)

TLC (EtOAc:Hexane 30:70); Yield: 52%; White solid; mp: 154-156°C; IR (KBr, *v* cm^{-1}): 3001 (sharp, N–H str.), 2962, 2885, 2829, 2621, 2559 (aromatic C-H str.), 1745 (keto C=O str.), 1687 (amide C=O str.), 1573, 1514 (C=C, C=N ring str.), 1454 (CH_2 bend.), 1301, 1274, 1180, 1163, 1147 (C=C bend.), 1099, 1037 (ether C-O bend.); ^{1}H NMR (400 MHz, $CDCl_3$) δ 11.60 (s, 1H, amide), 8.25 (dd, *J* = 8.1, 1.2 Hz, 1H, quinoxaline), 7.82 – 7.68 (m, 1H, phenyl), 7.61 – 7.49 (m, 3H, (2H)-benzyl, (1H)-phenyl), 7.43 – 7.31 (m, 1H, phenyl), 7.32 – 7.15 (m, 3H, quinoxaline), 6.96 – 6.75 (m, 3H, (2H)-benzyl, (1H)-phenyl), 5.57 (s, 2H, benzylic methylene), 3.78 (s, 6H, OCH_3).

4-(4-methoxybenzyl)-*N*-(4-methoxyphenyl)-3-oxo-3,4-dihydroquinoxaline-2-carboxamide (QCB-4)

TLC (EtOAc:Hexane 30:70); Yield: 63%; White solid; mp: 168-170°C; IR (KBr, *v* cm^{-1}): 3388 (sharp, N–H str.), 3126, 3070, 3000, 2925, 2657 (aromatic C-H str.), 1689 (keto C=O str.), 1679 (amide C=O str.), 1552, 1510 (C=C, C=N ring str.), 1454 (CH_2 bend.), 1301, 1255, 1244, (C=C bend.), 1097, 1035 (ether C-O bend.); ^{1}H NMR (400 MHz, $CDCl_3$) δ 11.87 (s, 1H, amide), 8.23 (dd, *J* = 8.1, 1.3 Hz, 1H, quinoxaline), 7.82 – 7.73 (m, 2H, phenyl), 7.68 – 7.59 (m, 1H, benzyl), 7.45 (dd, *J* = 13.2, 7.8 Hz, 2H, (1H)-benzyl, (1H)-quinoxaline), 7.21 (d, *J* = 8.7 Hz, 2H, quinoxaline), 6.94 – 6.86 (m, 4H, (2H)-phenyl, (2H)-benzyl), 5.56 (s, 2H, benzylic methylene), 3.77 (s, 6H, OCH_3).

***N*-(2-ethylphenyl)-4-(4-methoxybenzyl)-3-oxo-3,4-dihydroquinoxaline-2-carboxamide (QCB-5)**

TLC (EtOAc:Hexane 30:70); Yield: 59%; White solid; mp: 148-150°C; IR (KBr, *v* cm^{-1}): 3061 (sharp, N–H str.), 3041, 2960, 2830 (aromatic C-H str.), 1693 (keto C=O str.), 1681 (amide C=O str.), 1573, 1546, 1512 (C=C, C=N ring str.), 1485, 1444 (CH_2 bend.), 1327, 1247, 1178, 1163 (C=C bend.), 1099, 1035 (ether C-O bend.); ^{1}H NMR (400 MHz, $CDCl_3$) δ 11.93 (s, 1H, amide), 8.26 (d, *J* = 7.2 Hz, 1H, quinoxaline), 7.63 (t, *J* = 7.8 Hz, 1H, phenyl), 7.45 (dd, *J* = 15.5, 7.9 Hz, 2H, phenyl), 7.32 – 7.19 (m, 5H, (2H)-benzyl, (3H)-quinoxaline), 7.15 (t, *J* = 7.0 Hz, 1H, phenyl), 6.87 (d, *J* = 8.7 Hz, 2H, benzyl), 5.59 (s, 2H, benzylic methylene), 3.78 (s, 3H, OCH_3), 2.84 (q, *J* = 7.5 Hz, 2H, CH_2CH_3), 1.33 (t, *J* = 7.5 Hz, 3H, CH_2CH_3).

_N_-(3-ethylphenyl)-4-(4-methoxybenzyl)-3-oxo-3,4-dihydroquinoxaline-2-carboxamide (QCB-6)

TLC (EtOAc:Hexane 30:70); Yield: 61%; White solid; mp: 140-142°C; IR (KBr, *v* cm^{-1}): 3076 (sharp, N–H str.), 3041, 2960, 2908, 2839 (aromatic C-H str.), 1693 (keto C=O str.), 1681 (amide C=O str.), 1650, 1612, 1556, 1514 (C=C, C=N ring str.), 1444 (CH_2 bend.), 1301, 1246, 1178, 1163, 1120 (C=C bend.), 1097, 1031 (ether C-O bend.); ^{1}H NMR (400 MHz, $CDCl_3$) δ 11.90 (s, 1H, amide), 8.25 – 8.19 (m, 1H, quinoxaline), 7.72 (d, *J* = 8.1 Hz, 1H, phenyl), 7.67 – 7.61 (m, 2H, phenyl), 7.49 – 7.41 (m, 2H, benzyl), 7.33 – 7.22 (m, 3H, quinoxaline), 7.02 (d, *J* = 7.7 Hz, 1H, phenyl), 6.90 – 6.85 (m, 2H, benzyl), 5.56 (s, 2H, benzylic methylene), 3.77 (s, 3H, OCH_3), 2.68 (d, *J* = 7.6 Hz, 2H, CH_2CH_3), 1.27 (t, *J* = 7.6 Hz, 3H, CH_2CH_3).

_N_-(3-chloro-2-methylphenyl)-4-(4-methoxybenzyl)-3-oxo-3,4-dihydroquinoxaline-2-carboxamide (QCB-7)

TLC (EtOAc:Hexane 30:70); Yield: 35%; White solid; mp: 162-164°C; IR (KBr, *v* cm^{-1}): 3063 (sharp, N–H str.), 2984, 2885, 2829, 2624, 2557 (aromatic C-H str.), 1693 (keto C=O str.), 1681 (amide C=O str.), 1573, 1514 (C=C, C=N ring str.), 1454 (CH_2 bend.), 1301, 1274, 1180, 1163 (C=C bend.), 1099, 1035 (ether C-O bend.); ^{1}H NMR (400 MHz, $CDCl_3$) δ 11.76 (s, 1H, amide), 8.13 (d, *J* = 7.0 Hz, 1H, quinoxaline), 7.44 – 7.29 (m, 3H, (1H)-phenyl, (2H)-benzyl), 7.22 (d, *J* = 8.8 Hz, 2H, phenyl), 7.18 (d, *J* = 8.5 Hz, 1H, quinoxaline), 6.97 (d, *J* = 8.8 Hz, 2H, benzyl), 5.57 (s, 2H, benzylic methylene), 3.75 (s, 3H, OCH_3), 2.37 (s, 3H, CH_3).

4-(4-methoxybenzyl)-3-oxo-_N_-(2-propylphenyl)-3,4-dihydroquinoxaline-2-carboxamide (QCB-8)

TLC (EtOAc:Hexane 30:70); Yield: 69%; White solid; mp: 120-122°C; IR (KBr, *v* cm^{-1}): 3061 (sharp, N–H str.), 3041, 2956, 2885, 2620, 2358 (aromatic C-H str.), 1693 (keto C=O str.), 1681 (amide C=O str.), 1573, 1514 (C=C, C=N ring str.), 1454 (CH_2 bend.), 1309, 1274, 1180, 1163 (C=C bend.), 1097, 1031 (ether C-O bend.); ^{1}H NMR (400 MHz, $CDCl_3$) δ 11.75 (s, 1H, amide), 8.15 (dd, *J* = 8.1, 1.4 Hz, 1H, quinoxaline), 7.54 (ddd, *J* = 8.6, 7.3, 1.5 Hz, 1H, phenyl), 7.42 – 7.36 (m, 2H, phenyl), 7.29 – 7.19 (m, 2H, benzyl), 7.15 (dd, *J* = 7.6, 1.4 Hz, 2H, (1H)-quinoxaline, (1H)-phenyl), 7.05 (td, *J* = 7.5, 1.2 Hz, 2H, quinoxaline), 6.90 – 6.85 (m, 2H, benzyl), 5.56 (s, 2H, benzylic methylene), 3.77 (s, 3H, OCH_3), 2.75 – 2.66 (m, 2H, $CH_2CH_2CH_3$), 1.65 – 1.59 (m, 2H, $CH_2CH_2CH_3$), 0.94 (t, *J* = 7.3 Hz, 3H, $CH_2CH_2CH_3$).

_N_-(2-isopropylphenyl)-4-(4-methoxybenzyl)-3-oxo-3,4-dihydroquinoxaline-2-carboxamide (QCB-9)

TLC (EtOAc:Hexane 30:70); Yield: 72%; White solid; mp: 160-162°C; IR (KBr, *v* cm^{-1}): 3061 (sharp, N–H str.), 3045, 2999, 2962, 2820 (aromatic C-H str.), 1693 (keto C=O str.), 1681 (amide C=O str.), 1573, 1531, 1514 (C=C, C=N ring str.), 1454 (CH_2 bend.), 1309, 1282, 1247, 1180, 1165 (C=C bend.), 1101, 1035 (ether C-O bend.); ^{1}H NMR (400 MHz, $CDCl_3$) δ 11.91 (s, 1H, amide), 8.24 (dd, *J* = 8.1, 1.2 Hz, 1H, quinoxaline), 7.66 – 7.59 (m, 1H, phenyl), 7.44 (dd, *J* = 12.9, 7.9 Hz, 2H, phenyl), 7.35 (dd, *J* = 7.7, 1.5 Hz, 1H, benzyl), 7.31 – 7.16 (m, 5H, (1H)-benzyl, (1H)-phenyl, (3H)-quinoxaline), 6.90 – 6.84 (m, 2H, benzyl), 5.58 (s, 2H, benzylic methylene), 3.77 (s, 3H, OCH_3), 3.34 (dd, *J* = 13.6, 6.8 Hz, 1H, $CH(CH_3)_2$), 1.33 (d, *J* = 6.8 Hz, 6H, $CH(CH_3)_2$).

_N_-(4-isopropylphenyl)-4-(4-methoxybenzyl)-3-oxo-3,4-dihydroquinoxaline-2-carboxamide (QCB-10)

TLC (EtOAc:Hexane 30:70); Yield: 79%; White solid; mp: 140-142°C; IR (KBr, *v* cm^{-1}): 3039 (sharp, N–H str.), 2960, 2870, 2820 (aromatic C-H str.), 1693 (keto C=O str.), 1681 (amide C=O str.), 1651, 1548, 1514 (C=C, C=N ring str.), 1485 (CH_2 bend.), 1415, 1294, 1251, 1180, 1163 (C=C bend.), 1091, 1026 (ether C-O bend.); ^{1}H NMR (400 MHz, $CDCl_3$) δ 11.58 (s, 1H, amide), 8.09 (dd, J = 8.1, 1.4 Hz, 1H, quinoxaline), 7.74 – 7.62 (m, 3H, phenyl), 7.55 – 7.40 (m, 2H, (1H)-phenyl, (1H)-benzyl), 7.26 (dd, J = 14.7, 8.6 Hz, 4H, (1H)-benzyl, (3H)-quinoxaline), 6.86 (d, J = 8.7 Hz, 2H, benzyl), 5.57 (s, 2H, benzylic methylene), 3.76 (s, 3H, OCH_3), 2.91 (dd, J = 13.8, 6.9 Hz, 1H, $CH(CH_3)_2$), 1.26 (d, J = 6.9 Hz, 6H, $CH(CH_3)_2$).

_N_-(2-chloro-4-methylphenyl)-4-(4-methoxybenzyl)-3-oxo-3,4-dihydroquinoxaline-2-carboxamide (QCB-11)

TLC (EtOAc:Hexane 30:70); Yield: 40%; White solid; mp: 206-208°C; IR (KBr, *v* cm^{-1}): 3039 (sharp, N–H str.), 2993, 2968, 2933, 2891, 2835 (aromatic C-H str.), 1703 (keto C=O str.), 1697 (amide C=O str.), 1531, 1514 (C=C, C=N ring str.), 1463, 1450 (CH_2 bend.), 1301, 1249, 1180, 1165 (C=C bend.), 1097, 1033 (ether C-O bend.); ^{1}H NMR (400 MHz, $CDCl_3$) δ 12.24 (s, 1H, amide), 8.27 – 8.19 (m, 1H, quinoxaline), 7.63 (dd, *J* = 12.2, 5.1 Hz, 2H, phenyl), 7.44 (dd, *J* = 16.3, 8.0 Hz, 3H, (2H)-benzyl, (1H)-phenyl), 7.22 (d, *J* = 8.8 Hz, 2H, quinoxaline), 7.15 (d, *J* = 8.5 Hz, 1H, quinoxaline), 6.87 (d, *J* = 8.8 Hz, 2H, benzyl), 5.59 (s, 2H, benzylic methylene), 3.77 (s, 3H, OCH_3), 2.34 (s, 3H, CH_3).

***N*-(2-chloro-5-methylphenyl)-4-(4-methoxybenzyl)-3-oxo-3,4-dihydroquinoxaline-2-carboxamide (QCB-12)**

TLC (EtOAc:Hexane 30:70); Yield: 44%; White solid; mp: 186-188°C; IR (KBr, *v* cm^{-1}): 3043 (sharp, N–H str.), 2960, 2918, 2823 (aromatic C-H str.), 1697 (keto C=O str.), 1692 (amide C=O str.), 1573, 1531, 1516 (C=C, C=N ring str.), 1438, 1444, 1415 (CH_2 bend.), 1310, 1257, 1182, 1153 (C=C bend.), 1097, 1051 (ether C-O bend.); ^{1}H NMR (400 MHz, $CDCl_3$) δ 12.20 (s, 1H, amide), 8.23 (d, *J* = 7.0 Hz, 1H, quinoxaline), 7.67 – 7.60 (m, 1H, phenyl), 7.45 (dd, *J* = 16.2, 7.9 Hz, 2H, (1H)-phenyl, (1H)-benzyl), 7.33 – 7.23 (m, 4H, (1H)-benzyl, (3H)-quinoxaline), 6.92 (dd, *J* = 8.2, 1.5 Hz, 1H, phenyl), 6.89 – 6.84 (m, 2H, benzyl), 5.59 (s, 2H, benzylic methylene), 3.77 (s, 3H, OCH_3), 2.39 (s, 3H, CH_3).

***N*-(2-chloro-6-methylphenyl)-4-(4-methoxybenzyl)-3-oxo-3,4-dihydroquinoxaline-2-carboxamide (QCB-13)**

TLC (EtOAc:Hexane 30:70); Yield: 49%; White solid; mp: 148-150°C; IR (KBr, *v* cm^{-1}): 2927 (sharp, N–H str.), 2835, 2763, 2655, 2557, 2493, 2453, 2285 (aromatic C-H str.), 1742 (keto C=O str.), 1687 (amide C=O str.), 1571, 1514 (C=C, C=N ring str.), 1492, 1473, 1454 (CH_2 bend.), 1301, 1259, 1230, 1163 (C=C bend.), 1097, 1039 (ether C-O bend.); ^{1}H NMR (400 MHz, $CDCl_3$) δ 11.49 (s, 1H, amide), 8.26 (d, *J* = 8.0 Hz, 1H, quinoxaline), 7.65 (t, *J* = 7.7 Hz, 1H, phenyl), 7.46 (t, *J* = 7.8 Hz, 2H, benzyl), 7.32 (d, *J* = 7.6 Hz, 1H, phenyl), 7.28 – 7.22 (m, 3H, quinoxaline), 7.16 (t, *J* = 7.7 Hz, 1H, phenyl), 6.88 (d, *J* = 8.6 Hz, 2H, benzyl), 5.58 (s, 2H, benzylic methylene), 3.78 (s, 3H, OCH_3), 2.40 (s, 3H, CH_3).

***N*-(4-chloro-2-methylphenyl)-4-(4-methoxybenzyl)-3-oxo-3,4-dihydroquinoxaline-2-carboxamide (QCB-14)**

TLC (EtOAc:Hexane 30:70); Yield: 51%; White solid; mp: 196-198°C; IR (KBr, *v* cm^{-1}): 3053 (sharp, N–H str.), 2958, 2899, 2830 (aromatic C-H str.), 1705 (keto C=O str.), 1698 (amide C=O str.), 1587, 1573, 1537, 1512 (C=C, C=N ring str.), 1483, 1467, 1440 (CH_2 bend.), 1321, 1303, 1249, 1182 (C=C bend.), 1089, 1035 (ether C-O bend.); ^{1}H NMR (400 MHz, $CDCl_3$) δ 11.84 (s, 1H, amide), 8.13 (dd, *J* = 8.1, 1.4 Hz, 1H, quinoxaline), 7.69 (ddd, *J* = 8.6, 7.3, 1.5 Hz, 1H, phenyl), 7.56 (d, *J* = 8.0 Hz, 1H, phenyl), 7.52 – 7.45 (m, 1H, phenyl), 7.31 – 7.19 (m, 5H, (2H)-benzyl, (3H)-quinoxaline), 6.89 – 6.83 (m, 2H, benzyl), 5.60 (s, 2H, benzylic methylene), 3.76 (s, 3H, OCH_3), 2.44 (s, 3H, CH_3).

4-(4-methoxybenzyl)-3-oxo-*N*-(2-(trifluoromethyl)phenyl)-3,4-dihydroquinoxaline-2-carboxamide (QCB-15)

TLC (EtOAc:Hexane 30:70); Yield: 54%; White solid; mp: 170-172°C; IR (KBr, *v* cm^{-1}): 3076 (sharp, N–H str.), 2962, 2885, 2829, 2657, 2557, 2499, 2328, 2287 (aromatic C-H str.), 1735 (keto C=O str.), 1684 (amide C=O str.), 1573, 1514 (C=C, C=N ring str.), 1454, 1421 (CH_2 bend.), 1276, 1259, 1176, 1160 (C=C bend.), 1099, 1037 (ether C-O bend.); ^{1}H NMR (400 MHz, $CDCl_3$) δ 11.90 (s, 1H, amide), 8.16 (d, *J* = 7.7 Hz, 1H, quinoxaline), 7.75 (d, *J* = 7.7 Hz, 1H, phenyl), 7.45 (t, *J* = 7.7 Hz, 3H, phenyl), 7.22 (dt, *J* = 15.7, 7.6 Hz, 2H, benzyl), 7.17 (d, *J* = 8.6 Hz, 1H, quinoxaline), 7.05 (t, *J* = 7.4 Hz, 2H, quinoxaline), 6.88 (d, *J* = 8.7 Hz, 2H, benzyl), 5.57 (s, 2H, benzylic methylene), 3.78 (s, 3H, OCH_3).

***N*-(2-chlorophenyl)-4-(4-methoxybenzyl)-3-oxo-3,4-dihydroquinoxaline-2-carboxamide (QCB-16)**

TLC (EtOAc:Hexane 30:70); Yield: 59%; White solid; mp: 206-208°C; IR (KBr, *v* cm^{-1}): 3034 (sharp, N–H str.), 2981, 2885, 2833, 2355, 2324 (aromatic C-H str.), 1697 (keto C=O str.), 1685 (amide C=O str.), 1643, 1573, 1514 (C=C, C=N ring str.), 1481, 1438 (CH_2 bend.), 1325, 1288, 1251, 1180, 1161 (C=C bend.), 1101, 1026 (ether C-O bend.); ^{1}H NMR (400 MHz, $CDCl_3$) δ 12.27 (s, 1H, amide), 8.64 (dd, *J* = 8.3, 1.4 Hz, 1H, quinoxaline), 8.14 (dd, *J* = 8.1, 1.2 Hz, 1H, phenyl), 7.73 – 7.66 (m, 1H, phenyl), 7.55 (d, *J* = 8.4 Hz, 1H, phenyl), 7.51 – 7.46 (m, 2H, benzyl), 7.37 (dd, *J* = 11.4, 4.3 Hz, 1H, phenyl), 7.28 (d, *J* = 8.7 Hz, 2H, quinoxaline), 7.15 (td, *J* = 7.7, 1.5 Hz, 1H, quinoxaline), 6.86 (d, *J* = 8.7 Hz, 2H, benzyl), 5.61 (s, 2H, benzylic methylene), 3.75 (s, 3H, OCH_3).

***N*-(3-chlorophenyl)-4-(4-methoxybenzyl)-3-oxo-3,4-dihydroquinoxaline-2-carboxamide (QCB-17)**

TLC (EtOAc:Hexane 30:70); Yield: 64%; White solid; mp: 182-184°C; IR (KBr, *v* cm^{-1}): 3267 (sharp, N–H str.), 3182, 3113, 2999, 2927, 2831, 2673, 2071 (aromatic C-H str.), 1680 (keto C=O str.), 1631 (amide C=O str.), 1589, 1535, 1510 (C=C, C=N ring str.), 1477, 1467 (CH_2 bend.), 1411, 1327, 1271, 1246 (C=C bend.), 1101, 1041 (ether C-O bend.); ^{1}H NMR (400 MHz, $CDCl_3$) δ 8.36 (d, *J* = 8.1 Hz, 1H, amide), 8.06 (d, *J* = 7.8 Hz, 1H, quinoxaline), 7.89 (dd, *J* = 12.8, 5.4 Hz, 1H, phenyl), 7.69 – 7.63 (m, 1H, phenyl), 7.49 (d, *J* = 22.4 Hz, 1H, phenyl), 7.39 (d, *J* = 8.8 Hz, 2H, phenyl), 7.31 – 7.19 (m, 5H, (2H)-benzyl, (3H)-quinoxaline), 6.94 – 6.87 (m, 2H, benzyl), 5.30 (s, 2H, benzylic methylene), 3.81 (s, 3H, OCH_3).

_N_-(4-chlorophenyl)-4-(4-methoxybenzyl)-3-oxo-3,4-dihydroquinoxaline-2-carboxamide (QCB-18)

TLC (EtOAc:Hexane 30:70); Yield: 64%; White solid; mp: 188-190°C; IR (KBr, *v* cm^{-1}): 3103 (sharp, N–H str.), 3012, 2885, 2825 (aromatic C-H str.), 1697 (keto C=O str.), 1685 (amide C=O str.), 1573, 1546, 1514 (C=C, C=N ring str.), 1489, 1463 (CH_2 bend.), 1296, 1249, 1228, 1178, 1161 (C=C bend.), 1087, 1036 (ether C-O bend.); ^{1}H NMR (400 MHz, $CDCl_3$) δ 11.17 (s, 1H, amide), 7.96 (t, *J* = 1.9 Hz, 1H, quinoxaline), 7.62 – 7.56 (m, 2H, phenyl), 7.46 – 7.36 (m, 2H, phenyl), 7.30 (d, *J* = 8.7 Hz, 2H, benzyl), 7.17 (dd, *J* = 8.0, 1.3 Hz, 3H, quinoxaline), 6.87 (d, *J* = 8.7 Hz, 2H, benzyl), 5.51 (s, 2Hbenzylic methylene), 3.73 (s, 3H, OCH_3).

4.3.3. Series-3: 4-(4-cyanobenzyl)-3-oxo-*N*-phenyl-3,4-dihydroquinoxaline-2-carboxamide analogues (QCC-1 to 19)

Ethyl 4-(4-cyanobenzyl)-3-oxo-3,4-dihydroquinoxaline-2-carboxylate (QC-2C)

5 g (0.023 mol) of ethyl 3-oxo-3,4-dihydroquinoxaline-2-carboxylate was taken in a 250 ml RBF and dissolved in 75 ml of DMF by stirring at room temperature for 30 min. To the above solution, 9.50 g (0.069 mol) of potassium carbonate was added and the reaction mixture stirred at room temperature for 1 hr. 4.49 g (0.023 mol) of 4-cyanobenzyl bromide was gradually added in portions and stirring was continued at room temperature overnight. The obtained suspension was poured into 200 ml of cold water and product extracted with ethylacetate (3 × 25 ml). The combined extracts were washed with brine solution and dried over sodium sulfate. Evaporation of solvent gave crude compound and the resultant solid residue was then washed with hexane, filtered, to afford the desired compound. TLC (EtOAc:Hexane 50:50); Yield: 69%; Pale yellow solid; mp: 204-206 °C; IR (KBr, *v* cm^{-1}): 3260, 3186, 3114, 3075, 2380 (aromatic C-H str.), 2227 (nitrile -C≡N str.), 1740 (ester C=O str.), 1680 (keto C=O str.), 1570, 1486 (C=C, C=N ring str.), 1454, 1420 (CH_2 bend), 1336, 1294, 1198, 1159 (C=C bend), 1095, 1044 (ether C-O bend.); ^{1}H NMR (400 MHz, $CDCl_3$) δ 7.86 (dd, *J* = 8.0, 1.4 Hz, 1H, quinoxaline), 7.44 (m, *J* = 8.7, 7.3, 1.5 Hz, 2H, benzyl), 7.25 (d, *J* = 8.6 Hz, 2H, benzyl), 7.28 – 7.20 (m, 1H, quinoxaline), 6.92 – 6.84 (m, 2H, quinoxaline), 5.52 (s, 2H, benzylic methylene), 4.40 (q, *J* = 7.1 Hz, 2H, OCH_2CH_3), 1.35 (t, *J* = 7.1 Hz, 3H, OCH_2CH_3).

4-(4-cyanobenzyl)-3-oxo-3,4-dihydroquinoxaline-2-carboxylic acid (QC-3C)

1 g (0.0030 mol) of ethyl 4-(4-cyanobenzyl)-3-oxo-3,4-dihydroquinoxaline-2-carboxylate was dissolved in 5 ml of dry THF in a 100 ml RBF. To the reaction mixture, 50% aqueous sodium hydroxide solution (*pH*>10) was added and stirred at room temperature for 2 hr. The solvent was removed under vacuum; residue washed with ethylacetate and the aqueous portion acidified with dil. HCl (*pH*=5). The obtained solid residue was washed with cold water, filtered and recrystallized with EtOH to afford the desired compound. TLC (EtOAc:Hex 30:70); Yield: 78%; Pale Yellow solid; mp: 184-186 °C; IR (KBr, *v* cm^{-1}): 3147 (broad O–H str. COOH), 3066, 2875, 2546, 2455 (aromatic C-H str.), 2339 (nitrile -C≡N str.), 1764 (acid C=O str.), 1707 (keto C=O str.), 1566 (C=C, C=N ring str.), 1460 (CH_2 bend.), 1328, 1292 (C=C bend.); ^{1}H NMR (400 MHz, $CDCl_3$) δ 12.70 (s, 1H, acid), 8.59 (d, *J* = 7.6 Hz, 1H, quinoxaline), 7.59 – 7.47 (m, 4H, benzyl), 7.39 – 7.31 (m, 1H, quinoxaline), 7.24 – 7.08 (m, 2H, quinoxaline), 5.71 (s, 2H, benzylic methylene).

General procedure for the synthesis of New Chemical Entity's (NCE's) i.e. quinoxaline-2-carboxamide analogues (QCC-1 to 19)

To 0.5 g (0.0016 mol) of 4-(4-cyanobenzyl)-3-oxo-3,4-dihydroquinoxaline-2-carboxylic acid taken in a 100 ml RBF, 0.38 g (0.0020 mol) of EDC·HCl was added and stirred with 5 ml of dry THF in an inert atmosphere (nitrogen) at 0 °C for 15 min. To the above reaction mixture, 0.38 g (0.0025 mol) HOBt was added and stirred for another 45 min. To the above mixture, 1 equivalent of appropriate amines were added and stirred continuously for 6 hr. The reaction mixture was concentrated under reduced pressure; resultant mass diluted with DCM or ethyl acetate, washed with aqueous sodium bicarbonate (2 × 50 ml), saturated brine solution (2 × 50 ml) and dried over anhydrous sodium sulfate. The solvent was then evaporated under reduced pressure to afford the desired compounds. The crude compounds were purified by recrystallization with EtOH/MeOH/column chromatography over silica gel.

4-(4-cyanobenzyl)-3-oxo-*N*-phenyl-3,4-dihydroquinoxaline-2-carboxamide (QCC-1)

TLC (EtOAc:Hexane 30:70); Yield: 72%; White solid; mp: 216-218°C; IR (KBr, *v* cm^{-1}): 3261 (sharp, N–H str.), 3192, 3120, 3065, 2360 (aromatic C-H str.), 2227 (nitrile -C≡N str.), 1693 (keto C=O str.), 1678 (amide C=O str.), 1539 (C=C, C=N ring str.), 1442, 1415 (CH_2 bend.), 1327, 1161, 1099, 1026 (C=C bend.); ^{1}H NMR (400 MHz, $CDCl_3$) δ 9.85 (s, 1H, amide), 8.12 (d, *J* = 8.3 Hz, 1H, quinoxaline), 7.59 – 7.47 (m, 2H, phenyl), 7.39 – 7.31 (m, 4H, (2H)-phenyl, (2H)-benzyl), 7.24 – 7.08 (m, 2H, (1H)-quinoxaline, (1H)-phenyl), 6.95 – 6.87 (m, 2H, quinoxaline), 5.56 (s, 2H, benzylic methylene).

4-(4-cyanobenzyl)-*N*-(2-methoxyphenyl)-3-oxo-3,4-dihydroquinoxaline-2-carboxamide (QCC-2)

TLC (EtOAc:Hexane 30:70); Yield: 30%; White solid; mp: 198-200 °C; IR (KBr, *v* cm^{-1}): 3205 (sharp, N–H str.), 3062, 2990, 2965, 2360 (aromatic C-H str.), 2227 (nitrile -C≡N str.), 1687 (keto C=O str.), 1678 (amide C=O str.), 1595, 1531 (C=C, C=N ring str.), 1485, 1462, 1415 (CH_2 bend.), 1332, 1290, 1265, 1220 (C=C bend.), 1095, 1044 (ether C-O bend.); ^{1}H NMR (400 MHz, $CDCl_3$) δ 10.12 (s, 1H, amide), 8.17 (d, *J* = 7.2 Hz, 1H, quinoxaline), 7.96 (d, *J* = 8.4 Hz, 1H, phenyl), 7.69 (d, *J* = 7.4 Hz, 2H, benzyl), 7.60 (d, *J* = 7.4 Hz, 2H, benzyl), 7.42 (t, *J* = 8.0 Hz, 1H, quinoxaline), 7.39 – 7.27 (m, 4H, (2H)-quinoxaline, (2H)-phenyl), 7.20 – 7.15 (m, 1H, phenyl), 5.76 (s, 2H, benzylic methylene), 3.89 (s, 3H, OCH_3).

4-(4-cyanobenzyl)-*N*-(3-methoxyphenyl)-3-oxo-3,4-dihydroquinoxaline-2-carboxamide (QCC-3)

TLC (EtOAc:Hexane 30:70); Yield: 35%; White solid; mp: 242-244°C; IR (KBr, *v* cm^{-1}): 3307 (sharp, N–H str.), 3076, 2960, (aromatic C-H str.), 2227 (nitrile -C≡N str.), 1693 (keto C=O str.), 1681 (amide C=O str.), 1556, 1530 (C=C, C=N ring str.), 1485, 1462, 1415 (CH_2 bend.), 1334, 1292, 1211, 1163 (C=C bend.), 1087, 1039 (ether C-O bend.); ^{1}H NMR (400 MHz, $CDCl_3$) δ 9.73 (s, 1H, amide), 8.12 (d, *J* = 8.3 Hz, 1H, quinoxaline), 7.90 (d, *J* = 8.4 Hz, 1H, benzyl), 7.85 – 7.75 (m, 3H, benzyl), 7.72 – 7.66 (m, 3H, (2H)-phenyl, (1H)-quinoxaline), 7.57 (t, *J* = 2.2 Hz, 1H, phenyl), 7.31 (t, *J* = 8.0 Hz, 2H, quinoxaline), 6.79 – 6.71 (m, 1H, phenyl), 5.78 (s, 2H, benzylic methylene), 3.88 (s, 3H, OCH_3).

4-(4-cyanobenzyl)-*N*-(4-methoxyphenyl)-3-oxo-3,4-dihydroquinoxaline-2-carboxamide (QCC-4)

TLC (EtOAc:Hexane 30:70); Yield: 54%; White solid; mp: 176-178°C; IR (KBr, *v* cm^{-1}): 3255 (sharp, N–H str.), 3197, 3130, 3064 (aromatic C-H str.), 2227 (nitrile -C≡N str.), 1680 (keto C=O str.), 1645, (amide C=O str.), 1600, 1539, 1510 (C=C, C=N ring str.), 1485, 1462, 1415 (CH_2 bend.), 1328, 1242, 1210, 1165 (C=C bend.), 1092, 1048 (ether C-O bend.); ^{1}H NMR (400 MHz, $CDCl_3$) δ 9.60 (s, 1H, amide), 8.11 (d, *J* = 8.3 Hz, 1H, quinoxaline), 7.89 (d, *J* = 7.4 Hz, 1H, benzyl), 7.83 – 7.77 (m, 3H, (1H)-benzyl, (2H)-phenyl), 7.73 – 7.66 (m, 5H, (2H)-benzyl, (3H)-quinoxaline), 6.96 (d, *J* = 9.0 Hz, 2H, phenyl), 5.68 (s, 2H, benzylic methylene), 3.84 (s, 3H, OCH_3).

***N*-(2-chlorophenyl)-4-(4-cyanobenzyl)-3-oxo-3,4-dihydroquinoxaline-2-carboxamide (QCC-5)**

TLC (EtOAc:Hexane 30:70); Yield: 32%; White solid; mp: 234-236°C; IR (KBr, *v* cm^{-1}): 3321 (sharp, N–H str.), 3064, 2970 (aromatic C-H str.), 2227 (nitrile -C≡N str.), 1693 (keto C=O str.), 1670 (amide C=O str.), 1575, 1531 (C=C, C=N ring str.), 1485, 1462, 1442 (CH_2 bend.), 1334, 1292, 1209, 1163 (C=C bend.); ^{1}H NMR (400 MHz, $CDCl_3$) δ 10.54 (s, 1H, amide), 8.13 (dd, J = 8.3, 1.2 Hz, 2H, (1H)-quinoxaline, (1H)-phenyl), 7.94 (d, *J* = 8.4 Hz, 1H, phenyl), 7.81 (d, *J* = 8.9 Hz, 2H, benzyl), 7.69 (d, *J* = 8.2 Hz, 2H, benzyl), 7.58 – 7.53 (m, 1H, phenyl), 7.40 – 7.28 (m, 4H, (3H)-quinoxaline, (1H)-phenyl), 5.65 (s, 2H, benzylic methylene).

_N_-(3-chlorophenyl)-4-(4-cyanobenzyl)-3-oxo-3,4-dihydroquinoxaline-2-carboxamide (QCC-6)

TLC (EtOAc:Hexane 30:70); Yield: 38%; White solid; mp: 240-242°C; IR (KBr, *v* cm^{-1}): 3358 (sharp, N–H str.), 3261, 3180, 3070, 2962 (aromatic C-H str.), 2225 (nitrile -C≡N str.), 1680 (keto C=O str.), 1637 (amide C=O str.), 1591, 1537 (C=C, C=N ring str.), 1467, 1415 (CH_2 bend.), 1336, 1271, 1209, 1157 (C=C bend.); ^{1}H NMR (400 MHz, $CDCl_3$) δ 10.24 (s, 1H, amide), 8.21 (d, *J* = 7.0 Hz, 1H, quinoxaline), 8.02 (d, *J* = 8.4 Hz, 1H, phenyl), 7.75 – 7.65 (m, 3H, (2H)-benzyl, (1H)-phenyl), 7.52 – 7.46 (m, 3H, (2H)-benzyl, (1H)-phenyl), 7.36 (t, *J* = 2.2 Hz, 1H, phenyl), 7.24 (d, *J* = 7.4 Hz, 1H, quinoxaline), 7.15 (t, *J* = 8.0 Hz, 2H, quinoxaline), 5.78 (s, 2H, benzylic methylene).

_N_-(4-chlorophenyl)-4-(4-cyanobenzyl)-3-oxo-3,4-dihydroquinoxaline-2-carboxamide (QCC-7)

TLC (EtOAc:Hexane 30:70); Yield: 58%; White solid; mp: 174-176°C; IR (KBr, *v* cm^{-1}): 3182 (sharp, N–H str.), 3109, 3057, 2951 (aromatic C-H str.), 2227 (nitrile -C≡N str.), 1693 (keto C=O str.), 1680 (amide C=O str.), 1537, 1531 (C=C, C=N ring str.), 1492, 1415 (CH_2 bend.), 1402, 1327, 1234, 1211, 1160 (C=C bend.); ^{1}H NMR (400 MHz, $CDCl_3$) δ 10.79 (s, 1H, amide), 8.01 – 7.97 (d, *J* = 7.4 Hz, 1H, quinoxaline), 7.72 (d, *J* = 8.9 Hz, 2H, phenyl), 7.52 (d, *J* = 8.2 Hz, 2H, benzyl), 7.46 (dd, *J* = 9.5, 4.9 Hz, 2H, phenyl), 7.43 – 7.37 (m, 2H, benzyl), 7.36 (d, *J* = 8.8 Hz, 3H, quinoxaline), 5.68 (s, 2H, benzylic methylene).

4-(4-cyanobenzyl)-_N_-(2-ethylphenyl)-3-oxo-3,4-dihydroquinoxaline-2-carboxamide (QCC-8)

TLC (EtOAc:Hexane 30:70); Yield: 62%; White solid; mp: 126-128°C; IR (KBr, *v* cm^{-1}): 3597 (sharp, N–H str.), 3502, 3439, 3250, 3203, 2972 (aromatic C-H str.), 2231 (nitrile -C≡N str.), 1697 (keto C=O str.), 1681 (amide C=O str.), 1645, 1581, 1529 (C=C, C=N ring str.), 1487, 1446, 1415 (CH_2 bend.), 1328, 1161 (C=C bend.); ^{1}H NMR (400 MHz, $CDCl_3$) δ 9.86 (s, 1H, amide), 8.09 (dd, J = 8.3, 0.9 Hz, 1H, quinoxaline), 7.91 (dd, J = 8.4, 0.9 Hz, 1H, benzyl), 7.86 – 7.75 (m, 2H, benzyl), 7.74 – 7.60 (m, 3H, (1H)-benzyl, (2H)-phenyl), 7.56 – 7.45 (m, 1H, phenyl), 7.39 – 7.28 (m, 3H, (1H)-phenyl, (2H)-quinoxaline), 7.18 (dd, J = 11.3, 3.9 Hz, 1H, quinoxaline), 5.78 (s, 2H, benzylic methylene), 2.80 (tt, J = 12.6, 6.3 Hz, 2H, CH_2CH_3), 1.25 (s, 3H, CH_2CH_3).

4-(4-cyanobenzyl)-*N*-(3-ethylphenyl)-3-oxo-3,4-dihydroquinoxaline-2-carboxamide (QCC-9)

TLC (EtOAc:Hexane 30:70); Yield: 64%; White solid; mp: 188-190 °C; IR (KBr, *v* cm^{-1}): 3280 (sharp, N–H str.), 3076, 2964, 2872 (aromatic C-H str.), 2227 (nitrile -C≡N str.), 1693 (keto C=O str.), 1678 (amide C=O str.), 1639, 1556, 1537 (C=C, C=N ring str.), 1487, 1444, 1415 (CH_2 bend.), 1336, 1174 (C=C bend.); ^{1}H NMR (400 MHz, $CDCl_3$) δ 9.86 (s, 1H, amide), 8.09 (dd, *J* = 8.3, 0.9 Hz, 1H, quinoxaline), 7.82 (ddd, *J* = 6.9, 5.9, 1.5 Hz, 2H, phenyl), 7.53 – 7.47 (m, 2H, benzyl), 7.37 – 7.30 (m, 3H, (2H)-benzyl, (1H)-phenyl), 7.09 (d, *J* = 7.4 Hz, 1H, quinoxaline), 7.01 (dd, *J* = 8.7, 1.1 Hz, 2H, quinoxaline), 6.95 – 6.83 (m, 1H, phenyl), 5.78 (s, 2H, benzylic methylene), 2.79 (dd, *J* = 10.1, 5.0 Hz, 2H, CH_2CH_3), 1.25 (d, *J* = 5.2 Hz, 3H, CH_2CH_3).

4-(4-cyanobenzyl)-3-oxo-*N*-(2-propylphenyl)-3,4-dihydroquinoxaline-2-carboxamide (QCC-10)

TLC (EtOAc:Hexane 30:70); Yield: 55%; White solid; mp: 166-168 °C; IR (KBr, *v* cm^{-1}): 3201 (sharp, N–H str.), 3130, 3062, 2960, 2868 (aromatic C-H str.), 2225 (nitrile -C≡N str.), 1693 (keto C=O str.), 1678 (amide C=O str.), 1640, 1556, 1537 (C=C, C=N ring str.), 1454, 1411 (CH_2 bend.), 1336, 1159 (C=C bend.); ^{1}H NMR (400 MHz, $CDCl_3$) δ 10.44 (s, 1H, amide), 8.21 (d, *J* = 8.3 Hz, 1H, quinoxaline), 7.80 (d, *J* = 8.4 Hz, 2H, benzyl), 7.71 – 7.62 (m, 3H, (2H)-benzyl, (1H)-phenyl), 7.39 – 7.26 (m, 4H, (3H)-phenyl, (1H)-quinoxaline), 7.21 (t, *J* = 8.0 Hz, 2H, quinoxaline), 5.72 (s, 2H, benzylic methylene), 2.76 – 2.68 (m, 2H, $CH_2CH_2CH_3$), 1.01 (t, J = 7.3 Hz, 2H, $CH_2CH_2CH_3$), 0.89 (t, J = 7.3 Hz, 3H, $CH_2CH_2CH_3$).

4-(4-cyanobenzyl)-*N*-(2-isopropylphenyl)-3-oxo-3,4-dihydroquinoxaline-2-carboxamide (QCC-11)

TLC (EtOAc:Hexane 30:70); Yield: 63%; White solid; mp: 140-142 °C; IR (KBr, *v* cm^{-1}): 3194 (sharp, N–H str.), 3126, 3059, 2962, 2868 (aromatic C-H str.), 2229 (nitrile -C≡N str.), 1693 (keto C=O str.), 1678 (amide C=O str.), 1640, 1556, 1519 (C=C, C=N ring str.), 1489, 1454, 1415 (CH_2 bend.), 1371, 1330, 1282 (C=C bend.); ^{1}H NMR (400 MHz, $CDCl_3$) δ 10.75 (s, 1H, amide), 8.15 (d, *J* = 8.3 Hz, 1H, quinoxaline), 7.74 (d, *J* = 8.4 Hz, 2H, benzyl), 7.70 – 7.65 (m, 2H, benzyl), 7.58 – 7.49 (m, 3H, phenyl), 7.44 (t, *J* = 2.2 Hz, 2H, (1H)-quinoxaline, (1H)-phenyl), 7.27 (t, *J* = 8.0 Hz, 2H, quinoxaline), 5.77 (s, 2H, benzylic methylene), 2.85 (dt, *J* = 13.7, 6.9 Hz, 1H, $CH(CH_3)_2$), 1.27 (d, *J* = 6.7 Hz, 6H, $CH(CH_3)_2$).

4-(4-cyanobenzyl)-*N*-(4-isopropylphenyl)-3-oxo-3,4-dihydroquinoxaline-2-carboxamide (QCC-12)

TLC (EtOAc:Hexane 30:70); Yield: 71%; White solid; mp: 124-126 °C; IR (KBr, *v* cm^{-1}): 3250 (sharp, N–H str.), 3192, 3118, 3053, 2958, 2870 (aromatic C-H str.), 2227 (nitrile -C≡N str.), 1693 (keto C=O str.), 1678 (amide C=O str.), 1640, 1556, 1514 (C=C, C=N ring str.), 1489, 1454, 1415 (CH_2 bend.), 1371, 1325, 1286 (C=C bend.); ^{1}H NMR (400 MHz, $CDCl_3$) δ 10.48 (s, 1H, amide), 8.27 (d, *J* = 7.1 Hz, 1H, quinoxaline), 7.94 (d, *J* = 8.7 Hz, 2H, phenyl), 7.80 – 7.68 (m, 2H, benzyl), 7.64 – 7.56 (m, 2H, benzyl), 7.44 (t, *J* = 2.2 Hz, 2H, phenyl), 7.37 (d, *J* = 7.4 Hz, 1H, quinoxaline), 7.27 (t, *J* = 8.0 Hz, 2H, quinoxaline), 5.75 (s, 2H, benzylic methylene), 2.90 (dt, *J* = 13.7, 6.9 Hz, 1H, $CH(CH_3)_2$), 1.27 (d, *J* = 6.7 Hz, 6H, $CH(CH_3)_2$).

***N*-(2-chloro-4-methylphenyl)-4-(4-cyanobenzyl)-3-oxo-3,4-dihydroquinoxaline-2-carboxamide (QCC-13)**

TLC (EtOAc:Hexane 30:70); Yield: 59%; White solid; mp: 174-176°C; IR (KBr, *v* cm^{-1}): 3050 (sharp, N–H str.), 2966, 2920, 2870 (aromatic C-H str.), 2225 (nitrile -C≡N str.), 1693 (keto C=O str.), 1678 (amide C=O str.), 1537, 1514 (C=C, C=N ring str.), 1489, 1454, 1415 (CH_2 bend.), 1371, 1332, 1311, 1284 (C=C bend.); ^{1}H NMR (400 MHz, $CDCl_3$) δ 10.65 (s, 1H, amide), 8.22 (d, *J* = 8.3 Hz, 1H, quinoxaline), 7.93 (d, *J* = 8.9 Hz, 1H, phenyl), 7.82 (d, *J* = 8.2 Hz, 2H, benzyl), 7.71 (dd, *J* = 9.5, 4.9 Hz, 3H, (2H)-benzyl, (1H)-phenyl), 7.39 (d, *J* = 7.4 Hz, 1H, quinoxaline), 7.28 (t, *J* = 8.0 Hz, 2H, quinoxaline), 7.20 – 7.09 (m, 1H, phenyl), 5.72 (s, 2H, benzylic methylene), 2.54 (s, 3H, CH_3).

***N*-(2-chloro-5-methylphenyl)-4-(4-cyanobenzyl)-3-oxo-3,4-dihydroquinoxaline-2-carboxamide (QCC-14)**

TLC (EtOAc:Hexane 30:70); Yield: 59%; White solid; mp: 130-132 °C; IR (KBr, *v* cm^{-1}): 3050 (sharp, N–H str.), 2966, 2970, 2870, 2357 (aromatic C-H str.), 2227 (nitrile -C≡N str.), 1693 (keto C=O str.), 1678 (amide C=O str.), 1537, 1531, 1514 (C=C, C=N ring str.), 1454, 1415 (CH_2 bend.), 1371, 1336, 1311, 1286 (C=C bend.); ^{1}H NMR (400 MHz, $CDCl_3$) δ 10. 56 (s, 1H, amide), 8.16 (d, *J* = 8.3 Hz, 1H, quinoxaline), 7.89 (d, *J* = 8.9 Hz, 1H, phenyl), 7.79 (d, *J* = 8.2 Hz, 2H, benzyl), 7.67 (dd, *J* = 9.5, 4.9 Hz, 3H, (2H)-benzyl, (1H)-phenyl), 7.43 (d, *J* = 7.4 Hz, 1H, quinoxaline), 7.31 (t, *J* = 8.0 Hz, 2H, quinoxaline), 7.26 – 7.19 (m, 1H, phenyl), 5.74 (s, 2H, benzylic methylene), 2.44 (s, 3H, CH_3).

_N_-(2-chloro-6-methylphenyl)-4-(4-cyanobenzyl)-3-oxo-3,4-dihydroquinoxaline-2-carboxamide (QCC-15)

TLC (EtOAc:Hexane 30:70); Yield: 61%; White solid; mp: 208-210°C; IR (KBr, *v* cm^{-1}): 3238 (sharp, N–H str.), 3197, 3055, 3022, 2873 (aromatic C-H str.), 2227 (nitrile -C≡N str.), 1693 (keto C=O str.), 1666 (amide C=O str.), 1560, 1556, 1519 (C=C, C=N ring str.), 1489, 1454, 1415 (CH_2 bend.), 1336, 1286, 1267 (C=C bend.); ^{1}H NMR (400 MHz, $CDCl_3$) δ 10. 48 (s, 1H, amide), 8.20 (d, *J* = 7.1 Hz, 1H, quinoxaline), 7.68 (d, *J* = 8.9 Hz, 2H, benzyl), 7.56 (dd, *J* = 9.5, 4.9 Hz, 3H, (1H)-phenyl, (2H)-benzyl), 7.38 (d, *J* = 7.1 Hz, 1H, phenyl), 7.29 (d, *J* = 7.4 Hz, 1H, quinoxaline), 7.22 (t, *J* = 8.0 Hz, 2H, quinoxaline), 7.16 – 7.10 (m, 1H, phenyl), 5.79 (s, 2H, benzylic methylene), 2.47 (s, 3H, CH_3).

_N_-(3-chloro-2-methylphenyl)-4-(4-cyanobenzyl)-3-oxo-3,4-dihydroquinoxaline-2-carboxamide (QCC-16)

TLC (EtOAc:Hexane 30:70); Yield: 65%; White solid; mp: 204-206°C; IR (KBr, *v* cm^{-1}): 3435 (sharp, N–H str.), 3371, 3174, 3041, 2966 (aromatic C-H str.), 2233 (nitrile -C≡N str.), 1693 (keto C=O str.), 1672 (amide C=O str.), 1531 (C=C, C=N ring str.), 1440, 1417 (CH_2 bend.), 1392, 1313, 1271 (C=C bend.); ^{1}H NMR (400 MHz, $CDCl_3$) δ 10.37 (s, 1H, amide), 8.19 (d, *J* = 8.3 Hz, 1H, quinoxaline), 7.78 (d, *J* = 8.4 Hz, 2H, benzyl), 7.69 – 7.59 (m, 3H, (2H)-benzyl, (1H)-phenyl), 7.37 – 7.28 (m, 3H, (1H)-quinoxaline, (2H)-phenyl), 7.19 (t, *J* = 8.0 Hz, 2H, quinoxaline), 5.69 (s, 2H, benzylic methylene), 2.45 (s, 3H, CH_3).

4-(4-cyanobenzyl)-3-oxo-_N_-(piperidin-1-yl)-3,4-dihydroquinoxaline-2-carboxamide (QCC-17)

TLC (EtOAc:Hexane 30:70); Yield: 60%; White solid; mp: 158-160°C; IR (KBr, *v* cm^{-1}): 3207 (sharp, N–H str.), 3059, 2939, 2856, 2810 (aromatic C-H str.), 2229 (nitrile -C≡N str.), 1666 (keto C=O str.), 1645 (amide C=O str.), 1508 (C=C, C=N ring str.), 1440, 1415 (CH_2 bend.), 1332, 1315, 1267, 1220 (C=C bend.); ^{1}H NMR (400 MHz, $CDCl_3$) δ 11.58 (s, 1H, amide), 8.21 (d, *J* = 8.3 Hz, 1H, quinoxaline), 7.87 (d, *J* = 8.4 Hz, 2H, benzyl), 7.69 – 7.59 (m, 2H, benzyl), 7.52 – 7.47 (m, 1H, quinoxaline), 7.35 (t, *J* = 8.0 Hz, 2H, quinoxaline), 5.72 (s, 2H, benzylic methylene), 4.72 (dd, *J* = 9.5, 4.9 Hz, 2H, piperidine), 2.16 (m, 3H, piperidine).

_N_-(4-chloro-2-methylphenyl)-4-(4-cyanobenzyl)-3-oxo-3,4-dihydroquinoxaline-2-carboxamide (QCC-18)

TLC (EtOAc:Hexane 30:70); Yield: 29%; White solid; mp: 196-198°C; IR (KBr, *v* cm^{-1}): 3250 (sharp, N–H str.), 3192, 3118, 3053, 2958, 2870 (aromatic C-Hstr.), 2227 (nitrile -C≡N str.), 1693 (keto C=O str.), 1678 (amide C=O str.), 1640, 1556, 1514 (C=C, C=N ring str.), 1489, 1454, 1415 (CH_2 bend.), 1371, 1325, 1286 (C=C bend.); ^{1}H NMR (400 MHz, $CDCl_3$) δ 10.95 (s, 1H, amide), 8.15 (d, *J* = 8.3 Hz, 1H, quinoxaline), 7.86 (d, *J* = 8.9 Hz, 1H, phenyl), 7.75 (d, *J* = 8.2 Hz, 2H, benzyl), 7.64 (dd, *J* = 9.5, 4.9 Hz, 3H, (2H)-benzyl, (1H)-phenyl), 7.48 (t, *J* = 2.2 Hz, 1H, phenyl), 7.32 (d, *J* = 7.4 Hz, 1H, quinoxaline), 7.21 (t, *J* = 8.0 Hz, 2H, quinoxaline), 5.84 (s, 2H, benzylic methylene), 2.24 (s, 3H, CH_3).

4-(4-cyanobenzyl)-3-oxo-_N_-(2-(trifluoromethyl)phenyl)-3,4-dihydroquinoxaline-2-carboxamide (QCC-19)

TLC (EtOAc:Hexane 30:70); Yield: 32%; White solid; mp: 170-172 °C; IR (KBr, *v* cm^{-1}): 3205 (sharp, N–H str.), 3062, 2990, 2965, 2360 (aromatic C-H str.), 2227 (nitrile -C≡N str.), 1687 (keto C=O str.), 1678 (amide C=O str.), 1595, 1531 (C=C, C=N ring str.), 1485, 1462, 1415 (CH_2 bend), 1332, 1290, 1265, 1220 (C=C bend); ^{1}H NMR (400 MHz, $CDCl_3$) δ 11.27 (s, 1H, amide), 8.12 (d, *J* = 8.3 Hz, 1H, quinoxaline), 7.76 (d, *J* = 8.9 Hz, 1H, phenyl), 7.67 (d, *J* = 8.2 Hz, 2H, benzyl), 7.55 – 7.45 (m, 3H, phenyl), 7.42 (d, *J* = 8.2 Hz, 2H, benzyl), 7.32 – 7.27 (m, 1H, quinoxaline), 7.22 (t, *J* = 8.0 Hz, 2H, quinoxaline), 5.54 (s, 2H, benzylic methylene).

4.3.4. Series-4: 4-benzoyl-3-oxo-*N*-phenyl-3,4-dihydroquinoxaline-2-carboxamide analogues (QCD-1 to 18)

Ethyl 4-benzoyl-3-oxo-3,4-dihydroquinoxaline-2-carboxylate (QC-2D)

5 g (0.023 mol) of ethyl 3-oxo-3,4-dihydroquinoxaline-2-carboxylate was dissolved in 75 ml of DMF in a 250 ml RBF and stirred at room temperature for 30 min. To the above solution, 9.50 g (0.069 mol) of potassium carbonate was added and the mixture stirred at room temperature for 1 hr. 3.22 g (0.023 mol) of benzoyl chloride was gradually added in portions and stirring was continued at room temperature overnight. The obtained suspension was poured into 200 ml of cold water and product extracted with ethylacetate (3 × 25 ml). The combined extracts were washed with brine solution and dried over sodium sulfate. Evaporation of solvent gave crude compound and the resultant solid residue was then washed with hexane, filtered, to afford the desired pure compound. TLC (EtOAc:Hex 50:50); Yield: 78%; Pale yellow solid; mp: 168-170 °C; IR (KBr, *v* cm^{-1}): 3300 (quinoxaline N-H str.), 3062, 2987, 2939, 2904, 2677, 2490 (aromatic C-H str.), 1745 (benzoyl keto C=O str.), 1724 (ester C=O str.), 1714 (keto C=O str.), 1568, 1490 (C=C, C=N ring str.), 1446 (CH_2 bend), 1327 (CH_3 bend), 1240, 1211, 1172 (C=C bend), 1098, 1039 (ether C-O bend.); ^{1}H NMR (400 MHz, DMSO) δ 8.30 (d, *J* = 8.2 Hz, 1H, quinoxaline), 8.23 (d, *J* = 7.5 Hz, 2H, benzoyl), 8.11 (t, *J* = 7.6 Hz, 1H, benzoyl), 8.00 (ddd, *J* = 15.2, 14.1, 6.9 Hz, 2H, benzoyl), 7.78 (t, *J* = 7.4 Hz, 1H, quinoxaline), 7.64 (t, *J* = 7.7 Hz, 2H, quinoxaline), 4.34 (q, *J* = 7.1 Hz, 2H, OCH_2CH_3), 1.20 (t, *J* = 7.1 Hz, 3H, OCH_2CH_3).

4-benzoyl-3-oxo-3,4-dihydroquinoxaline-2-carboxylic acid (QC-3D)

1 g (0.00310 mol) of ethyl 4-benzoyl-3-oxo-3,4-dihydroquinoxaline-2-carboxylate was dissolved in 5 ml of dry THF in a 100 ml RBF. To this mixture, 50% aqueous sodium hydroxide solution (*pH*>10) was added and stirred at room temperature for 2 hr. The solvent was removed under vacuum; residue washed with ethylacetate and the aqueous portion acidified with dil. HCl (*pH*=5). The obtained solid residue was washed with cold water, filtered and recrystallized with EtOH to afford the desired compound. TLC (EtOAc:Hex 25:75); Yield: 70%; Pale Yellow solid; mp: 184-186 °C; IR (KBr, *v* cm^{-1}): 3084, 3012 (broad O–H str. COOH), 2885, 2831, 2681, 2656, 2507, 2343 (aromatic C-H str.), 1745 (benzoyl keto C=O str.), 1724 (acid C=O str.), 1693 (keto C=O str.), 1643, 1627, 1494, 1421 (C=C, C=N ring str.), 1290, 1260, 1147 (C=C bend.); ^{1}H NMR (400 MHz, DMSO) δ 8.88 (s, 1H, acid), 7.99 – 7.93 (m, 1H, benzoyl), 7.86 (d, *J* = 8.1 Hz, 1H, benzoyl), 7.67 – 7.55 (m, 2H, (1H)-quinoxaline, (1H)-benzoyl), 7.47 (t, *J* = 7.6 Hz, 2H, benzoyl), 7.42 – 7.38 (m, 3H, quinoxaline).

General procedure for the synthesis of New Chemical Entity's (NCE's) i.e. quinoxaline-2-carboxamide analogues (QCD-1 to 18)

To 0.5 g (0.0017 mol) of 4-benzoyl-3-oxo-3,4-dihydroquinoxaline-2-carboxylic acid taken in a 100 ml RBF, 0.39 g (0.0020 mol) of EDC·HCl was added and stirred with 5 ml of dry THF in an inert atmosphere (nitrogen) at 0 °C for 15 min. To the above reaction mixture, 0.39 g (0.0025 mol) HOBt was added and stirred for another 45 min. To the above mixture, 1 equivalent of appropriate amines were added and stirred continuously for 6 hr. The reaction mixture was concentrated under reduced pressure; resultant mass diluted with DCM/ethyl acetate, washed with aqueous sodium bicarbonate (2 × 50 ml), saturated brine solution (2 × 50 ml) and dried over anhydrous sodium sulfate. The solvent was then evaporated under reduced pressure to afford the desired compounds. The obtained compounds were purified by recrystallization with EtOH/MeOH/column chromatography over silica gel.

4-benzoyl-3-oxo-*N*-phenyl-3,4-dihydroquinoxaline-2-carboxamide (QCD-1)

TLC (EtOAc:Hexane 30:70); Yield: 84%; White solid; mp: 240-242°C; IR (KBr, *v* cm^{-1}): 3342 (sharp, N–H str.), 3051, 2995, 2939, 2873, 2831, 2713 (aromatic C-H str.), 1732 (benzoyl keto C=O str.), 1685 (keto C=O str.), 1654 (amide C=O str.), 1598, 1556 (C=C, C=N ring str.), 1529, 1490, 1440, 1425 (CH_2 bend.), 1323, 1261 (C=C bend.); ^{1}H NMR (400 MHz, DMSO) δ 10.12 (s, 1H, amide), 7.96 (d, *J* = 7.2 Hz, 2H, benzoyl), 7.78 (d, *J* = 8.0 Hz, 2H, (1H)-quinoxaline, (1H)-benzoyl), 7.52 (dt, *J* = 24.7, 7.1 Hz, 4H, (2H)-benzoyl, (2H)-phenyl), 7.44 – 7.25 (m, 5H, (3H)-phenyl, (2H)-quinoxaline), 7.11 (dt, *J* = 22.7, 7.4 Hz, 1H, quinoxaline).

4-benzoyl-*N*-(4-methoxyphenyl)-3-oxo-3,4-dihydroquinoxaline-2-carboxamide (QCD-2)

TLC (EtOAc:Hexane 30:70); Yield: 74%; White solid; mp: 146-148°C; IR (KBr, *v* cm^{-1}): 3329 (sharp, N–H str.), 3049, 2962, 2837 (aromatic C-H str.), 1705 (benzoyl keto C=O str.), 1647 (keto C=O str.), 1640 (amide C=O str.), 1616, 1514, 1492 (C=C, C=N ring str.), 1470, 1408 (CH_2 bend.), 1373, 1317, 1303, 1269 (C=C bend.), 1089, 1035 (ether C-O bend.); ^{1}H NMR (400 MHz, DMSO) δ 10.04 (s, 1H, amide), 7.95 (d, J = 7.0 Hz, 2H, benzoyl), 7.71– 7.65 (m, 3H, (1H)-quinoxaline, (2H)-benzoyl)), 7.57 – 7.45 (m, 5H, (1H)-benzoyl, (2H)-phenyl, (2H)-quinoxaline), 6.91 – 6.85 (m, 3H, (1H)-quinoxaline, (2H)-phenyl), 3.76 (s, 3H, OCH_3).

4-benzoyl-3-oxo-*N*-p-tolyl-3,4-dihydroquinoxaline-2-carboxamide (QCD-3)

TLC (EtOAc:Hexane 30:70); Yield: 72%; White solid; mp: 148-150°C; IR (KBr, *v* cm^{-1}): 3307 (sharp, N–H str.), 3068, 3032, 3010, 2916, 2860 (aromatic C-H str.), 1705 (benzoyl keto C=O str.), 1647 (keto C=O str.), 1640 (amide C=O str.), 1597, 1514, 1490 (C=C, C=N ring str.), 1444, 1404 (CH_2 bend.), 1373, 1317, 1298, 1265 (C=C bend.); ^{1}H NMR (400 MHz, DMSO) δ 10.04 (s, 1H, amide), 7.98 – 7.93 (m, 3H, (2H)-benzoyl, (1H)-quinoxaline), 7.65 (d, *J* = 8.4 Hz, 3H, benzoyl), 7.53 (d, *J* = 7.1 Hz, 1H, quinoxaline), 7.50 – 7.45 (m, 3H, phenyl), 7.12 (d, *J* = 8.3 Hz, 3H, (1H)-phenyl, (2H)-quinoxaline), 2.30 (s, 3H, CH_3).

4-benzoyl-*N*-(4-chlorophenyl)-3-oxo-3,4-dihydroquinoxaline-2-carboxamide (QCD-4)

TLC (EtOAc:Hexane 30:70); Yield: 61%; White solid; mp: 178-180 °C; IR (KBr, *v* cm^{-1}): 3348 (sharp, N–H str.), 3300, 3103, 3034, 2983, 2763, 2627 (aromatic C-H str.), 1705 (benzoyl keto C=O str.), 1656 (keto C=O str.), 1650 (amide C=O str.), 1595, 1517, 1494 (C=C, C=N ring str.), 1446, 1398 (CH_2 bend.), 1359, 1315, 1288, 1257 (C=C bend.); ^{1}H NMR (400 MHz, DMSO) δ 10.29 (s, 1H, amide), 7.98 – 7.93 (m, 3H, (2H)-benzoyl, (1H)-quinoxaline), 7.86 – 7.80 (m, 3H, benzoyl), 7.56 (dd, *J* = 6.0, 3.8 Hz, 1H, quinoxaline), 7.50 (t, *J* = 7.3 Hz, 3H, phenyl), 7.37 – 7.31 (m, 3H, (1H)-phenyl, (2H)-quinoxaline).

4-benzoyl-*N*-(3-methoxyphenyl)-3-oxo-3,4-dihydroquinoxaline-2-carboxamide (QCD-5)

TLC (EtOAc:Hexane 30:70); Yield: 70%; White solid; mp: 116-118°C; IR (KBr, *v* cm^{-1}): 3304 (sharp, N–H str.), 3207, 3134, 3059, 2968, 2910, 2831 (aromatic C-H str.), 1705 (benzoyl keto C=O str.), 1656 (keto C=O str.), 1648 (amide C=O str.), 1604, 1531, 1492 (C=C, C=N ring str.), 1446, 1415, (CH_2 bend.), 1373, 1309, 1271, 1261 (C=C bend.), 1093, 1040 (ether C-O bend.); ^{1}H NMR (400 MHz, DMSO) δ 10.13 (s, 1H, amide), 7.96 (d, *J* = 7.2 Hz, 2H, benzoyl), 7.50 (d, *J* = 7.4 Hz, 4H, (1H)-quinoxaline, (3H)-benzoyl), 7.47 (s, 1H, quinoxaline), 7.37 (d, *J* = 8.0 Hz, 2H, phenyl), 7.21 (t, *J* = 8.1 Hz, 2H, (1H)-quinoxaline, (1H)-phenyl), 6.65 (dd, *J* = 8.1, 2.0 Hz, 2H, (1H)-quinoxaline, (1H)-phenyl), 3.77 (s, 3H, OCH_3).

4-benzoyl-3-oxo-*N*-m-tolyl-3,4-dihydroquinoxaline-2-carboxamide (QCD-6)

TLC (EtOAc:Hexane 30:70); Yield: 60%; White solid; mp: 114-116°C; IR (KBr, *v* cm^{-1}): 3271 (sharp, N–H str.), 3261, 3138, 3059, 2912, 2860, 2791, 2735 (aromatic C-H str.), 1705 (benzoyl keto C=O str.), 1656 (keto C=O str.), 1651 (amide C=O str.), 1604, 1537,

1492 (C=C, C=N ring str.), 1446, 1427, (CH_2 bend.), 1373, 1300, 1259 (C=C bend.); ^{1}H NMR (400 MHz, DMSO) δ 10.07 (s, 1H, amide), 7.96 (d, *J* = 7.0 Hz, 2H, benzoyl), 7.57 – 7.52 (m, 3H, (1H)-quinoxaline, (2H)-benzoyl), 7.51 – 7.46 (m, 4H, (3H)-phenyl, (1H)-benzoyl), 7.19 (t, *J* = 7.8 Hz, 2H, quinoxaline), 6.90 (d, *J* = 7.5 Hz, 2H, (1H)-quinoxaline, (1H)-phenyl), 2.33 (s, 3H, CH_3).

4-benzoyl-*N*-(3-chlorophenyl)-3-oxo-3,4-dihydroquinoxaline-2-carboxamide (QCD-7)

TLC (EtOAc:Hexane 30:70); Yield: 49%; White solid; mp: 186-188 °C; IR (KBr, *v* cm^{-1}): 3284 (sharp, N–H str.), 3076, 3055, 2995, 2947, 2900, 2887, 2831 (aromatic C-H str.), 1732 (benzoyl keto C=O str.), 1693 (keto C=O str.), 1681 (amide C=O str.), 1651, 1593, 1531 (C=C, C=N ring str.), 1475, 1427, (CH_2 bend.), 1359, 1290, 1260 (C=C bend.); ^{1}H NMR (400 MHz, DMSO) δ 10.34 (s, 1H, amide), 8.02 – 7.88 (m, 3H, (2H)-benzoyl, (1H)-phenyl), 7.73 – 7.62 (m, 2H, (1H)-quinoxaline, (1H)-benzoyl), 7.55 (dt, *J* = 15.0, 8.0 Hz, 3H, (2H)-benzoyl, (1H)-phenyl), 7.44 – 7.30 (m, 4H, (2H)-phenyl, (2H)-quinoxaline), 7.14 (dd, *J* = 22.7, 8.0 Hz, 1H, quinoxaline).

4-benzoyl-3-oxo-*N*-o-tolyl-3,4-dihydroquinoxaline-2-carboxamide (QCD-8)

TLC (EtOAc:Hexane 30:70); Yield: 54%; White solid; mp: 158-160 °C; IR (KBr, *v* cm^{-1}): 3234 (sharp, N–H str.), 3128, 3103, 3059, 2951, 2827, 2673, 2630 (aromatic C-H str.), 1743 (benzoyl keto C=O str.), 1697 (keto C=O str.), 1685 (amide C=O str.), 1651, 1593, 1519 (C=C, C=N ring str.), 1487, 1471, 1421 (CH_2 bend.), 1359, 1309, 1240 (C=C bend.);^{1}H NMR (400 MHz, DMSO) δ 9.77 (s, 1H, amide), 7.99 (d, *J* = 7.4 Hz, 2H, benzoyl), 7.89 (dd, *J* = 22.2, 8.3 Hz, 1H, quinoxaline), 7.70 – 7.59 (m, 1H, benzoyl), 7.59 – 7.45 (m, 4H, (2H)-benzoyl, (2H)-phenyl), 7.39 (dd, *J* = 18.0, 9.6 Hz, 2H, quinoxaline), 7.19 (ddd, *J* = 21.2, 15.9, 7.3 Hz, 3H, (2H)-phenyl, (1H)-quinoxaline), 2.27 (s, 3H, CH_3).

4-benzoyl-*N*-(2-chlorophenyl)-3-oxo-3,4-dihydroquinoxaline-2-carboxamide (QCD-9)

TLC (EtOAc:Hexane 30:70); Yield: 42%; White solid; mp: 156-158 °C; IR (KBr, *v* cm^{-1}): 3256 (sharp, N–H str.), 3078, 3060, 2986, 2934, 2912, 2855, 2822 (aromatic C-H str.), 1738 (benzoyl keto C=O str.), 1695 (keto C=O str.), 1679 (amide C=O str.), 1660, 1587, 1527 (C=C, C=N ring str.), 1475, 1427, (CH_2 bend.), 1359, 1290, 1260 (C=C bend.); ^{1}H NMR (400 MHz, DMSO) δ 10.12 (s, 1H, amide), 8.02 – 7.88 (m, 3H, (2H)-benzoyl, (1H)-phenyl), 7.78 – 7.62 (m, 2H, (1H)-quinoxaline, (1H)-benzoyl), 7.55 (dt, *J* = 15.0, 8.0 Hz, 3H, (2H)-benzoyl, (1H)-phenyl), 7.44 – 7.30 (m, 4H, (2H)-phenyl, (2H)-quinoxaline), 7.14 (dd, *J* = 22.7, 8.0 Hz, 1H, quinoxaline).

4-benzoyl-*N*-(2-methoxyphenyl)-3-oxo-3,4-dihydroquinoxaline-2-carboxamide (QCD-10)

TLC (EtOAc:Hexane 30:70); Yield: 68%; White solid; mp: 152-154°C; IR (KBr, *v* cm^{-1}): 3226 (sharp, N–H str.), 3112, 3039, 2960, 2827, 2673, 2630 (aromatic C-H str.), 1745 (benzoyl keto C=O str.), 1692 (keto C=O str.), 1685 (amide C=O str.), 1651, 1590, 1522 (C=C, C=N ring str.), 1487, 1471, 1421 (CH_2 bend.), 1359, 1309, 1240 (C=C bend.), 1099, 1037 (ether C-O bend.); ^{1}H NMR (400 MHz, DMSO) δ 10.13 (s, 1H, amide), 8.02 (d, *J* = 7.2 Hz, 2H, benzoyl), 7.80 (d, *J* = 7.4 Hz, 4H, (1H)-quinoxaline, (3H)-benzoyl), 7.77 (s, 1H, quinoxaline), 7.57 (d, *J* = 8.0 Hz, 2H, phenyl), 7.41 (t, *J* = 8.1 Hz, 2H, (1H)-quinoxaline, (1H)-phenyl), 6.85 (dd, *J* = 8.1, 2.0 Hz, 2H, (1H)-quinoxaline, (1H)-phenyl), 3.77 (s, 3H, OCH_3).

4-benzoyl-3-oxo-*N*-(2-propylphenyl)-3,4-dihydroquinoxaline-2-carboxamide (QCD-11)

TLC (EtOAc:Hexane 30:70); Yield: 59%; White solid; mp: 224-226 °C; IR (KBr, *v* cm^{-1}): 3244 (sharp, N–H str.), 3226, 3168, 3132, 3064, 2950, 2836, 2684, 2650 (aromatic C-H str.), 1745 (benzoyl keto C=O str.), 1692 (keto C=O str.), 1683 (amide C=O str.), 1665, 1595, 1522 (C=C, C=N ring str.), 1487, 1471, 1421 (CH_2 bend.), 1360, 1309, 1238 (C=C bend.); ^{1}H NMR (400 MHz, DMSO) δ 9.81 (s, 1H, amide), 8.02 – 7.96 (m, 2H, benzoyl), 7.70 – 7.64 (m, 1H, quinoxaline), 7.53 – 7.43 (m, 3H, benzoyl), 7.34 – 7.30 (m, 1H, quinoxaline), 7.28 – 7.18 (m, 5H, (4H)-phenyl, (1H)-quinoxaline), 7.14 – 7.08 (m, 1H, quinoxaline), 2.76 – 2.68 (m, 2H, $CH_2CH_2CH_3$), 1.01 (t, J = 7.3 Hz, 2H, $CH_2CH_2CH_3$), 0.89 (t, J = 7.3 Hz, 3H, $CH_2CH_2CH_3$).

4-benzoyl-*N*-(2-isopropylphenyl)-3-oxo-3,4-dihydroquinoxaline-2-carboxamide (QCD-12)

TLC (EtOAc:Hexane 30:70); Yield: 60%; White solid; mp: 240-242 °C; IR (KBr, *v* cm^{-1}): 3268 (sharp, N–H str.), 3124, 3115, 3066, 2974, 2839, 2686, 2650 (aromatic C-H str.), 1745 (benzoyl keto C=O str.), 1690 (keto C=O str.), 1682 (amide C=O str.), 1656, 1597, 1520 (C=C, C=N ring str.), 1475, 1468, 1420 (CH_2 bend.), 1360, 1312, 1240 (C=C bend.); ^{1}H NMR (400 MHz, DMSO) δ 11.54 (s, 1H, amide), 7.99 (dd, *J* = 11.7, 7.9 Hz, 2H, benzoyl), 7.67 (t, *J* = 7.4 Hz, 1H, quinoxaline), 7.55 – 7.40 (m, 3H, benzoyl), 7.35 (d, *J* = 7.0 Hz, 2H, (1H)-quinoxaline, (1H)-phenyl), 7.29 – 7.15 (m, 5H, (2H)-quinoxaline, (3H)-pheny), 2.85 (dt, *J* = 13.7, 6.9 Hz, 1H, $CH(CH_3)_2$), 1.27 (d, *J* = 6.7 Hz, 6H, $CH(CH_3)_2$).

4-benzoyl-*N*-(4-isopropylphenyl)-3-oxo-3,4-dihydroquinoxaline-2-carboxamide (QCD-13)

TLC (EtOAc:Hexane 30:70); Yield: 75%; White solid; mp: 242-244 °C; IR (KBr, *v* cm^{-1}): 3245 (sharp, N–H str.), 3226, 3174, 3082, 2985, 2857, 2783, 2680 (aromatic C-H str.), 1745 (benzoyl keto C=O str.), 1697 (keto C=O str.), 1685 (amide C=O str.), 1651, 1593, 1519 (C=C, C=N ring str.), 1487, 1471, 1421 (CH_2 bend.), 1359, 1309, 1240 (C=C bend.); ^{1}H NMR (400 MHz, DMSO) δ 10.08 (s, 1H, amide), 7.96 (d, *J* = 7.2 Hz, 2H, benzoyl), 7.68 (d, *J* = 8.4 Hz, 1H, quinoxaline), 7.55 – 7.40 (m, 3H, benzoyl), 7.49 (d, *J* = 7.5 Hz, 2H, phenyl), 7.29 – 7.20 (m, 3H, (1H)-quinoxaline, (2H)-pheny), 7.15 (d, *J* = 8.3 Hz, 2H, quinoxaline), 2.88 (dt, *J* = 13.7, 6.9 Hz, 1H, $CH(CH_3)_2$), 1.22 (d, *J* = 6.9 Hz, 6H, $CH(CH_3)_2$).

4-benzoyl-*N*-(2-chloro-4-methylphenyl)-3-oxo-3,4-dihydroquinoxaline-2-carboxamide (QCD-14)

TLC (EtOAc:Hexane 30:70); Yield: 40%; White solid; mp: >250 °C; IR (KBr, *v*cm^{-1}): 3275 (sharp, N–H str.), 3284, 3176, 3040, 2975, 2837, 2755, 2679 (aromatic C-H str.), 1745 (benzoyl keto C=O str.), 1695 (keto C=O str.), 1665 (amide C=O str.), 1630, 1590, 1520 (C=C, C=N ring str.), 1490, 1472, 1421 (CH_2 bend.), 1359, 1321, 1264, 1170 (C=C bend.); ^{1}H NMR (400 MHz, DMSO) δ 10.18 (s, 1H, amide), 8.12 (d, *J* = 7.2 Hz, 2H, benzoyl), 7.80 – 7.74 (m, 1H, quinoxaline), 7.65 – 7.50 (m, 4H, (3H)-benzoyl,. (1H)-phenyl), 7.39 (d, *J* = 7.5 Hz, 2H, (1H)-quinoxaline, (1H)-phenyl), 7.15 – 7.05 (m, 3H, (2H)-quinoxaline, (1H)-phenyl), 2.33 (s, 3H, CH_3).

4-benzoyl-*N*-(2-chloro-5-methylphenyl)-3-oxo-3,4-dihydroquinoxaline-2-carboxamide (QCD-15)

TLC (EtOAc:Hexane 30:70); Yield: 30%; White solid; mp: >250 °C; IR (KBr, *v* cm^{-1}): 3300 (sharp, N–H str.), 3284, 3236, 3153, 3122, 3045, 2920, 2844, 2674, 2630 (aromatic C-H str.), 1745 (benzoyl keto C=O str.), 1695 (keto C=O str.), 1685 (amide C=O str.), 1660, 1595, 1522 (C=C, C=N ring str.), 1487, 1469, 1420 (CH_2 bend.), 1360, 1310, 1235 (C=C bend.); ^{1}H NMR (400 MHz, DMSO) δ 10.22 (s, 1H, amide), 8.08 (d, *J* = 7.2 Hz, 2H, benzoyl), 7.85 – 7.79 (m, 1H, quinoxaline), 7.75 – 7.60 (m, 4H, (3H)-benzoyl, (1H)-phenyl), 7.50 (d, *J* = 7.5 Hz, 2H, (1H)-quinoxaline, (1H)-phenyl), 7.29 (t, *J* = 7.8 Hz, 1H, quinoxaline), 7.25 – 7.10 (m, 2H, (1H)-quinoxaline, (1H)-phenyl), 2.33 (s, 3H, CH_3).

4-benzoyl-*N*-(2-chloro-6-methylphenyl)-3-oxo-3,4-dihydroquinoxaline-2-carboxamide (QCD-16)

TLC (EtOAc:Hexane 30:70); Yield: 45%; White solid; mp: >250 °C; IR (KBr, *v* cm^{-1}): 3284 (sharp, N–H str.), 3226, 3138, 3100, 3055, 2950, 2836, 2650 (aromatic C-H str.), 17453 (benzoyl keto C=O str.), 1695 (keto C=O str.), 1685 (amide C=O str.), 1660, 1595, 1520 (C=C, C=N ring str.), 1487, 1471, 1421 (CH_2 bend.), 1360, 1310, 1240 (C=C bend.); ^{1}H NMR (400 MHz, DMSO) δ 10.08 (s, 1H, amide), 8.05 (d, *J* = 7.2 Hz, 2H, benzoyl), 7.89 – 7.79 (m, 1H, quinoxaline), 7.75 – 7.65 (m, 3H, benzoyl, 7.48 (d, *J* = 7.5 Hz, 2H, (1H)-quinoxaline, (1H)-phenyl), 7.32 – 7.17 (m, 2H, (1H)-phenyl, (1H)-quinoxaline), 7.10 – 6.98 (m, 2H, (1H)-quinoxaline, (1H)-phenyl), 2.20 (s, 3H, CH_3).

4-benzoyl-*N*-(3-chloro-2-methylphenyl)-3-oxo-3,4-dihydroquinoxaline-2-carboxamide (QCD-17)

TLC (EtOAc:Hexane 30:70); Yield: 48%; White solid; mp: >250 °C; IR (KBr, *v* cm^{-1}): 3266 (sharp, N–H str.), 3214, 3136, 3115, 3065, 2847, 2764, 2632, 2559 (aromatic C-H str.), 1747 (benzoyl keto C=O str.), 1694 (keto C=O str.), 1679 (amide C=O str.), 1669, 1594, 1521 (C=C, C=N ring str.),1475, 1463, 1429 (CH_2 bend.), 1359, 1310, 1240 (C=C bend.); ^{1}H NMR (400 MHz, DMSO) δ 10.12 (s, 1H, amide), 8.06 (d, *J* = 7.2 Hz, 2H, benzoyl), 7.87 – 7.80 (m, 1H, quinoxaline), 7.77 – 7.57 (m, 3H, benzoyl), 7.48 (d, *J* = 7.5 Hz, 2H, (1H)-quinoxaline, (1H)-phenyl), 7.29 – 7.10 (m, 4H, (2H)-quinoxaline, (2H)-phenyl), 2.27 (s, 3H, CH_3).

4-benzoyl-3-oxo-*N*-(2-(trifluoromethyl)phenyl)-3,4-dihydroquinoxaline-2-carboxamide (QCD-18)

TLC (EtOAc:Hexane 30:70); Yield: 28%; White solid; mp: 204-206 °C; IR (KBr, *v* cm^{-1}): 3320 (sharp, N–H str.), 3226, 3168, 3132, 3064, 2950, 2836, 2684, 2650 (aromatic C-H str.), 1745 (benzoyl keto C=O str.), 1692 (keto C=O str.), 1683 (amide C=O str.), 1665, 1595, 1522 (C=C, C=N ring str.), 1487, 1471, 1421 (CH_2 bend.), 1360, 1309, 1238 (C=C bend.); ^{1}H NMR (400 MHz, DMSO) δ 10.16 (s, 1H, amide), 8.05 (d, *J* = 7.6 Hz, 2H, benzoyl), 7.85 – 7.78 (m, 1H, quinoxaline), 7.80 – 7.60 (m, 4H, (3H)-benzoyl, (1H)-phenyl), 7.50 – 7.30 (m, 4H, (3H)-phenyl, (1H)-quinoxaline), 7.12 (d, *J* = 8.3 Hz, 2H, quinoxaline).

4.3.5. Series-5: 3-oxo-*N*-phenyl-4-(2-phenylacetyl)-3,4-dihydroquinoxaline-2-carboxamide analogues (QCE-1 to 19)

Ethyl 3-oxo-4-(2-phenylacetyl)-3,4-dihydroquinoxaline-2-carboxylate (QC-2E)

5 g (0.023 mol) of ethyl 3-oxo-3,4-dihydroquinoxaline-2-carboxylate was dissolved in 75 ml of DMF in a 250 ml RBF and stirred at room temperature for 30 min. To the above solution, 9.50 g (0.069 mol) of potassium carbonate was added and the mixture stirred at room temperature for 1 hr. 4.56 g (0.023 mol) of phenacyl bromide was gradually added in portions and stirring was continued at room temperature overnight. The obtained suspension was poured into 200 ml of cold water and product extracted with ethylacetate (3 × 25 ml). The combined extracts were washed with brine solution and dried with sodium sulfate. Evaporation of solvent gave crude compound and the resultant solid residue was then washed with hexane, filtered, to afford the desired compound. TLC (EtOAc:Hex 50:50); Yield: 62%; Pale yellow solid; mp: 210-212 °C; IR (KBr, *v* cm^{-1}): 3283, 3165, 3076, 2945 (aromatic C-H str.), 2875, 2734, 2637 (aromatic C-H str.), 1735 (phenacyl C=O str.), 1721 (keto C=O str.), 1687 (amide C=O str.), 1587, 1518 (C=C, C=N ring str.), 1484, 1465 (CH_2 bend), 1394 (CH_3 bend), 1283, 1224, 1139 (C=C bend), 1095, 1044 (ether C-O bend.); ^{1}H NMR (400 MHz, DMSO) δ 7.96 (dd, *J* = 8.1, 1.4 Hz, 1H, quinoxaline), 7.67 (dtd, *J* = 8.6, 7.3, 1.6 Hz, 1H, quinoxaline), 7.47 – 7.39 (m, 2H, phenacyl), 7.34 – 7.25 (m, 3H, phenacyl), 7.15 (t, *J* = 7.4 Hz, 2H, quinoxaline), 4.41 (q, *J* = 7.1 Hz, 2H, OCH_2CH_3), 3.34 (s, 2H, benzylic methylene), 1.34 (t, *J* = 7.1 Hz, 3H, OCH_2CH_3).

3-oxo-4-(2-phenylacetyl)-3,4-dihydroquinoxaline-2-carboxylic acid (QC-3E)

1 g (0.0030 mol) of ethyl 3-oxo-4-(2-phenylacetyl)-3,4-dihydroquinoxaline-2-carboxylate was dissolved in 5 ml of dry THF in a 100 ml RBF. To this mixture, 50% aqueous sodium hydroxide solution (*pH*>10) was added and stirred at room temperature for 2 hr. The solvent was removed under vacuum; residue washed with ethylacetate and the aqueous portion was acidified with dil. HCl (*pH*=5). The obtained solid residue was washed with cold water, filtered and recrystallized with EtOH to afford the desired compound. TLC (EtOAc:Hex 30:70); Yield: 60%; Pale Yellow solid; mp: 184-186 °C; IR (KBr, *v* cm^{-1}): 3478 (broad O–H str. COOH), 3316, 3245, 3196, 3154, 3062, 2861 (aromatic C-H str.), 1732 (phenacyl C=O str.), 1714 (keto C=O str.), 1680 (amide C=O str.), 1597, 1520 (C=C, C=N ring str.), 1432, 1385, 1273, 1100 (C=C bend); ^{1}H NMR (400 MHz, DMSO) δ 12.24 (s, 1H, acid), 8.18 (dd, *J* = 8.1, 1.4 Hz, 1H, quinoxaline), 7.84 (dtd, *J* = 8.6, 7.3, 1.6 Hz, 1H, quinoxaline), 7.68 – 7.57 (m, 2H, phenacyl), 7.54 – 7.45 (m, 3H, phenacyl), 7.36 (t, *J* = 7.4 Hz, 2H, quinoxaline), 3.38 (s, 2H, benzylic methylene).

General procedure for the synthesis of New Chemical Entity's (NCE's) i.e. quinoxaline-2-carboxamide analogues (QCE-1 to 19)

To 0.5 g (0.0016 mol) of 3-oxo-4-(2-phenylacetyl)-3,4-dihydroquinoxaline-2-carboxylic acid taken in a 100 ml RBF, 0.37 g (0.0019 mol) of EDC·HCl was added and stirred with 5 ml of dry THF in an inert atmosphere (nitrogen) at 0 °C for 15 min. To the above reaction mixture, 0.37 g (0.0024 mol) HOBt was added and stirred for another 45 min. To the above mixture, 1 equivalent of appropriate amines were added and stirred continuously for 6 hr. The reaction mixture was concentrated under reduced pressure; resultant mass diluted with DCM/ethyl acetate, washed with aqueous sodium bicarbonate (2 × 50 ml), saturated brine solution (2 × 50 ml) and dried over anhydrous sodium sulfate. The solvent was then evaporated under reduced pressure to afford the desired compounds. The obtained compounds were purified by recrystallization with EtOH/MeOH/column chromatography over silica gel.

3-oxo-*N*-phenyl-4-(2-phenylacetyl)-3,4-dihydroquinoxaline-2-carboxamide (QCE-1)

TLC (EtOAc:Hexane 30:70); Yield: 66%; White solid; mp: 184-186 °C; IR (KBr, *v* cm^{-1}): 3474 (sharp, N–H str.), 3287, 3176, 2962, 2895, 2797 (aromatic C-H str.), 1745 (phenacyl keto C=O str.), 1702 (keto C=O str.), 1687 (amide C=O str.), 1586, 1544 (C=C, C=N ring str.), 1426, 1394, 1376 (CH_2 bend), 1284, 1168, 1045 (C=C bend); ^{1}H NMR (400 MHz, DMSO) δ 11.06 (s, 1H, amide), 7.97 (d, *J* = 7.9 Hz, 1H, quinoxaline), 7.72 (t, *J* = 7.4 Hz, 2H, phenyl), 7.68 – 7.63 (m, 3H, (1H)-quinoxaline, (2H)-phenyl), 7.56 – 7.42 (m, 5H, phenacyl), 7.32 – 7.30 (m, 2H, (1H)-quinoxaline, (1H)-phenyl), 7.24 (dd, *J* = 20.3, 11.7 Hz, 1H, quinoxaline), 3.35 (s, 2H, benzylic methylene).

***N*-(2-methoxyphenyl)-3-oxo-4-(2-phenylacetyl)-3,4-dihydroquinoxaline-2-carboxamide (QCE-2)**

TLC (EtOAc:Hexane 30:70); Yield: 40%; White solid; mp: 158-160 °C; IR (KBr, *v* cm^{-1}): 3482 (sharp, N–H str.), 3373, 3291, 3185, 2963, 2897, 2781 (aromatic C-H str.), 1747 (phenacyl keto C=O str.), 1700 (keto C=O str.), 1680 (amide C=O str.), 1585, 1557 (C=C, C=N ring str.), 1440, 1386, 1375 (CH_2 bend), 1289, 1177, 1149 (C=C bend), 1093, 1057 (ether C-O bend.); ^{1}H NMR (400 MHz, DMSO) δ 11.12 (s, 1H, amide), 8.12 – 8.05 (m, 2H, (1H)-phenyl, (1H)-quinoxaline), 7.75 (dd, *J* = 8.0, 1.3 Hz, 1H, quinoxaline), 7.66 – 7.53 (m, 5H, phenacyl), 7.48 (t, *J* = 7.4 Hz, 1H, quinoxaline), 7.37 – 7.22 (m, 4H, (1H)-quinoxaline, (3H)-phenyl), 3.77 (s, 2H, benzylic methylene), 3.35 (s, 3H, OCH_3).

***N*-(3-methoxyphenyl)-3-oxo-4-(2-phenylacetyl)-3,4-dihydroquinoxaline-2-carboxamide (QCE-3)**

TLC (EtOAc:Hexane 30:70); Yield: 44%; White solid; mp: 166-168 °C; IR (KBr, *v* cm^{-1}): 3456 (sharp, N–H str.), 3275, 3189, 2965, 2898, 2785 (aromatic C-H str.), 1740 (phenacyl keto C=O str.), 1710 (keto C=O str.), 1695 (amide C=O str.), 1587, 1560 (C=C, C=N ring str.), 1446, 1385, 1374 (CH_2 bend), 1290, 1187, 1125 (C=C bend), 1087, 1065 (ether C-O bend.); ^{1}H NMR (400 MHz, DMSO) δ 11.19 (s, 1H, amide), 8.16 (d, *J* = 7.4 Hz, 2H, quinoxaline), 8.07 – 7.98 (m, 1H, phenyl), 7.78 – 7.54 (m, 4H, phenacyl), 7.51 – 7.42 (m, 3H, (1H)-phenacyl, (2H)-phenyl), 7.23 (d, *J* = 5.0 Hz, 2H, quinoxaline), 6.68 (dd, *J* = 7.5, 4.0 Hz, 1H, phenyl), 3.79 (s, 2H, benzylic methylene), 3.36 (s, 3H, OCH_3).

***N*-(4-methoxyphenyl)-3-oxo-4-(2-phenylacetyl)-3,4-dihydroquinoxaline-2-carboxamide (QCE-4)**

TLC (EtOAc:Hexane 30:70); Yield: 56%; White solid; mp: 174-176 °C; IR (KBr, *v* cm^{-1}): 3465 (sharp, N–H str.), 3315, 3276, 3185, 2962, 2867 (aromatic C-H str.), 1742 (phenacyl keto C=O str.), 1710 (keto C=O str.), 1695 (amide C=O str.), 1586, 1565 (C=C, C=N ring str.), 1426, 1390, 1366 (CH_2 bend), 1287, 1162, 1114 (C=C bend) 1097, 1021 (ether C-O bend.); ^{1}H NMR (400 MHz, DMSO) δ 10.98 (s, 1H, amide), 8.21 – 8.14 (m, 2H, (1H)-phenyl, (1H)-quinoxaline), 8.01 (dd, *J* = 8.0, 1.3 Hz, 1H, quinoxaline), 7.73 (t, *J* = 7.4 Hz, 1H, phenacyl), 7.70 – 7.57 (m, 6H, (4H)-phenacyl, (2H)-quinoxaline), 7.55 – 7.44 (m, 2H, phenyl), 6.90 (dd, *J* = 9.7, 2.6 Hz, 1H, phenyl), 3.77 (s, 2H, benzylic methylene), 3.35 (s, 3H, OCH_3).

3-oxo-4-(2-phenylacetyl)-*N*-o-tolyl-3,4-dihydroquinoxaline-2-carboxamide (QCE-5)

TLC (EtOAc:Hexane 30:70); Yield: 44%; White solid; mp: 162-164 °C; IR (KBr, *v* cm^{-1}): 3490, 3426 (sharp, N–H str.), 3330, 3255, 3176, 2960, 2892, 2797 (aromatic C-H str.), 1749 (phenacyl keto C=O str.), 1710 (keto C=O str.), 1687 (amide C=O str.),1586, 1554 (C=C, C=N ring str.), 1435, 1390, 1376 (CH_2 bend), 1279, 1167, 1045, 965 (C=C bend); ^{1}H NMR (400 MHz, DMSO) δ 10.09 (s, 1H, amide), 7.95 (d, *J* = 7.9 Hz, 1H, quinoxaline), 7.49 (d, *J* = 18.6 Hz, 1H, quinoxaline), 7.48 – 7.36 (m, 4H, (2H)-phenyl, (2H)-phenacyl), 7.17 (t, *J* = 7.7 Hz, 4H, (1H)-phenyl, (3H)-phenacyl), 7.09 – 7.02 (m, 1H, quinoxaline), 7.02 (d, *J* = 13.8 Hz, 2H, (1H)-quinoxaline, (1H)-phenyl), 3.54 (s, 2H, benzylic methylene), 2.14 (s, 3H, CH_3).

3-oxo-4-(2-phenylacetyl)-*N*-m-tolyl-3,4-dihydroquinoxaline-2-carboxamide (QCE-6)

TLC (EtOAc:Hexane 30:70); Yield: 40%; White solid; mp: 162-194 °C; IR (KBr, *v* cm^{-1}): 3487, 3424 (sharp, N–H str.), 3285, 3163, 2971, 2890, 2700 (aromatic C-H str.), 1747 (phenacyl keto C=O str.), 1715 (keto C=O str.), 1680 (amide C=O str.), 1575, 1536 (C=C, C=N ring str.), 1428, 1395, 1364 (CH_2 bend), 1280, 1172, 1049, 967 (C=C bend); ^{1}H NMR (400 MHz, DMSO) δ 10.57 (s, 1H, amide), 7.74 (t, *J* = 7.3 Hz, 2H, (1H)-quinoxaline, (1H)-phenyl), 7.61 (d, *J* = 7.6 Hz, 2H, (1H)-phenyl, (1H)-quinoxaline), 7.58 – 7.44 (m, 6H, (5H)-phenacyl, (1H)-phenyl), 7.23 (t, *J* = 7.8 Hz, 2H, quinoxaline), 6.94 (d, *J* = 7.4 Hz, 1H, phenyl), 3.32 (s, 2H, benzylic methylene), 2.34 (s, 3H, CH_3).

3-oxo-4-(2-phenylacetyl)-*N*-p-tolyl-3,4-dihydroquinoxaline-2-carboxamide (QCE-7)

TLC (EtOAc:Hexane 30:70); Yield: 62%; White solid; mp: 206-208 °C; IR (KBr, *v* cm^{-1}): 3470 (sharp, N–H str.), 3292, 3179, 2960, 2899, 2785 (aromatic C-H str.), 1738 (phenacyl keto C=O str.), 1710 (keto C=O str.), 1680 (amide C=O str.), 1585, 1547 (C=C, C=N ring str.), 1425, 1392, 1360 (CH_2 bend), 1282, 1166, 1047, 984 (C=C bend); ^{1}H NMR (400 MHz, DMSO) δ 10.58 (s, 1H, amide), 7.99 (dd, *J* = 8.0, 1.2 Hz, 2H, quinoxaline), 7.46 (t, *J* = 7.6 Hz, 2H, phenacyl), 7.29 – 7.15 (m, 8H, (3H)-phenacyl, (4H)-phenyl, (1H)-quinoxaline), 7.08 (s, 1H, quinoxaline), 4.04 (q, *J* = 7.1 Hz, 2H, benzylic methylene), 2.46 (s, 3H, CH_3).

***N*-(2-chlorophenyl)-3-oxo-4-(2-phenylacetyl)-3,4-dihydroquinoxaline-2-carboxamide (QCE-8)**

TLC (EtOAc:Hexane 30:70); Yield: 46%; White solid; mp: 160-162 °C; IR (KBr, *v* cm^{-1}): 3490, 3426 (sharp, N–H str.), 3330, 3255, 3176, 2960, 2892, 2797 (aromatic C-H str.), 1749 (phenacyl keto C=O str.), 1710 (keto C=O str.), 1687 (amide C=O str.), 1575, 1536 (C=C, C=N ring str.), 1428, 1395, 1364 (CH_2 bend), 1280, 1172, 1049, 967 (C=C bend); ^{1}H NMR (400 MHz, DMSO) δ 10.56 (s, 1H, amide), 8.57 – 8.47 (m, 1H, phenyl), 8.12 (d, *J* = 7.9 Hz, 1H, quinoxaline), 7.72 (d, *J* = 8.4 Hz, 1H, phenyl), 7.49 (dd, *J* = 8.0, 1.3 Hz, 1H, quinoxaline), 7.38 (t, *J* = 8.5 Hz, 2H, phenacyl), 7.39 – 7.18 (m, 2H, (1H)-phenyl, (1H)-phenacyl), 7.20 – 7.09 (m, 2H, phenacyl), 7.05 – 6.98 (m, 2H, (1H)-quinoxaline, (1H)-phenyl), 6.85 (dd, *J* = 20.3, 11.7 Hz, 1H, quinoxaline), 3.31 (s, 2H, benzylic methylene).

_N_-(3-chlorophenyl)-3-oxo-4-(2-phenylacetyl)-3,4-dihydroquinoxaline-2-carboxamide (QCE-9)

TLC (EtOAc:Hexane 30:70); Yield: 44%; White solid; mp: 180-182 °C; IR (KBr, *v* cm^{-1}): 3456 (sharp, N–H str.), 3275, 3189, 2965, 2898, 2785 (aromatic C-H str.), 1740 (phenacyl keto C=O str.), 1710 (keto C=O str.), 1695 (amide C=O str.), 1586, 1565 (C=C, C=N ring str.), 1426, 1390, 1366 (CH_2 bend), 1287, 1162, 1041 (C=C bend); ^{1}H NMR (400 MHz, DMSO) δ 10.59 (s, 1H, amide), 7.99 (dd, *J* = 8.0, 1.4 Hz, 1H, phenyl), 7.94 (t, *J* = 2.0 Hz, 1H, quinoxaline), 7.62 – 7.55 (m, 2H, (1H)-phenyl, (1H)-quinoxaline), 7.53 – 7.43 (m, 5H, (2H)-phenyl, (3H)-phenacyl), 7.37 (t, *J* = 8.1 Hz, 2H, phenacyl), 7.16 (ddd, *J* = 8.0, 2.0, 0.8 Hz, 2H, quinoxaline), 3.31 (s, 2H, benzylic methylene).

_N_-(4-chlorophenyl)-3-oxo-4-(2-phenylacetyl)-3,4-dihydroquinoxaline-2-carboxamide (QCE-10)

TLC (EtOAc:Hexane 30:70); Yield: 70%; White solid; mp: 198-200 °C; IR (KBr, *v* cm^{-1}): 3490 (sharp, N–H str.), 3330, 3255, 3176, 2960, 2892, 2797 (aromatic C-H str.), 1749 (phenacyl keto C=O str.), 1710 (keto C=O str.), 1687 (amide C=O str.), 1585, 1557 (C=C, C=N ring str.), 1440, 1386, 1375 (CH_2 bend), 1289, 1177, 1049 (C=C bend); ^{1}H NMR (400 MHz, DMSO) δ 10.58 (s, 1H, amide), 8.17 (d, *J* = 7.3 Hz, 1H, quinoxaline), 7.99 (dd, *J* = 8.0, 1.1 Hz, 2H, phenyl), 7.55 (d, *J* = 8.3 Hz, 2H, phenyl), 7.47 (t, *J* = 7.5 Hz, 1H, quinoxaline), 7.36 (dd, *J* = 8.2, 5.3 Hz, 5H, phenacyl), 7.18 (d, *J* = 8.7 Hz, 1H, quinoxaline), 6.79 (d, *J* = 7.5 Hz, 1H, quinoxaline), 3.44 (s, 2H, benzylic methylene).

3-oxo-4-(2-phenylacetyl)-_N_-(2-propylphenyl)-3,4-dihydroquinoxaline-2-carboxamide (QCE-11)

TLC (EtOAc:Hexane 30:70); Yield: 58%; White solid; mp: 210-212 °C; IR (KBr, *v* cm^{-1}): 3485, 3417 (sharp, N–H str.), 3325, 3247, 3168, 2953, 2874, 2796 (aromatic C-H str.), 1742 (phenacyl keto C=O str.), 1706 (keto C=O str.), 1686 (amide C=O str.), 1587, 1549 (C=C, C=N ring str.), 1436, 1382, 1375 (CH_2 bend), 1289, 1165, 1050, 956 (C=C bend); ^{1}H NMR (400 MHz, DMSO) δ 10.60 (s, 1H, amide), 8.06 (dd, *J* = 8.0, 1.3 Hz, 1H, quinoxaline), 7.96 (d, *J* = 9.7 Hz, 1H, quinoxaline), 7.78 – 7.66 (m, 3H, phenacyl), 7.62 (dt, *J* = 10.5, 7.1 Hz, 3H, (2H)-phenacyl, (1H)-phenyl), 7.55 – 7.47 (m, 2H, phenyl), 7.30 – 7.19 (m, 2H, (1H)-quinoxaline, (1H)-phenyl), 7.14 (dd, *J* = 11.0, 3.7 Hz, 1H, quinoxaline), 3.36 (s, 2H, benzylic methylene), 2.69 – 2.60 (m, 2H, $CH_2CH_2CH_3$), 1.60 (dq, *J* = 14.7, 7.3 Hz, 2H, $CH_2CH_2CH_3$), 0.90 (t, *J* = 7.3 Hz, 3H, $CH_2CH_2CH_3$).

_N_-(2-isopropylphenyl)-3-oxo-4-(2-phenylacetyl)-3,4-dihydroquinoxaline-2-carboxamide (QCE-12)

TLC (EtOAc:Hexane 30:70); Yield: 54%; White solid; mp: 220-222 °C; IR (KBr, *v* cm^{-1}): 3470 (sharp, N–H str.), 3292, 3179, 2960, 2899, 2785 (aromatic C-H str.), 1738 (phenacyl keto C=O str.), 1710 (keto C=O str.), 1680 (amide C=O str.), 1586, 1544 (C=C, C=N ring str.), 1426, 1394, 1376 (CH_2 bend), 1284, 1168, 1045, 958 (C=C bend); ^{1}H NMR (400 MHz, DMSO) δ 11.02 (s, 1H, amide), 8.06 (dd, *J* = 8.0, 1.1 Hz, 1H, quinoxaline), 7.87 – 7.83 (m, 1H, quinoxaline), 7.67 – 7.59 (m, 5H, phenacyl), 7.56 (d, *J* = 8.4 Hz, 2H, phenyl), 7.49 (t, *J* = 7.5 Hz, 1H, phenyl), 7.34 (dd, *J* = 7.0, 2.3 Hz, 2H, (1H)-quinoxaline, (1H)-phenyl), 7.23 – 7.19 (m, 1H, quinoxaline), 3.31 (s, 1H, benzylic methylene), 2.55 – 2.48 (m, 1H, $CH(CH_3)_2$), 1.23 (d, *J* = 6.8 Hz, 6H, $CH(CH_3)_2$).

_N_-(4-isopropylphenyl)-3-oxo-4-(2-phenylacetyl)-3,4-dihydroquinoxaline-2-carboxamide (QCE-13)

TLC (EtOAc:Hexane 30:70); Yield: 72%; White solid; mp: 240-242 °C; IR (KBr, *v* cm^{-1}): 3485, 3427 (sharp, N–H str.), 3289, 3165, 2970, 2892, 2713 (aromatic C-H str.), 1745 (phenacyl keto C=O str.), 1715 (keto C=O str.), 1680 (amide C=O str.), 1575, 1536 (C=C, C=N ring str.), 1430, 1395, 1365 (CH_2 bend), 1280, 1172, 1049, 967 (C=C bend); ^{1}H NMR (400 MHz, DMSO) δ 10.96 (s, 1H, amide), 8.00 (dd, *J* = 8.0, 1.3 Hz, 1H, quinoxaline), 7.75 (t, *J* = 7.4 Hz, 2H, phenyl), 7.68 (d, *J* = 1.4 Hz, 1H, quinoxaline), 7.64 (ddd, *J* = 15.6, 8.0, 4.5 Hz, 5H, phenacyl), 7.55 (d, *J* = 8.4 Hz, 2H, phenyl), 7.47 (t, *J* = 7.2 Hz, 1H, quinoxaline), 7.21 (d, *J* = 8.5 Hz, 1H, quinoxaline), 3.33 (s, 2H, benzylic methylene), 2.89 (dt, *J* = 13.7, 6.8 Hz, 1H, $CH(CH_3)_2$), 1.22 (d, *J* = 6.9 Hz, 6H, $CH(CH_3)_2$).

_N_-(2-chloro-4-methylphenyl)-3-oxo-4-(2-phenylacetyl)-3,4-dihydroquinoxaline-2-carboxamide (QCE-14)

TLC (EtOAc:Hexane 30:70); Yield: 32%; White solid; mp: >250 °C; IR (KBr, *v* cm^{-1}): 3470 (sharp, N–H str.), 3292, 3179, 2960, 2899, 2785 (aromatic C-H str.), 1738 (phenacyl keto C=O str.), 1710 (keto C=O str.), 1680 (amide C=O str.), 1585, 1547 (C=C, C=N ring str.), 1425, 1392, 1360 (CH_2 bend), 1282, 1166, 1047, 984 (C=C bend); ^{1}H NMR (400 MHz, DMSO) δ 10.65 (s, 1H, amide), 7.97 (d, *J* = 7.3 Hz, 1H, quinoxaline), 7.89 (dd, *J* = 7.0, 1.1 Hz, 1H, phenyl), 7.71 (d, *J* = 7.6 Hz, 2H, (1H)-quinoxaline, (1H)-phenyl), 7.67 – 7.59 (m, 5H, phenacyl), 7.54 (t, *J* = 7.2 Hz, 1H, quinoxaline), 7.42 (d, *J* = 8.5 Hz, 2H, (1H)-quinoxaline, (1H)-phenyl), 3.45 (s, 2H, benzylic methylene), 2.36 (s, 3H, CH_3).

***N*-(2-chloro-5-methylphenyl)-3-oxo-4-(2-phenylacetyl)-3,4-dihydroquinoxaline-2-carboxamide (QCE-15)**

TLC (EtOAc:Hexane 30:70); Yield: 35%; White solid; mp: >250 °C; IR (KBr, *v* cm^{-1}): 3487, 3424 (sharp, N–H str.), 3285, 3179, 2970, 2890, 2782 (aromatic C-H str.), 1747 (phenacyl keto C=O str.), 1715 (keto C=O str.), 1680 (amide C=O str.), 1586, 1544 (C=C, C=N ring str.), 1426, 1394, 1376 (CH_2 bend), 1284, 1168, 1045, 958 (C=C bend); ^{1}H NMR (400 MHz, DMSO) δ 10.78 (s, 1H, amide), 7.95 (d, *J* = 7.3 Hz, 1H, quinoxaline), 7.86 (dd, *J* = 7.0, 1.1 Hz, 1H, phenyl), 7.78 (d, *J* = 1.4 Hz, 1H, quinoxaline), 7.71 – 7.64(m, 3H, (1H)-phenyl, (2H)-phenacyl), 7.57 – 7.49 (m, 3H, phenacyl), 7.34 (t, *J* = 7.2 Hz, 1H, quinoxaline), 7.22 (d, *J* = 8.5 Hz, 2H, (1H)-quinoxaline, (1H)-phenyl), 3.39 (s, 2H, benzylic methylene), 2.35 (s, 3H, CH_3).

***N*-(2-chloro-6-methylphenyl)-3-oxo-4-(2-phenylacetyl)-3,4-dihydroquinoxaline-2-carboxamide (QCE-16)**

TLC (EtOAc:Hexane 30:70); Yield: 42%; White solid; mp: >250 °C; IR (KBr, *v* cm^{-1}): 3475, 3420 (sharp, N–H str.), 3332, 3256, 3145, 2968, 2846, 2750 (aromatic C-H str.), 1748 (phenacyl keto C=O str.), 1718 (keto C=O str.), 1676 (amide C=O str.), 1582, 1545 (C=C, C=N ring str.), 1430, 1398, 1375 (CH_2 bend), 1287, 1154, 1042, 962 (C=C bend); ^{1}H NMR (400 MHz, DMSO) δ 10.85 (s, 1H, amide), 7.62 – 7.55 (m, 2H, (1H)-phenyl, (1H)-quinoxaline), 7.57 – 7.42 (m, 5H, phenacyl), 7.37 (t, *J* = 7.2 Hz, 1H, phenyl), 7.34 (t, *J* = 7.2 Hz, 1H, quinoxaline), 7.22 (d, *J* = 8.5 Hz, 2H, quinoxaline), 7.18 (d, *J* = 7.4 Hz, 1H, phenyl), 3.37 (s, 2H, benzylic methylene), 2.24 (s, 3H, CH_3).

***N*-(3-chloro-2-methylphenyl)-3-oxo-4-(2-phenylacetyl)-3,4-dihydroquinoxaline-2-carboxamide (QCE-17)**

TLC (EtOAc:Hexane 30:70); Yield: 46%; White solid; mp: >250 °C; IR (KBr, *v* cm^{-1}): 3432 (sharp, N–H str.), 3278, 3039, 2970, 2875, 2748 (aromatic C-H str.), 1744 (phenacyl keto C=O str.), 1720 (keto C=O str.), 1678 (amide C=O str.), 1576, 1558 (C=C, C=N ring str.), 1421, 1325 (CH_2 bend), 1285, 1170, 1035, 964 (C=C bend); ^{1}H NMR (400 MHz, DMSO) δ 10.70 (s, 1H, amide), 7.92 (d, *J* = 7.3 Hz, 1H, quinoxaline), 7.68 – 7.63 (m, 1H, quinoxaline), 7.57 – 7.49 (m, 3H, (1H)-phenyl, (2H)-phenacyl), 7.46 (dd, *J* = 8.0, 2.3 Hz, 3H, phenacyl), 7.40 – 7.44 (m, 3H, (2H)-phenyl, (1H)-quinoxaline), 7.28 (d, *J* = 7.4 Hz, 1H, phenyl), 3.39 (s, 2H, benzylic methylene), 2.25 (s, 3H, CH_3).

_N_-(4-chloro-2-methylphenyl)-3-oxo-4-(2-phenylacetyl)-3,4-dihydroquinoxaline-2-carboxamide (QCE-18)

TLC (EtOAc:Hexane 30:70); Yield: 45%; White solid; mp: >250 °C; IR (KBr, *v* cm^{-1}): 3456 (sharp, N–H str.), 3275, 3189, 2965, 2898, 2785 (aromatic C-H str.), 1740 (phenacyl keto C=O str.), 1710 (keto C=O str.), 1695 (amide C=O str.), 1585, 1547 (C=C, C=N ring str.), 1425, 1392, 1360 (CH_2 bend), 1282, 1166, 1047, 984 (C=C bend); ^{1}H NMR (400 MHz, DMSO) δ 10.89 (s, 1H, amide), 8.15 (d, *J* = 7.3 Hz, 1H, quinoxaline), 7.88(d, *J* = 9.7 Hz, 1H, phenyl), 7.65 – 7.58 (m, 2H, (1H)-quinoxaline, (1H)-phenyl), 7.53 – 7.44 (m, 5H, phenacyl), 7.42 (t, *J* = 7.2 Hz, 1H, phenyl), 7.38 (d, *J* = 8.5 Hz, 2H, quinoxaline), 3.39 (s, 2H, benzylic methylene), 2.25 (s, 3H, CH_3).

3-oxo-4-(2-phenylacetyl)-_N_-(2-(trifluoromethyl)phenyl)-3,4-dihydroquinoxaline-2-carboxamide (QCE-19)

TLC (EtOAc:Hexane 30:70); Yield: 42%; White solid; mp: >250 °C; IR (KBr, *v* cm^{-1}): 3487, 3424 (sharp, N–H str.), 3285, 3163, 2971, 2890, 2700 (aromatic C-H str.), 1747 (phenacyl keto C=O str.), 1715 (keto C=O str.), 1680 (amide C=O str.), 1587, 1549 (C=C, C=N ring str.), 1436, 1382, 1375 (CH_2 bend), 1289, 1165, 1050, 956 (C=C bend); ^{1}H NMR (400 MHz, DMSO) δ 10.96 (s, 1H, amide), 8.17 (d, *J* = 7.3 Hz, 1H, quinoxaline), 7.99 (dd, *J* = 7.0, 1.1 Hz, 1H, phenyl), 7.58 – 7.46 (m, 4H, (3H)-phenyl, (1H)-quinoxaline), 7.39 – 7.25 (m, 5H, phenacyl), 7.17 (t, *J* = 7.2 Hz, 1H, quinoxaline), 7.11 (d, *J* = 8.5 Hz, 1H, quinoxaline), 3.32 (s, 2H, benzylic methylene).

4.3.6. Series-6: 3-oxo-4-phenethyl-N-phenyl-3,4-dihydroquinoxaline-2-carboxamide analogues (QCF-1 to 19)

Ethyl 3-oxo-4-phenethyl-3,4-dihydroquinoxaline-2-carboxylate (QC-2F)

5 g (0.023 mol) of ethyl 3-oxo-3,4-dihydroquinoxaline-2-carboxylate was dissolved in 75 ml of DMFin a 250 ml RBF and stirred at room temperature for 30 min. To the above solution, 9.50 g (0.069 mol) of potassium carbonate was added and the mixture stirred at room temperature for 1 hr. 4.24 g (0.023 mol) of phenethyl bromide was gradually added in portions and stirring was continued at room temperature overnight. The obtained suspension was poured into 200 ml of cold water and product extracted with ethylacetate (3 × 25 ml). The combined extracts were washed with brine solution and dried over sodium sulfate. Evaporation of solvent gave crude compound and the resultant solid residue was then washed with hexane, filtered, to afford the desired compound. TLC (EtOAc:Hex 50:50); Yield: 65%; Pale yellow solid; mp: 234-236 °C; IR (KBr, *v* cm^{-1}): 3326, 3284, 3176 (aromatic C-H str.), 2426, 2365 (aromatic C-H str.), 1730 (ester C=O), 1675 (keto C=O str.), 1570, 1490 (C=C, C=N ring str.), 1465, 1420 (CH_2 bend), 1375 (CH_3 bend), 1300, 1100 (C=C bend), 1099, 1034 (ether C-O bend.); ^{1}H NMR (400 MHz, DMSO) δ 8.01 (dd, *J* = 8.2, 0.7 Hz, 1H, quinoxaline), 7.82 (dd, *J* = 8.3, 0.9 Hz, 1H, phenethyl), 7.79 – 7.72 (m, 1H, phenethyl), 7.67 – 7.59 (m, 1H), 7.36 – 7.26 (m, 4H), 7.22 (dt, *J* = 9.2, 4.3 Hz, 1H), 4.69 (t, *J* = 6.7 Hz, 2H, benzylic ethylene), 4.43 (q, *J* = 7.1 Hz, 2H, OCH_2CH_3), 3.12 (t, *J* = 6.7 Hz, 2H, benzylic ethylene), 1.37 (t, *J* = 7.1 Hz, 3H, OCH_2CH_3).

3-oxo-4-phenethyl-3,4-dihydroquinoxaline-2-carboxylic acid (QC-3F)

1 g (0.0031 mol) of ethyl 3-oxo-4-phenethyl-3,4-dihydroquinoxaline-2-carboxylate was dissolved in 5 ml of dry THF in a 100 ml RBF. To this mixture, 50% aqueous sodium hydroxide solution (*pH*>10) was added and stirred at room temperature for 2 hr. The solvent was removed under vacuum; residue washed with ethylacetate and the aqueous portion acidified with dil. HCl (*pH*=5). The obtained solid residue was washed with cold water, filtered and recrystallized with EtOH to afford the desired compound. TLC (EtOAc:Hex 25:75); Yield: 76%; Pale Yellow solid; mp: 220-222 °C; IR (KBr, *v* cm^{-1}): 3520 (broad O–H str. COOH), 3230, 3116, 3040, 2842 (aromatic C-H str.), 1736 (acid C=O str.), 1698 (keto C=O str.), 1540, 1490, 1427 (C=C, C=N ring str.), 1260, 1156 (C=C bend); ^{1}H NMR (400 MHz, DMSO) δ 8.13 (s, 1H, quinoxaline), 8.00 (dd, *J* = 8.3, 1.0 Hz, 1H, phenethyl), 7.90 (dd, *J* = 8.0, 1.4 Hz, 1H, phenethyl), 7.83 (dd, *J* = 8.4, 1.0 Hz, 2H, phenethyl), 7.77 (dt, *J* = 2.9, 1.4 Hz, 1H, phenethyl), 7.75 – 7.60 (m, 3H, quinoxaline), 4.69 (t, *J* = 6.9 Hz, 2H, benzylic ethylene), 3.05 – 2.94 (m, 2H, benzylic ethylene).

General procedure for the synthesis of New Chemical Entity's (NCE's) i.e. quinoxaline-2-carboxamide analogues (QCF-1 to 19)

To 0.5 g (0.0017 mol)of 3-oxo-4-phenethyl-3,4-dihydroquinoxaline-2-carboxylic acid taken in a 100 ml RBF, 0.39 g (0.0020 mol) of EDC·HCl was added and stirred with 5 ml of dry THF in an inert atmosphere (nitrogen) at 0 °C for 15 min. To the above reaction mixture, 0.39 g (0.0025 mol) HOBt was added and stirred for another 45 min. To the above mixture, 1 equivalent of appropriate amines were added and stirred continuously for 6 hr. The reaction mixture was concentrated under reduced pressure; resultant mass diluted with DCM/ethyl acetate, washed with aqueous sodium bicarbonate (2 × 50 ml), saturated brine solution (2 × 50 ml) and dried over anhydrous sodium sulfate. The solvent was then evaporated under reduced pressure to afford the desired compounds. The obtained compounds were purified by recrystallization with EtOH/MeOH/column chromatography over silica gel.

3-oxo-4-phenethyl-*N*-phenyl-3,4-dihydroquinoxaline-2-carboxamide (QCF-1)

TLC (EtOAc:Hexane 25:75); Yield: 70%; White solid; mp: 174-176 °C; IR (KBr, *v* cm^{-1}): 3320 (sharp, N–H str.), 3154, 2960, 2758 (aromatic C-H str.), 1747 (keto C=O str.), 1690 (amide C=O str.), 1580, 1545 (C=C, C=N ring str.), 1420, 1378 (CH_2 bend), 1280, 1040 (C=C bend); ^{1}H NMR (400 MHz, DMSO) δ 10.63 (s, 1H, amide), 8.10 – 8.01 (m, 1H, quinoxaline), 7.83 – 7.71 (m, 4H, phenyl), 7.38 (dd, *J* = 13.3, 5.1 Hz, 3H, phenethyl), 7.33 – 7.26 (m, 2H, phenethyl), 7.20 – 7.12 (m, 4H, (3H)-quinoxaline, (1H)-phenyl), 4.69 (t, *J* = 6.7 Hz, 2H, benzylic ethylene), 3.11 (t, *J* = 6.7 Hz, 2H, benzylic ethylene).

***N*-(2-methoxyphenyl)-3-oxo-4-phenethyl-3,4-dihydroquinoxaline-2-carboxamide (QCF-2)**

TLC (EtOAc:Hexane 25:75); Yield: 50%; White solid; mp: 168-170 °C; IR (KBr, *v* cm^{-1}): 3362 (sharp, N–H str.), 3284, 3176, 3055, 2954, 2780 (aromatic C-H str.), 1740 (keto C=O str.), 1700 (amide C=O str.), 1640, 1591, 1558 (C=C, C=N ring str.), 1412 (CH_2 bend), 1344, 1290 (C=C bend), 1095, 1044 (ether C-O bend.); ^{1}H NMR (400 MHz, DMSO) δ 10.09 (s, 1H, amide), 8.49 (dd, *J* = 8.0, 1.5 Hz, 1H, quinoxaline), 8.37 (dd, *J* = 8.0, 1.5 Hz, 1H, phenyl), 8.09 – 8.00 (m, 2H, phenethyl), 7.93 – 7.84 (m, 2H, phenethyl), 7.85 – 7.70 (m, 1H, phenethyl), 7.54 – 7.45 (m, 2H, quinoxaline), 7.13 – 7.05 (m, (1H)-quinoxaline, (2H)-phenyl), 7.04 – 6.95 (m, 1H, phenyl), 4.72 (t, *J* = 6.9 Hz, 2H, benzylic ethylene), 3.95 (s, 3H, OCH_3), 3.15 (t, *J* = 6.9 Hz, 2H, benzylic ethylene).

_N_-(3-methoxyphenyl)-3-oxo-4-phenethyl-3,4-dihydroquinoxaline-2-carboxamide (QCF-3)

TLC (EtOAc:Hexane 25:75); Yield: 54%; White solid; mp: 174-176 °C; IR (KBr, *v* cm^{-1}): 3360 (sharp, N–H str.), 3286, 3170, 3062, 2974, 2770 (aromatic C-H str.), 1744 (keto C=O str.), 1697 (amide C=O str.), 1595, 1560 (C=C, C=N ring str.), 1400, 1375 (CH_2 bend), 1295, 1147 (C=C bend), 1092, 1038 (ether C-O bend.); ^{1}H NMR (400 MHz, DMSO) δ 10.61 (s, 1H, amide), 8.05 (d, *J* = 8.1 Hz, 1H, quinoxaline), 7.97 (d, *J* = 7.9 Hz, 1H, phenethyl), 7.87 (d, *J* = 8.1 Hz, 1H, phenethyl), 7.78 (dd, *J* = 14.6, 7.2 Hz, 1H, phenyl), 7.74 – 7.63 (m, 3H, (1H)-phenyl, (2H)-phenethyl), 7.47 (s, 3H, (1H)-phenethyl, (2H)-quinoxaline), 7.17 (d, *J* = 6.6 Hz, 2H, (1H)-quinoxaline, (1H)-phenyl), 6.72 (d, *J* = 2.6 Hz, 1H, phenyl), 4.69 (t, *J* = 6.7 Hz, 2H, benzylic ethylene), 3.80 (d, *J* = 2.9 Hz, 3H, OCH_3), 3.11 (t, *J* = 6.6 Hz, 2H, benzylic ethylene).

_N_-(4-methoxyphenyl)-3-oxo-4-phenethyl-3,4-dihydroquinoxaline-2-carboxamide (QCF-4)

TLC (EtOAc:Hexane 25:75); Yield: 68%; White solid; mp: 188-190 °C; IR (KBr, *v* cm^{-1}): 3356 (sharp, N–H str.), 3187, 3060, 2956, 2779 (aromatic C-H str.), 1745 (keto C=O str.), 1692 (amide C=O str.), 1605, 1556 (C=C, C=N ring str.), 1402, 1378 (CH_2 bend), 1290, 1145 (C=C bend), 1095, 1037 (ether C-O bend.); ^{1}H NMR (400 MHz, DMSO) δ 10.44 (s, 1H, amide), 8.12 (d, *J* = 8.1 Hz, 1H, quinoxaline), 8.08 – 7.96 (m, 2H, phenyl), 7.86 –7.69 (m, 5H, phenethyl), 7.17 (d, *J* = 7.5 Hz, 3H, quinoxaline), 6.93 (d, *J* = 7.7 Hz, 2H, phenyl), 4.70 (s, 2H, benzylic ethylene), 3.80 (s, 3H, OCH_3), 3.12 (s, 2H, benzylic ethylene).

3-oxo-4-phenethyl-_N_-o-tolyl-3,4-dihydroquinoxaline-2-carboxamide (QCF-5)

TLC (EtOAc:Hexane 25:75); Yield: 48%; White solid; mp: 178-180 °C; IR (KBr, *v* cm^{-1}): 3367 (sharp, N–H str.), 3254, 3165, 3047, 2974, 2781 (aromatic C-H str.), 1747 (keto C=O str.), 1705 (amide C=O str.), 1605, 1598, 1556 (C=C, C=N ring str.), 1402, 1374 (CH_2 bend), 1287, 1039 (C=C bend); ^{1}H NMR (400 MHz, DMSO) δ 10.02 (s, 1H, amide), 8.07 (d, *J* = 8.3 Hz, 1H, quinoxaline), 7.88 (d, *J* = 7.4 Hz, 1H, phenethyl), 7.83 – 7.75 (m, 1H, phenethyl), 7.67 (dd, *J* = 7.5, 5.9 Hz, 3H, phenethyl), 7.33 (d, *J* = 7.0 Hz, 3H, phenyl), 7.21 (ddd, *J* = 17.8, 12.9, 7.6 Hz, 4H, (3H)-quinoxaline, (1H)-phenyl), 4.73 (t, *J* = 6.8 Hz, 2H, benzylic ethylene), 3.15 (t, *J* = 6.8 Hz, 2H, benzylic ethylene), 2.30 (s, 3H, CH_3).

3-oxo-4-phenethyl-*N*-m-tolyl-3,4-dihydroquinoxaline-2-carboxamide (QCF-6)

TLC (EtOAc:Hexane 25:75); Yield: 50%; White solid; mp: 192-194 °C; IR (KBr, *v* cm^{-1}): 3369 (sharp, N–H str.), 3284, 3216, 3176, 3065, 2976, 2781 (aromatic C-H str.), 1745 (keto C=O str.), 1715 (amide C=O str.), 1591, 1556 (C=C, C=N ring str.), 1405, 1378 (CH_2 bend), 1290, 1039 (C=C bend); ^{1}H NMR (400 MHz, DMSO) δ 10.49 (s, 1H, amide), 8.04 (d, *J* = 7.4 Hz, 1H, quinoxaline), 7.86 (d, *J* = 7.4 Hz, 1H, phenyl), 7.62 – 7.55 (m, 1H, phenyl), 7.35 (t, *J* = 7.4 Hz, 2H, phenethyl), 7.33 – 7.26 (m, 4H, (1H)-phenyl, (3H)-phenethyl), 7.24 (dt, *J* = 8.5, 4.1 Hz, 1H, quinoxaline), 7.17 (d, *J*= 6.3 Hz, 2H, quinoxaline), 7.00 – 6.93 (m, 1H, phenyl), 4.69 (t, *J* = 6.7 Hz, 2H, benzylic ethylene), 3.11 (t, *J* = 6.7 Hz, 2H, benzylic ethylene), 2.37 (s, 3H, CH_3).

3-oxo-4-phenethyl-*N*-p-tolyl-3,4-dihydroquinoxaline-2-carboxamide (QCF-7)

TLC (EtOAc:Hexane 25:75); Yield: 72%; White solid; mp: 198-200 °C; IR (KBr, *v* cm^{-1}): 3370 (sharp, N–H str.), 3286, 3220, 3182, 3065, 2974, 2785 (aromatic C-H str.), 1745 (keto C=O str.), 1715 (amide C=O str.), 1591, 1556 (C=C, C=N ring str.), 1402, 1376 (CH_2 bend), 1294, 1032 (C=C bend); ^{1}H NMR (400 MHz, DMSO) δ 10.52 (s, 1H, amide), 8.04 (d, *J* = 7.8 Hz, 1H, quinoxaline), 7.40 – 7.31 (m, 2H, phenethyl), 7.31 (dd, *J* = 5.9, 3.5 Hz, 5H, (3H)-phenethyl, (2H)-phenyl), 7.21 – 7.14 (m, 5H, (3H)-quinoxaline, (2H)-phenyl), 4.68 (t, *J* = 6.7 Hz, 2H, benzylic ethylene), 3.11 (t, *J* = 6.7 Hz, 2H, benzylic ethylene), 2.33 (s, 3H, CH_3).

***N*-(2-chlorophenyl)-3-oxo-4-phenethyl-3,4-dihydroquinoxaline-2-carboxamide (QCF-8)**

TLC (EtOAc:Hexane 25:75); Yield: 46%; White solid; mp: 166-168 °C; IR (KBr, *v* cm^{-1}): 3356 (sharp, N–H str.), 3236, 3195, 3056, 2979, 2779 (aromatic C-H str.), 1744 (keto C=O str.), 1709 (amide C=O str.), 1595, 1553 (C=C, C=N ring str.), 1402, 1385 (CH_2 bend), 1294, 1032, 971 (C=C bend); ^{1}H NMR (400 MHz, DMSO) δ 10.31 (s, 1H, amide), 8.06 (t, *J* = 7.1 Hz, 2H, (1H)-quinoxaline, (1H)-phenyl), 7.69 (d, *J* = 8.4 Hz, 1H, phenyl), 7.41 (t, *J* = 8.5 Hz, 2H, phenethyl), 7.33 (dd, *J* = 14.8, 7.1 Hz, 4H, (1H)-phenyl, (3H)-phenethyl), 7.22 (dd, *J* = 15.6, 8.5 Hz, 4H, (3H)-quinoxaline, (1H)-phenyl), 4.74 (t, *J* = 6.8 Hz, 2H, benzylic ethylene), 3.17 (t, *J* = 6.8 Hz, 2H, benzylic ethylene).

***N*-(3-chlorophenyl)-3-oxo-4-phenethyl-3,4-dihydroquinoxaline-2-carboxamide (QCF-9)**

TLC (EtOAc:Hexane 25:75); Yield: 54%; White solid; mp: 172-174 °C; IR (KBr, *v* cm^{-1}): 3362 (sharp, N–H str.), 3238, 3187, 3064, 2985, 2780 (aromatic C-H str.), 1740 (keto C=O str.), 1710 (amide C=O str.), 1590, 1545 (C=C, C=N ring str.), 1400, 1386 (CH_2

bend), 1295, 1035, 965 (C=C bend); ^{1}H NMR (400 MHz, DMSO) δ 10.81 (s, 1H, amide), 8.06 (d, *J* = 7.5 Hz, 1H, quinoxaline), 7.97 (d, *J* = 2.1 Hz, 1H, phenyl), 7.47 (t, *J* = 7.3 Hz, 1H, phenyl), 7.41 – 7.35 (m, 3H, (2H)-phenethyl, (1H)-phenyl), 7.34 – 7.26 (m, 4H, (3H)-phenethyl, (1H)-phenyl), 7.17 (dt, *J* = 11.5, 5.6 Hz, 3H, quinoxaline), 4.70 (t, *J* = 6.7 Hz, 2H, benzylic ethylene), 3.11 (t, *J* = 6.6 Hz, 2H, benzylic ethylene).

_N_-(4-chlorophenyl)-3-oxo-4-phenethyl-3,4-dihydroquinoxaline-2-carboxamide (QCF-10)

TLC (EtOAc:Hexane 25:75); Yield: 70%; White solid; mp: 194-196 °C; IR (KBr, *v* cm^{-1}): 3360 (sharp, N–H str.), 3189, 3074, 2969, 2780 (aromatic C-H str.), 1742 (keto C=O str.), 1709 (amide C=O str.), 1590, 1545 (C=C, C=N ring str.), 1400, 1386 (CH_2 bend), 1295, 1035, 965 (C=C bend); ^{1}H NMR (400 MHz, DMSO) δ 10.75 (s, 1H, amide), 8.05 (d, *J* = 7.4 Hz, 1H, quinoxaline), 7.79 (d, *J* = 8.7 Hz, 2H, phenyl), 7.42 – 7.38 (m, 2H, phenyl), 7.39 – 7.35 (m, 2H, phenethyl), 7.32 – 7.27 (m, 3H, phenethyl), 7.17 (q, *J* = 5.1 Hz, 3H, quinoxaline), 4.69 (t, *J* = 6.7 Hz, 2H, benzylic ethylene), 3.11 (t, *J* = 6.7 Hz, 2H, benzylic ethylene).

3-oxo-4-phenethyl-_N_-(2-propylphenyl)-3,4-dihydroquinoxaline-2-carboxamide (QCF-11)

TLC (EtOAc:Hexane 25:75); Yield: 58%; White solid; mp: 202-204 °C; IR (KBr, *v* cm^{-1}): 3368 (sharp, N–H str.), 3072, 2969, 2777 (aromatic C-H str.), 1746 (keto C=O str.), 1710 (amide C=O str.), 1587, 1545 (C=C, C=N ring str.), 1398, 1367 (CH_2 bend), 1285, 1022, 962 (C=C bend); ^{1}H NMR (400 MHz, DMSO) δ 10.00 (s, 1H, amide), 8.05 (d, *J* = 7.5 Hz, 1H, quinoxaline), 7.33 (t, *J* = 6.6 Hz, 3H, (2H)-phenethyl, (1H)-phenyl), 7.30 – 7.22 (m, 5H, (3H)-phenethyl, (2H)-phenyl), 7.24 – 7.07 (m, 4H, (3H)-quinoxaline, (1H)-phenyl), 4.73 (t, *J* = 7.0 Hz, 2H, benzylic ethylene), 3.15 (t, *J* = 6.9 Hz, 2H, benzylic ethylene), 2.73 – 2.61 (m, 2H, $CH_2CH_2CH_3$), 1.65 (dd, *J* = 15.1, 7.5 Hz, 2H, $CH_2CH_2CH_3$), 0.96 (t, *J* = 7.3 Hz, 3H, $CH_2CH_2CH_3$).

_N_-(2-isopropylphenyl)-3-oxo-4-phenethyl-3,4-dihydroquinoxaline-2-carboxamide (QCF-12)

TLC (EtOAc:Hexane 25:75); Yield: 64%; White solid; mp: 220-222 °C; IR (KBr, *v* cm^{-1}): 3374 (sharp, N–H str.), 3064, 2972, 2780 (aromatic C-H str.), 1748 (keto C=O str.), 1695 (amide C=O str.), 1590, 1549 (C=C, C=N ring str.), 1395, 1322 (CH_2 bend), 1290, 1066, 954 (C=C bend); ^{1}H NMR (400 MHz, DMSO) δ 10.09 (s, 1H, amide), 8.08 (d, *J* = 7.7 Hz, 1H, quinoxaline), 7.36 (dd, *J* = 12.6, 8.5 Hz, 3H, (2H)-phenethyl, (1H)-phenyl), 7.33 – 7.24 (m, 5H, (3H)-phenethyl, (2H)-phenyl), 7.28 – 7.16 (m, 4H, (3H)-quinoxaline, (1H)-

phenyl), 4.73 (t, *J* = 6.9 Hz, 2H, benzylic ethylene), 3.15 (t, *J* = 6.9 Hz, 2H, benzylic ethylene), 3.10 – 2.98 (m, 1H, $CH(CH_3)_2$), 1.22 (d, *J* = 6.8 Hz, 6H, $CH(CH_3)_2$).

_N_-(4-isopropylphenyl)-3-oxo-4-phenethyl-3,4-dihydroquinoxaline-2-carboxamide (QCF-13)

TLC (EtOAc:Hexane 25:75); Yield: 78%; White solid; mp: 238-240 °C; IR (KBr, *v* cm^{-1}): 3320 (sharp, N–H str.), 3224, 3185, 3046, 2927, 2710 (aromatic C-H str.), 1744 (keto C=O str.), 1701 (amide C=O str.), 1594, 1535 (C=C, C=N ring str.), 1405, 1255, 1312 (CH_2 bend), 1279, 1056, 926 (C=C bend); ^{1}H NMR (400 MHz, DMSO) δ 10.05 (s, 1H, amide), 8.07 (d, *J* = 7.3 Hz, 1H, quinoxaline), 7.73 – 7.62 (m, 2H, phenyl), 7.41 – 7.34 (m, 2H, phenethyl), 7.37 – 7.25 (m, 5H, (3H)-phenethyl, (2H)-phenyl), 7.25 – 7.16 (m, 3H, quinoxaline), 4.74 (t, *J* = 6.9 Hz, 2H, benzylic ethylene), 3.16 (t, *J* = 6.9 Hz, 2H, benzylic ethylene), 3.10 – 2.99 (m, 1H, $CH(CH_3)_2$), 1.23 (d, *J* = 6.8 Hz, 6H, $CH(CH_3)_2$).

_N_-(2-chloro-4-methylphenyl)-3-oxo-4-phenethyl-3,4-dihydroquinoxaline-2-carboxamide (QCF-14)

TLC (EtOAc:Hexane 25:75); Yield: 36%; White solid; mp: >250 °C; IR (KBr, *v* cm^{-1}): 3338 (sharp, N–H str.), 3206, 3166, 3010, 2895, 2720 (aromatic C-H str.), 1747 (keto C=O str.), 1709 (amide C=O str.), 1589, 1544 (C=C, C=N ring str.), 1402, 1305, 1266 (CH_2 bend), 1210, 1054, 974 (C=C bend); ^{1}H NMR (400 MHz, DMSO) δ 10.24 (s, 1H, amide), 8.07 (dd, *J* = 8.3, 1.0 Hz, 1H, quinoxaline), 7.68 (ddd, *J* = 8.3, 6.9, 1.4 Hz, 1H, phenyl), 7.38 – 7.33 (m, 3H, (2H)-phenethyl, (1H)-phenyl), 7.33 – 7.23 (m, 3H, phenethyl), 7.24 – 7.15 (m, 4H, (3H)-quinoxaline, (1H)-phenyl), 4.72 (t, *J* = 6.8 Hz, 2H, benzylic ethylene), 3.15 (t, *J* = 6.8 Hz, 2H, benzylic ethylene), 2.33 (s, 3H, CH_3).

_N_-(2-chloro-5-methylphenyl)-3-oxo-4-phenethyl-3,4-dihydroquinoxaline-2-carboxamide (QCF-15)

TLC (EtOAc:Hexane 25:75); Yield: 30%; White solid; mp: 234-236 °C; IR (KBr, *v* cm^{-1}): 3360 (sharp, N–H str.), 3174, 3065, 2960, 2894 (aromatic C-H str.), 1745 (keto C=O str.), 1698 (amide C=O str.), 1595, 1548 (C=C, C=N ring str.), 1410, 1325 (CH_2 bend), 1286, 1055 (C=C bend); ^{1}H NMR (400 MHz, DMSO) δ 10.25 (s, 1H, amide), 8.07 (d, *J* = 7.5 Hz, 1H, quinoxaline), 7.70 (dd, *J* = 5.7, 2.6 Hz, 1H, phenyl), 7.43 – 7.33 (m, 3H, (2H)-phenethyl, (1H)-phenyl), 7.27 – 7.19 (m, 3H, phenethyl), 7.18 (dd, *J* = 8.4, 5.9 Hz, 3H, quinoxaline), 7.04 (dd, *J* = 8.1, 1.6 Hz, 1H, phenyl), 4.74 (t, *J* = 6.8 Hz, 2H, benzylic ethylene), 3.16 (t, *J* = 6.8 Hz, 2H, benzylic ethylene), 2.39 (s, 3H, CH_3).

***N*-(2-chloro-6-methylphenyl)-3-oxo-4-phenethyl-3,4-dihydroquinoxaline-2-carboxamide (QCF-16)**

TLC (EtOAc:Hexane 25:75); Yield: 46%; White solid; mp: 238-240 °C; IR (KBr, *v* cm^{-1}): 3365 (sharp, N–H str.), 3259, 3145, 3059, 2954, 2761 (aromatic C-H str.), 1742 (keto C=O str.), 1695 (amide C=O str.), 1590, 1548 (C=C, C=N ring str.), 1410 (CH_2 bend), 1322, 1264, 1022, 965 (C=C bend); ^{1}H NMR (400 MHz, DMSO) δ 10.77 (s, 1H, amide), 8.01 (d, *J* = 7.6 Hz, 1H, quinoxaline), 7.49 (t, *J* = 7.3 Hz, 1H, phenyl), 7.36 (d, *J* = 5.1 Hz, 2H, phenethyl), 7.35 – 7.26 (m, 4H, (3H)-phenethyl, (1H)-phenyl), 7.27 – 7.15 (m, 4H, (3H)-quinoxaline, (1H)-phenyl), 4.62 – 4.51 (m, 2H, benzylic ethylene), 3.10 – 2.98 (m, 2H, benzylic ethylene), 2.36 (s, 3H, CH_3).

***N*-(3-chloro-2-methylphenyl)-3-oxo-4-phenethyl-3,4-dihydroquinoxaline-2-carboxamide (QCF-17)**

TLC (EtOAc:Hexane 25:75); Yield: 35%; White solid; mp: 212-215 °C; IR (KBr, *v* cm^{-1}): 3380 (sharp, N–H str.), 3276, 3224, 3157, 3048, 2956, 2787 (aromatic C-H str.), 1748 (keto C=O str.), 1692 (amide C=O str.), 1584, 1529 (C=C, C=N ring str.), 1395 (CH_2 bend), 1268, 1130, 1038 (C=C bend); ^{1}H NMR (400 MHz, DMSO) δ 10.30 (s, 1H, amide), 8.07 (dd, *J* = 8.2, 1.0 Hz, 1H, quinoxaline), 7.37 – 7.31 (m, 3H, (2H)-phenethyl, (1H)-phenyl), 7.31 – 7.23 (m, 3H, phenethyl), 7.26 – 7.13 (m, 5H, (3H)-quinoxaline, (2H)-phenyl), 4.74 (t, *J* = 6.8 Hz, 2H,benzylic ethylene), 3.15 (t, *J* = 6.8 Hz, 2H, benzylic ethylene), 2.31 (s, 3H, CH_3).

***N*-(4-chloro-2-methylphenyl)-3-oxo-4-phenethyl-3,4-dihydroquinoxaline-2-carboxamide (QCF-18)**

TLC (EtOAc:Hexane 25:75); Yield: 34%; White solid; mp: 203-206 °C; IR (KBr, *v* cm^{-1}): 3355 (sharp, N–H str.), 3235, 3127, 3062, 2970, 2718 (aromatic C-H str.), 1745 (keto C=O str.), 1710 (amide C=O str.), 1622, 1574, 1526 (C=C, C=N ring str.), 1390 (CH_2 bend), 1265, 1180, 1127, 1035, 986, 957 (C=C bend); ^{1}H NMR (400 MHz, DMSO) δ 10.07 (s, 1H, amide), 8.08 – 8.04 (m, 1H, quinoxaline), 7.71 – 7.68 (m, 1H, phenyl), 7.36 – 7.28 (m, 3H, (2H)-phenethyl, (1H)-phenyl), 7.25 (ddd, *J* = 14.1, 8.1, 4.9 Hz, 4H, (3H)-phenethyl, (1H)-phenyl), 7.23 – 7.13 (m, 3H, quinoxaline), 4.74 (t, *J* = 6.8 Hz, 2H, benzylic ethylene), 3.15 (t, *J* = 6.8 Hz, 2H, benzylic ethylene), 2.28 (s, 3H, CH_3).

3-oxo-4-phenethyl-*N*-(2-(trifluoromethyl)phenyl)-3,4-dihydroquinoxaline-2-carboxamide (QCF-19)

TLC (EtOAc:Hexane 25:75); Yield: 40%; White solid; mp: 208-210 °C; IR (KBr, *v* cm^{-1}): 3385, 3364, 3345 (sharp, N–H str.), 3221, 3164, 3057, 2974 (aromatic C-H str.), 1748 (keto C=O str.), 1712 (amide C=O str.), 1622, 1587, 1547 (C=C, C=N ring str.), 1410, 1345 (CH_2 bend), 1277, 1159, 1029 (C=C bend); ^{1}H NMR (400 MHz, DMSO) δ 10.22 (s, 1H, amide), 8.08 (d, *J* = 7.5 Hz, 1H, quinoxaline), 7.71 – 7.68 (m, 1H, phenyl), 7.36 – 7.24 (m, 5H, (2H)-phenethyl, (3H)-phenyl), 7.22 – 7.15 (m, 3H, phenethyl), 7.14 (dd, *J* = 8.4, 5.9 Hz, 3H, quinoxaline), 4.68 (t, *J* = 6.8 Hz, 2H, benzylic ethylene), 3.09 (t, *J* = 6.8 Hz, 2H, benzylic ethylene).

4.4. Synthesis of different 3-substituted 4-oxo-3,4-dihydroquinazoline-2-carboxamides (QZA – QZB series)

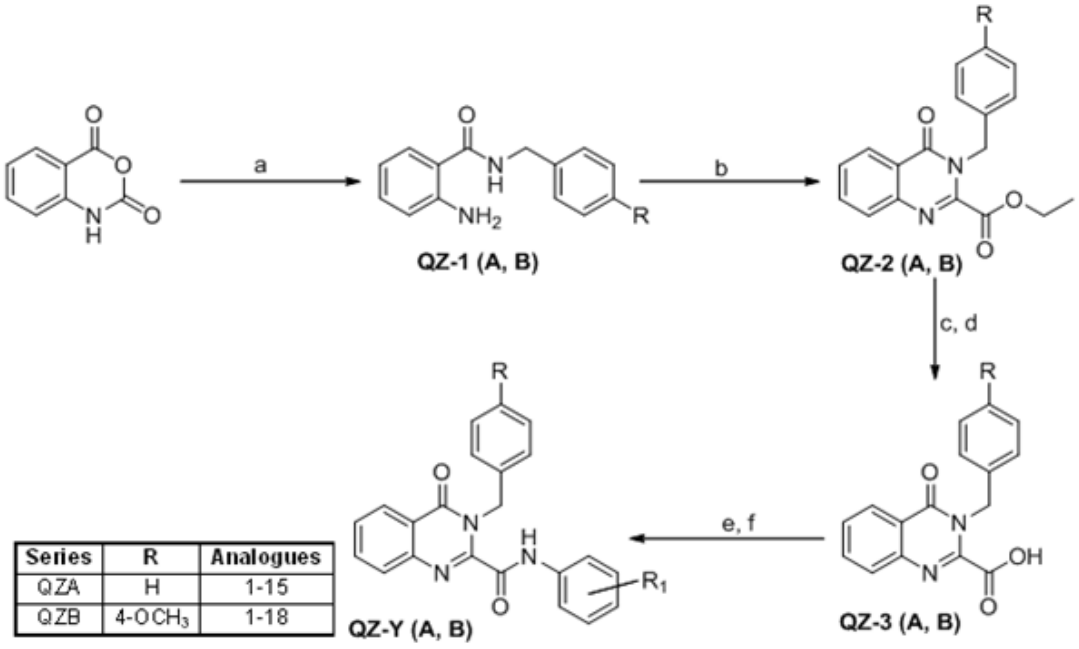

Series	R	Analogues
QZA	H	1-15
QZB	4-OCH_3	1-18

Reagents and conditions: (**a**) $C_6H_5CH_2NH_2$, DMF, 45-50°C, 3h., 50% NaOH, 1hr.; (**b**) Melt, Diethyloxalate, 6hr., then EtOH, rt, 6 hr.; (**c**) 10% aq. NaOH, rt, 2hr.; or Na_2CO_3, reflux, 6 hr; (**d**) Conc. HCl, 50%; (**e**) EDC·HCl, HOBt, THF, N_2, 0 °C–rt, 1hr; (**f**) amines, rt, 6 hr.

4.4.1. Series-7: 3-benzyl-4-oxo-N-phenyl-3,4-dihydroquinazoline-2-carboxamide analogues (QZA-1 to 15)

2-amino-*N*-benzylbenzamide (QZ-1A)

A solution of 2.25 g (0.021 mole) of benzylamine in 4 ml of DMF was added to a stirred solution of 3.26 g (0.020 mole) of isatoic anhydride in 10 ml of DMF maintained at 45-50 °C in a 100 ml RBF. Stirring and heating were continued for 3 hr. The cooled mixture was poured into 100 ml water, basified with 50% sodium hydroxide (*pH* = 9), filtered and washed with water to afford the desired compound. TLC (EtOAc:Hex 30:70); Yield: 91%; Grey-colored solid; mp: 121-122 °C; IR (KBr, *v* cm^{-1}): 3467 (N-H str. of primary -NH_2), 3359 (N-H str.), 3301 (aromatic C-H str.), 1660 (amide C=O str.), 1570, 1490 (C=C, C=N ring str.), 1465 (CH_2 bend), 1375 (CH_3 bend), 1300, 1100 (C=C bend.); ^{1}H NMR (400 MHz, $CDCl_3$) δ 10.86 (s, 1H, amide), 7.41 – 7.38 (m, 3H, (1H)-benzene, (2H)-phenyl), 7.36 – 7.33 (m, 2H, phenyl), 7.26 – 7.22 (m, 1H, phenyl), 7.20 (dd, *J* = 7.5, 6.4 Hz, 1H, benzene), 6.67 (d, *J* = 8.2 Hz, 1H, benzene), 6.61 (d, *J* = 8.1 Hz, 1H, benzene), 6.38 (s, 2H, amine), 4.59 (d, *J* = 5.7 Hz, 2H, benzylic methylene); MS (EI): *m/z* [M^+] for $C_{14}H_{14}N_2O$ = 226.

Ethyl 3-benzyl-4-oxo-3,4-dihydroquinazoline-2-carboxylate (QZ-2A)

A mixture of 2.26 g (0.01 mol) of *O*-Amino-*N*-benzylbenzamide and 4.38 g (0.03 mol) of diethyl oxalate were heated for 30 min in a 100 ml RBF. The above mixture was cooled, 5 ml of EtOH was added, and the obtained precipitate filtered off, dried and recrystallized with EtOH to afford the desired compound. TLC (EtOAc:Hexane 30:70); Yield 72%; Pale white solid; mp: 210-212 °C; IR (KBr, *v* cm^{-1}): 3043 (aromatic C-H str.), 2357, 2339 (aromatic C-H str.), 1732 (ester C=O Keto), 1680 (keto C=O str.), 1570, 1490 (C=C, C=N ring str.), 1465 (CH_2 bend), 1375 (CH_3 bend), 1300, 1100 (C=C bend), 1093, 1044 (ether C-O bend.); ^{1}H NMR (400 MHz, $CDCl_3$) δ 8.66 (s, 1H, quinazoline), 7.52 (dd, *J* = 16.5, 7.7 Hz, 2H, quinazoline), 7.40 – 7.23 (m, 6H, benzyl), 4.66 (s, 2H, benzylic methylene), 4.42 (q, *J* = 7.1 Hz, 2H, OCH_2CH_3), 1.43 (t, *J* = 7.1 Hz, 3H, OCH_2CH_3).

3-benzyl-4-oxo-3,4-dihydroquinazoline-2-carboxylic acid (QZ-3A)

3.1 g (0.01 mol) of Ethyl 3-benzyl-4-oxo-3,4-dihydroquinazoline-2-carboxylate was dissolved in 5 ml of dry THF in a 100 ml RBF. To this mixture, 50% aqueous sodium hydroxide solution (*pH*>10) was added and stirred at room temperature for 2 hr. The solvent was removed under vacuum; residue washed with ethylacetate and the aqueous portion acidified with dil. HCl (*pH* = 5). The obtained solid residue was washed with cold water, filtered and recrystallized with EtOH to afford the desired compound. TLC (EtOAc:Hexane 25:75); Yield: 80%; White solid; mp: 224-227 °C; IR (KBr, *v* cm^{-1}): 3460 (broad O–H str. COOH), 3043, 2561 (aromatic C-H str.), 1732 (acid C=O str.), 1692 (keto C=O str.), 1537, 1490 (C=C, C=N ring str.), 1273, 1100 (C=C bend.); ^{1}H NMR (400 MHz, DMSO) δ 12.86 (s, 1H, acid), 8.65 (d, *J* = 8.3 Hz, 1H, quinazoline), 7.86 (d, *J* = 7.8 Hz, 1H, quinazoline), 7.71 (d, *J* = 2.7 Hz, 1H, quinazoline), 7.50 (t, *J* = 7.8 Hz, 1H, quinazoline), 7.34 (q, *J* = 7.7 Hz, 3H, benzyl), 7.26 (d, *J* = 7.0 Hz, 1H, benzyl), 7.18 (t, *J* = 7.6 Hz, 1H, benzyl), 4.60 (s, 2H, benzylic methylene).

General procedure for the synthesis of New Chemical Entity's (NCE's) i.e. quinazoline-2-carboxamide analogues (QZA-1 to 15)

To 0.5 g (0.0018 mol) of 3-benzyl-4-oxo-3,4-dihydroquinazoline-2-carboxylic acid taken in a 100 ml RBF, 0.41 g (0.0021 mol) of EDC·HCl was added and stirred with 5 ml of dry THF in an inert atmosphere (nitrogen) at 0 °C for 15 min. To the above reaction mixture, 0.41 g (0.0027 mol) HOBt was added and stirred for another 45 min. To the above mixture, 1 equivalent of appropriate amines were added and stirred continuously for 6 hr. The reaction mixture was concentrated under reduced pressure; resultant mass diluted with DCM/ethyl acetate, washed with aqueous sodium bicarbonate (2 × 50 ml), saturated brine solution (2 × 50 ml) and dried over anhydrous sodium sulfate. The solvent was then

evaporated under reduced pressure to afford the desired compounds. The obtained compounds were purified by recrystallization with EtOH/MeOH/column chromatography over silica gel.

3-benzyl-4-oxo-*N*-phenyl-3,4-dihydroquinazoline-2-carboxamide (QZA-1)

TLC (EtOAc:Hexane 25:75); Yield: 74%; White solid; mp: 196-198 °C; IR (KBr, *v* cm^{-1}): 3250 (sharp, N–H str.), 3126, 3068 (aromatic C-H str.), 1693 (keto C=O str.), 1675 (amide C=O str.), 1591, 1556 (C=C, C=N ring str.), 1465 (CH_2 bend), 1325, 1165 (C=C bend.); ^{1}H NMR (400 MHz, DMSO) δ 10.55 (s, 1H, amide), 8.70 (d, *J* = 8.2 Hz, 1H, quinoxaline), 7.89 (t, *J* = 9.2 Hz, 3H, quinoxaline), 7.54 (t, *J* = 7.7 Hz, 1H, phenyl), 7.40 – 7.29 (m, 6H, (3H)-phenyl, (3H)-benzyl), 7.28 – 7.19 (m, 2H, benzyl), 7.14 (t, *J* = 7.3 Hz, 1H, phenyl), 4.59 (s, 2H, benzylic methylene).

3-benzyl-*N*-(2-methoxyphenyl)-4-oxo-3,4-dihydroquinazoline-2-carboxamide (QZA-2)

TLC (EtOAc:Hexane 25:75); Yield: 78%; White solid; mp: 188-189 °C; IR (KBr, *v* cm^{-1}): 3182 (sharp, N–H str.), 3059, 2916 (aromatic C-H str.), 1703 (keto C=O str.), 1643 (amide C=O str.), 1573, 1462 (C=C, C=N ring str.), 1415 (CH_2 bend), 1172, 1129 (C=C bend), 1085, 1034 (ether C-O bend.); ^{1}H NMR (400 MHz, DMSO) δ 9.91 (s, 1H, amide), 8.67 (d, *J* = 8.4 Hz, 1H, quinoxaline), 8.43 (d, *J* = 8.0 Hz, 1H, phenyl), 7.89 (d, *J* = 7.7 Hz, 1H, quinoxaline), 7.54 (t, *J* = 7.7 Hz, 1H, quinoxaline), 7.41 – 7.29 (m, 4H, (1H)-quinoxaline, (3H)-benzyl), 7.20 (ddd, *J* = 27.2, 15.2, 7.4 Hz, 3H, (2H)-benzyl, (1H)-phenyl), 6.99 (d, *J* = 7.5 Hz, 2H, phenyl), 4.63 (d, *J* = 5.5 Hz, 2H, benzylic methylene), 3.97 (s, 3H, OCH_3).

3-benzyl-*N*-(3-methoxyphenyl)-4-oxo-3,4-dihydroquinazoline-2-carboxamide (QZA-3)

TLC (EtOAc:Hexane 25:75); Yield: 82%; White solid; mp: 180-182 °C; IR (KBr, *v* cm^{-1}): 3190 (sharp, N–H str.), 3039, 2875 (aromatic C-H str.), 1681 (keto C=O str.), 1633 (amide C=O str.), 1598, 1525 (C=C, C=N ring str.), 1421 (CH_2 bend), 1321, 1170 (C=C bend), 1092, 1039 (ether C-O bend.); ^{1}H NMR (400 MHz, DMSO) δ 10.42 (s, 1H, amide), 8.70 (d, *J* = 8.4 Hz, 1H, quinoxaline), 7.95 – 7.83 (m, 3H, quinoxaline), 7.54 (t, *J* = 7.7 Hz, 1H, phenyl), 7.45 – 7.27 (m, 5H, benzyl), 7.25 (dd, *J* = 7.6, 4.4 Hz, 2H, phenyl), 6.70 (d, *J* = 8.2 Hz, 1H, phenyl), 4.61 (d, *J* = 5.8 Hz, 2H, benzylic methylene), 3.80 (s, 3H, OCH_3).

3-benzyl-*N*-(4-methoxyphenyl)-4-oxo-3,4-dihydroquinazoline-2-carboxamide (QZA-4)

TLC (EtOAc:Hexane 25:75); Yield: 84%; White solid; mp: 198-200 °C; IR (KBr, *v* cm^{-1}): 3250 (sharp, N–H str.), 3128, 3074 (aromatic C-H str.), 1693 (keto C=O str.), 1680 (amide C=O str.), 1587, 1537 (C=C, C=N ring str.), 1462 (CH_2 bend), 1323, 1166 (C=C bend), 1099, 1049 (ether C-O bend.); ^{1}H NMR (400 MHz, DMSO) δ 9.91 (s, 1H, amide), 8.67 (d, *J* = 8.4 Hz, 1H, quinoxaline), 8.43 (d, *J* = 8.0 Hz, 1H, quinoxaline), 7.89 (d, *J* = 7.7 Hz, 1H, quinoxaline), 7.54 (t, *J* = 7.7 Hz, 1H, quinoxaline), 7.41 – 7.29 (m, 4H, (2H)-phenyl, (2H)-benzyl), 7.20 (ddd, *J* = 27.2, 15.2, 7.4 Hz, 3H, benzyl), 6.99 (d, *J* = 7.5 Hz, 2H, phenyl), 4.63 (s, 2H, benzylic methylene), 3.97 (s, 3H, OCH_3).

3-benzyl-*N*-(2-ethylphenyl)-4-oxo-3,4-dihydroquinazoline-2-carboxamide (QZA-5)

TLC (EtOAc:Hexane 25:75); Yield: 75%; White solid; mp: 170-172 °C; IR (KBr, *v* cm^{-1}): 3300 (sharp, N–H str.), 3086, 3030 (aromatic C-H str.), 1737 (keto C=O str.), 1651 (amide C=O str.), 1587, 1537 (C=C, C=N ring str.), 1469 (CH_2 bend), 1346 (CH_3 bend), 1257, 1095 (C=C bend.); ^{1}H NMR (400 MHz, DMSO) δ 10.42 (s, 1H, amide), 8.70 (d, *J* = 8.3 Hz, 1H, quinoxaline), 7.90 (d, *J* = 7.9 Hz, 1H, quinoxaline), 7.77 (s, 1H, quinoxaline), 7.64 (d, *J* = 8.1 Hz, 1H, quinoxaline), 7.54 (t, *J* = 7.7 Hz, 1H, phenyl), 7.42 – 7.16 (m, 7H, (5H)-benzyl, (2H)-phenyl), 6.99 (d, *J* = 7.6 Hz, 1H, phenyl), 4.59 (s, *J* = 5.7 Hz, 2H, benzylic methylene), 2.64 (q, *J* = 7.5 Hz, 2H, CH_2CH_3), 1.24 (t, *J* = 7.6 Hz, 3H, CH_2CH_3).

3-benzyl-*N*-(3-ethylphenyl)-4-oxo-3,4-dihydroquinazoline-2-carboxamide (QZA-6)

TLC (EtOAc:Hexane 25:75); Yield: 77%; White solid; mp: 162-165 °C; IR (KBr, *v* cm^{-1}): 3321 (sharp, N–H str.), 3010, 2308 (aromatic C-H str.), 1726 (keto C=O str.), 1680 (amide C=O str.), 1593, 1515 (C=C, C=N ring str.), 1435 (CH_2 bend), 1253, 1028 (C=C bend.); ^{1}H NMR (400 MHz, DMSO) δ 9.76 (s, 1H, amide), 8.69 (d, *J* = 8.4 Hz, 1H, quinoxaline), 8.05 – 7.83 (m, 2H, phenyl), 7.53 (dd, *J* = 11.5, 4.3 Hz, 1H, quinoxaline), 7.45 – 7.10 (m, 9H, (2H)-quinoxaline, (5H)-benzyl, (2H)-phenyl), 4.60 (d, *J* = 5.8 Hz, 2H, benzylic methylene), 2.73 (d, *J* = 7.6 Hz, 2H, CH_2CH_3), 1.27 (t, *J* = 7.6 Hz, 3H, CH_2CH_3).

3-benzyl-*N*-(2-chlorophenyl)-4-oxo-3,4-dihydroquinazoline-2-carboxamide (QZA-7)

TLC (EtOAc:Hexane 25:75); Yield: 71%; White solid; mp: 182-184 °C; IR (KBr, *v* cm^{-1}): 3344 (sharp, N–H str.), 3062, 2974, 2781 (aromatic C-H str.), 1760 (keto C=O str.), 1703 (amide C=O str.), 1591, 1556 (C=C, C=N ring str.), 1402 (CH_2 bend), 1290, 1035 (C=C bend.); ^{1}H NMR (400 MHz, DMSO) δ 10.08 (s, 1H, amide), 8.62 (dd, *J* = 30.2, 8.2 Hz, 1H, phenyl), 8.30 (d, *J* = 7.7 Hz, 1H, quinoxaline), 7.89 (dd, *J* = 33.9, 22.6 Hz, 1H,

quinoxaline), 7.62 – 7.45 (m, 2H, quinoxaline), 7.34 (dt, *J* = 15.1, 7.4 Hz, 5H, benzyl), 7.28 – 7.16 (m, 3H, phenyl), 4.58 (d, *J* = 5.9 Hz, 2H, benzylic methylene).

3-benzyl-*N*-(3-chlorophenyl)-4-oxo-3,4-dihydroquinazoline-2-carboxamide (QZA-8)

TLC (EtOAc:Hexane 25:75); Yield: 68%; White solid; mp: 188-190 °C; IR (KBr, *v* cm^{-1}): 3323 (sharp, N–H str.), 3140, 2954 (aromatic C-H str.), 1739 (keto C=O str.), 1685 (amide C=O str.), 1485, 1454 (C=C, C=N ring str.), 1321 (CH_2 bend), 1166, 1099 (C=C bend.); ^{1}H NMR (400 MHz, DMSO) δ 10.75 (s, 1H, amide), 9.12 (s, 1H, quinoxaline), 8.70 (d, *J* = 8.3 Hz, 1H, phenyl), 7.86 (s, 1H, quinoxaline), 7.77 (d, *J* = 8.2 Hz, 1H, quinoxaline), 7.54 (t, *J* = 7.7 Hz, 1H, quinoxaline), 7.44 – 7.29 (m, 5H, benzyl), 7.29 – 7.19 (m, 2H, phenyl), 7.12 (d, *J* = 7.2 Hz, 1H, phenyl), 4.61 (d, *J* = 5.8 Hz, 2H, benzylic methylene).

3-benzyl-*N*-(4-chlorophenyl)-4-oxo-3,4-dihydroquinazoline-2-carboxamide (QZA-9)

TLC (EtOAc:Hexane 25:75); Yield: 73%; White solid; mp: 224-227 °C; IR (KBr, *v* cm^{-1}): 3200 (sharp, N–H str.), 3040, 2860 (aromatic C-H str.), 1710 (keto C=O str.), 1660 (amide C=O str.), 1574, 1480 (C=C, C=N ring str.), 1354 (CH_2 bend), 1266, 1100 (C=C bend.); ^{1}H NMR (400 MHz, DMSO) δ 10.90 (s, 1H, amide), 9.27 (t, *J* = 5.8 Hz, 1H, quinoxaline), 8.68 (d, *J* = 8.0 Hz, 1H, phenyl), 7.92 (t, *J* = 8.2 Hz, 3H, (1H)-phenyl, (2H)-quinoxaline), 7.55 (t, *J* = 7.3 Hz, 1H, quinoxaline), 7.39 – 7.30 (m, 6H, (5H)-benzyl, (1H)-phenyl), 7.25 (d, *J* = 6.9 Hz, 1H, phenyl), 4.57 (d, *J* = 5.9 Hz, 2H, benzylic methylene).

3-benzyl-*N*-(2-isopropylphenyl)-4-oxo-3,4-dihydroquinazoline-2-carboxamide (QZA-10)

TLC (EtOAc:Hexane 25:75); Yield: 74%; White solid; mp: 172-174 °C; IR (KBr, *v* cm^{-1}): 3000 (sharp, N–H str.), 2949, 2360, 1975 (aromatic C-H str.), 1745 (keto C=O str.), 1697 (amide C=O str.), 1539, 1455 (C=C, C=N ring str.), 1350 (CH_2 bend), 1197, 1056 (C=C bend.); ^{1}H NMR (400 MHz, DMSO) δ 10.06 (s, 1H, amide), 8.70 (d, *J* = 8.4 Hz, 1H, quinoxaline), 7.90 (d, *J* = 8.0 Hz, 1H, quinoxaline), 7.64 (d, *J* = 8.7 Hz, 1H, quinoxaline), 7.54 (t, *J* = 7.8 Hz, 1H, quinoxaline), 7.42 – 7.28 (m, 6H, (1H)-phenyl, (5H)-benzyl), 7.26 – 7.20 (m, 3H, phenyl), 4.57 (d, *J* = 5.6 Hz, 2H, benzylic methylene), 3.17 (dt, *J* = 13.7, 6.7 Hz, 1H, $CH(CH_3)_2$), 1.25 (d, *J* = 6.8 Hz, 6H, $CH(CH_3)_2$).

3-benzyl-*N*-(4-isopropylphenyl)-4-oxo-3,4-dihydroquinazoline-2-carboxamide (QZA-11)

TLC (EtOAc:Hexane 25:75); Yield: 77%; White solid; mp: 164-166 °C; IR (KBr, *v* cm^{-1}): 3242 (sharp, N–H str.), 2924, 2840 (aromatic C-H str.), 1741 (keto C=O str.), 1651 (amide C=O str.), 1556, 1469 (C=C, C=N ring str.), 1348 (CH_2 bend), 1259, 1163 (C=C

bend.); ^{1}H NMR (400 MHz, DMSO) δ 10.60 (s, 1H, amide), 9.25 (s, 1H, quinoxaline), 8.69 (d, *J* = 8.3 Hz, 1H, quinoxaline), 7.91 (d, *J* = 7.4 Hz, 1H, quinoxaline), 7.78 (d, *J* = 8.4 Hz, 1H, quinoxaline), 7.55 (t, *J* = 7.5 Hz, 1H, phenyl), 7.34 (dt, *J* = 15.0, 7.4 Hz, 4H, (1H)-phenyl, (3H)-benzyl), 7.28 – 7.15 (m, 4H, (2H)-phenyl, (2H)-benzyl), 4.58 (d, *J* = 5.8 Hz, 2H, benzylic methylene), 2.89 (dt, *J* = 13.8, 6.8 Hz, 1H, $CH(CH_3)_2$), 1.23 (d, *J* = 6.9 Hz, 6H, $CH(CH_3)_2$).

3-benzyl-4-oxo-*N*-(2-propylphenyl)-3,4-dihydroquinazoline-2-carboxamide (QZA-12)

TLC (EtOAc:Hexane 25:75); Yield: 85%; White solid; mp: 138-140 °C; IR (KBr, *v* cm^{-1}): 3203 (sharp, N–H str.), 3032, 2970 (aromatic C-H str.), 1691 (keto C=O str.), 1694 (amide C=O str.), 1587, 1524 (C=C, C=N ring str.), 1371 (CH_3, CH_2 bend), 1165, 1074 (C=C bend.); ^{1}H NMR (400 MHz, DMSO) δ 9.68 (s, 1H, amide), 8.69 (d, *J* = 8.3 Hz, 1H, quinoxaline), 8.03 (d, *J* = 8.3 Hz, 1H, quinoxaline), 7.89 (d, *J* = 7.5 Hz, 1H, quinoxaline), 7.53 (t, *J* = 7.6 Hz, 1H, quinoxaline), 7.41 – 7.29 (m, 4H, phenyl), 7.27 – 7.22 (m, 3H, benzyl), 7.21 – 7.08 (m, 2H, benzyl), 4.61 (d, *J* = 5.7 Hz, 2H, benzylic methylene), 2.68 (t, *J* = 7.6 Hz, 2H, $CH_2CH_2CH_3$), 1.68 (dd, *J* = 14.9, 7.6 Hz, 2H, $CH_2CH_2CH_3$), 1.01 (t, *J* = 7.3 Hz, 3H, $CH_2CH_2CH_3$).

3-benzyl-*N*-(2-chloro-4-methylphenyl)-4-oxo-3,4-dihydroquinazoline-2-carboxamide (QZA-13)

TLC (EtOAc:Hexane 25:75); Yield: 65%; White solid; mp: 162-166 °C; IR (KBr, *v* cm^{-1}): 3473 (sharp, N–H str.), 3290, 2956 (aromatic C-H str.), 1745 (keto C=O str.), 1600 (amide C=O str.), 1587, 1504 (C=C, C=N ring str.), 1392 (CH_2 bend), 1257, 1170 (C=C bend.); ^{1}H NMR (400 MHz, DMSO) δ 10.00 (s, 1H, amide), 8.66 (d, *J* = 8.4 Hz, 1H, quinoxaline), 8.15 (d, *J* = 8.3 Hz, 1H, quinoxaline), 7.93 (d, *J* = 8.0 Hz, 1H, quinoxaline), 7.75 (d, *J* = 8.6 Hz, 1H, quinoxaline), 7.56 (t, *J* = 7.6 Hz, 1H, phenyl), 7.35 (dd, *J* = 13.1, 7.2 Hz, 6H, (1H)-phenyl, (5H)-benzyl), 7.17 (d, *J* = 8.7 Hz, 1H, phenyl), 4.58 (d, *J* = 5.8 Hz, 2H, benzylic methylene), 2.35 (s, 3H, CH_3).

3-benzyl-*N*-(3-chloro-2-methylphenyl)-4-oxo-3,4-dihydroquinazoline-2-carboxamide (QZA-14)

TLC (EtOAc:Hexane 25:75); Yield: 64%; White solid; mp: 166-168 °C; IR (KBr, *v* cm^{-1}): 3321 (sharp, N–H str.), 3010, 2308 (aromatic C-H str.), 1685 (keto C=O str.), 1680 (amide C=O str.), 1593, 1515 (C=C, C=N ring str.), 1435 (CH_2 bend), 1253, 1028 (C=C bend.); ^{1}H NMR (400 MHz, DMSO) δ 10.37 (s, 1H, amide), 9.23 (t, *J* = 5.7 Hz, 1H, quinoxaline), 8.69 (d, *J* = 8.3 Hz, 1H, quinoxaline), 7.90 (d, *J* = 7.9 Hz, 1H, quinoxaline), 7.53 (dd, *J* = 7.5, 4.6 Hz, 2H, (1H)-quinoxaline, (1H)-phenyl), 7.39 – 7.27 (m, 5H,

benzyl), 7.26 – 7.21 (m, 2H, phenyl), 4.56 (d, *J* = 5.8 Hz, 2H, benzylic methylene), 2.33 (s, 3H, CH_3).

3-benzyl-*N*-(4-chloro-2-methylphenyl)-4-oxo-3,4-dihydroquinazoline-2-carboxamide (QZA-15)

TLC (EtOAc:Hexane 25:75); Yield: 60%; White solid; mp: 192-194 °C; IR (KBr, *v* cm^{-1}): 3344 (sharp, N–H str.), 3062, 2974, 2781 (aromatic C-H str.), 1760 (keto C=O str.), 1703 (amide C=O str.), 1591, 1556 (C=C, C=N ring str.), 1402 (CH_2 bend), 1290, 1035 (C=C bend.); ^{1}H NMR (400 MHz, DMSO) δ 10.01 (s, 1H, amide), 8.68 (d, *J* = 8.5 Hz, 1H, quinoxaline), 7.90 (d, *J* = 7.9 Hz, 1H, quinoxaline), 7.74 (d, *J* = 8.6 Hz, 1H, quinoxaline), 7.54 (t, *J* = 7.7 Hz, 1H, quinoxaline), 7.34 (dd, *J* = 13.1, 7.2 Hz, 4H, (2H)-phenyl, (2H)-benzyl), 7.26 (t, *J* = 12.3 Hz, 2H, (1H)-phenyl, (1H)-benzyl), 7.05 – 6.83 (m, 1H, benzyl), 6.61 (d, *J* = 8.4 Hz, 1H, benzyl), 4.58 (d, *J* = 5.6 Hz, 2H, benzylic methylene), 2.33 (s, 3H, CH_3).

4.4.2. Series-8: 3-(4-methoxybenzyl)-4-oxo-N-phenyl-3,4-dihydroquinazoline-2-carboxamide analogues (QZB-1 to 19)

2-amino-*N*-(4-methoxybenzyl)benzamide (QZ-1B)

A solution of 3 g (0.022 mole) of 4-methoxybenzylamine in 4 ml of DMF was added to a stirred solution of 3.26 g (0.020 mole) of isatoic anhydride in 50 ml of THF maintained at 45-50 °C in a 100 ml RBF. Stirring and heating were continued for 8 hours. The cooled mixture was poured into 100 ml water, basified with 50% sodium hydroxide (*pH* = 9), filtered and washed with water to afford the desired compound. TLC (EtOAc:Hex 30:70); Yield: 98%; Colorless solid; mp: 104-105 °C; IR (KBr, *v* cm^{-1}): 3450 (N-H str. of primary - NH_2), 3350 (N-H str.), 3300 (aromatic C-H str.), 1678 (amide C=O str.), 1580, 1530 (C=C, C=N ring str.), 1510, 1465 (CH_2 bend), 1380 (CH_3 bend), 1300, 1100 (C=C bend), 1095, 1027 (ether C-O bend.); ^{1}H NMR (400 MHz, $CDCl_3$) δ 7.15-7.34 (m, 4H, (1H)-amide, (1H)-benzene, (2H)-phenyl), 6.89 (d, *J* = 8.2 Hz, 2H, benzene), 6.58-6.73 (m, 2H, phenyl), 6.25 (s, 1H, benzene), 5.56 (s, 2H, amine), 4.54 (d, *J* = 5.4 Hz, 2H, benzylic methylene), 3.81 (s, 3H, OCH_3).

Ethyl 3-(4-methoxybenzyl)-4-oxo-3,4-dihydroquinazoline-2-carboxylate (QZ-2B)

A mixture of 2.56 g (0.01 mol) of 2-amino-*N*-(4-methoxybenzyl)benzamide and 4.38 g (0.03 mol) of diethyl oxalate were heated for 30 min in a 100 ml RBF. The above mixture was cooled, 5 ml of EtOH was added, and the obtained precipitate filtered off, dried and recrystallized with ethanol to afford the desired compound. TLC (MeOH:$CHCl_3$ 30:70); Yield 72%; Pale white solid; mp: 210-212 °C; IR (KBr, *v* cm^{-1}): 3043 (aromatic C-H str.), 2357, 2339 (aromatic C-H str.), 1732 (ester C=O), 1680 (keto C=O str.), 1570, 1490 (C=C, C=N ring str.), 1465 (CH_2 bend), 1375 (CH_3 bend), 1310, 1100 (C=C bend), 1097, 1035 (ether C-O bend.); ^{1}H NMR (400 MHz, $CDCl_3$) δ 8.17 (dd, *J* = 8.5, 1.4 Hz, 1H, quinoxaline), 7.78 – 7.65 (m, 3H, quinoxaline), 7.45 (dd, *J* = 7.8, 6.6 Hz, 2H, benzyl), 6.92 – 6.84 (m, 2H, benzyl), 5.32 (s, 2H, benzylic methylene), 4.40 (q, *J* = 7.1 Hz, 2H, OCH_2CH_3), 3.78 (s, 3H, OCH_3), 1.35 (t, *J* = 7.1 Hz, 3H, OCH_2CH_3).

3-(4-methoxybenzyl)-4-oxo-3,4-dihydroquinazoline-2-carboxylic acid (QZ-3B)

3.3 g (0.01 mol) of ethyl 3-(4-methoxybenzyl)-4-oxo-3,4-dihydroquinazoline-2-carboxylate was dissolved in 5 ml of dry THF in a 100 ml RBF. To this mixture, 50% aqueous sodium hydroxide solution (*pH*>10) was added and stirred at room temperature for 2 hr. The solvent was removed under vacuum; residue washed with ethylacetate and the aqueous portion acidified with dil. HCl (*pH* = 5). The obtained solid residue was washed with cold water, filtered and recrystallized with EtOH to afford the desired compound.

TLC (EtOAc:Hexane 40:60); Yield: 85%; White solid; mp: 184-187 °C; IR (KBr, *v* cm^{-1}): 3384 (broad O–H str. COOH), 3218, 3175, 3066, 2947, 2858, 2644 (aromatic C-H str.), 1745 (acid C=O str.), 1715 (keto C=O str.), 1694, 1578, 1535 (C=C, C=N ring str.), 1460 (CH_2 bend), 1332, 1146 (C=C bend), 1095, 1040 (ether C-O bend.); ^{1}H NMR (400 MHz, $CDCl_3$) δ 10.24 (s, 1H, acid), 8.27 (d, *J* = 8.5 Hz, 1H, quinoxaline), 7.49 – 7.35 (m, 2H, benzyl), 7.28 – 7.18 (m, 3H, quinoxaline), 6.92 – 6.84 (m, 2H, benzyl), 5.58 (s, 2H, benzylic methylene), 3.83 (s, 3H, OCH_3).

General procedure for the synthesis of New Chemical Entity's (NCE's) i.e. quinazoline-2-carboxamide analogues (QZB-1 to 19)

To 0.5 g (0.0016 mol) of 3-(4-methoxybenzyl)-4-oxo-3,4-dihydroquinazoline-2-carboxylic acid taken in a 100 ml RBF, 0.37 g (0.0019 mol) of EDC·HCl was added and stirred with 5 ml of dry THF in an inert atmosphere (nitrogen) at 0 °C for 15 min. To the above reaction mixture, 0.37 g (0.0024 mol) HOBt was added and stirred for another 45 min. To the above mixture, 1 equivalent of appropriate amines were added and stirred continuously for 6 hr. The reaction mixture was concentrated under reduced pressure; resultant mass diluted with DCM/ethyl acetate, washed with aqueous sodium bicarbonate (2 × 50 ml), saturated brine solution (2 × 50 ml) and dried over anhydrous sodium sulfate. The solvent was then evaporated under reduced pressure to afford the desired compounds. The obtained compounds were purified by recrystallization with EtOH/MeOH/column chromatography over silica gel.

3-(4-methoxybenzyl)-4-oxo-*N*-phenyl-3,4-dihydroquinazoline-2-carboxamide (QZB-1)

TLC (EtOAc:Hexane 40:60); Yield: 77%; White solid; mp: 197-200 °C; IR (KBr, *v* cm^{-1}): 3374, 3290, (sharp, N–H str.), 3147, 3054, 2972, 2829 (aromatic C-H str.), 1698 (keto C=O str.), 1668 (amide C=O str.), 1635, 1584 (C=C, C=N ring str.), 1440 (CH_2 bend), 1383, 1248, 1184, 1157 (C=C bend), 1085, 1030 (ether C-O bend.); ^{1}H NMR (400 MHz, $CDCl_3$) δ 11.95 (s, 1H, amide), 8.15 (d, *J* = 7.7 Hz, 1H, quinoxaline), 7.70 – 7.65 (m, 5H, (3H)-quinoxaline, (2H)-phenyl), 7.40 (dt, *J* = 15.7, 7.6 Hz, 2H, phenyl), 7.25 (d, *J* = 8.6 Hz, 2H, benzyl), 7.19 (t, *J* = 7.4 Hz, 1H, phenyl), 6.85 (d, *J* = 8.7 Hz, 2H, benzyl), 5.57 (s, 2H, benzylic methylene), 3.78 (s, 3H, OCH_3).

3-(4-methoxybenzyl)-*N*-(2-methoxyphenyl)-4-oxo-3,4-dihydroquinazoline-2-carboxamide (QZB-2)

TLC (EtOAc:Hexane 40:60); Yield: 44%; White solid; mp: 164-166°C; IR (KBr, *v* cm^{-1}): 3354, 3265, 3105 (sharp, N–H str.), 2926, 2858, 2812, 2635, 2561 (aromatic C-H str.), 1715 (keto C=O str.), 1697 (amide C=O str.), 1565, 1512 (C=C, C=N ring str.), 1457

(CH_2 bend), 1322, 1276, 1184, 1165 (C=C bend), 1085, 1032 (ether C-O bend.); ^{1}H NMR (400 MHz, $CDCl_3$) δ 10.95 (s, 1H, amide), 8.25 (d, *J* = 7.7 Hz, 1H, quinoxaline), 7.82 (d, *J* = 7.7 Hz, 1H, phenyl), 7.70 – 7.65 (m, 3H, quinoxaline), 7.22 (d, *J* = 8.6 Hz, 2H, benzyl), 7.17 – 7.02 (m, 3H, phenyl), 6.88 (d, *J* = 8.7 Hz, 2H, benzyl), 5.57 (s, 2H, benzylic methylene), 3.78 (s, 6H, OCH_3).

3-(4-methoxybenzyl)-*N*-(3-methoxyphenyl)-4-oxo-3,4-dihydroquinazoline-2-carboxamide (QZB-3)

TLC (EtOAc:Hexane 40:60); Yield: 40%; White solid; mp: 157-160°C; IR (KBr, *v* cm^{-1}): 3344, 3257, 3125 (sharp, N–H str.), 2967, 2858, 2845, 2627, 2562 (aromatic C-H str.), 1726 (keto C=O str.), 1687 (amide C=O str.), 1585, 1534 (C=C, C=N ring str.), 1445 (CH_2 bend), 1324, 1277, 1186, 1165, 1152 (C=C bend), 1088, 1026 (ether C-O bend.); ^{1}H NMR (400 MHz, $CDCl_3$) δ 10.56 (s, 1H, amide), 8.12 (dd, *J* = 8.1, 1.2 Hz, 1H, quinoxaline), 7.82 – 7.68 (m, 3H, quinoxaline), 7.43 – 7.31 (m, 2H, benzyl), 7.32 – 7.15 (m, 3H, phenyl), 6.96 – 6.75 (m, 3H, (2H)-benzyl, (1H)-phenyl), 5.52 (s, 2H, benzylic methylene), 3.78 (s, 6H, OCH_3).

3-(4-methoxybenzyl)-*N*-(4-methoxyphenyl)-4-oxo-3,4-dihydroquinazoline-2-carboxamide (QZB-4)

TLC (EtOAc:Hexane 40:60); Yield: 60%; White solid; mp: 165-168°C; IR (KBr, *v* cm^{-1}): 3279, 3240 (sharp, N–H str.), 3139, 3066, 2995, 2927, 2765 (aromatic C-H str.), 1697 (keto C=O str.), 1685 (amide C=O str.), 1568, 1524 (C=C, C=N ring str.), 1459 (CH_2 bend), 1311, 1245, 1248, (C=C bend), 1090, 1032 (ether C-O bend.); ^{1}H NMR (400 MHz, $CDCl_3$) δ 10.85 (s, 1H, amide), 8.13 (dd, *J* = 8.1, 1.3 Hz, 1H, quinoxaline), 7.82 – 7.73 (m, 3H, quinoxaline), 7.45 (dd, *J* = 13.2, 7.8 Hz, 2H, phenyl), 7.21 (d, *J* = 8.7 Hz, 2H, benzyl), 6.94 – 6.86 (m, 2H, phenyl), 6.85 – 6.79 (m, 2H, benzyl), 5.56 (s, 2H, benzylic methylene), 3.77 (s, 6H, OCH_3).

***N*-(2-ethylphenyl)-3-(4-methoxybenzyl)-4-oxo-3,4-dihydroquinazoline-2-carboxamide (QZB-5)**

TLC (EtOAc:Hexane 40:60); Yield: 54%; White solid; mp: 156-158°C; IR (KBr, *v* cm^{-1}): 3312, 3256, 3165 (sharp, N–H str.), 3057, 2966, 2824 (aromatic C-H str.), 1705 (keto C=O str.), 1685 (amide C=O str.), 1586, 1554, 1525 (C=C, C=N ring str.), 1467, 1453 (CH_2 bend), 1329, 1240, 1165, 1127 (C=C bend), 1085, 1039 (ether C-O bend.); ^{1}H NMR (400 MHz, $CDCl_3$) δ 10.95 (s, 1H, amide), 8.16 (d, *J* = 7.2 Hz, 1H, quinoxaline), 7.82 – 7.68 (m, 3H, quinoxaline), 7.45 (d, *J* = 7.2 Hz, 1H, phenyl), 7.32 – 7.19 (m, 4H, (2H)-phenyl, (2H)-benzyl), 7.15 (t, *J* = 7.0 Hz, 1H, phenyl), 6.87 (d, *J* = 8.7 Hz, 2H,

benzyl), 5.59 (s, 2H, benzylic methylene), 3.78 (s, 3H, OCH_3), 2.84 (q, *J* = 7.5 Hz, 2H, CH_2CH_3), 1.33 (t, *J* = 7.5 Hz, 3H, CH_2CH_3).

***N*-(3-ethylphenyl)-3-(4-methoxybenzyl)-4-oxo-3,4-dihydroquinazoline-2-carboxamide (QZB-6)**

TLC (EtOAc:Hexane 40:60); Yield: 59%; White solid; mp: 152-154°C; IR (KBr, *v* cm^{-1}): 3276, 3165, 3067 (sharp, N–H str.), 3047, 2957, 2839 (aromatic C-H str.), 1699 (keto C=O str.), 1685 (amide C=O str.), 1646, 1605, 1548, 1513 (C=C, C=N ring str.), 1439 (CH_2 bend), 1299, 1242, 1175, 1158, 1118 (C=C bend), 1084, 1025 (ether C-O bend.); ^{1}H NMR (400 MHz, $CDCl_3$) δ 10.90 (s, 1H, amide), 8.19 (d, *J* = 7.2 Hz, 1H, quinoxaline), 7.72 (d, *J* = 8.1 Hz, 2H, phenyl), 7.67 – 7.58 (m, 3H, quinoxaline), 7.49 – 7.41 (m, 1H, phenyl), 7.33 – 7.22 (m, 2H, benzyl), 7.02 (d, *J* = 7.7 Hz, 1H, phenyl), 6.90 – 6.85 (m, 2H, benzyl), 5.56 (s, 2H, benzylic methylene), 3.77 (s, 3H, OCH_3), 2.68 (d, *J* = 7.6 Hz, 2H, CH_2CH_3), 1.27 (t, *J* = 7.6 Hz, 3H, CH_2CH_3).

***N*-(3-chloro-2-methylphenyl)-3-(4-methoxybenzyl)-4-oxo-3,4-dihydroquinazoline-2-carboxamide (QZB-7)**

TLC (EtOAc:Hexane 40:60); Yield: 27%; White solid; mp: 178-180°C; IR (KBr, *v* cm^{-1}): 3269, 3162, 3059 (sharp, N–H str.), 2978, 2897, 2819, 2647, 2575 (aromatic C-H str.), 1692 (keto C=O str.), 1686 (amide C=O str.), 1605, 1573, 1514 (C=C, C=N ring str.), 1454 (CH_2 bend), 1301, 1274, 1180, 1163 (C=C bend), 1099, 1035 (ether C-O bend.); ^{1}H NMR (400 MHz, $CDCl_3$) δ 10.87 (s, 1H, amide), 8.13 (d, *J* = 7.0 Hz, 1H, quinoxaline), 7.64 – 7.49 (m, 3H, quinoxaline), 7.42 (dd, *J* = 11.4, 4.3 Hz, 1H, phenyl), 7.38 – 7.25 (m, 4H, (2H)-benzyl, (2H)-phenyl), 7.07 (d, *J* = 8.8 Hz, 2H, benzyl), 5.57 (s, 2H, benzylic methylene), 3.75 (s, 3H, OCH_3), 2.37 (s, 3H, CH_3).

***N*-(2-chlorophenyl)-3-(4-methoxybenzyl)-4-oxo-3,4-dihydroquinazoline-2-carboxamide (QZB-8)**

TLC (EtOAc:Hexane 40:60); Yield: 52%; White solid; mp: 215-218°C; IR (KBr, *v* cm^{-1}): 3265, 3158, 3047 (sharp, N–H str.), 2985, 2881, 2816, 2375, 2311 (aromatic C-H str.), 1695 (keto C=O str.), 1683 (amide C=O str.), 1643, 1573, 1514 (C=C, C=N ring str.), 1481, 1438 (CH_2 bend), 1325, 1288, 1251, 1180, 1161 (C=C bend), 1105, 1026 (ether C-O bend.); ^{1}H NMR (400 MHz, $CDCl_3$) δ 11.15 (s, 1H, amide), 8.44 (dd, *J* = 8.3, 1.4 Hz, 2H, (1H)-phenyl, (1H)-quinoxaline), 7.75 – 7.60 (m, 4H, (3H)-quinoxaline, (1H)-phenyl), 7.37 (dd, *J* = 11.4, 4.3 Hz, 1H, phenyl), 7.28 (d, *J* = 8.7 Hz, 2H, benzyl), 7.15 (td, *J* = 7.7, 1.5 Hz, 1H, phenyl), 6.86 (d, *J* = 8.7 Hz, 2H, benzyl), 5.61 (s, 2H, benzylic methylene), 3.75 (s, 3H, OCH_3).

_N_-(3-chlorophenyl)-3-(4-methoxybenzyl)-4-oxo-3,4-dihydroquinazoline-2-carboxamide (QZB-9)

TLC (EtOAc:Hex 40:60); Yield: 59%; White solid; mp: 198-200°C; IR (KBr, *v* cm^{-1}): 3297, 3176 (sharp, N–H str.), 3182, 3113, 3054, 2930, 2834, 2678, 2070 (aromatic C-H str.), 1704 (keto C=O str.), 1681 (amide C=O str.), 1598, 1535, 1510 (C=C, C=N ring str.), 1479, 1467 (CH_2 bend), 1411, 1327, 1271, 1246 (C=C bend), 1101, 1041 (ether C-O bend.); ^{1}H NMR (400 MHz, $CDCl_3$) δ 10.98 (s, 1H, amide), 8.35 (dd, *J* = 8.3, 1.4 Hz, 2H, (1H)-quinoxaline, (1H)- phenyl), 7.89 – 7.81 (m, 3H, quinoxaline), 7.69 (d, *J* = 22.4 Hz, 1H, phenyl), 7.59 (d, *J* = 8.8 Hz, 1H, phenyl), 7.51 – 7.43 (m, 3H, (2H)-benzyl, (1H)-phenyl), 7.14 – 7.07 (m, 2H, benzyl), 5.30 (s, 2H, benzylic methylene), 3.81 (s, 3H, OCH_3).

_N_-(4-chlorophenyl)-3-(4-methoxybenzyl)-4-oxo-3,4-dihydroquinazoline-2-carboxamide (QZB-10)

TLC (EtOAc:Hexane 40:60); Yield: 60%; White solid; mp: 194-196°C; IR (KBr, *v* cm^{-1}): 3284, 3103 (sharp, N–H str.), 3012, 2885, 2825, (aromatic C-H str.), 1717 (keto C=O str.), 1689 (amide C=O str.), 1570, 1544, 1517 (C=C, C=N ring str.), 1489, 1463 (CH_2 bend), 1296, 1249, 1228, 1178, 1161 (C=C bend), 1087, 1036 (ether C-O bend.); ^{1}H NMR (400 MHz, $CDCl_3$) δ 10.57 (s, 1H, amide), 7.96 (d, *J* = 7.1 Hz, 1H, quinoxaline), 7.62 – 7.56 (m, 2H, phenyl), 7.46 – 7.32 (m, 3H, quinoxaline), 7.30 (d, *J* = 8.7 Hz, 2H, benzyl), 6.87 (d, *J* = 8.7 Hz, 2H, benzyl), 5.51 (s, 2H, benzylic methylene), 3.73 (s, 3H, OCH_3).

3-(4-methoxybenzyl)-4-oxo-_N_-o-tolyl-3,4-dihydroquinazoline-2-carboxamide (QZB-11)

TLC (EtOAc:Hexane 40:60); Yield: 48%; White solid; mp: 224-226 °C; IR (KBr, *v* cm^{-1}): 3326, 3265, 3142 (sharp, N–H str.), 3084, 2962, 2824 (aromatic C-H str.), 1712 (keto C=O str.), 1688 (amide C=O str.), 1585, 1544, 1512 (C=C, C=N ring str.), 1437, 1393 (CH_2 bend), 1329, 1240, 1165, 1127 (C=C bend), 1085, 1039 (ether C-O bend.); ^{1}H NMR (400 MHz, $CDCl_3$) δ 10.65 (s, 1H, amide), 8.16 (d, *J* = 7.1 Hz, 1H, quinoxaline), 7.74 – 7.60 (m, 3H, quinoxaline), 7.54 – 7.42 (m, 3H, phenyl), 7.38 – 7.26 (m, 2H, benzyl), 7.09 (dd, *J* = 7.6, 1.4 Hz, 1H, phenyl), 6.90 – 6.84 (m, 2H, benzyl), 5.58 (s, 2H, benzylic methylene), 3.79 (s, 3H, OCH_3), 2.14 (s, 3H, CH_3).

3-(4-methoxybenzyl)-4-oxo-*N*-m-tolyl-3,4-dihydroquinazoline-2-carboxamide (QZB-12)

TLC (EtOAc:Hexane 40:60); Yield: 40%; White solid; mp: 217-220 °C; IR (KBr, *v* cm^{-1}): 3345, 3254, 3137 (sharp, N–H str.), 3079, 2965, 2890 (aromatic C-H str.), 1716 (keto C=O str.), 1685 (amide C=O str.), 1584, 1548, 1510 (C=C, C=N ring str.), 1451, 1358 (CH_2 bend), 1329, 1240, 1165, 1127 (C=C bend), 1085, 1039 (ether C-O bend.); ^{1}H NMR (400 MHz, $CDCl_3$) δ 10.84 (s, 1H, amide), 8.12 (d, *J* = 7.1 Hz, 1H, quinoxaline), 7.82 (d, *J* = 7.7 Hz, 1H, phenyl), 7.70 – 7.65 (m, 3H, quinoxaline), 7.54 – 7.49 (m, 1H, phenyl), 7.38 – 7.26 (m, 3H, (1H)-phenyl, (2H)-benzyl), 7.09 (dd, *J* = 7.6, 1.4 Hz, 1H, phenyl), 6.90 – 6.84 (m, 2H, benzyl), 5.58 (s, 2H, benzylic methylene), 3.77 (s, 3H, OCH_3), 2.34 (s, 3H, CH_3).

3-(4-methoxybenzyl)-4-oxo-*N*-p-tolyl-3,4-dihydroquinazoline-2-carboxamide (QZB-13)

TLC (EtOAc:Hexane 40:60); Yield: 58%; White solid; mp: 208-210 °C; IR (KBr, *v* cm^{-1}): 3344, 3254, 3137 (sharp, N–H str.), 3062, 2974, 2781 (aromatic C-H str.), 1720 (ester C=O Keto), 1683 (C=O str.), 1591, 1556 (C=C, C=N ring str.), 1402 (CH_2 bend), 1370, 1245, 1167, 1135 (C=C bend), 1089, 1045 (ether C-O bend.); ^{1}H NMR (400 MHz, $CDCl_3$) δ 10.75 (s, 1H, amide), 8.15 (d, *J* = 7.1 Hz, 1H, quinoxaline), 7.74 – 7.59 (m, 3H, quinoxaline), 7.43 – 7.31 (m, 2H, benzyl), 7.32 – 7.15 (m, 4H, phenyl), 6.96 – 6.80 (m, 2H, benzyl), 5.54 (s, 2H, benzylic methylene), 3.77 (s, 3H, OCH_3), 2.36 (s, 3H, CH_3).

3-(4-methoxybenzyl)-4-oxo-*N*-(2-propylphenyl)-3,4-dihydroquinazoline-2-carboxamide (QZB-14)

TLC (EtOAc:Hexane 40:60); Yield: 65%; White solid; mp: 146-148°C; IR (KBr, *v* cm^{-1}): 3279, 3125 3064 (sharp, N–H str.), 3044, 2960, 2878, 2628, 2362 (aromatic C-H str.), 1703 (keto C=O str.), 1686 (amide C=O str.), 1573, 1514 (C=C, C=N ring str.), 1454 (CH_2 bend), 1309, 1274, 1180, 1163 (C=C bend), 1097, 1031 (ether C-O bend.); ^{1}H NMR (400 MHz, $CDCl_3$) δ 10.75 (s, 1H, amide), 8.15 (d, *J* = 7.1 Hz, 1H, quinoxaline), 7.74 – 7.59 (m, 3H, quinoxaline), 7.52 – 7.46 (m, 1H, phenyl), 7.39 – 7.25 (m, 4H, (2H)-phenyl, (2H)-benzyl), 7.15 (dd, *J* = 7.6, 1.4 Hz, 1H, phenyl), 6.90 – 6.85 (m, 2H, benzyl), 5.56 (s, 2H, benzylic methylene), 3.77 (s, 3H, OCH_3), 2.75 – 2.66 (m, 2H, $CH_2CH_2CH_3$), 1.65 – 1.59 (m, 2H, $CH_2CH_2CH_3$), 0.94 (t, *J* = 7.3 Hz, 3H, $CH_2CH_2CH_3$).

_N_-(2-isopropylphenyl)-3-(4-methoxybenzyl)-4-oxo-3,4-dihydroquinazoline-2-carboxamide (QZB-15)

TLC (EtOAc:Hexane 40:60); Yield: 69%; White solid; mp: 175-178°C; IR (KBr, *v* cm^{-1}): 3272, 3118 3084 (sharp, N–H str.), 3034, 2997, 2932, 2825 (aromatic C-H str.), 1713 (keto C=O str.), 1685 (amide C=O str.), 1578, 1520, 1504 (C=C, C=N ring str.), 1451 (CH_2 bend), 1309, 1282, 1247, 1180, 1165 (C=C bend), 1101, 1035 (ether C-O bend.); ^{1}H NMR (400 MHz, $CDCl_3$) δ 10.95 (s, 1H, amide), 8.24 (d, *J* = 7.1 Hz, 1H, quinoxaline), 7.66 – 7.52 (m, 3H, quinoxaline), 7.44 – 7.31 (m, 3H, phenyl), 7.28 – 7.16 (m, 2H, benzyl), 7.09 (dd, *J* = 7.6, 1.4 Hz, 1H, phenyl), 6.90 – 6.84 (m, 2H, benzyl), 5.58 (s, 2H, benzylic methylene), 3.77 (s, 3H, OCH_3), 3.34 (dd, *J* = 13.6, 6.8 Hz, 1H, $CH(CH_3)_2$), 1.33 (d, *J* = 6.8 Hz, 6H, $CH(CH_3)_2$).

_N_-(4-isopropylphenyl)-3-(4-methoxybenzyl)-4-oxo-3,4-dihydroquinazoline-2-carboxamide (QZB-16)

TLC (EtOAc:Hexane 40:60); Yield: 66%; White solid; mp: 170-172°C; IR (KBr, *v* cm^{-1}): 3265, 3147 3056 (sharp, N–H str.), 2958, 2866, 2817 (aromatic C-H str.), 1715 (keto C=O str.), 1688 (amide C=O str.), 1651, 1548, 1514 (C=C, C=N ring str.), 1485 (CH_2 bend), 1415, 1294, 1251, 1180, 1163 (C=C bend), 1091, 1026 (ether C-O bend.); ^{1}H NMR (400 MHz, $CDCl_3$) δ 10.85 (s, 1H, amide), 8.09 (d, *J* = 7.1 Hz, 1H, quinoxaline), 7.74 – 7.59 (m, 5H, (3H)-quinoxaline, (2H)-phenyl), 7.30 – 7.16 (m, 4H, (2H)-phenyl, (2H)- benzyl), 6.86 (d, *J* = 8.7 Hz, 2H, benzyl), 5.57 (s, 2H, benzylic methylene), 3.76 (s, 3H, OCH_3), 2.91 (dd, J = 13.8, 6.9 Hz, 1H, $CH(CH_3)_2$), 1.26 (d, *J* = 6.9 Hz, 6H, $CH(CH_3)_2$).

_N_-(2-chloro-4-methylphenyl)-3-(4-methoxybenzyl)-4-oxo-3,4-dihydroquinazoline-2-carboxamide (QZB-17)

TLC (EtOAc:Hexane 40:60); Yield: 24%; White solid; mp: 234-236°C; IR (KBr, *v* cm^{-1}): 3279, 3127 3042 (sharp, N–H str.), 2973, 2948, 2913, 2871, 2815 (aromatic C-H str.), 1703 (keto C=O str.), 1685 (amide C=O str.), 1531, 1514 (C=C, C=N ring str.), 1463, 1450 (CH_2 bend), 1301, 1249, 1180, 1165 (C=C bend), 1097, 1033 (ether C-O bend.); ^{1}H NMR (400 MHz, $CDCl_3$) δ 10.24 (s, 1H, amide), 8.19 (d, *J* = 7.1 Hz, 1H, quinoxaline), 7.75 – 7.60 (m, 4H, (3H)-quinoxaline, (1H)-phenyl), 7.44 (d, *J* = 7.0 Hz, 1H, phenyl), 7.22 (d, *J* = 8.8 Hz, 2H, benzyl), 7.15 (d, *J* = 8.5 Hz, 1H, phenyl), 6.87 (d, *J* = 8.8 Hz, 2H, benzyl), 5.59 (s, 2H, benzylic methylene), 3.77 (s, 3H, OCH_3), 2.34 (s, 3H, CH_3).

_N_-(2-chloro-5-methylphenyl)-3-(4-methoxybenzyl)-4-oxo-3,4-dihydroquinazoline-2-carboxamide (QZB-18)

TLC (EtOAc:Hexane 40:60); Yield: 35%; White solid; mp: 206-208°C; IR (KBr, *v* cm^{-1}): 3272, 3120 3045 (sharp, N–H str.), 2960, 2928, 2825, (aromatic C-H str.), 1707 (keto C=O str.), 1682 (amide C=O str.), 1575, 1531, 1516 (C=C, C=N ring str.), 1438, 1444, 1415 (CH_2 bend), 1310, 1257, 1182, 1153 (C=C bend), 1097, 1051 (ether C-O bend.); ^{1}H NMR (400 MHz, $CDCl_3$) δ 10.20 (s, 1H, amide), 8.23 (d, *J* = 7.0 Hz, 1H, quinoxaline), 7.67 – 7.52 (m, 4H, (3H)-quinoxaline, (1H)-phenyl), 7.45 (d, *J* = 7.0 Hz, 1H, phenyl), 7.23 (d, *J* = 8.8 Hz, 2H, benzyl), 6.92 (dd, *J* = 8.2, 1.5 Hz, 1H, phenyl), 6.89 – 6.84 (m, 2H, benzyl), 5.59 (s, 2H, benzylic methylene), 3.77 (s, 3H, OCH_3), 2.39 (s, 3H, CH_3).

_N_-(2-chloro-6-methylphenyl)-3-(4-methoxybenzyl)-4-oxo-3,4-dihydroquinazoline-2-carboxamide (QZB-19)

TLC (EtOAc:Hexane 40:60); Yield: 39%; White solid; mp: 178-180°C; IR (KBr, *v* cm^{-1}): 3267, 3158, 3040 (sharp, N–H str.), 2902, 2835, 2763, 2655 (aromatic C-H str.), 1742 (keto C=O str.), 1687 (amide C=O str.), 1570, 1512 (C=C, C=N ring str.), 1487, 1453, 1414 (CH_2 bend), 1301, 1259, 1230, 1163 (C=C bend), 1097, 1039 (ether C-O bend.); ^{1}H NMR (400 MHz, $CDCl_3$) δ 10.28 (s, 1H, amide), 8.26 (d, *J* = 8.0 Hz, 1H, quinoxaline), 7.65 – 7.49 (m, 3H, quinoxaline) 7.42 (t, *J* = 7.7 Hz, 1H, phenyl), 7.36 (t, *J* = 7.8 Hz, 3H, (1H)-phenyl, (2H)-benzyl), 7.22 (d, *J* = 7.6 Hz, 1H, phenyl), 6.88 (d, *J* = 8.6 Hz, 2H, benzyl), 5.58 (s, 2H, benzylic methylene), 3.78 (s, 3H, OCH_3), 2.40 (s, 3H, CH_3).

4.5. Assay for PDE4 inhibitory activity

All the synthesized compounds were subjected to *in-vitro* evaluation (assay) using PDE4D and PDE4B isoform elisa kits. PDE4 assay kit used in the assay was PDE4B2 (Catalog number # 60343)[264] and PDE4D2 (Catalog number # 60345)[44b] obtained from BPS Bioscience, SanDiego, CA, USA.

The assay Kit is intended for recognition of inhibitors by fluorescence polarization (FP).[265] The assay is based on the binding of a fluorescent nucleotide monophosphate produced by PDE4B and PDE4D to the binding agent. The standard assay protocol provided by the supplier was followed.

The chemicals used were PDE4D2 or PDE4B2 recombinant enzyme, carboxyfluorescein (FAM)-Cyclic-3´, 5´-AMP (20 µM), PDE assay buffer, binding agent, binding agent diluent along with black, low binding NUNC microtiter plate which were provided with the elisa kit and dimethylsulfoxide (DMSO).

PDEs catalyze the hydrolysis of the phosphodiester bond in dye-labeled cyclic monophosphates. Beads selectively bind to the phosphate group in the nucleotide product. This increases the size of the nucleotide relative to unreacted cyclic monophosphate. In the polarization assay, dye molecules with absorption transition vectors parallel to the linearly-polarized excitation light are selectively excited. Dyes attached to the rapidly-rotating cyclic monophosphates will obtain random orientations and emit light with low polarization. Dyes attached to the slowly-rotating nucleotide-bead complexes will not have time to reorient and therefore will emit highly polarized light. **(Fig. 23)**

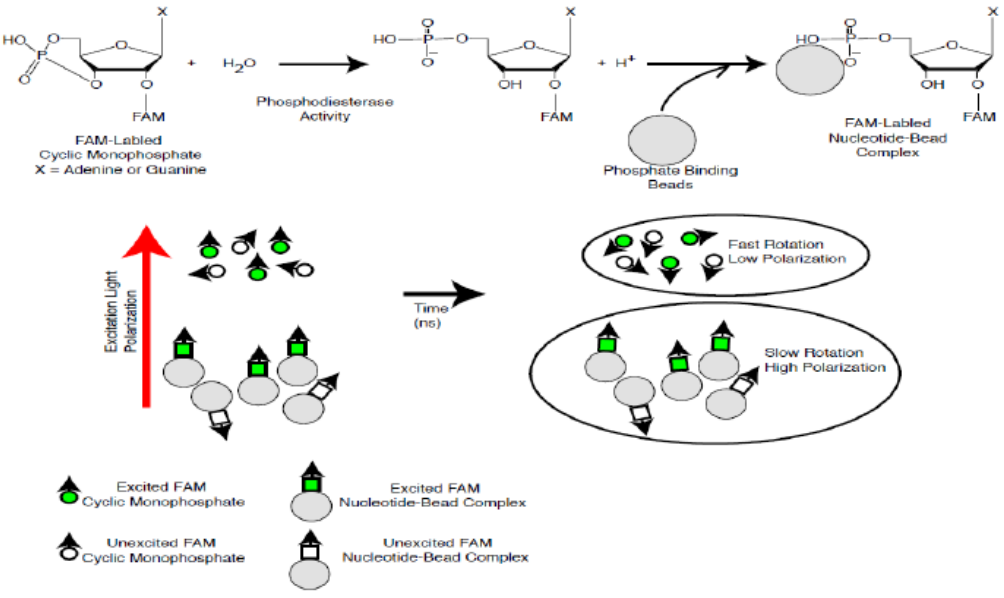

Fig. 23: Assay by fluorescent polarization principle (*BPS Bioscience*)

100 µM solutions of the test compounds and rolipram as standard were prepared with 10% DMSO in PDE assay bufferso that the final concentration of DMSO is 1% in all the reaction mixtures. DMSO does not affect enzyme activity at this concentration. The enzymatic reactions were conducted at room temperature for 60 min in a 50 µl mixture containing 25 µl of 200 nM FAM-cAMP (fluorescently labeled PDE4B/PDE4D substrate), 20 µl of PDE4B2/PDE4D2 enzyme and 5 µl of the test compound solution in PDE assay buffer. After the enzymatic reaction, 100 µl of a binding solution (1:100 dilution of the binding agent with the binding agent diluent) was added to each reaction well and the reaction was performed at room temperature for 60 min. Fluorescence intensity was measured at an excitation of 485 nm and an emission of 528 nm using a SpectroMax *M5* microplate reader (Molecular Device, USA). All samples and controls were tested in duplicates and blank values subtracted from all other values.[266] The percent activity in the presence of the compound was calculated according to the following equation

$$Percentage\ Inhibitory\ Activity = \frac{FP - FP_b}{FP_t - FP_b} \times 100$$

Where, *FP* is the fluorescence polarization in the presence of the compound, FP_t is the positive controland FP_b is blank.

The percentage of PDE4B and PDE4D inhibitory activity of the synthesized compounds were subsequently calculated. The term “affinity” was used to distinguish among the PDE4 isoform (PDE4B and PDE4D) while the term “activity” was used to describe the extent to which it binds to the enzyme to elicit the pharmacological response as depicted by the following **fig. 24**.[267]

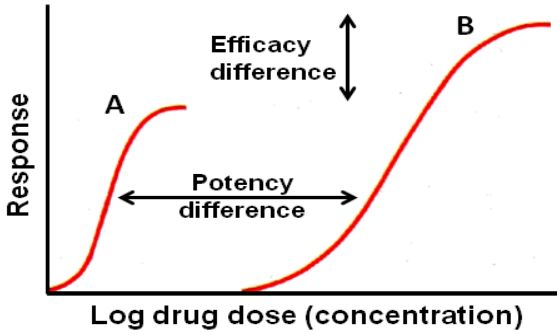

Fig. 24: Difference between ‘potency’ (*affinity*) and ‘efficacy’ (*activity*)

4.6. Rational and design

Molecular docking studies of the synthesized compounds were performed in order to rationalize the obtained biological results and also help us to understand the various interactions between the ligands and enzyme active sites in detail.

4.6.1. Ligand Preparation

A total of 143 ligands were used for this study. The structures of these ligands were sketched in DS 3.5 and the 3D structure generated using catalyst and saved in .sd format. To these ligands, hydrogen bonds were added and energy minimized using CHARMm force field. The proposed compounds were optimized by semi-empirical method (AM1) using Chem3D to eliminate bond length and bond angle biases and saved to be used in the docking steps. All the designed molecules adhered to "Lipinski's rule of 5" and were calculated for the ligands used in this study.

4.6.2. Protein structure preparation

The PDE4 protein-ligand complex crystal structure for PDE4B (PDB ID: 1XMY)[30] and PDE4D (PDB ID: 1Q9M)[38] were chosen as templates for docking analysis. The coordinates for the protein structure was obtained from the RCSB Protein Data Bank (PDB). All molecular simulations were performed on Dell workstation. Protein Structure was prepared using DS 3.5 software package.[262b] The original crystal ligand and water molecules were removed from the protein-ligand complexes, the invalid or missing residues were added and the structures aligned using the protein structure alignment module. Hydrogen atoms were added and the structures were energy minimized using CHARMm force field which is explained by the equation below and Momany-Rone charge as a default setting in DS 3.5, to relax the backbone and to remove the clashes. The prepared protein structures were saved in .dsv format.

$$E = Eb + Eq + Ef + Ew + Evdw + Eel + Ehb + Ecr + Ecj$$

Where E = total energy; Eb = Bond potential energy; Eq & Ef = bond angle potential energy; Ew = torsion energy; Evdw = vanderwaals interaction energy; Eel = electrostatic potential energy; Ehb = hydrogen bond energy; Ecr = energy constraints; Ecj = energy function.

The rational for the selection of these proteins was that it contains rolipram as co-crystallized ligand. The PDB structure chosen for PDE4B (PDB ID: 1XMY) had a good resolution of 2.40 Å with R-value of 0.245 and R-free of 0.298 while, the PDB structure chosen for PDE4D (PDB ID: 1Q9M) had a good resolution of 2.30 Å with R-value of 0.224 and R-free of 0.259 and both these proteins had RMSD value below 2 Å.

4.6.3. Material and method – Molecular Docking

LigandFit (DS 3.5) software was used in this study for docking studies.[262] LigandFit was executed for accurate orientation of the ligands into the protein active site. The binding sites of the proteins were identified based on a cavity detection algorithm from the

receptor site parameter of the tool which allows us to predict the strongest binders based on various scoring function. Monte Carlo conformational search algorithm was applied for generating ligand poses consistent with the active site shape. The ligand pose (or) pose optimization i.e., fine-tuning of fine energy in ligandfit occurs by Broyden-Flecher Gold Farbshanno (BFGS) method. Throughout the docking process top ten conformations were generated for each ligand after the energy minimization using the smart minimize method, which begins with steepest descent method followed by conjugate gradient method.

To execute docking process, a protocol called “Dockligands” (LigandFit) was selected under receptor-ligand interaction protocol cluster. The ligand compound was given as input in the parameter “input ligands” and the protocol run for each of the proteins selected for the study. The determination of the ligand binding affinity was calculated using LigScore and PLP, Jain and Dock score. The ligand binding energies were calculated based on high Dock score of best conformation.

The active site was identified by the volume occupied by co-crystal. The critical residues were selected by examining the PDE4 co-crystal structures from PDB.The binding sites of the proteins were analyzed and were identified based on a cavity detection algorithm by selecting amino acids nearby the original ligands.[262a] In the present study, for PDE4B **site 2**, a defined cavity size of **2281 points, 285.125 Å^3** and for PDE4D **site 4**, a defined cavity size of **3663 point units, 457.875 Å^3** were chosen as the binding site as they were in close proximity to that of the co-crystallized rolipram which was followed by site sphere definition. The site partition was defined and was set to 5.

For the study, the molecular docking analysis of PDE4 with ligands was carried out using ‘dreiding’ parameter. In this energy grid parameter, the Gasteiger charging method is employed to calculate the partial charges of target protein and ligand. The energy grid extension was set to 3.0 Á and the conformation search number of Monte-carlo trial to ‘15000’. The number of poses for ligands in receptor cavity was set to 10. Apart from these, other input parameters for docking were set as default options. The docked poses were minimized using CHARMm force field and evaluated with a set of scoring functions. Thebinding modes were calculated using intermolecular flexible docking simulations of ligandFit program.

Validation of the function implemented in ligandfit was done by docking of the native ligand into its binding site. The docked results were compared to the crystal structure of the bound ligand–protein complex. The RMSD of the docked ligand for PDE4B and PDE4D was 0.96 Á and 0.60 Á respectively, as it seems exactly superimposed on the

native bound one. **(Fig. 25)** In the interpretation of docked molecules, Dockscore scoring function was able to retrieve reasonable pose of the active molecules. These results indicated high accuracy of the ligandfit simulation in comparison with biological methods.

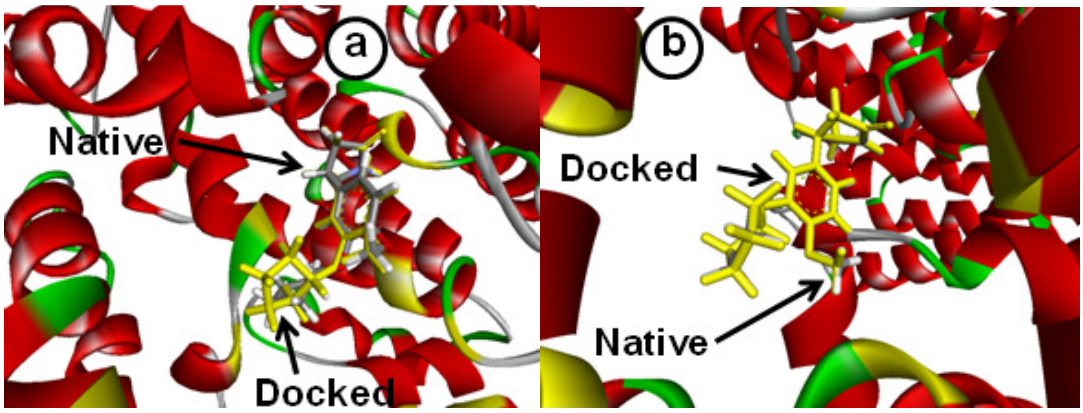

Fig. 25: Validation of docking methodology **(a)** RMSD of PDE4B (1XMY)=0.96 Å **(b)** RMSD of PDE4D (1Q9M)=0.60 Å. Redocked mode of rolipram (yellow) superimposed with the co-crystallized ligand (gray). The rest of the protein component is suppressed for clarification purposes.

Next, docking studies were performed for the synthesized compounds and the final docked complexes of ligand–enzyme were selected according to the criteria of interaction energy combined with geometrical matching quality. Top ten scored docking complex were extracted for conformational cluster analysis in order to find the docking results with the highest probability. Each of the saved conformation was evaluated and ranked using the scoring functions including LigScore1, LigScore2, Piecewise Linear Potential (PLP1 and PLP2), PMF, JAIN, and Dockscore, which were used for the detection of potential inhibitors. Consensus score was computed after scoring all the poses which improves the accuracy of docking simulation and *in-silico* screening. Ligscores indicates the protein ligand affinity energy; higher PLP score indicates stronger receptor-ligand binding, high PMF score indicates a stronger receptor-ligand binding affinity and DockScore was used to estimate the ligand-binding energies.

4.6.4. Predicting ADME properties: *ADMET descriptors using Accelrys software*

The ADMET properties of designed molecules was computed using the ADME descriptors module available in Discovery Studio (D.S) 3.5 software package (Accelrys)[262b] to predict a range of drug-like properties of compounds. This protocol uses the QSAR models and is suitable to estimate the ADME related properties for designed small molecules. The following properties can be computed such as aqueous solubility, blood-brain barrier penetration (BBB), cytochrome P450 (CYP450) *2D6* inhibition, hepatotoxicity, human intestinal absorption (HIA), and plasma protein binding.

Furthermore, key issue was to calculate the BBB penetration of these compounds, as it should cross the BBB to react with the receptor protein to treat central nervous system (CNS) disorders. The obtained data are listed.

4.6.4.1. *Aqueous Solubility*

This model uses linear regression to predict the solubility of each compound in water at 25 ˚C. A predictive model for aqueous solubility was generated using a dataset containing 775 compounds (MW between 50 and 800).[268] This model classifies the compounds as six prediction levels: 0 (Extremely low), 1 (very low, but possible), 2 (low), 3 (good), 4 (optimal), 5 (too soluble), 6 (Warning: molecules with one or more unknown AlogP98 types).

4.6.4.2. *Blood-brain barrier (BBB)*

This model predicts BBB after oral administration. It is a quantitative linear regression model comprised of 95 and 99% confidence ellipses in the ADMET_PSA_2D, ADMET_AlogP98 plane. These ellipses are not the same as those associated with the ADMET-HIA, although they have an analogous interpretation. They were derived from over 800 compounds that are known to enter the CNS after oral administration.[269] There are four prediction levels within the 95% and 99% confidence ellipsoids: 0 (Very high penetrant), 1 (High), 2 (Medium), 3 (Low), 4 (Undefined).

4.6.4.3. *Cytochrome P450 (CYP450)*

The CYP450 *2D6* model predicts CYP*2D6* enzyme inhibition using 2D chemical structure as input. The model was developed from known CYP*2D6* inhibition data on a diverse set of 151 compounds.[270] An ensemble of recursive partitioning trees was trained against 2D descriptors and 1D similarity data. The model classifies compounds as either 0 or 1 for non-inhibitor or inhibitor and provides an average-class-value estimate of confidence.

4.6.4.4. *Hepatotoxicity*

A computational model for predicting potential liver toxicity for a wide range of structurally diverse compounds was reported.[271] Using literature data of 436 compounds which exhibited liver toxicity, or trigger elevated dose-related aminotransferase levels in more than 10% of the human population. These compounds were classified using SAR technique that uses modified Bayesian learning and later using recursive partitioning.[272] Using only 2D information from the compounds provided, the model predicts, with greater than 80% accuracy, the potential occurrence of dose-dependent human hepatotoxicity of any compound. The model classifies compounds either as 0 or 1 for ‘nontoxic’ or ‘toxic’ and offers a confidence level indicator of the probability of the predictive accuracy of the model.

Each marker molecule has a characteristic 1D similarity threshold which determines whether predicted compound is sufficiently similar to bind at that marker's associated level (90 or 95%). Binding level predictions is also augmented by circumstances on AlogP98.[273]

4.6.4.5. *Human intestinal absorption (HIA)*

Egan et al. reported a computational model for predicting HIA after oral administration. Intestinal absorption is defined as a percentage absorbed rather than, as a ratio of concentrations (BBB penetration). The model was developed using 182 compounds in the training set, with descriptors that include AlogP98 and 2D polar surface area (PSA_2D).[269, 274] Well absorbed compounds have at least 90% absorption into human bloodstream, and by this model will generally reside within the ellipse regions of 95% and 99% confidence levels. This model classifies compounds as four prediction levels: 0 (Good), 1 (Moderate), 2 (Poor) and 3 (Very poor) thereby providing an average-class-value estimate of confidence.

4.6.4.6. *Plasma Protein Binding (PPB)*

The PPB model predicts whether a compound is likely to be highly bound (>= 90% bound) to carrier proteins in the blood. Plasma protein binding of drug molecules can affect the efficiency of a drug, because the bound fraction is temporarily shielded from metabolism. On the other hand, only the unbound fraction exhibits pharmacological effects. The model was developed using 854 compounds in the training set and using a cutoff binding level of 90%, the training set was divided into 329 binders and 525 non-binders.[273, 275] A modified Bayesian learning was used to create a binary classification model and was validated.[272] The model classifies compounds as either 0 or 1 for less than 90% or greater than 90% and provides an average-class-value estimate of confidence.

4.7. Pharmacology

All the animals were obtained from Hissar Agricultural University, Hissar, Haryana, India, and were maintained in colony cages at 23 ± 2 °C, relative humidity of 45 to 55% under a 12-h light/dark cycle, fed with standard animal feed and water *ad libitum*. The Institutional Animal Ethics Committee of the Birla Institute of Technology & Science, Pilani, India, approved the experimentation on animals (Protocol No. IAEC/RES/14/03 and IAEC/RES/Rev/16/08) and compounds were assessed for their anti-depressant and anxiolytic potential in Swiss Albino mice (18-25 g).

4.7.2. Spontaneous locomotor activity (SLA)

SLA was assessed using the actophotometer, which contained a square arena (30 × 30 cm) with walls that were fitted with photocells just above the floor level. The photocells were tested before the start of the experiment. The drug (1 mg/Kg, i.p.)/vehicle treated mice (n = 6/8) were then individually placed in the arena. After a two minute adaptation period, the digital locomotor scores were recorded for the next 10 min.[276]

4.7.2. Anti-depressant screening

FST and TST were used for screening anti-depressant properties of the synthesized compounds.

4.7.2.1. Force swim test (FST)

The FST was slightly modified[276] from the originally described method.[277] In brief, each mouse was placed individually in a glass cylinder (diameter 22.5 cm, height 30 cm) filled with water at a height of 15 cm. The floor of the cylinder was demarcated into four equal quadrants. The mice were forced to swim for 15 min on the 1st day. Mice were then allowed to return to their home cage. On the 2nd day, each mouse [vehicle/drug (1 mg/Kg, i.p.) treated] was placed again in the water and forced to swim for 6 min. The duration of immobility during the last 4 min was measured. The mouse was considered as immobile when it stopped struggling and passively moved to remain floating by keeping its head above water. Water was changed between trials and temperature was maintained at 22–23 °C. The parameter recorded was the number of seconds spent immobile, and fluoxetine for FST (10 mg/kg i.p.) was used as a standard drug.

4.7.2.2. Tail suspension test (TST)

In TST, the mouse was suspended on the edge of a shelf 50 cm above a table top by adhesive tape placed approximately 1 cm from the tip of the tail and duration of immobility being recorded. The total duration of the test (6 min) can be divided into periods of agitation and immobility. Mice were considered immobile only when they were completely motionless. The parameter recorded was the number of seconds spent immobile, and bupropion (20 mg/kg i.p.) for TST was used as a standard drug.[278]

4.7.3. Anxiolytic Screening

The compounds that exhibited better anti-depressant activity (FST and TST) were evaluated for their anxiolytic activity in mice using elevated plus-maze (EPM) model. Compounds which showed significant anxiolytic effect in EPM test were subjected to open field test (OFT), another standard animal model for anxiolytic screening, to confirm their anxiolytic effects. Diazepam (2 mg/kg i.p.) was used as a positive control, a standard anxiolytic agent.

4.7.3.1. Elevated Plus-Maze (EPM) test

EPM is a simple apparatus to study anxiolytic response of anti-anxiety agents. It consists of two opposed open arms (16 x 5 cm) at right angles with two opposed enclosed arms (16 x 5 x 12 cm). This method was used to evaluate the anxiolytic effects of the new chemical entities.[279] The rodents (mice) were treated with vehicle or test compounds (0.5 - 2 mg/Kg, i.p.) or diazepam (2 mg/Kg, i.p.). After 30 min, animals were placed individually at the center of the plus-maze with head facing towards the open arm at the beginning of the test and the time spent in each arm (open/closed) were recorded for 5 min.It is calculated using the formula:

$$\%\ of\ Open\ arm\ entries = \frac{time\ spent\ in\ open\ arm}{total\ time\ \ (5\ min)} \times\ 100$$

$$\%\ of\ time\ spent\ in\ Open\ arm = \frac{time\ spent\ in\ open\ arm - closed\ arm}{time\ spent\ in\ open\ arm} \times 100$$

4.7.3.2. Light /dark Aversion Test (L/D)

The apparatus comprised of a box divided into two separate compartments, occupying two-third and one-third of the total size, respectively. The large chamber was brightly illuminated, while the smaller compartment was entirely dark. The chambers are separated by a partition with a tunnel to allow Mice to move freely between the two chambers.[263] The mice were treatedwith vehicle or test compounds (0.5-1 mg/kg i.p.) or diazepam (2 mg/kg i.p.) and placed at the center of the light compartment facing towards the tunnel and allowed to explore, while the latency time to leave the light compartment, total time spent in light compartment and number of transitions between L/D compartments is recorded for 5 min. Floor was cleaned with 50% aqueous EtOH and dried between each trial.

4.7.3.3. Open Field Test (OFT)

The apparatus consisted of a wooden box with dimension of 68 cm × 68 cm and 45 cm high wall. The walls and floor were painted black; the floor was divided into 100 squares. The experimental place was very dimly illuminated and sound attenuated. The open field was illuminated with 60 Watts bulb, which was suspended at a height of 75 cm.[263] Mice were treated with vehicle or test compounds (2 mg/Kg, i.p.) or diazepam (2 mg/Kg, i.p.). After 30 min, animals were placed individually in one of the corner square. The number of squares crossed and number of rearing were recorded for the period of 5 min. Floor was cleaned with 50% aqueous EtOH and dried between each trial.

4.7.4. Statistical analysis

Statistical analyses were done by using Graph pad prism (version 3) software and Microsoft Office Excel (MS Office 2007). The results of anti-depressant, locomotor and anxiolytic activities are expressed as the mean ± SEM. Experimental data were analyzed through one way ANOVA followed by post hoc Dunnett's test. Statistical significance was set at $p<0.05$.

5. RESULTS AND DISCUSSION

5.1. Pharmacophore and Chemistry

5.1.1. Pharmacophore design

A common pharmacophore from compounds topologically associated to nitraquazone and its analogues were preferred for the pharmacophoric assessment. **(Fig. 26)** A meticulous logical conformational exploration on the preferred compounds was executed to establish their lowest energy conformations. Calculations were performed using CHARMm force field in D.S ver 3.5 or ACDLABS-12.0/3D. Identifying the common features of nitraquazone derivative PDE4 inhibitors, the interfeature distances were measured and considered for designing novel modified pharmacophore model. Slight modification was attempted to incorporate the benzyl group instead of phenyl group in the pharmacophore to reduce emetogenic effect.[280] Using this model, novel PDE4 inhibitors were designed which may be potent, better isoform selective and plausibly with minimum side effects.

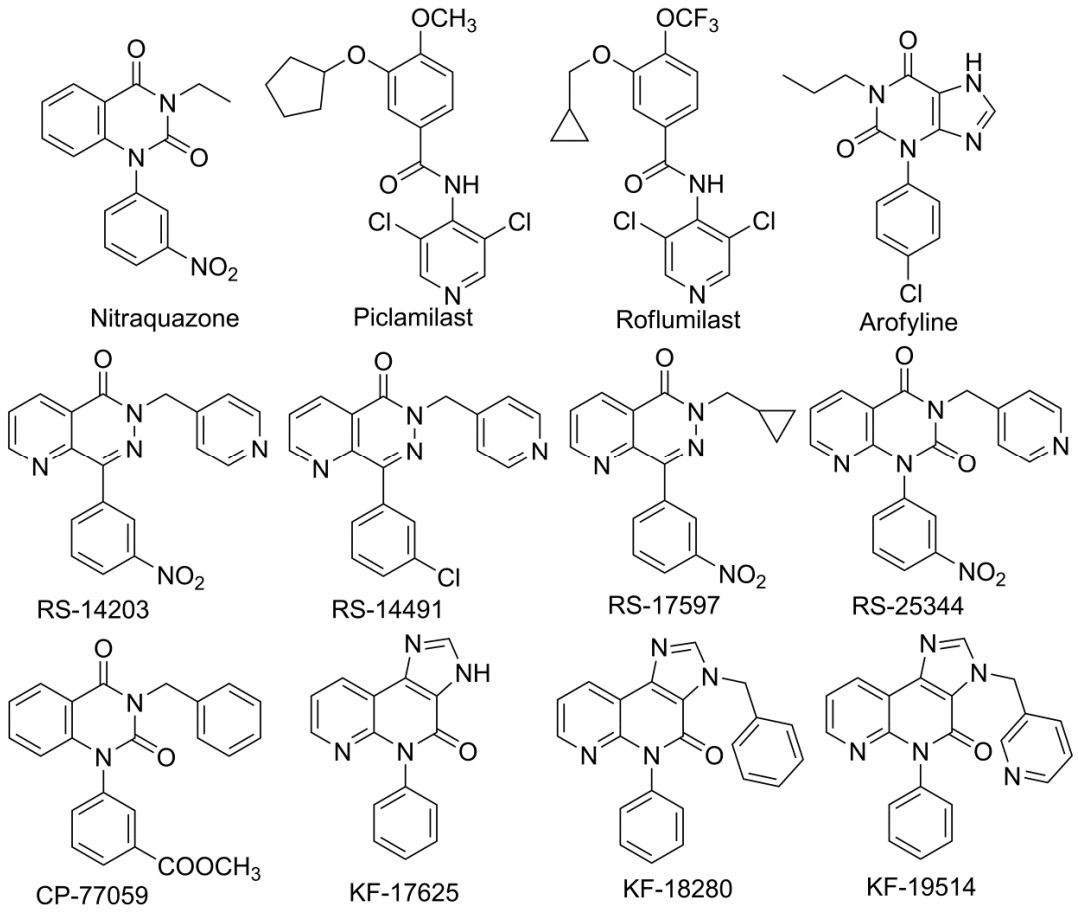

Fig. 26: Nitraquazone derivatives selected for building pharmacophore model[226]

3D Pharmacophore Model: The aforementioned compounds were used as template for making a pharmacophore model for PDE4 inhibitors. The least energy conformation for each compound was generated and the pharmacophoric distances were measured by ACDLABS-12.0/3D Viewer (CHARMM Parameterizations). The important structural components that were included in the three-point pharmacophore model were the aryl group with electron withdrawing group(s) **[B]**; planar scaffold with a hydrogen bond acceptor (HBA) atom **[A]** and a hydrophobic aliphatic or aromatic group **[C]**. The distances between the centroid of planar scaffold with HBA **[A]** to centroid of the aryl group containing electron withdrawing group(s) [**B]**, centroid of planar scaffold with HBA **[A]** to centroid of hydrophobic aliphatic or aromatic group **[C]** and centroid of aryl group **[B]** to centroid of the hydrophobic aliphatic or aromatic group **[C]** were measured, the obtained average distances between the pharmacophoric elements were considered for building this model. **(Table 4)**

Table 4: Distances between the pharmacophoric elements of selected nitraquazone derivatives and standard PDE4 inhibitors **[A]**, **[B]**, **[C]*.**

Compound	**[A]-[B]** Å	**[A]-[C]** Å	**[B]-[C]** Å
Nitraquazone	6.702	5.346	6.528
Piclamilast	4.823	6.904	9.921
Roflumilast	5.411	6.944	8.966
Arofyline	5.814	6.741	7.855
RS-14203	6.560	6.523	7.915
RS-14491	6.762	6.510	7.983
RS-17597	6.560	5.925	7.827
RS-25344	6.573	6.917	8.374
CP-77059	6.916	6.856	8.272
KF-17625	6.224	7.350	9.211
KF-18280	6.439	7.939	9.952
KF-19514	6.322	7.923	9.916
Average Distance	**6.259** Å	**6.823** Å	**8.560** Å

* Distances were calculated for 3D optimized structures, using ACDLABS-12.0/3D Viewer (CHARMM Parametrization).

The novel designed pharmacophore model includes the interfeature distances between

a) Planar scaffold providing a hydrogen bond acceptor (HBA) and the hydrophobe connected through linker-1 **(A-B)** (~6.574 Å to ~8.405 Å),
b) Planar scaffold with HBA and hydrophobe connected through linker-2 **(A-C)** (~6.820 to ~7.696 Å) and
c) Between the two hydrophobes **(B-C)** (~8.5 to ~9.136 Å), respectively.

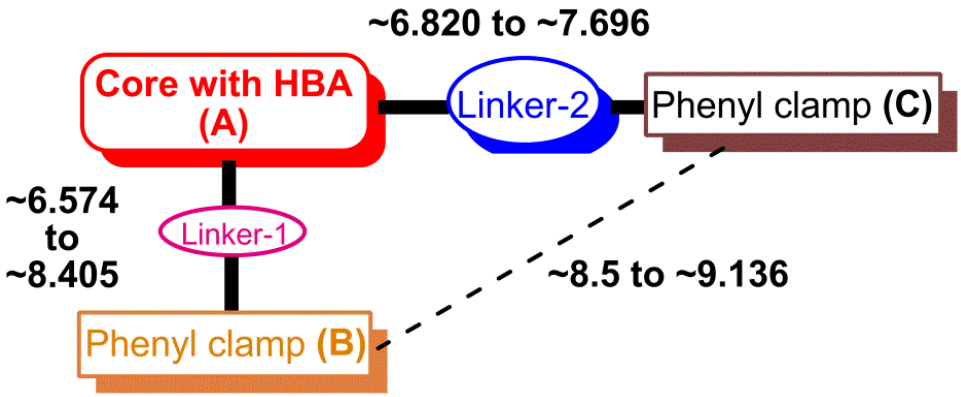

Fig. 27: Novel pharmacophoric model for designing novel PDE4 inhibitors

The novel pharmacophore consists of key elements: a) a planar scaffold providing a HBA **(A)** and b) two hydrophobic substituent's **(B and C)** with their corresponding linker (1 and 2) respectively. **(Fig. 27)** On the basis of the proposed pharmacophore, quinoxaline or quinazoline moieties were selected as the basic core with HBA, varying the linker-1 with different alkyl or carbonyl group or both, carboxamide was preferably selected a linker-2 as in roflumilast and piclamilast with two bulky aromatic hydrophobic substituents that can create a clamp to hold it in closed conformation. Based on this pharmacophore model, New Chemical Entities (NCE's) were planned, synthesized and assessed for their PDE4 inhibitory activity.

5.1.2. Design of novel series of compounds

Once the pharmacophoric model was defined, several condensed heterocyclic systems were assessed. After extensive evaluation quinoxaline and quinazoline moieties were selected consisting of a central planar template along with hydrogen bond acceptors (HBA). The interfeature distances were measured and reported. **(Table 5)** The structural and electronic profile compatibility of these novel molecules with the proposed pharmacophore was further explored.

Using the nitraquazone derivatives derived modified pharmacophore model, the proposed compounds were mapped, In order to find the best fit among compounds that are capable ofbinding to PDE4 with a similar or better set of interactions. On comparison

between nitraquazone derivative and the designed series (QCA–QCF and QZA–QZB), the RMSD value were QCA – 0.7123 Å, QCB – 0.8478 Å, QCC – 2.5511 Å, QCD – 1.7695 Å, QCE – 1.981 Å, QCF – 1.6454 Å, QZA – 2.0466 Å, QZB – 2.0035 Å, respectively indicating that all the proposed compounds had high fit value as illustrated in **fig. 28**.

Table 5: Distances between the pharmacophoric elements of the designed series **[A]**, **[B]**, **[C]*** .

Compound	**[A]-[B]** Å	**[A]-[C]** Å	**[B]-[C]** Å
QCA Series	6.481	7.610	8.753
QCB Series	7.803	7.672	8.822
QCC Series	7.012	7.691	9.225
QCD Series	6.924	7.675	9.782
QCE Series	8.411	7.714	10.104
QCF Series	8.522	7.705	10.243
QZA Series	7.324	7.710	8.041
QZB Series	7.918	7.789	8.120
Average Distance	**7.549** Å	**7.696** Å	**9.136** Å

* Distances were calculated for 3D optimized structures, using ACDLABS-12.0/3D Viewer (CHARMM Parametrization).

The novel designed NCE's adhered to the pharmacophoric features and distances in accordance with the designed pharmacophoric model as desired. Further, “Lipinski’s rule of five”, i.e. hydrogen bond donor (HBD) atom not more than 5, hydrogen bond acceptor (HBA) atom not more than 10, log P value not more than 5 and molecular weight not more than 500 daltons were considered to attain better pharmacokinetic profile (absorption, distribution, metabolism and excretion). The designed NCE's were then synthesized and evaluated for their PDE4 inhibitory activity.

Pharmacophoric comparison

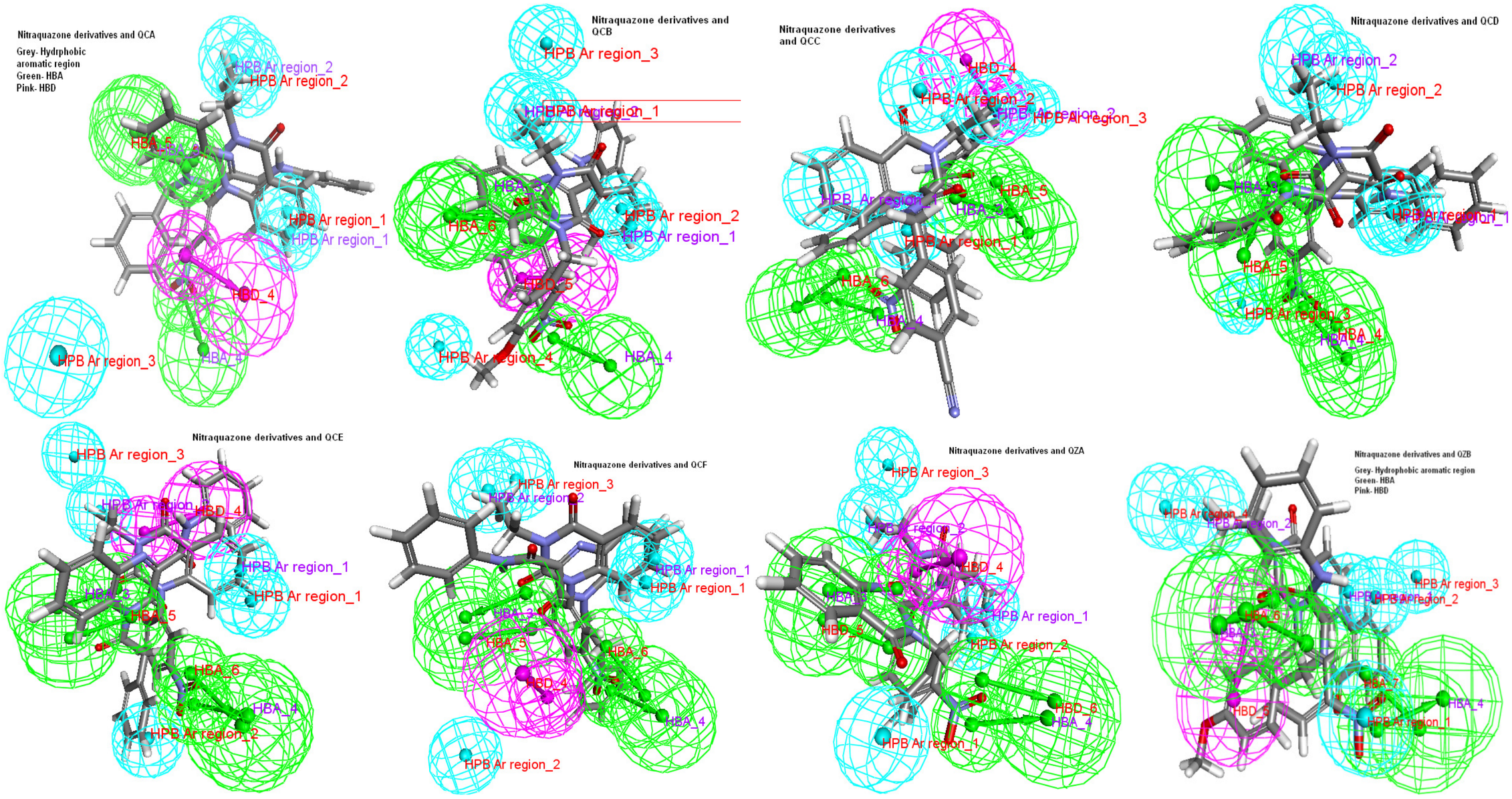

Fig. 28: Pharmacophoric comparison of Nitraquazone derivatives and QC (A – F) series and QZ (A – B) series

Grey – Hydrophobic aromatic region, Green – Hydrogen bond acceptor (HBA), Pink – Hydrogen bond donor (HBD)

5.1.3. Chemistry of series 1-6

5.1.3.1. Mechanism of ethyl 3-oxo-3,4-dihydroquinoxaline-2-carboxylate

Cyclic condensation of *o*-phenylenediamine with diethyl ketomalonate furnished the ethyl 3,4-dihydro-3-oxoquinoxalin-2-carboxylate. IR spectra of the compound showed absorption bands at 1750 cm^{-1} and 1660 cm^{-1} indicating the presence of lactam carbonyl and ester carbonyl groups, respectively. A sharp absorption, band at 3460 cm^{-1} indicated the presence of NH group. In proton NMR spectra, a singlet signal corresponding to one proton at δ 12.95 indicated the presence of lactam NH proton in compound. Three proton triplet at δ 1.46 and two proton quartet at δ 4.54 confirmed the presence of ethyl ester group. The schematic representation of mechanism of product formation is depicted in **Fig. 29**.

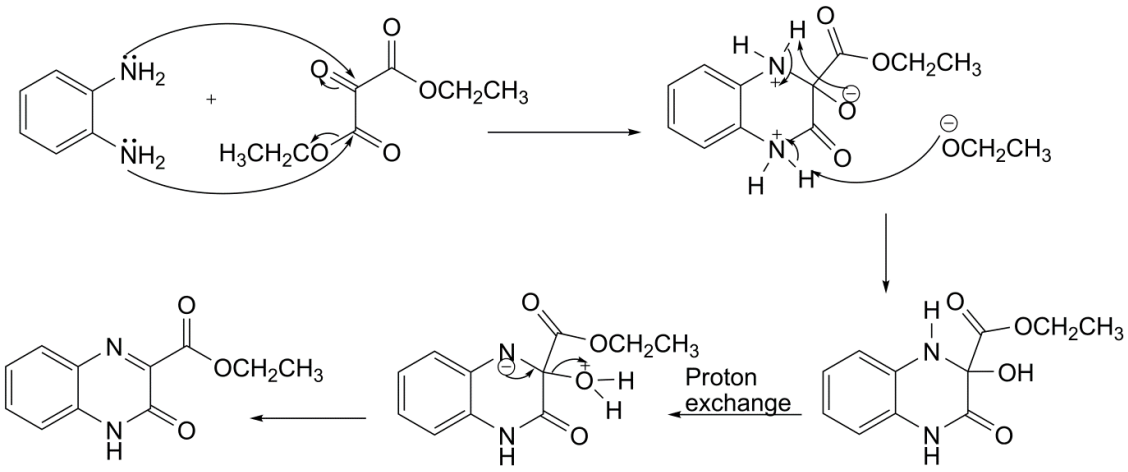

Fig. 29: Mechanism of ethyl 3-oxo-3,4-dihydroquinoxaline-2-carboxylate formation

5.1.3.2 Mechanism of ethyl 4-benzyl/substituted benzyl 3-oxo-3,4-dihydroquinoxaline-2-carboxylate

Quinoxaline-2-carboxylate on *N*-alkylation with benzyl bromide or substituted benzyl chloride/bromide in the presence of strong base like potassium carbonate as catalyst in DMF provided the *N*-alkylated compound in quantitative yield. Nucleophilic aliphatic substitution of the halide was the reaction product resulting in a higher substituted amine. The disappearance of NH group stretching absorption bands in IR spectra indicated the formation of *N*-alkylated compound. Disappearance of NH proton signal (NMR spectra) at δ 12.95 and appearance of CH_2 (benzylic methylene) proton signal (NMR spectra) at δ 5.40 ~ 5.64 confirmed the formation of *N*-alkylated compound. The mechanism of product formation is given in **Fig. 30**.

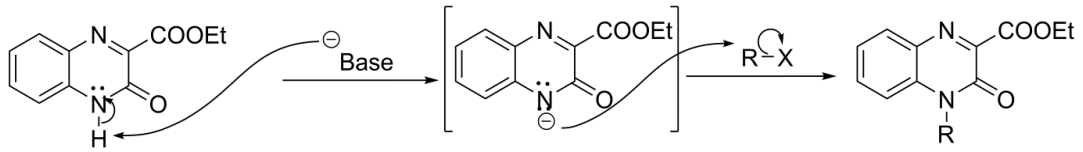

Fig. 30: Mechanism of ethyl 4-benzyl/substituted benzyl 3-oxo-3,4-dihydroquinoxaline-2-carboxylate formation

The carboxylic acid group of the key intermediate was coupled with appropriate primary amines using coupling agents EDC·HCl and HOBt in an inert atmosphere, (nitrogen gas). This method furnished desired product, particularly when different substituted aromatic amines (aniline, *p*-toludine, *p*-anisidine etc.) were coupled with carboxylic acid. Using column chromatography or recrystallization technique, the pure compounds were obtained and impurities if any were isolated, wherever desired and characterized by proton NMR.

5.1.4. Chemistry for series QZA-QZB series

5.1.4.1. Mechanism of 2-amino-*N*-benzyl/substituted benzylbenzamide

When isatoic anhydride was refluxed in alkali (like benzyl amine or substituted benzyl amine) it became highly susceptible to cleavage, forming *N*-substituted compounds with ring opening by quantitative liberation of carbon dioxide. The appearance of -NH_2 group stretching absorption bands at 3467 cm^{-1} in IR spectra indicated the ring opening and formation of *N*-alkylated compound. Appearance of amide and amine proton signal (NMR spectra) at δ 10.86 and δ 6.38, respectively and also appearance of CH_2 (benzylic methylene) proton signal (NMR spectra) at δ 4.59 confirmed the formation of *N*-alkylated compound. The mechanism of product formation is given in **Fig. 31**.

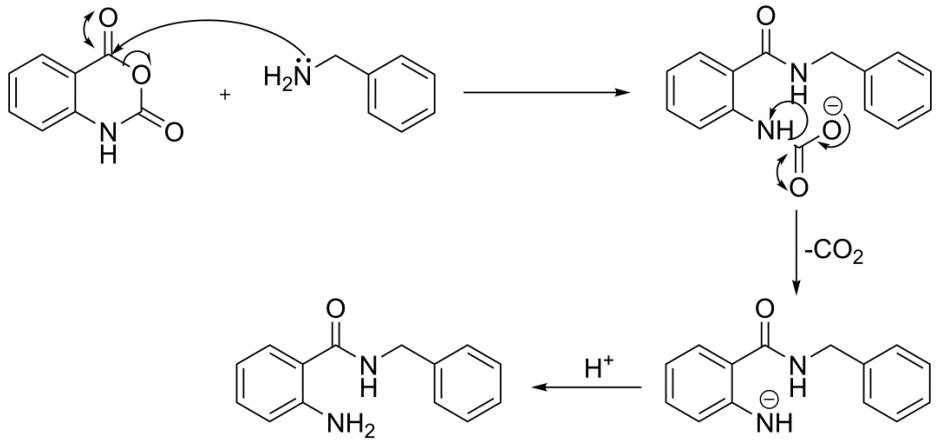

Fig. 31: Mechanism of 2-amino-*N*-benzyl/substituted benzylbenzamide formation

5.1.4.2. Mechanism of ethyl 3-benzyl/substituted benzyl-4-oxo-3,4-dihydroquinazoline-2-carboxylate

Cyclic condensation of 2-amino-*N*-benzyl/substituted benzylbenzamide with diethyl oxalate furnished the ethyl 3-benzyl/substituted benzyl-4-oxo-3,4-dihydroquinazoline-2-carboxylate. IR spectra of the compound showed absorption bands at 1732 cm^{-1} and 1680 cm^{-1} indicating the presence of carbonyl and ester carbonyl groups, respectively. Disappearance of sharp stretching bands at 3467 cm^{-1} and 3359 cm^{-1} indicated the absence of primary $-NH_2$ and NH group respectively. In proton NMR spectra, disappearance of singlet signal corresponding to one proton at δ 10.86 and two protons at δ 6.38 indicated the absence of NH and $-NH_2$ in compound. Three proton triplet at δ 1.43 and two proton quartet at δ 4.42 confirmed the presence of ethyl ester group. The schematic representation of mechanism of product formation is depicted in **Fig. 32**.

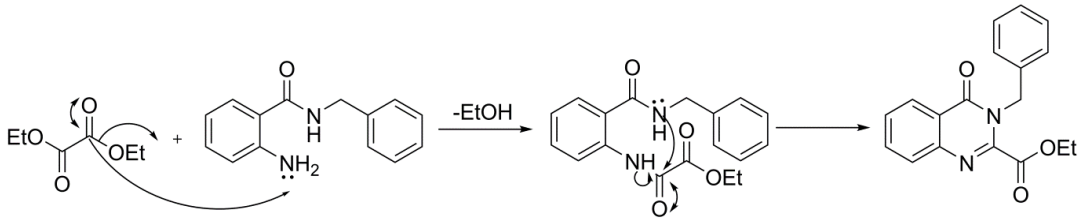

Fig. 32: Mechanism of ethyl 3-benzyl/substituted benzyl-4-oxo-3,4-dihydroquinazoline-2-carboxylate formation

The carboxylic acid group of the key intermediate was coupled with appropriate primary amines using coupling agents EDC·HCl and HOBt in an inert atmosphere, (nitrogen gas) to furnish desired compounds as mentioned earlier.

5.1.5. Assay for PDE4 inhibitory activity

The synthesized compounds were further subjected to *in-vitro* assay by PDE4D and PDE4B isoform elisa-kit using fluorescence polarization (FP) principle based on the binding of a fluorescent nucleotide monophosphate generated by PDE4B and PDE4D to the binding agent.Fluorescence intensity was measured at an excitation of 485 nm and an emission of 528 nm using elisa microplate reader. All samples and controls were tested in duplicates and blank values subtracted from all other values. The standard assay protocol was followed as provided by the supplier and the percent activity was calculated for the designed analogues and standard and has been reported.

5.1.6. Docking studies

PDE4 is a tetramer of identical, catalytically active subunits. When the heteroatoms were verified in the protein downloaded from protein data bank (PDB), it had 4 co-crystallized ligands i.e., rolipram in different chains of the protein. On further analysis, the ligand in chain 'B' formed two hydrogen bonds with the side chain of Gln369 while the other rolipram in chain A, C, D formed only one hydrogen bond with the side chain Gln369. Chain 'B' displayed all the necessary amino acids in close proximity to the plausible binding sites. For PDE4D, thirty one active sites were identified according to the volume of their binding cavity. Among the thirty one active sites – site 4 was chosen for our study, as the catalytic site were coordinated by key amino acids like histidine, phenylalanine, glutamine, asparagine and aspartic acid as found in PDE4D-rolipram co-crystallized structure. As a result, docking was performed for all 142 ligands in site 4 **(3663 point units, 457.875 Å^3)** of PDE4D.[48] Similarly when PDE4B when analyzed, twenty one active sites were identified among them site 2 **(2281 points, 285.125 Å^3)** was chosen for the study as the catalytic site were coordinated by key amino acids like leucine, glutamine, histidine, threonine and/or Cysteine, aspartic acid, Isoleucine and additionally tyrosine as found in PDE4B-rolipram co-crystallized structure.[34b] After docking, best poses of these ligands were evaluated using different energy parameters and scoring functions. The docked poses are ranked based on different scoring functions and their consensus scores.

In the current study, candidate ligand poses were prioritized according to the Dockscore and were selected as lead for further evaluation by visual examination for their protein-ligand interactions. All these ligands, formed good hydrophobic and/or hydrogen bond interactions with His160, His204, Asn209, His233, Met273, Asn283, Asp318, Phe340, Ile336, Glu369, Phe372, Phe414 and Phe446 respectively, were preferred as potent leads for further development as PDE4 inhibitors. Docking calculations were performed with other parameters of ligandfit set in their default values, unless specified.

5.2. Biological activities/Pharmacology for QCA Series

4-benzyl-3-oxo-*N*-phenyl-3,4-dihydroquinoxaline-2-carboxamide analogues (QCAseries) were synthesized and subjected for their inhibitory properties through *in-vitro* studies at 10 µM using PDE4B or PDE4D enzyme assay using rolipram as a reference standard.

Compound QCA-1, QCA-8 and QCA-14 showed pronounced inhibitory activity whereas compound QCA-4, QCA-10, QCA-11 and QCA-13 exhibited moderate inhibitory activity for PDE4D enzyme. Rest of the tested compounds exhibited poor inhibition. Except compound QCA-15 which displayed a very less moderate activity for PDE4B enzyme, while other compounds displayed poor inhibitory activity. **(Table 6)**

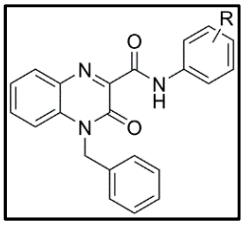

Compound QCA-8 was the most active compound in this series with better inhibitory activity for PDE4D exhibiting more than 2-fold affinity, whereas compound QCA-1 expressed more than 3-fold affinity for PDE4D than PDE4B enzyme. Compounds QCA-4, QCA-10 and QCA-14 showed better affinity for PDE4D and while, compounds like QCA-11 and QCA-13 displayed lower affinity among its isoform i.e., PDE4D and PDE4B. **(Table 6)**

Table 6: In-vitro data of QCA series

Compound	R	PDE4B[a]	SD	PDE4D[a]	SD	Selectivity[b]
QCA-1	Phenyl	18.55	1.43	66.03	1.22	3.6
QCA-2	4-methoxyphenyl	39.09	0.52	38.57	0.86	-
QCA-3	2-ethylphenyl	44.01	1.48	45.36	0.92	-
QCA-4	2-chloro-4-methylphenyl	18.12	2.21	51.22	1.12	2.8
QCA-5	2-chloro-5-methylphenyl	21.13	0.32	45.66	1.43	-
QCA-6	2-methyl-3-chlorophenyl	29.09	0.62	46.28	0.54	-
QCA-7	2-methyl-4-chlorophenyl	41.38	1.14	31.78	0.86	-
QCA-8	2-propylphenyl	30.63	0.53	67.57	0.53	2.2
QCA-9	3-chlorophenyl	34.13	0.86	44.74	1.32	-
QCA-10	1-morpholino	28.18	3.20	56.16	2.15	2.0
QCA-11	2-isopropylphenyl	44.00	2.85	58.62	1.16	1.3
QCA-12	4-isopropylphenyl	41.33	1.62	28.08	1.48	-
QCA-13	2-trifluoromethylphenyl	35.36	0.33	50.91	0.22	1.4
QCA-14	2-methoxyphenyl	24.48	0.58	63.87	1.10	2.6
QCA-15	3-methoxyphenyl	48.01	1.26	44.74	1.98	-
QCA-16	2-choro-6-methylphenyl	45.32	1.54	46.70	1.86	-
Rolipram		90.27	0.22	96.54	0.14	1.1

[a] Average percentage inhibition – Values that are the mean of two or more experiments are shown with their standard deviations (SD)
[b] Ratio of PDE4D/PDE4B

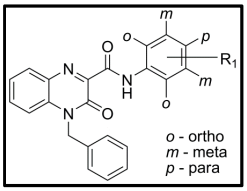

The SAR of these synthesized compounds indicates that the unsubstituted phenyl group as in compound QCA-1 or if substituted, the *ortho*-position on the phenyl ring was better favored for PDE4D inhibitory activity as evident from compound QCA-4, QCA-8, QCA-11, QCA-13 and QCA-14. These analogues with variable substitution on different positions of the phenyl group had markedly lower affinity for PDE4B enzyme.

Introduction of a better lipophilic group at *ortho*-position on the phenyl ring, like propyl or isopropyl group which is weak ring activators enhances the PDE4D inhibitory activity as in compound QCA-8 and QCA-11. As compared to the initial compound QCA-1, compound QCA-8 showed slight improvement in inhibition ofPDE4D enzyme. In the homologous series, the linear propyl group as in compound QCA-8 was better tolerated as compared to ethyl group as in compound QCA-3. However, introduction of isopropyl group in *ortho*-position expressed slight decrease in the activity as in compound QCA-11 whereas, when substituted at *para*-position lead to further decrease in the activity as in compound QCA-12. When the interactions inside the active site of these compounds QCA-8 and QCA-11 were analyzed they showed very similar interactions with His160, His233, Phe340 and Phe372. **(Fig. 35 and 39)** However, the only difference between these compounds were QCA-8 had an additional σ-π interaction with Ile336 which could plausibly better stabilize the moiety inside the active site.

Introduction of a strong activating group preferably methoxy group in *ortho*-position on the phenyl ring as in compound QCA-14 was well tolerated and restored the activity. Whereas, when substituted at *meta* or *para*-position as in compound QCA-15 and QCA-2 was not tolerated. Substituting phenyl group with basic moiety like morpholino group as in compound QCA-10 restored the activity. Compound like QCA-4 which has a substituent at *ortho*-position preferably chlorine (weak deactivator) and at *para*-position preferably methyl group (weak activator) displayed moderate activity. Swapping of these functional groups to other positions markedly affected the activity as in compound QCA-5, QCA-6 and QCA-7. However, when a strong deactivating group preferably trifluoromethyl introduced at *ortho*-position as in compound QCA-13, restored the inhibitory activity but was moderately active.

In order to understand the nature of interactions of these molecules, rolipram as standard and nitraquazone as the molecules synthesized are its derivatives within the active site of PDE4D and PDE4B, docking studies were carried out for all these compounds. The dockscore and other scores obtained after docking of these molecules into the PDE4D and PDE4B proteins are summarized in **Table 7** and **8** respectively.

Table 7: Docking results of QCA series for PDE4D (PDB: 1Q9M)

Compound	LigScore_1	LigScore_2	-PLP1	-PLP2	Jain	-PMF	-PMF04	Dockscore	Ludi_3	Consensus
QCA-1	3.52	4.79	57.75	45.60	2.56	132.00	69.48	68.21	550	1
QCA-2	2.08	5.09	65.68	62.42	0.96	132.20	74.76	67.54	672	1
QCA-3	3.14	5.54	87.66	84.16	5.07	188.66	91.87	68.33	978	6
QCA-4	2.13	4.82	60.98	62.38	2.06	123.30	75.99	69.59	642	1
QCA-5	3.18	5.60	84.66	81.71	4.85	178.73	97.56	70.78	901	2
QCA-6	2.33	5.12	85.29	85.03	2.29	137.32	74.70	59.83	857	2
QCA-7	3.46	5.99	85.79	82.48	5.20	185.92	91.47	70.62	931	4
QCA-8	2.94	5.45	83.68	80.00	4.17	194.87	97.32	69.36	915	3
QCA-9	3.26	5.82	85.92	83.28	4.60	185.13	87.42	68.76	895	1
QCA-10	2.99	5.28	79.18	75.40	3.82	157.79	102.95	67.58	770	2
QCA-11	2.39	5.33	62.29	58.54	1.21	144.05	69.91	68.64	848	2
QCA-12	3.03	5.62	78.16	79.79	3.14	156.77	82.30	66.92	930	2
QCA-13	2.85	5.12	87.51	83.78	3.30	183.63	94.66	68.85	943	7
QCA-14	3.26	5.62	93.41	88.95	4.80	205.42	111.12	70.58	839	4
QCA-15	2.93	5.38	83.50	78.71	4.31	169.16	106.54	69.93	876	6
QCA-16	3.30	5.50	85.20	82.81	4.35	187.76	100.13	70.03	926	5
Rolipram	3.82	4.54	48.46	48.38	2.78	118.37	64.25	46.866	456	1
Nitraquazone	4.24	4.73	52.53	50.68	1.71	158.56	94.33	56.384	701	3

Table 8: Docking results of QCA series for PDE4B (PDB: 1XMY)

Compound	LigScore_1	LigScore_2	-PLP1	-PLP2	Jain	-PMF	-PMF04	Dockscore	Ludi_3	Consensus
QCA-1	4.21	4.88	63.18	62.40	3.01	119.32	69.64	62.93	839	3
QCA-2	1.96	4.88	77.47	71.20	1.14	97.08	71.25	66.76	637	4
QCA-3	2.09	5.17	67.51	63.70	0.94	123.09	93.56	64.14	570	3
QCA-4	2.09	5.20	75.23	70.76	1.02	114.57	92.17	69.50	645	4
QCA-5	1.99	4.93	78.68	72.33	2.11	167.17	124.61	65.84	826	6
QCA-6	2.18	5.42	77.11	73.56	1.21	122.60	88.72	59.30	676	4
QCA-7	2.05	5.05	68.46	64.87	0.91	109.87	87.27	68.48	635	1
QCA-8	2.02	5.02	68.64	66.09	0.98	129.66	89.10	64.94	593	1
QCA-9	1.85	4.70	65.58	67.32	0.98	95.02	77.16	66.41	627	1
QCA-10	3.84	4.40	57.07	47.49	3.45	132.02	81.91	66.04	675	2
QCA-11	1.97	4.95	56.68	50.99	1.25	130.07	87.11	64.37	654	1
QCA-12	1.72	4.53	65.01	61.19	1.36	132.13	89.01	62.92	846	2
QCA-13	2.11	5.06	68.93	68.24	1.75	137.66	102.17	68.99	656	4
QCA-14	2.19	5.21	65.23	63.18	2.21	109.34	82.11	67.50	647	5
QCA-15	2.23	5.12	69.58	65.85	1.58	112.01	81.97	69.92	625	4
QCA-16	2.04	5.20	67.78	61.61	1.36	144.14	108.37	67.05	626	3
Rolipram	2.23	4.39	54.3	46.79	2.51	141.03	107.36	45.193	608	2
Nitraquazone	1.78	4.61	68.64	51.8	1.44	139.65	96.4	57.033	708	0

The interaction of compound QCA-1 within the active site of PDE4D protein **(Fig. 33)** is mainly contributed by (i) two H-bonds, one between the keto group of the quinoxaline ring with His160 at a distance of 4.6 Å and other between -NH of the amide linker and Glu230 at a distance of 4.1 Å, (ii) a π-π stacking interaction between the centroid of the benzyl ring and Phe340, (iii) cationic-π interaction between His160 and the centroid of the benzene ring of the quinoxaline scaffold. However, it did not have any interactions with PDE4B protein **(Fig. 34)** plausibly attributing to its poor inhibitory activity. This suggests that this moiety could be considered as a lead, and on appropriate modification may possibly lead to a better PDE4D selective inhibitor devoid of PDE4B inhibitory activity.

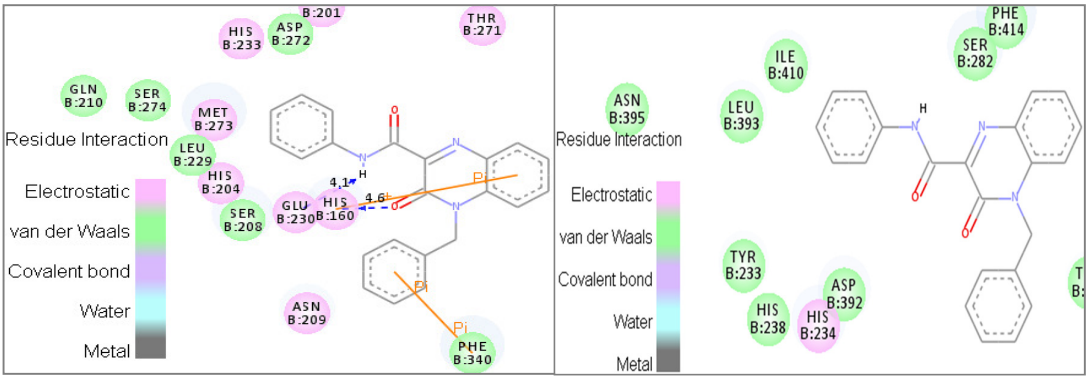

Fig. 33 and 34: QCA-1 at the active site of PDE4D and PDE4B

Similarly, the interaction of compound QCA-8 within the active site of PDE4D protein **(Fig. 35)** is contributed by (i) H-bond between *N1* of the quinoxaline ring with His160 at a distance of 5.4 Å, (ii) three π-π stacking interactions, two between centroid of the benzyl ring with His160 and Phe340 while another between the centroid of the phenyl ring on the amide linker with Phe372, (iii) σ-π interaction between Ile336 and the centroid of the phenyl ring on the amide linker, (iv) cationic-π interaction between the centroid of benzene ring of the quinoxaline scaffold and His233. Whereas, the interaction of compound QCA-14 within the active site of PDE4D protein **(Fig. 36)** is mainly contributed by (i) H-bond between the 2-OCH_3 substitution on the phenyl ring attached to the amide linker and His160 at a distance of 4.8 Å, (ii) π-π stacking interaction between centroid of the benzyl ring and Phe340, (iii) cationic-π interaction between His160 and centroid of the benzene ring of the quinoxaline scaffold.

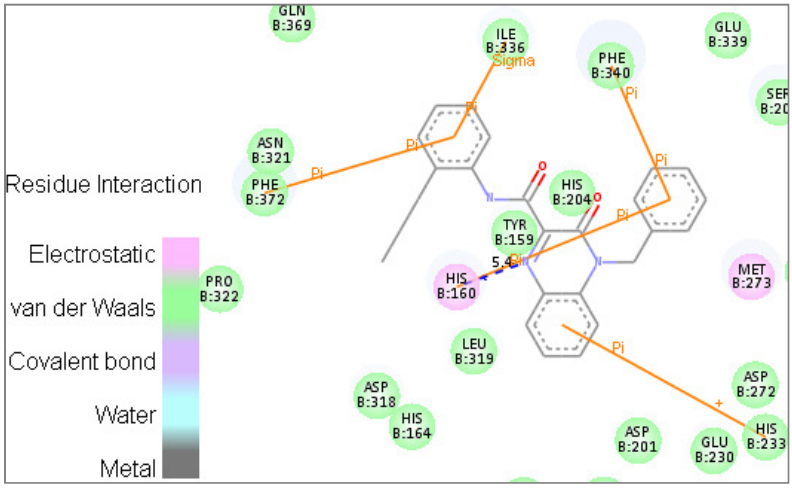

Fig. 35: QCA-8 at the active site of PDE4D

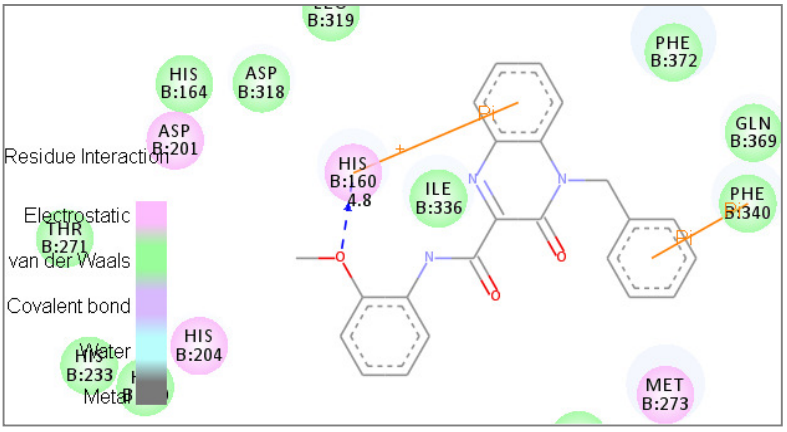

Fig. 36: QCA-14 at the active site of PDE4D

The interaction of compound QCA-4 within the active site of PDE4D protein **(Fig. 37)** is mainly contributed by (i) H-bond between *N1* of the quinoxaline ring with His160 at a distance of 5.5 Á, (ii) two π-π stacking interactions, one between the centroid of the phenyl ring on the amide linker while, another with the centroid of the benzyl ring and His160, (iii) σ-π interaction with Ile336 and the centroid of the phenyl ring on the amide linker. Similarly, the interaction of compound QCA-10 within the active site of PDE4D protein **(Fig. 38)** is contributed by (i) H-bond between oxygen of the morpholine ring with His160 at a distance of 4.9 Á, (ii) π-π stacking interaction between the centroid of the benzyl ring and Phe340, (iii) cationic-π interaction between His160 and the centroid of the benzene ring of the quinoxaline scaffold.

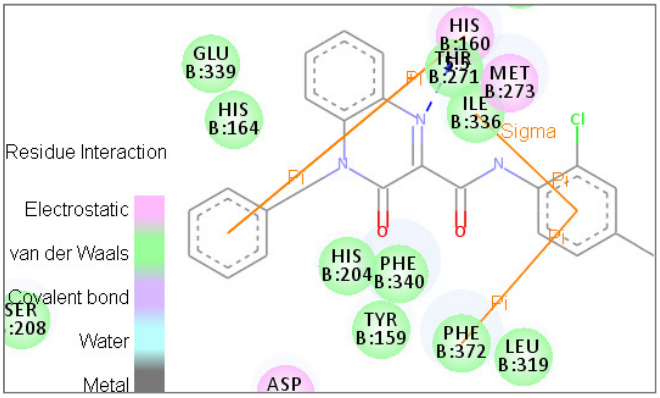

Fig. 37: QCA-4 at the active site of PDE4D

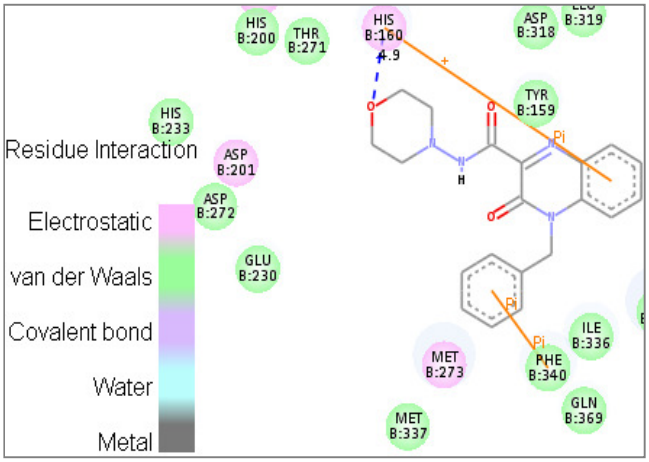

Fig. 38: QCA-10 at the active site of PDE4D

The interaction of compound QCA-11 within the active site of PDE4D protein **(Fig. 39)** is mainly contributed by (i) H-bond between *N1* of the quinoxaline ring with His160 at a distance of 5.5 Å, (ii) three π-π stacking interactions, two between His160 and Phe340 with the centroid of the benzyl ring and another between the centroid of the phenyl ring on the amide linker and Phe372 (iii) cationic-π interaction between His233 and the centroid of the benzene ring of the quinoxaline scaffold. Whereas, the interaction of compound QCA-13 within the active site of PDE4D protein **(Fig. 40)** is mainly contributed by (i) H-bond between *N1* of the quinoxaline ring with His160 at a distance of 5.4 Å, (ii) π-π stacking interaction between the centroid of the phenyl ring on the amide linker with Phe372, (iii) cationic-π interaction between His160 and the centroid of the benzyl ring. While the interaction of compound QCA-15 within the active site of PDE4B protein **(Fig. 41)** was mainly contributed by (i) π-π stacking interaction between the centroid of the phenyl ring on the amide linker with Phe446, (ii) cationic-π interaction between His307 and the centroid of the benzyl ring.

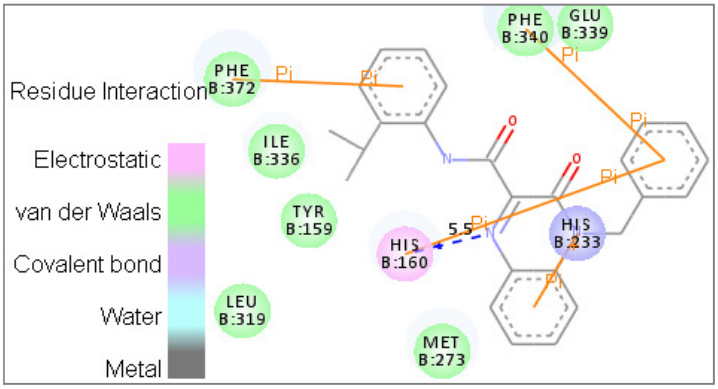

Fig. 39: QCA-11 at the active site of PDE4D

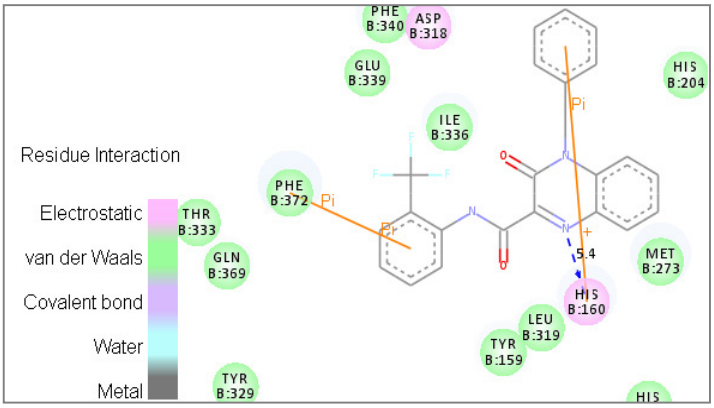

Fig. 40: QCA-13 at the active site of PDE4D

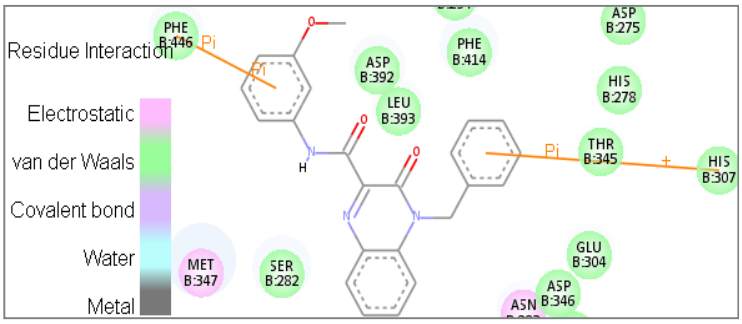

Fig. 41: QCA-15 at the active site of PDE4DB

Overall, the present 4-benzyl-3-oxo-quinoxaline-2-carboxamide analogues displayed better interactions with PDE4D enzyme exhibiting their inhibitory activity. This indicates that the pharmacophoric elements like the central quinoxaline ring with a keto group which acts as a hydrogen bond acceptor (HBA), the benzyl moiety, diverse substituted phenyl ring and the amide linker plays substantial roles in forming various interactions with the active site.

5.2.1. ADME properties

The analysis showed that the compounds of this series, when administered orally might show better intestinal absorption, as well as good blood–brain barrier (BBB) permeability. Their aqueous solubility and drug–likeness properties were envisaged to be very low.In addition, these compounds arelikely to inhibit enzyme such as CYP450 *2D6*. Most of these compounds are predicted to be hepatotoxic. It was also found that the inhibitor-plasma protein binding is not more than 90%, indicating that these compounds are likely to be less bound to plasma protein present in the blood. **(Table 9)**

Nevertheless, It is a common understanding that ADME profiles are complex to envisage accurately just by *in-silico* and so the envisaged profiles must be utilized with care. For our study, further testing ought to be done to investigate the actual profiles of these compounds as an extension of this work.

In the ADMET plot, since all the molecule are inside the 99% confidence ellipse of BBB and HIAmodel, the predictions are considered reliable and therefore the BBB and HIA predictions are made for these ligands respectively. **(Fig. 42)**

Table 9: ADME properties of QCA Series

QCA	Aqueous solubility[a]		BBB[b]		CYP450 *2D6*[c]		Hepatotoxicity[d]		HIA[e]		PPB[g]		AlogP98[g]	
	Value	Level	Value	Level	Value	Level	Value	Level	Value	Level	Value	Level	Value	Level
1	-4.857	2	-0.038	2	-3.810	1	-3.522	0	NV[f]	0	3.433	0	3.553	0
2	-4.825	2	-0.185	2	-5.177	1	-3.549	0	NV[f]	0	1.141	0	3.537	0
3	-5.619	2	0.253	1	-3.737	1	-6.423	1	NV[f]	0	4.559	0	4.496	0
4	-6.016	1	0.317	1	-3.683	1	-4.073	0	NV[f]	0	6.188	0	4.704	0
5	-6.026	1	0.317	1	-3.690	1	-4.177	1	NV[f]	0	6.702	0	4.704	0
6	-6.027	1	0.317	1	-3.115	1	-4.885	1	NV[f]	0	6.508	0	4.704	0
7	-6.016	1	0.317	1	-3.675	1	-4.060	0	NV[f]	0	8.145	0	4.704	0
8	-5.895	2	0.394	1	-3.558	1	-5.820	1	NV[f]	0	5.103	0	4.952	0
9	-5.558	2	0.167	1	-3.507	1	-2.489	0	NV[f]	0	7.003	0	4.218	0
10	-3.467	3	-0.185	2	-5.164	1	-8.480	1	NV[f]	0	1.128	0	1.767	1
11	-5.870	2	0.331	1	-3.319	1	-4.569	1	NV[f]	0	3.871	0	4.747	0
12	-5.808	2	0.331	1	-3.236	1	-2.998	0	NV[f]	0	3.892	0	4.747	0
13	-6.075	1	0.253	1	-1.690	1	-8.030	1	NV[f]	0	4.681	0	4.496	0
14	-4.867	2	-0.185	2	-3.937	1	-4.395	1	NV[f]	0	3.623	0	3.537	0
15	-4.846	2	-0.185	2	-5.177	1	-4.256	1	NV[f]	0	3.751	0	3.537	0
16	-6.037	1	0.317	1	-3.971	1	-3.674	0	NV[f]	0	6.113	0	4.704	0

[a] Level 2 means the aqueous solubility of inhibitor is not very good and its drug-likeness properties are low, while Level 1 means the aqueous solubility of inhibitor is very poor.
[b] Level 2 means inhibitor has medium ability and Level 1 means inhibitor has high ability to cross the blood-brain barrier (BBB).
[c] Level 1 means inhibitor likely to inhibit CYP*2D6* enzyme.
[d] Level 0 means inhibitor not likely to be hepatotoxic, while Level 1 means inhibitor are likely to be hepatotoxic.
[e] Level 0 means inhibitor has good human intestinal absorption (HIA) after oral administration.
[f] NV means no value was given.
[g] Level 0 means the binding between inhibitor and plasma protein (PPB) is less than 90% (No markers flagged and AlogP98 < 5.0).

ADMET PLOT

The ADMET plot is a 2D chart of ADMET_PSA_2D versus ADMET_AlogP98. The two sets of ellipses are for the prediction confidence space (95% and 99%) for the Blood Brain Barrier Penetration and Human Intestinal Absorption models, respectively.

Since the molecule is outside of the 99% BBB model confidence ellipse, the prediction is considered unreliable and no BBB prediction is made for this ligand.

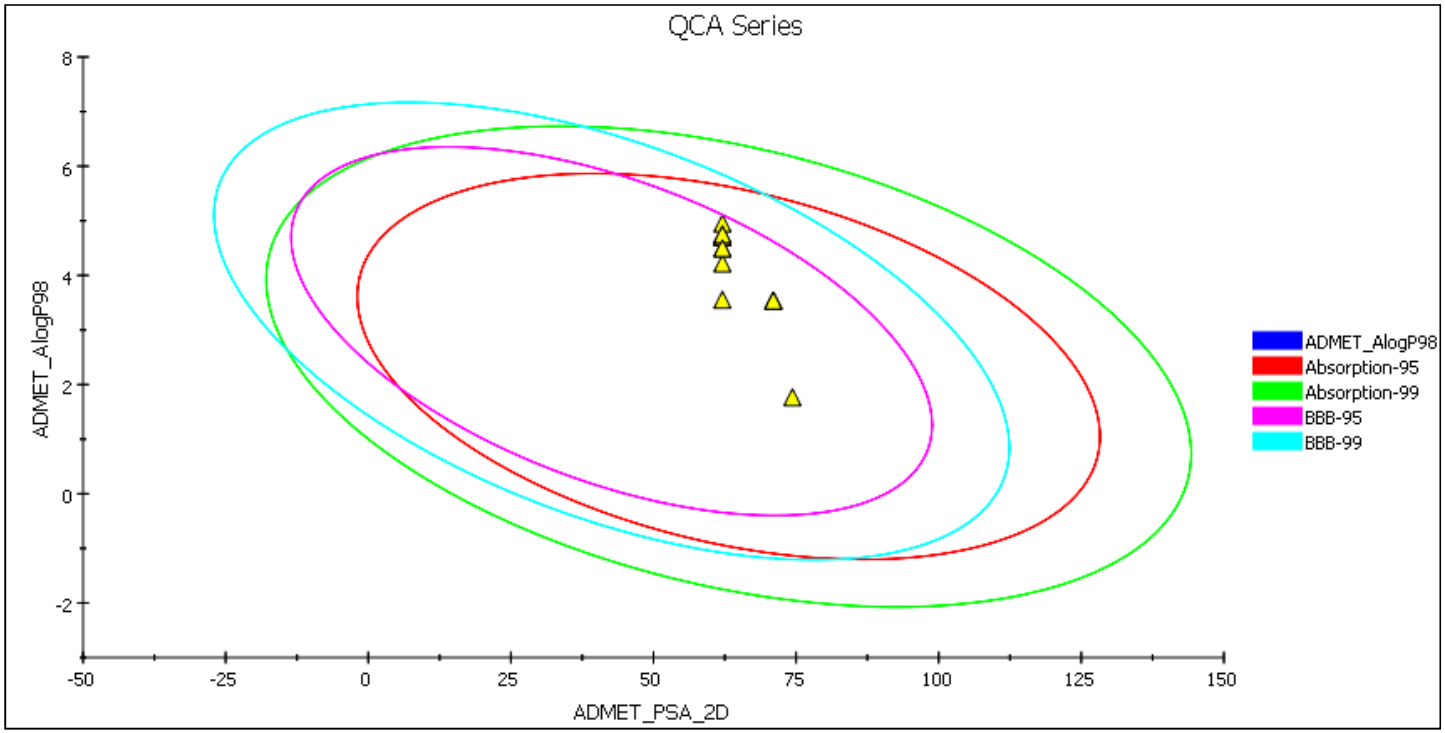

Fig. 42: ADMET Plot for QCA Series

5.2.2. Preliminary screening of NCE's as potential anti-depressants

Based on the encouraging results obtained from *in-vitro* screening, further preliminary screenings of these NCE's were carried out on the standardized rodent models for depression and anxiety.

Irrespective of the PDE4 inhibitory activity, to assess their potential as anti-depressants, all the compounds of QCA series were subjected to FST and TST in mice model. Anti-depressant activity was estimated as mean of immobility time in seconds. The anti-depressant activity data from FST and TST are shown as Mean ± S.E.M. in **Table 10** and **11** respectively.

In order to ascertain the possible occurrence of drug induced changes (stimulation/suppression) in the locomotor activity of mice, which may contribute to their behavioral changes in FST and TST, all the compounds were subjected to spontaneous locomotor activity study using actophotometer. Neither standard, nor test compounds were found to cause pronounced changes in the locomotor activity of mice when compared to the control as shown in **Table 10**. Therefore, the results obtained from the actophotometer study eliminate the possible existence of any false positive and (or) false negative result in FST and TST.

1. Force Swim Test (FST)

In the preliminary anti-depressant screening by FST, all the compounds were administered at a dose of 1 mg/kg, i.p. in mice **(Table 10)**. Among the fifteen compounds screened, three compounds (QCA-1, QCA-8, QCA-14 and QCA-15) showed prominent anti-depressant like activities as indicated by marked [$P < 0.05$] reduction in immobility time compared to the control, whereas five compounds (QCA-4, QCA-6, QCA-10 and QCA-11) showed moderate anti-depressant like activities.

Supported by preliminary anti-depressant study, these compounds were chosen for profiling in a dose–response assay of mice in FST. In dose-response assay (0.5, 1 and 2 mg/kg), five compounds (QCA-1, QCA-8, QCA-12, QCA-14 and QCA-15) demonstrated a statistically pronounced reduction in immobility time compared to control, in a dose-dependent manner. These compounds emerged as better potential derivatives as they markedly [$P < 0.05$] reduced the immobility time compared to the control at all the three tested dose levels (0.5, 1 and 2 mg/kg).

Table 10: Pharmacological data of QCA series analogues for spontaneous locomotor activity (SLA) and its anti-depressant activity in Force Swim Test (FST) mice model

Compounds	Locomotor scores[b] (10 min) Dose, mg/kg (ip)			Duration of immobility in seconds (FST)[b] Dose, mg/kg (ip)		
	2	1	0.5	2	1	0.5
QCA-1	406.17±22.22	411.33±23.01	441.33±19.71	84.66 ±4.67*	99.3 ±7.14*	107.5 ±7.39*
QCA-2	371.50±26. 52	413.50±20.30	388.83±29.01	133.17 ±13.54	133.33 ±11.23	138 ±6.88
QCA-3	435.33±19.68	501.17±28.88	412±26.62	123.67 ±12.66*	124.00±11.72*	138.25 ±9.45
QCA-4	411.83±19.57	422.50±15.56	408.00± 18.45	104.67 ±10.44*	110.83 ±11.98*	133.2 ±10.21
QCA-5	374.00±24.52	400.00±19.00	402.00±29.24	122.67 ±15.34*	135.50 ±13.13	134 ±12.74
QCA-6	511.83±20.89	495±21.32	420.83±19.34	94 ±8.06*	105.17 ±9.22*	151.67 ±10.37
QCA-7	486.33±23.45	430.33±15.50	419.83±19.34	103 ±7.28*	136±8.58	151.4±16.87
QCA-8	422.00±16.47	488.50±10.12	440.67±20.26	84.25 ±8.54*	100.6 ±11.59*	108 ±8.66*
QCA-9	383.17±24.63	402.86±29.04	384.57±19.39	122.5 ±7.77*	148 ±8.92	143 ±7.22
QCA-10	402.17±17.26	397.50±30.59	399.21± 22.28	89.80±11.19*	102.83±13.01*	140.12 ±7.12
QCA-11	452.00±12.07	472.67± 27.80	424.17±24.97	122.20±7.25*	119.33 ±11.02*	153.2 ±10.75
QCA-12	443.60±19.99	426.20±20.12	394.50±21.82	116.80 ±11.16*	124.50±9.16*	125.83±15.09*
QCA-13	431.67±22.07	405.83±16.92	401.83±12.23	135.0±12	149.83 ±14.09	160.50 ±6.66
QCA-14	423.33±22.32	459.5±22.12	437±18.14	72.5 ±9.07*	84.33 ±6.78*	111.83 ±6.77*
QCA-15	399.33±23.88	440.50± 16.63	393.83±20.08	65.67 ±11.79*	67.17 ±6.87*	100.17±11.08*
Fluoxetine[#]				**90.5 ± 9.05***		
Control	**445.0±35.81**			**157.23± 12.91**		

[#]Fluoxetine (10 mg/kg) i.p.

All values represent mean ± SEM. Data were analyzed by graph pad prism (3) software through one way ANOVA followed by post hoc Dunnett's test. *p < 0.05 when compared with vehicle-treated group; n = 6/group *P < 0.05

2. Tail Suspension Test (TST)

To assess and further ascertain the anti-depressant like activity, all the compounds were also subjected to TST in mice at a dose of 1 mg/kg, i.p. **(Table 11)** Among the fifteen compounds screened, four compounds (QCA-1, QCA-8, QCA-14 and QCA-15) exhibited good anti-depressant activities as indicated by marked [$P < 0.05$] reduction in immobility time as compared to the control, while seven compounds (QCA-3, QCA-4, QCA-6, QCA-10, QCA-11 and QCA-12) showed moderate anti-depressant like activities. Subsequently, a dose-response assay (0.5 and 2 mg/kg, i.p.) was performed with some promising compounds. In dose-response assay four compounds (QCA-1, QCA-8, QCA-14 and QCA-15) dose-dependently reduced the immobility time which were statistically pronounced compared to the vehicle. These compounds were found to be the most promising as they markedly reduced immobility time compared to the control at all the three (0.5, 1 and 2 mg/kg) tested doses.

Analogues containing unsubstituted phenyl group as in compound QCA-1 and if substituted, the *ortho*-position, are better favoured for their potential as anti-depressants which are evident from compounds QCA-8 and QCA-14. Weak ring activators which are electron donating substituents on the phenyl ring, such as 2-propyl (QCA-8) and strong ring activators which are electron withdrawing substituents on the phenyl ring, such as 2-methoxy (QCA-14) and in *meta*-position as in 3-methoxy compound (QCA-15), exhibited better potential for their anti-depressant like activity than other compounds in FST and TST.

Table 11: Anti-depressant activity of QCA series analogues in Tail Suspension Test (TST) mice model

Compounds	Duration of immobility in seconds (TST)[b] Dose, mg/kg (ip)		
	2	**1**	**0.5**
QCA-1	155.67 ±10.30*	162.67 ±16.26*	182.5 ±16.77*
QCA-2	198.33 ±11.10		
QCA-3	173.67 ±14.15*	182.14±10.90*	206.33 ±19.89
QCA-4	171.00 ±18.26*	187.83 ±12.55*	
QCA-5	184.83 ±510.42*		
QCA-6	168.5 ±12.65*	189.67 ±10.60*	203.0 ±13.20
QCA-7	177.33 ±11.22*		
QCA-8	158.0 ±16.22*	179.67 ±21.19*	190.67±18.90*
QCA-9	177.33±14.48*	203.17 ±8.02	
QCA-10	164.0±11.55*	160.83±14.53*	195.33 ±10.59
QCA-11	175.50±13.77*	177.0 ±17.58*	201.17 ±10.79
QCA-12	178.80 ±6.30*	179.0±8.12*	200.17±10.14
QCA-13	192.5±11.92		
QCA-14	157.67 ±14.02*	171.5 ±17.17*	180.17 ±6.73*
QCA-15	117.5 ±11.79*	140.7 ±12.15*	137.67±12.86*
Bupropion[#]	**122.37 ± 9.38***		
Control	**218.5± 11.25**		

[#]Bupropion (20 mg/kg) i.p.

All values represent mean ± SEM. Data were analyzed by graph pad prism (3) software through one way ANOVA followed by post hoc Dunnett's test. *p < 0.05 when compared with vehicle-treated group; n = 6/group *P < 0.05

5.2.3. Preliminary screening of NCE's as potential anxiolytics

1. Elevated Plus Maze (EPM) test

The effects of NCE's and diazepam on the behavior of mice in the EPM test are summarized in **Table 12**. Treatment with compound QCA-11 (0.5 and 1 mg/kg, i.p.) and diazepam (1 mg/kg, i.p.) markedly [$P < 0.05$] increased the time spent in the open arm as compared to the vehicle. Compounds QCA-1, QCA-11 and QCA-14 (dose only at 1 mg/kg, i.p.) markedly [$P < 0.05$] increased the open arm entries as well as time spent in the open arm. Diazepam (1mg/kg, i.p.) treatment markedly [$P < 0.05$] increased the open arm entries and time spent in the open arm as compared to the vehicle control. Compounds QCA-1, QCA-11 and QCA-14 showed only pronounced [$P < 0.05$] increase in time spent in the open arms at 1 mg/kg, i.p. Compound QCA-11 showed marked [$P < 0.05$] change in the open arm entries at lower dose of compound (0.5 mg/kg, i.p.) as compared to the vehicle. Compounds QCA-1, QCA-11 and QCA-14 (1mg/kg, i.p.) treatment markedly increased the percentage open arm entries and percentage time spent in open arm as compared to vehicle.

Table 12: Effect of QCA series analogues and diazepam on the behavior of mice in elevated plus maze (EPM) test

Compounds	Percentage of Open Arm Entries Dose (mg/kg)		Percentage of Time Spent in Open Arm Entries Dose (mg/kg)	
	0.5	1	0.5	1
QCA-1	19.90±5.52	28.91±2.66*	19.87±2.98	33.60±1.52*
QCA-4	15.67±6.74	17.00±7.68	15.20±3.18	13.47±5.48
QCA-8	23.79±3.09	26.67±9.65	15.13±3.01	20.40±7.50
QCA-9	14.76±6.41	25.00±8.33	13.73±2.09	14.87±5.37
QCA-10	19.88±6.05	20.67±5.59	16.60±3.17	13.00±1.21
QCA-11	21.36±4.89	30.79±1.03*	21.53± 2.02*	22.20±3.37*
QCA-14	26.27±3.77	34.03±2.62*	18.60±4.41	26.27±2.03*
Diazepam#	60.01±5.53*		41.50±4.38*	
Control	**20.38±4.93**		**16.43±1.55**	

#Diazepam (2 mg/kg) i.p.

All values represent mean ± SEM. Data were analyzed by graph pad prism (3) software through one way ANOVA followed by post hoc Dunnett's test. *p < 0.05 when compared with vehicle-treated group; n = 6/group *P < 0.05

2. Light /dark Aversion Test

The effects of NCE's and diazepam on the behaviour of mice in the L/D test are presented in **Table 13**. Compounds QCA-1, QCA-8, QCA-11 and QCA-14 (1 mg/kg, i.p.), and diazepam (1 mg/kg, i.p.) treatment markedly [$P < 0.05$] increased the time spent in the lit area and number of transitions as compared to vehicle control. In addition, diazepam (1 mg/kg, i.p.) treatment markedly [$P < 0.05$] increased the latency to enter into the dark chamber. Treatment with compounds QCA-1, QCA-4, QCA-8, QCA-11 and QCA-14 (only at 1 mg/kg, i.p.) markedly [$P < 0.05$] increased the latency to enter into the dark chamber. Lower dose of NCE's (0.5 mg/kg, i.p.) did not produce any pronounced change in the latency to leave the light compartment as compared to vehicle control. In case of all the tested compounds, the anxiolytic like effect was more predominant at higher dose (1 mg/kg) level.

Compounds QCA-1, QCA-8 and QCA-14 and diazepam treatment markedly increased the number of transitions and time spent in the lit area, suggesting anti-anxiety like effect which is also exhibited by various anxiolytics and 5-HT_3 receptor antagonists.

Table 13: Effect of QCA series analogues and diazepam in dark-light mice model

Compounds	Latency time		Time spent (Light)		Transition	
	1	0.5	1	0.5	1	0.5
QCA-1	22.00±2.34*	16.50±1.29	94.25±10.80*	77.17±7.35	15.00±0.97*	12.33±3.54
QCA-4	20.80±2.13*	15.40±2.20	69.60±12.87	76.00±9.48	7.80±1.59	7.00±2.00
QCA-8	34.00±4.30*	20.60±3.33	116.80±10.37*	84.60±10.76	14.60±1.57*	11.20±1.02
QCA-9	16.20±12.80	15.00±2.17	69.80±17.80	72.20±8.00	9.20±2.78	8.80±2.85
QCA-10	16.40±2.71	20.00±2.88	75.40±10.68	80.00±11.61	6.20±1.59	6.40±2.60
QCA-11	33±6.45*	14±5.22	114±5.65*	83.60±9.37	15±0.67	8.20± 1.77
QCA-14	55±6.63*	20.60±6.22	101±8.94*	115.40±12.36*	15±1.75*	14.60±1.12*
Diazepam[#]	73.83 ± 8.90*		164.83 ± 5.50*		17.16 ± 9.00*	
Control	**16.17 ± 2.11**		**70.17 ± 6.34**		**9.33 ± 1.47**	

[#]Diazepam (2 mg/kg) i.p.

All values represent mean ± SEM. Data were analyzed by graph pad prism (3) software through one way ANOVA followed by post hoc Dunnett's test. *p < 0.05 when compared with vehicle-treated group; n = 6/group *P < 0.05

3. Open Field Test (OFT)

The results of the OFT are shown in **Table 14**. Treatment with compound QCA-1 (at 0.5 and 1 mg/kg, i.p.), and diazepam (2 mg/kg, i.p.) markedly [$P < 0.05$] increased the ambulation scores as compared to the vehicle control. Moreover, Compound QCA-1 (at 0.5 and 1 mg/kg, i.p.) and compound QCA-8 and QCA-14 (only at 1 mg/kg, i.p.) markedly [$P < 0.05$] increased the number of rearing as compared to the vehicle control. Treatment with compounds QCA-1, QCA-8 and QCA-14 increased the ambulation score and rearing number in the open field arena indicating the anxiolytic effect of these compounds.

Analogues that contain unsubstituted phenyl group (QCA-1) and if substituted at *ortho*-position are better favoured for their potential as anxiolytics which is evident from compounds QCA-8 and QCA-14. Weak ring activators which are electron donating substituents on the phenyl ring, such as 2-propyl (QCA-8) and strong ring activators which are electron withdrawing substituents on the phenyl ring, such as 2-methoxy (QCA-14), induced better anxiolytic like activity than other compounds in L/D and OFT. The results indicate that the selected compounds exhibited moderate potential for their anxiolytic like activity.

Table 14: Effect QCA series analogues and diazepam on the behavior of mice in open field test (OFT)

Compounds	Ambulation Score Dose (mg/kg)		Rearing number Dose (mg/kg)		Fecal pellets Dose (mg/kg)	
	1	0.5	1	0.5	1	0.5
QCA-1	257.60±14.58*	243.60±14.46*	18.60±5.82*	12.00±1.92*	0.60±0.40*	1.00±0.45
QCA-4	222.80±8.78*	219.40±8.53	7.20±1.32	7.40±0.98	1.60±0.40	1.40±0.68
QCA-8	233.60±10.98*	211.60±20.75	13.40±1.81*	8.60±2.06	1.60±0.68	1.40±0.40
QCA-9	197.60±14.79	190.2±13.6	6.60±1.63	7.2±2.4	1.00±0.45	2.4±1.0
QCA-10	194.00±6.95	188.60±30.39	9.00±1.97	8.60±2.69	1.20±0.58	1.00±0.45
QCA-11	222.80±6.69*	206.60±12.17	10.20±1.39	10.80±2.89	1.40±0.51	1.80±0.37
QCA-14	303.60±15.33*	203.40±22.14	15.80±1.50*	9.40±2.50	1.80±0.37	2.00±0.43
Diazepam[#]	**367.50 ± 15.19***		**29.50 ± 1.02***		**0.50±0.11**	
Control	200.20± 10.37		8.60± 1.17		1.80±0.66	

[#]Diazepam (2 mg/kg) i.p.

All values represent mean ± SEM. Data were analyzed by graph pad prism (3) software through one way ANOVA followed by post hoc Dunnett's test. *p < 0.05 when compared with vehicle-treated group; n = 6/group *P < 0.05

5.3. Biological activities/Pharmacology for QCB Series

Modification on the benzyl ring of the QCA series by introducing a strong activating group like methoxy group (-OCH_3) at the *para*-position lead to 4-(4-methoxybenzyl)-3-oxo-*N*-phenyl-3,4-dihydroquinoxaline-2-carboxamide analogues (QCB-series), were synthesized and subjected for their inhibitory properties through *in-vitro* studies at 10 µM using PDE4B or PDE4D enzyme assay using rolipram as a reference compound.

Compound QCB-6, QCB-7, QCB-11, QCB-12, QCB-13, QCB-16 and QCB-18 showed pronounced inhibitory activity whereas compound QCB-18 exhibited moderate inhibitory activity and compound QCB-1, QCB-2 and QCB-3 displayed weak inhibitory activity for PDE4D enzyme. Compound QCB-6, QCB-9, QCB-10, QCB-13, QCB-14 and QCB-18 displayed moderate PDE4B inhibitory activity, while rest of the tested compounds exhibited poor inhibition. **(Table 15)**

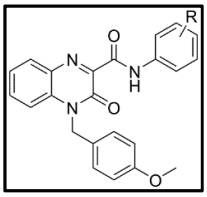

Compound QCB-7, QCB-11, QCB-12 and QCB-16 are the most active compound in this series which displayed comparatively more than 2-fold affinity for PDE4D than PDE4B enzyme. However, compound QCB-2 and QCB-3 exhibited 3-fold affinity for PDE4D than PDE4B but were inactive. Since, compound QCB-6, QCB-13 and QCB-18 displayed moderate activity for PDE4B enzyme indicating that these compounds are non-selective. Whereas, compounds like QCB-1 and QCB-17 had equally affinity for PDE4D and PDE4B enzymes, respectively. **(Table 15)**

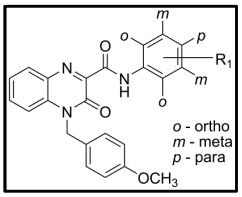

The SAR of these synthesized compounds indicates that substitutions preferably at *ortho*-position was more favored on the phenyl ring for PDE4D inhibitory activity as evident from compounds QCB-2, QCB-7, QCB-11, QCB-12, QCB-13 and QCB-16. Similarly for PDE4B enzyme, substitutions either at *ortho*, *para* or both the positions on the phenyl ringwere tolerated as marked by compounds QCB-9, QCB-10, QCB-13, QCB-14 and QCB-18 which displayed better to moderate inhibitory activity.

Introduction of a weak deactivating substituent like halogen especially chlorine is preferred at *ortho*-position on the phenyl ring along with a weak activating substituent like alkyl group especially methyl as in compounds QCB-11, QCB-12, and QCB-13, while swapping the position of these groups as in compound QCB-7 retained the activity; whereas, devoid of alkyl group there was slight decrease in the inhibitory activity as in compound QCB-16. Strong ring activator like methoxy group was tolerated as in compound QCB-2 and QCB-3 displayed moderate PDE4D inhibitory activity and were inactive for PDE4B. Unsubstituted phenyl group as in compound QCB-1 showed weak PDE4D and PDE4B inhibitory activity.

When substituents like alkyl group especially ethyl was introduced at *meta*-position as in compound QCB-6 enhanced PDE4D and moderate PDE4B inhibitory activity. Further, when a chlorine group was introduced at *ortho*-position on the phenyl ring as in compounds like QCB-12, QCB-13, QCB-16, QCB-17 and QCB-18 displayed moderate PDE4D and PDE4B inhibitory activities, respectively indicating that these compounds were non-selective.

Introduction of weak activating bulkier lipophilic group preferably isopropyl at *ortho*- or *para*-position on the phenyl ring as in compounds like QCB-9 and QCB-10 rather displayed moderate PDE4B inhibitory activity eroding the PDE4D inhibitory activity. Similarly when weak activating alkyl group particularly methyl was introduced at *ortho*-position along with weak deactivating halogen group particularly chlorine as in compound QCB-14retained the PDE4B inhibitory activity.

Table 15: In-vitro data of QCB series

Compound	R	PDE4B[a]	SD	PDE4D[a]	SD	Selectivity[b]
QCB-1	Phenyl	43.73	1.66	49.06	1.32	1.1
QCB-2	2-methoxyphenyl	16.58	0.55	48.44	1.29	3.0
QCB-3	3-methoxyphenyl	17.58	2.10	45.05	2.08	2.6
QCB-4	4-methoxyphenyl	30.71	1.82	33.94	1.95	-
QCB-5	2-ethylphenyl	41.22	1.74	41.65	1.84	-
QCB-6	3-ethylphenyl	57.88	2.22	72.2	0.94	1.3
QCB-7	3-chloro-2-methylphenyl	33.85	1.96	73.13	0.72	2.2
QCB-8	2-propylphenyl	25.61	1.12	39.95	0.84	-
QCB-9	2-isopropylphenyl	54.67	0.65	41.71	0.23	-
QCB-10	4-isopropylphenyl	55.81	1.52	40.04	1.22	-
QCB-11	2-chloro-4-methylphenyl	32.31	1.44	75.15	1.10	2.3
QCB-12	2-chloro-5-methylphenyl	46.25	1.32	69.34	0.84	1.5
QCB-13	2-chloro-6-methylphenyl	53.01	0.54	70.46	0.42	1.3
QCB-14	4-chloro-2-methylphenyl	57.67	1.20	37.30	1.36	-
QCB-15	2-trifluoromethylphenyl	11.85	2.42	19.51	0.96	-
QCB-16	2-chlorophenyl	44.01	2.18	71.16	0.99	1.6
QCB-17	3-chlorophenyl	42.06	1.24	54.95	1.12	1.3
QCB-18	4-chlorophenyl	50.71	0.95	64.07	0.98	1.3
Rolipram		90.27	0.22	96.54	0.14	1.1

[a] Average percentage inhibition – Values that are the mean of two or more experiments are shown with their standard deviations (SD)
[b] Ratio of PDE4D/PDE4B

In order to understand the nature of interactions of these molecules, rolipram and nitraquazone as standards within the active site of PDE4D and PDE4B, docking studies were carried out for all these compounds. The dockscore and other scores obtained after docking of these molecules into the PDE4D and PDE4B proteins are summarized in **Table 16** and **17** respectively. The interaction of compound QCB-11 within the active site of PDE4D protein **(Fig. 43)** is mainly contributed by (i) a π-π stacking interaction between the centroid of the phenyl ring on the amide linker and Phe340, (ii) two cationic-π interactions with His160, one with centroid of the benzene ring of the quinoxaline scaffold and other with the centroid of substituted benzyl group. Similarly, the interaction of compound QCB-7 within the active site of PDE4D protein **(Fig. 44)** is contributed by (i) H-bond interaction between the keto group of the quinoxaline ring with His160 at a distance of 5.2 Á, (ii) π-π stacking interaction between the centroid of the substituted benzyl ring and Phe372, (iii) σ-π interaction between the centroid of the centroid of the phenyl ring on the amide linker and Met273, (iv) two cationic-π interactions with His160, one between the centroid of the benzene ring of the quinoxaline scaffold and other with the centroid of the substituted benzyl ring.

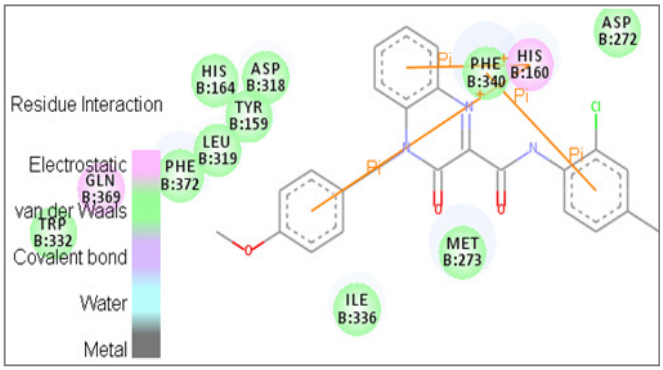

Fig. 43: QCB-11 at the active site of PDE4D

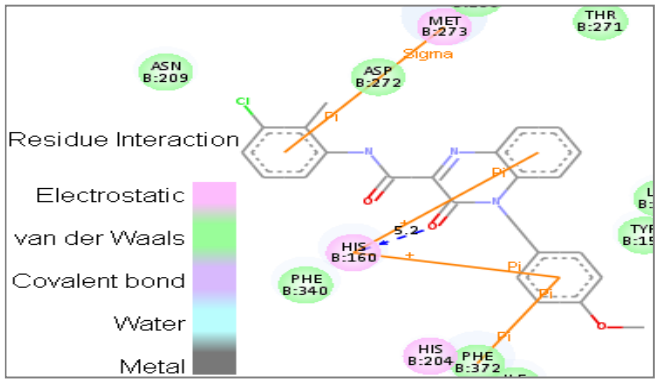

Fig. 44: QCB-7 at the active site of PDE4D

The interaction of compound QCB-6 within the active site of PDE4D protein **(Fig. 45)** is mainly contributed by (i) a π-π stacking interaction between the centroid of the substituted benzyl ring with Phe372, (ii) cationic-π interaction between the centroid of the substituted benzyl ring with His160. While, with PDE4B protein the interaction within the active site **(Fig. 46)** is mainly contributed by (i) two π-π stacking interactions, one between the centroid of the phenyl ring on the amide linker with Phe446, while another between the centroid of the substituted benzyl ring and Phe414, (ii) cationic-π interaction between the centroid of the benzene ring of the quinoxaline scaffold and His307.

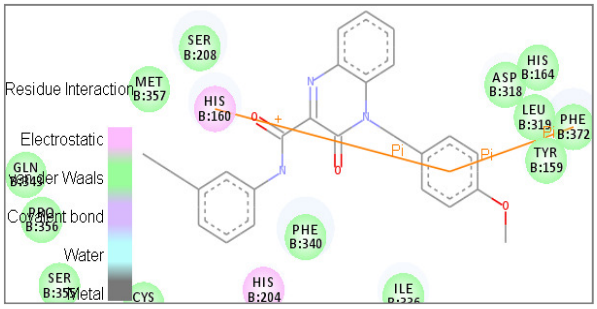

Fig. 45: QCB-6 at the active site of PDE4D

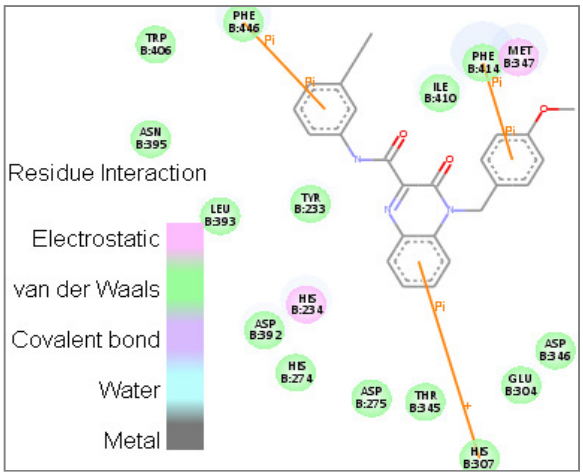

Fig. 46: QCB-6 at the active site of PDE4B

The interaction of compound QCB-16 within the active site of PDE4D protein **(Fig. 47)** is mainly contributed by (i) two π-π stacking interactions, one between the centroid of the phenyl ring on the amide linker with Phe340, while another between the centroid of the substituted benzyl ring and Phe372, (ii) two cationic-π interactions with His160, one between the centroid of the benzene ring of the quinoxaline scaffold and other with the centroid of the substituted benzyl ring. Similarly, the interaction of compound QCB-13 within the active site of PDE4D protein **(Fig. 48)** is mainly contributed by (i) H-bond interaction between the keto group of the quinoxaline ring with His160 at a distance of 5.2 Å, (ii) π-π stacking interaction between the centroid of the substituted benzyl ring

with Phe372, (iii) two cationic-π interactions with His160, one between the centroid of the benzene ring of the quinoxaline scaffold and other with the centroid of the substituted benzyl ring.

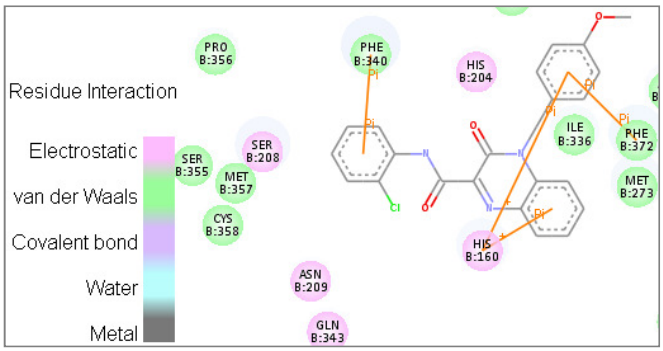

Fig. 47: QCB-16 at the active site of PDE4D

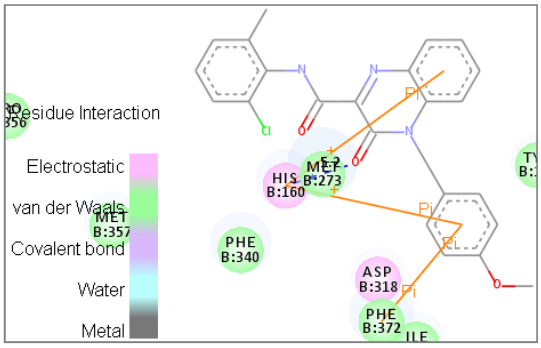

Fig. 48: QCB-13 at the active site of PDE4D

The interaction of compound QCB-12 within the active site of PDE4D protein **(Fig. 49)** is mainly contributed by (i) two π-π stacking interactions, one between the centroid of the centroid of the phenyl ring on the amide linker with Phe340, while another between the centroid of the substituted benzyl ring and Phe372, (ii) two cationic-π interactions with His160, one between the centroid of the benzene ring of the quinoxaline scaffold and other with the centroid of the substituted benzyl ring. Whereas, the interaction of compound QCB-18 within the active site of PDE4D protein **(Fig. 50)** is mainly contributed by (i) π-π stacking interaction between the centroid of the substituted benzyl ring with Phe372, (iii) two cationic-π interactions with His160, one between the centroid of the benzene ring of the quinoxaline scaffold and other with the centroid of the substituted benzyl ring. While, the interaction of compound QCB-14 within the active site of PDE4B protein **(Fig. 51)** is mainly contributed by (i) π-π stacking interaction between the centroid of the substituted benzyl ring with Phe446.

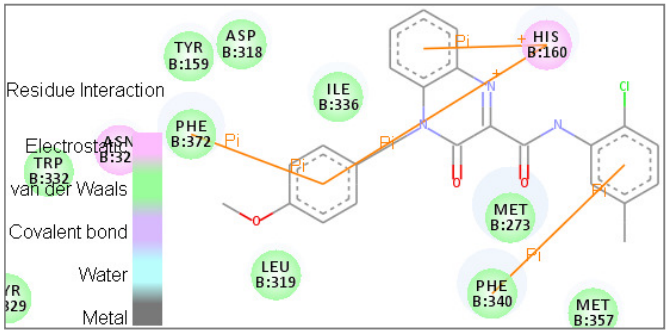

Fig. 49: QCB-12 at the active site of PDE4D

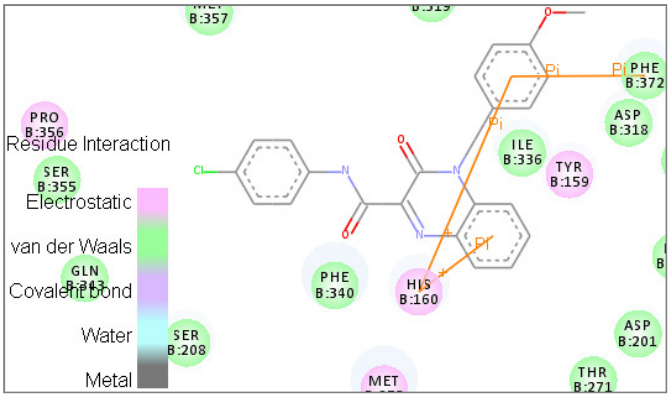

Fig. 50: QCB-18 at the active site of PDE4D

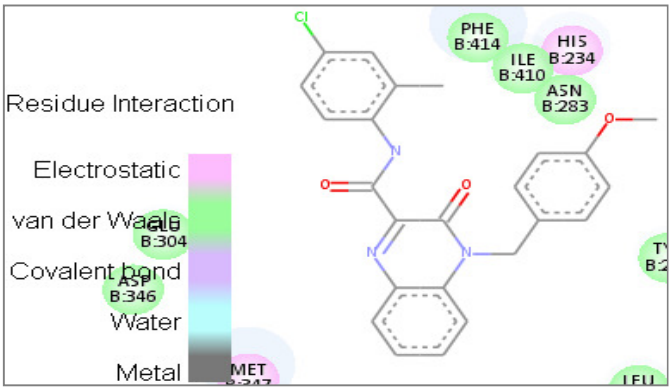

Fig. 51: QCB-14 at the active site of PDE4B

Overall, the present 4-(4-methoxybenzyl)-3-oxo-quinoxaline-2-carboxamide analogues displayed better interactions with PDE4D enzyme exhibiting their inhibitory activity. This indicates that the pharmacophoric elements like the central quinoxaline ring with a keto group which acts as a hydrogen bond acceptor (HBA), the benzyl moiety, diverse substituted phenyl ring and the amide linker played a substantial role in forming various interactions within the active site.

Table 16: Docking results of QCB series for PDE4D (PDB: 1Q9M)

Compound	LigScore_1	LigScore_2	-PLP1	-PLP2	Jain	-PMF	-PMF04	Dockscore	Ludi_3	Consensus
QCB-1	3.25	5.43	66.77	65.79	3.65	179.51	98.90	63.10	994	6
QCB-2	2.75	4.85	84.62	83.15	3.75	148.29	91.83	72.68	743	5
QCB-3	2.68	5.28	74.61	67.82	2.11	149.84	83.39	72.36	789	2
QCB-4	2.78	5.69	72.52	66.12	1.99	145.06	78.77	72.05	712	3
QCB-5	2.60	5.41	70.79	65.43	1.72	151.32	76.97	71.22	748	2
QCB-6	2.88	5.50	73.21	67.48	2.48	150.06	80.94	72.55	786	2
QCB-7	2.67	5.29	74.92	70.39	2.23	112.22	55.57	71.94	673	1
QCB-8	3.20	6.28	97.36	92.49	2.63	168.57	92.88	69.79	780	7
QCB-9	2.35	5.28	57.47	51.74	0.09	147.84	80.74	71.17	762	2
QCB-10	4.06	5.05	84.56	71.31	3.28	167.46	92.98	71.96	900	9
QCB-11	2.58	5.48	77.79	72.47	2.41	156.38	82.50	72.04	787	3
QCB-12	2.78	5.52	72.42	68.87	1.60	138.30	81.77	75.11	734	1
QCB-13	2.54	5.11	60.02	59.65	1.44	135.77	80.66	71.90	598	1
QCB-14	2.61	5.07	64.15	62.88	2.23	147.97	74.30	70.99	656	0
QCB-15	2.14	5.21	69.04	63.90	1.72	160.55	100.75	69.93	736	2
QCB-16	2.35	5.24	71.85	64.49	1.21	150.39	80.14	71.58	638	2
QCB-17	2.63	5.28	67.26	63.83	1.24	138.94	72.55	71.59	712	2
QCB-18	2.73	5.34	72.12	69.19	2.64	147.77	77.54	71.65	783	2
Rolipram	3.82	4.54	48.46	48.38	2.78	118.37	64.25	46.866	456	1
Nitraquazone	4.24	4.73	52.53	50.68	1.71	158.56	94.33	56.384	701	3

Table 17: Docking results of QCB series for PDE4B (PDB: 1XMY)

Compound	LigScore_1	LigScore_2	-PLP1	-PLP2	Jain	-PMF	-PMF04	Dockscore	Ludi_3	Consensus
QCB-1	2.65	5.13	81.79	72.62	2.02	69.42	54.93	56.56	424	5
QCB-2	1.94	4.85	71.29	64.91	1.21	170.77	122.60	66.85	717	4
QCB-3	1.95	5.07	63.67	58.09	0.11	136.30	96.01	65.61	749	2
QCB-4	1.75	4.68	53.94	53.91	1.77	134.22	89.83	64.05	609	2
QCB-5	1.90	5.03	52.07	43.96	0.23	136.55	95.88	65.01	769	4
QCB-6	2.37	5.24	59.93	55.13	0.53	119.72	83.06	66.18	644	4
QCB-7	1.97	5.06	73.32	71.17	3.20	122.57	78.38	64.09	842	4
QCB-8	2.22	5.37	68.49	60.74	0.75	154.64	112.60	64.87	786	7
QCB-9	2.03	5.32	67.26	64.10	1.19	137.84	92.56	63.97	696	6
QCB-10	2.84	4.52	80.17	62.47	3.01	157.31	107.98	64.56	824	9
QCB-11	2.06	4.93	58.36	56.04	1.79	120.50	86.07	66.16	569	2
QCB-12	2.04	5.34	72.61	69.81	0.42	117.98	87.28	64.34	641	3
QCB-13	2.07	5.12	68.65	64.34	1.74	156.57	109.86	68.71	792	5
QCB-14	1.82	4.86	57.58	51.02	0.71	111.48	86.40	63.26	632	0
QCB-15	1.88	4.91	65.57	55.89	0.87	145.35	109.06	63.97	800	6
QCB-16	2.02	5.12	73.30	66.52	1.02	125.09	100.50	65.98	590	4
QCB-17	2.06	5.17	64.73	62.02	0.37	113.99	79.10	65.68	612	2
QCB-18	2.03	5.05	63.27	59.62	1.26	119.89	78.61	68.20	624	2
Rolipram	2.23	4.39	54.3	46.79	2.51	141.03	107.36	45.193	608	2
Nitraquazone	1.78	4.61	68.64	51.8	1.44	139.65	96.4	57.033	708	0

5.3.1. ADME properties

The analysis showed that the compounds of this series, when administered orally might show better intestinal absorption, as well as good blood–brain barrier (BBB) permeability. Their aqueous solubility and drug–likeness properties were predicted be very low. In addition, these compounds are likely to inhibit enzyme such as CYP450 *2D6*. Most of these compounds are expected to be non-hepatotoxic. It was also found that the inhibitor-plasma protein binding is not more than 90%, indicating that these compounds are likely to be less bound to plasma protein present in the blood. **(Table 18)**

Nevertheless, It is a familiar understanding that ADME profiles are complex to envisage accurately just by *in-silico* and so the envisaged profiles should be employed with care. For our study, further testing ought to be done to investigate the actual profiles of these compounds as an extension of this work.

In the ADMET plot, since all the molecule are inside the 99% confidence ellipse of BBB and HIA model, the predictions are considered reliable and therefore the BBB and HIA predictions are made for these ligands respectively. **(Fig. 52)**

Table 18: ADME properties of QCB Series

QCB	Aqueous solubility[a]		BBB[b]		CYP450 *2D6*[c]		Hepatotoxicity[d]		HIA[e]		PPB[g]		AlogP98[g]	
	Value	Level	Value	Level	Value	Level	Value	Level	Value	Level	Value	Level	Value	Level
1	-4.834	2	-0.185	2	-4.750	1	-2.725	0	NV[f]	0	3.946	0	3.537	0
2	-4.816	2	-0.331	2	-4.854	1	-2.921	0	NV[f]	0	3.809	0	3.520	0
3	-4.793	2	-0.331	2	-5.845	1	-2.875	0	NV[f]	0	3.652	0	3.520	0
4	-4.771	2	-0.331	2	-5.845	1	-1.949	0	NV[f]	0	1.597	0	3.520	0
5	-5.568	2	0.107	1	-4.568	1	-6.211	1	NV[f]	0	5.084	0	4.479	0
6	-5.546	2	0.107	1	-5.389	1	-3.939	0	NV[f]	0	5.002	0	4.479	0
7	-5.976	2	0.171	1	-4.345	1	-2.933	0	NV[f]	0	6.505	0	4.687	0
8	-5.829	2	0.248	1	-4.588	1	-5.540	1	NV[f]	0	5.362	0	4.935	0
9	-5.805	2	0.185	1	-4.440	1	-4.356	1	NV[f]	0	4.314	0	4.731	0
10	-5.738	2	0.185	1	-4.638	1	-1.624	0	NV[f]	0	4.335	0	4.731	0
11	-5.965	2	0.171	1	-4.913	1	-2.122	0	NV[f]	0	6.186	0	4.687	0
12	-5.975	2	0.171	1	-4.920	1	-2.225	0	NV[f]	0	6.700	0	4.687	0
13	-5.987	2	0.171	1	-5.201	1	-1.723	0	NV[f]	0	6.110	0	4.687	0
14	-5.965	2	0.171	1	-4.905	1	-2.109	0	NV[f]	0	8.143	0	4.687	0
15	-5.995	2	0.107	1	-2.811	1	-7.817	1	NV[f]	0	4.970	0	4.479	0
16	-5.532	2	0.021	1	-3.588	1	-2.507	0	NV[f]	0	5.854	0	4.201	0
17	-5.520	2	0.021	1	-4.005	1	-0.636	0	NV[f]	0	7.083	0	4.201	0
18	-5.509	2	0.021	1	-2.962	1	-1.835	0	NV[f]	0	7.021	0	4.201	0

[a] Level 2 means the aqueous solubility of inhibitor is not very good and its drug-likeness properties are low.
[b] Level 2 means inhibitor has medium ability and Level 1 means inhibitor has high ability to cross the blood-brain barrier (BBB).
[c] Level 1 means inhibitor likely to inhibit CYP*2D6* enzyme.
[d] Level 0 means inhibitor not likely to be hepatotoxic, while Level 1 means inhibitor are likely to be hepatotoxic.
[e] Level 0 means inhibitor has good human intestinal absorption (HIA) after oral administration.
[f] NV means no value was given.
[g] Level 0 means the binding between inhibitor and plasma protein (PPB) is less than 90% (No markers flagged and AlogP98 < 5.0).

ADMET PLOT

The ADMET plot is a 2D chart of ADMET_PSA_2D versus ADMET_AlogP98. The two sets of ellipses are for the prediction confidence space (95% and 99%) for the Blood Brain Barrier Penetration and Human Intestinal Absorption models, respectively.

Since the molecule is outside of the 99% BBB model confidence ellipse, the prediction is considered unreliable and no BBB prediction is made for this ligand.

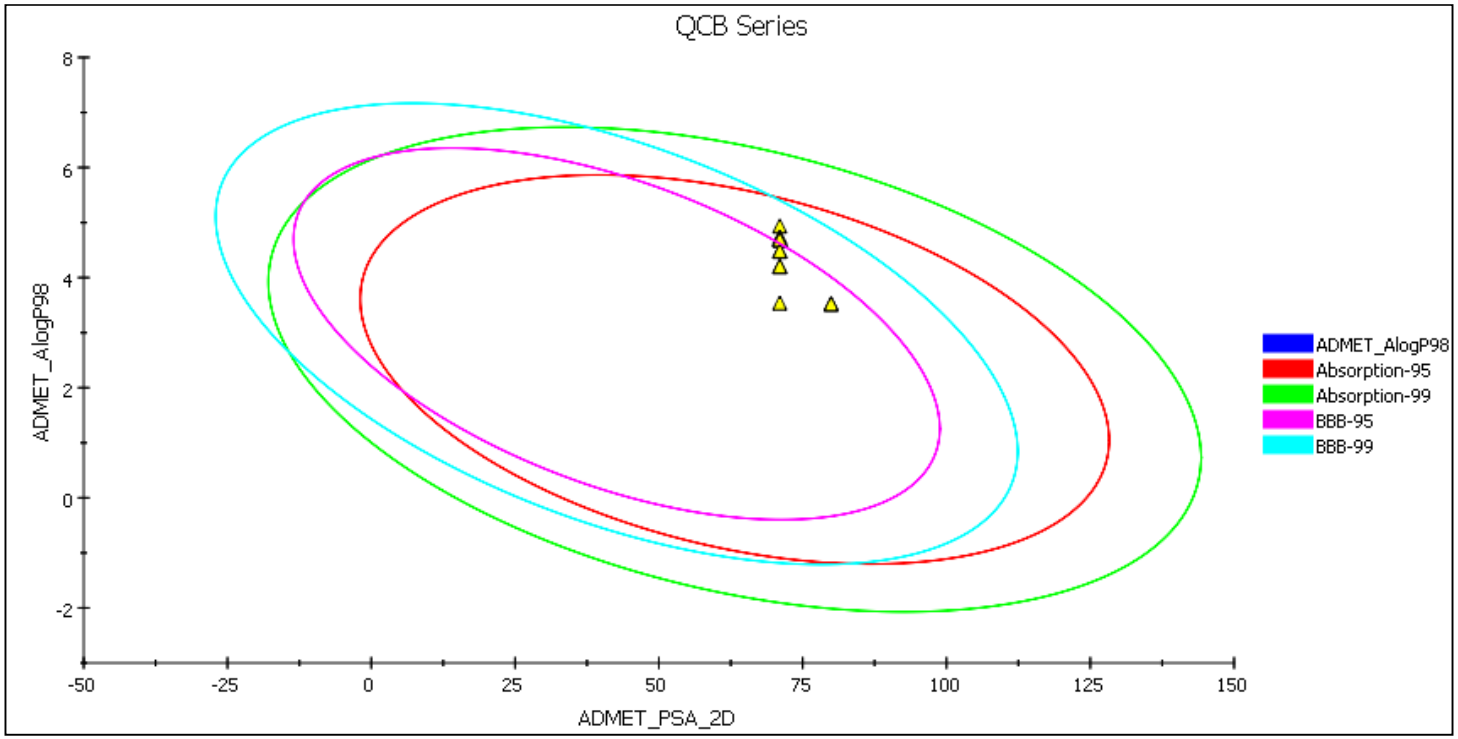

Fig. 52: ADMET Plot for QCB Series

5.3.2. Preliminary screening of NCE's as potential anti-depressants

Based on the encouraging results obtained from *in-vitro* screening, further preliminary screening of these new chemical entities (NCE's) were carried out on the standardized rodent models for depression and anxiety.

Irrespective of the PDE4 inhibitory activity, to assess their potential for their anti-depressant activity, all the compounds of QCB series were subjected to FST and TST in mice model. Anti-depressant activity was estimated as mean immobility time in seconds. The anti-depressant activity data from FST and TST are shown as Mean ± S.E.M. in **Table 19**.

In order to ascertain the possible occurrence of drug induced changes (stimulation/suppression) in the locomotor activity of mice, which may contribute to their behavioral changes in FST and TST, all the compounds were subjected to spontaneous locomotor activity study using actophotometer. Neither standard, nor test compounds were found to cause pronounced changes in the locomotor activity of mice when compared to the control as shown in **Table 19**. Therefore, the results obtained from the actophotometer study eliminate the possible existence of any false positive and (or) false negative result in FST and TST.

1. Force Swim Test (FST)

In the preliminary anti-depressant screening by FST, initially all the compounds were administered intra-peritoneally (i.p.) at a dose of 1 mg/kg body weight of mice. **(Table 19)** Among the fifteen compounds screened, four compounds QCB-3, QCB-5, QCB-12 and QCB-15 showed prominent anti-depressant like activities as indicated by marked [$P < 0.05$] reduction in immobility time compared to the control, while five compounds QCB-7, QCB-8, QCB-9, QCB-11, QCB-13 and QCB-14 showed moderate anti-depressant like activities.

Supported by preliminary anti-depressant study, these compounds were chosen for profiling in a dose–response assay of mice FST. In dose-response assay (0.5 and 1 mg/kg), four compounds QCB-3, QCB-5, QCB-12and QCB-15 demonstrated a statistically pronounced reduction in immobility time compared to control, in a dose-dependent manner. These compounds emerged as better potential derivatives as they markedly [$P < 0.05$] reduced the immobility time compared to the control at two test dose levels (0.5 and 1 mg/kg).

2. Tail Suspension Test (TST)

In order to further ascertain the anti-depressant like activity, all the compounds were also subjected to TST in mice at a dose of 0.5 and 1 mg/kg, i.p. **(Table 19)** Among the fifteen compounds screened, five compounds QCB-2, QCB-3, QCB-7, QCB-8 and QCB-15 exhibited good anti-depressant activities as indicated by marked [$P < 0.05$] reduction in immobility time as compared to the control, while four compounds QCB-5, QCB-9, QCB-12 and QCB-13 showed moderate anti-depressant like activities. Subsequently, a dose-response assay (0.5 and 2 mg/kg, i.p) was performed with some promising compounds. In dose-response assay five compounds QCB-2, QCB-3, QCB-7, QCB-8 and QCB-15 dose dependently reduced the immobility time which was statistically pronounced compared to the vehicle. These compoundswere found to be the better derivatives as they markedly reduced immobility time compared to the control at two (0.5 and 1 mg/kg) test dose levels.

Analogues which contain substitution at *ortho*-position are better favoured for their potential as anti-depressants which are evident from compounds QCB-5, QCB-7, QCB-8, QCB-9, QCB-12 and QCB-15. Weak ring activators which are electron donating substituents on the phenyl ring, such as 2-methyl (QCB-7), 2-ethyl (QCB-5), 2-propyl (QCB-8) and 2-isopropyl (QCB-9), whereas strong deactivator which are strong electron withdrawing such as 2-trifluoromethyl (QCB-15) and strong ring activator which are electron withdrawing, at *meta*-position such as 3-methoxy (QCB-3) or weak deactivator which are strong electron withdrawing such as 3-chloro (QCB-7) or activator which are weak donating such as 5-methyl (QCB-12), exhibited better potential for their anti-depressant like activity than other compounds in FST and TST.

Table 19: Pharmacological data of QCB series analogues for spontaneous locomotor activity (SLA) and its anti-depressant activity in Force Swim Test (FST) and Tail Suspension Test (TST) mice model

Compounds	Locomotor scores[b] (10 min) Dose, mg/kg (ip)		Duration of immobility in sec (FST)[b] Dose, mg/kg (ip)		Duration of immobility in sec (TST) [b] Dose, mg/kg (ip)	
	1	0.5	1	0.5	1	0.5
QCB-1	410.33 ± 25.30	360.50 ± 22.68	129.33 ± 10.52*	140.17 ± 5.23	169.83 ± 18.54*	190.83 ± 11.48
QCB-2	359.00 ± 25.25	391.50 ± 11.27	114.33 ± 13.31*	141.33 ± 5.92	139.17 ± 20.20*	176.33 ± 13.97*
QCB-3	386.00 ± 23.66	356.83 ± 27.75	95.67 ± 4.65*	114.57 ± 11.75*	167.50 ± 8.69*	182.17 ± 7.76*
QCB-4	371.00 ± 16.70	400.50 ± 23.49	157.67 ± 12.13	172.83 ± 4. 86	197.50 ± 7.29	216.33 ± 16.93
QCB-5	397.20 ± 21.44	341.00 ± 37.35	84.83 ± 8.46*	107.67 ± 5.53*	173.33 ± 9.15*	176.00 ± 8.99*
QCB-6	382.43 ± 12.32	364.13 ± 19.21	134.20 ± 6.90*	148.60 ± 8.48	229.60 ± 8.37	237.83 ± 15.01
QCB-7	417.00 ± 11.41	424.00 ± 17.72	116.33 ± 9.83*	128.00 ± 6.25*	158.67 ± 8.81*	171.50 ± 10.59*
QCB-8	378.83 ± 15.12	384.00 ± 29.49	127.50 ± 3.99*	114.17 ± 6.34*	143.51 ± 1.82*	164.00 ± 7.14*
QCB-9	417.17 ± 14.16	380.83 ± 12.62	116.50 ± 7.17*	134.50 ± 5.11*	178.5 ± 10.49*	191.50 ± 9.38*
QCB-10	380.33 ± 15.05	398.33 ± 14.83	126.83 ± 9.48*	139.40 ± 5.98	176.14 ± 19.95	196.57 ± 11.99
QCB-11	376.67 ± 17.40	357.00 ± 35.29	119.33 ± 11.02*	122.20 ± 7.25*	190.00 ± 11.50*	198.50 ± 10.21
QCB-12	381.33 ± 12.77	369.67 ± 15.42	98.00 ± 7.04*	118.80 ± 6.05*	168.50 ± 13.10*	183.17 ± 12.98*
QCB-13	382.50 ± 17.37	356.40 ± 19.08	106.67 ± 7.70*	128.00 ± 8.98*	174.40 ± 5.75*	187.60 ± 14.42*
QCB-14	363.00 ± 18.69	378.17 ± 15.32	114.83 ± 7.22*	129.33 ± 6.97*	166.50 ± 10.12*	186.67 ± 15.90
QCB-15	393.80 ± 21.82	344.33 ± 12.12	81.33 ± 7.22*	119.50 ± 9.08*	147.17 ± 9.62*	165.20 ± 11.01*
Fluoxetine[#]			**90.5 ± 9.05***			
Bupropion[#]					**122.37 ± 9.38***	
Control	**383.00 ± 18.37**		**157.23 ± 12.91**		**218.5 ± 11.25**	

[#]Fluoxetine (10 mg/kg) i.p. and [#]Bupropion (20 mg/kg) i.p.

All values represent mean ± SEM. Data were analyzed by graph pad prism (3) software through one way ANOVA followed by post hoc Dunnet's test. *p < 0.05 when compared with vehicle-treated group; n = 6/group *p < 0.05

5.4. Biological activities/Pharmacology for QCC Series

Modification on the benzyl ring of the QCA series by introducing a strong deactivating group like nitrile group (-CN) at the *para*-position lead to 4-(4-nitrilebenzyl)-3-oxo-*N*-phenyl-3,4-dihydroquinoxaline-2-carboxamide analogues (QCC-series), which were synthesized and subjected for their inhibitory properties through *in-vitro* studies at 10 µM using PDE4B or PDE4D enzyme assay using rolipram as a reference compound.

In this series, compound QCC-2, QCC-3, QCC-5, QCC-10, QCC-11 and QCC-12 showed pronounced inhibitory activity whereas compound QCC-1 and QCC-16 exhibited moderate inhibitory activity for PDE4D enzyme. Compound QCC-1, QCC-8 and QCC-10 displayed moderate PDE4B inhibitory activity, while rest of the tested compounds exhibited poor inhibition. **(Table 20)**

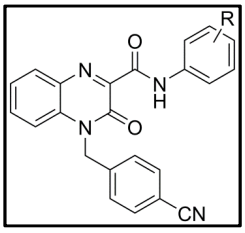

Compound QCC-12 showed better PDE4D inhibitory activity but compound QCC-2 has relatively more than 4-fold affinity, while compound QCC-11 has 3-fold affinity for PDE4D compared to PDE4B isozyme for its inhibitory activity. Compound QCC-16 has shown moderate activity but has relatively 4-fold affinity for PDE4D than PDE4B enzyme. Whereas, compound QCC-10 and QCC-3 exhibited better inhibitory activity; while compound QCC-1 displayed moderate inhibitory activity; however, all these compounds showed equal affinity for both the isoform indicating there non-selectivity. Compound QCC-5 exhibited a 64-fold affinity for PDE4D with better inhibitory activity. **(Table 20)** This suggests that this moiety could be considered as a lead, and on appropriate modification may possibly enhance the PDE4D selective inhibition and also devoid of its PDE4B inhibitory activity.

Table 20: In-vitro data of QCC series

Compound	R	PDE4B[a]	SD	PDE4D[a]	SD	Selectivity[b]
QCC-1	Phenyl	56.21	0.33	59.15	1.43	1.1
QCC-2	2-methoxyphenyl	15.16	0.58	69.19	0.52	4.6
QCC-3	3-methoxyphenyl	43.93	1.26	63.72	1.48	1.5
QCC-4	4-methoxyphenyl	30.98	1.54	32.07	2.21	-
QCC-5	**2-chlorophenyl**	**0.00**	1.66	**64.30**	0.32	**64**
QCC-6	3-chlorophenyl	49.04	0.55	45.23	0.62	-
QCC-7	4-chlorophenyl	19.93	2.10	45.23	1.14	-
QCC-8	2-ethylphenyl	54.07	1.82	46.22	0.53	-
QCC-9	3-ethylphenyl	43.61	1.74	42.69	0.86	-
QCC-10	2-propylphenyl	52.74	2.22	72.92	3.20	1.4
QCC-11	2-isopropylphenyl	22.02	1.96	67.46	2.85	3.1
QCC-12	4-isopropylphenyl	33.45	1.12	77.37	1.62	2.3
QCC-13	2-chloro-4-methylphenyl	11.72	1.14	35.92	1.22	-
QCC-14	2-chloro-5-methylphenyl	32.39	0.94	28.84	0.89	-
QCC-15	2-chloro-6-methylphenyl	27.52	1.12	36.14	1.21	-
QCC-16	3-chloro-2-methylphenyl	15.14	0.95	57.07	1.26	3.8
QCC-17	1-amino piperidine	9.38	1.54	47.79	2.22	5.10
QCC-18	4-chloro-2-methylphenyl	17.11	1.66	44.53	0.84	-
QCC-19	2-trifluoromethylphenyl	16.10	0.89	32.30	0.99	-
Rolipram		90.27	0.22	96.54		1.1

[a] Average percentage inhibition – Values that are the mean of two or more experiments are shown with their standard deviations (SD)
[b] Ratio of PDE4D/PDE4B

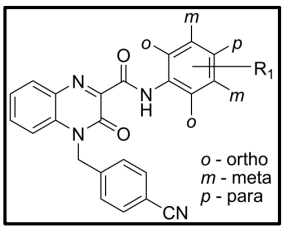

The SAR of these synthesized compounds indicates that substitution preferably at *ortho* or *para*-position on the phenyl ring was more favored for pronounced PDE4D inhibitory activity as evident from compounds QCC-2, QCC-5, QCC-10, QCC-11, QCC-12 and QCC-16. Similarly for PDE4B enzyme, substitution at *ortho*-position on the phenyl ring was favored which displayed moderate PDE4B inhibitory activity as marked from compounds QCC-8 and QCC-10. The initial compound QCC-1 showed moderate PDE4D inhibitory activity and was equipotent for its PDE4B isoform.

A bulkier and better lipophilic group especially isopropyl at *para*-position was better tolerated as evident from compound QCC-12 which displayed prominent inhibition for PDE4D enzyme. However, when it was introduced at the *ortho*-position as in compound

QCC-11 there was slight decrease in the PDE4D inhibitory activity but retained PDE4D better inhibitory activity. When a weak deactivating bulkier lipophilic group especially propyl and strong activating group mainly methoxy was introduced at *ortho*-position as in compound QCC-10 and QCC-2, respectively restored and markedly improved the activity. Interestingly, when methoxy was introduced at *meta*-position as in compound QCC-3 also retained the activity. When weak deactivating group like halogen particularly chloro at *ortho*-position as evident in compound QCC-5 was predominantly tolerated and displayed higher selectivity for its PDE4D inhibitory activity and eroding its PDE4B inhibitory activity.

Introduction of weak activating substituent like alkyl group preferably methyl at *ortho*-position along with a weak deactivating substituent like halogen mainly chlorine preferably at *meta*-position on the phenyl ring as in compound QCC-16 exhibited moderate but markedly selective PDE4D inhibiton than PDE4B isoform. When a weak activating substituent like alkyl group preferably ethyl or isopropyl at *ortho*-position on the phenyl ring as in compound QCC-8 and QCC-10 showed moderate PDE4B inhibition and were non-selective.

Notably this indicates that the weak deactivating group like halogen especially chloro at *ortho*-position will be better favored in the pharmacophore for designing further novel selective PDE4D inhibitors.

In order to understand the nature of interactions of these molecules, rolipram and nitraquazone as standards within the active site of PDE4D and PDE4B, docking studies were carried out for all these compounds. The dockscore and other scores obtained after docking of these molecules into the PDE4D and PDE4B proteins are summarized in **Table 21** and **22** respectively.

Table 21: Docking results of QCC series for PDE4D (PDB: 1Q9M)

Compound	LigScore_1	LigScore_2	-PLP1	-PLP2	Jain	-PMF	-PMF04	Dockscore	Ludi_3	Consensus
QCC-1	3.21	5.38	88.91	80.73	2.43	164.09	78.28	59.52	839	4
QCC-2	3.39	5.73	79.10	74.82	2.46	169.65	85.12	74.97	722	4
QCC-3	4.69	6.44	90.71	85.42	2.21	206.30	114.05	74.89	928	9
QCC-4	2.67	5.27	81.04	72.38	1.70	157.10	71.03	70.52	773	1
QCC-5	3.40	5.57	67.35	66.97	3.49	163.09	73.04	69.76	749	1
QCC-6	2.68	5.39	74.37	75.02	1.72	155.17	59.45	70.50	712	0
QCC-7	2.44	5.30	69.32	66.80	0.98	131.13	43.53	70.22	666	0
QCC-8	3.01	5.45	74.61	71.39	2.61	167.74	71.07	67.34	738	3
QCC-9	3.42	5.66	67.08	65.10	3.93	158.86	76.64	71.21	681	3
QCC-10	3.20	5.77	72.95	66.75	0.59	144.46	71.52	68.62	609	1
QCC-11	3.11	5.65	71.58	68.82	2.48	161.17	70.26	69.98	732	1
QCC-12	2.49	5.17	65.09	59.62	1.98	152.68	64.11	64.47	704	2
QCC-13	3.18	5.87	77.52	77.21	1.97	165.86	93.09	73.96	746	3
QCC-14	2.62	5.14	66.05	63.88	3.56	152.40	72.38	68.76	736	1
QCC-15	3.54	5.79	83.08	84.83	2.64	157.38	56.85	75.54	793	5
QCC-16	3.15	5.63	64.28	62.14	0.98	144.12	73.08	70.46	651	1
QCC-17	2.66	5.32	70.74	67.13	2.15	159.18	71.68	68.97	623	1
QCC-18	3.22	5.92	77.66	79.11	1.88	163.21	90.15	74.60	737	4
QCC-19	3.99	5.80	84.34	83.09	4.90	159.25	77.61	70.97	718	6
Rolipram	3.82	4.54	48.46	48.38	2.78	118.37	64.25	46.866	456	1
Nitraquazone	4.24	4.73	52.53	50.68	1.71	158.56	94.33	56.384	701	3

Table 22: Docking results of QCC series for PDE4B (PDB: 1XMY)

Compound	LigScore_1	LigScore_2	-PLP1	-PLP2	Jain	-PMF	-PMF04	Dockscore	Ludi_3	Consensus
QCC-1	2.52	5.07	81.81	66.50	1.95	157.44	107.02	56.78	820	5
QCC-2	2.82	5.41	75.19	68.66	1.57	147.87	92.26	71.06	703	6
QCC-3	1.98	4.65	76.87	68.08	0.60	138.13	97.60	66.90	761	4
QCC-4	3.07	5.12	75.09	67.38	1.79	63.19	31.46	61.98	570	2
QCC-5	3.17	5.16	78.58	75.90	4.33	140.80	100.87	67.81	843	8
QCC-6	2.18	5.56	69.34	63.38	1.86	158.11	105.59	70.40	655	4
QCC-7	2.87	4.93	76.02	62.71	1.35	156.58	105.86	67.33	772	4
QCC-8	2.39	5.18	67.70	63.20	1.67	109.52	69.13	62.95	815	4
QCC-9	3.34	5.33	81.92	78.66	4.67	115.60	77.11	66.93	791	8
QCC-10	2.27	5.42	74.45	65.38	1.72	128.38	81.10	64.95	926	4
QCC-11	2.44	5.21	62.23	62.15	1.09	131.34	83.50	64.19	777	2
QCC-12	2.54	5.35	72.80	68.02	1.01	117.32	76.12	61.60	589	4
QCC-13	2.07	5.19	68.99	62.41	1.91	125.53	92.51	67.77	666	3
QCC-14	2.64	4.90	69.04	64.20	1.32	128.99	72.32	64.98	699	1
QCC-15	2.75	5.82	97.73	94.68	2.33	135.60	95.24	77.03	891	8
QCC-16	2.05	5.28	66.42	60.81	0.37	135.44	82.37	66.58	669	3
QCC-17	1.95	4.82	62.66	54.52	1.27	131.82	88.44	64.51	894	2
QCC18	2.15	5.13	65.79	59.96	0.61	111.32	72.40	68.79	710	2
QCC-19	2.01	4.95	69.09	61.00	0.52	104.68	76.70	64.37	690	1
Rolipram	2.23	4.39	54.3	46.79	2.51	141.03	107.36	45.193	608	2
Nitraquazone	1.78	4.61	68.64	51.8	1.44	139.65	96.4	57.033	708	0

The interaction of compound QCC-12 within the active site of PDE4D protein **(Fig. 53)** is mainly contributed by (i) H-bond between the keto group of the quinoxaline ring with His160 at a distance of 4.9 Á, (ii) a π-π stacking interaction between the centroid of the substituted benzyl ring and Phe340, (iii) three cationic-π interactions, two cationic-π interactions with His160, one between the centroid of the benzene ring of the quinoxaline scaffold and other with the centroid of the substituted benzyl ring, while the third one between the centroid of the benzene ring of the quinoxaline scaffold and His233. Whereas, the interaction of compound QCC-10 within the active site of PDE4D protein **(Fig. 54)** is mainly contributed by (i) π-π stacking interaction between the centroid of the substituted benzyl ring and Phe372, (ii) cationic-π interaction between His160 and the centroid of the benzene ring of the quinoxaline scaffold.

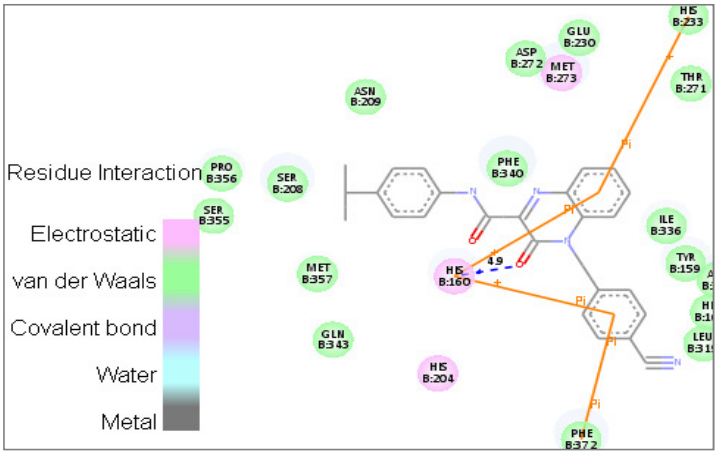

Fig. 53: QCC-12 at the active site of PDE4D

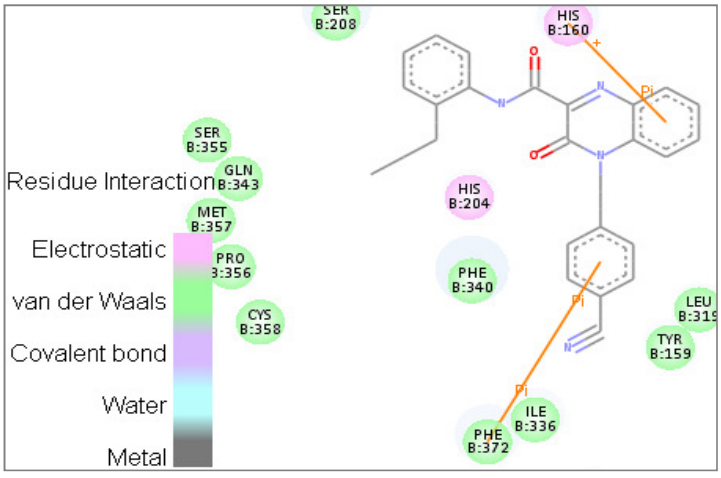

Fig. 54: QCC-10 at the active site of PDE4D

The interaction of compound QCC-2 within the active site of PDE4D protein **(Fig. 55)** is mainly contributed by (i) H-bond between the nitrile substitution on the benzyl ring with Glu369 at a distance of 5.4 Å, (ii) π-π stacking interaction between the centroid of the substituted benzyl ring and Phe372. Whereas, the interaction of compound QCC-11 within the active site of PDE4D protein **(Fig. 56)** is mainly contributed only by, (i) π-π stacking interaction between the centroid of the substituted benzyl ring and Phe372. Similarly, the interaction of compound QCC-5 within the active site of PDE4D protein **(Fig. 57)** is mainly contributed by, (i) two H-bonds, one between the keto group of the quinoxaline ring with His160 at a distance of 5.2 Å and other between the nitrile substitution on the benzyl ring with Glu369 at a distance of 5.5 Å, and (ii) π-π stacking interaction between the centroid of the substituted benzyl ring and Phe372. While, the interaction of compound QCC-3 within the active site of PDE4D protein **(Fig. 58)** is mainly contributed by, (i) two H-bonds, one between the keto group of the amide linker with His160 at a distance of 5.1 Å and other between the *para*-methoxy substituent on the phenyl ring on amide linker with His204 at a distance of 5.7 Å, and (ii) cationic-π interaction between His160 and the centroid of the phenyl ring on amide linker.

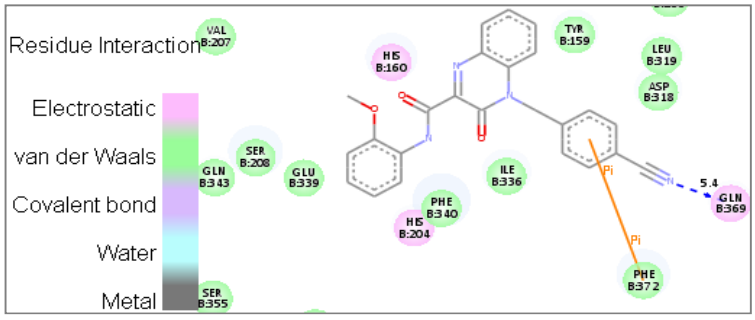

Fig. 55: QCC-2 at the active site of PDE4D

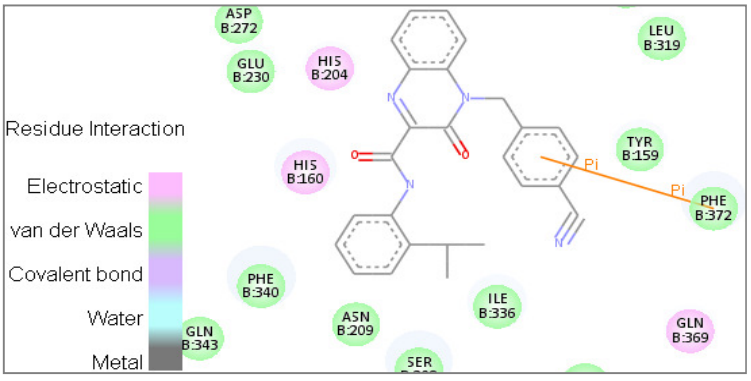

Fig. 56: QCC-11 at the active site of PDE4D

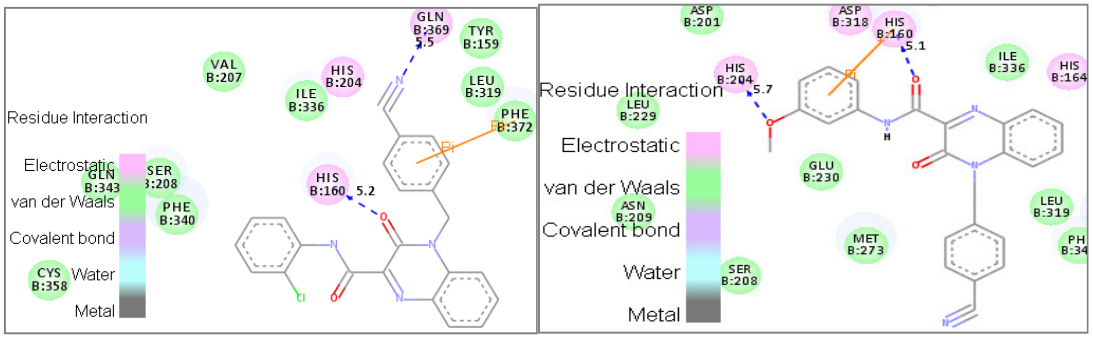

Fig. 57 and 58: QCC-5 and QCC-3 at the active site of PDE4D

The interaction of compound QCC-1 within the active site of PDE4D protein **(Fig. 59)** is mainly contributed by (i) H-bond between *N1* of the quinoxaline ring with His204 at a distance of 5.8 Á, (ii) four cationic-π interactions, two between the centroid of the benzene ring of the quinoxaline scaffold with His160 and His200, while the other two between His160 with the centroid of the pyrazine ring of the quinoxaline scaffold, and between the substituted benzyl ring. While, the compound QCC-1 did not show any interaction within the active site of PDE4B protein **(Fig. 60)**, whereas the interaction of compound QCC-16 within the active site of PDE4D protein **(Fig. 61)** is mainly contributed by (i) H-bond between the keto group of the quinoxaline ring with His160 at a distance of 5.2 Á, (ii) two π-π stacking interactions, one between the centroid of the phenyl ring on the amide linker with Phe340 while, another with the centroid of the benzyl ring and Phe372, (iii) cationic-π interaction between His160 and the centroid of the benzene ring of the quinoxaline scaffold. While the interaction of compound QCC-8 within the active site of PDE4B protein **(Fig. 62)** is mainly contributed by (i) π-π stacking interaction between the centroid of the substituted benzyl ring and Phe446.

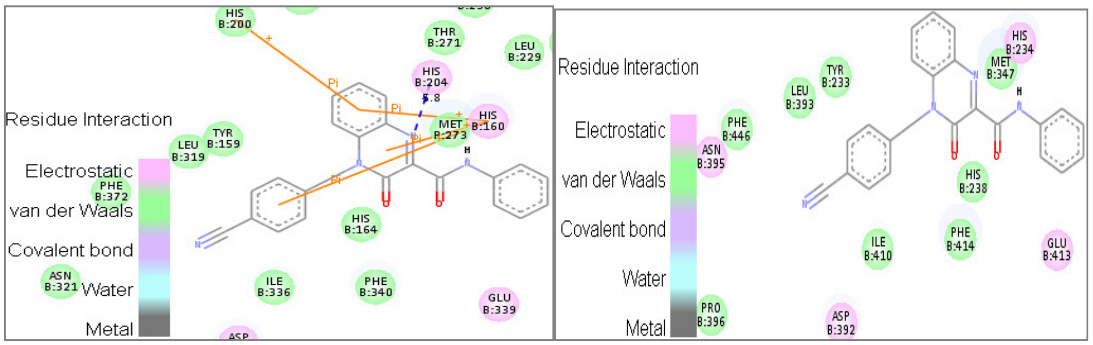

Fig. 59 and 60: QCC-1 at the active site of PDE4D and PDE4B

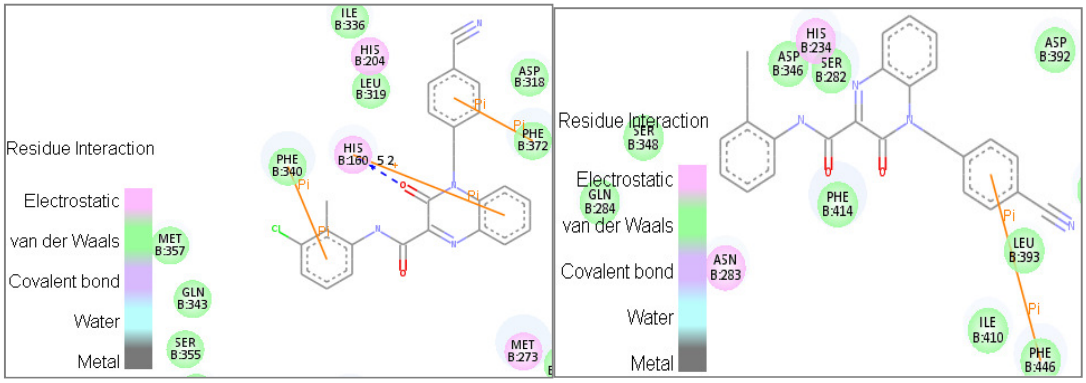

Fig. 61 and 62: QCC-16 at the active site of PDE4D and QCC-8 at PDE4B

Overall, the present 4-(4-nitrilebenzyl)-3-oxo-quinoxaline-2-carboxamide analogues displayed better interactions with PDE4D enzyme exhibiting their inhibitory activity. This indicates that the pharmacophoric elements like the central quinoxaline ring with a keto group which acts as a hydrogen bond acceptor (HBA), the benzyl moiety, diverse substituted phenyl ring and the amide linker played a substantial role in forming various interactions within the active site.

5.4.1. ADME properties

The analysis showed that the compounds of this series,when administered orally might show better intestinal absorption,as well as good blood–brain barrier (BBB) permeability, whereas for compounds containing polar group where, (n > 2) it could not compute the ability to cross the BBB. Their aqueous solubility and drug–likeness properties were envisaged to be low. In addition, these compounds are likely to inhibit enzyme such as CYP450 *2D6*. Most of these compounds are predicted to be non-hepatotoxic. It was also found that the inhibitor-plasma protein binding is not more than 90%, indicating that these compounds are likely to be less bound to plasma protein present in the blood. **(Table 23)**

Nevertheless, It is a familiar understanding that ADME profiles are complex to envisage accurately just by *in-silico* and so the envisaged profiles must be utilized with care. For our study, further testing ought to be done to investigate the actual profiles of these compounds as an extension of this work.

In the ADMET plot, since some of the molecule are inside and some outside the 99% confidence ellipse of BBB and HIA model, the prediction for those molecules inside are considered reliable, whereas for those molecules outside are considered unreliable and no BBB predictions are made for these ligands respectively. **(Fig. 63)**

Table 23: ADME properties of QCC Series

QCC	Aqueous solubility[a]		BBB[b]		CYP450 *2D6*[c]		Hepatotoxicity[d]		HIA[e]		PPB[g]		AlogP98[g]	
	Value	Level	Value	Level	Value	Level	Value	Level	Value	Level	Value	Level	Value	Level
1	-4.743	2	-0.438	2	-5.605	1	-2.042	0	NV[f]	0	2.953	0	3.432	0
2	-4.724	2	-0.585	3	-6.540	1	-2.180	0	NV[f]	0	3.201	0	3.416	0
3	-4.702	2	-0.585	3	-7.780	1	-2.041	0	NV[f]	0	3.328	0	3.416	0
4	-4.679	2	-0.585	3	-7.780	1	-1.335	0	NV[f]	0	0.718	0	3.416	0
5	-5.440	2	-0.233	2	-4.425	1	-2.230	0	NV[f]	0	4.861	0	4.097	0
6	-5.429	2	-0.233	2	-4.843	1	-0.359	0	NV[f]	0	6.090	0	4.097	0
7	-5.418	2	-0.233	2	-3.800	1	-1.558	0	NV[f]	0	6.027	0	4.097	0
8	-5.477	2	-0.147	2	-5.234	1	-5.357	1	NV[f]	0	3.749	0	4.375	0
9	-5.454	2	-0.147	2	-6.055	1	-3.085	0	NV[f]	0	3.666	0	4.375	0
10	-5.738	2	NV[f]	4	-5.345	1	-4.840	1	NV[f]	0	4.292	0	4.831	0
11	-5.714	2	NV[f]	4	-5.019	1	-3.741	0	NV[f]	0	3.061	0	4.626	0
12	-5.646	2	NV[f]	4	-5.217	1	-1.009	0	NV[f]	0	3.082	0	4.626	0
13	-5.873	2	NV[f]	4	-5.664	1	-1.998	0	NV[f]	0	5.378	0	4.583	0
14	-5.884	2	NV[f]	4	-5.671	1	-2.101	0	NV[f]	0	5.892	0	4.583	0
15	-5.896	2	NV[f]	4	-5.952	1	-1.599	0	NV[f]	0	5.302	0	4.583	0
16	-5.885	2	NV[f]	4	-5.095	1	-2.809	0	NV[f]	0	5.697	0	4.583	0
17	-4.341	2	-0.664	3	-4.850	1	-5.277	1	NV[f]	0	4.251	0	2.875	1
18	-5.873	2	NV[f]	4	-5.656	1	-1.985	0	NV[f]	0	7.335	0	4.583	0
19	-5.904	2	-0.147	2	-3.478	1	-6.964	1	NV[f]	0	3.717	0	4.374	0

[a] Level 2 means the aqueous solubility of inhibitor is not very good and its drug-likeness properties are low.
[b] Level 2 means inhibitor has medium ability, Level 3 means inhibitor has low ability and Level 4 means inhibitor has undefined ability to cross the blood-brain barrier (BBB).
[c] Level 1 means inhibitor likely to inhibit CYP*2D6* enzyme.
[d] Level 0 means inhibitor not likely to be hepatotoxic, while Level 1 means inhibitor are likely to be hepatotoxic.
[e] Level 0 means inhibitor has good human intestinal absorption (HIA) after oral administration.
[f] NV means no value was given.
[g] Level 0 means the binding between inhibitor and plasma protein (PPB) is less than 90% (AlogP98 < 5.0), while Level 1 means PPB more than 90% (Marker flagged).

ADMET PLOT

The ADMET plot is a 2D chart of ADMET_PSA_2D versus ADMET_AlogP98. The two sets of ellipses are for the prediction confidence space (95% and 99%) for the Blood Brain Barrier Penetration and Human Intestinal Absorption models, respectively.

Since the molecule is outside of the 99% BBB model confidence ellipse, the prediction is considered unreliable and no BBB prediction is made for this ligand.

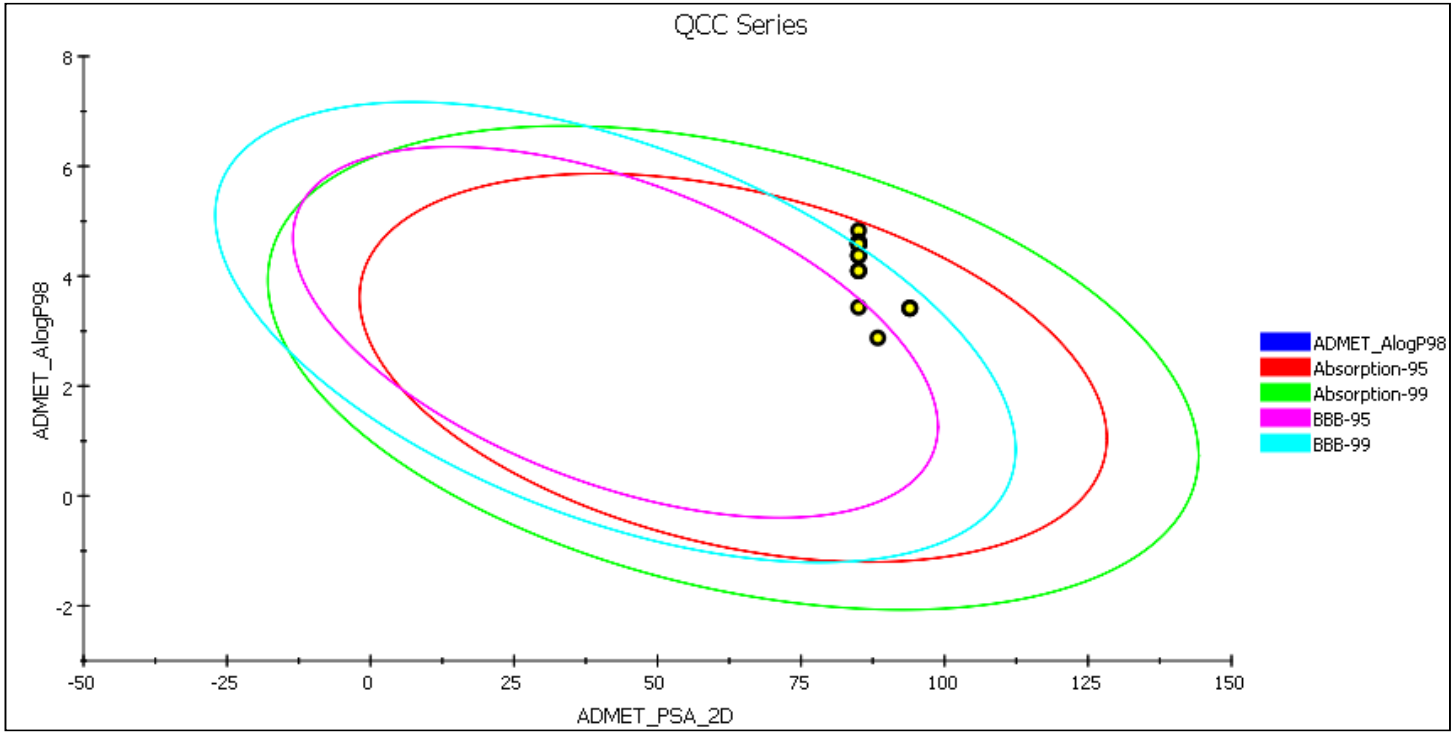

Fig. 63: ADMET Plot for QCC Series

5.5. Biological activities/Pharmacology for QCD Series

On the basis of encouraging results obtained from synthesized analogues bearing benzyl group (QCA series) and its substituted variants at *para*-positions (QCB and QCC series) at *N4* position of the quinoxaline scaffold, further modification was attempted to understand the significance of the methylene (-CH_2-) group of the benzyl moiety which was suitably replaced with the carbonyl (>C=O) group i.e., benzoyl moiety lead to 4-benzoyl-3-oxo-*N*-phenyl-3,4-dihydroquinoxaline-2-carboxamide analogues (QCD series). All these compounds were subjected for their inhibitory properties through *in-vitro* studies at 10 µM using PDE4B or PDE4D enzyme assay using rolipram as a reference standard.

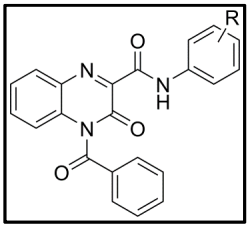

In this series, compound QCD-3, QCD-4, and QCD-16 showed pronounced inhibitory activity whereas compound QCD-5, QCD-8 and QCD-15 exhibited moderate inhibitory activity for PDE4D enzyme, while rest of the tested compounds exhibited poor inhibition. Except compound QCD-16 which displayed a very less moderate activity for PDE4B enzyme, rest all the compounds displayed poor inhibitory activity. **(Table 24)**

Compound QCD-16 showed better PDE4D enzyme inhibitory activity and has similar affinity for PDE4B isoform indicating that these compounds are non-selective. However, compounds QCD-3, QCC-4, QCD-5, QCD-8 and QCD-15 were relatively 2-fold more active against PDE4D as compared to PDE4B for its inhibitory activity. **(Table 24)**

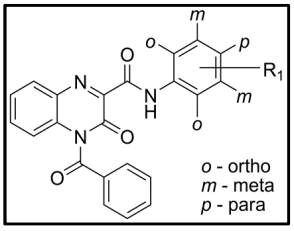

The SAR of these synthesized compounds indicates that substitution at *ortho*- or *para*-position on the phenyl ring was more favored for PDE4D inhibitory activity as marked by compounds QCD-3, QCD-4, QCD-8, QCD-15 and QCD-16. Similarly for PDE4B enzyme, substitution at *ortho*-position on the phenyl ring was favored which displayed moderate PDE4B inhibitory activity as marked from compound QCD-16.

Introduction of a weak activating substituent like alkyl group preferably methyl along with or without a weak deactivating substituent like halogen mainly chlorine at *ortho*-position on the phenyl ring as in compound QCD-8 and QCD-16 exhibited better PDE4D inhibition but were relatively non-selective among PDE4B and PDE4D isoform. Similarly, weak activating or deactivating group like alkyl especially methyl or halogen like chlorine at *para*-position on the phenyl ring is better tolerated as in compound QCD-3 and QCD-4 which retained better PDE4D inhibition and displayed weak PDE4B inhibition.

Interestingly, in compound QCD-5 strong activating group like methoxy was introduced at *meta*-position which moderately restored the activity. Whereas, when a weak deactivating substituent like halogen preferably chlorine at *ortho*-position along with a weak activating substituent like alkyl group mainly methyl at *meta*-position on the phenyl ring as in compound QCD-15 retain its moderate PDE4D inhibitory activity and was equipotent for PDE4B isoform.

Table 24: In-vitro data of QCD series

Compound	R	PDE4B[a]	SD	PDE4D[a]	SD	Selectivity[b]
QCD-1	Phenyl	46.15	0.55	32.88	0.10	-
QCD-2	4-methoxyphenyl	39.17	1.21	39.40	1.16	-
QCD-3	4-methylphenyl	30.97	1.23	59.65	1.20	1.9
QCD-4	4-chlorophenyl	38.59	0.92	60.59	0.66	1.6
QCD-5	3-methoxyphenyl	41.34	1.20	52.79	2.72	1.9
QCD-6	3-methylphenyl	27.49	1.53	43.92	3.12	-
QCD-7	3-chlorophenyl	24.77	0.64	47.77	2.44	-
QCD-8	2-methylphenyl	28.92	2.15	55.19	1.35	1.9
QCD-9	2-chlorophenyl	19.98	1.40	34.07	1.62	-
QCD-10	2-methoxyphenyl	22.24	1.72	28.26	0.88	-
QCD-11	2-propylphenyl	24.44	0.90	42.80	0.76	-
QCD-12	2-isopropylphenyl	30.82	1.48	46.01	1.44	-
QCD-13	4-isopropylphenyl	16.50	1.43	35.56	1.74	-
QCD-14	2-chloro-4-methylphenyl	17.69	0.12	28.53	0.29	-
QCD-15	2-chloro-5-methylphenyl	31.53	0.54	53.67	1.63	1.7
QCD-16	2-chloro-6-methylphenyl	51.96	0.33	64.77	2.12	1.3
QCD-17	3-chloro-2-methylphenyl	26.73	1.32	37.76	1.97	-
QCD-18	2-trifluoromethylphenyl	21.54	0.86	32.48	0.86	-
Rolipram		90.27	0.22	96.54	0.14	1.1

[a] Average percentage inhibition – Values that are the mean of two or more experiments are shown with their standard deviations (SD)
[b] Ratio of PDE4D/PDE4B

In order to understand the nature of interactions of these molecules, rolipram and nitraquazone as standards within the active site of PDE4D and PDE4B, docking studies were carried out for all these compounds. The dockscore and other scores obtained after docking of these molecules into the PDE4D and PDE4B proteins are summarized in **Table 25** and **26** respectively.

Table 25: Docking results of QCD series for PDE4D (PDB: 1Q9M)

Compound	LigScore_1	LigScore_2	-PLP1	-PLP2	Jain	-PMF	-PMF04	Dockscore	Ludi_3	Consensus
QCD-1	2.63	4.93	79.75	80.33	2.56	162.52	83.32	58.94	896	2
QCD-2	2.71	5.46	71.80	68.88	2.32	117.10	76.61	60.47	639	4
QCD-3	2.24	4.86	73.46	75.39	3.35	112.93	64.90	58.98	684	0
QCD-4	2.25	4.99	72.27	76.03	3.12	98.80	58.50	58.19	682	0
QCD-5	3.13	4.93	79.93	80.32	4.47	136.56	95.02	63.01	934	7
QCD-6	2.22	4.85	79.29	78.64	2.68	120.21	80.08	59.70	767	0
QCD-7	2.16	5.32	80.54	79.37	2.61	126.63	75.95	61.23	712	1
QCD-8	2.57	5.14	83.23	82.33	2.80	166.33	85.94	61.55	878	5
QCD-9	2.63	5.05	83.02	85.43	2.86	155.24	87.68	62.62	897	5
QCD-10	2.81	4.92	71.70	72.48	4.19	133.38	89.55	66.64	749	5
QCD-11	2.25	5.24	81.52	80.35	2.58	131.15	80.12	66.13	714	2
QCD-12	2.31	5.15	76.95	78.70	2.08	124.40	73.15	63.18	768	2
QCD-13	2.42	4.58	79.89	83.16	4.44	122.57	69.22	57.79	735	4
QCD-14	2.11	5.44	81.57	82.10	1.73	90.58	70.64	60.36	582	2
QCD-15	2.43	4.97	81.69	81.55	3.53	120.40	81.27	62.87	832	3
QCD-16	2.22	5.05	78.76	78.74	2.97	136.16	80.31	64.47	735	3
QCD-17	3.31	5.57	76.71	72.73	3.68	130.51	75.43	62.86	713	4
QCD-18	2.64	5.13	85.25	85.76	2.96	176.08	100.84	62.97	860	9
Rolipram	3.82	4.54	48.46	48.38	2.78	118.37	64.25	46.866	456	1
Nitraquazone	4.24	4.73	52.53	50.68	1.71	158.56	94.33	56.384	701	3

Table 26: Docking results of QCD series for PDE4B (PDB: 1XMY)

Compound	LigScore_1	LigScore_2	-PLP1	-PLP2	Jain	-PMF	-PMF04	Dockscore	Ludi_3	Consensus
QCD-1	3.15	5.16	72.28	59.04	3.01	138.42	92.45	64.01	797	3
QCD-2	3.10	5.15	77.75	64.03	3.27	137.06	91.56	65.48	742	4
QCD-3	2.71	5.03	70.65	58.48	1.59	125.31	81.98	61.21	632	0
QCD-4	3.18	5.09	75.66	63.27	3.51	138.68	86.79	65.89	765	4
QCD-5	3.16	5.17	77.87	65.41	3.36	132.35	89.93	66.48	751	5
QCD-6	3.03	5.21	77.41	65.26	2.30	137.71	92.69	64.57	749	5
QCD-7	3.12	5.16	75.91	64.21	2.63	137.25	86.18	65.90	738	2
QCD-8	3.14	5.26	80.40	67.68	2.99	130.49	88.78	64.61	769	3
QCD-9	3.10	5.21	78.39	66.28	3.39	131.82	85.97	66.16	765	5
QCD-10	3.49	5.47	77.82	64.20	3.00	134.34	94.87	65.36	740	7
QCD-11	3.53	5.53	79.25	65.50	3.61	133.00	91.84	70.08	737	8
QCD-12	2.94	5.19	74.70	61.74	1.50	123.67	80.71	64.25	687	1
QCD-13	3.18	5.30	75.11	62.64	2.80	135.46	89.70	58.77	737	2
QCD-14	3.12	5.47	66.95	56.68	2.70	137.18	81.84	62.94	742	1
QCD-15	3.30	5.28	81.41	68.41	3.19	133.94	83.43	65.36	753	5
QCD-16	3.10	5.20	69.46	59.08	3.16	133.39	93.35	65.72	757	4
QCD-17	1.82	4.69	71.61	66.72	2.30	80.49	63.65	58.82	573	2
QCD-18	3.17	5.30	76.62	62.50	2.09	124.71	91.75	63.39	722	2
Rolipram	2.23	4.39	54.3	46.79	2.51	141.03	107.36	45.193	608	2
Nitraquazone	1.78	4.61	68.64	51.8	1.44	139.65	96.4	57.033	708	0

The interaction of compound QCD-16 within the active site of PDE4D protein **(Fig. 64)** is mainly contributed by (i) two π-π stacking interactions with Phe372, one between the centroid of the benzene ring and other with the pyrazine ring of the quinoxaline scaffold, (ii) cationic-π interaction between the centroid of the phenyl ring on the amide linker with His160. Whereas, the interaction within the active site of PDE4B protein **(Fig. 65)** is mainly contributed by (i) H-bond between the keto group of the amide linker with Asn283 at a distance of 3.6 Å.

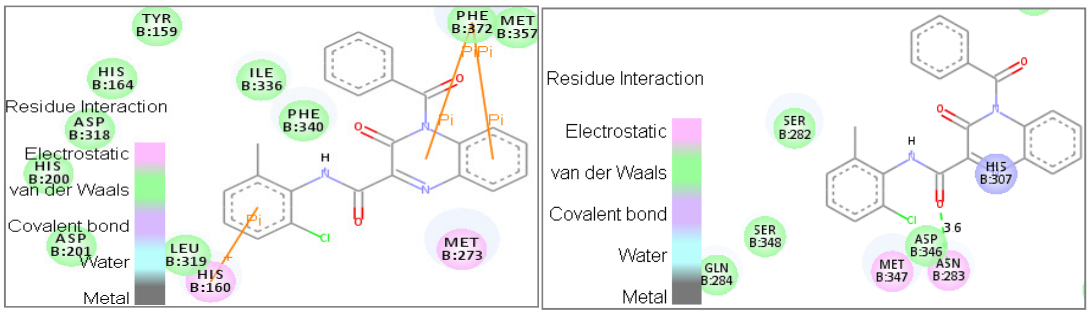

Fig. 64 and 65: QCD-16 at the active site of PDE4D and PDE4B

The interaction of compound QCD-4 within the active site of PDE4D protein **(Fig. 66)** is mainly contributed by (i) two π-π stacking interactions with Phe372, one between the centroid of the benzene ring and other with the pyrazine ring of the quinoxaline scaffold, (ii) cationic-π interaction between the centroid of the phenyl ring on the amide linker with His160. Whereas, the interaction of compound QCD-3 within the active site of PDE4D protein **(Fig. 67)** is mainly contributed by (i) two π-π stacking interactions with Phe372, one between the centroid of the benzene ring and other with the pyrazine ring of the quinoxaline scaffold, (ii) cationic-π interaction between the centroid of the phenyl ring on the amide linker with His160.

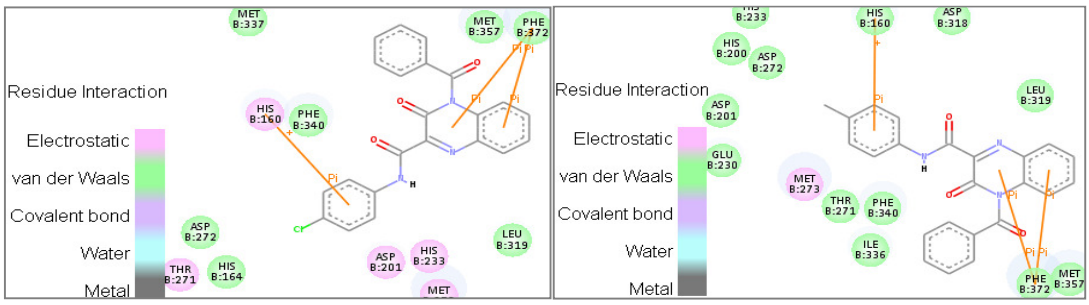

Fig. 66 and 67: QCD-4 and QCD-3 at the active site of PDE4D

The interaction of compound QCD-8 within the active site of PDE4D protein **(Fig. 68)** is mainly contributed by (i) H-bond between the *N1* of the quinoxaline ring with His160 at a distance of 5.8Å, (ii) π-π stacking interaction between the centroid of the phenyl ring on the amide linker with Phe372, (iii) two cationic-π interactions with His160, one

between the centroid of the benzene ring and other with the pyrazine ring of the quinoxaline scaffold. Whereas, the interaction of compound QCD-15 within the active site of PDE4D protein **(Fig. 69)** is mainly contributed by (i) two π-π stacking interactions with Phe372, one between the centroid of the benzene ring and other with the pyrazine ring of the quinoxaline scaffold, (ii) cationic-π interaction between the centroid of the phenyl ring on the amide linker with His160. Similarly, the interaction of compound QCD-5 within the active site of PDE4D protein **(Fig. 70)** is mainly contributed by (i) H-bond between the 2-OCH_3 substituent on the phenyl ring with His204 at a distance of 5.5Å, (ii) two π-π stacking interactions with Phe372, one between the centroid of the benzene ring and other with the pyrazine ring of the quinoxaline scaffold, (iii) cationic-π interaction between the centroid of the phenyl ring on the amide linker with His160.

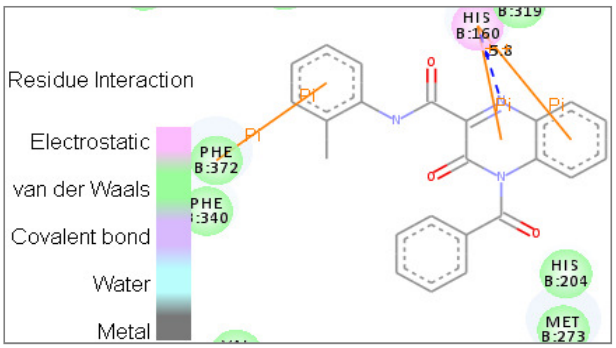

Fig. 68: QCD-8 at the active site of PDE4D

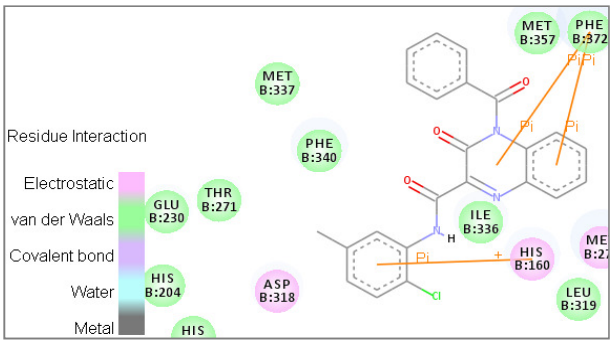

Fig. 69: QCD-15 at the active site of PDE4D

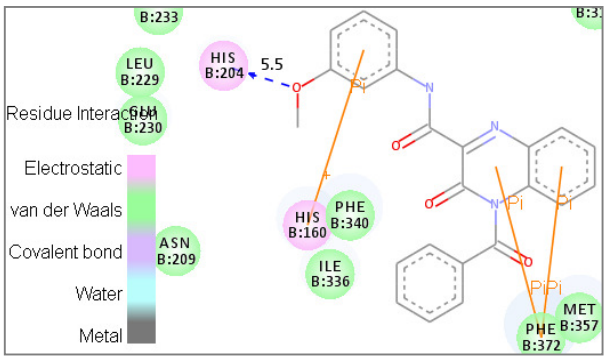

Fig. 70: QCD-5 at the active site of PDE4D

Overall, the present 4-benzoyl-3-oxo-quinoxaline-2-carboxamide analogues displayed better interactions with PDE4D enzyme exhibiting their inhibitory activity. This indicates that the pharmacophoric elements like the central quinoxaline ring with a keto group which acts as a hydrogen bond acceptor (HBA), diverse substituted phenyl ring and the amide linker played a substantial role in forming various interactions within the active site. Interestingly, it is observed that the benzoyl group did not form any interactions with the active site of both the PDE4B/D enzyme. This could the possibly reason for its lesser activity than its counterpart the QCA series.

5.5.1. ADME properties

The analysis showed that the compounds of this series,when administered orally might show better intestinal absorption, as well as good blood–brain barrier (BBB) permeability, whereas for compounds containing polar group where, (n > 2) it could not compute the ability to cross the BBB. Their aqueous solubility and drug–likeness properties were envisaged to be very low. In addition, these compounds are likely to inhibit enzyme such as CYP450 *2D6*. Most of these compounds are predicted to be non-hepatotoxic. It was also found that the inhibitor-plasma protein binding is not more than 90%, indicating that these compounds are likely to be less bound to plasma protein present in the blood. **(Table 27)**

Nevertheless, It is a common understanding that ADME profiles are complex to envisage accurately just by *in-silico* and so the envisaged profiles must be utilized with care. For our study, further testing ought to be done to investigate the actual profiles of these compounds as an extension of this work.

In the ADMET plot, since some of the molecule are inside and some outside the 99% confidence ellipse of BBB and HIA model, the prediction for those molecules inside are considered reliable, whereas for those molecules outside are considered unreliable and no BBB predictions are made for these ligands respectively. **(Fig. 71)**

Table 27: ADME properties of QCD Series

QCD	Aqueous solubility[a]		BBB[b]		CYP450 *2D6*[c]		Hepatotoxicity[d]		HIA[e]		PPB[g]		AlogP98[g]	
	Value	Level	Value	Level	Value	Level	Value	Level	Value	Level	Value	Level	Value	Level
1	-5.434	2	-0.162	2	-5.523	1	-0.242	0	NV[f]	0	3.326	0	4.038	0
2	-5.39	2	-0.308	2	-8.456	1	-1.003	0	NV[f]	0	1.552	0	4.022	0
3	-5.878	2	-0.012	2	-5.871	1	-2.963	0	NV[f]	0	4.677	0	4.524	0
4	-6.118	1	0.043	1	-4.264	1	-0.409	0	NV[f]	0	6.555	0	4.703	0
5	-5.412	2	-0.308	2	-8.456	1	-1.709	0	NV[f]	0	4.162	0	4.022	0
6	-5.889	2	-0.012	2	-5.871	1	-2.200	0	NV[f]	0	5.087	0	4.524	0
7	-6.129	1	0.043	1	-5.307	1	0.791	0	NV[f]	0	6.618	0	4.703	0
8	-5.900	2	-0.012	2	-6.935	1	-3.623	0	NV[f]	0	3.889	0	4.524	0
9	-6.140	1	0.043	1	-4.889	1	-1.080	0	NV[f]	0	5.389	0	4.703	0
10	-5.433	2	-0.308	2	-7.216	1	-1.848	0	NV[f]	0	4.035	0	4.022	0
11	-6.457	1	NV[f]	4	-5.349	1	-4.536	1	NV[f]	1	5.141	0	5.437	0
12	-6.432	1	NV[f]	4	-5.194	1	-4.014	0	NV[f]	1	4.355	0	5.232	0
13	-6.367	1	NV[f]	4	-5.391	1	-1.282	0	NV[f]	1	4.376	0	5.232	0
14	-6.583	1	NV[f]	4	-5.539	1	-1.830	0	NV[f]	0	6.097	0	5.189	0
15	-6.593	1	NV[f]	4	-5.547	1	-1.934	0	NV[f]	0	6.611	0	5.189	0
16	-6.604	1	NV[f]	4	-5.827	1	-1.431	0	NV[f]	0	6.021	0	5.189	0
17	-6.594	1	NV[f]	4	-5.272	1	-2.222	0	NV[f]	0	6.288	0	5.189	0
18	-6.632	1	NV[f]	4	-3.652	1	-7.322	1	NV[f]	0	5.165	0	4.980	0

[a] Level 2 means the aqueous solubility of inhibitor is not very good and its drug-likeness properties are low, while Level 1 means the aqueous solubility of inhibitor is very poor.
[b] Level 2 means inhibitor has medium ability, Level 1 means inhibitor has high ability and Level 4 means inhibitor has undefined ability to cross the blood-brain barrier (BBB).
[c] Level 1 means inhibitor likely to inhibit CYP*2D6* enzyme.
[d] Level 0 means inhibitor not likely to be hepatotoxic, while Level 1 means inhibitor are likely to be hepatotoxic.
[e] Level 0 means inhibitor has good, while Level 1 means inhibitor has moderate human intestinal absorption (HIA) after oral administration.
[f] NV means no value was given.
[g] Level 0 means the binding between inhibitor and plasma protein (PPB) is less than 90% (No markers flagged and AlogP98 < 5.0).

ADMET PLOT

The ADMET plot is a 2D chart of ADMET_PSA_2D versus ADMET_AlogP98. The two sets of ellipses are for the prediction confidence space (95% and 99%) for the Blood Brain Barrier Penetration and Human Intestinal Absorption models, respectively.

Since the molecule is outside of the 99% BBB model confidence ellipse, the prediction is considered unreliable and no BBB prediction is made for this ligand.

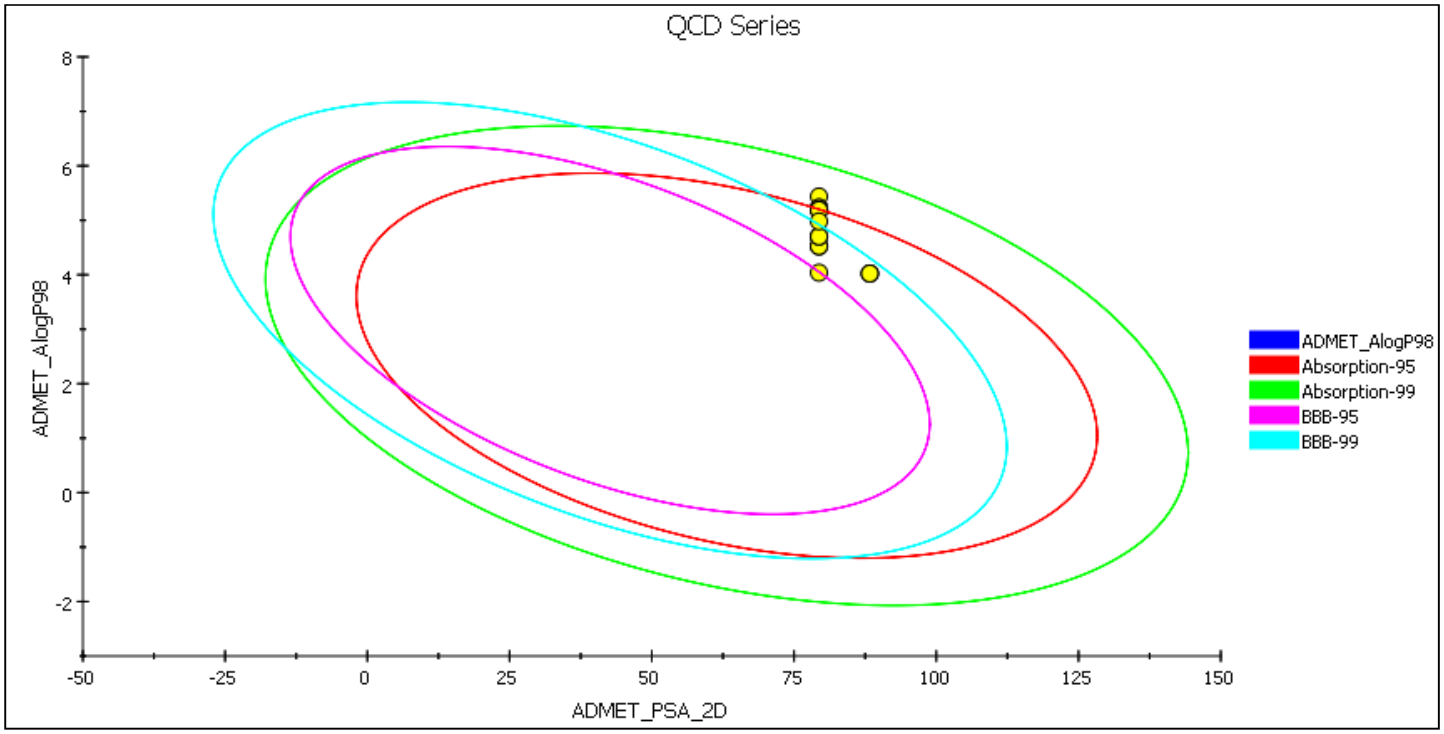

Fig. 71: ADMET Plot for QCD Series

5.6. Biological activities/Pharmacology for QCE Series

On the basis of encouraging results obtained from synthesized analogues bearing benzyl group (QCA series) and benzoyl group (QCD series) at *N4* position of the quinoxaline scaffold, further modification was attempted to understand the significance of both these functional group i.e., the methylene (-CH_2-) and carbonyl (>C=O) group in the pharmacophore by introducing phenacyl group lead to series of 3-oxo-*N*-phenyl-4-(2-phenylacetyl)-3,4-dihydroquinoxaline-2-carboxamide analogues (QCE series). All these compounds were subjected for their inhibitory properties through *in-vitro* studies at 10 µM using PDE4B or PDE4D enzyme assay using rolipram as a reference compound.

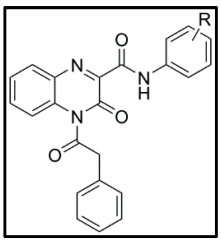

In this series, most of the compounds QCE-5, QCE-6, QCE-7, QCE-8, QCE-10, QCE-11, QCE-12, QCE-13 and QCE-18 were highly active which showed very pronounced inhibitory activity whereas, compounds QCE-1, QCE-2, QCE-9 and QCE-14 displayed moderate inhibitory activity for PDE4D enzyme. For PDE4B enzyme, compounds QCE-5, QCE-6 and QCE-7 showed moderate inhibitory activity, while rest of the tested compounds displayed poor inhibitory activity. **(Table 28)**

Compound QCE-5 is the most active compound in this series, while compounds QCE-7, QCE-6, QCE-13, QCE-8, QCE-18, QCE-10, QCE-12 and QCE-11 showed prominent PDE4D enzyme inhibitory activity and has similar affinity for PDE4B isoform indicating that these compounds are non-selective. **(Table 28)**

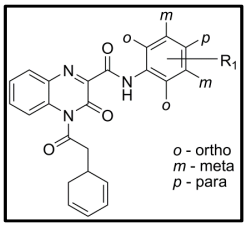

The SAR of these synthesized compounds indicates that substitution at *ortho*- or *para*-position on the phenyl ring was more favored for PDE4D inhibitory activity as evident from compounds QCE-1, QCE-2, QCE-5, QCE-6, QCE-7, QCE-8, QCE-9, QCE-10, QCE-11, QCE-12, QCE-13, QCE-14 and QCE-18. Similarly for PDE4B enzyme, substitution at *ortho*- or *para*-position on the phenyl ring was favored which displayed better to moderate inhibitory activity as marked from compounds 1-QCE, 5-QCE, 6-QCE, 7-QCE, 8-QCE, 10-QCE and 13-QCE.

The initial compound QCE-1 showed moderate PDE4D inhibitory activity and was equipotent for its PDE4B isoform. Introduction of a weak activating substituent like alkyl group preferably propyl or isopropyl at *ortho*-position or methyl at *ortho*-, *meta*- or *para*-position on the phenyl ring as in compounds QCE-5, QCE-6, QCE-7, QCE-11, QCE-12, QCE-14 and QCE-18 exhibited better PDE4D inhibition and was equally active for its PDE4B isoform. Whereas alkyl group like isopropyl at *para*-positions as in compound QCE-13 was also well tolerated and displayed better activity for both isoform.

Weak deactivating substituent like halogen group preferably chlorine at *ortho*-position or *para*-position as in compounds QCE-8, QCE-10, QCE-14 and QCE-18 and at

meta-position as in compound QCE-9 displayed equal activity for both PDE4D and PDE4B isoform. Interestingly, when strong activating group like methoxy was introduced at *ortho*-position as in compound QCE-2 retained the activity for both isoform. The results indicate that most of these compounds has similar affinity for both isoform and are non-selective.

Table 28: In-vitro data of QCE series

Compound	R	PDE4B[a]	SD	PDE4D[a]	SD	Selectivity[b]
QCE-1	phenyl	62.45	1.16	72.84	1.82	1.2
QCE-2	2-methoxyphenyl	55.96	1.09	76.10	1.17	1.4
QCE-3	3-methoxyphenyl	48.10	1.21	52.50	1.42	-
QCE-4	4-methoxyphenyl	50.13	0.94	63.15	1.22	-
QCE-5	2-methylphenyl	68.23	0.57	88.91	2.14	1.3
QCE-6	3-methylphenyl	69.15	0.74	86.83	1.95	1.3
QCE-7	4-methylphenyl	67.99	0.06	87.40	1.84	1.3
QCE-8	2-chlorophenyl	64.40	0.12	81.86	1.77	1.3
QCE-9	3-chlorophenyl	59.68	1.60	77.97	2.21	1.3
QCE-10	4-chlorophenyl	60.33	2.15	80.53	2.56	1.3
QCE-11	2-propylphenyl	57.26	2.06	79.97	2.82	1.4
QCE-12	2-isopropylphenyl	57.77	0.44	80.13	0.83	1.4
QCE-13	4-isopropylphenyl	62.86	3.22	83.47	2.52	1.3
QCE-14	2-chloro-4-methylphenyl	51.09	0.63	69.62	1.99	1.4
QCE-15	2-chloro-5-methylphenyl	44.90	1.88	55.57	1.55	-
QCE-16	2-chloro-6-methylphenyl	3.81	2.26	19.98	0.09	-
QCE-17	3-chloro-2-methylphenyl	48.57	1.83	43.49	1.32	-
QCE-18	4-chloro-2-methylphenyl	58.27	1.77	81.38	1.88	1.4
QCE-19	2-trifluoromethylphenyl	20.40	1.32	42.64	0.94	-
Rolipram		90.27	0.22	96.54	0.14	1.1

[a] Average percentage inhibition – Values that are the mean of two or more experiments are shown with their standard deviations (SD)
[b] Ratio of PDE4D/PDE4B

In order to understand the nature of interactions of these molecules, within the active site of PDE4D and PDE4B, docking studies were carried out for all these compounds. The dockscore and other scores obtained after docking of these molecules into the PDE4D and PDE4B proteins are summarized in **Table 29** and **30** respectively.

Table 29: Docking results of QCE series for PDE4D (PDB: 1Q9M)

Compound	LigScore_1	LigScore_2	-PLP1	-PLP2	Jain	-PMF	-PMF04	Dockscore	Ludi_3	Consensus
QCE-1	2.11	4.85	73.21	73.73	3.02	131.52	77.71	57.00	767	1
QCE-2	2.68	5.18	94.97	92.37	3.58	128.85	74.28	56.67	740	5
QCE-3	3.12	5.33	92.99	91.07	2.79	131.10	72.14	63.97	771	6
QCE-4	2.56	5.18	90.55	86.88	1.67	89.87	54.33	58.42	574	4
QCE-5	2.17	5.02	84.55	82.93	1.93	95.10	58.24	57.05	585	0
QCE-6	3.06	5.48	85.09	83.29	2.65	146.47	77.36	63.73	764	4
QCE-7	2.65	4.73	88.33	85.57	3.01	146.28	76.02	58.14	749	2
QCE-8	2.25	5.15	80.61	82.57	2.25	79.25	49.72	59.17	579	1
QCE-9	3.00	5.55	88.26	87.21	3.44	136.06	73.16	63.45	722	6
QCE-10	2.89	5.06	85.74	87.91	3.52	145.86	79.58	59.03	781	5
QCE-11	2.25	5.08	86.43	85.45	2.52	102.52	59.89	63.00	601	3
QCE-12	2.87	5.41	89.21	85.52	3.34	155.95	86.98	62.21	710	8
QCE-13	2.14	4.47	86.11	86.03	4.08	87.04	47.81	51.20	648	4
QCE-14	2.03	4.57	85.61	84.12	2.46	78.94	58.11	58.73	587	1
QCE-15	2.82	5.12	91.55	90.00	3.01	126.28	76.26	63.66	783	4
QCE-16	2.71	5.43	85.08	84.13	2.45	115.54	74.46	60.76	638	3
QCE-17	3.30	5.90	80.03	80.31	2.69	150.29	76.23	64.55	754	6
QCE-18	3.14	5.80	68.33	71.79	1.05	137.58	84.03	58.63	589	5
QCE-19	2.40	5.04	92.78	87.27	2.11	120.13	77.12	56.96	596	3
Rolipram	3.82	4.54	48.46	48.38	2.78	118.37	64.25	46.866	456	1
Nitraquazone	4.24	4.73	52.53	50.68	1.71	158.56	94.33	56.384	701	3

Table 30: Docking results of QCE series for PDE4B (PDB: 1XMY)

Compound	LigScore_1	LigScore_2	-PLP1	-PLP2	Jain	-PMF	-PMF04	Dockscore	Ludi_3	Consensus
QCE-1	3.50	4.57	73.51	65.38	2.68	85.49	62.11	55.22	808	4
QCE-2	2.63	5.25	70.15	60.87	1.79	133.21	93.61	56.64	616	4
QCE-3	1.74	4.38	60.31	55.23	1.80	116.64	76.14	54.70	533	1
QCE-4	1.81	4.79	61.32	60.43	-0.10	130.54	90.92	49.29	724	2
QCE-5	1.96	5.13	73.95	69.44	1.72	122.36	83.26	55.97	706	1
QCE-6	2.18	4.92	62.53	57.94	1.93	141.81	91.41	54.08	596	1
QCE-7	1.73	4.64	61.05	62.85	0.04	142.65	97.42	52.40	701	2
QCE-8	2.60	5.30	89.91	87.39	3.29	52.45	36.86	57.47	608	6
QCE-9	2.35	5.11	84.41	81.22	2.66	38.96	22.50	55.79	624	5
QCE-10	1.86	4.97	70.17	62.95	1.18	133.63	86.06	53.08	582	1
QCE-11	2.14	4.86	63.41	60.09	2.29	127.69	87.51	58.87	600	3
QCE-12	2.23	5.24	69.21	64.53	1.57	120.34	79.74	61.62	597	3
QCE-13	2.64	4.30	55.18	52.06	0.89	84.96	50.08	26.93	551	2
QCE-14	2.10	5.29	81.59	77.99	0.99	117.76	81.01	58.50	667	4
QCE-15	2.15	4.88	66.22	60.59	1.96	130.01	91.63	56.25	554	1
QCE-16	2.00	4.79	63.87	64.41	1.17	138.56	94.31	55.09	717	3
QCE-17	2.07	5.08	86.51	88.34	4.03	79.66	52.27	57.22	663	5
QCE-18	2.06	5.41	81.07	78.09	1.41	126.54	88.52	53.83	726	4
QCE-19	3.22	5.59	82.18	67.56	2.39	138.74	102.49	58.67	663	9
Rolipram	2.23	4.39	54.3	46.79	2.51	141.03	107.36	45.193	608	2
Nitraquazone	1.78	4.61	68.64	51.8	1.44	139.65	96.4	57.033	708	0

The interaction of compound QCE-5 within the active site of PDE4D protein **(Fig. 72)** is mainly contributed by (i) π-π stacking interaction between the centroid of the phenyl ring on the amide linker and Phe372. Whereas, the interaction within the active site of PDE4B protein **(Fig. 73)** is mainly contributed by (i) H-bond between the *N1* of the quinoxaline ring with Asn283 at a distance of 4.3 Å, (ii) a π-π stacking interaction between the centroid of the phenacyl ring and Phe446.

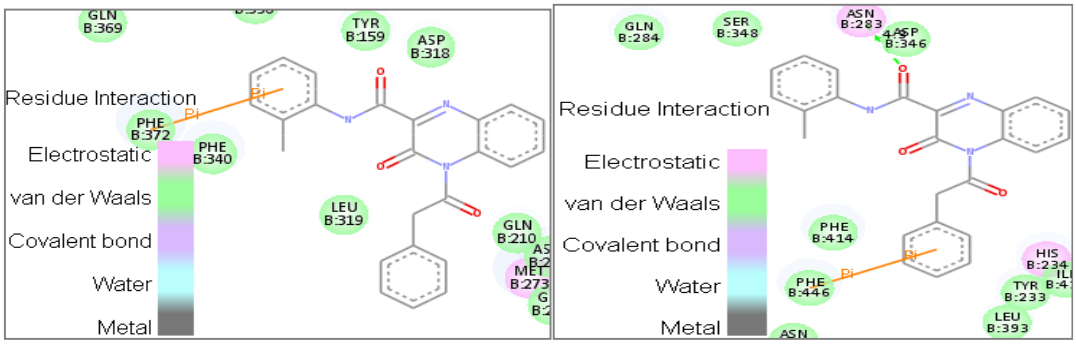

Fig. 72 and 73: QCE-5 at the active site of PDE4D and PDE4B

The interaction of compound QCE-7 within the active site of PDE4D protein **(Fig. 74)** is mainly contributed by (i) H-bond between the *N1* of the quinoxaline ring with His160 at a distance of 5.7 Å, (ii) two cationic-π interactions, one between His160 and the centroid of the pyrazine ring of the quinoxaline scaffold, while another between His233 and the centroid of the benzene ring of the quinoxaline scaffold. Whereas, the interaction within the active site of PDE4B protein **(Fig. 75)** is mainly contributed by (i) H-bond between the keto group of the amide linker with Asn283 at a distance of 3.0 Å, (ii) a π-π stacking interaction between the centroid of the phenacyl ring and Phe414.

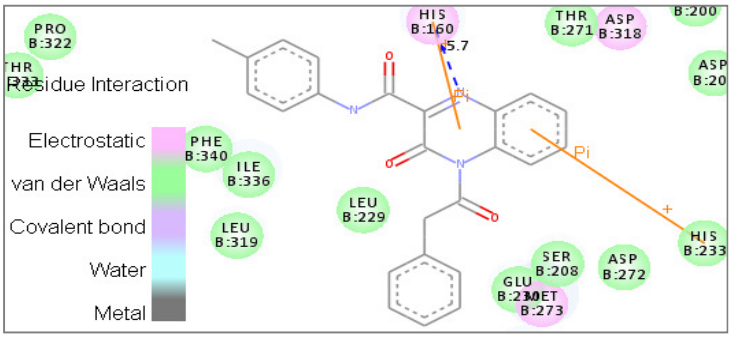

Fig. 74: QCE-7 at the active site of PDE4D

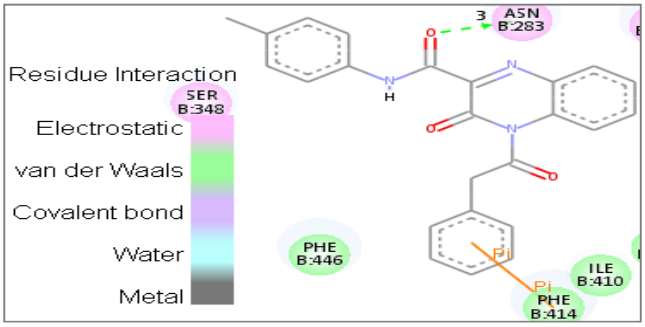

Fig. 75: QCE-7 at the active site of PDE4B

The interaction of compound QCE-6 within the active site of PDE4D protein **(Fig. 76)** is mainly contributed by (i) H-bond between the *N1* of the quinoxaline ring with His160 at a distance of 5.6 Á, (ii) π-π stacking interaction between the centroid of the phenyl ring on the amide linker and Phe372, (iii) cationic-π interaction between His233 and the centroid of the benzene ring of the quinoxaline scaffold. Whereas, the interaction within the active site of PDE4B protein **(Fig. 77)** is mainly contributed by (i) H-bond between the keto group of the amide linker with Asn283 at a distance of 3.9 Á, (ii) σ-π interaction between Asn283 and the centroid of the phenyl ring on the amide linker.

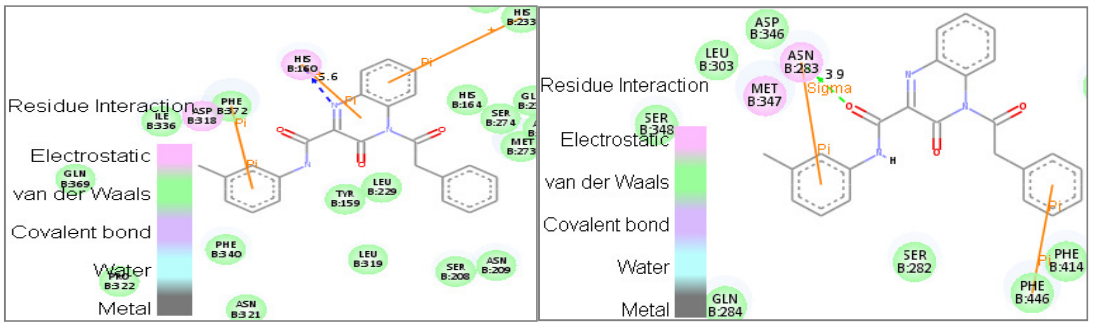

Fig. 76 and 77: QCE-6 at the active site of PDE4D and PDE4B

The interaction of compound QCE-13 within the active site of PDE4D protein **(Fig. 78)** is mainly contributed by (i) π-π stacking interaction between the centroid of the phenyl ring on the amide linker and Phe372, (ii) σ-π interaction between Asn209 and the centroid of the phenacyl ring, (iii) two cationic-π interactions, one between His160 and the centroid of the pyrazine ring of the quinoxaline scaffold, while another between His233 and the centroid of the benzene ring of the quinoxaline scaffold. While compound QCE-8 did not show any interaction within the active site of PDE4D protein **(Fig. 79)**.

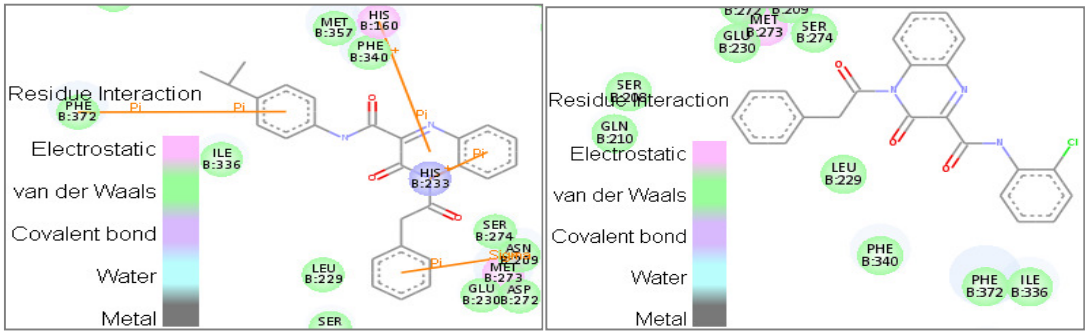

Fig. 78 and 79: QCE-13 and QCE-8 at the active site of PDE4D

The interaction of compound QCE-18 within the active site of PDE4D protein **(Fig. 80)** is mainly contributed by (i) H-bond between the *N1* of the quinoxaline ring with His160 at a distance of 5.7 Å, (ii) π-π stacking interaction between the centroid of the phenyl ring on the amide linker and Phe372. Whereas, the interaction of compound QCE-10 within the active site of PDE4D protein **(Fig. 81)** is mainly contributed by (i) H-bond between the *N1* of the quinoxaline ring with His160 at a distance of 5.7 Å, (ii) cationic-π interaction between His160 and the centroid of the pyrazine ring of the quinoxaline scaffold.

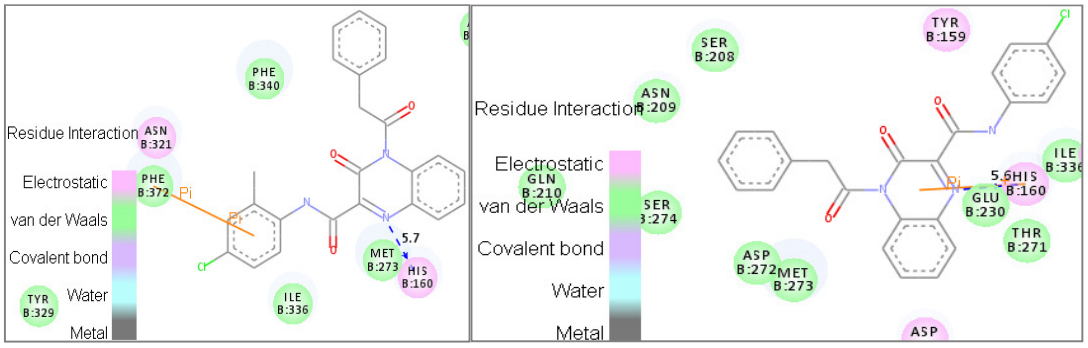

Fig. 80 and 81: QCE-18 and QCE-10 at the active site of PDE4D

The interaction of compound QCE-12 within the active site of PDE4D protein **(Fig. 82)** is mainly contributed by (i) H-bond between the *N1* of the quinoxaline ring with His160 at a distance of 5.7 Å, (ii) π-π stacking interaction between the centroid of the phenyl ring on the amide linker and Phe372, (iii) cationic-π interaction between His160 and the centroid of the pyrazine ring of the quinoxaline scaffold. Whereas, the interaction of compound QCE-11 within the active site of PDE4D protein **(Fig. 83)** is mainly contributed by (i) π-π stacking interaction between the centroid of the phenyl ring on the amide linker and Phe372, (ii) σ-π interaction between Asn209 and the centroid of the phenacyl ring.

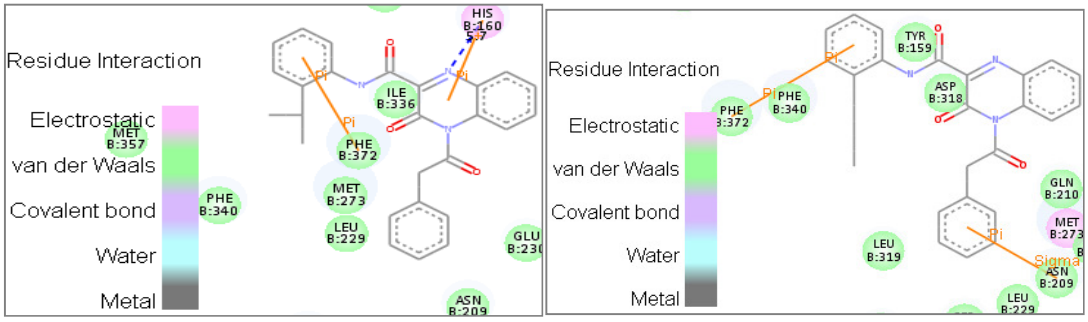

Fig. 82 and 83: QCE-12 and QCE-11 at the active site of PDE4D

Overall, the present 3-oxo-4-(2-phenylacetyl)-quinoxaline-2-carboxamide analogues displayed better interactions with PDE4D enzyme exhibiting their inhibitory activity. This indicates that the pharmacophoric elements like the central quinoxaline ring with a keto group which acts as a hydrogen bond acceptor (HBA), the phenacyl moiety, diverse substituted phenyl ring and the amide linker played a substantial role in forming various interactions within the active site.

5.6.1. ADME properties

The analysis showed that the compounds of this series,when administered orally might show better intestinal absorption, as well as good blood–brain barrier (BBB) permeability, whereas for compounds containing polar group where, (n > 2) it could not compute the ability to cross the BBB. Their aqueous solubility and drug–likeness properties were envisaged to be very low. In addition, these compounds are likely to inhibit enzyme such as CYP450 *2D6*. Most of these compounds are predicted to be non-hepatotoxic. It was also found that the inhibitor-plasma protein binding is not more than 90%, indicating that these compounds are likely to be less bound to plasma protein present in the blood. **(Table 31)**

Nevertheless, It is a common understanding that ADME profiles are complex to envisage accurately just by *in-silico* and so the envisaged profiles must be utilized with care. For our study, further testing ought to be done to investigate the actual profiles of these compounds as an extension of this work.

In the ADMET plot, since some of the molecule are inside and some outside the 99% confidence ellipse of BBB and HIA model, the prediction for those molecules inside are considered reliable, whereas for those molecules outside are considered unreliable and no BBB predictions are made for these ligands respectively. **(Fig. 83)**

Table 31: ADME properties of QCE Series

QCE	Aqueous solubility[a]		BBB[b]		CYP450 *2D6*[c]		Hepatotoxicity[d]		HIA[e]		PPB[g]		AlogP98[g]	
	Value	Level	Value	Level	Value	Level	Value	Level	Value	Level	Value	Level	Value	Level
1	-5.33	2	-0.151	2	-4.069	1	-3.131	0	NV[f]	0	1.264	0	4.073	0
2	-5.314	2	-0.298	2	-5.004	1	-3.514	0	NV[f]	0	1.451	0	4.057	0
3	-5.292	2	-0.298	2	-6.244	1	-3.375	0	NV[f]	0	1.578	0	4.057	0
4	-5.269	2	-0.298	2	-6.244	1	-2.668	0	NV[f]	0	-1.032	0	4.057	0
5	-5.788	2	-0.001	2	-6.704	1	-4.133	1	NV[f]	0	1.738	0	4.559	0
6	-5.777	2	-0.001	2	-5.359	1	-3.873	0	NV[f]	0	2.936	0	4.559	0
7	-5.766	2	-0.001	2	-5.359	1	-4.635	1	NV[f]	0	2.527	0	4.559	0
8	-6.029	1	0.054	1	-3.348	1	-3.649	0	NV[f]	0	3.430	0	4.737	0
9	-6.017	1	0.054	1	-3.766	1	-1.778	0	NV[f]	0	4.658	0	4.737	0
10	-6.006	1	0.054	1	-2.723	1	-2.978	0	NV[f]	0	4.596	0	4.737	0
11	-6.329	1	NV[f]	4	-4.674	1	-5.011	1	NV[f]	1	2.758	0	5.472	0
12	-6.305	1	NV[f]	4	-4.435	1	-3.913	0	NV[f]	1	1.527	0	5.267	0
13	-6.237	1	NV[f]	4	-4.352	1	-2.342	0	NV[f]	1	1.548	0	5.267	0
14	-6.463	1	NV[f]	4	-4.712	1	-3.417	0	NV[f]	1	3.844	0	5.224	0
15	-6.474	1	NV[f]	4	-4.719	1	-3.521	0	NV[f]	1	4.358	0	5.224	0
16	-6.485	1	NV[f]	4	-5.000	1	-3.018	0	NV[f]	1	3.768	0	5.224	0
17	-6.475	1	NV[f]	4	-4.144	1	-4.229	1	NV[f]	1	4.163	0	5.224	0
18	-6.463	1	NV[f]	4	-4.704	1	-3.404	0	NV[f]	1	5.801	0	5.224	0
19	-6.497	1	NV[f]	4	-2.681	1	-7.221	1	NV[f]	0	2.183	0	5.015	0

[a] Level 2 means the aqueous solubility of inhibitor is not very good and its drug-likeness properties are low, while Level 1 means the aqueous solubility of inhibitor is very poor.
[b] Level 2 means inhibitor has medium ability, Level 1 means inhibitor has high ability and Level 4 means inhibitor has undefined ability to cross the blood-brain barrier (BBB).
[c] Level 1 means inhibitor likely to inhibit CYP*2D6* enzyme.
[d] Level 0 means inhibitor not likely to be hepatotoxic, while Level 1 means inhibitor are likely to be hepatotoxic.
[e] Level 0 means inhibitor has good, while Level 1 means inhibitor has moderate human intestinal absorption (HIA) after oral administration.
[f] NV means no value was given.
[g] Level 0 means the binding between inhibitor and plasma protein (PPB) is less than 90% (No markers flagged and AlogP98 < 5.0).

ADMET PLOT

The ADMET plot is a 2D chart of ADMET_PSA_2D versus ADMET_AlogP98. The two sets of ellipses are for the prediction confidence space (95% and 99%) for the Blood Brain Barrier Penetration and Human Intestinal Absorption models, respectively.

Since the molecule is outside of the 99% BBB model confidence ellipse, the prediction is considered unreliable and no BBB prediction is made for this ligand.

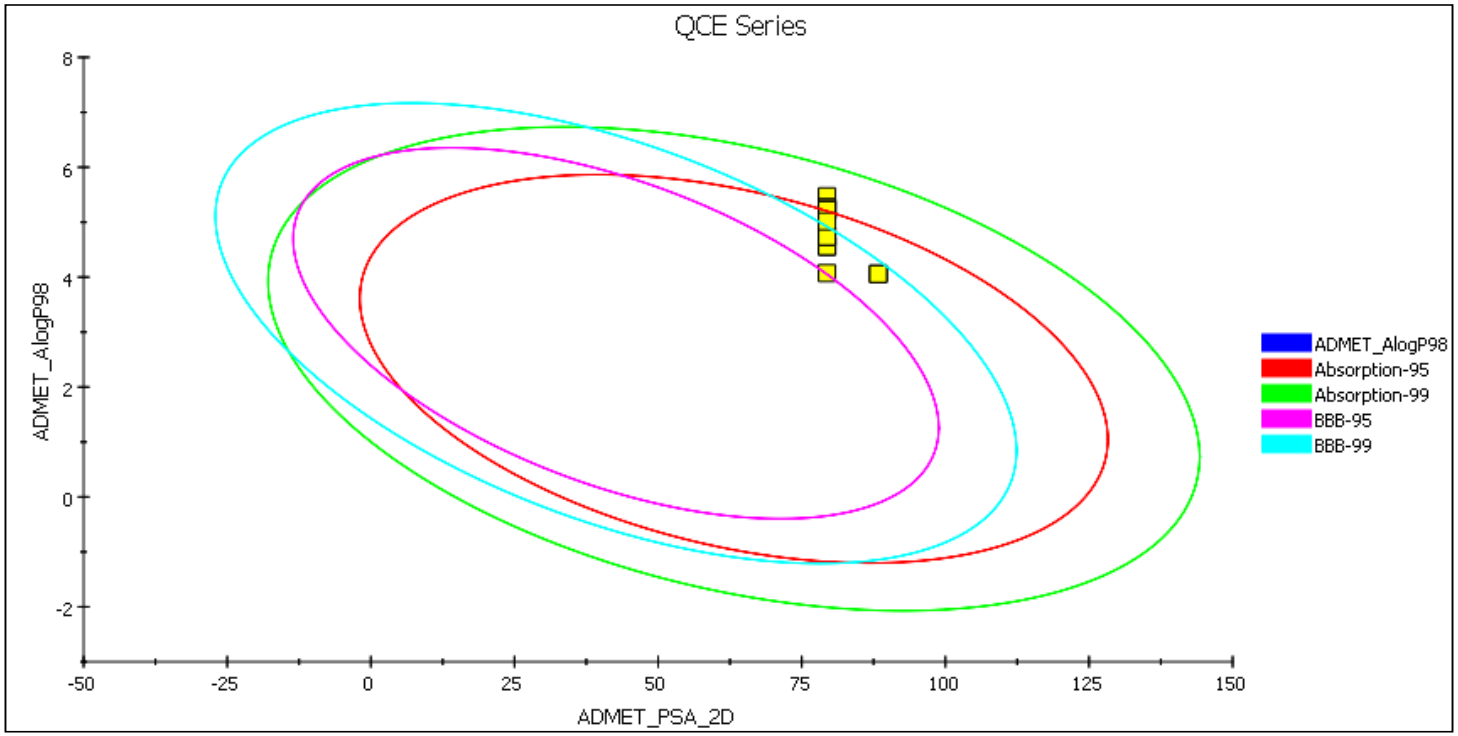

Fig. 83: ADMET Plot for QCE Series

5.7. Biological activities/Pharmacology for QCF Series

On the basis of encouraging results obtained from synthesized analogues bearing benzyl group (QCA series) and substituted benzyl group (QCB and QCC series) at *N4* position of the quinoxaline scaffold, further modification was attempted to understand the significance of the chain length between the quinoxaline core and the hydrophobe in the pharmacophore by substituting methylene ($-CH_2-$) with ethylene group $(-CH_2-)_2$ i.e., phenethyl group lead to 3-oxo-4-phenethyl-*N*-phenyl-3,4-dihydroquinoxaline-2-carboxamide analogues (QCF series). All these compounds were subjected for their inhibitory properties through *in-vitro* studies at 10 µM using PDE4B or PDE4D enzyme assay using rolipram as a reference compound.

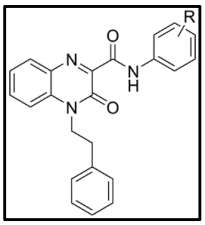

In this series, most of the compounds QCF-2, QCF-4, QCF-5, QCF-8, QCF-10, QCF-16, QCF-17 and QCF-18 showed pronounced inhibitory activity, while compounds QCF-11, QCF-12 and QCF-13 displayed moderate inhibitory activity for PDE4D isoform. Compounds QCF-5 and QCF-10 displayed moderate PDE4B inhibitory activity. Finally, the rest of the tested compounds exhibited poor inhibition. **(Table 32)**

Compounds QCF-5, QCF-8, QCF-10 and QCF-16 showed better PDE4D enzyme inhibitory activity and have similar affinity for PDE4B isoform indicating that this compound is non-selective. However, compounds QCF-2, QCF-4, QCF-17 and QCF-18 which also displayed better PDE4 inhibitory activity but have more than 2-fold affinity for PDE4D as compared to PDE4B isoform. **(Table 32)**

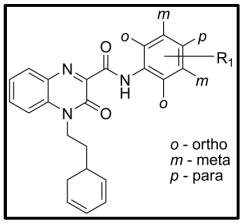

The SAR of these synthesized compounds indicates that substitution at *ortho*- or *para*-position on the phenyl ring was more favored for PDE4D inhibitory activity as evident from compounds QCF-2, QCF-4, QCF-5, QCF-8, QCF-10, QCF-16, QCF-17 and QCF-18. Similarly for PDE4B enzyme, substitution at *ortho*- or *para*-position on the phenyl ring was favored which displayed moderate inhibitory activity as marked from compounds QCF-5 and QCE-10.

The initial compound QCF-1 showed moderate PDE4D inhibitory activity and was equipotent for its PDE4B isoform. Introduction of a weak deactivating substituent like halogen group preferably chlorine at *ortho*-position or *para*-position on the phenyl ring as in compounds QCF-8, QCF-10, QCF-16 and QCF-18 and at *meta*-position as in compound QCF-17 displayed better activity for PDE4D than PDE4B isoform, except compound QCF-10 which exhibited equal activity for both isoform. The chloro possibly at *para*-position as in analogue QCF-10 and QCF-18 was better tolerated. Similarly, weak activating substituent like alkyl group preferably methyl at *ortho*-position on the phenyl ring as in compounds QCF-5, QCF-16, QCF-17 and QCF-18 exhibited better PDE4D

inhibition than its PDE4B isoform, except compound QCF-5 which exhibited equal activity for both isoform.

Interestingly, when strong activating group like methoxy was introduced at *ortho*-position or *para*-position on the phenyl ring as in compounds QCF-2 and QCF-4 retained the activity for PDE4D than PDE4B isoform. However, *ortho*-position was better tolerated displaying better PDE4D activity while at *para*-position it exhibited moderate PDE4 activity.

Table 32: In-vitro data of QCF series

Compound	R	PDE4B[a]	SD	PDE4D[a]	SD	Selectivity[b]
QCF-1	phenyl	39.46	2.06	58.16	1.96	-
QCF-2	2-methoxyphenyl	39.24	1.95	78.54	2.22	2.0
QCF-3	3-methoxyphenyl	26.74	2.14	59.79	1.34	-
QCF-4	4-methoxyphenyl	37.48	1.57	72.19	0.86	2.0
QCF-5	2-methylphenyl	50.71	1.66	73.58	1.58	1.5
QCF-6	3-methylphenyl	28.01	1.76	57.05	1.26	-
QCF-7	4-methylphenyl	24.83	1.54	52.19	0.62	-
QCF-8	2-chlorophenyl	45.64	1.06	70.38	3.22	1.5
QCF-9	3-chlorophenyl	28.33	1.40	55.65	2.66	-
QCF-10	4-chlorophenyl	52.92	0.56	83.83	1.52	1.6
QCF-11	2-propylphenyl	22.58	1.44	67.79	1.44	-
QCF-12	2-isopropylphenyl	33.70	0.63	65.23	2.14	-
QCF-13	4-isopropylphenyl	30.26	1.22	63.76	1.18	-
QCF-14	2-chloro-4-methylphenyl	8.66	1.12	27.70	1.43	-
QCF-15	2-chloro-5-methylphenyl	30.00	0.32	44.80	1.15	-
QCF-16	2-chloro-6-methylphenyl	42.22	1.43	75.48	0.92	1.8
QCF-17	3-chloro-2-methylphenyl	31.02	2.92	76.65	3.11	2.5
QCF-18	4-chloro-2-methylphenyl	38.59	2.36	80.37	1.48	2.1
QCF-19	2-trifluoromethylphenyl	30.22	0.93	36.53	1.16	-
Rolipram		90.27	0.22	96.54	0.14	1.1

[a] Average percentage inhibition – Values that are the mean of two or more experiments are shown with their standard deviations (SD)
[b] Ratio of PDE4D/PDE4B

In order to understand the nature of interactions of these molecules within the active site of PDE4D and PDE4B, docking studies were carried out for all the compounds. The dockscore and other scores obtained after docking of these molecules into the PDE4D and PDE4B proteins are summarized in **Table 33** and **34** respectively.

Table 33: Docking results of QCF series for PDE4D (PDB: 1Q9M)

Compound	LigScore_1	LigScore_2	-PLP1	-PLP2	Jain	-PMF	-PMF04	Dockscore	Ludi_3	Consensus
QCF-1	2.82	5.16	78.64	72.67	2.41	155.17	83.03	62.13	740	0
QCF-2	2.34	5.18	68.43	70.33	1.71	169.22	91.38	65.06	689	1
QCF-3	2.88	5.54	85.90	82.89	3.21	176.81	84.34	66.62	901	3
QCF-4	2.08	5.04	65.10	64.38	1.90	124.47	73.24	63.69	693	1
QCF-5	3.02	5.80	87.49	84.84	2.69	193.01	92.82	68.14	942	6
QCF-6	3.16	5.72	86.00	83.17	2.42	188.78	89.13	68.44	1,017	4
QCF-7	3.03	5.47	85.37	83.46	3.03	196.63	93.03	65.69	892	3
QCF-8	2.90	5.76	86.13	82.64	2.14	178.95	91.21	68.42	916	2
QCF-9	3.31	5.92	89.68	88.11	2.24	183.88	89.85	65.80	1,008	7
QCF-10	2.21	5.66	82.86	80.75	1.83	147.96	68.73	65.91	822	0
QCF-11	2.78	5.66	71.66	71.00	3.71	153.03	81.79	69.01	752	3
QCF-12	2.43	5.34	68.64	70.82	1.88	170.74	88.88	66.33	674	1
QCF-13	2.53	5.34	67.08	63.67	1.78	161.24	78.56	66.20	760	1
QCF-14	3.20	5.56	79.32	79.29	3.27	174.82	95.01	66.69	891	3
QCF-15	2.66	5.38	71.50	68.39	2.24	158.81	80.84	71.38	691	1
QCF-16	2.89	5.55	76.98	74.18	1.88	169.61	90.43	65.23	781	1
QCF-17	2.81	5.80	87.50	86.42	2.14	159.65	81.01	72.04	788	5
QCF-18	3.21	5.88	77.79	77.28	2.70	177.73	84.57	65.63	839	3
QCF-19	3.13	5.76	90.35	85.99	2.80	207.45	109.69	69.41	937	8
Rolipram	3.82	4.54	48.46	48.38	2.78	118.37	64.25	46.866	456	1
Nitraquazone	4.24	4.73	52.53	50.68	1.71	158.56	94.33	56.384	701	3

Table 34: Docking results of QCF series for PDE4B (PDB: 1XMY)

Compound	LigScore_1	LigScore_2	-PLP1	-PLP2	Jain	-PMF	-PMF04	Dockscore	Ludi_3	Consensus
QCF-1	1.88	4.97	62.23	56.39	1.32	128.32	83.60	58.71	557	0
QCF-2	2.04	5.13	60.89	58.08	1.58	143.01	102.50	64.79	627	3
QCF-3	2.26	5.02	78.10	73.35	4.17	166.17	99.39	63.27	1,017	6
QCF-4	1.96	4.83	82.28	76.46	2.97	120.42	89.93	54.04	691	5
QCF-5	2.01	4.40	56.60	58.88	3.80	162.19	99.27	58.88	773	2
QCF-6	2.13	5.14	63.91	59.44	2.10	165.49	110.35	61.68	663	3
QCF-7	1.65	4.45	74.71	69.98	2.85	118.11	85.49	57.72	666	1
QCF-8	2.03	5.12	81.67	78.20	2.83	132.36	108.56	59.01	783	4
QCF-9	2.09	5.57	87.14	83.92	2.32	134.20	98.16	65.93	791	5
QCF-10	2.11	5.44	80.88	77.37	2.81	97.64	47.41	56.11	681	6
QCF-11	2.20	5.42	75.62	76.26	0.99	124.65	90.88	63.55	657	5
QCF-12	2.21	5.46	70.51	64.07	0.64	137.66	88.06	61.86	705	5
QCF-13	1.94	5.09	60.09	54.16	0.76	144.27	96.58	64.31	605	2
QCF-14	2.07	4.99	60.68	58.16	2.23	166.98	113.58	61.26	699	2
QCF-15	2.00	4.87	78.67	74.15	2.26	127.53	89.64	67.80	751	1
QCF-16	2.23	5.40	81.14	74.01	2.50	130.92	101.72	61.09	812	7
QCF-17	1.90	5.11	61.23	59.70	0.14	128.97	87.49	59.53	720	1
QCF-18	3.18	5.52	78.14	67.00	1.65	121.70	82.92	64.08	666	4
QCF-19	2.03	5.04	79.26	75.99	2.92	145.76	111.79	59.54	765	5
Rolipram	2.23	4.39	54.3	46.79	2.51	141.03	107.36	45.193	608	2
Nitraquazone	1.78	4.61	68.64	51.8	1.44	139.65	96.4	57.033	708	0

The interaction of compound QCF-10 within the active site of PDE4D protein **(Fig. 85)** is mainly contributed by (i) π-π stacking interaction between the centroid of the phenyl ring on the amide linker and Phe372, (ii) two cationic-π interactions between His160 and the centroid of the pyrazine ring of the quinoxaline scaffold and another with the centroid of the benzene ring of the quinoxaline scaffold. While, the interaction within the active site of PDE4B protein **(Fig. 86)** is mainly contributed by (i) π-π stacking interaction between the centroid of the phenyl ring on the amide linker and Phe446.

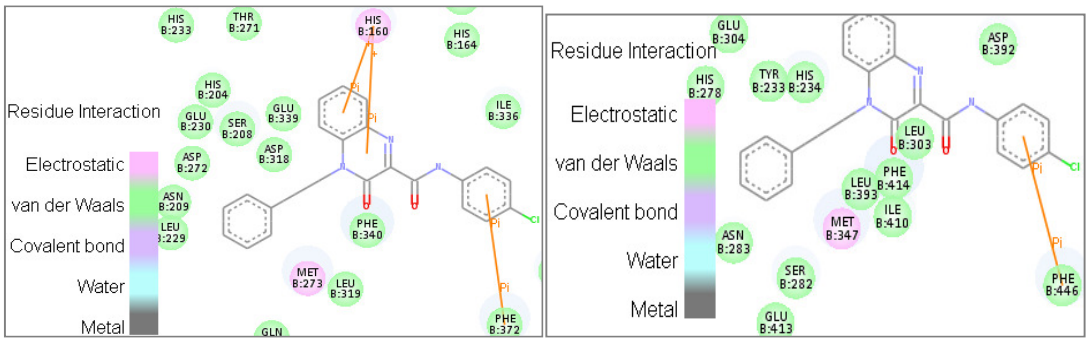

Fig. 85 and 86: QCF-10 at the active site of PDE4D and PDE4B

The interaction of compound QCF-18 within the active site of PDE4D protein **(Fig. 87)** is mainly contributed by (i) H-bond between the *N1* of the quinoxaline ring with His160 at a distance of 5.6 Á, (ii) cationic-π interaction between His160 and the centroid of the pyrazine ring of the quinoxaline scaffold. While, the interaction of compound QCF-2 within the active site of PDE4D protein **(Fig. 88)** is mainly contributed by (i) π-π stacking interaction between the centroid of the phenethyl ring and Phe372, (ii) two cationic-π interactions, one between His160 and the centroid of the pyrazine ring of the quinoxaline scaffold, while another between His233 and the centroid of the benzene ring of the quinoxaline scaffold.

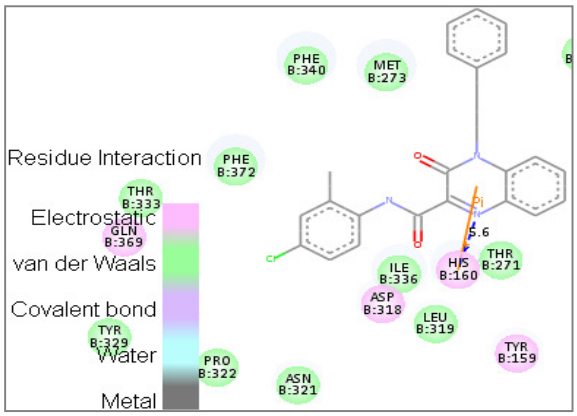

Fig. 87: QCF-18 at the active site of PDE4D

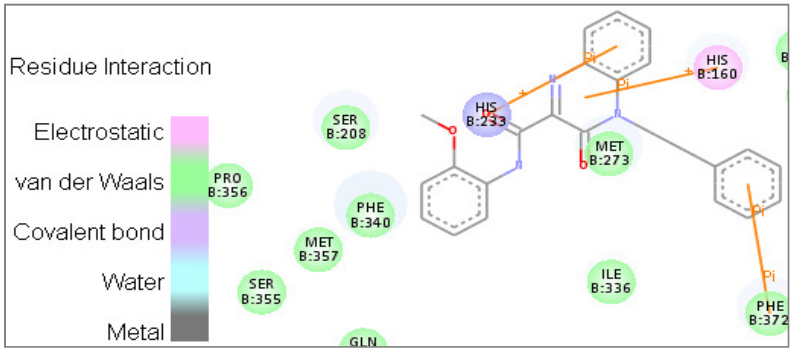

Fig. 88: QCF-2 at the active site of PDE4D

The compound QCF-17 did not show any interaction within the active site of PDE4D protein **(Fig. 89)**. The interaction of compound QCF-16 within the active site of PDE4D protein **(Fig. 90)** is mainly contributed by (i) H-bond between the *N1* of the quinoxaline ring with His160 at a distance of 5.8 Á, (ii) π-π stacking interaction between the centroid of the phenyl ring on the amide linker and Phe372, (iii) cationic-π interaction between His160 and the centroid of the pyrazine ring of the quinoxaline scaffold. Similarly, the interaction of compound QCF-5 within the active site of PDE4D protein **(Fig. 91)** is mainly contributed by (i) H-bond between the *N1* of the quinoxaline ring with His160 at a distance of 5.7 Á, (ii) two π-π stacking interactions, one between Phe372 and the centroid of the phenyl ring on the amide linker while, another between the centroid of the phenethyl ring and His160, (iii) two cationic-π interactions, one between His160 and the centroid of the pyrazine ring of the quinoxaline scaffold, while another between His233 and the centroid of the benzene ring of the quinoxaline scaffold. Whereas, the interaction within the active site of PDE4B protein **(Fig. 92)** was mainly contributed by (i) H-bond between the keto group of the amide linker with Asn283 at a distance of 4.2 Á.

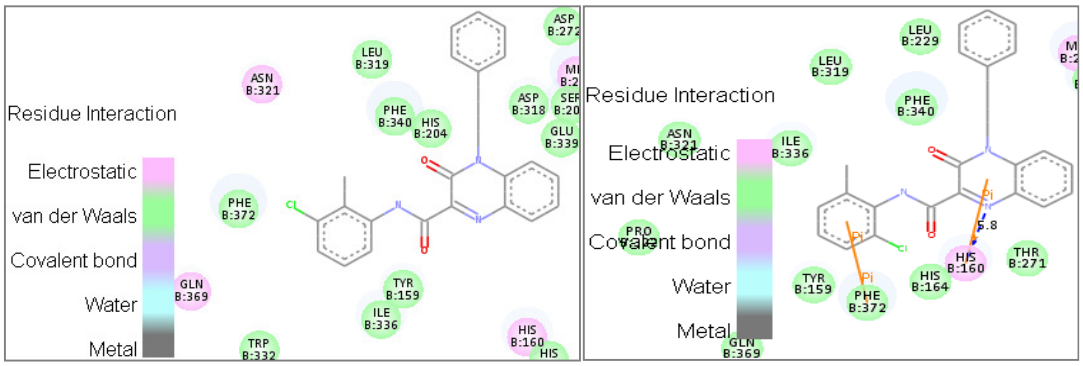

Fig. 89 and 90: QCF-17 and QCF-16 at the active site of PDE4D

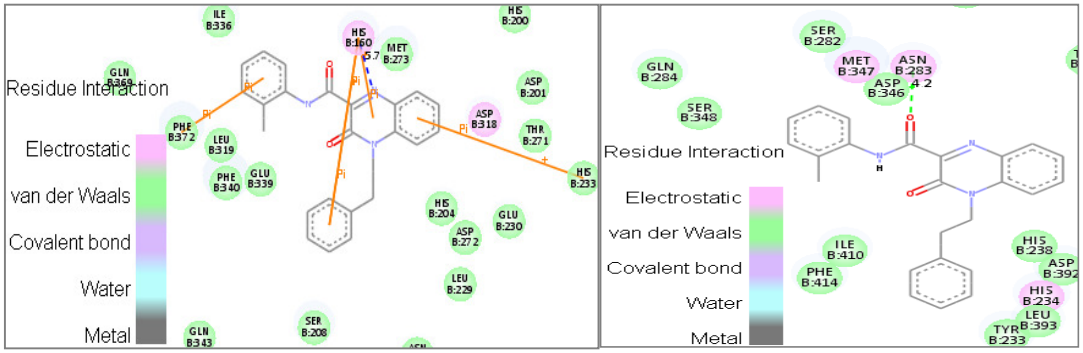

Fig. 91 and 92: QCF-5 at the active site of PDE4D and PDE4B

The interaction of compound QCF-4 within the active site of PDE4D protein **(Fig. 93)** is mainly contributed by (i) two cationic-π interactions between His160 and the centroid of the phenyl ring on the amide linker and another with the centroid of the phenethyl ring. While, the interaction of compound QCF-8 within the active site of PDE4D protein **(Fig. 94)** is mainly contributed by (i) H-bond between the *N1* of the quinoxaline ring with His160 at a distance of 5.9 Á, (ii) π-π stacking interaction between the centroid of the phenyl ring on the amide linker and Phe372, (iii) two cationic-π interactions, one between His160 and the centroid of the pyrazine ring of the quinoxaline scaffold, while another between His233 and the centroid of the benzene ring of the quinoxaline scaffold.

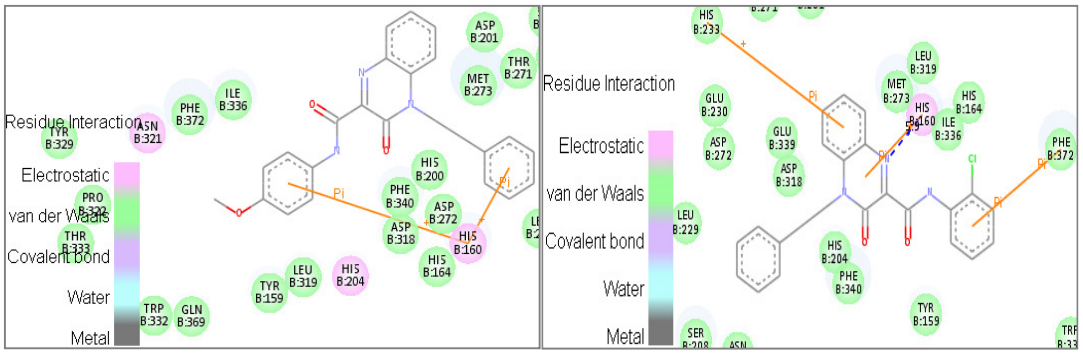

Fig. 93 and 94: QCF-4 and QCF-8 at the active site of PDE4D

Overall, the present 3-oxo-4-phenethyl-quinoxaline-2-carboxamide analogues showed better interactions with PDE4D enzyme exhibiting their inhibitory activity. This indicates that the pharmacophoric elements like the central quinoxaline ring with a keto group which acts as a hydrogen bond acceptor (HBA), the benzyl moiety, diverse substituted phenyl ring and the amide linker played a substantial role in forming various interactions within the active site.

5.7.1. ADME properties

The analysis showed that the compounds of this series when administered orally might show better intestinal absorption, as well as good blood–brain barrier (BBB) permeability. Their aqueous solubility and drug–likeness properties were envisaged to be very low. In addition, these compounds are likely to inhibit enzyme such as CYP450 *2D6*. These compounds are predicted to be hepatotoxic. It was also found that the inhibitor-plasma protein binding is not more than 90%, indicating that these compounds are likely to be less bound to plasma protein present in the blood. **(Table 35)**

Nevertheless, It is a common understanding that ADME profiles are complex to envisage accurately just by *in-silico* and so the envisaged profiles must be utilized with care. For our study, further testing ought to be done to investigate the actual profiles of these compounds as an extension of this work.

In the ADMET plot, since all the molecule are inside the 99% confidence ellipse of BBB and HIA model, the predictions are considered reliable and thereby the BBB and HIA predictions are made for these ligands respectively. **(Fig. 95)**

Table 35: ADME properties of QCF Series

QCF	Aqueous solubility[a]		BBB[b]		CYP450 *2D6*[c]		Hepatotoxicity[d]		HIA[e]		PPB[g]		AlogP98[g]	
	Value	Level	Value	Level	Value	Level	Value	Level	Value	Level	Value	Level	Value	Level
1	-5.007	2	0.061	1	-5.620	1	-4.748	1	NV[f]	0	5.867	0	3.874	0
2	-5.001	2	-0.085	2	-5.918	1	-6.198	1	NV[f]	0	6.141	0	3.858	0
3	-4.980	2	-0.085	2	-7.158	1	-6.058	1	NV[f]	0	6.269	0	3.858	0
4	-4.958	2	-0.085	2	-7.158	1	-5.352	1	NV[f]	0	3.658	0	3.858	0
5	-5.471	2	0.211	1	-7.822	1	-6.477	1	NV[f]	0	6.155	0	4.361	0
6	-5.460	2	0.211	1	-6.477	1	-6.216	1	NV[f]	0	7.353	0	4.361	0
7	-5.449	2	0.211	1	-6.477	1	-6.979	1	NV[f]	0	6.944	0	4.361	0
8	-5.711	2	0.266	1	-4.263	1	-5.993	1	NV[f]	0	7.989	0	4.539	0
9	-5.700	2	0.266	1	-4.681	1	-4.122	1	NV[f]	0	9.217	0	4.539	0
10	-5.689	2	0.266	1	-3.638	1	-5.322	1	NV[f]	0	9.155	0	4.539	0
11	-6.022	1	0.493	1	-5.543	1	-7.734	1	NV[f]	0	7.292	0	5.273	0
12	-5.997	2	0.43	1	-5.395	1	-6.680	1	NV[f]	0	6.389	0	5.069	0
13	-5.932	2	0.43	1	-5.313	1	-5.110	1	NV[f]	0	6.410	0	5.069	0
14	-6.150	1	0.417	1	-5.588	1	-5.608	1	NV[f]	0	8.261	0	5.025	0
15	-6.161	1	0.417	1	-5.596	1	-5.712	1	NV[f]	0	8.775	0	5.025	0
16	-6.172	1	0.417	1	-5.876	1	-5.209	1	NV[f]	0	8.185	0	5.025	0
17	-6.162	1	0.417	1	-5.020	1	-6.419	1	NV[f]	0	8.580	0	5.025	0
18	-6.150	1	0.417	1	-5.580	1	-5.595	1	NV[f]	0	10.218	0	5.025	0
19	-6.194	1	0.352	1	-3.854	1	-9.989	1	NV[f]	0	7.341	0	4.817	0

[a] Level 2 means the aqueous solubility of inhibitor is not very good and its drug-likeness properties are low, while Level 1 means the aqueous solubility of inhibitor is very poor.
[b] Level 2 means inhibitor has medium ability and Level 1 means inhibitor has high ability to cross the blood-brain barrier (BBB).
[c] Level 1 means inhibitor likely to inhibit CYP*2D6* enzyme.
[d] Level 1 means inhibitor are likely to be hepatotoxic.
[e] Level 0 means inhibitor has good human intestinal absorption (HIA) after oral administration.
[f] NV means no value was given.
[g] Level 0 means the binding between inhibitor and plasma protein (PPB) is less than 90% (No markers flagged and AlogP98 < 5.0).

ADMET PLOT

The ADMET plot is a 2D chart of ADMET_PSA_2D versus ADMET_AlogP98. The two sets of ellipses are for the prediction confidence space (95% and 99%) for the Blood Brain Barrier Penetration and Human Intestinal Absorption models, respectively.

Since the molecule is outside of the 99% BBB model confidence ellipse, the prediction is considered unreliable and no BBB prediction is made for this ligand.

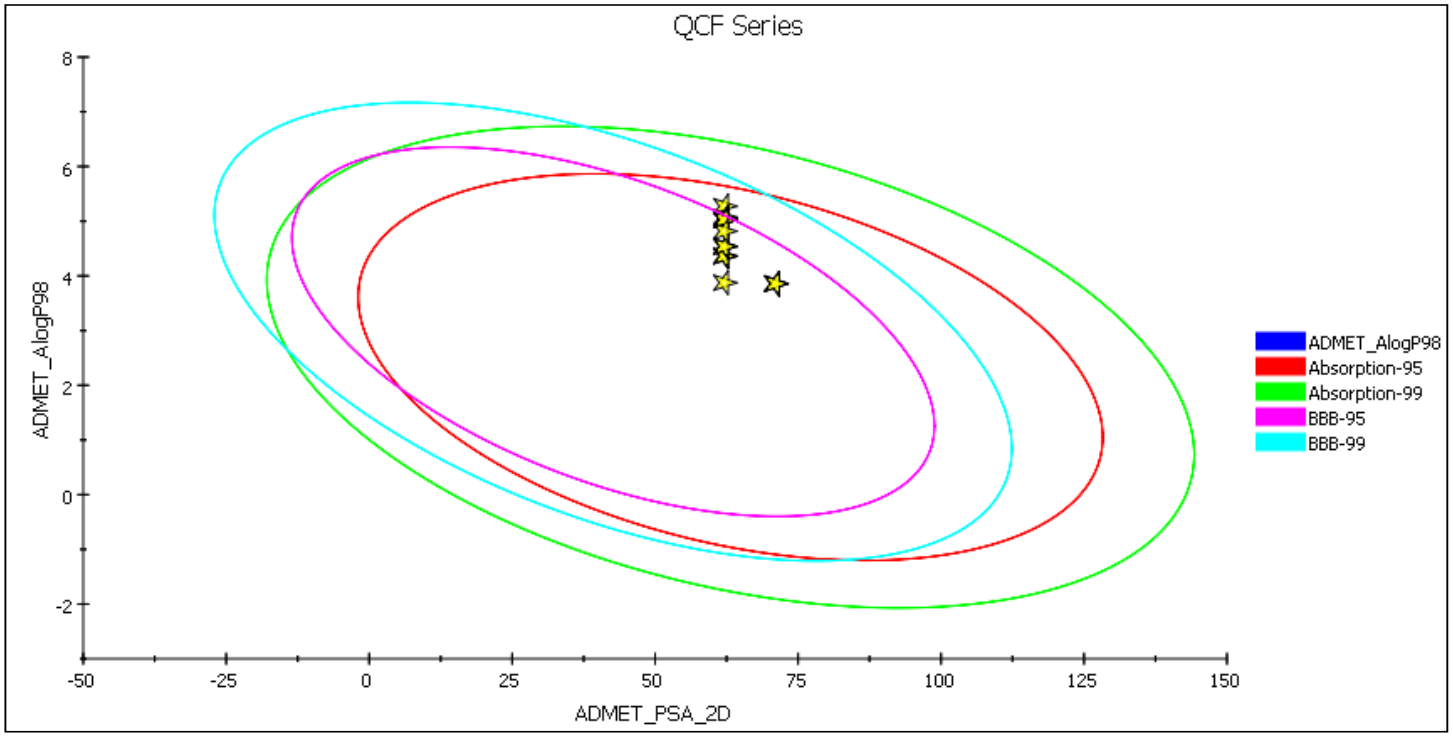

Fig. 95: ADMET Plot for QCF Series

5.8. Biological activities/Pharmacology for QZA Series

On the basis of encouraging results obtained from synthesized analogues bearing benzyl group (QCA series) and its substituted variants at *para*-positions (QCB and QCC series) at *N4* position of the quinoxaline scaffold, further modification was attempted to the basic scaffold i.e., substituting the quinoxaline scaffold with a positional isomeric quinazoline scaffold resulting in positional isomeric analogues of QCA series lead to 3-benzyl-4-oxo-*N*-phenyl-3,4-dihydroquinazoline-2-carboxamide analogues (QZA series). All these compounds were subjected for their inhibitory properties through *in-vitro* studies at 10 µM using PDE4B or PDE4D enzyme assay using rolipram as a reference compound. This series will help us to understand the significance of the basic scaffold in the pharmacophore.

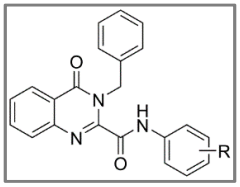

In this series, compound QZA-10, QZA-14 and QZA-15 showed pronounced inhibitory activity whereas compound QZA-3, QZA-4, QZA-6, QZA-12 and QZA-13 exhibited moderate inhibitory activity for PDE4D enzyme. Finally, the rest of the tested compounds exhibited poor inhibition. These compounds exhibited poor inhibitory activity for PDE4B enzyme, indicating that this series is selective. **(Table 36)**

Compound QZA-10 is the most active compound in this series which displayed comparatively more than 6-fold affinity for PDE4D than PDE4B enzyme. Similarly, compound QZA-6 which exhibited moderate inhibitory activity also displayed 6-fold affinity for PDE4D than its isoform. Whereas, compound QZA-4 and QZA-14 exhibited more than 31-fold affinity, while compound QZA-7 and QZA-15 displayed more than 11-fold affinity for PDE4D isoform.

Compound QZA-3, QZA-12, QZA-13 displayed 3-fold affinity and QZA-11 exhibited 2-fold more affinity for PDE4D isoform than PDE4B isoform. The results indicate that these compounds were more specific for PDE4D compared to PDE4B isoform. **(Table 36)** This suggests that this moiety could be considered as a lead, and on appropriate modification may possibly enhance the PDE4D selective inhibition and also devoid of its PDE4B inhibitory activity.

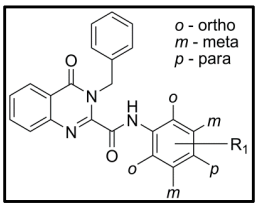

The SAR of these synthesized compounds indicates that substitution at *ortho*- or *para*-position on the phenyl ring was more favored for PDE4D inhibitory activity as evident from compounds QZA-4, QZA-7, QZA-10, QZA-11, QZA-12, QZA-13, QZA-14 and QZA-15. These analogues with variable substitution on various positions on the phenyl group had markedly lower affinity for PDE4B enzyme.

Introduction of a weak activating substituent like alkyl group preferably methyl, propyl or isopropyl at *ortho*-positionas in compounds QZA-10, QZA-12, QZA-14 and QZA-15 or at *para*-position on the phenyl ring as in compound QZA-11 and QZA-13 exhibited better to moderate PDE4D inhibition and was poorly active for its PDE4B isoform. This indicates that these compounds were moderately PDE4D selective. Whereas, when alkyl group like ethyl as in compound QZA-6 was introduced at *meta*-position exhibited moderate PDE4D inhibitory activity.

Similarly, weak deactivating substituent like halogen group preferably chlorine at *ortho*-position on the phenyl ring as in compound QZA-7 and QZA-13 or at *meta*- or *para*-position as in compound QZA-14 and QZA-15 was better tolerated and showed moderate PDE4D activity. Interestingly, when strong activating group like methoxy on the phenyl ring was introduced at *meta*- or *para*-position as in compounds QZA-3 and QZA-4 retained the moderate PDE4D inhibitory activity with decrease in PDE4B inhibitory activity.

Table 36: In-vitro data of QZA series

Compound	R	PDE4B[a]	SD	PDE4D[a]	SD	Selectivity[b]
QZA-1	phenyl	16.15	1.22	32.1	1.49	-
QZA-2	2-methoxyphenyl	8.27	1.48	38.6	1.15	-
QZA-3	3-methoxyphenyl	16.79	1.16	59.2	1.44	3.5
QZA-4	4-methoxyphenyl	1.79	0.44	58.3	2.60	32.6
QZA-5	2-ethylphenyl	10.74	0.62	5.86	2.56	-
QZA-6	3-ethylphenyl	9.21	1.98	53.4	2.33	5.8
QZA-7	2-chlorophenyl	4.40	1.59	49.4	1.17	11.2
QZA-8	3-chlorophenyl	27.14	2.64	40.1	3.12	-
QZA-9	4-chlorophenyl	19.23	2.11	37.64	1.17	-
QZA-10	2-isopropylphenyl	11.50	0.86	77.75	1.28	6.7
QZA-11	4-isopropylphenyl	21.02	3.21	46.59	3.67	2.2
QZA-12	2-propylphenyl	14.13	1.32	58.93	3.56	4.2
QZA-13	2-chloro-4-methylphenyl	13.99	2.51	49.98	1.12	3.6
QZA-14	3-chloro-2-methylphenyl	1.89	1.23	58.62	0.59	31.0
QZA-15	2-methyl-4-chlorophenyl	4.89	1.15	62.94	0.74	12.9
Rolipram		90.27	0.22	96.54	0.14	1.1

[a] Average percentage inhibition – Values that are the mean of two or more experiments are shown with their standard deviations (SD)
[b] Ratio of PDE4D/PDE4B

In order to understand the nature of interactions of these molecules within the active site of PDE4D and PDE4B, docking studies were carried out for all the compounds. The dockscore and other scores obtained after docking of these molecules into the PDE4D and PDE4B proteins are summarized in **Table 37** and **38** respectively.

Table 37: Docking results of QZA series for PDE4D (PDB: 1Q9M)

Compound	LigScore_1	LigScore_2	-PLP1	-PLP2	Jain	-PMF	-PMF04	Dockscore	Ludi_3	Consensus
QZA-1	3.77	4.58	73.29	63.92	5.09	152.68	76.62	67.60	807	0
QZA-2	1.94	5.10	76.63	77.01	1.92	132.02	81.06	65.03	717	2
QZA-3	3.98	4.49	79.89	70.49	5.66	151.81	76.43	71.63	898	4
QZA-4	3.99	4.50	77.39	68.80	5.82	152.76	75.39	71.04	896	4
QZA-5	2.00	5.16	78.04	79.32	2.89	132.20	79.34	67.07	842	2
QZA-6	3.64	4.15	78.95	69.01	5.94	163.16	81.22	66.44	881	5
QZA-7	2.00	5.43	77.66	79.40	2.91	129.25	67.69	65.61	908	3
QZA-8	3.80	4.76	73.18	66.38	4.80	150.69	86.75	69.08	810	3
QZA-9	3.99	4.51	77.45	69.09	5.53	149.00	77.35	71.49	905	3
QZA-10	2.37	5.14	69.49	67.18	1.96	130.75	58.95	63.30	628	1
QZA-11	3.95	4.59	85.77	76.03	5.67	171.71	87.31	71.06	916	7
QZA-12	2.09	5.28	80.45	81.07	2.62	137.99	75.82	68.19	641	4
QZA-13	3.75	5.49	82.97	75.87	2.27	94.46	43.37	67.96	584	3
QZA-14	2.27	5.09	77.62	78.90	2.81	143.88	74.84	64.56	866	2
QZA-15	2.06	5.34	79.25	74.70	2.13	135.58	70.63	65.41	885	2
Rolipram	3.82	4.54	48.46	48.38	2.78	118.37	64.25	46.866	456	1
Nitraquazone	4.24	4.73	52.53	50.68	1.71	158.56	94.33	56.384	701	3

Table 38: Docking results of QZA series for PDE4B (PDB: 1XMY)

Compound	LigScore_1	LigScore_2	-PLP1	-PLP2	Jain	-PMF	-PMF04	Dockscore	Ludi_3	Consensus
QZA-1	2.06	5.08	75.25	69.48	3.29	151.69	95.03	63.23	908	5
QZA-2	2.13	5.39	80.45	79.38	2.44	136.23	98.84	65.44	883	8
QZA-3	1.96	4.67	74.80	71.11	2.22	90.41	70.92	63.09	497	1
QZA-4	2.25	3.86	69.46	52.56	3.66	158.36	102.80	61.52	776	5
QZA-5	2.01	5.26	75.39	75.35	2.01	137.59	93.23	64.53	745	5
QZA-6	1.89	4.93	70.25	68.25	1.35	101.02	72.95	64.63	703	2
QZA-7	1.75	4.08	77.23	79.30	3.40	94.41	70.88	63.32	858	3
QZA-8	1.94	5.08	76.70	72.91	2.63	128.16	78.40	62.47	847	0
QZA-9	1.99	5.15	73.44	72.90	2.94	118.07	80.48	62.77	845	1
QZA-10	2.78	5.34	78.92	76.60	4.42	124.35	78.80	65.01	628	7
QZA-11	3.42	5.39	94.09	87.26	3.29	86.03	57.63	62.59	485	7
QZA-12	2.14	5.40	77.27	77.38	2.82	140.61	97.05	65.46	832	9
QZA-13	1.98	5.13	77.61	76.38	2.94	123.84	91.62	64.47	845	2
QZA-14	2.25	4.91	73.32	75.80	3.03	134.06	92.66	63.49	872	5
QZA-15	1.89	5.02	70.19	66.52	2.14	124.96	95.26	62.26	792	2
Rolipram	2.23	4.39	54.3	46.79	2.51	141.03	107.36	45.193	608	2
Nitraquazone	1.78	4.61	68.64	51.8	1.44	139.65	96.4	57.033	708	0

The interaction of compound QZA-10 within the active site of PDE4D protein **(Fig. 96)** is mainly contributed by (i) a π-π stacking interaction between the centroid of the benzyl ring and His160.

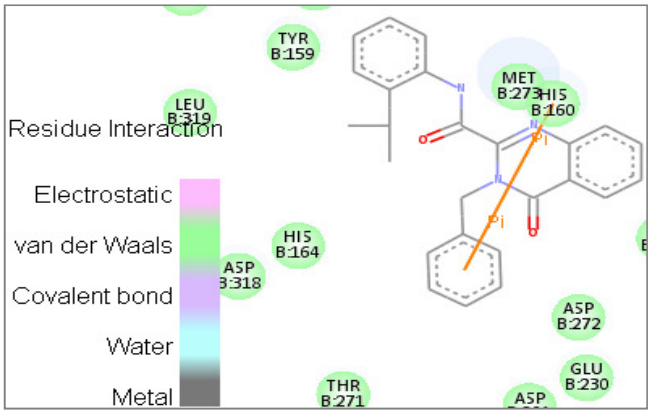

Fig. 96: QZA-10 at the active site of PDE4D

The interaction of compound QZA-15 within the active site of PDE4D protein **(Fig. 97)** is mainly contributed by (i) two π-π stacking interactions between the centroid of the phenyl ring on the amide linker with His160 and Phe340 (ii) cationic-π interaction between His160 and the centroid of the benzene ring of the quinazoline scaffold. Whereas, the interaction of compound QZA-3 within the active site of PDE4D protein **(Fig. 98)** is mainly contributed by (i) three H-bonds, one between the *N1* of the quinazoline ring with His160 at a distance of 5.4 Å, while one between the keto group of the quinazoline ring with His204 at a distance of 5.2 Å and another between -NH of the amide linker and Asp318 at a distance of 3.5 Å, (ii) σ-π interaction between Met273 and the centroid of the benzyl ring, (iii) cationic-π interaction between His160 and the centroid of the phenyl ring on the amide linker.

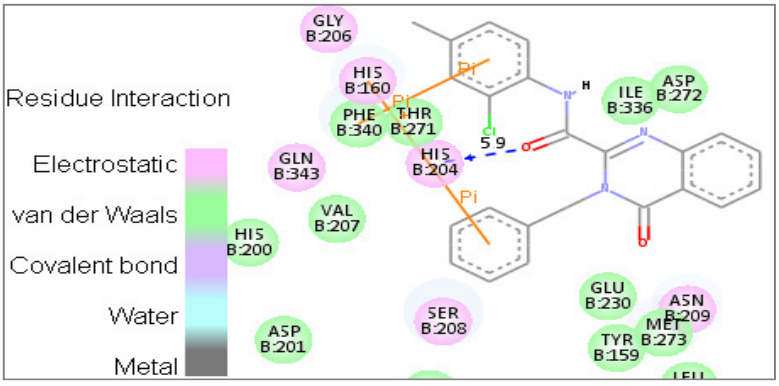

Fig. 97: QZA-15 at the active site of PDE4D

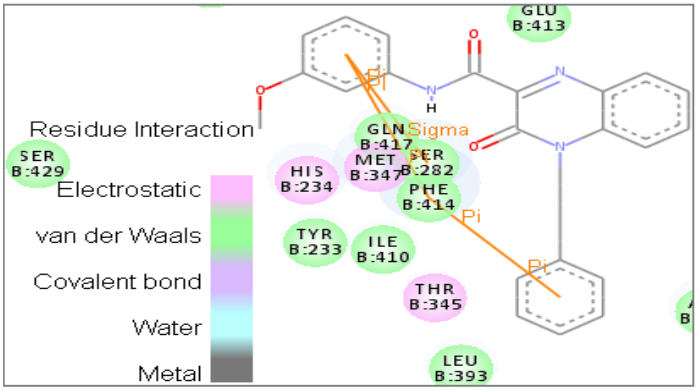

Fig. 98: QZA-3 at the active site of PDE4D

The interaction of compound QZA-12 within the active site of PDE4D protein **(Fig. 99)** is mainly contributed by (i) π-π stacking interaction between the centroid of the phenyl ring on the amide linker and Phe340, (ii) cationic-π interaction between His160 and the centroid of the benzene ring of the quinazoline scaffold. Similarly, the interaction of compound QZA-14 within the active site of PDE4D protein **(Fig. 100)** is mainly contributed by (i) two π-π stacking interactions, one between Phe372 and the centroid of the phenyl ring on the amide linker while, another between the centroid of the benzene ring of the quinazoline scaffold, (ii) two cationic-π interactions between His160 and the centroid of the phenyl ring on the amide linker, and with the centroid of the benzyl ring. Whereas, the interaction of compound QZA-4 within the active site of PDE4D protein **(Fig. 101)** is mainly contributed by (i) three H-bonds, one between the *N1* of the quinazoline ring with His160 at a distance of 5.4 Å, while one between the keto group of the quinazoline ring with His204 at a distance of 5.2 Å and another between -NH of the amide linker and Asp318 at a distance of 3.5 Å, (ii) σ-π interaction between Met273 and the centroid of the benzyl ring, (iii) cationic-π interaction between His160 and the centroid of the phenyl ring on the amide linker.

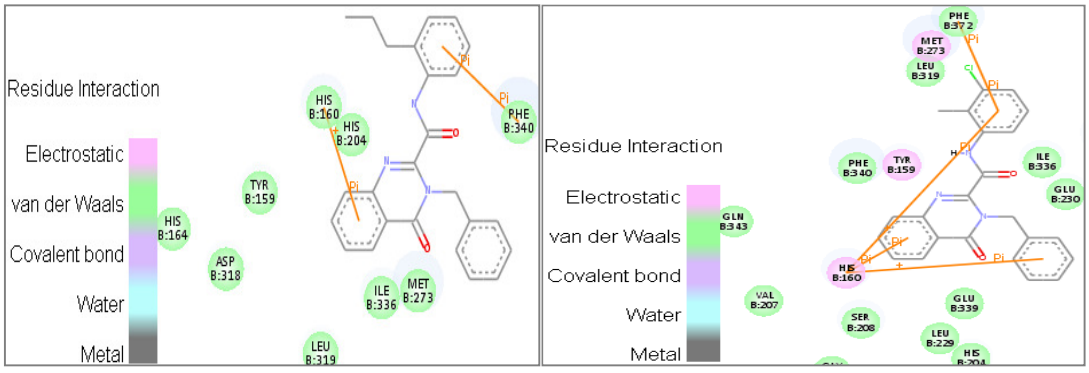

Fig. 99 and 100: QZA-12 and QZA-14 at the active site of PDE4D

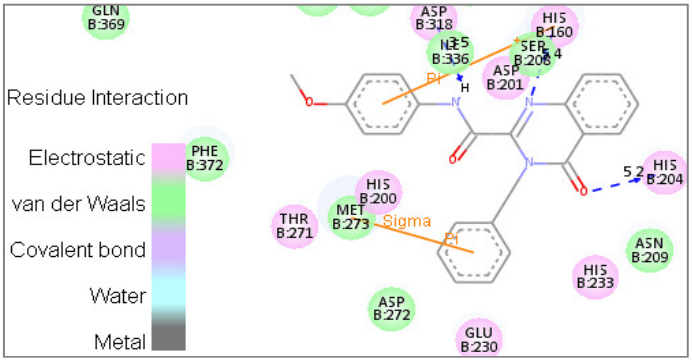

Fig. 101: QZA-4 at the active site of PDE4D

Overall, the present 3-benzyl-4-oxo-quinazoline-2-carboxamide analogues showed better interactions with PDE4D enzyme exhibiting their inhibitory activity. This indicates that the pharmacophoric elements like the central quinazoline ring with a keto group which acts as a hydrogen bond acceptor (HBA), the benzyl moiety, diverse substituted phenyl ring and the amide linker played a substantial role in forming various interactions within the active site.

5.8.1. ADME properties

The analysis showed that the compound of this series when administered orally might show better intestinal absorption, as well as good blood–brain barrier (BBB) permeability. Their aqueous solubility and drug–likeness properties were envisaged to be very low. In addition, these compounds are likely to inhibit enzyme like CYP450 *2D6*. Most of these compounds are predicted to be non-hepatotoxic. It was also found that the inhibitor-plasma protein binding is not more than 90%, indicating that these compounds are likely to be less bound to plasma protein present in the blood. **(Table 39)**

Nevertheless, It is a common understanding that ADME profiles are complex to envisage accurately just by *in-silico* and so the envisaged profiles must be utilized with care. For our study, further testing ought to be done to investigate the actual profiles of these compounds as an extension of this work.

In the ADMET plot, since all the molecule are inside the 99% confidence ellipse of BBB and HIA model, the predictions are considered reliable and thereby the BBB and HIA predictions are made for these ligands respectively. **(Fig. 102)**

Table 39: ADME properties of QZA Series

QZA	Aqueous solubility[a]		BBB[b]		CYP450 *2D6*[c]		Hepatotoxicity[d]		HIA[e]		PPB[g]		AlogP98[g]	
	Value	Level	Value	Level	Value	Level	Value	Level	Value	Level	Value	Level	Value	Level
1	-4.868	2	-0.04	2	-4.293	1	-1.833	0	NV[f]	0	2.921	0	3.549	0
2	-4.883	2	-0.186	2	-4.420	1	-2.706	0	NV[f]	0	3.111	0	3.532	0
3	-4.863	2	-0.186	2	-5.962	1	-2.859	0	NV[f]	0	2.881	0	3.532	0
4	-4.842	2	-0.186	2	-5.962	1	-2.152	0	NV[f]	0	0.271	0	3.532	0
5	-5.636	2	0.252	1	-4.220	1	-4.735	1	NV[f]	0	4.047	0	4.491	0
6	-5.615	2	0.252	1	-5.062	1	-3.917	0	NV[f]	0	3.607	0	4.491	0
7	-5.582	2	0.166	1	-3.573	1	-2.671	0	NV[f]	0	5.262	0	4.213	0
8	-5.572	2	0.166	1	-4.292	1	-1.092	0	NV[f]	0	6.133	0	4.213	0
9	-5.561	2	0.166	1	-3.249	1	-2.292	0	NV[f]	0	6.071	0	4.213	0
10	-5.890	2	0.330	1	-3.802	1	-2.880	0	NV[f]	0	3.359	0	4.743	0
11	-5.828	2	0.330	1	-4.021	1	-1.601	0	NV[f]	0	3.022	0	4.743	0
12	-5.915	2	0.393	1	-4.041	1	-4.132	1	NV[f]	0	4.591	0	4.947	0
13	-6.033	1	0.316	1	-4.467	1	-2.676	0	NV[f]	0	5.319	0	4.699	0
14	-6.044	1	0.316	1	-3.899	1	-3.488	0	NV[f]	0	5.638	0	4.699	0
15	-6.033	1	0.316	1	-4.460	1	-2.663	0	NV[f]	0	7.275	0	4.699	0

[a] Level 2 means the aqueous solubility of inhibitor is not very good and its drug-likeness properties are low, while Level 1 means the aqueous solubility of inhibitor is very poor.
[b] Level 2 means inhibitor has medium ability and Level 1 means inhibitor has high ability to cross the blood-brain barrier (BBB).
[c] Level 1 means inhibitor likely to inhibit CYP*2D6* enzyme.
[d] Level 0 means inhibitor not likely to be hepatotoxic, while Level 1 means inhibitor are likely to be hepatotoxic.
[e] Level 0 means inhibitor has good human intestinal absorption (HIA) after oral administration.
[f] NV means no value was given.
[g] Level 0 means the binding between inhibitor and plasma protein (PPB) is less than 90% (No markers flagged and AlogP98 < 5.0).

ADMET PLOT

The ADMET plot is a 2D chart of ADMET_PSA_2D versus ADMET_AlogP98. The two sets of ellipses are for the prediction confidence space (95% and 99%) for the Blood Brain Barrier Penetration and Human Intestinal Absorption models, respectively.

Since the molecule is outside of the 99% BBB model confidence ellipse, the prediction is considered unreliable and no BBB prediction is made for this ligand.

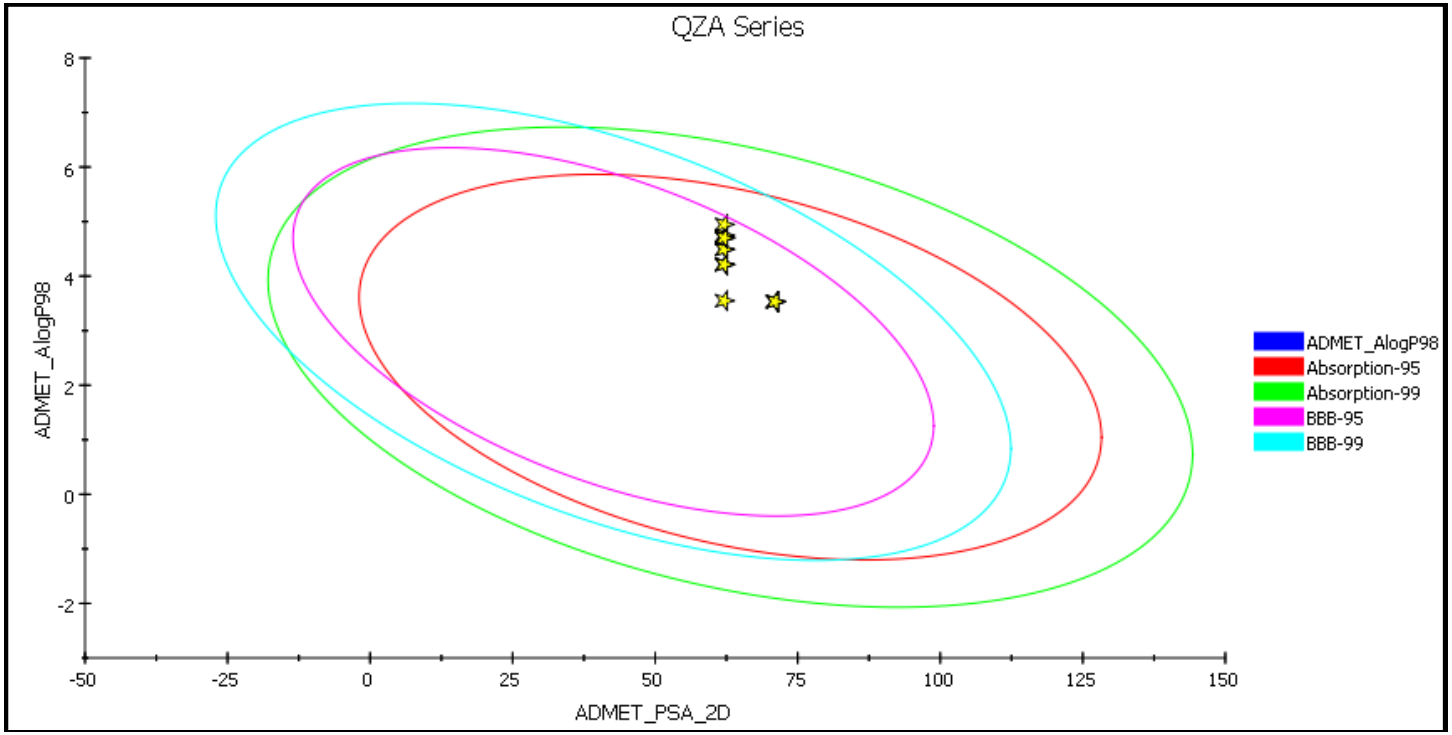

Fig. 102: ADMET Plot for QZA Series

5.9. Biological activities/Pharmacology for QZB Series

On the basis of encouraging results obtained from synthesized analogues bearing benzyl group (QZA series) at *N3* position of the quinazoline scaffold, further modification on the benzyl ring by introducing a strong activating group like methoxy group (-OCH_3) at the *para*-position lead to 3-(4-methoxybenzyl)-4-oxo-*N*-phenyl-3,4-dihydroquinazoline-2-carboxamide analogues (QZB-series). All these compounds were subjected for their inhibitory properties through *in-vitro* studies at 10 µM using PDE4B or PDE4D enzyme assay using rolipram as a reference compound.

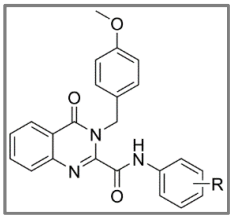

In this series, compounds QZB-2, QZB-5 and QZB-11 showed moderate inhibitory activity whereas compound QZB-3, QZB-6 and QZB-17 exhibited moderately poor inhibitory activity for PDE4D enzyme. Compound QZB-4 and QZB-6 displayed moderate PDE4B enzyme inhibition. Rest of the tested compounds exhibited very poor inhibition. **(Table 40)**

Compound QZB-5 is the most active compound in this series which displayed comparatively equal affinity for PDE4D and PDE4B enzyme. Similarly, despite compound QZB-11 and QZB-3 exhibited 5-fold affinity; while QZB-2 and QZB-17 exhibited more than 7-fold affinity, these compounds displayed moderate inhibitory activity for PDE4D than its isoform. The results indicate that these compounds were more specific for PDE4D compared to PDE4B isoform. Except compound QZB-4 and QZB-6 which showed moderate activity for PDE4B enzyme, while the rest of the compounds shown weak enzyme inhibition. Compound QZB-10 exhibited a selective inhibition for PDE4D, but with poor inhibitory activity. **(Table 40)** This suggests that this moiety could be considered as a lead, and on appropriate modification may possibly enhance the PDE4D selective inhibition and also devoid of its PDE4B inhibitory activity.

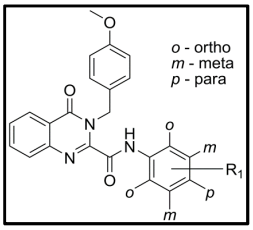

The SAR of these synthesized compounds indicates that substitution at *ortho*-position on the phenyl ring was more favored for moderate PDE4D inhibitory activity as evident from compounds QZB-2, QZB-5, and QZB-11. Similarly for PDE4B enzyme, substitution at *para*- or *meta*-position on the phenyl ring was better tolerated which displayed predominantly moderate inhibitory activity as marked from compounds QZB-4 and QZB-6.

Introduction of a weak activating substituent like alkyl group preferably methyl or ethyl at *ortho*-position as in compound QZB-11 and QZB-5 exhibited moderate PDE4D inhibition and was poorly active for its PDE4B isoform. Interestingly, when strong activating group like methoxy on the phenyl ring was introduced at *ortho*- or *meta*-position as in

compound QZB-2 and QZB-3 retained the moderate PDE4D inhibitory activity and showed poor PDE4B inhibitory activity. This indicates that these compounds were moderately PDE4D selective and poorly active for PDE4B inhibitory activity.

However, when methoxy group was introduced at *para*-position as in compound QZB-4 it was better tolerated but resulted in predominantly moderate PDE4B inhibitory activity and poor PDE4D activity. Similarly, when alkyl group like ethyl was introduced at *meta*-position as in compound QZB-6 displayed moderate activity for PDE4B and PDE4D indicating its non-selectivity.

Table 40: In-vitro data of QZB series

Compound	R	PDE4B[a]	SD	PDE4D[a]	SD	Selectivity[b]
QZB-1	phenyl	1.24	0.92	33.63	0.74	-
QZB-2	2-methoxyphenyl	6.95	0.21	50.29	0.46	7.2
QZB-3	3-methoxyphenyl	8.59	0.28	47.21	1.32	5.5
QZB-4	4-methoxyphenyl	54.94	0.54	27.20	1.20	-
QZB-5	2-ethylphenyl	34.28	0.97	57.70	2.32	1.7
QZB-6	3-ethylphenyl	52.07	1.12	43.80	1.56	-
QZB-7	3-chloro-2-methylphenyl	42.50	1.44	36.68	1.45	-
QZB-8	2-chlorophenyl	11.85	0.26	34.78	2.68	-
QZB-9	3-chlorophenyl	13.73	0.56	27.43	1.84	-
QZB-10	4-chlorophenyl	0.00	0.33	25.48	1.48	-
QZB-11	2-methylphenyl	10.80	1.84	54.44	3.16	5.0
QZB-12	3-methylphenyl	4.67	0.39	18.48	0.39	-
QZB-13	4-methylphenyl	5.76	1.66	38.68	0.83	-
QZB-14	2-propylphenyl	13.72	2.15	30.99	3.31	-
QZB-15	2-isopropylphenyl	9.73	1.78	20.01	1.23	-
QZB-16	4-isopropylphenyl	5.70	2.26	23.12	0.53	-
QZB-17	2-chloro-4-methylphenyl	5.60	1.77	42.73	2.15	7.6
QZB-18	2-chloro-5-methylphenyl	2.36	1.12	38.07	2.63	-
QZB-19	2-chloro-6-methylphenyl	20.40	0.84	22.64	0.94	-
Rolipram		90.27	0.22	96.54	0.14	1.1

[a] Average percentage inhibition – Values that are the mean of two or more experiments are shown with their standard deviations (SD)
[b] Ratio of PDE4D/PDE4B

In order to understand the nature of interactions of these molecules within the active site of PDE4D and PDE4B, docking studies were carried out for all the compounds. The dockscore and other scores obtained after docking of these molecules into the PDE4D and PDE4B proteins are summarized in **Table 41** and **42** respectively.

Table 41: Docking results of QZB series for PDE4D (PDB: 1Q9M)

Compound	LigScore_1	LigScore_2	-PLP1	-PLP2	Jain	-PMF	-PMF04	Dockscore	Ludi_3	Consensus
QZB-1	3.34	5.47	88.93	86.37	3.82	175.03	105.83	65.10	839	4
QZB-2	2.48	5.12	84.86	84.40	2.66	152.39	89.83	70.71	1,019	6
QZB-3	2.59	5.19	74.52	71.66	2.37	110.74	81.96	62.43	654	2
QZB-4	4.09	4.61	79.64	70.08	4.80	150.86	77.63	68.18	930	5
QZB-5	2.16	5.45	75.76	69.41	1.55	124.29	78.70	63.48	677	1
QZB-6	4.11	4.59	76.18	67.80	4.54	157.15	76.62	70.41	853	3
QZB-7	2.72	5.51	75.46	68.15	1.27	175.05	87.49	65.30	899	4
QZB-8	2.46	5.29	86.31	82.92	2.64	136.30	75.59	69.74	962	4
QZB-9	3.84	4.69	75.07	65.60	5.22	146.96	81.52	73.27	820	3
QZB-10	3.94	4.84	76.32	66.52	5.10	150.28	84.78	71.22	880	3
QZB-11	2.54	5.44	88.70	87.28	2.73	129.33	78.77	70.41	949	4
QZB-12	3.52	4.34	71.06	65.18	4.82	151.26	78.16	69.35	798	1
QZB-13	4.10	4.61	76.89	67.15	5.26	153.51	75.33	69.47	906	3
QZB-14	2.82	5.64	84.65	85.43	3.08	136.64	81.19	69.03	917	5
QZB-15	2.19	5.06	81.09	79.44	3.26	143.75	75.16	62.90	993	3
QZB-16	3.20	5.28	82.29	73.76	2.94	128.06	64.58	65.53	906	3
QZB-17	2.96	5.60	86.97	86.77	3.59	128.99	74.47	70.35	976	6
QZB-18	2.86	5.63	99.38	95.74	3.12	135.90	79.86	71.68	929	6
QZB-19	2.57	5.38	81.53	78.72	3.29	117.51	73.64	70.23	794	2
Rolipram	3.82	4.54	48.46	48.38	2.78	118.37	64.25	46.866	456	1
Nitraquazone	4.24	4.73	52.53	50.68	1.71	158.56	94.33	56.384	701	3

Table 42: Docking results of QZB series for PDE4B (PDB: 1XMY)

Compound	LigScore_1	LigScore_2	-PLP1	-PLP2	Jain	-PMF	-PMF04	Dockscore	Ludi_3	Consensus
QZB-1	2.04	5.07	67.54	58.54	1.74	118.76	82.12	62.68	776	2
QZB-2	2.27	5.02	78.64	69.83	1.98	101.75	79.64	64.77	751	3
QZB-3	2.22	5.38	79.38	62.67	1.01	155.56	116.92	62.34	903	5
QZB-4	1.83	4.68	71.97	61.23	0.76	98.93	70.76	63.73	670	7
QZB-5	2.39	5.43	82.68	77.03	2.59	99.61	63.92	65.61	601	3
QZB-6	1.93	4.89	61.13	55.39	0.80	92.56	65.13	63.77	576	2
QZB-7	2.17	5.29	81.69	67.35	1.41	152.90	104.18	66.53	887	6
QZB-8	2.41	5.37	78.00	77.22	2.01	112.92	83.21	64.90	659	4
QZB-9	2.54	5.38	82.83	76.35	1.67	128.31	91.21	66.28	822	8
QZB-10	2.86	5.38	71.95	65.28	3.08	154.90	115.94	68.10	866	7
QZB-11	2.42	5.32	81.77	77.83	1.74	144.59	93.47	65.14	881	7
QZB-12	2.08	4.87	75.97	69.62	2.41	76.71	50.67	64.70	731	1
QZB-13	1.81	4.55	79.29	69.48	2.07	96.87	65.11	64.14	632	1
QZB-14	2.70	4.89	71.37	63.59	1.63	87.62	61.75	62.89	616	2
QZB-15	2.30	4.79	61.82	60.27	1.89	93.08	64.00	59.75	525	5
QZB-16	2.71	5.44	80.79	75.28	1.12	46.73	36.92	63.36	495	6
QZB-17	2.73	5.48	90.38	85.41	3.83	118.57	84.11	67.66	899	10
QZB-18	1.78	4.51	82.52	83.24	2.43	89.05	67.97	64.06	649	4
QZB-19	1.75	4.38	72.89	67.06	3.10	154.94	99.84	63.73	957	7
Rolipram	2.23	4.39	54.3	46.79	2.51	141.03	107.36	45.193	608	2
Nitraquazone	1.78	4.61	68.64	51.8	1.44	139.65	96.4	57.033	708	0

The interaction of compound QZB-5 within the active site of PDE4D protein **(Fig. 103)** is mainly contributed by (i) π-π stacking interaction between the centroid of the substituted benzyl ring and Phe372, (ii) cationic-π interaction between His160 and the centroid of the substituted benzyl ring. While, the interaction of compound QZB-11 within the active site of PDE4D protein **(Fig. 104)** is mainly contributed by (i) three H-bonds, one between the *N1* of the quinazoline ring with His160 at a distance of 5.2 Á, while one between the keto group of the quinazoline ring with His204 at a distance of 5.0 Á and another between -NH of the amide linker and Asp318 at a distance of 3.4 Á, (ii) cationic-π interaction between His160 and the centroid of the phenyl ring on the amide linker.

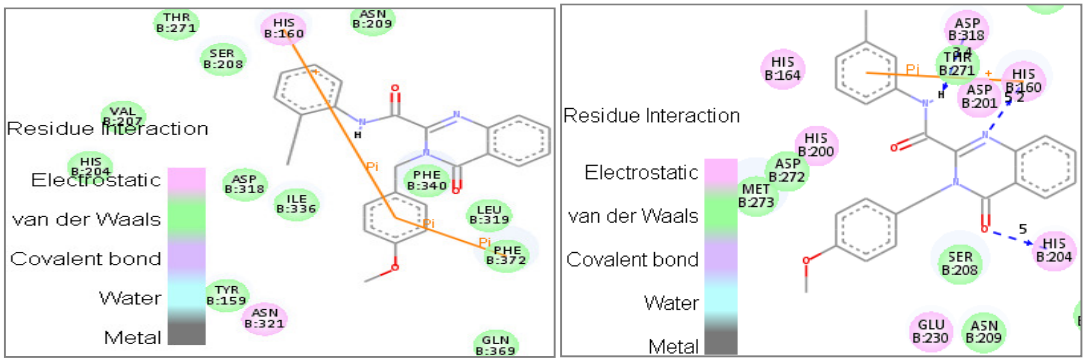

Fig. 103 and 104: QZB-5 and QZB-11 at the active site of PDE4D

The interaction of compound QZB-2 within the active site of PDE4D protein **(Fig. 105)** is mainly contributed by (i) three π-π stacking interactions, two between the centroid of the phenyl ring on the amide linker with His160 and Phe340 while another between the centroid of the benzyl ring with Phe372, (ii) cationic-π interaction between the centroid of benzene ring of the quinazoline scaffold and His160. Whereas, the interaction of compound QZB-3 within the active site of PDE4D protein **(Fig. 106)** is mainly contributed by (i) H-bond between the $–OCH_3$ substituent on the benzyl ring with His160 at a distance of 5.2 Å, (ii) three π-π stacking interactions, two between Phe340 with the centroid of the benzene ring and pyrimidine ring of the quinazoline scaffold, while another between the centroid of the phenyl ring on the amide linker and Phe372.

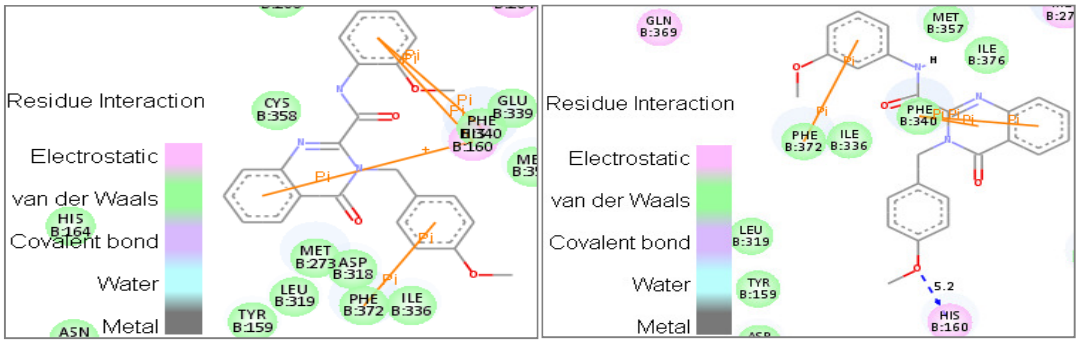

Fig. 105 and 106: QZB-2 and QZB-3 at the active site of PDE4D

The interaction of compound QZB-4 within the active site of PDE4B protein **(Fig. 107)** is mainly contributed by (i) H-bond between the $–OCH_3$ group of the substituted benzyl ring with Asn283 at a distance of 3.8 Á. Whereas, the compound QZB-6 did not show any interaction within the active site of PDE4B protein.**(Fig. 108)**

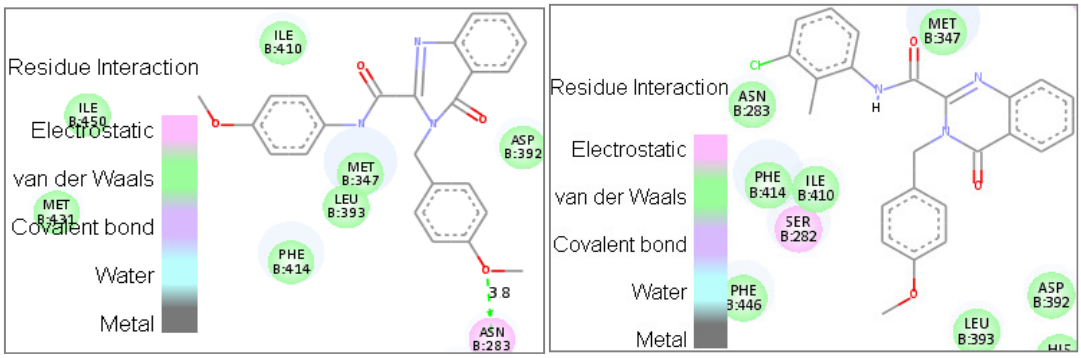

Fig. 107 and 108: QZB-4 and QZB-6 at the active site of PDE4B

Overall, the present 3-(4-methoxybenzyl)-4-oxo-quinazoline-2-carboxamide analogues showed better interactions with PDE4D enzyme exhibiting their inhibitory activity. This indicates that the pharmacophoric elements like the central quinazoline ring with a keto group which acts as a hydrogen bond acceptor (HBA), the benzyl moiety, diverse substituted phenyl ring and the amide linker played a substantial role in forming various interactions within the active site.

5.9.1. ADME properties

The analysis showed that the compound of this series when administered orally might show better intestinal absorption, as well as good blood–brain barrier (BBB) permeability. Their aqueous solubility and drug–likeness properties were envisaged to be very low. In addition, these compounds are likely to inhibit enzyme such as CYP450 *2D6*. Most of these compounds are predicted to be non-hepatotoxic. It was also found that the inhibitor-plasma protein binding is not more than 90%, indicating that these compounds are likely to be less bound to plasma protein present in the blood. **(Table 43)**

Nevertheless, It is a common understanding that ADME profiles are complex to envisage accurately just by *in-silico* and so the envisaged profiles must be utilized with care. For our study, further testing ought to be done to investigate the actual profiles of these compounds as an extension of this work.

In the ADMET plot, since all the molecule are inside the 99% confidence ellipse of BBB and HIA model, the predictions are considered reliable and therefore the BBB and HIA predictions are made for these ligands respectively. **(Fig. 109)**

Table 43: ADME properties of QZB Series

QZB	Aqueous solubility[a]		BBB[b]		CYP450 *2D6*[c]		Hepatotoxicity[d]		HIA[e]		PPB[g]		AlogP98[g]	
	Value	Level	Value	Level	Value	Level	Value	Level	Value	Level	Value	Level	Value	Level
1	-4.850	2	-0.186	2	-5.233	1	-1.036	0	NV[f]	0	3.434	0	3.532	0
2	-4.839	2	-0.332	2	-5.337	1	-1.233	0	NV[f]	0	3.297	0	3.516	0
3	-4.817	2	-0.332	2	-6.629	1	-1.478	0	NV[f]	0	2.783	0	3.516	0
4	-4.794	2	-0.332	2	-6.629	1	-0.552	0	NV[f]	0	0.727	0	3.516	0
5	-5.592	2	0.105	1	-5.051	1	-4.522	1	NV[f]	0	4.573	0	4.475	0
6	-5.569	2	0.105	1	-6.174	1	-2.542	0	NV[f]	0	4.132	0	4.475	0
7	-6.000	2	0.170	1	-5.129	1	-1.536	0	NV[f]	0	5.635	0	4.683	0
8	-5.551	2	0.019	1	-4.071	1	-0.818	0	NV[f]	0	5.343	0	4.197	0
9	-5.540	2	0.019	1	-4.790	1	0.761	0	NV[f]	0	6.213	0	4.197	0
10	-5.529	2	0.019	1	-3.747	1	-0.438	0	NV[f]	0	6.151	0	4.197	0
11	-5.311	2	-0.036	2	-7.147	1	-2.464	0	NV[f]	0	3.651	0	4.019	0
12	-5.300	2	-0.036	2	-6.384	1	-1.333	0	NV[f]	0	4.491	0	4.019	0
13	-5.289	2	-0.036	2	-6.384	1	-2.095	0	NV[f]	0	4.082	0	4.019	0
14	-5.857	2	0.246	1	-5.071	1	-3.851	0	NV[f]	0	4.851	0	4.931	0
15	-5.833	2	0.183	1	-4.923	1	-2.667	0	NV[f]	0	3.802	0	4.727	0
16	-5.765	2	0.183	1	-5.422	1	-0.227	0	NV[f]	0	3.465	0	4.727	0
17	-5.988	2	0.170	1	-5.698	1	-0.725	0	NV[f]	0	5.316	0	4.683	0
18	-5.999	2	0.170	1	-5.043	1	-0.828	0	NV[f]	0	5.605	0	4.683	0
19	-6.011	1	0.170	1	-5.324	1	-0.326	0	NV[f]	0	5.015	0	4.683	0

[a] Level 2 means the aqueous solubility of inhibitor is not very good and its drug-likeness properties are low.
[b] Level 2 means inhibitor has medium ability and Level 1 means inhibitor has high ability to cross the blood-brain barrier (BBB).
[c] Level 1 means inhibitor likely to inhibit CYP*2D6* enzyme.
[d] Level 0 means inhibitor not likely to be hepatotoxic, while Level 1 means inhibitor are likely to be hepatotoxic.
[e] Level 0 means inhibitor has good human intestinal absorption (HIA) after oral administration.
[f] NV means no value was given.
[g] Level 0 means the binding between inhibitor and plasma protein (PPB) is less than 90% (No markers flagged and AlogP98 < 5.0).

ADMET PLOT

The ADMET plot is a 2D chart of ADMET_PSA_2D versus ADMET_AlogP98. The two sets of ellipses are for the prediction confidence space (95% and 99%) for the Blood Brain Barrier Penetration and Human Intestinal Absorption models, respectively.

Since the molecule is outside of the 99% BBB model confidence ellipse, the prediction is considered unreliable and no BBB prediction is made for this ligand.

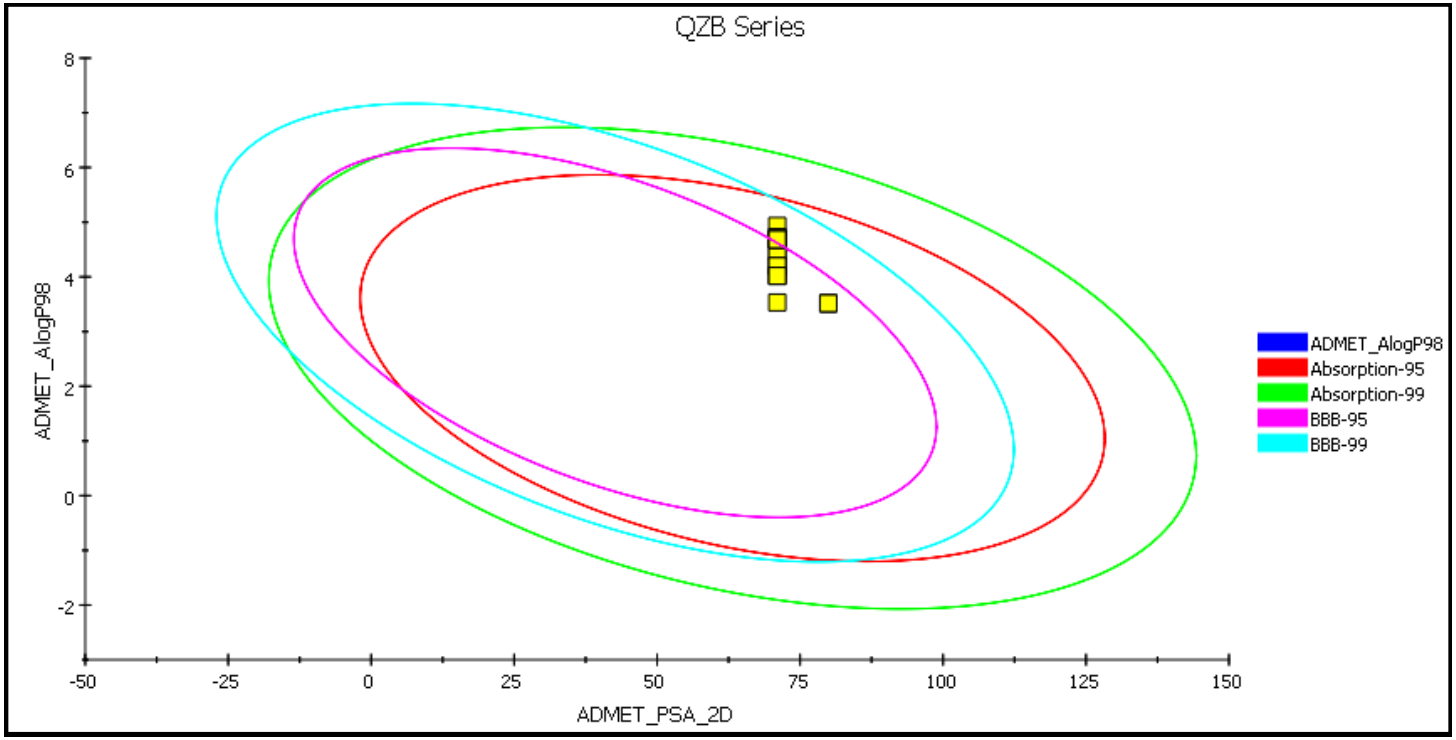

Fig. 109: ADMET Plot for QZB Series

Summary and Conclusions

Based on the novel designed pharmacophore requirement, and the results obtained from docking and ADMET studies, six different series of N4 substituted quinoxaline based carboxamides with variations on linker-1 and/or unsubstituted/substituted hydrophobe, like linker-1 having alkyl group i.e., benzyl (QCA), strong activating group (OCH_3) at para-position i.e., 4-methoxybenzyl (QCB), strong deactivating group (CN) at para-position i.e., 4-cyanobenzyl (QCC), linker-1 having carbonyl group viz., benzoyl (QCD), linker-1 having both alkyl and carbonyl group i.e., 2-phenylacetyl (QCE), linker-1 having increased alkyl chain length i.e., phenethyl (QCF), while two series of N3 substituted quinazoline based carboxamides which are positional isomer of QCA and QCB series viz. benzyl (QZA), 4-methoxybenzyl (QZB) were synthesized and evaluated as PDE4 inhibitors for their anti-depressant and anxiolytic potential.

The aforementioned target quinoxaline-2-carboxamides were synthesized from *o*-phenylenediamine as the starting material, while the quinazoline-2-carboxamides were synthesized from isatoic anhydride in a sequence of reaction. For quinoxaline-2-carboxamides, the starting material was condensed with diethyl ketomalonate and the resultant ester compound was subsequently benzylated under basic condition; then saponified with alkali followed by acidification resulted in the formation of corresponding 4-benzylated quinoxalin-2-carboxylic acid, which on coupling with appropriate amines yielded the 4-quinoxalin-2-carboxamides. For quinazoline-2-carboxamides, the starting material isatoic anhydride in the presence of alkali (like benzyl amine or substituted benzyl amine) underwent cleavage forming *N*-substituted compounds which were subsequently cyclic condensed with diethyl oxalate; then saponified with alkali followed by acidification resulting in 3-benzylated quinazolin-2-carboxylic acid, which on coupling with appropriate amines yielded the 3-benzylated-quinazolin-2-carboxamides.

The purity of the synthesized molecules were assessed by TLC, in at least in two different solvent systems and detected by UV/I_2 chamber using ninhydrin reagent. IR, ^1H NMR and Mass spectral data were used for characterization of the synthesized molecules. The synthesized compounds were further subjected to *in-vitro* assay by PDE4D and PDE4B isoform elisa-kit using fluorescence polarization (FP) principle based on the binding of a fluorescent nucleotide monophosphate generated by PDE4B and PDE4D to the binding agent. Fluorescence intensity was measured at an excitation of 485 nm and an emission of 528 nm using elisa microplate reader. All samples and controls were tested in duplicates and blank values subtracted from all other values. The standard assay protocol was followed as provided by the supplier and the percent activity was calculated for the designed analogues and standard and has been reported.

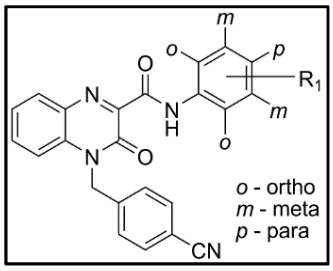

All the synthesized compounds showed varied PDE4 inhibitoryactivity, most of these compounds showed equal affinity for both the isoforms. However, they displayed better PDE4D inhibitory activity as compared to PDE4B. Among different series of quinoxaline-2-carboxamides, QCC series analogues like QCC-5 and QCC-2 containing strong deactivating group i.e., 4-cyanobenzyl substitution at *N4* position exhibited prominent inhibition and better affinity for PDE4D than PDE4B isoform. These moieties could be considered as a lead, and an appropriate modification may possibly enhance the PDE4D selective inhibition and also devoid of its PDE4B inhibitory activity. Rest of the molecules showed better activity but possess equal affinity for both the isoforms (**Table 18**).

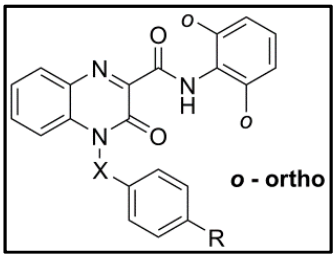

The SAR studies of the analogues synthesized indicate that the substitution at *ortho*-position on the phenyl ring is better tolerated for PDE4D inhibitory activity. These moieties have markedly lower affinity and inhibitory activity for PDE4B isoform. The interactions of these ligands were analyzed inside the binding site and reported.

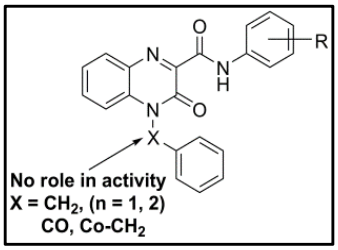

Among the quinoxaline-2-carboxamide series, modification on the linker-1 with alkyl or carbonyl group does not play any crucial role in the activity or affinity. Nevertheless, introduction of both the carbonyl and alkyl group enhance the inhibitory activity for both the isoform and are non-selective.

Among the regioisomeric series, (QCA and QZA) and (QCB and QZB) the quinazoline planar scaffold with HBA is preferred over the quinoxaline scaffold for selective PDE4D isoform inhibition. However, these analogues showed weak inhibitory activity. This indicates that the position of nitrogen and keto group in the planar scaffold including the benzyl group plays a major role in defining the potency andaffinity among the isoform. Among the quinazoline-2-carboxamides, compounds of QZA and QZB series displayed notable affinity for PDE4D but were moderate to weak PDE4 inhibitors (**Table 4 and 38**).

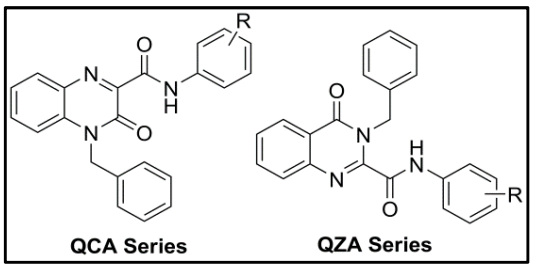

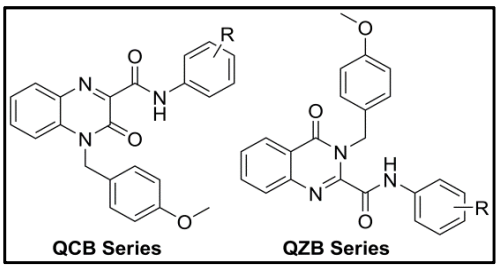

Regardless of their antagonistic potentials, the synthesized molecules (QCA and QCB series) were screened for their anti-depressant potentials by using various rodents' test battery like FST, TST in mice model, etc.; interestingly none of the tested compounds affected the baseline locomotion of mice at tested dose levels. Compounds with better PDE4 inhibition exhibited good anti-depressant-like activity as compared to the vehicle treated group. The compounds with better PDE4 inhibition and significant anti-depressant effects were selected for their anxiolytic study using elevated plus-maze test, L/D model and open field test.

Among the tested moieties in both FST and TST, few compounds (QCA-1, QCA-8, QCA-14, QCA-15, QCB-3, QCB-5, QCB-12 and QCB-15) showed better anti-depressant activity as compared to vehicle treated group. Compounds QCA-1, QCA-8, QCA-11 and QCA-14 exhibited pronounced potential for their anxiolytic like activityas compared to vehicle treated group in EPM. Further, when subjected to open field test (OFT), compounds QCA-1, QCA-8 and QCA-14 exhibited pronounced effect compared to control.

Overall SAR studies of the analogues synthesized indicate that the basic pharmacophoric baggage include a) basic core as flat heterocyclic aromatic region - bicyclic ring containing nitrogen at (1,4) or (1,3) position, b) a hydrogen bond acceptor (HBA) at third or fourth position, c) flexible pendant benzyl ring which fits into the pocket of the binding site along at third or fourth position, d) the phenyl group attached with the amido group on second position. The amido group may also acts as a metabophore. Substitution on this phenyl group is highly preferred on the *ortho*-position for better PDE4D inhibitory activity.

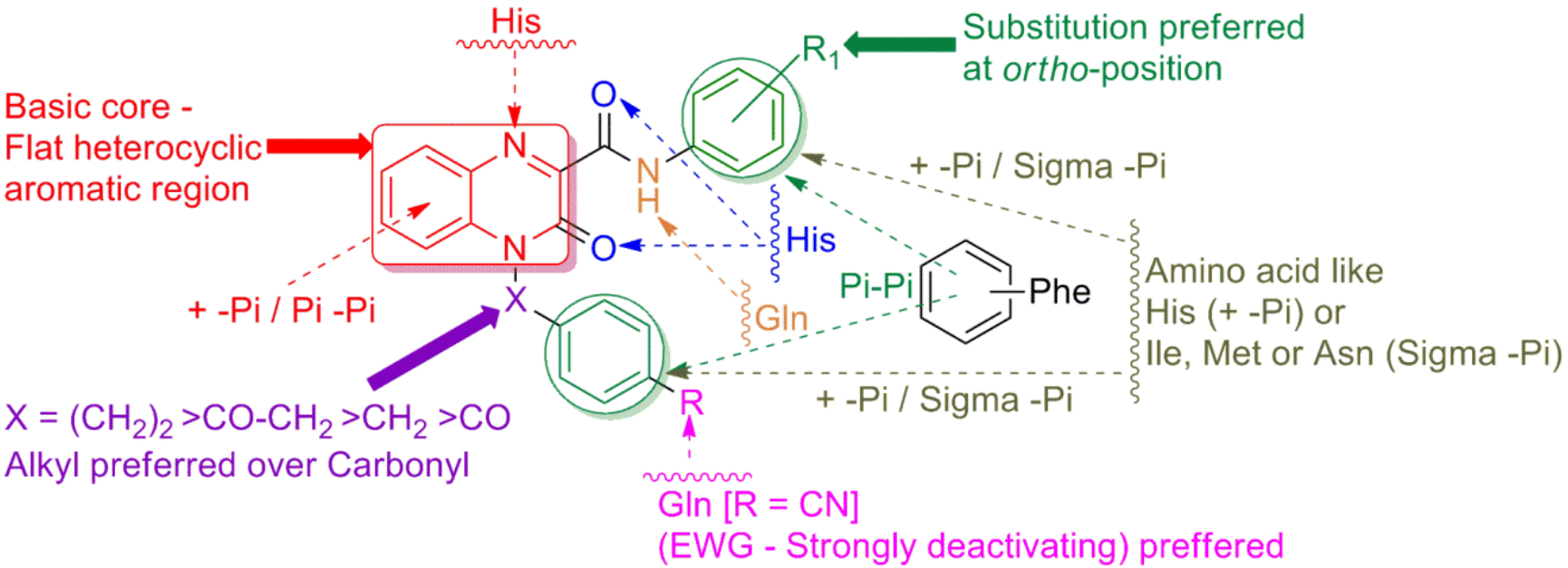

Structural activity relationship of Quinoxaline series – QC(A-F)

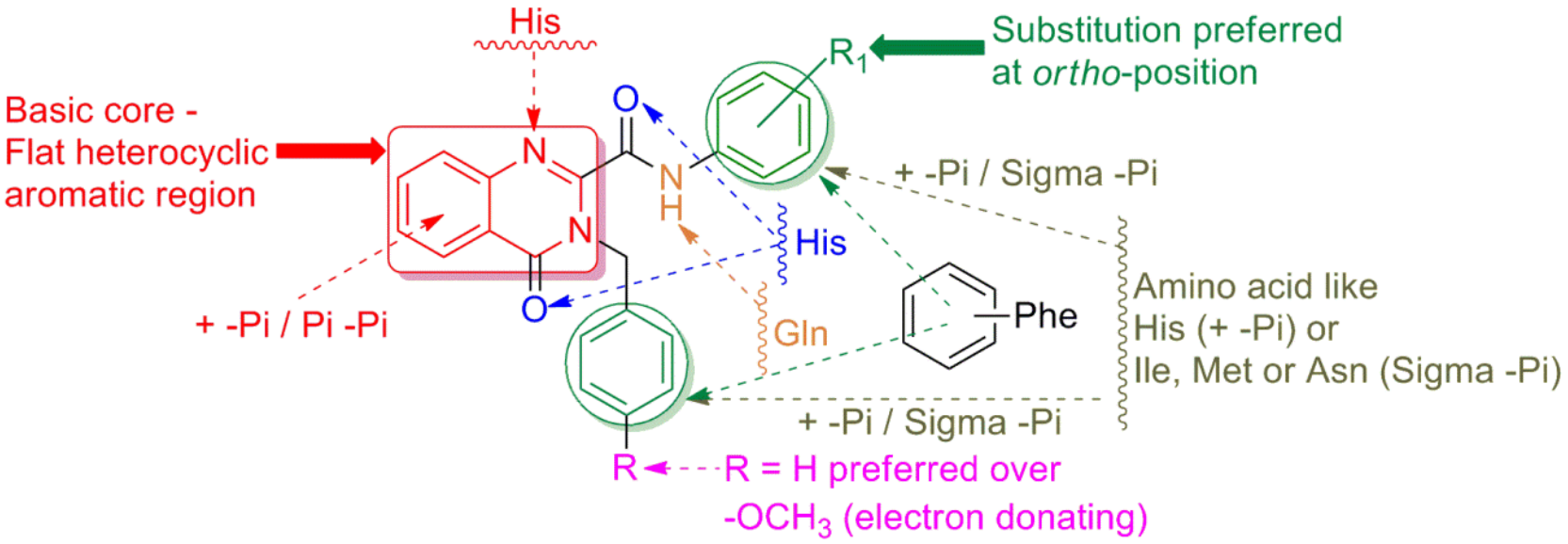

Structural activity relationship of Quinazoline series – QZ(A-B)

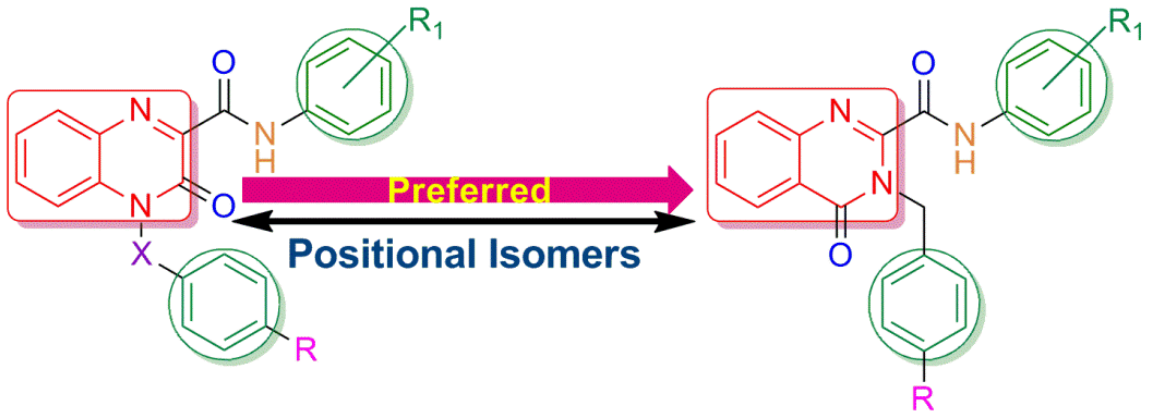

Based on the overall study, the following conclusions were drawn:

1. Among the synthesized moieties most of them showed equal affinity and moderate inhibitory activity for both the isoform.
2. QCC analogues QCC-5, and QCC-17 containing strong deactivating group like cyano at *para*-position of the benzyl ring at *N4* position of the quinoxaline-2-carboxamide exhibited prominent inhibition and better affinity for PDE4D than PDE4B isoform.
3. In QZA series, analogues 4, 14, 6, 7, 10 and 15 exhibited better inhibition and selectivity for PDE4D than 4B.
4. These moieties especially QCC-5 could be considered as a lead, and an appropriate modification may possibly enhance the PDE4D selective inhibition and also devoid of its PDE4B inhibitory activity.
5. Among the regioisomeric series, (QCA and QZA) and (QCB and QZB) the quinazoline planar scaffold with HBA is preferred over the quinoxaline scaffold with HBA for selective PDE4D isoform inhibition.
6. Modification on the linker-1 with alkyl or carbonyl group does not play any crucial role in the activity or affinity, but alkyl is preferred over the carbonyl group.
7. The SAR studies of the analogues synthesized indicate that the substitution at *ortho*-position on the phenyl ring is better tolerated for PDE4D inhibitory activity than for PDE4B isoform.
8. The results obtained from docking studies indicate that these ligands formed key interactions with important amino acids inside the binding pocket.
9. The ADMET profile of the designed ligands were computed to predict a range of drug-like properties and reported
10. The beneficial effect of PDE4 inhibition in depression and anxiety were correlated.

Future scope of work

- To further confirm the role of planar scaffold with HBA for PDE4 inhibitory activity, the core can be further modified by positioning the nitrogen at different positions which could be synthesized and screened for their potential PDE4 inhibitory activity.
- Neurochemical and extensive neuropharmacological evaluation on the promising compounds will be carried out to discover the involvement of monoamine(s) for the anti-depressant and anxiolytic effects.
- Extensive *in-vivo* pharmacological studies are to be carried out on the promising molecules to uncover the exact mechanism implicated for the anti-depressant and anxiolytic potentials.
- Sub-acute and acute toxicological studies on the selected compounds (active molecules) to observe the safety profile are to be carried out.
- Extensive pharmacokinetic profile could be studied on the compounds with good safety margin.

REFERENCES

1. Dousa, T. P., Cyclic-3',5'-nucleotide phosphodiesterase isozymes in cell biology and pathophysiology of the kidney. *Kidney Int.* **1999,***55* (1), 29-62.

2. Self, D. W.; Genova, L. M.; Hope, B. T.; Barnhart, W. J.; Spencer, J. J.; Nestler, E. J., Involvement of cAMP-dependent protein kinase in the nucleus accumbens in cocaine self-administration and relapse of cocaine-seeking behavior. *J. Neuro. Sci.* **1998,***18* (5), 1848-1859.

3. (a) Houslay, M. D.; Milligan, G., Tailoring cAMP-signalling responses through isoform multiplicity. *Trends Biochem. Sci.* **1997,***22* (6), 217-224;(b) Francis, S. H.; Corbin, J. D., Structure and function of cyclic nucleotide-dependent protein kinases. *Annu. Rev. Physiol.* **1994,***56* (1), 237-272;(c) Francis, S. H.; Turko, I. V.; Corbin, J. D., Cyclic nucleotide phosphodiesterases: relating structure and function. In *Prog. Nucleic Acid Res. Mol. Biol.*, Academic Press: **2000**; 65, 1-52;(d) Esposito, K.; Reierson, G. W.; Luo, H. R.; Wu, G. S.; Licinio, J.; Wong, M.-L., Phosphodiesterase genes and antidepressant treatment response: a review. *Ann. Med.* **2009,***41* (3), 177-185.

4. (a) Kresge, N.; Simoni, R. D.; Hill, R. L., Earl W. Sutherland's discovery of cyclic adenine monophosphate and the second messenger system. *J. Biol. Chem.* **2005,***280* (42), e39;(b) Rall, T.; Sutherland, E., Fractionation and characterization of a cyclic adenine ribonucleotide formed by tissue particles. *J. Chem. Biol.* **1958,***232*, 1077-1092.

5. (a) Lohse, M. J.; Nikolaev, V. O.; Hein, P.; Hoffmann, C.; Vilardaga, J.-P.; Bünemann, M., Optical techniques to analyze real-time activation and signaling of G-protein-coupled receptors. *Trends Pharmacol. Sci.* **2008,***29* (3), 159-165;(b) Lohse, M. J.; Maiellaro, I.; Calebiro, D., Kinetics and mechanism of G protein-coupled receptor activation. *Curr. Opin. Cell Biol.* **2014,***27*, 87-93;(c) Hill, S. J.; Williams, C.; May, L. T., Insights into GPCR pharmacology from the measurement of changes in intracellular cyclic AMP; advantages and pitfalls of differing methodologies. *Br. J. Pharmacol.* **2010,***161* (6), 1266-1275;(d) Beavo, J. A.; Brunton, L. L., Cyclic nucleotide research – still expanding after half a century. *Nat. Rev. Mol. Cell Biol.* **2002,***3* (9), 710-718.

6. (a) Bender, A. T.; Beavo, J. A., Cyclic nucleotide phosphodiesterases: molecular regulation to clinical use. *Pharmacol. Rev.* **2006,***58* (3), 488-520;(b) Beavo, J. A., Cyclic nucleotide phosphodiesterases: Functional implications of multiple isoforms. *Physiol. Rev.* **1995,***75* (4), 725-748;(c) Press, N. J.; Banner, K. H., 2. PDE4 Inhibitors - A review of the current field. In *Prog. Med. Chem.*, Lawton, G.; Witty, D. R., Eds. Elsevier: **2009**; 47, 37-74.

7. (a) Soderling, S. H.; Beavo, J. A., Regulation of cAMP and cGMP signaling: new phosphodiesterases and new functions. *Curr. Opin. Cell Biol.* **2000,***12* (2), 174-179;(b) Lau, J. K.-C.; Cheng, Y.-K., An update view on the substrate recognition mechanism of phosphodiesterases: a computational study of PDE10 and PDE4 bound with cyclic nucleotides. *Biopolymers.* **2012,***97* (11), 910-922.

8. (a) Houslay, M. D.; Kolch, W., Cell-type specific integration of cross-talk between extracellular signal-regulated kinase and cAMP signaling. *Mol. Pharmacol.* **2000,***58* (4), 659-668;(b) Conti, M.; Richter, W.; Mehats, C.; Livera, G.; Park, J.-Y.; Jin, C., Cyclic AMP-specific PDE4 phosphodiesterases as critical components of cyclic AMP signaling. *J. Biol. Chem.* **2003,***278* (8), 5493-5496;(c) Zheng, Z.; Zhu, M.; He, Y.; Li, N.; Guo, T.;

Chen, Y.; Wu, J.; Ying, H.; Xie, J., Gene cloning, expression, and characterization of a cyclic nucleotide phosphodiesterase from Arthrobacter sp. CGMCC 3584. *Appl. Biochem. Biotechnol.* **2013,***169* (8), 2442-2456.

9. (a) Hanoune, J.; Defer, N., Regulation and role of adenylyl cyclase isoforms. *Annu. Rev. Pharmacol. Toxicol.* **2001,***41* (1), 145-174;(b) Boswell-Smith, V.; Spina, D.; Page, C. P., Phosphodiesterase inhibitors. *Br. J. Pharmacol.* **2006,***147* (S1), S252-S257.

10. (a) Karin, M., Signal transduction from cell surface to nucleus in development and disease. *FASEB J.* **1992,***6* (8), 2581-2590;(b) Sunahara, R. K.; Taussig, R., Isoforms of mammalian adenylyl cyclase: multiplicities of signaling. *Mol. Interv.* **2002,***2* (3), 168-184;(c) Tang, W.-J.; Hurley, J. H., Catalytic mechanism and regulation of mammalian adenylyl cyclases. *Mol. Pharmacol.* **1998,***54* (2), 231-240;(d) McCahill, A. C.; Huston, E.; Li, X.; Houslay, M. D., PDE4 associates with different scaffolding proteins: modulating interactions as treatment for certain diseases. In *Protein-Protein Interactions as New Drug Targets*, Klussmann, E.; Scott, J., Eds. Springer Berlin Heidelberg: **2008**; 186, 125-166.

11. (a) Zaccolo, M., cAMP signal transduction in the heart: understanding spatial control for the development of novel therapeutic strategies. *Br. J. Pharmacol.* **2009,***158* (1), 50-60;(b) Kritzer, M. D.; Li, J.; Dodge-Kafka, K.; Kapiloff, M. S., AKAPs: The architectural underpinnings of local cAMP signaling. *J. Mol. Cell. Cardiol.* **2012,***52* (2), 351-358.

12. (a) Oldenburger, A.; Maarsingh, H.; Schmidt, M., Multiple facets of cAMP signalling and physiological impact: cAMP compartmentalization in the lung. *Pharmaceuticals.* **2012,***5* (12), 1291-1331;(b) Chen, H.; Wild, C.; Zhou, X.; Ye, N.; Cheng, X.; Zhou, J., Recent advances in the discovery of small molecules targeting exchange proteins directly activated by cAMP (EPAC). *J. Med. Chem.* **2014,***57* (9), 3651-3665;(c) Billington, C. K.; Hall, I. P., Novel cAMP signalling paradigms: therapeutic implications for airway disease. *Br. J. Pharmacol.* **2012,***166* (2), 401-410;(d) Houslay, M. D., Underpinning compartmentalised cAMP signalling through targeted cAMP breakdown. *Trends Biochem. Sci.* **2010,***35* (2), 91-100.

13. (a) McCudden, C. R.; Hains, M. D.; Kimple, R. J.; Siderovski, D. P.; Willard, F. S., G-protein signaling: back to the future. *Cell. Mol. Life Sci.* **2005,***62* (5), 551-577;(b) Edwards, H. V.; Christian, F.; Baillie, G. S., cAMP: novel concepts in compartmentalised signalling. *Semin. Cell Dev. Biol.* **2012,***23* (2), 181-190;(c) Houslay, M. D., Gi-2 at the centre of an active phosphorylation/dephosphorylation cycle in hepatocytes: the fine-tuning of stimulatory and inhibitory inputs into adenylate cyclase in normal and diabetic states. *Cell. Signal.* **1991,***3* (1), 1-9.

14. (a) Latini, S.; Pedata, F., Adenosine in the central nervous system: release mechanisms and extracellular concentrations. *J. Neurochem.* **2001,***79* (3), 463-484;(b) Sudlow, L. C.; Gillette, R., Cyclic AMP levels, adenylyl cyclase activity, and their stimulation by serotonin quantified in intact neurons. *J. Gen. Physiol.* **1997,***110* (3), 243-255.

15. (a) Xu, Y.; Zhang, H.-T.; O'Donnell, J. M., Phosphodiesterases in the central nervous system: implications in mood and cognitive disorders; In *Phosphodiesterases as drug targets*. Francis, S. H.; Conti, M.; Houslay, M. D., Eds. Springer Berlin Heidelberg: **2011**; 204, 447-485;(b) Zhang, H. T., Cyclic AMP-specific phosphodiesterase-4 as a target for the development of antidepressant drugs. *Curr. Pharm. Des.* **2009,***15* (14), 1688-1698.

16. (a) Hebb, A. L. O.; Robertson, H. A., Role of phosphodiesterases in neurological and psychiatric disease. *Curr. Opin. Pharmacol.* **2007,***7* (1), 86-92;(b) Reneerkens, O.; Rutten, K.; Steinbusch, H.; Blokland, A.; Prickaerts, J., Selective phosphodiesterase inhibitors: a promising target for cognition enhancement. *Psychopharmacology.* **2009,***202* (1), 419-443.

17. Malberg, J. E.; Blendy, J. A., Antidepressant action: to the nucleus and beyond. *Trends Pharmacol. Sci.* **2005,***26* (12), 631-638.

18. (a) Ghosh, M.; Pearse, D., Cyclic AMP-specific PDEs: a promising therapeutic target for CNS repair. *Translat.Neurosci.* **2010,***1* (2), 101-105;(b) Menniti, F. S.; Faraci, W. S.; Schmidt, C. J., Phosphodiesterases in the CNS: targets for drug development. *Nat. Rev. Drug Discov.* **2006,***5* (8), 660-670;(c) Wong, M.-L.; Whelan, F.; Deloukas, P.; Whittaker, P.; Delgado, M.; Cantor, R. M.; McCann, S. M.; Licinio, J., Phosphodiesterase genes are associated with susceptibility to major depression and antidepressant treatment response. *Proc. Natl. Acad. Sci.* **2006,***103* (41), 15124-15129.

19. Sinsheimer, R. L.; Koerner, J. F., A purification of venom phosphodiesterase. *J. Biol. Chem.* **1952,***198* (1), 293-296.

20. Thompson, W. J.; Appleman, M. M., Characterization of cyclic nucleotide phosphodiesterases of rat tissues. *J. Biol. Chem.* **1971,***246* (10), 3145-3150.

21. (a) Mika, D.; Leroy, J.; Vandecasteele, G.; Fischmeister, R., PDEs create local domains of cAMP signaling. *J. Mol. Cell. Cardiol.* **2012,***52* (2), 323-329;(b) Beavo, J. A.; Francis, S. H.; Houslay, M. D., *Cyclic nucleotide phosphodiesterases in health and disease*. Taylor & Francis: **2010**.

22. (a) Lugnier, C., Cyclic nucleotide phosphodiesterase (PDE) superfamily: a new target for the development of specific therapeutic agents. *Pharmacol. Ther.* **2006,***109* (3), 366-398;(b) Jeon, Y. H.; Heo, Y. S.; Kim, C. M.; Hyun, Y. L.; Lee, T. G.; Ro, S.; Cho, J. M., Phosphodiesterase: overview of protein structures, potential therapeutic applications and recent progress in drug development. *Cell. Mol. Life Sci.* **2005,***62* (11), 1198-1220.

23. (a) Omori, K.; Kotera, J., Overview of PDEs and their regulation. *Circ. Res.* **2007,***100* (3), 309-327;(b) Houslay, M. D.; Adams, D. R., PDE4 cAMP phosphodiesterases: modular enzymes that orchestrate signalling cross-talk, desensitization and compartmentalization. *Biochem. J.* **2003,***370* (1), 1-18.

24. (a) Soderling, S. H.; Bayuga, S. J.; Beavo, J. A., Identification and characterization of a novel family of cyclic nucleotide phosphodiesterases. *J. Biol. Chem.* **1998,***273* (25), 15553-15558;(b) Dyke, H. J.; Montana, J. G., The therapeutic potential of PDE4 inhibitors. *Expert Opin. Investig. Drugs.* **1999,***8* (9), 1301-1325;(c) Essayan, D. M., Cyclic nucleotide phosphodiesterases. *J. Allergy Clin. Immunol.* **2001,***108* (5), 671-680;(d) Thompson, W. J., Cyclic nucleotide phosphodiesterases: pharmacology, biochemistry and function. *Pharmacol. Ther.* **1991,***51* (1), 13-33;(e) Conti, M.; Nemoz, G.; Sette, C.; Vicini, E., Recent progress in understanding the hormonal regulation of phosphodiesterases. *Endocr. Rev.* **1995,***16* (3), 370-389;(f) Keravis, T.; Lugnier, C., Cyclic nucleotide phosphodiesterase (PDE) isozymes as targets of the intracellular signalling network: benefits of PDE inhibitors in various diseases and perspectives for future therapeutic developments. *Br. J. Pharmacol.* **2012,***165* (5), 1288-1305.

25. (a) Bolger, G.; Michaeli, T.; Martins, T.; St John, T.; Steiner, B.; Rodgers, L.; Riggs, M.; Wigler, M.; Ferguson, K., A family of human phosphodiesterases homologous to the dunce learning and memory gene product of drosophila melanogaster are potential targets for antidepressant drugs. *Mol. Cell. Biol.* **1993,***13* (10), 6558-6571;(b) Beavo, J. A.; Reifsnyder, D. H., Primary sequence of cyclic nucleotide phosphodiesterase isozymes and the design of selective inhibitors. *Trends Pharmacol. Sci.* **1990,***11* (4), 150-155.

26. (a) Maurice, D. H.; Palmer, D.; Tilley, D. G.; Dunkerley, H. A.; Netherton, S. J.; Raymond, D. R.; Elbatarny, H. S.; Jimmo, S. L., Cyclic nucleotide phosphodiesterase activity, expression, and targeting in cells of the cardiovascular system. *Mol. Pharmacol.* **2003,***64* (3), 533-546;(b) Francis, S. H.; Blount, M. A.; Corbin, J. D., Mammalian cyclic nucleotide phosphodiesterases: molecular mechanisms and physiological functions. *Physiol. Rev.* **2011,***91* (2), 651-690.

27. Conti, M.; Beavo, J., Biochemistry and physiology of cyclic nucleotide phosphodiesterases: essential components in cyclic nucleotide signaling. *Annu. Rev. Biochem.* **2007,***76* (1), 481-511.

28. Conti, M.; Mika, D.; Richter, W., Cyclic AMP compartments and signaling specificity: role of cyclic nucleotide phosphodiesterases. *J. Gen. Physiol.* **2014,***143* (1), 29-38.

29. (a) Kapiloff, M. S.; Rigatti, M.; Dodge-Kafka, K. L., Architectural and functional roles of A kinase–anchoring proteins in cAMP microdomains. *J. Gen. Physiol.* **2014,***143* (1), 9-15;(b) Ke, H.; Wang, H., Crystal structures of phosphodiesterases and implications on substrate specificity and inhibitor selectivity. *Curr. Top. Med. Chem.* **2007,***7* (4), 391-403.

30. Card, G. L.; England, B. P.; Suzuki, Y.; Fong, D.; Powell, B.; Lee, B.; Luu, C.; Tabrizizad, M.; Gillette, S.; Ibrahim, P. N.; Artis, D. R.; Bollag, G.; Milburn, M. V.; Kim, S.-H.; Schlessinger, J.; Zhang, K. Y. J., Structural basis for the activity of drugs that inhibit phosphodiesterases. *Structure.* **2004,***12* (12), 2233-2247.

31. (a) Conti, M.; Jin, S. L. C., The molecular biology of cyclic nucleotide phosphodiesterases. In *Prog. Nucleic Acid Res. Mol. Biol.*, Kivie, M., Ed. Academic Press: **1999**; 63, 1-38;(b) Nankervis, J. L.; Feil, S. C.; Hancock, N. C.; Zheng, Z.; Ng, H.-L.; Morton, C. J.; Holien, J. K.; Ho, P. W. M.; Frazzetto, M. M.; Jennings, I. G.; Manallack, D. T.; John Martin, T.; Thompson, P. E.; Parker, M. W., Thiophene inhibitors of PDE4: crystal structures show a second binding mode at the catalytic domain of PDE4D2. *Bioorg. Med. Chem. Lett.* **2011,***21* (23), 7089-7093.

32. Xu, R. X.; Hassell, A. M.; Vanderwall, D.; Lambert, M. H.; Holmes, W. D.; Luther, M. A.; Rocque, W. J.; Milburn, M. V.; Zhao, Y.; Ke, H.; Nolte, R. T., Atomic structure of PDE4: insights into phosphodiesterase mechanism and specificity. *Science.* **2000,***288* (5472), 1822-1825.

33. Wang, H.; Peng, M.-S.; Chen, Y.; Geng, J.; Robinson, H.; Houslay, M. D.; Cai, J.; Ke, H., Structures of the four subfamilies of phosphodiesterase-4 provide insight into the selectivity of their inhibitors. *Biochem. J.* **2007,***408* (2), 193-201.

34. (a) Zhang, K. Y. J.; Card, G. L.; Suzuki, Y.; Artis, D. R.; Fong, D.; Gillette, S.; Hsieh, D.; Neiman, J.; West, B. L.; Zhang, C.; Milburn, M. V.; Kim, S.-H.; Schlessinger, J.; Bollag, G., A glutamine switch mechanism for nucleotide selectivity by phosphodiesterases. *Mol. Cell.* **2004,***15* (2), 279-286;(b) Dym, O.; Xenarios, I.; Ke, H.;

Colicelli, J., Molecular docking of competitive phosphodiesterase inhibitors. *Mol. Pharmacol.* **2002,***61* (1), 20-25;(c) Xu, R. X.; Rocque, W. J.; Lambert, M. H.; Vanderwall, D. E.; Luther, M. A.; Nolte, R. T., Crystal structures of the catalytic domain of phosphodiesterase 4B complexed with AMP, 8-Br-AMP, and rolipram. *J. Mol. Biol.* **2004,***337* (2), 355-365.

35. Neale, D. S.; Thompson, P. E.; White, P. J.; Chalmers, D. K.; Yuriev, E.; Manallack, D. T., Binding mode prediction of PDE4 inhibitors: a comparison of modelling methods. *Aust. J. Chem.* **2010,***63* (3), 396-404.

36. (a) Lee, M. E.; Markowitz, J.; Lee, J.-O.; Lee, H., Crystal structure of phosphodiesterase 4D and inhibitor complex. *FEBS Lett.* **2002,***530* (1–3), 53-58;(b) Wang, H.; Liu, Y.; Chen, Y.; Robinson, H.; Ke, H., Multiple elements jointly determine inhibitor selectivity of cyclic nucleotide phosphodiesterases 4 and 7. *J. Biol. Chem.* **2005,***280* (35), 30949-30955.

37. (a) Baillie, G. S.; Sood, A.; McPhee, I.; Gall, I.; Perry, S. J.; Lefkowitz, R. J.; Houslay, M. D., β-Arrestin-mediated PDE4 cAMP phosphodiesterase recruitment regulates β-adrenoceptor switching from Gs to Gi. *Proc. Natl. Acad. Sci.* **2003,***100* (3), 940-945;(b) Shepherd, M.; McSorley, T.; Olsen, A. E.; Johnston, L. A.; Thomson, N. C.; Baillie, G. S.; Houslay, M. D.; Bolger, G. B., Molecular cloning and subcellular distribution of the novel PDE4B4 cAMP-specific phosphodiesterase isoform. *Biochem. J.* **2003,***370* (2), 429-438.

38. Huai, Q.; Wang, H.; Sun, Y.; Kim, H.-Y.; Liu, Y.; Ke, H., Three-dimensional structures of PDE4D in complex with roliprams and implication on inhibitor selectivity. *Structure.* **2003,***11* (7), 865-873.

39. Baillie, G. S.; Adams, D. R.; Bhari, N.; Houslay, T. M.; Vadrevu, S.; Meng, D.; Li, X.; Dunlop, A.; Milligan, G.; Bolger, G. B.; Klussmann, E.; Houslay, M. D., Mapping binding sites for the PDE4D5 cAMP-specific phosphodiesterase to the N- and C-domains of β-arrestin using spot-immobilized peptide arrays. *Biochem. J.* **2007,***404* (1), 71-80.

40. Huai, Q.; Colicelli, J.; Ke, H., The crystal structure of AMP-bound PDE4 suggests a mechanism for phosphodiesterase catalysis. *Biochemistry.* **2003,***42* (45), 13220-13226.

41. Richter, W.; Conti, M., The oligomerization state determines regulatory properties and inhibitor sensitivity of type 4 cAMP-specific phosphodiesterases. *J. Biol. Chem.* **2004,***279* (29), 30338-30348.

42. (a) Sette, C.; Conti, M., Phosphorylation and activation of a cAMP-specific phosphodiesterase by the cAMP-dependent protein kinase. Involvement of serine 54 in the enzyme activation. *J. Biol. Chem.* **1996,***271* (28), 16526-16534;(b) Huai, Q.; Liu, Y.; Francis, S. H.; Corbin, J. D.; Ke, H., Crystal structures of phosphodiesterases 4 and 5 in complex with inhibitor 3-isobutyl-1-methylxanthine suggest a conformation determinant of inhibitor selectivity. *J. Biol. Chem.* **2004,***279* (13), 13095-13101.

43. Wallace, D. A.; Johnston, L. A.; Huston, E.; MacMaster, D.; Houslay, T. M.; Cheung, Y.-F.; Campbell, L.; Millen, J. E.; Smith, R. A.; Gall, I.; Knowles, R. G.; Sullivan, M.; Houslay, M. D., Identification and characterization of PDE4A11, a novel, widely expressed long isoform encoded by the human PDE4A cAMP phosphodiesterase gene. *Mol. Pharmacol.* **2005,***67* (6), 1920-1934.

44. (a) Houslay, M. D.; Sullivan, M.; Bolgerz, G. B., The multienzyme PDE4 cyclic adenosine monophosphate-specific phosphodiesterase family: intracellular targeting, regulation, and selective inhibition by compounds exerting anti-inflammatory and antidepressant actions. In *Advances in Pharmacology*, J. Thomas August, M. W. A. F. M.; Joseph, T. C., Eds. Academic Press: **1998**; 44, 225-342;(b) Chandrasekaran, A.; Toh, K. Y.; Low, S. H.; Tay, S. K. H.; Brenner, S.; Goh, D. L. M., Identification and characterization of novel mouse PDE4D isoforms: Molecular cloning, subcellular distribution and detection of isoform-specific intracellular localization signals. *Cell. Signal.* **2008,***20* (1), 139-153.

45. (a) Bolger, G. B., Molecular biology of the cyclic AMP-specific cyclic nucleotide phosphodiesterases: A diverse family of regulatory enzymes. *Cell. Signal.* **1994,***6* (8), 851-859;(b) Livi, G. P.; Kmetz, P.; McHale, M. M.; Cieslinski, L. B.; Sathe, G. M.; Taylor, D. P.; Davis, R. L.; Torphy, T. J.; Balcarek, J. M., Cloning and expression of cDNA for a human low-Km, rolipram-sensitive cyclic AMP phosphodiesterase. *Mol. Cell. Biol.* **1990,***10* (6), 2678-2686.

46. Reeves, M. L.; Leigh, B. K.; England, P. J., The identification of a new cyclic nucleotide phosphodiesterase activity in human and guinea-pig cardiac ventricle. Implications for the mechanism of action of selective phosphodiesterase inhibitors. *Biochem. J.* **1987,***241* (2), 535-541.

47. (a) Bolger, G. B.; Rodgers, L.; Riggs, M., Differential CNS expression of alternative mRNA isoforms of the mammalian genes encoding cAMP-specific phosphodiesterases. *Gene.* **1994,***149* (2), 237-244;(b) Bolger, G. B.; Erdogan, S.; Jones, R. E.; Loughney, K.; Scotland, G.; Hoffmann, R.; Wilkinson, I.; Farrell, C.; Houslay, M. D., Characterization of five different proteins produced by alternatively spliced mRNAs from the human cAMP-specific phosphodiesterase PDE4D gene. *Biochem. J.* **1997,***328* (2), 539-548.

48. Burgin, A. B.; Magnusson, O. T.; Singh, J.; Witte, P.; Staker, B. L.; Bjornsson, J. M.; Thorsteinsdottir, M.; Hrafnsdottir, S.; Hagen, T.; Kiselyov, A. S.; Stewart, L. J.; Gurney, M. E., Design of phosphodiesterase 4D (PDE4D) allosteric modulators for enhancing cognition with improved safety. *Nat. Biotechnol.* **2010,***28* (1), 63-70.

49. Altar, C. A.; Vawter, M. P.; Ginsberg, S. D., Target identification for CNS diseases by transcriptional profiling. *Neuropsychopharmacology.* **2008,***34* (1), 18-54.

50. Nakagawa, S.; Kim, J.-E.; Lee, R.; Chen, J.; Fujioka, T.; Malberg, J.; Tsuji, S.; Duman, R. S., Localization of phosphorylated cAMP response element-binding protein in immature neurons of adult hippocampus. *J. Neuro. Sci.* **2002,***22* (22), 9868-9876.

51. (a) Alessandri, A. L.; Sousa, L. P.; Lucas, C. D.; Rossi, A. G.; Pinho, V.; Teixeira, M. M., Resolution of inflammation: Mechanisms and opportunity for drug development. *Pharmacol. Ther.* **2013,***139* (2), 189-212;(b) Pruniaux, M.-P.; Lagente, V.; Ouaged, M.; Bertin, B.; Moreau, F.; Julien-Larose, C.; Rocher, M.-N.; Leportier, C.; Martin, B.; Bouget, A.; Dubuit, J.-P.; Burnouf, C.; Doherty, A. M.; Bertrand, C. P., Relationship between phosphodiesterase type 4 inhibition and anti-inflammatory activity of CI-1044 in rat airways. *Fundam. Clin. Pharmacol.* **2010,***24* (1), 73-82.

52. (a) Izquierdo, I.; Bevilaqua, L. R. M.; Rossato, J. I.; Bonini, J. S.; Medina, J. H.; Cammarota, M., Different molecular cascades in different sites of the brain control memory consolidation. *Trends Neurosci.* **2006,***29* (9), 496-505;(b) Müller, G.; Grey, S.;

Jung, C.; Bandlow, W., Insulin-like signaling in yeast: modulation of protein phosphatase 2A, protein kinase A, cAMP-specific phosphodiesterase, and glycosyl-phosphatidylinositol-specific phospholipase C activities. *Biochemistry.* **2000,***39* (6), 1475-1488.

53. (a) Sartorius, N.; Baghai, T. C.; Baldwin, D. S.; Barrett, B.; Brand, U.; Fleischhacker, W.; Goodwin, G.; Grunze, H.; Knapp, M.; Leonard, B. E., Antidepressant medications and other treatments of depressive disorders: A CINP Task Force report based on a review of evidence. *Int. J. Neuropsychopharmacol.* **2007,***10* (Suppl. 1), 1-207;(b) Li, Y.-F.; Huang, Y.; Amsdell, S. L.; Xiao, L.; O'Donnell, J. M.; Zhang, H.-T., Antidepressant- and anxiolytic-like effects of the phosphodiesterase-4 inhibitor rolipram on behavior depend on cyclic AMP response element binding protein-mediated neurogenesis in the hippocampus. *Neuropsychopharmacology.* **2009,***34* (11), 2404-2419.

54. (a) Pagès, L.; Gavaldà, A.; Lehner, M. D., PDE4 inhibitors: a review of current developments (2005-2009). *Expert Opin. Ther. Pat.* **2009,***19* (11), 1501-1519;(b) Gavalda, A.; Richard, R. S., Phosphodiesterase-4 inhibitors: a review of current developments (2010-2012). *Expert Opin. Ther. Pat.* **2013,***23* (8), 997-1016.

55. Gallant, M.; Aspiotis, R.; Day, S.; Dias, R.; Dubé, D.; Dubé, L.; Friesen, R. W.; Girard, M.; Guay, D.; Hamel, P.; Huang, Z.; Lacombe, P.; Laliberté, S.; Lévesque, J.-F.; Liu, S.; Macdonald, D.; Mancini, J.; Nicholson, D. W.; Styhler, A.; Townson, K.; Waters, K.; Young, R. N.; Girard, Y., Discovery of MK-0952, a selective PDE4 inhibitor for the treatment of long-term memory loss and mild cognitive impairment. *Bioorg. Med. Chem. Lett.* **2010,***20* (22), 6387-6393.

56. Zeller, E.; Stief, H. J.; Pflug, B.; Sastre-y-Hernández, M., Results of a phase II study of the antidepressant effect of rolipram. *Pharmacopsychiatry.* **1984,***17* (6), 188-190.

57. (a) Shpakov, A. O.; Derkach, K. V., The functional state of hormone-sensitive adenylyl cyclase signaling system in diabetes mellitus. *J. Signal Transduct.* **2013,***2013:594213*, 1-16;(b) Shpakov, A.; Derkach, K.; Chistyakova, O.; Sukhov, I.; Shipilov, V.; Bondareva, V., The brain adenylyl cyclase signaling system and cognitive functions in rat with neonatal diabetes under the influence of intranasal serotonin. *J. Metabolic Synd.* **2012,***1* (2), 1-9;(c) García-Osta, A.; Cuadrado-Tejedor, M.; García-Barroso, C.; Oyarzábal, J.; Franco, R., Phosphodiesterases as therapeutic targets for alzheimer's disease. *ACS Chem. Neurosci.* **2012,***3* (11), 832-844.

58. Houslay, M. D.; Schafer, P.; Zhang, K. Y. J., Keynote review: phosphodiesterase-4 as a therapeutic target. *Drug Discov. Today.* **2005,***10* (22), 1503-1519.

59. (a) Kodimuthali, A.; Jabaris, S. S.; Pal, M., Recent advances on phosphodiesterase 4 inhibitors for the treatment of asthma and chronic obstructive pulmonary disease. *J. Med. Chem.* **2008,***51* (18), 5471-5489;(b) Baumer, W.; Hoppmann, J.; Rundfeldt, C.; Kietzmann, M., Highly selective phosphodiesterase 4 inhibitors for the treatment of allergic skin diseases and psoriasis. *Inflamm. Allergy Drug Targets.* **2007,***6* (1), 17-26.

60. Rabe, K. F., Update on roflumilast, a phosphodiesterase 4 inhibitor for the treatment of chronic obstructive pulmonary disease. *Br. J. Pharmacol.* **2011,***163* (1), 53-67.

61. (a) Montana, J. G.; Dyke, H. J., Update on the therapeutic potential of PDE4 inhibitors. *Expert Opin. Investig. Drugs.* **2002,***11* (1), 1-13;(b) Teixeira, M. M.; Gristwood, R. W.; Cooper, N.; Hellewell, P. G., Phosphodiesterase (PDE)4 inhibitors: anti-

inflammatory drugs of the future? *Trends Pharmacol. Sci.* **1997,***18* (5), 164-171;(c) Kelly, V.; Genovese, M., Novel small molecule therapeutics in rheumatoid arthritis. *Rheumatology.* **2013,***52* (7), 1155-1162.

62. Norman, P., PDE4 inhibitors 2001. Patent and literature activity 2000 - September 2001. *Expert Opin. Ther. Pat.* **2002,***12* (1), 93-112.

63. (a) Mehats, C.; Andersen, C. B.; Filopanti, M.; Jin, S. L. C.; Conti, M., Cyclic nucleotide phosphodiesterases and their role in endocrine cell signaling. *Trends Endocrinol. Metab.* **2002,***13* (1), 29-35;(b) Leibowitz, M. D.; Biswas, C.; Brady, E. J.; Conti, M.; Cullinan, C. A.; Hayes, N. S.; Manganiello, V. C.; Saperstein, R.; Wang, L.-h.; Zafian, P. T.; Berger, J., A novel insulin secretagogue is a phosphodiesterase inhibitor. *Diabetes.* **1995,***44* (1), 67-74;(c) Furman, B.; Ong, W.; Pyne, N., Cyclic AMP signaling in pancreatic islets. In *The islets of langerhans*, Islam, M. S., Ed. Springer Netherlands: **2010**; 654, 281-304.

64. Kley, H.-P. Use of PDE4 inhibitors for the treatment of diabetes mellitus. US 7,776,893, 17 Aug., **2010**.

65. (a) Pittenger, C.; Duman, R. S., Stress, depression, and neuroplasticity: a convergence of mechanisms. *Neuropsychopharmacology.* **2007,***33* (1), 88-109;(b) Ayalew, M.; Le-Niculescu, H.; Levey, D. F.; Jain, N.; Changala, B.; Patel, S. D.; Winiger, E.; Breier, A.; Shekhar, A.; Amdur, R.; Koller, D.; Nurnberger, J. I.; Corvin, A.; Geyer, M.; Tsuang, M. T.; Salomon, D.; Schork, N. J.; Fanous, A. H.; O'Donovan, M. C.; Niculescu, A. B., Convergent functional genomics of schizophrenia: from comprehensive understanding to genetic risk prediction. *Mol. Psychiatry.* **2012,***17* (9), 887-905;(c) Thome, J.; Sakai, N.; Shin, K.-H.; Steffen, C.; Zhang, Y.-J.; Impey, S.; Storm, D.; Duman, R. S., cAMP response element-mediated gene transcription is upregulated by chronic antidepressant treatment. *J. Neuro. Sci.* **2000,***20* (11), 4030-4036.

66. (a) Murray, C. J. L.; Lopez, A. D., Alternative projections of mortality and disability by cause 1990–2020: Global burden of disease study. *Lancet.* **1997,***349* (9064), 1498-1504;(b) Nestler, E. J.; Barrot, M.; DiLeone, R. J.; Eisch, A. J.; Gold, S. J.; Monteggia, L. M., Neurobiology of depression. *Neuron.* **2002,***34* (1), 13-25;(c) Catalá-López, F.; Gènova-Maleras, R.; Vieta, E.; Tabarés-Seisdedos, R., The increasing burden of mental and neurological disorders. *Eur. Neuropsychopharmacol.* **2013,***23* (11), 1337-1339;(d) Miret, M.; Ayuso-Mateos, J. L.; Sanchez-Moreno, J.; Vieta, E., Depressive disorders and suicide: epidemiology, risk factors, and burden. *Neurosci. Biobehav. Rev.* **2013,***37* (10, 1), 2372-2374;(e) Albert, P. R.; Benkelfat, C.; Descarries, L., The neurobiology of depression—revisiting the serotonin hypothesis. I. Cellular and molecular mechanisms. *Philos. Trans. R. Soc. B: Biol. Sci.* **2012,***367* (1601), 2378-2381;(f) Wittchen, H. U.; Jacobi, F.; Rehm, J.; Gustavsson, A.; Svensson, M.; Jönsson, B.; Olesen, J.; Allgulander, C.; Alonso, J.; Faravelli, C.; Fratiglioni, L.; Jennum, P.; Lieb, R.; Maercker, A.; van Os, J.; Preisig, M.; Salvador-Carulla, L.; Simon, R.; Steinhausen, H. C., The size and burden of mental disorders and other disorders of the brain in Europe 2010. *Eur. Neuropsychopharmacol.* **2011,***21* (9), 655-679;(g) Krishnan, V.; Nestler, E. J., Linking molecules to mood: new insight into the biology of depression. *Am. J. Psychiatry.* **2010,***167* (11), 1305-1320;(h) Donohue, J.; Pincus, H., Reducing the societal burden of depression. *Pharmacoeconomics.* **2007,***25* (1), 7-24.

67. (a) Manji, H. K.; Drevets, W. C.; Charney, D. S., The cellular neurobiology of depression. *Nat. Med.* **2001,***7* (5), 541-547;(b) Chochinov, H. M.; Wilson, K. G.; Enns, M.; Lander, S., Depression, Hopelessness, and suicidal ideation in the terminally ill. *Psychosomatics.* **1998,***39* (4), 366-370;(c) Dumesnil, H.; Verger, P., Public awareness campaigns about depression and suicide: a review. *Psychiatr. Serv.* **2009,***60* (9), 1203-1213;(d) Dwivedi, Y., Brain-derived neurotrophic factor: role in depression and suicide. *Neuropsychiatr. Dis. Treat.* **2009,***5*, 433-449.

68. Armstrong, G.; Nuken, A.; Samson, L.; Singh, S.; Jorm, A.; Kermode, M., Quality of life, depression, anxiety and suicidal ideation among men who inject drugs in Delhi, India. *BMC Psychiatry.* **2013,***13* (1), 1-11.

69. (a) Stewart, J. W.; McGrath, P. J.; Quitkin, F. M.; Klein, D. F., DSM-IV depression with atypical features: is it valid? *Neuropsychopharmacology.* **2009,***34* (13), 2625-2632;(b) Klein, D. N., Classification of depressive disorders in the DSM-V: proposal for a two-dimension system. *J. Abnorm. Psychol.* **2008,***117* (3), 552-560;(c) Shorter, E., The doctrine of the two depressions in historical perspective. *Acta Psychiatr. Scand.* **2007,***433*, 5-13;(d) Ohmae, S., The difference between depression and melancholia: two distinct conditions that were combined into a single category in DSM-III. *Seishin Shinkeigaku Zasshi.* **2012,***114* (8), 886-905.

70. (a) Manji, H. K.; Duman, R. S., Impairments of neuroplasticity and cellular resilience in severe mood disorders: implications for the development of novel therapeutics. *Psychopharmacol. Bull.* **2001,***35* (2), 5-49;(b) Duman, R., Role of neurotrophic factors in the etiology and treatment of mood disorders. *Neuromol. Med.* **2004,***5* (1), 11-25;(c) Duman, R. S.; Monteggia, L. M., A neurotrophic model for stress-related mood disorders. *Biol. Psychiatry.* **2006,***59* (12), 1116-1127.

71. (a) Dzirasa, K.; Covington, H. E., Increasing the validity of experimental models for depression. *Ann. NY Acad. Sci.* **2012,***1265* (1), 36-45;(b) Post, R., Mechanisms of illness progression in the recurrent affective disorders. *Neurotox. Res.* **2010,***18* (3-4), 256-271.

72. (a) Manji, H. K.; Moore, G. J.; Rajkowska, G.; Chen, G., Neuroplasticity and cellular resilience in mood disorders. *Mol. Psychiatry.* **2000,***5* (6), 578-593;(b) Charney, D. S.; DeJesus, G.; Manji, H. K., Cellular plasticity and resilience and the pathophysiology of severe mood disorders. *Dialogues Clin. Neurosci.* **2004,***6* (2), 217-225;(c) Bachmann, R.; Schloesser, R.; Gould, T.; Manji, H., Mood stabilizers target cellular plasticity and resilience cascades: implications for the development of novel therapeutics. *Mol. Neurobiol.* **2005,***32* (2), 173-202.

73. Miller, G. A.; Rockstroh, B., Endophenotypes in psychopathology research: where do we stand? *Annu. Rev. Clin. Psychol.* **2013,***9*, 177-213.

74. (a) Naismith, S. L.; Norrie, L. M.; Mowszowski, L.; Hickie, I. B., The neurobiology of depression in later-life: clinical, neuropsychological, neuroimaging and pathophysiological features. *Prog. Neurobiol.* **2012,***98* (1), 99-143;(b) Koolschijn, P. C. M. P.; van Haren, N. E. M.; Lensvelt-Mulders, G. J. L. M.; Hulshoff Pol, H. E.; Kahn, R. S., Brain volume abnormalities in major depressive disorder: a meta-analysis of magnetic resonance imaging studies. *Hum. Brain Mapp.* **2009,***30* (11), 3719-3735;(c) Taylor, S. B.; Lewis, C.; Olive, M., The neurocircuitry of illicit psychostimulant addiction: acute and chronic effects in humans. *Subst. Abuse Rehabil.* **2013,***4*, 29-43;(d) Vago, R. D.; Epstein, J.; Catenaccio, E.; Stern, E., Identification of neural targets for the treatment

of psychiatric disorders: the role of functional neuroimaging. *Neurosurg. Clin. N. Am.* **2011,***22* (2), 279-305;(e) Entis, J. J.; Doerga, P.; Barrett, L. F.; Dickerson, B. C., A reliable protocol for the manual segmentation of the human amygdala and its subregions using ultra-high resolution MRI. *Neuroimage.* **2012,***60* (2), 1226-1235;(f) Stockmeier, C. A.; Rajkowska, G., Cellular abnormalities in depression: evidence from postmortem brain tissue. *Dialogues Clin. Neurosci.* **2004,***6* (2), 185-197.

75. (a) Linden, D. E. J., How psychotherapy changes the brain - the contribution of functional neuroimaging. *Mol. Psychiatry.* **2006,***11* (6), 528-538;(b) Drevets, W. C., Orbitofrontal cortex function and structure in depression. *Ann. NY Acad. Sci.* **2007,***1121* (1), 499-527;(c) Rigucci, S.; Serafini, G.; Pompili, M.; Kotzalidis, G. D.; Tatarelli, R., Anatomical and functional correlates in major depressive disorder: the contribution of neuroimaging studies. *World J. Biol. Psychiatry.* **2010,***11* (2_2), 165-180;(d) Berton, O.; Nestler, E. J., New approaches to antidepressant drug discovery: beyond monoamines. *Nat. Rev. Neurosci.* **2006,***7* (2), 137-151;(e) Drevets, W. C., Neuroimaging abnormalities in the amygdala in mood disorders. *Ann. NY Acad. Sci.* **2003,***985* (1), 420-444;(f) Jappe, L. M.; Klimes-Dougan, B.; Cullen, K. R., Brain imaging and the prediction of treatment outcomes in mood and anxiety disorders. In *Functional Brain Mapping and the Endeavor to Understand the Working Brain*, Signorelli, F.; Chirchiglia, D., Eds. InTech: **2013**; 279-300.

76. Pariante, C. M.; Lightman, S. L., The HPA axis in major depression: classical theories and new developments. *Trends Neurosci.* **2008,***31* (9), 464-468.

77. (a) Rush, A. J.; Weissenburger, J. E., Melancholic symptom features and DSM-IV. *Am. J. Psychiatry.* **1994,***151* (4), 489-498;(b) Ozminkowski, R. J.; Musich, S.; Bottone, F. G.; Hawkins, K.; Bai, M.; Unützer, J.; Hommer, C. E.; Migliori, R. J.; Yeh, C. S., The burden of depressive symptoms and various chronic conditions and health concerns on the quality of life among those with Medicare Supplement Insurance. *Int. J. Geriatr. Psychiatry.* **2012,***27* (9), 948-958;(c) Ayuso-Mateos, J. L.; Nuevo, R.; Verdes, E.; Naidoo, N.; Chatterji, S., From depressive symptoms to depressive disorders: the relevance of thresholds. *Br. J. Psychiatry.* **2010,***196* (5), 365-371.

78. (a) Baldwin, D. S.; Pallanti, S.; Zwanzger, P., Developing a European research network to address unmet needs in anxiety disorders. *Neurosci. Biobehav. Rev.* **2013,***37* (10_1), 2312–2317;(b) Haber, S.; Safadi, Z.; Milad, M., Meeting report: “Depression and Anxiety Spectrum disorders: from basic science to the clinic and back”. *Biol. Mood Anxiety Disord.* **2013,***3* (1), 1-9.

79. Yorbik, Ö.; Birmaher, B., Pharmacological treatment of anxiety disorders in children and adolescents. *BCP.* **2003,***13* (3), 133-141.

80. Williams, M., Anxioselective anxiolytics. *J. Med. Chem.* **1983,***26* (5), 619-628.

81. Middeldorp, C. M.; Cath, D. C.; Van Dyck, R.; Boomsma, D. I., The co-morbidity of anxiety and depression in the perspective of genetic epidemiology. A review of twin and family studies. *Psychol. Med.* **2005,***35* (5), 611-624.

82. López-Muñoz, F.; Álamo, C.; García-García, P., The discovery of chlordiazepoxide and the clinical introduction of benzodiazepines: half a century of anxiolytic drugs. *J. Anxiety Disord.* **2011,***25* (4), 554-562.

83. Mitchell, P., The pharmacological treatment of tricyclic-resistant depression: review and management guidelines. *Aust. N Z. J. Psychiatry.* **1987,***21* (4), 442-451.

84. McGlynn, F. D., Research methods in psychopathology. In *Advanced abnormal psychology*, Springer: **1994**; 45-66.

85. (a) Leichsenring, F.; Hiller, W.; Weissberg, M.; Leibing, E., Cognitive-behavioral therapy and psychodynamic psychotherapy: techniques, efficacy, and indications. *Am. J. Psychother.* **2006,***60* (3), 233-259;(b) Stiles, W. B.; Honos-Webb, L.; Surko, M., Responsiveness in psychotherapy. *Clin. Psychol. Sci. Pract.* **1998,***5* (4), 439-458;(c) Prochaska, J. O.; Norcross, J. C., *Systems of psychotherapy: a transtheoretical analysis*. Brooks/Cole Publishing Company: **2013**.

86. Otto, M. W.; Smits, J. A.; Reese, H. E., Combined psychotherapy and pharmacotherapy for mood and anxiety disorders in adults: review and analysis. *FOCUS: The Journal of Lifelong Learning in Psychiatry.* **2006,***4* (2), 204-214.

87. Freud, F., A Psychotherapy for the People. *Contemporary Psychoanalysis.* **2012,***48* (2), 141-165.

88. Holtzheimer, P. E., Advances in the management of treatment-resistant depression. *FOCUS: The Journal of Lifelong Learning in Psychiatry.* **2010,***8* (4), 488-500.

89. Anderson, R. J.; Frye, M. A.; Abulseoud, O. A.; Lee, K. H.; McGillivray, J. A.; Berk, M.; Tye, S. J., Deep brain stimulation for treatment-resistant depression: efficacy, safety and mechanisms of action. *Neurosci. Biobehav. Rev.* **2012,***36* (8), 1920-1933.

90. (a) Popoli, M.; Brunello, N.; Perez, J.; Racagni, G., Second messenger-regulated protein kinases in the brain: their functional role and the action of antidepressant drugs. *J. Neurochem.* **2000,***74* (1), 21-33;(b) Quesseveur, G.; Gardier, A. M.; Guiard, B. P., The monoaminergic tripartite synapse: a putative target for currently available antidepressant drugs. *Curr. Drug Targets.* **2013,***14* (11), 1272-1289;(c) Millan, M. J.; Agid, Y.; Brüne, M.; Bullmore, E. T.; Carter, C. S.; Clayton, N. S.; Connor, R.; Davis, S.; Deakin, B.; DeRubeis, R. J.; Dubois, B.; Geyer, M. A.; Goodwin, G. M.; Gorwood, P.; Jay, T. M.; Joëls, M.; Mansuy, I. M.; Meyer-Lindenberg, A.; Murphy, D.; Rolls, E.; Saletu, B.; Spedding, M.; Sweeney, J.; Whittington, M.; Young, L. J., Cognitive dysfunction in psychiatric disorders: characteristics, causes and the quest for improved therapy. *Nat. Rev. Drug Discov.* **2012,***11* (2), 141-168.

91. Ravindran, A. V.; da Silva, T. L., Complementary and alternative therapies as add-on to pharmacotherapy for mood and anxiety disorders: a systematic review. *J. Affect. Disord.* **2013,***150* (3), 707-719.

92. (a) da Silva, T. L.; Ravindran, L. N.; Ravindran, A. V., Yoga in the treatment of mood and anxiety disorders: A review. *Asian J. Psychiatr.* **2009,***2* (1), 6-16;(b) Pilkington, K.; Kirkwood, G.; Rampes, H.; Richardson, J., Yoga for depression: the research evidence. *J. Affect. Disord.* **2005,***89* (1–3), 13-24.

93. Qureshi, N. A.; Al-Bedah, A. M., Mood disorders and complementary and alternative medicine: a literature review. *Neuropsychiatr. Dis. Treat.* **2013,***9*, 639-658.

94. Emmelkamp, P. M., Behavior therapy with adults. In *Handbook of psychotherapy and behavior change*, 4 ed.; A. E. Bergin & S. L. Garfield, Ed. New York: John Wiley & Sons.: **1994**; 379-427.

95. (a) Gillman, P. K., Tricyclic antidepressant pharmacology and therapeutic drug interactions updated. *Br. J. Pharmacol.* **2007,***151* (6), 737-748;(b) Papakostas, G. I., Augmentation strategies in the treatment of major depressive disorder. Examining the evidence on augmentation with atypical antipsychotics. *CNS Spectr.* **2007,***12* (12 Suppl. 22), 10-12.

96. (a) Cowen, P., Pharmacotherapy for anxiety disorders: drugs available. *Adv. Psychiatr. Treat.* **1997,***3* (2), 66-71;(b) Nash, J.; Nutt, D., Psychopharmacology of anxiety. *Psychiatry.* **2007,***6* (4), 143-148.

97. Schildkraut, J. J., The catecholamine hypothesis of affective disorders: a review of supporting evidence. *Am. J. Psychiatry.* **1965,***122* (5), 509-522.

98. Blier, P., The pharmacology of putative early-onset antidepressant strategies. *Eur. Neuropsychopharmacol.* **2003,***13* (2), 57-66.

99. Kharade, S.; Gumate, D.; Naikwade, N., A review: hypothesis of depression and role of antidepressant drugs. *Int. J. Pharm. Pharm. Sci.* **2010,***2* (Suppl.4), 3-6.

100. Lopez-Munoz, F.; Alamo, C., Monoaminergic neurotransmission: the history of the discovery of antidepressants from 1950s until today. *Curr. Pharm. Des.* **2009,***15* (14), 1563-1586.

101. Blanco, C.; Bragdon, L. B.; Schneier, F. R.; Liebowitz, M. R., The evidence-based pharmacotherapy of social anxiety disorder. *Int. J. Neuropsychopharmacol.* **2013,***16* (1), 235-249.

102. (a) Wimbiscus, M.; Kostenko, O.; Malone, D., MAO inhibitors: Risks, benefits, and lore. *Cleve. Clin. J. Med.* **2010,***77* (12), 859-882;(b) Wang, C.; Billett, E.; Borchert, A.; Kuhn, H.; Ufer, C., Monoamine oxidases in development. *Cell. Mol. Life Sci.* **2013,***70* (4), 599-630.

103. Farach, F. J.; Pruitt, L. D.; Jun, J. J.; Jerud, A. B.; Zoellner, L. A.; Roy-Byrne, P. P., Pharmacological treatment of anxiety disorders: current treatments and future directions. *J. Anxiety Disord.* **2012,***26* (8), 833-843.

104. Liebelt, E. L., An update on antidepressant toxicity: an evolution of unique toxicities to master. *Clin. Pediatr. Emerg. Med.* **2008,***9* (1), 24-34.

105. (a) López-Muñoz, F.; Álamo, C.; Juckel, G.; Assion, H.-J., Half a century of antidepressant drugs: on the clinical introduction of monoamine oxidase inhibitors, tricyclics, and tetracyclics. Part I: monoamine oxidase inhibitors. *J. Clin. Psychopharmacol.* **2007,***27* (6), 555-559;(b) Fangmann, P.; Assion, H.-J.; Juckel, G.; González, C. Á.; López-Muñoz, F., Half a century of antidepressant drugs: on the clinical introduction of monoamine oxidase inhibitors, tricyclics, and tetracyclics. Part II: tricyclics and tetracyclics. *J. Clin. Psychopharmacol.* **2008,***28* (1), 1-4

106. (a) Overall, K. L., Pharmacological treatment in behavioural medicine: the importance of neurochemistry, molecular biology and mechanistic hypotheses. *Vet. J.* **2001,***162* (1), 9-23;(b) Grados, M. A.; Riddle, M. A., Pharmacological treatment of childhood obsessive-compulsive disorder: from theory to practice. *J. Clin. Child Psychol.* **2001,***30* (1), 67-79.

107. Barlow, D. H.; Gorman, J. M.; Shear, M.; Woods, S. W., Cognitive-behavioral therapy, imipramine, or their combination for panic disorder: a randomized controlled trial. *JAMA.* **2000,***283* (19), 2529-2536.

108. Nutt, D. J.; Glue, P., Clinical pharmacology of anxiolytics and antidepressants: a psychopharmacological perspective. *Pharmacol. Ther.* **1989,***44* (3), 309-334.

109. Maubach, K. A.; Rupniak, N. M. J.; Kramer, M. S.; Hill, R. G., Novel strategies for pharmacotherapy of depression. *Curr. Opin. Chem. Biol.* **1999,***3* (4), 481-488.

110. Pacher, P.; Kecskemeti, V., Trends in the development of new antidepressants. Is there a light at the end of the tunnel? *Curr. Med. Chem.* **2004,***11* (7), 925-943.

111. Baldwin, D.; Woods, R.; Lawson, R.; Taylor, D., Efficacy of drug treatments for generalised anxiety disorder: systematic review and meta-analysis. *BMJ.* **2011,***342*, 1-11.

112. Den Boer, J. A.; Bosker, F. J.; Slaap, B. R., Serotonergic drugs in the treatment of depressive and anxiety disorders. *Hum. Psychopharmacol.* **2000,***15* (5), 315-336.

113. (a) Walker, F. R., A critical review of the mechanism of action for the selective serotonin reuptake inhibitors: do these drugs possess anti-inflammatory properties and how relevant is this in the treatment of depression? *Neuropharmacology.* **2013,***67*, 304-317;(b) Greener, M., Beyond serotonin: new approaches to the management of depression. *Prog. Neurol. Psychiatry.* **2013,***17* (4), 23-25.

114. Wensel, T. M.; Powe, K. W.; Cates, M. E., Pregabalin for the treatment of generalized anxiety disorder. *Ann. Pharmacother.* **2012,***46* (3), 424-429.

115. Stahl, S. M., Mechanism of action of serotonin selective reuptake inhibitors: Serotonin receptors and pathways mediate therapeutic effects and side effects. *J. Affect. Disord.* **1998,***51* (3), 215-235.

116. (a) Boyer, E. W.; Shannon, M., The serotonin syndrome. *N. Engl. J. Med.* **2005,***352* (11), 1112-1120;(b) Ener, R. A.; Meglathery, S. B.; Decker, W. A. V.; Gallagher, R. M., Serotonin syndrome and other serotonergic disorders. *Pain Med.* **2003,***4* (1), 63-74.

117. (a) Black, K.; Shea, C.; Dursun, S.; Kutcher, S., Selective serotonin reuptake inhibitor discontinuation syndrome: proposed diagnostic criteria. *J. Psychiatry Neurosci.* **2000,***25* (3), 255-261;(b) Renoir, T., Selective serotonin reuptake inhibitor (SSRI) antidepressant treatment discontinuation syndrome: a review of the clinical evidence and the possible mechanisms involved. *Front. Pharmacol.* **2013,***4:45*, 1-10.

118. (a) Sepede, G.; Corbo, M.; Fiori, F.; Martinotti, G., Reboxetine in clinical practice: a review. *Clin. Ther.* **2012,***163*, e255-262;(b) Whiskey, E.; Taylor, D., A review of the adverse effects and safety of noradrenergic antidepressants. *J. Psychopharmacol.* **2013,***27* (8), 732-739.

119. Horst, W. D.; Preskorn, S. H., Mechanisms of action and clinical characteristics of three atypical antidepressants: venlafaxine, nefazodone, bupropion. *J. Affect. Disord.* **1998,***51* (3), 237-254.

120. Nelson, J. C., Managing treatment-resistant major depression. *J. Clin. Psychiatry.* **2003,***64* (1), 5-12.

121. Pleuvry, B. J., Anxiolytics and hypnotics. *Anaesthesia & Intensive Care Medicine.* **2004,***5* (8), 252-256.

122. (a) Davidson, J. T.; Potts, N.; Richichi, E.; Krishnan, R.; Ford, S. M.; Smith, R.; Wilson, W. H., Treatment of social phobia with clonazepam and placebo. *J. Clin. Psychopharmacol.* **1993,***13* (6), 423-428;(b) Aswar, M. K.; Bidkar, A. A.; Gujar, K. N.; Athawale, T. G., Anxiolytic like effects of leaves extract of Vitex negundo (L)_(Fam:-verbaceae) in Elevated Plus Maze test. *JNR.* **2012,***12* (2), 141-150.

123. Marchand, A.; Todorov, C.; Borgeat, F.; Pelland, M.-E., Effectiveness of a brief cognitive behavioural therapy for panic disorder with agoraphobia and the impact of partner involvement. *Behav. Cogn. Psychother.* **2007,***35* (5), 613-629.

124. (a) Argyropoulos, S. V.; Nutt, D. J., The use of benzodiazepines in anxiety and other disorders. *Eur. Neuropsychopharmacol.* **1999,***9, Supl. 6*, S407-S412;(b) Haller, J., The link between stress and the efficacy of anxiolytics. A new avenue of research. *Physiol. Behav.* **2001,***73* (3), 337-342.

125. (a) Lader, M., Clinical pharmacology of non-benzodiazepine anxiolytics. *Pharmacol. Biochem. Behav.* **1988,***29* (4), 797-798;(b) Young, R.; Urbancic, A.; Emrey, T. A.; Hall, P. C.; Metcalf, G., Behavioral effects of several new anxiolytics and putative anxiolytics. *Eur. J. Pharmacol.* **1987,***143* (3), 361-371.

126. (a) Kennett, G. A.; Dourish, C. T.; Curzon, G., Antidepressant-like action of 5-HT1A agonists and conventional antidepressants in an animal model of depression. *Eur. J. Pharmacol.* **1987,***134* (3), 265-274;(b) Blier, P.; Ward, N. M., Is there a role for 5-HT1A agonists in the treatment of depression? *Biol. Psychiatry.* **2003,***53* (3), 193-203.

127. Sivaraman, P.; Curran, S.; Musa, S., 5 - Hypnosedatives and anxiolytics. In *Side Effects of Drugs Annual*, Aronson, J. K., Ed. Elsevier: **2012**; 34, 45-50.

128. Blier, P.; Bergeron, R.; de Montigny, C., Selective activation of postsynaptic 5-HT1A receptors induces rapid antidepressant response. *Neuropsychopharmacology.* **1997,***16* (5), 333-338.

129. Angrini, M.; Leslie, J. C.; Shephard, R. A., Effects of propranolol, buspirone, pCPA, reserpine, and chlordiazepoxide on open-field behavior. *Pharmacol. Biochem. Behav.* **1998,***59* (2), 387-397.

130. Baldwin, D. S.; Anderson, I. M.; Nutt, D. J.; Bandelow, B.; Bond, A.; Davidson, J. R.; den Boer, J. A.; Fineberg, N. A.; Knapp, M.; Scott, J., Evidence-based guidelines for the pharmacological treatment of anxiety disorders: recommendations from the British Association for Psychopharmacology. *J. Psychopharmacol.* **2005,***19* (6), 567-596.

131. Argyropoulos, S. V.; Sandford, J. J.; Nutt, D. J., The psychobiology of anxiolytic drug. Part 2: Pharmacological treatments of anxiety. *Pharmacol. Ther.* **2000,***88* (3), 213-227.

132. (a) Najjar, F.; Weller, R.; Weisbrot, J.; Weller, E., Post-traumatic stress disorder and its treatment in children and adolescents. *Curr. Psychiatry Rep.* **2008,***10* (2), 104-108;(b) Kaminer, D.; Seedat, S.; Stein, D. J., Post-traumatic stress disorder in children. *World Psychiatry.* **2005,***4* (2), 121-125.

133. (a) Gupta, S.; Popli, A.; Bathurst, E.; Hennig, L.; Droney, T.; Keller, P., Efficacy of cyproheptadine for nightmares associated with posttraumatic stress disorder. *Compr. Psychiatry.* **1998,***39* (3), 160-164;(b) Albucher, R. C.; Liberzon, I., Psychopharmacological treatment in PTSD: a critical review. *J. Psychiatr. Res.* **2002,***36* (6), 355-367.

134. Thase, M. E.; Howland, R. H.; Friedman, E. S., Treating antidepressant nonresponders with augmentation strategies: an overview. *J. Clin. Psychiatry.* **1998,***59* (Suppl. 5:5-12), 13-15.

135. Blier, P., Pharmacology of rapid-onset antidepressant treatment strategies. *J. Clin. Psychiatry.* **2001,***62* (Suppl.15), 12-17.

136. Lucas, G., Fast-acting antidepressants: are we nearly there? *Expert Rev. Neurother.* **2007,***8* (1), 1-3.

137. Newhouse, P. A.; Kelton, M., Nicotinic systems in central nervous systems disease: degenerative disorders and beyond. *Pharm. Acta Helv.* **2000,***74* (2-3), 91-101.

138. (a) Schmidt, H. D.; Duman, R. S., Peripheral BDNF produces antidepressant-like effects in cellular and behavioral models. *Neuropsychopharmacology.* **2010,***35* (12), 2378-2391;(b) Duman, R. S.; Li, N.; Liu, R.-J.; Duric, V.; Aghajanian, G., Signaling pathways underlying the rapid antidepressant actions of ketamine. *Neuropharmacology.* **2012,***62* (1), 35-41.

139. (a) Yirmiya, R.; Goshen, I., Immune modulation of learning, memory, neural plasticity and neurogenesis. *Brain Behav. Immun.* **2011,***25* (2), 181-213;(b) Day, J. J.; Sweatt, J. D., Cognitive neuroepigenetics: a role for epigenetic mechanisms in learning and memory. *Neurobiol. Learn. Mem.* **2011,***96* (1), 2-12;(c) Dubnau, J.; Tully, T., Gene discovery in Drosophila: new insights for learning and memory. *Annu. Rev. Neurosci.* **1998,***21* (1), 407-444;(d) Silva, A. J.; Kogan, J. H.; Frankland, P. W.; Kida, S., CREB and memory. *Annu. Rev. Neurosci.* **1998,***21* (1), 127-148.

140. (a) Kandel, E. R., The molecular biology of memory: cAMP, PKA, CRE, CREB-1, CREB-2, and CPEB. *Mol. Brain.* **2012,***5* (14), 1-12;(b) Duman, R. S.; Heninger, G. R.; Nestler, E. J., A molecular and cellular theory of depression. *Arch Gen. Psychiatry.* **1997,***54* (7), 597-606;(c) Gelowitz, D. L.; Berger, S. P., Signal transduction mechanisms and behavioral sensitization to stimulant drugs: an overview of cAMP and PLA2. *J. Addict. Dis.* **2001,***20* (3), 33-42.

141. Mathew, S. J.; Manji, H. K.; Charney, D. S., Novel drugs and therapeutic targets for severe mood disorders. *Neuropsychopharmacology.* **2008,***33* (9), 2080-2092.

142. Van der Mey, M.; Hatzelmann, A.; Van der Laan, I. J.; Sterk, G. J.; Thibaut, U.; Timmerman, H., Novel selective PDE4 inhibitors. 1. Synthesis, structure-activity relationships, and molecular modeling of 4-(3,4-dimethoxyphenyl)-2H-phthalazin-1-ones and analogues. *J. Med. Chem.* **2001,***44* (16), 2511-2522.

143. Schwabe, U.; Miyake, M.; Ohga, Y.; Daly, J. W., 4-(3-Cyclopentyloxy-4-methoxyphenyl)-2-pyrrolidone (ZK 62711): a potent inhibitor of adenosine cyclic 3',5'-monophosphate phosphodiesterases in homogenates and tissue slices from rat brain. *Mol. Pharmacol.* **1976,***12* (6), 900-910.

144. (a) Komas, N.; Lugnier, C.; Bec, A. L.; Gal, C. S.-L.; Barthélémy, G.; Stoclet, J. C., Differential sensitivity to cardiotonic drugs of cyclic AMP phosphodiesterases isolated from canine ventricular and sinoatrial-enriched tissues. *J. Cardiovasc. Pharmacol.* **1989,***14* (2), 213-220;(b) Lugnier, C.; Schoeffter, P.; Le Bec, A.; Strouthou, E.; Stoclet, J. C., Selective inhibition of cyclic nucleotide phosphodiesterases of human, bovine and rat aorta. *Biochem. Pharmacol.* **1986,***35* (10), 1743-1751;(c) Lugnier, C.; Stierlé, A.; Beretz, A.; Schoeffter, P.; Lebec, A.; Wermuth, C.-G.; Cazenave, J.-P.; Stoclet, J.-C., Tissue and substrate specificity of inhibition by alkoxy-aryl-lactams of platelet and arterial smooth muscle cyclic nucleotide phosphodiesterases relationship to pharmacological activity. *Biochem. Biophys. Res. Commun.* **1983,***113* (3), 954-959.

145. Dinter, H.; Tse, J.; Halks-Miller, M.; Asarnow, D.; Onuffer, J.; Faulds, D.; Mitrovic, B.; Kirsch, G.; Laurent, H.; Esperling, P., The type IV phosphodiesterase specific inhibitor mesopram inhibits experimental autoimmune encephalomyelitis in rodents. *J. Neuroimmunol.* **2000,***108* (1), 136-146.

146. (a) Brackeen, M. F.; Stafford, J. A.; Cowan, D. J.; Brown, P. J.; Domanico, P. L.; Feldman, P. L.; Rose, D.; Strickland, A. B.; Veal, J. M.; Verghese, M., Design and synthesis of conformationally constrained analogs of 4-(3-Butoxy-4-methoxybenzyl)imidazolidin-2-one (Ro 20-1724) as potent inhibitors of cAMP-specific phosphodiesterase. *J. Med. Chem.* **1995,***38* (24), 4848-4854;(b) Torphy, T. J.; Undem, B., Phosphodiesterase inhibitors: new opportunities for the treatment of asthma. *Thorax.* **1991,***46* (7), 512-523.

147. (a) Gruenman, V.; Hoffer, M. N-[(1-cyano-2-phenyl) ethyl] carbamates. US Patent 3,923,833, 2 Dec., **1975**;(b) Sheppard, H.; Wiggan, G., Analogues of 4-(3,4-dimethoxybenzyl)-2-imidazolidinone as potent inhibitors of rat erythrocyte adenosine cyclic 3',5'-phosphate phosphodiesterase. *Mol. Pharmacol.* **1971,***7* (1), 111-115.

148. Christensen, S. B.; Torphy, T. J., Isozyme-selective phosphodiesterase inhibitors as antiasthmatic agents. *Annu. Rep. Med. Chem.* **1994,***29*, 185-194.

149. Hatzelmann, A.; Schudt, C., Anti-inflammatory and immunomodulatory potential of the novel PDE4 inhibitor roflumilast in vitro. *J. Pharmacol. Exp. Ther.* **2001,***297* (1), 267-279.

150. Giembycz, M. A.; Field, S. K., Roflumilast: first phosphodiesterase 4 inhibitor approved for treatment of COPD. *Drug Des. Devel. Ther.* **2010,***2010* (4), 147-158.

151. Rhee, C. K.; Kim, J. H.; Sub, B.-C.; Xiang, M. X.; Youn, Y. S.; Bang, W. Y.; Kim, E.; Shin, J. K.; Lee, Y., Synthesis and biological studies of catechol ether type derivatives as potential phosphodiesterase (PDE) IV inhibitors. *Arch. Pharm. Res.* **1999,***22* (2), 202-207.

152. Christensen, S. B.; Guider, A.; Forster, C. J.; Gleason, J. G.; Bender, P. E.; Karpinski, J. M.; DeWolf, W. E.; Barnette, M. S.; Underwood, D. C.; Griswold, D. E.; Cieslinski, L. B.; Burman, M.; Bochnowicz, S.; Osborn, R. R.; Manning, C. D.; Grous, M.; Hillegas, L. M.; Bartus, J. O. L.; Ryan, M. D.; Eggleston, D. S.; Haltiwanger, R. C.; Torphy, T. J., 1,4-Cyclohexanecarboxylates: potent and selective inhibitors of phosophodiesterase 4 for the treatment of asthma. *J. Med. Chem.* **1998,***41* (6), 821-835.

153. Regan, J.; Bruno, J.; McGarry, D.; Poli, G.; Hanney, B.; Bower, S.; Travis, J.; Sweeney, D.; Miller, B.; Souness, J.; Djuric, S., 2-Substituted-4-methoxybenzimidazole-based PDE4 inhibitors. *Bioorg. Med. Chem. Lett.* **1998,***8* (19), 2737-2742.

154. Kleinman, E. F.; Campbell, E.; Giordano, L. A.; Cohan, V. L.; Jenkinson, T. H.; Cheng, J. B.; Shirley, J. T.; Pettipher, E. R.; Salter, E. D.; Hibbs, T. A.; DiCapua, F. M.; Bordner, J., Striking effect of hydroxamic acid substitution on the phosphodiesterase type 4 (PDE4) and TNF alpha inhibitory activity of two series of rolipram analogues: implications for a new active site model of PDE4. *J. Med. Chem.* **1998,***41* (3), 266-270.

155. Bacher, E.; Boer, C.; Bray-French, K.; Demnitz, F. W. J.; Keller, T. H.; Mazzoni, L.; Müller, T.; Walker, C., N-Arylrolipram derivatives as potent and selective PDE4 inhibitors. *Bioorg. Med. Chem. Lett.* **1998,***8* (22), 3229-3234.

156. Li, C.; Chauret, N.; Trimble, L. A.; Nicoll-Griffith, D. A.; Silva, J. M.; MacDonald, D.; Perrier, H.; Yergey, J. A.; Parton, T.; Alexander, R. P.; Warrellow, G. J., Investigation of the in vitro metabolism profile of a phosphodiesterase-IV inhibitor, CDP-840: leading to structural optimization. *Drug Metab. Dispos.* **2001,***29* (3), 232-241.

157. Hughes, B.; Owens, R.; Perry, M.; Warrellow, G.; Allen, R., PDE 4 inhibitors: the use of molecular cloning in the design and development of novel drugs. *Drug Discov. Today.* **1997,***2* (3), 89-101.

158. Perry, M. J.; O'Connell, J.; Walker, C.; Crabbe, T.; Baldock, D.; Russell, A.; Lumb, S.; Huang, Z.; Howat, D.; Allen, R.; Merriman, M.; Walls, J.; Daniel, T.; Hughes, B.; Laliberte, F.; Higgs, G. A.; Owens, R. J., CDP840: a novel inhibitor of PDE-4. *Cell Biochem. Biophys.* **1998,***29* (1-2), 113-132.

159. Guay, D.; Hamel, P.; Blouin, M.; Brideau, C.; Chan, C. C.; Chauret, N.; Ducharme, Y.; Huang, Z.; Girard, M.; Jones, T. R.; Laliberté, F.; Masson, P.; McAuliffe, M.; Piechuta, H.; Silva, J.; Young, R. N.; Girard, Y., Discovery of L-791,943: a potent, selective, non emetic and orally active phosphodiesterase-4 inhibitor. *Bioorg. Med. Chem. Lett.* **2002,***12* (11), 1457-1461.

160. Frenette, R.; Blouin, M.; Brideau, C.; Chauret, N.; Ducharme, Y.; Friesen, R. W.; Hamel, P.; Jones, T. R.; Laliberté, F.; Li, C.; Masson, P.; McAuliffe, M.; Girard, Y., Substituted 4-(2,2-diphenylethyl)pyridine-N-oxides as phosphodiesterase-4 inhibitors: SAR study directed toward the improvement of pharmacokinetic parameters. *Bioorg. Med. Chem. Lett.* **2002,***12* (20), 3009-3013.

161. Côté, B.; Frenette, R.; Prescott, S.; Blouin, M.; Brideau, C.; Ducharme, Y.; Friesen, R. W.; Laliberté, F.; Masson, P.; Styhler, A.; Girard, Y., Substituted aminopyridines as potent and selective phosphodiesterase-4 inhibitors. *Bioorg. Med. Chem. Lett.* **2003,***13* (4), 741-744.

162. Hulme, C.; Poli, G. B.; Fu-Chih, H.; Souness, J. E.; Djuric, S. W., Quaternary substituted PDE4 inhibitors I: the synthesis and in vitro evaluation of a novel series of oxindoles. *Bioorg. Med. Chem. Lett.* **1998,***8* (2), 175-178.

163. Hulme, C.; Moriarty, K.; Huang, F.-C.; Mason, J.; McGarry, D.; Labaudiniere, R.; Souness, J.; Djuric, S., Quaternary substituted PDE IV inhibitors II: the synthesis and in vitro evaluation of a novel series of γ-lactams. *Bioorg. Med. Chem. Lett.* **1998,***8* (4), 399-404.

164. Hulme, C.; Moriarty, K.; Miller, B.; Mathew, R.; Ramanjulu, M.; Cox, P.; Souness, J.; Page, K. M.; Uhl, J.; Travis, J.; Huang, F.-c.; Labaudiniere, R.; Djuric, S. W., The synthesis and biological evaluation of a novel series of indole PDE4 inhibitors I. *Bioorg. Med. Chem. Lett.* **1998,***8* (14), 1867-1872.

165. Marfat, A. Therapeutically active compounds based on indazole bioisostere replacement of catechol in PDE4 inhibitors. US 2002/0058687, 16 May., **1998**.

166. Stafford, J. A.; Feldman, P. L.; Marron, B. E.; Schoenen, F. J.; Valvano, N. L.; Unwalla, R. J.; Domanico, P. L.; Brawley, E. S.; Leesnitzer, M. A.; Rose, D. A.; Dougherty, R. W., Structure-activity relationships involving the catechol subunit of rolipram. *Bioorg. Med. Chem. Lett.* **1994,***4* (15), 1855-1860.

167. (a) Buckley, G.; Cooper, N.; Dyke, H. J.; Galleway, F.; Gowers, L.; Gregory, J. C.; Hannah, D. R.; Haughan, A. F.; Hellewell, P. G.; Kendall, H. J.; Lowe, C.; Maxey, R.; Montana, J. G.; Naylor, R.; Picken, C. L.; Runcie, K. A.; Sabin, V.; Tuladhar, B. R.; Warneck, J. B., 7-Methoxybenzofuran-4-carboxamides as PDE 4 inhibitors: a potential treatment for asthma. *Bioorg. Med. Chem. Lett.* **2000,***10* (18), 2137-40;(b) McGarry, D. G.; Regan, J. R.; Volz, F. A.; Hulme, C.; Moriarty, K. J.; Djuric, S. W.; Souness, J. E.; Miller, B. E.; Travis, J. J.; Sweeney, D. M., Benzofuran based PDE4 inhibitors. *Bioorg. Med. Chem.* **1999,***7* (6), 1131-1139.

168. Buckley, G. M.; Cooper, N.; Davenport, R. J.; Dyke, H. J.; Galleway, F. P.; Gowers, L.; Haughan, A. F.; Kendall, H. J.; Lowe, C.; Montana, J. G.; Oxford, J.; Peake, J. C.; Picken, C. L.; Richard, M. D.; Sabin, V.; Sharpe, A.; Warneck, J. B. H., 7-Methoxyfuro[2,3-c]pyridine-4-carboxamides as PDE4 inhibitors: A potential treatment for asthma. *Bioorg. Med. Chem. Lett.* **2002,***12* (3), 509-512.

169. Montana, J. G.; Buckley, G. M.; Cooper, N.; Dyke, H. J.; Gowers, L.; Gregory, J. P.; Hellewell, P. G.; Kendall, H. J.; Lowe, C.; Maxey, R.; Miotla, J.; Naylor, R. J.; Runcie, K. A.; Tuladhar, B.; Warneck, J. B. H., Aryl sulfonamides as selective PDE4 inhibitors. *Bioorg. Med. Chem. Lett.* **1998,***8* (19), 2635-2640.

170. (a) Nielson, S. F. Benzodioxole or benzodioxepine heterocyclic compounds as phosphodiesterase inhibitors. US 2013/0123291, 16 May., **2011**;(b) Nielsen, S. F.; Horneman, A. M.; Lau, J.; Larsen, J. C. H. Biaryl phosphodiesterase inhibitors. US 2013/0059853, 7 Mar., **2011**.

171. Schudt, C.; Winder, S.; Müller, B.; Ukena, D., Zardaverine as a selective inhibitor of phosphodiesterase isozymes. *Biochem. Pharmacol.* **1991,***42* (1), 153-162.

172. (a) Macor, J. E., *Annual Reports in Medicinal Chemistry*. Elsevier Science, Academic Press: **2011**;(b) Kümmerle, A. E.; Schmitt, M.; Cardozo, S. V. S.; Lugnier, C.; Villa, P.; Lopes, A. B.; Romeiro, N. C.; Justiniano, H.; Martins, M. A.; Fraga, C. A. M.; Bourguignon, J.-J.; Barreiro, E. J., Design, synthesis, and pharmacological evaluation of N-acylhydrazones and novel conformationally constrained compounds as selective and potent orally active phosphodiesterase-4 inhibitors. *J. Med. Chem.* **2012,***55* (17), 7525-7545.

173. Cheng, J. B.; Cooper, K.; Duplantier, A. J.; Eggler, J. F.; Kraus, K. G.; Marshall, S. C.; Marfat, A.; Masamune, H.; Shirley, J. T.; Tickner, J. E.; Umland, J. P., Synthesis and in vitro profile of a novel series of catechol benzimidazoles. The discovery of potent,

selective phosphodiesterase type IV inhibitors with greatly attenuated affinity for the [3H]rolipram binding site. *Bioorg. Med. Chem. Lett.* **1995,***5* (17), 1969-1972.

174. (a) Cohan, V. L.; Showell, H. J.; Fisher, D. A.; Pazoles, C. J.; Watson, J. W.; Turner, C. R.; Cheng, J. B., In vitro pharmacology of the novel phosphodiesterase type 4 inhibitor, CP-80633. *J. Pharmacol. Exp. Ther.* **1996,***278* (3), 1356-1361;(b) Turner, C. R.; Cohan, V. L.; Cheng, J. B.; Showell, H. J.; Pazoles, C. J.; Watson, J. W., The in vivo pharmacology of CP-80, 633, a selective inhibitor of phosphodiesterase 4. *J. Pharmacol. Exp. Ther.* **1996,***278* (3), 1349-1355.

175. Lombardo, L. J. Oxime-carbamates and oxime-carbonates as bronchodilators and anti-inflammatory agents. 5,124,455, 23 Jun., **1992**.

176. Ho, P. P. K.; Bertsch, B.; Esterman, M.; Panetta, J. A., Tibenelast, 5,6-diethoxybenzo (B) thiophebe-2-carboxylic acid, sodium salt (LY 186655), is an orally active anti-asthma compound in the guinea pig. *Life Sci.* **1990,***46* (13), 917-925.

177. Duplantier, A. J.; Biggers, M. S.; Chambers, R. J.; Cheng, J. B.; Cooper, K.; Damon, D. B.; Eggler, J. F.; Kraus, K. G.; Marfat, A.; Masamune, H.; Pillar, J. S.; Shirley, J. T.; Umland, J. P.; Watson, J. W., Biarylcarboxylic acids and -amides: inhibition of phosphodiesterase type IV versus [3H]rolipram binding activity and their relationship to emetic behavior in the ferret. *J. Med. Chem.* **1996,***39* (1), 120-125.

178. Bickston, S. J.; Snider, K. R.; Kappus, M. R., Tetomilast: new promise for phosphodiesterase-4 inhibitors? *Expert Opin. Investig. Drugs.* **2012,***21* (12), 1845-1849.

179. Matera, M. G.; Page, C. P.; Cazzola, M., Novel bronchodilators for the treatment of chronic obstructive pulmonary disease. *Trends Pharmacol. Sci.* **2011,***32* (8), 495-506.

180. Barnette, M. S.; Christensen, S. B.; Essayan, D. M.; Grous, M.; Prabhakar, U.; Rush, J. A.; Kagey-Sobotka, A.; Torphy, T. J., SB 207499 (Ariflo), a potent and selective second-generation phosphodiesterase 4 inhibitor: in-vitro anti-inflammatory actions. *J. Pharmacol. Exp. Ther.* **1998,***284* (1), 420-426.

181. Schmidt, D.; Dent, G.; Rabe, K. F., Selective phosphodiesterase inhibitors for the treatment of bronchial asthma and chronic obstructive pulmonary disease. *Clin. Exp. Allergy.* **1999,***29* (Suppl. 2), 99-109.

182. Pinto, I. L.; Buckle, D. R.; Readshaw, S. A.; Smith, D. G., The selective inhibition of phosphodiesterase IV by benzopyran derivatives of rolipram. *Bioorg. Med. Chem. Lett.* **1993,***3* (8), 1743-1746.

183. Marivet, M. C.; Bourguignon, J. J.; Lugnier, C.; Mann, A.; Stoclet, J. C.; Wermuth, C. G., Inhibition of cyclic adenosine-3',5'-monophosphate phosphodiesterase from vascular smooth muscle by rolipram analogs. *J. Med. Chem.* **1989,***32* (7), 1450-1457.

184. Chong, J.; Poole, P.; Leung, B.; Black, P. N., Phosphodiesterase 4 inhibitors for chronic obstructive pulmonary disease. *Cochrane Database Syst. Rev.* **2011,***5*.

185. Egerland, U.; Höfgen, N.; Kuss, H.; Olbrich, M.; Rundfeldt, C.; Schindler, R.; Steinike, K. 7-azaindoles and the use thereof as therapeutic agents. US 7,947,705, 24 May., **2011**.

186. Bäumer, W.; Gorr, G.; Hoppmann, J.; Ehinger, A. M.; Rundfeldt, C.; Kietzmann, M., AWD 12–281, a highly selective phosphodiesterase 4 inhibitor, is effective in the

prevention and treatment of inflammatory reactions in a model of allergic dermatitis. *J. Pharm. Pharmacol.* **2003,***55* (8), 1107-1114.

187. He, W.; Huang, F.-C.; Hanney, B.; Souness, J.; Miller, B.; Liang, G.; Mason, J.; Djuric, S., Novel cyclic compounds as potent phosphodiesterase 4 inhibitors. *J. Med. Chem.* **1998,***41* (22), 4216-4223.

188. Armani, E.; Amari, G.; Rizzi, A.; Fanti, R. D.; Ghidini, E.; Capaldi, C.; Carzaniga, L.; Caruso, P.; Guala, M.; Peretto, I.; La Porta, E.; Bolzoni, P. T.; Facchinetti, F.; Carnini, C.; Moretto, N.; Patacchini, R.; Bassani, F.; Cenacchi, V.; Volta, R.; Amadei, F.; Capacchi, S.; Delcanale, M.; Puccini, P.; Catinella, S.; Civelli, M.; Villetti, G., Novel class of benzoic acid ester derivatives as potent PDE4 inhibitors for inhaled administration in the treatment of respiratory diseases. *J. Med. Chem.* **2014,***57* (3), 793-816.

189. Hester, J. B.; Rudzik, A. D.; Veldkamp, W., Pyrrolo[3,2,1-jk][1,4]benzodiazepines and pyrrolo[1,2,3-ef][1,5]benzodiazepines which have central nervous system activity. *J. Med. Chem.* **1970,***13* (5), 827-835.

190. Devillers, I.; Pevet, I.; Jacobelli, H.; Durand, C.; Fasquelle, V.; Puaud, J.; Gaudillière, B.; Idrissi, M.; Moreau, F.; Wrigglesworth, R., New substituted triaza-benzo[cd]azulen-9-ones as promising phosphodiesterase-4 inhibitors. *Bioorg. Med. Chem. Lett.* **2004,***14* (12), 3303-3306.

191. Pascal, Y.; Andrianjara, C. R.; Auclair, E.; Avenel, N.; Bertin, B.; Calvet, A.; Féru, F.; Lardon, S.; Moodley, I.; Ouagued, M.; Payne, A.; Pruniaux, M.-P.; Szilagyi, C., Synthesis and structure–activity relationships of 4-oxo-1-phenyl-3,4,6,7-tetrahydro-[1,4]diazepino[6,7,1-hi]indoles: novel PDE4 inhibitors. *Bioorg. Med. Chem. Lett.* **2000,***10* (1), 35-38.

192. Burnouf, C.; Auclair, E.; Avenel, N.; Bertin, B.; Bigot, C.; Calvet, A.; Chan, K.; Durand, C.; Fasquelle, V.; Féru, F.; Gilbertsen, R.; Jacobelli, H.; Kebsi, A.; Lallier, E.; Maignel, J.; Martin, B.; Milano, S.; Ouagued, M.; Pascal, Y.; Pruniaux, M.-P.; Puaud, J.; Rocher, M.-N.; Terrasse, C.; Wrigglesworth, R.; Doherty, A. M., Synthesis, structure–activity relationships, and pharmacological profile of 9-amino-4-oxo-1-phenyl-3,4,6,7-tetrahydro[1,4]diazepino[6,7,1-hi]indoles: discovery of potent, selective phosphodiesterase type 4 inhibitors. *J. Med. Chem.* **2000,***43* (25), 4850-4867.

193. Muller, G. W.; Shire, M. G.; Wong, L. M.; Corral, L. G.; Patterson, R. T.; Chen, Y.; Stirling, D. I., Thalidomide analogs and PDE4 inhibition. *Bioorg. Med. Chem. Lett.* **1998,***8* (19), 2669-2674.

194. Man, H.-W.; Schafer, P.; Wong, L. M.; Patterson, R. T.; Corral, L. G.; Raymon, H.; Blease, K.; Leisten, J.; Shirley, M. A.; Tang, Y.; Babusis, D. M.; Chen, R.; Stirling, D.; Muller, G. W., Discovery of (S)-N-[2-[1-(3-ethoxy-4-methoxyphenyl)-2-methanesulfonylethyl]-1,3-dioxo-2,3-dihydro-1H-isoindol-4-yl] acetamide (apremilast), a potent and orally active phosphodiesterase 4 and tumor necrosis factor-alpha inhibitor. *J. Med. Chem.* **2009,***52* (6), 1522-1524.

195. http://www.wikinvest.com/stock/Memory_Pharmaceuticals_(MEMY)/Pde4_Inhibitor_Program_Mem_1414_1917.

196. Palfreyman, M. N., Phosphodiesterase type IV inhibitors as antiinflammatory agents. *Drugs Future.* **1995,***20* (8), 793-804.

197. Dal Piaz, V.; Giovannoni, M. P., Phosphodiesterase 4 inhibitors, structurally unrelated to rolipram, as promising agents for the treatment of asthma and other pathologies. *Eur. J. Med. Chem.* **2000,***35* (5), 463-480.

198. Lowe, J. A.; Archer, R. L.; Chapin, D. S.; Cheng, J. B.; Helweg, D.; Johnson, J. L.; Koe, B. K.; Lebel, L. A.; Moore, P. F., Structure-activity relationship of quinazolinedione inhibitors of calcium-independent phosphodiesterase. *J. Med. Chem.* **1991,***34* (2), 624-628.

199. Alvarez, R.; Wilhelm, R.; Shelton, E.; Daniels, D.; Yang, D.; Kelly, K.; Eglen, R., Potent and selective inhibition of cyclic AMP specific phosphodiesterase (PDE IV) by structural analogs of nitraquazone. *Can. J. Physiol. Pharmacol.* **1994,***72* (Sup. 1), 510.

200. Dal Piaz, V.; Giovannoni, M. P.; Castellana, C.; Palacios, J. M.; Beleta, J.; Doménech, T.; Segarra, V., Novel heterocyclic-fused pyridazinones as potent and selective phosphodiesterase IV inhibitors. *J. Med. Chem.* **1997,***40* (10), 1417-1421.

201. Page, C.; Schudt, C.; Dent, G.; Rabe, K. F., *Phosphodiesterase Inhibitors*. Elsevier Science: **1996**.

202. Lombardo, L. J., Phosphodiesterase-IV inhibitors: novel therapeutics for the treatment of inflammatory diseases. *Curr. Pharm. Des.* **1995,***1* (2), 255-268.

203. (a) Tralau-Stewart, C. J.; Williamson, R. A.; Nials, A. T.; Gascoigne, M.; Dawson, J.; Hart, G. J.; Angell, A. D.; Solanke, Y. E.; Lucas, F. S.; Wiseman, J., GSK256066, an exceptionally high-affinity and selective inhibitor of phosphodiesterase 4 suitable for administration by inhalation: in vitro, kinetic, and in vivo characterization. *J. Pharmacol. Exp. Ther.* **2011,***337* (1), 145-154;(b) Nials, A. T.; Tralau-Stewart, C. J.; Gascoigne, M. H.; Ball, D. I.; Ranshaw, L. E.; Knowles, R. G., In vivo characterization of GSK256066, a high-affinity inhaled phosphodiesterase 4 inhibitor. *J. Pharmacol. Exp. Ther.* **2011,***337* (1), 137-144.

204. Benzofuran and quinoline carboxamides and quinoline sulfonamides as TNF inhibitors and as PDE4 inhibitors. *Expert Opin. Ther. Pat.* **1998,***8* (7), 899-905.

205. Dyke, H. J.; Montana, J. G. Heterocyclic compounds and their therapeutic use. US 6,642,254, 4 Nov., **2003**.

206. Macdonald, D.; Mastracchio, A.; Perrier, H.; Dubé, D.; Gallant, M.; Lacombe, P.; Deschênes, D.; Roy, B.; Scheigetz, J.; Bateman, K.; Li, C.; Trimble, L. A.; Day, S.; Chauret, N.; Nicoll-Griffith, D. A.; Silva, J. M.; Huang, Z.; Laliberté, F.; Liu, S.; Ethier, D.; Pon, D.; Muise, E.; Boulet, L.; Chan, C. C.; Styhler, A.; Charleson, S.; Mancini, J.; Masson, P.; Claveau, D.; Nicholson, D.; Turner, M.; Young, R. N.; Girard, Y., Discovery of a substituted 8-arylquinoline series of PDE4 inhibitors: structure-activity relationship, optimization, and identification of a highly potent, well tolerated, PDE4 inhibitor. *Bioorg. Med. Chem. Lett.* **2005,***15* (23), 5241-5246.

207. Huang, Z.; Dias, R.; Jones, T.; Liu, S.; Styhler, A.; Claveau, D.; Otu, F.; Ng, K.; Laliberte, F.; Zhang, L.; Goetghebeur, P.; Abraham, W. M.; Macdonald, D.; Dubé, D.; Gallant, M.; Lacombe, P.; Girard, Y.; Young, R. N.; Turner, M. J.; Nicholson, D. W.; Mancini, J. A., L-454,560, a potent and selective PDE4 inhibitor with in vivo efficacy in animal models of asthma and cognition. *Biochem. Pharmacol.* **2007,***73* (12), 1971-1981.

208. Gallant, M.; Chauret, N.; Claveau, D.; Day, S.; Deschênes, D.; Dubé, D.; Huang, Z.; Lacombe, P.; Laliberté, F.; Lévesque, J.-F.; Liu, S.; Macdonald, D.; Mancini, J.; Masson, P.; Mastracchio, A.; Nicholson, D.; Nicoll-Griffith, D. A.; Perrier, H.; Salem, M.; Styhler, A.; Young, R. N.; Girard, Y., Design, synthesis, and biological evaluation of 8-biarylquinolines: a novel class of PDE4 inhibitors. *Bioorg. Med. Chem. Lett.* **2008,***18* (4), 1407-1412.

209. Aspiotis, R.; Deschênes, D.; Dubé, D.; Girard, Y.; Huang, Z.; Laliberté, F.; Liu, S.; Papp, R.; Nicholson, D. W.; Young, R. N., The discovery and synthesis of highly potent subtype selective phosphodiesterase 4D inhibitors. *Bioorg. Med. Chem. Lett.* **2010,***20* (18), 5502-5505.

210. Crespo, M. a. I.; Gràcia, J.; Puig, C.; Vega, A.; Bou, J.; Beleta, J.; Doménech, T.; Ryder, H.; Segarra, V. c.; Palacios, J. M., Synthesis and biological evaluation of 2,5-dihydropyrazolo[4,3-c]quinolin-3-ones, a novel series of PDE 4 inhibitors with low emetic potential and antiasthmatic properties. *Bioorg. Med. Chem. Lett.* **2000,***10* (23), 2661-2664.

211. Atta-ur-Rahman.; Reitz, A. B.; Choudhary, I., *Frontiers in Medicinal Chemistry*. Bentham Science Publishers: **2004**; 1.

212. Suzuki, F.; Kuroda, T.; Nakasato, Y.; Manabe, H.; Ohmori, K.; Kitamura, S.; Ichikawa, S.; Ohno, T., New bronchodilators. 1. 1,5-Substituted 1H-imidazo[4,5-c]quinolin-4(5H)-ones. *J. Med. Chem.* **1992,***35* (22), 4045-4053.

213. Boswell-Smith, V.; Spina, D.; Oxford, A. W.; Comer, M. B.; Seeds, E. A.; Page, C. P., The pharmacology of two novel long-acting phosphodiesterase 3/4 inhibitors, RPL554 [9,10-dimethoxy-2(2,4,6-trimethylphenylimino)-3-(N-carbamoyl-2-aminoethyl)-3,4,6,7-tetrahydro-2H-pyrimido[6,1-a]isoquinolin-4-one] and RPL565 [6,7-dihydro-2-(2,6-diisopropylphenoxy)-9,10-dimethoxy-4H-pyrimido[6,1-a]isoquinolin-4-one]. *J. Pharmacol. Exp. Ther.* **2006,***318* (2), 840-848.

214. Hersperger, R.; Bray-French, K.; Mazzoni, L.; Müller, T., Palladium-catalyzed cross-coupling reactions for the synthesis of 6, 8-disubstituted 1,7-naphthyridines: a novel class of potent and selective phosphodiesterase type 4D inhibitors. *J. Med. Chem.* **2000,***43* (4), 675-682.

215. Hersperger, R.; Dawson, J.; Mueller, T., Synthesis of 4-(8-benzo[1,2,5]oxadiazol-5-yl-[1,7]naphthyridine-6-yl)-benzoic acid: a potent and selective phosphodiesterase type 4D inhibitor. *Bioorg. Med. Chem. Lett.* **2002,***12* (2), 233-235.

216. Trifilieff, A.; Wyss, D.; Walker, C.; Mazzoni, L.; Hersperger, R., Pharmacological profile of a novel phosphodiesterase 4 inhibitor, 4-(8-benzo[1,2,5]oxadiazol-5-yl-[1,7]naphthyridin-6-yl)-benzoic acid (NVP-ABE171), a 1,7-naphthyridine derivative, with anti-inflammatory activities. *J. Pharmacol. Exp. Ther.* **2002,***301* (1), 241-248.

217. Norman, P., PDE4 inhibitors: sustained patenting activity as leading drugs near the market. *Expert Opin. Ther. Pat.* **2000,***10* (9), 1415-1427.

218. Li, C.; Girard, M.; Hamel, P.; Laliberte, S.; Friesen, R.; Girard, Y.; Guay, D. 1-biaryl-1, 8-naphthyridin-4-one phosphodiesterase-4 inhibitors. US 6,677,351, 13 Jan., **2004**.

219. Kuroda, T.; Suzuki, F.; Tamura, T.; Ohmori, K.; Hosoe, H., A novel synthesis and potent antiinflammatory activity of 4-hydroxy-2(1H)-oxo-1-phenyl-1,8-naphthyridine-3-carboxamides. *J. Med. Chem.* **1992,***35* (6), 1130-1136.

220. Suzuki, F.; Kuroda, T.; Tamura, T.; Sato, S.; Ohmori, K.; Ichikawa, S., New antiinflammatory agents. 2. 5-Phenyl-3H-imidazo[4,5-c][1,8]naphthyridin-4(5H)-ones: a new class of nonsteroidal antiinflammatory agents with potent activity like glucocorticoids. *J. Med. Chem.* **1992,***35* (15), 2863-2870.

221. Suzuki, F.; Kuroda, T.; Kawakita, T.; Manabe, H.; Kitamura, S.; Ohmori, K.; Ichimura, M.; Kase, H.; Ichikawa, S., New bronchodilators. 3. Imidazo[4,5-c][1,8]naphthyridin-4(5H)-ones. *J. Med. Chem.* **1992,***35* (26), 4866-4874.

222. Piaz, V. D.; Giovannoni, M. P.; Castellana, C.; Palacios, J. M.; Beleta, J.; Doménech, T.; Segarra, V., Heterocyclic-fused 3(2H)-pyridazinones as potent and selective PDE IV inhibitors: further structure-activity relationships and molecular modelling studies. *Eur. J. Med. Chem.* **1998,***33* (10), 789-797.

223. Vinick, F. J.; Saccomano, N. A.; Koe, B. K.; Nielsen, J. A.; Williams, I. H.; Thadeio, P. F.; Jung, S.; Meltz, M.; Johnson, J.; Lebel, L. A.; Russo, L. L.; Helweg, D., Nicotinamide ethers: novel inhibitors of calcium-independent phosphodiesterase and [3H]rolipram binding. *J. Med. Chem.* **1991,***34* (1), 86-89.

224. Macdonald, D.; Perrier, H.; Liu, S.; Laliberté, F.; Rasori, R.; Robichaud, A.; Masson, P.; Huang, Z., Hunting the emesis and efficacy targets of PDE4 inhibitors: identification of the photoaffinity probe 8-(3-azidophenyl)-6- [(4-iodo-1H-1-imidazolyl)methyl]quinoline (APIIMQ). *J. Med. Chem.* **2000,***43* (21), 3820-3823.

225. (a) Van der Mey, M.; Boss, H.; Couwenberg, D.; Hatzelmann, A.; Sterk, G. J.; Goubitz, K.; Schenk, H.; Timmerman, H., Novel selective phosphodiesterase (PDE4) inhibitors. 4. Resolution, absolute configuration, and PDE4 inhibitory activity of cis-tetra- and cis-hexahydrophthalazinones. *J. Med. Chem.* **2002,***45* (12), 2526-2533;(b) Van der Mey, M.; Hatzelmann, A.; Van Klink, G. P. M.; Van der Laan, I. J.; Sterk, G. J.; Thibaut, U.; Ulrich, W. R.; Timmerman, H., Novel selective PDE4 inhibitors. 2. Synthesis and structure-activity relationships of 4-aryl-substituted cis-tetra- and cis-hexahydrophthalazinones. *J. Med. Chem.* **2001,***44* (16), 2523-2535.

226. Van der Mey, M.; Bommelé, K. M.; Boss, H.; Hatzelmann, A.; Van Slingerland, M.; Sterk, G. J.; Timmerman, H., Synthesis and structure-activity relationships of cis-tetrahydrophthalazinone/pyridazinone hybrids: a novel series of potent dual PDE3/PDE4 inhibitory agents. *J. Med. Chem.* **2003,***46* (10), 2008-2016.

227. Crespo, M. I.; Pagès, L.; Vega, A.; Segarra, V.; López, M.; Doménech, T.; Miralpeix, M.; Beleta, J.; Ryder, H.; Palacios, J. M., Design, synthesis, and biological activities of new thieno[3,2-d] pyrimidines as selective type 4 phosphodiesterase inhibitors. *J. Med. Chem.* **1998,***41* (21), 4021-4035.

228. Merz, K.-H.; Marko, D.; Regiert, T.; Reiss, G.; Frank, W.; Eisenbrand, G., Synthesis of 7-benzylamino-6-chloro-2-piperazino-4-pyrrolidinopteridine and novel derivatives free of positional isomers. Potent inhibitors of cAMP-specific phosphodiesterase and of malignant tumor cell growth. *J. Med. Chem.* **1998,***41* (24), 4733-4743.

229. (a) Beasley, S. C.; Cooper, N.; Gowers, L.; Gregory, J. P.; Haughan, A. F.; Hellewell, P. G.; Macari, D.; Miotla, J.; Montana, J. G.; Morgan, T.; Naylor, R.; Runcie, K. A.; Tuladhar, B.; Warneck, J. B. H., Synthesis and evaluation of a novel series of phosphodiesterase IV inhibitors. A potential treatment for asthma. *Bioorg. Med. Chem. Lett.* **1998,***8* (19), 2629-2634;(b) Gupta, R.; Kumar, G.; Kumar, R. S., An update on cyclic nucleotide phosphodiesterase (PDE) inhibitors: phosphodiesterases and drug selectivity. *Methods Find. Exp. Clin. Pharmacol.* **2005,***27* (2), 101-118.

230. Iwasaki, T.; Kondo, K.; Kuroda, T.; Moritani, Y.; Yamagata, S.; Sugiura, M.; Kikkawa, H.; Kaminuma, O.; Ikezawa, K., Novel selective PDE IV inhibitors as antiasthmatic agents. Synthesis and biological activities of a series of 1-aryl-2,3-bis(hydroxymethyl)naphthalene lignans. *J. Med. Chem.* **1996,***39* (14), 2696-2704.

231. Sugahara, M.; Moritani, Y.; Terakawa, Y.; Ogiku, T.; Ukita, T.; Iwasaki, T., A synthesis of 1-pyridylnaphthalene lignan analogs. *Tetrahedron Lett.* **1998,***39* (11), 1377-1380.

232. Ukita, T.; Sugahara, M.; Terakawa, Y.; Kuroda, T.; Wada, K.; Nakata, A.; Ohmachi, Y.; Kikkawa, H.; Ikezawa, K.; Naito, K., Novel, potent, and selective phosphodiesterase-4 inhibitors as antiasthmatic agents: synthesis and biological activities of a series of 1-pyridylnaphthalene derivatives. *J. Med. Chem.* **1999,***42* (6), 1088-1099.

233. Wells, J. N.; Kramer, G. L., Phosphodiesterase inhibitors as tools in cyclic nucleotide research: a precautionary comment. *Mol. Cell. Endocrinol.* **1981,***23* (1), 1-9.

234. Wells, J. N.; Miller, J. R., 46. Methylxanthine inhibitors of phosphodiesterases. In *Methods in Enzymology*, Jackie D. Corbin, R. A. J., Ed. Academic Press: **1988**; 159, 489-496.

235. Barnes, P., Cyclic nucleotides and phosphodiesterases and airway function. *Eur. Respir. J.* **1995,***8* (3), 457-462.

236. Banner, K.; Page, C., Theophylline and selective phosphodiesterase inhibitors as anti-inflammatory drugs in the treatment of bronchial asthma. *Eur. Respir. J.* **1995,***8* (6), 996-1000.

237. Miyamoto, K.; Kurita, M.; Ohmae, S.; Sakai, R.; Sanae, F.; Takagi, K., Selective tracheal relaxation and phosphodiesterase-IV inhibition by xanthine derivatives. *Eur. J. Pharmacol.* **1994,***267* (3), 317-322.

238. Sawanishi, H.; Suzuki, H.; Yamamoto, S.; Waki, Y.; Kasugai, S.; Ohya, K.; Suzuki, N.; Miyamoto, K.-i.; Takagi, K., Selective inhibitors of cyclic AMP-specific phosphodiesterase: heterocycle-condensed purines. *J. Med. Chem.* **1997,***40* (20), 3248-3253.

239. Suzuki, F.; Kuroda, T.; Hayashi, H.; Nakasato, Y.; Manabe, H.; Ohmori, K.; Kitamura, S., New bronchodilators. II. 3H-imidazo[4,5-c]quinolin-4(5H)-ones. *Chem. Pharm. Bull.* **1992,***40* (12), 3245-3252.

240. Miyamoto, K.; Yamamoto, Y.; Kurita, M.; Sakai, R.; Konno, K.; Sanae, F.; Ohshima, T.; Takagi, K.; Hasegawa, T., Bronchodilator activity of xanthine derivatives substituted with functional groups at the 1-or 7-position. *J. Med. Chem.* **1993,***36* (10), 1380-1386.

241. Sakai, R.; Konno, K.; Yamamoto, Y.; Sanae, F.; Takagi, K.; Hasegawa, T.; Iwasaki, N.; Kakiuchi, M.; Kato, H.; Miyamoto, K., Effects of alkyl substitutions of xanthine skeleton on bronchodilation. *J. Med. Chem.* **1992,***35* (22), 4039-4044.
242. Nicholson, C. D.; Jackman, S. A.; Wilke, R., The ability of denbufylline to inhibit cyclic nucleotide phosphodiesterase and its affinity for adenosine receptors and the adenosine re-uptake site. *Br. J. Pharmacol.* **1989,***97* (3), 889-897.
243. Ellis, G. P.; Luscombe, D. K., *Progress Medicinal Chemistry PMC33*. Elsevier Science: **1996**.
244. Buckle, D. R.; Arch, J. R. S.; Connolly, B. J.; Fenwick, A. E.; Foster, K. A.; Murray, K. J.; Readshaw, S. A.; Smallridge, M.; Smith, D. G., Inhibition of cyclic nucleotide phosphodiesterase by derivatives of 1,3-Bis(cyclopropylmethyl)xanthine. *J. Med. Chem.* **1994,***37* (4), 476-485.
245. Regnier, G. L.; Guillonneau, C. G.; Duhault, J. L.; Tisserand, F. P.; Saint-Romas, G.; Holstorp, S. M., New xanthine derivatives with potent and long lasting anti-bronchoconstrictive activity. *Eur. J. Med. Chem.* **1987,***22* (3), 243-250.
246. Busk, M. F.; Flavahan, N. A.; Vanhoutte, P. M., Effects of the methyl xanthine S 9795 on isolated bronchi of the dog. *J. Pharmacol. Exp. Ther.* **1990,***254* (3), 1045-1053.
247. Bourguignon, J.-J.; Désaubry, L.; Raboisson, P.; Wermuth, C.-G.; Lugnier, C., 9-Benzyladenines: Potent and selective cAMP phosphodiesterase inhibitors. *J. Med. Chem.* **1997,***40* (12), 1768-1770.
248. Butt, E.; Beltman, J.; Becker, D. E.; Jensen, G. S.; Rybalkin, S. D.; Jastorff, B.; Beavo, J. A., Characterization of cyclic nucleotide phosphodiesterases with cyclic AMP analogs: topology of the catalytic sites and comparison with other cyclic AMP-binding proteins. *Mol. Pharmacol.* **1995,***47* (2), 340-347.
249. Subrahmanyam, V.; Renwick, A. B.; Walters, D. G.; Price, R. J.; Tonelli, A. P.; Lake, B. G., Metabolism of a novel phosphodiesterase-IV inhibitor (V11294) by human hepatic cytochrome P450 forms. *Xenobiotica.* **2002,***32* (6), 521-534.
250. Whitehead, J. W.; Lee, G. P.; Gharagozloo, P.; Hofer, P.; Gehrig, A.; Wintergerst, P.; Smyth, D.; McCoull, W.; Hachicha, M.; Patel, A.; Kyle, D. J., 8-Substituted analogues of 3-(3-cyclopentyloxy-4-methoxy-benzyl)-8-isopropyl-adenine: highly potent and selective PDE4 inhibitors. *J. Med. Chem.* **2005,***48* (4), 1237-1243.
251. Schneller, S. W.; Ibay, A. C.; Martinson, E. A.; Wells, J. N., Inhibition of cyclic nucleotide phosphodiesterases from pig coronary artery by benzo-separated analogs of 3-isobutyl-1-methylxanthine. *J. Med. Chem.* **1986,***29* (6), 972-978.
252. (a) Gibson, L. C. D.; Hastings, S. F.; McPhee, I.; Clayton, R. A.; Darroch, C. E.; Mackenzie, A.; MacKenzie, F. L.; Nagasawa, M.; Stevens, P. A.; MacKenzie, S. J., The inhibitory profile of Ibudilast against the human phosphodiesterase enzyme family. *Eur. J. Pharmacol.* **2006,***538* (1–3), 39-42;(b) Huang, Z.; Liu, S.; Zhang, L.; Salem, M.; Greig, G. M.; Chi Chung, C.; Natsumeda, Y.; Noguchi, K., Preferential inhibition of human phosphodiesterase 4 by ibudilast. *Life Sci.* **2006,***78* (23), 2663-2668.

253. Parra, S.; Laurent, F.; Subra, G.; Deleuze-Masquefa, C.; Benezech, V.; Fabreguettes, J.-R.; Vidal, J.-P.; Pocock, T.; Elliott, K.; Small, R.; Escale, R.; Michel, A.; Chapat, J.-P.; Bonnet, P.-A., Imidazo[1,2-a]quinoxalines: synthesis and cyclic nucleotide phosphodiesterase inhibitory activity. *Eur. J. Med. Chem.* **2001,***36* (3), 255-264.

254. Vitse, O.; Laurent, F.; Pocock, T. M.; Bénézech, V.; Zanik, L.; Elliott, K. R. F.; Subra, G.; Portet, K.; Bompart, J.; Chapat, J.-P.; Small, R. C.; Michel, A.; Bonnet, P.-A.,

New imidazo[1,2-a]pyrazine derivatives with bronchodilatory and cyclic nucleotide phosphodiesterase inhibitory activities. *Bioorg. Med. Chem.* **1999,***7* (6), 1059-1065.

255. Makhay, M.; Houslay, M.; O'Donnell, J., Discriminative stimulus effects of the type-4 phosphodiesterase inhibitor rolipram in rats. *Psychopharmacology.* **2001,***158* (3), 297-304.

256. Zhang, H.-T.; Zhao, Y.; Huang, Y.; Deng, C.; Hopper, A.; De Vivo, M.; Rose, G.; O'Donnell, J., Antidepressant-like effects of PDE4 inhibitors mediated by the high-affinity rolipram binding state (HARBS) of the phosphodiesterase-4 enzyme (PDE4) in rats. *Psychopharmacology.* **2006,***186* (2), 209-217.

257. Gale, D. D.; Hofer, P.; Spina, D.; Seeds, E. A.; Banner, K. H.; Harrison, S.; Douglas, G.; Matsumoto, T.; Page, C. P.; Wong, R. H.; Jordan, S.; Smith, F.; Banik, N.; Halushka, P. V.; Cavalla, D.; Rotshteyn, Y.; Kyle, D. J.; Burch, R. M.; Chasin, M., Pharmacology of a new cyclic nucleotide phosphodiesterase type 4 inhibitor, V11294. *Pulm. Pharmacol. Ther.* **2003,***16* (2), 97-104.

258. Novel 4-aminopyrazolo[3,4-b]pyridine PDE4 inhibitors. *Expert Opin. Ther. Pat.* **2005,***15* (1), 111-114.

259. (a) Kumar, N.; Goldminz, A. M.; Kim, N.; Gottlieb, A. B., Phosphodiesterase 4-targeted treatments for autoimmune diseases. *BMC Med.* **2013,***11* (1), 96;(b) Nazarian, R.; Weinberg, J. M., AN-2728, a PDE4 inhibitor for the potential topical treatment of psoriasis and atopic dermatitis. *Curr. Opin. Investig. Drugs.* **2009,***10* (11), 1236-1242.

260. Huang, Z.; Ducharme, Y.; Macdonald, D.; Robichaud, A., The next generation of PDE4 inhibitors. *Curr. Opin. Chem. Biol.* **2001,***5* (4), 432-438.

261. Lerner, A.; Epstein, P. M., Cyclic nucleotide phosphodiesterases as targets for treatment of haematological malignancies. *Biochem Journal* **2006,***393* (1), 21-41.

262. (a) Venkatachalam, C. M.; Jiang, X.; Oldfield, T.; Waldman, M., LigandFit: a novel method for the shape-directed rapid docking of ligands to protein active sites. *J. Mol. Graph. Model.* **2003,***21* (4), 289-307;(b) Discovery Studio 3.5. Accelrys Software Inc., San Diego, CA, USA.

263. Vogel, H., *Drug discovery and evaluation: pharmacological assays*. springer: **2007**; 1.

264. Cullen, M. D.; Cheung, Y.-F.; Houslay, M. D.; Hartman, T. L.; Watson, K. M.; Buckheit Jr, R. W.; Pannecouque, C.; De Clercq, E.; Cushman, M., Investigation of the alkenyldiarylmethane non-nucleoside reverse transcriptase inhibitors as potential cAMP phosphodiesterase-4B2 inhibitors. *Bioorg. Med. Chem. Lett.* **2008,***18* (4), 1530-1533.

265. Lea, W. A.; Simeonov, A., Fluorescence polarization assays in small molecule screening. *Expert Opin. Drug Discov.* **2011,***6* (1), 17-32.

266. Elansary, A.; Kadry, H.; Ahmed, E.; Sonousi, A., Design, synthesis and in vitro PDE4 inhibition activity of certain quinazolinone derivatives for treatment of asthma. *Med. Chem. Res.* **2012,***21* (11), 3327-3335.

267. http://www.dr-green.co.uk/Powerpoint/Analgesics%20and%20pain%20web%20fin/sld040.htm.

268. Cheng, A.; Merz, K. M., Prediction of aqueous solubility of a diverse set of compounds using quantitative structure-property relationships. *J. Med. Chem.* **2003,***46* (17), 3572-3580.

269. Egan, W. J.; Lauri, G., Prediction of intestinal permeability. *Adv. Drug Deliv. Rev.* **2002,***54* (3), 273-289.

270. Susnow, R. G.; Dixon, S. L., Use of robust classification techniques for the prediction of human cytochrome P450 2D6 inhibition. *J. Chem. Inf. Comput. Sci.* **2003,***43* (4), 1308-1315.

271. Cheng, A.; Dixon, S., In silico models for the prediction of dose-dependent human hepatotoxicity. *J. Comput. Aided Mol. Des.* **2003,***17* (12), 811-823.

272. Xia, X.; Maliski, E. G.; Gallant, P.; Rogers, D., Classification of kinase inhibitors using a Bayesian model. *J. Med. Chem.* **2004,***47* (18), 4463-4470.

273. Dixon, S. L.; Merz, K. M., One-dimensional molecular representations and similarity calculations: methodology and validation. *J. Med. Chem.* **2001,***44* (23), 3795-3809.

274. Egan, W. J.; Merz, K. M.; Baldwin, J. J., Prediction of drug absorption using multivariate statistics. *J. Med. Chem.* **2000,***43* (21), 3867-3877.

275. Votano, J. R.; Parham, M.; Hall, L. M.; Hall, L. H.; Kier, L. B.; Oloff, S.; Tropsha, A., QSAR modeling of human serum protein binding with several modeling techniques utilizing structure-information representation. *J. Med. Chem.* **2006,***49* (24), 7169-7181.

276. Mahesh, R.; Jindal, A.; Gautam, B.; Bhatt, S.; Pandey, D., Evaluation of anti-depressant-like activity of linezolid, an oxazolidinone class derivative - an investigation using behavioral tests battery of depression. *Biochem. Biophys. Res. Commun.* **2011,***409* (4), 723-726.

277. Porsolt, R. D.; Anton, G.; Blavet, N.; Jalfre, M., Behavioural despair in rats: a new model sensitive to antidepressant treatments. *Eur. J. Pharmacol.* **1978,***47* (4), 379-391.

278. Steru, L.; Chermat, R.; Thierry, B.; Simon, P., The tail suspension test: A new method for screening antidepressants in mice. *Psychopharmacology.* **1985,***85* (3), 367-370.

279. Kulkarni, S.; Sharma, K., Alprazolam modifies animal behaviour on elevated plus-maze. *Indian J. Exp. Biol.* **1993,***31* (11), 908-911.

280. (a) Lauener, R. W.; Burgoyne, D. L.; Rebstein, P. J.; Mackenzie, L. F.; Zhou, Y.; Shen, Y. Benzylated PDE4 inhibitors. U.S. Patent No. 7,446,129, 4 Nov. , **2008**;(b) Lauener, R. W.; Burgoyne, D. L.; Rebstein, P. J.; Mackenzie, L. F.; Zhou, Y.; Shen, Y. Benzylated PDE4 inhibitors. U.S. Patent No. 6,555,572, 29 Apr., **2003**.

List of Publications and Presentations from Thesis

Patent

- Filed national patent – Mahesh R., **Muthu Venkatesh S.,** *PDE4 inhibitor compounds for treating anti-depressant and anxiolytic related disorders.*Application No. **1290/DEL/2014** dated **15/05/2014**

Poster Presentations at National Conferences from Thesis

- Mahesh R, **Sudali MV**, Murugesan S, Dhar AK, Mundra S, Jindal A *Design and docking study of 4-benzyl-3-oxo-3,4-dihydroquinoxaline-2-carboxamide analogues as phosphodiestrase-IV (PDE-IV) inhibitors* Indian Pharmaceutical Association (IPA) Convention 17-18th March, 2012; Manipal, Karnataka, India
- **Muthu VS**, Mahesh R, Jindal A. *Design, synthesis and pharmacological evaluation of novel phosphodiesterases-4 inhibitors as potential anti-depressants* International Conference on Recent Advances in Molecular Mechanisms of Neurological Disorders, 21-23rd February, 2013; AIIMS, New Delhi, India

List of Other Publications

- Mahesh R, Devadoss T, Pandey DK, Dhar AK, **Sudali M**, Mundra S, Bhatt S, Jindal A *Ligand-Based Design, Synthesis and Pharmacological Evaluation of 3-Methoxyquinoxalin-2-Carboxamides as Structurally Novel Serotonin Type-3 Receptor Antagonists* Archiv. Der. Pharmazie, 2012; 345, 687-94 *(Wiley Online Library)*

List of Other Poster Presentations at National conference

- **S. Muthu Venkatesh**, R. Mahesh, Chandan Raychaudhury, F. Nawaz Khan D*ocking study of potential ligands on CYP 450 3A4 using Ligandfit*62nd Indian Pharmaceutical Congress 17-19th December, 2010; Manipal, Karnataka, India
- Mahesh R, Mundra S, Devadoss T, Dhar AK, **Sudali MV***Design and synthesis of pyrimidine scaffold for their kinase inhibitor activity* National conference of Pharmanext 19-20th February, 2012; Aligarh, U.P, India
- Mahesh R, Dhar AK, Jindal A, **Muthu VS**, Mundra S *Design, synthesis and pharmacological evaluation of Novel 2-(4-substituted piperazine 1-yl)-1,8-naphthyridine 3-carboxylic acids as 5-HT3 receptor antagonists for the management of depression* Indian Pharmaceutical association convention 17-18th March, 2012; Manipal, Karnataka, India

Biography of Prof. R. Mahesh

Dr. Mahesh is currently working as Professor, Department of Pharmacy and Dean, Faculty Affairs in BITS, Pilani. He was awarded Ph.D (Medicinal Chemistry) in 1997 from BITS, Pilani. He has been involved in teaching and research for past more than two decades. He has vast experience in the field of Molecular Modeling and Drug Design, Medicinal chemistry, Neuropharmacology and Clinical Pharmacy and Therapeutics. He has successfully completed several funded projects and some on-going projects as Principal Investigator by UGC, DBT, DST and ICMR. He has guided six Ph.D students and six students are pursuing. He has guided several postgraduate and undergraduate students on various projects. Several of his projects have won several awards in Academic Exhibitions. He has published several papers in peer reviewed international/national Journals and in conferences of international/national repute.He is life time member of Association of Pharmaceutical Teachers of India, Indian Pharmacological Society and Society of Neurochemistry, India.

Biography of Muthu Venkatesh S

Mr. Muthu Venkatesh S has completed his Bachelor of Pharmacy (B. Pharm) from K. M. College of Pharmacy, Madurai, affiliated to Dr. M. G. R Medical University, Chennai, Tamil Nadu in 2004, Master of Technology (M. Tech) from School of Advanced Science, VIT University, Tamil Nadu in 2008 and Postgraduate diploma in Intellectual property rights (IPR) from Nalsar, Hyderabad in 2013. He served as lecturer in Pharmacy College in Mahabubnagar and Ananthapur, A.P. He is the recipient of DBT-JRF and UGC-BSR fellowships during doctoral program. He has filed a national patent from his research work and presented papers in national conferences. He is a life time member of Association of Pharmaceutical Teachers of India (APTI) and Society of Neurochemistry in India (SNCI).